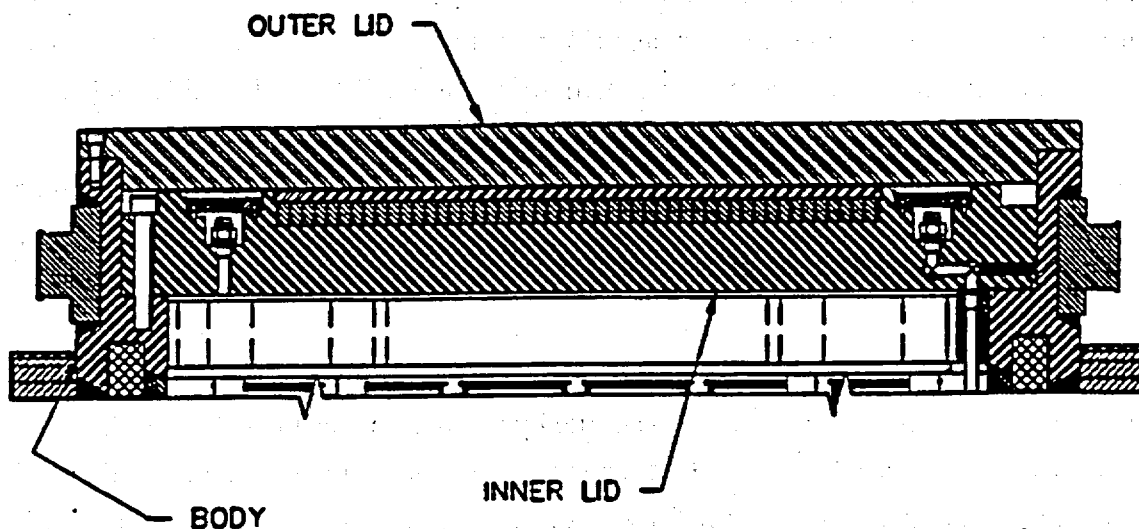


2.6.7.5 Closure Analysis - Normal Conditions of Transport

The main closure of the NAC-STC is effected by an assembly of a bolted inner lid and a bolted outer lid. The Type 304 stainless steel inner lid is bolted to the top forging by forty-two 1 1/2 - 8 UN bolts fabricated from SB-637, Grade N07718 nickel alloy bolting material and is sealed by two metallic o-rings. The SA-705, Type 630, 17-4 PH stainless steel outer lid is bolted to the end of the top forging by thirty-six 1 - 8 UNC bolts fabricated from SA-564, Type 630, 17-4 PH stainless steel, and is sealed to the top forging by one metallic o-ring.



Closure Assembly of NAC-STC Body and Lids

2.6.7.5.1 Closure Geometry

The main body of the inner lid is 9.0 inches thick and 79.0 inches in diameter. A 3.0-inch thick, 2.75-inch wide integral outer rim on the top of the inner lid encloses a 2.0-inch thick layer of NS-4-FR neutron shielding material and a 1.0-inch thick, Type 304 stainless steel coverplate. The inner lid provides the primary containment for the NAC-STC main closure.

The outer lid is a plate consisting of a 5.25-inch thick central body having a 79.08-inch diameter and a 2.50-inch thick integral outer flange having an outside diameter of 86.70 inches. There is a 0.06-inch gap between the inner lid and the outer lid.

2.6.7.5.2 Closure Analysis Considerations

The closure assembly analysis must demonstrate that the lids and bolts satisfy two criteria: (1) calculated maximum stresses must be less than the allowable stress limit (the material yield strength is conservatively selected) and (2) lid deformation and/or rotation at the o-ring locations must be less than the elastic rebound of the o-rings.

Finite element evaluations of the closure are performed using the ANSYS computer program and a two-dimensional axisymmetric model. The critical design load conditions for the NAC-STC closure are three 10 CFR 71 accident loading conditions: (1) impact limiter crush pressure on the outer lid; (2) pin puncture on the outer lid; and (3) impact of the cavity contents on the inner lid. These accident condition analyses are presented in Section 2.7.1.6. The lids and bolts are evaluated at a temperature of 200°F and 270°F, respectively. The impact stresses in the closure components for the normal conditions of transport 1-foot drop are calculated by ratioing the impact stresses calculated in Section 2.7.1.6 according to the g-loads documented in Table 2.6.7.4-3.

The package geometry, package weight, and contents weight are the parameters that control the closure design. This fact is demonstrated to be true by the analysis results in Tables 2.6.7.5-1, -2, -3, and -4, as well as Tables 2.7.1.6-2, -3, -4, and -5. The tables show that the inner lid and bolts (the containment boundary) are critical for end or "near end" impact load conditions and the outer lid bolts are critical for side or "near side" impact load conditions. The closure evaluation presented in this section is for the package (loaded NAC-STC cask with impact limiters as described on the drawings in Section 1.3.2) with a total weight of 260,000 pounds and a cavity contents weight of 67,196 pounds. This evaluation envelopes all of the NAC-STC cask configurations, i.e., the directly loaded fuel configuration, the canistered fuel configuration, and the canistered GTCC waste configuration. The package geometry is identical for all of the configurations, as is the package center of gravity location. Therefore, the closure analyses in this section and in Sections 2.7.1.6, 2.7.3.4, and 2.10.8 are applicable for the directly loaded and the canistered configurations of the NAC-STC.

2.6.7.5.3 Closure Analysis Results

2.6.7.5.3.1 Description

The critical normal conditions of transport loading for the inner lid is the 1-foot top end drop. Since the 45.3 psig maximum internal operating pressure (Section 3.4.4), MNOP = 12 psig produces a minimal portion of the inner lid stress, approximately 1,500 psi (Table 2.10.4-1, Sections U, V, W, and X), the maximum inner lid primary membrane plus bending stress for the 1-foot top end drop is calculated by ratioing from the 30-foot top end drop result shown in Table 2.7.1.6-1 (Load Condition 1):

$$S_{IL} = (18,088)(19.6/56.1) = 6,320 \text{ psi}$$

For the inner lid primary membrane plus primary bending stress ($P_m + P_b$) the allowable stress limit is $1.5 S_m$, which for Type 304 stainless steel is 30.0 ksi at 200°F.

Then,

$$MS = \frac{1.5S_m}{S_{IL}} - 1 = \underline{+Large}$$

The critical normal conditions of transport loading for the outer lid is also the 1-foot top end drop. The outer lid is loaded on its outer surface by the crush pressure of the upper impact limiter. The maximum outer lid primary membrane plus bending stress for the 1-foot top end drop is calculated by ratioing from the 30-foot top end drop result shown in Table 2.7.1.6-1 (Load Condition 1):

$$S_{OL} = (19,647)(19.6/56.1) = 6,864 \text{ psi}$$

For the outer lid primary membrane plus bending stress ($P_m + P_b$), the allowable stress limit is $1.5 S_m$, which for Type 17-4 PH, H1150 stainless steel is 67.5 ksi at 200°F.

Then,

$$MS = \frac{1.5S_m}{S_{OL}} - 1 = \underline{+Large}$$

2.6.7.5.4 Lid Bolt Analysis - Normal Conditions of Transport

The NAC-STC inner and outer lid bolts are preloaded at installation to ensure that the sealing function of the o-rings located in the inner and in the outer lids are maintained. The lid bolts are installed with a torque that is calculated to produce a total tensile load that is not less than the total load on the lid; that is, the sum of: (1) internal pressure force on the lid; (2) o-ring compression force; (3) inertial weight of the lid (calculated weight multiplied by the impact load factor); and (4) inertial weight of any other components that can contact the lid (calculated weight multiplied by the impact load factor). Since the total bolt preload exceeds the total load on the lid, there is no movement of the lid relative to its mating component and the status of the seal at the o-ring(s) is maintained.

The bounding load condition for the NAC-STC inner lid bolt evaluation is the combined weight of the loaded Yankee-MPC canister, canister spacers, and inner lid multiplied by the acceleration factors applicable to the redwood impact limiter as summarized in Tables 2.6.7.4.1-1 through 2.6.7.4.1-3. Although the loaded CY-MPC canister configuration is heavier, the lower acceleration factor developed by the balsa impact limiters (Tables 2.6.7.4.2-1 and 2.6.7.4.2-2) results in a lower impact load on the inner lid bolts. Using the values from the tables, the Yankee-MPC end drop impact load is $(66,690 \times 19.6g =) 1.31 \times 10^6$ lbs. The corresponding CY-MPC impact load is $(77,885 \times 15.2 =) 1.18 \times 10^6$ lbs. The internal pressure of the CY-MPC configuration is also less than that of the directly loaded and Yankee-MPC configurations. Therefore, the directly loaded and Yankee-MPC configurations are bounding for the inner lid bolt analysis. Since the redwood impact limiter is heavier than the balsa impact limiter, the directly loaded and Yankee-MPC configurations are also bounding for the outer lid bolt analysis.

2.6.7.5.4.1 Inner Lid Bolts

The inner lid of the NAC-STC is bolted to the top forging of the cask body by forty-two 1 1/2 - 8 UN bolts that are fabricated from SB-637, Grade N07718 nickel alloy bolting material.

Since the coefficient of thermal expansion for the SB-637, Grade N07718 nickel alloy bolting material is lower than that of the Type 304 stainless steel inner lid, the inner lid expands faster than the bolts during normal transport heat-up, and the bolt preload increases. The differential thermal expansion between the inner lid and the bolts results in an increase in the bolt tensile stress of 9,184 psi is calculated below.

The required preload on the inner lid bolts considers the following factors: (1) an internal pressure force on the inner lid of 45.3 psig (60 psia); (2) the o-ring compression force due to the two metallic o-rings for the inner lid; (3) the inertial weight of the inner lid, basket, and fuel due to the 30-foot accident drop conditions; and (4) the differential thermal expansion between the inner lid material and the bolt. Based on the above considerations, an installation torque of 2,540 \pm 200 foot-pounds is conservatively selected for the inner lid bolts. The maximum torque value, 2,740 foot-pounds, develops a tensile force of 115,066 pounds based on the following relationship:

$$T = \left[\left(\frac{d_m}{2d} \right) \left(\frac{\tan \lambda + \mu \sec \alpha}{1 - \mu \tan \lambda \sec \alpha} \right) + 0.625 \mu \right] (F)(d)$$

where:

- T = applied torque in inch-pounds
- F = preload force in pounds
- d = bolt diameter = 1.50 in
- d_m = mean diameter of threads = 1.4375 in
- α = one-half the thread angle = 30°
- μ = coefficient of friction = 0.15
- $\tan \lambda = 1 / (\pi d_m n)$
- n = 8 threads per inch

Therefore, the bolt preload, F_{bp}, due to a 2,740 foot-pound torque for each inner lid bolt, is determined as:

$$\begin{aligned} T &= (0.1905)F_{bp}d \\ F_{bp} &= (2,740)(12)/(0.1905)(1.5) \\ F_{bp} &= 115,066 \text{ lbs} \end{aligned}$$

The tensile stress due to the differential expansion of the bolt and the lid is:

$$\begin{aligned} S_{dt} &= \Delta T(\alpha_L - \alpha_B)E_B \\ &= 9,184 \text{ psi} \end{aligned}$$

where:

$$\begin{aligned} \Delta T &= 270^\circ\text{F} - 70^\circ\text{F} \\ &= 200^\circ\text{F} \end{aligned}$$

α_L = 8.94×10^{-6} in/in/°F, coefficient of expansion of Type 304 stainless steel lid

α_B = 7.30×10^{-6} in/in/°F, coefficient of expansion of SB-637, Grade N07718 nickel alloy bolting material

E_B = 28.0×10^6 psi, modulus of elasticity of SB-637, Grade N07718 nickel alloy bolting material

The average tensile stress in the inner lid bolt is:

$$S_t = \frac{F_{bp}}{A_t} + S_{dt}$$

$$= 86,306 \text{ psi}$$

where:

$$A_t = \text{tensile stress area for } 1 \frac{1}{2} - 8 \text{ UN thread} = 1.492 \text{ in}^2$$

The margin of safety is:

$$MS = \frac{2S_m}{S_t} - 1 = +0.09$$

where:

$$2 S_m = 94.5 \text{ ksi @ } 270^\circ\text{F (SB-637, Grade N07718 nickel alloy bolting material)}$$

In general, the lid impact loads may impose unequal individual forces, or loadings, in each of the inner lid bolts. This NAC-STC evaluation conservatively assumes a set of impact forces that induce maximum containment closure separation forces and bolt loadings.

With this conservative assumption, the external impact force is presumed to be located at a point where it cannot restrain those forces that tend to separate the cask lid from the cask body. This assumption locates the external impact force at the lower corner of the lid-body interface. With this assumption, the lower corner of the lid is assumed to be pinned (by the impact forces), and bolt tension forces are assumed to vary linearly from zero at this pinned lower corner to a maximum value at the opposite, or upper, corner of the lid.

A complete range of impact orientations is evaluated, from an end impact at 0 degrees to a side impact at 90 degrees, using 5-degree increments. Loads are derived from the normal impact accelerations summarized within Table 2.6.7.4.1-1. Where necessary, impact accelerations have been interpolated at 5-degree increments from those values given in Table 2.6.7.4.1-1.

The details of this analytic evaluation are described and an example calculation is performed within Section 2.10.8 for the hypothetical accident condition. Normal conditions of transport results are summarized in Tables 2.6.7.5-1 and 2.6.7.5-2, corresponding to a "hot" condition and a "cold" condition, respectively. The hot condition bolt temperatures are assumed to be 200°F, as summarized in Table 3.4-5. The cold condition bolt temperatures are assumed to be -20°F, per regulatory requirements. Physical properties for the SB-637, Grade N07718 nickel alloy bolts are conservatively taken at 270°F for both the hot and cold conditions. As defined in Table 2.1.2-1, the allowable maximum bolt stress for normal conditions for primary membrane stress is two times the design stress intensity, $2S_m$, resulting in allowable direct tension stresses of 94.5 ksi at 270°F. Based on this thorough evaluation, the inner lid bolts incur a maximum stress intensity of 88,435 psi, which results in a minimum margin of safety of +0.07 (See Table 2.6.7.5-2, 5°).

$$MS = (94,500/88,435) - 1 = +0.07$$

The ultimate load capacity of the inner lid bolt/top forging threaded connection relative to the ultimate tensile load capacity of the inner lid bolt is evaluated to ensure that the length of engagement is sufficient to develop the full strength of the bolt. The inner lid bolt holes have threaded inserts to protect the threads during the likely numerous installations and removals of the bolts.

Component Description

Inner lid Bolt

- 1 1/2 - 8 UN
 - SB-637, Grade N07718 Nickel Alloy Steel Bolting
- Material

- Length in cask body = 2.63 inches
- $S_u = 174.7$ ksi at 270°F

Threaded Insert

- Helicoil #4190-24 CN x 2.50
- (AMS 7245) 18-8 Stainless Steel
- Length of insert = 2.50 inches
- O.D. = 1 5/8 - 8 UN Thread
- $S_u = 200.0$ ksi

Top Forging (Cask Body)

- Type 304 Stainless Steel
- Thread depth = $3.0 - 0.125 = 2.875$ in
- $S_u = 62.9$ ksi at 270°F

(Bolt Strength)

Tensile Area, A_t	=	1.492 in^2 (1 1/2 - 8 UN Thread)
Tensile Strength, S_u	=	174.8 ksi
Bolt-Tensile Load Capacity, P_{BLC}	=	$(1.492)(174,700)$ = 260,652 lbs

(Threaded Insert/Bolt Interface)

Thread Size	=	1 1/2 - 8 UN
Engaged Length	=	$2.50 - 0.12 = 2.38$ in
Bolt: S_u	=	174.7 ksi
Insert: S_u	=	200.0 ksi

External (Bolt) Thread Shear Area

$$AS_s = (\pi)(n)(L_e)(K_{nmax})[(1/2n) + (0.57735)(E_{Smin} - K_{nmax})]^*$$
$$= 6.123 \text{ in}^2$$

* FED-STD-H28 (1963), Page 103.

where:

$$n = 8 \text{ threads/in}$$

$$L_e = 2.38 \text{ in}$$

$$E_{smin} = 1.4093 \text{ in Min. Pitch Diameter of External Threads}$$

$$K_{nmax} = 1.390 \text{ in Max. Minor Diameter of Internal Threads}$$

$$\begin{aligned} \text{Bolt Thread-Tensile Load Capacity, } P_{BT} &= (6.123)(0.5^* \times 174,700) \\ &= 534,844 \text{ lbs} \end{aligned}$$

Internal (Insert) Thread Shear Area

$$\begin{aligned} AS_n &= (\pi)(n)(L_e)(D_{smin})[(1/2n) + (0.57735)(D_{smin} - E_{nmax})]** \\ &= 8.334 \text{ in}^2 \end{aligned}$$

where:

$$D_{smin} = 1.4828 \text{ in Min. Major Diameter of External Thread}$$

$$E_{nmax} = 1.4283 \text{ in Max. Pitch Diameter of Internal Thread}$$

$$\begin{aligned} \text{Insert Thread-Tensile Load Capacity, } P_{IT} &= (8.334)(0.5^* \times 200,000) \\ &= 833,430 \text{ lbs} \end{aligned}$$

(Threaded Insert/Top Forging Interface)

$$\text{Thread Size} = 1 \frac{5}{8} - 8 \text{ UN}$$

$$\text{Engaged Length} = 2.50 - 0.12 = 2.38 \text{ in}$$

$$\text{Insert: } S_u = 200 \text{ ksi}$$

$$\text{Top Forging: } S_u = 62.9 \text{ ksi}$$

* Shear Strength Conservatively Assumed = (0.5)(Tensile Strength).

** FED-STD-H28 (1963), page 103.

External (Insert) Thread Shear Area

$$\begin{aligned}AS_s &= (\pi)(n)(L_e)(K_{nmax})[(1/2n) + (0.57735)(E_{Smin} - K_{nmax})]^* \\ &= 6.668 \text{ in}^2\end{aligned}$$

where:

$$\begin{aligned}n &= 8 \text{ threads/inch} \\ L_e &= 2.38 \text{ in} \\ E_{smin} &= 1.5342 \text{ in Min. Pitch Diameter of External Threads} \\ K_{nmax} &= 1.515 \text{ in Max. Minor Diameter of Internal Threads}\end{aligned}$$

$$\begin{aligned}\text{Insert Thread-Tensile Load Capacity, } P_{ITO} &= (6.668)(0.5^{**} \times 200,000) \\ &= 666,800 \text{ lbs}\end{aligned}$$

Internal (Top Forging) Thread Shear Area

$$\begin{aligned}AS_n &= (\pi)(n)(L_e)(D_{Smin})[(1/2n) + (0.57735)(D_{Smin} - E_{nmax})]^* \\ &= 9.026 \text{ in}^2\end{aligned}$$

where:

$$\begin{aligned}D_{smin} &= 1.6078 \text{ in Min. Major Diameter of External Thread} \\ E_{nmax} &= 1.5535 \text{ in Max. Pitch Diameter of Internal Thread}\end{aligned}$$

$$\begin{aligned}\text{Top Forging Thread - Tensile Load Capacity, } P_{TFT} &= (9.026)(0.5^{**} \times 62,900) \\ &= 283,868 \text{ lbs}\end{aligned}$$

* FED-STD-H28 (1963), page 103.

** Shear Strength Conservatively Assumed = (0.5)(Tensile Strength).

<u>Component</u>	<u>Ultimate Load Capacity</u> <u>(lbs)</u>
Inner Lid Bolt	260,652
Bolt Thread	534,844
Insert I.D. Thread	833,430
Insert O.D. Thread	666,800
Top Forging Thread	283,868

$$MS = (283,868/260,652) - 1 = +0.09$$

Since the minimum Tensile Load Capacity of the threaded joint exceeds the maximum Tensile Load Capacity of the inner lid bolt, the design requirements are satisfied. The inner lid bolt threaded-joint design is satisfactory.

Using consistently conservative assumptions, the NAC-STC inner lid is shown to satisfy the performance and structural integrity requirements of 10 CFR 71.71(c)(7) for normal conditions of transport.

2.6.7.5.4.2 Outer Lid Bolts

The outer lid of the NAC-STC is bolted to the end of the top forging by thirty-six 1 - 8 UNC bolts that are fabricated from SA-564, Type 630, H1150, 17-4 PH stainless steel, which has mechanical properties that are identical to those of the material of the outer lid (SA-705, Type 630, H1150, 17-4 PH stainless steel). Thus, there is negligible differential thermal expansion between the outer lid bolts and the outer lid, since they are at essentially the same temperature and have the same mechanical properties.

The required preload on the outer lid bolts considers the following factors: (1) a conservative interlid pressure force on the outer lid of 7.35 psig (1.5 atm absolute) to provide operational flexibility; (2) the o-ring compression force due to the metallic o-ring located between the cask forging and the outer lid; and (3) the inertial weight of the outer lid and impact limiter, due to the 30-foot accident drop conditions, considering the impact limiter together with the outer lid for the 30-foot accident drop condition envelopes the transport conditions when the influence of the impact limiter is actually transmitted to the outer lid bolts. Based on these

loading conditions for the outer lid bolts, an installation torque of 550 ± 50 foot-pounds is conservatively selected for the outer lid bolts. The maximum torque value, 600 foot-pounds, develops a tensile force of 36,810 pounds based on the following relationship:

$$T = \left[\left(\frac{d_m}{2d} \right) \left(\frac{\tan \lambda + \mu \sec \alpha}{1 - \mu \tan \lambda \sec \alpha} \right) + 0.625 \mu \right] (F_{bp})(d) \quad (\text{Shigley})$$

where:

T = applied torque in inch-pounds

F_{bp} = preload force in pounds

d = bolt diameter = 1.00 in

d_m = mean diameter of thread = 0.9375 in

α = one-half the thread angle = 30°

μ = coefficient of friction = 0.15

$$\tan \lambda = 1 / (\pi d_m n)$$

n = 8 threads per inch

Therefore, the bolt preload, F_{bp} , due to a 600 foot-pound torque for each outer lid bolt, is determined as:

$$T = (0.1956)F_{bp}d$$

$$F_{bp} = (600)(12)/(0.1956)(1.0)$$

$$F_{bp} = 36,810 \text{ lbs}$$

The average tensile stress in the outer lid bolt is:

$$S_t = F_{bp} / A_t$$

$$= 60,743 \text{ psi}$$

where:

A_t = tensile stress area for 1 - 8 UNC thread

$$= 0.606 \text{ in}^2$$

The margin of safety is:

$$MS = (2S_m/S_t) - 1 = +0.48$$

where:

$$2S_m = 90.0 \text{ ksi at } 270^\circ\text{F (SA-564, Type 630, H1150, 17-4 PH stainless steel)}$$

The outer lid bolts are evaluated under normal transport conditions in the same manner as the inner lid bolts were evaluated in Section 2.6.7.5.4.1. The method of analysis used is described and an example calculation is performed in Section 2.10.8. The lid impact loads are assumed to impose unequal forces in the closure bolts. The loads are derived from the normal impact accelerations summarized in Table 2.6.7.4.1-1. A complete range of impact orientations is evaluated, from an end impact at 0 degrees to a side impact at 90 degrees, at 5-degree increments. Where necessary, impact accelerations have been interpolated at 5-degree increments from those given in Table 2.6.7.4.1-1.

Tables 2.6.7.5-3 and 2.6.7.5-4 summarize the results of the evaluation of the outer lid bolt stresses under the normal conditions of transport corresponding to a "hot" condition and a "cold" condition, respectively. The hot condition bolt temperature is taken at 200°F, as summarized in Table 3.4-5. The cold condition bolt temperature is assumed to be -20°F, per regulatory requirements. Physical properties for the SA-564, Type 630, H1150, 17-4 PH stainless steel bolt material are conservatively taken at 270°F for both the hot and cold condition. As defined in Table 2.1.2-1, the allowable primary membrane stress is taken as $2S_m$, resulting in allowable direct tension stresses of 90,000 psi. Based on this thorough evaluation, the outer lid bolts incur a maximum stress intensity of 62,698 psi, which results in a minimum margin of safety of + 0.44 (See Table 2.6.7.5-4, 90°):

$$MS = (90,000/62,698) - 1 = + 0.44$$

Bolt engagement may be evaluated by computing shear stresses within the SA-336, Type 304, inner lid. At 270°F, the allowable shear stress is $0.6S_m$, or 12.0 ksi, according to Table 2.3.2-2. The maximum tensile bolt load is found as the product of the maximum bolt stress intensity, noted above, and the bolt stress area ($62,518 \times 0.606 = 37,886$ lbs). The shear area per inch of

engagement for a 1 - 8 UNC internal thread is 2.325 square inches (Screw-Thread Standards for Federal Services). The resultant shear stress and margin of safety within the inner lid forging is:

$$\begin{aligned}\tau &= 37,886 / (2.325)(2.0) \\ &= 8,148 \text{ psi}\end{aligned}$$

$$MS = (12,000 / 8,148) - 1 = + 0.47$$

2.6.7.5.5 Conclusion

Using consistently conservative assumptions, the NAC-STC closure assembly has been shown to satisfy the performance and structural integrity requirements of 10 CFR 71.71(c)(7) for normal conditions of transport.

Table 2.6.7.5-1 NAC-STC "Hot" Inner Lid Bolt Analysis (Normal Conditions of Transport)

Nominal Bolt Diameter (in):	1.5	Longitudinal Weight (lb):	66,690
Number of Bolts:	42	Lateral Weight (lb):	10,690
Service Stress, 2Sm (psi):	94,400		
Bolt Expansion (in/in):	7.30E-06 at a 270°F		
Bolt Modulus of Elasticity (ksi):	27,950 Service Temp.		
Lid Expansion (in/in):	8.94E-06	CALCULATED LOADS & STIFFNESS	
Lid Modulus of Elasticity (ksi):	27,180	Bolt Thermal Load (lb):	13,703
Bolt Stress Area (in ²):	1.492	Bolt Preload (lb):	115,066
		Bolt Static Load (lb):	9,036
Maximum Pressure (psig):	45.3	Bolt Stiffness (lb/in):	4.57E+06
Seal Diameter (in):	73.247	Lid Stiffness (lb/in):	5.40E+07
Preload Torque (ft/lb):	2,740 at room temperature		
Nominal Room Temp. °F:	70		
Bolt Circle Diameter (in):	75.31		
Lid Diameter (in):	79.00		

Angle wrt. Vert. (deg)	Impact Accel. ¹ (g)	LOAD (lbs)				STRESS (psi)					Margin of Safety
		Impact		Bolt Tension		Direct Tension	Shear	Principal		Stress Intens.	
		Tension	Shear	Applied	Net			S2	S1		
0 End	17.7	37141	0	37141	131667	88249	0	0	88249	88249	0.07
5 (+)	14.9	31653	331	31653	131944	88434	222	-1	88435	88435	0.07
10 (+)	12.1	25411	535	25411	131457	88108	358	-1	88109	88111	0.07
15 (+)	9.3	19156	613	19156	130969	87781	411	-2	87783	87784	0.08
20 (+)	6.5	13025	566	13025	130490	87460	379	-2	87462	87463	0.08
24 Corner	4.3	8377	445	8377	130128	87217	298	-1	87218	87219	0.08
30 (+)	4.9	9049	624	9049	130180	87252	418	-2	87254	87256	0.08
35 (+)	5.4	9433	788	9433	130210	87272	528	-3	87275	87279	0.08
40 (+)	5.9	9638	965	9638	130226	87283	647	-5	87288	87292	0.08
45 (+)	6.5	9801	1170	9801	130239	87291	784	-7	87298	87306	0.08
50 (+)	7.0	9595	1365	9595	130223	87281	915	-10	87290	87300	0.08
55 (+)	7.5	9173	1564	9173	130190	87259	1048	-13	87271	87284	0.08
60 (+)	8.0	8530	1763	8530	130140	87225	1182	-16	87241	87257	0.08
65 (+)	8.5	7660	1961	7660	130072	87179	1314	-20	87199	87219	0.08
70 (+)	9.0	6564	2153	6564	129986	87122	1443	-24	87146	87170	0.08
75 (+)	9.6	5298	2360	5298	129887	87056	1582	-29	87085	87113	0.08
80 (+)	10.1	3740	2532	3740	129766	86974	1697	-33	87008	87041	0.08
85 (+)	10.6	1970	2688	1970	129628	86882	1801	-37	86919	86957	0.09
90 Side	11.1	0	2825	0	129474	86779	1894	-41	86820	86861	0.09

¹ See Section 2.6.7.4 for impact acceleration details.

Table 2.6.7.5-2 NAC-STC "Cold" Inner Lid Bolt Analysis (Normal Conditions of Transport)

Nominal Bolt Diameter (in):	1.5	Longitudinal Weight (lb):	66,690
Number of Bolts:	42	Lateral Weight (lb):	10,690
Service Stress, 2Sm (psi):	94,400		
Bolt Expansion (in/in):	7.30E-06 at a 270°F		
Bolt Modulus of Elasticity (ksi):	27,950 Service Temp.		
Lid Expansion (in/in):	8.94E-06		
Lid Modulus of Elasticity (ksi):	27,180		
Bolt Stress Area (in ²):	1.492		
		CALCULATED LOADS & STIFFNESS	
Maximum Pressure (psig):	45.3	Bolt Thermal Load (lb):	0
Seal Diameter (in):	73.247	Bolt Preload (lb):	115,066
Preload Torque (ft/lb):	2740 at room temperature	Bolt Static Load (lb):	9,036
Nominal Room Temp. °F:	70	Bolt Stiffness (lb/in):	4.57E+06
Bolt Circle Diameter (in):	75.31	Lid Stiffness (lb/in):	5.40E+07
Lid Diameter (in):	79.00		

Angle wrt. Vert. (deg)	Impact Accel. ¹ (g)	LOAD (lbs)				STRESS (psi)					Margin of Safety
		Impact		Bolt Tension		Direct Tension	Shear	Principal		Stress Intens.	
		Tension	Shear	Applied	Net			S2	S1		
0 End	19.6	40158	0	40158	118199	79222	0	0	79222	79222	0.19
5 (+)	16.6	35264	368	35264	118523	79439	247	-1	79439	79440	0.19
10 (+)	13.6	28561	601	28561	118000	79088	403	-2	79090	79092	0.19
15 (+)	10.6	21834	698	21834	117475	78736	468	-3	78739	78742	0.20
20 (+)	7.6	15229	662	15229	116959	78391	443	-3	78393	78396	0.20
24 Corner	5.2	10130	538	10130	116561	78124	361	-2	78126	78128	0.21
30 (+)	6.4	11819	814	11819	116693	78213	546	-4	78216	78220	0.21
35 (+)	7.4	12926	1080	12926	116780	78271	724	-7	78277	78284	0.21
40 (+)	8.3	13558	1358	13558	116829	78304	910	-11	78314	78325	0.21
45 (+)	9.3	14023	1674	14023	116865	78328	1122	-16	78344	78360	0.20
50 (+)	10.3	14118	2008	14118	116873	78333	1346	-23	78356	78379	0.20
55 (+)	11.3	13821	2356	13821	116849	78317	1579	-32	78349	78361	0.20
60 (+)	12.2	13008	2689	13008	116786	78275	1802	-41	78316	78358	0.20
65 (+)	13.2	11896	3045	11896	116699	78217	2041	-53	78270	78323	0.21
70 (+)	14.2	10357	3396	10357	116579	78136	2276	-66	78202	78269	0.21
75 (+)	15.2	8389	3737	8389	116426	78033	2505	-80	78114	78194	0.21
80 (+)	16.1	5962	4036	5962	116236	77906	2705	-94	78000	78094	0.21
85 (+)	17.1	3178	4336	3178	116019	77761	2906	-108	77869	77978	0.21
90 Side	18.1	0	4607	0	115771	77595	3088	-123	77717	77840	0.21

¹ See Section 2.6.7.4 for impact acceleration details.

Table 2.6.7.5-3 NAC-STC "Hot" Outer Lid Bolt Analysis (Normal Conditions of Transport)

Nominal Bolt Diameter (in):	1	Longitudinal Weight (lb):	16,985
Number of Bolts:	36	Lateral Weight (lb):	8,120
Service Stress, 2Sm (psi):	90,000		
Bolt Expansion (in/in):	5.90E-06 at a 270°F		
Bolt Modulus of Elasticity (ksi):	27,300 Service Temp.		
Lid Expansion (in/in):	5.90E-06	CALCULATED LOADS & STIFFNESS	
Lid Modulus of Elasticity (ksi):	27,300	Bolt Thermal Load (lb):	0
Bolt Stress Area (in ²):	0.606	Bolt Preload (lb):	36,810
		Bolt Static Load (lb):	4,000
Maximum Pressure (psig):	7.35	Bolt Stiffness (lb/in):	5.49E+06
Seal Diameter (in):	81.81	Lid Stiffness (lb/in):	6.83E+07
Preload Torque (ft/lb):	600		
Nominal Room Temp. °F:	70		
Bolt Circle Diameter (in):	83.7		
Lid Diameter (in):	86.7		

Angle wrt. Vert. (deg)	Impact Accel. ¹ (g)	LOAD (lbs)				STRESS (psi)					Margin of Safety
		Impact		Bolt Tension		Direct Tension	Shear	Principal		Stress Intens.	
		Tension	Shear	Applied	Net			S2	S1		
0 End	17.7	12351	0	12351	37729	62259	0	0	62259	62259	0.45
5 (+)	14.9	9388	293	9388	37806	62386	483	-4	62390	62393	0.44
10 (+)	12.1	7536	474	7536	37668	62159	782	-10	62168	62178	0.45
15 (+)	9.3	5681	543	5681	37530	61931	896	-13	61944	61957	0.45
20 (+)	6.5	3863	501	3863	37395	61708	827	-11	61719	61730	0.46
24 Corner	4.3	2484	394	2484	37292	61538	851	-7	61545	61552	0.46
30 (+)	4.9	2684	553	2684	37307	61563	912	-14	61576	61580	0.46
35 (+)	5.4	2798	699	2798	37316	61577	1153	-22	61598	61620	0.46
40 (+)	5.9	2858	855	2858	37320	61584	1412	-32	61617	61649	0.46
45 (+)	6.5	2907	1037	2907	37324	61590	1711	-47	61638	61685	0.46
50 (+)	7.0	2846	1209	2846	37319	61583	1996	-65	61647	61712	0.46
55 (+)	7.5	2721	1386	2721	37310	61567	2287	-85	61652	61737	0.46
60 (+)	8.0	2530	1563	2530	37296	61544	2579	-108	61652	61760	0.46
65 (+)	8.5	2272	1738	2272	37276	61512	2867	-133	61646	61779	0.46
70 (+)	9.0	1947	1908	1947	37252	61472	3148	-161	61633	61794	0.46
75 (+)	9.6	1571	2092	1571	37224	61426	3451	-193	61620	61813	0.46
80 (+)	10.1	1109	2244	1109	37190	61370	3702	-223	61592	61815	0.46
85 (+)	10.6	584	2382	584	37151	61305	3930	-251	61556	61807	0.46
90 Side	11.1	0	2504	0	37107	61233	4131	-277	61511	61788	0.46

¹ See Section 2.6.7.4 for impact acceleration details.

Table 2.6.7.5-4 NAC-STC "Cold" Outer Lid Bolt Analysis (Normal Conditions of Transport)

Nominal Bolt Diameter (in):	1	Longitudinal Weight (lb):	16,985
Number of Bolts:	36	Lateral Weight (lb):	8,120
Service Stress, 2Sm (psi):	90,000		
Bolt Expansion (in/in):	5.90E-06 at a 270°F		
Bolt Modulus of Elasticity (ksi):	27,300 Service Temp.		
Lid Expansion (in/in):	5.90E-06	CALCULATED LOADS & STIFFNESS	
Lid Modulus of Elasticity (ksi):	27,300	Bolt Thermal Load (lb):	0
Bolt Stress Area (in ²):	0.608	Bolt Preload (lb):	36,810
		Bolt Static Load (lb):	4,000
Maximum Pressure (psig):	7.35	Bolt Stiffness (lb/in):	5.49E+06
Seal Diameter (in):	81.81	Lid Stiffness (lb/in):	6.83E+07
Preload Torque (ft/lb):	600		
Nominal Room Temp. °F:	70		
Bolt Circle Diameter (in):	83.7		
Lid Diameter (in):	86.7		

Angle wrt. Vert. (deg)	Impact Accel. ¹ (g)	LOAD (lbs)				STRESS (psi)					Margin of Safety
		Impact		Bolt Tension		Direct	Shear	Principal		Stress Intens.	
		Tension	Shear	Applied	Net	Tension		S2	S1		
0 End	19.6	13247	0	13247	37795	62369	0	0	62369	62369	0.44
5 (+)	18.6	10459	326	10459	37886	62517	538	-5	62522	62527	0.44
10 (+)	13.6	8471	533	8471	37738	62273	879	-12	62286	62298	0.44
15 (+)	10.8	6476	619	6476	37589	62028	1021	-17	62045	62062	0.45
20 (+)	7.6	4517	586	4517	37443	61788	967	-15	61803	61818	0.46
24 Corner	5.2	3004	477	3004	37331	61602	787	-10	61612	61622	0.46
30 (+)	6.4	3505	722	3505	37368	61664	1191	-23	61687	61710	0.46
35 (+)	7.4	3834	957	3834	37393	61704	1580	-40	61744	61785	0.46
40 (+)	8.3	4021	1203	4021	37407	61727	1986	-64	61791	61855	0.46
45 (+)	9.3	4159	1483	4159	37417	61744	2448	-97	61841	61938	0.45
50 (+)	10.3	4187	1780	4187	37419	61747	2937	-139	61887	62026	0.45
55 (+)	11.3	4099	2088	4099	37412	61737	3445	-192	61928	62120	0.45
60 (+)	12.2	3858	2383	3858	37394	61707	3933	-250	61957	62206	0.45
65 (+)	13.2	3528	2698	3528	37370	61667	4453	-320	61986	62306	0.44
70 (+)	14.2	3072	3010	3072	37336	61610	4967	-398	62008	62406	0.44
75 (+)	15.2	2488	3312	2488	37293	61539	5485	-482	62020	62502	0.44
80 (+)	16.1	1768	3576	1768	37239	61450	5901	-562	62012	62574	0.44
85 (+)	17.1	943	3842	943	37178	61349	6340	-648	61998	62648	0.44
90 Side	18.1	0	4083	0	37107	61233	6737	-732	61966	62698	0.44

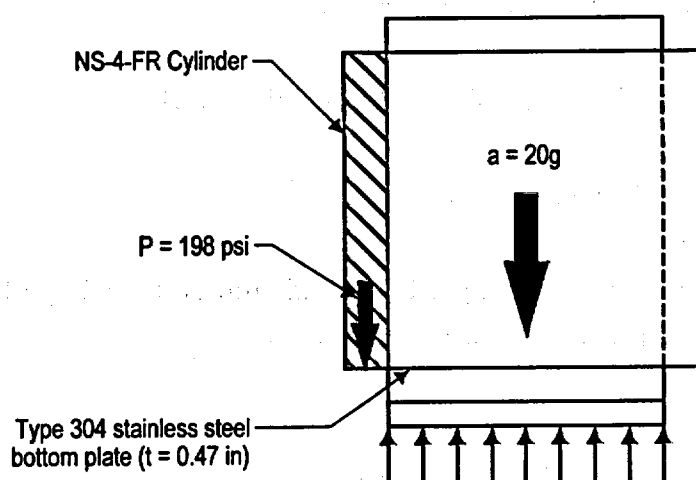
¹ See Section 2.6.7.4 for impact acceleration details.

2.6.7.6 Neutron Shield Analysis

The NAC-STC neutron shield is evaluated for two distributed-load conditions: a 1-foot end drop event and a 1-foot side drop event. For each of these conditions, the solid neutron shielding material applies a load on the neutron shield shell. The weights of the neutron shield shell and fins are included in the analysis. The neutron shield geometry is shown in Figure 2.6.7.6-1.

2.6.7.6.1 End Plate One-Foot End Drop Analysis

The primary loading on the neutron shield shell and end plates is the weight of the NS-4-FR neutron shielding material. The neutron shield is evaluated for the impact loading of the NS-4-FR during a 1-foot bottom end drop event.



The load on the bottom plate, including the weight of the plate itself, is calculated as:

$$\begin{aligned} p &= d_B L + d_p t \\ &= 9.89 \text{ psi} \end{aligned}$$

where:

$$d_B = (1.68) \frac{62.4}{1,728}$$

$$= 0.0607 \text{ lbs/in}^3, \text{ density of NS-4-FR}$$

$$\text{NS-4-FR specific gravity} = 1.68$$

$$L = 160.7 \text{ in, height of NS-4-FR material}$$

$$d_p = 0.288 \text{ lbs/in}^3, \text{ density of Type 304 stainless steel}$$

$$t = 0.472 \text{ in, plate thickness}$$

The deceleration of the package during a 1-foot end drop event is 20 g (Table 2.6.7.4.1-1). The impact load on the plate is calculated as:

$$P_i = p(20)$$

$$= 194 \text{ psi}$$

The material properties (conservatively taken at 300°F) for the Type 304 stainless steel shell, fins, and bottom plate are:

$$S_u = 66.0 \text{ ksi}$$

$$S_y = 22.5 \text{ ksi}$$

$$S_m = 20.0 \text{ ksi}$$

$$S_s = (0.60)S_m$$

$$= 12.0 \text{ ksi}$$

(Allowable Stresses)

The allowable stress intensity for the normal condition loading, according to Regulatory Guide 7.6, is:

$$\text{Axial + Bending } (S_{\text{allow}})_n = 1.5 S_m = 30.0 \text{ ksi}$$

where

$$S_m = 20.0 \text{ ksi for Type 304 stainless steel}$$

Stress Analysis

From Table 26, Case 1a, of Formulas for Stress and Strain, the stress in the end plate is:

$$\sigma_{\text{max}} = \frac{\beta P b^2}{t^2}$$

$$= 18,248 \text{ psi.}$$

where

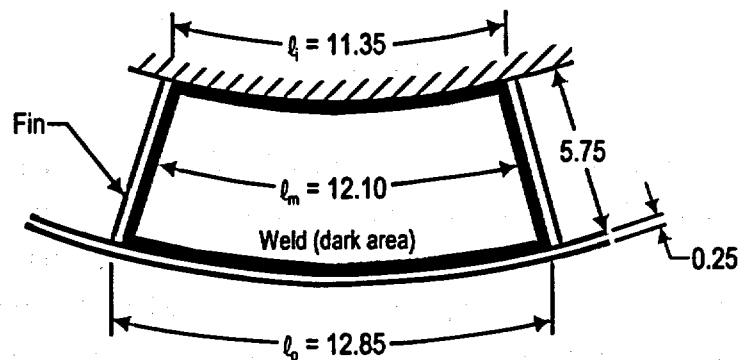
$$\begin{aligned} P &= P_1 = 198 \text{ psi} \\ a &= 12.1 \text{ in} \\ b &= 5.75 \text{ in} \\ t &= 0.472 \text{ in (12 mm)} \\ a/b &= 2.10 \\ \beta &= 0.621 \end{aligned}$$

The margin of safety is:

$$MS = \frac{(\sigma_{\text{allow}})_n}{\sigma_{\text{max}}} - 1 = +0.64$$

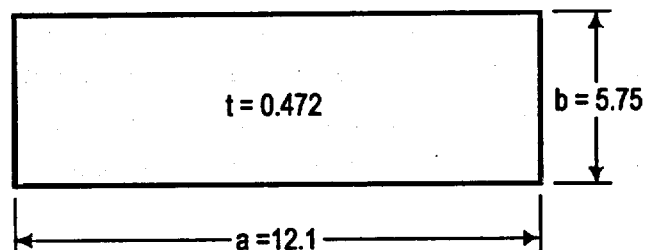
where

$$(\sigma_{\text{allow}})_n = 1.5 S_m = 30,000 \text{ psi}$$



(Dimensions in inches)

Neutron Shield Bottom Plate



(Dimensions in inches)

Equivalent Flat Plate Simply

For the reaction in the welds, assume all welds are quarter-inch fillets, which is conservative.

$$q_w = \frac{(198)(5.75)(12.1)}{(2)(5.75+12.1)}$$
$$= 386 \text{ lb/in}$$

$$q_i = \text{allowable shear/inch}$$
$$= (S_s)(0.707)(0.25)$$
$$= 2,121 \text{ lb/in}$$

The margin of safety is:

$$MS = \frac{q_i}{q_w} - 1 = + 4.49$$

2.6.7.6.2 Side Drop Analysis

This analysis assumes that the cask is subjected to a 1-foot side drop event. The side drop impact force is limited by the upper and lower impact limiters. For this analysis, an impact force that is equivalent to a 20 g side impact is used. The impact limiter stops the cask before the neutron shield contacts the impacted surface. Therefore, the impact force is distributed through the cask body from the impact limiters. The impact deceleration force of the weight of the neutron shielding material is reacted by the neutron shield shell and fins, which transfer the load to the cask body. The NS-4-FR neutron shielding material is assumed to act as an internal pressure on the shell.

Since the structural function of the neutron shield shell and radial heat transfer fin provides support for the NS-4-FR radial neutron shield, ASME Code Section III, Subsection NF, Component Supports, is used as governing structural criteria for the evaluation of the welds connecting the radial heat transfer fins to the neutron shield shell and cask outer shell.

In addition to assuming the conservative load combination resulting from cold impact loads and discontinuity thermal expansion between the NS-4-FR and radial fin from hot steady state conditions, an additional 3 psi pressure is assumed to have been created from potential gas loss from the NS4FR subjected to extended service in a high end temperature environment.

Load on the weld joints has been categorized into the following service level conditions following the methodology of ASME Section III criteria and cask design practice.

Service Level B

- 1) Pressure developed on the neutron shield shell from differential radial thermal expansion of the NS-4-FR neutron shield relative to the Type 304 stainless steel radial heat transfer fin. Considering differential thermal expansion and three percent initial compression of the HT800 expansion foam on the inside surface of the neutron shield shell, compression of the foam develops a service load of:

$$\begin{aligned}\text{Compression} &= 3\% (0.125) + 0.05143 \\ &= 0.05519\end{aligned}$$

$$\begin{aligned}\% \text{ Compression} &= \frac{0.05519}{0.125} \times 100 \\ &= 44.15\%\end{aligned}$$

From the manufacturer design information presented in Table 2.6.7.6-1, the equivalent pressure load developed on the neutron shield shell is 16.8 psi.

- 2) Potential pressure developed from extended service of the NS-4-FR neutron shield at highend temperature defined as 3 psi for this evaluation.

Service Level C

- 1) Service Level B loads plus dynamic induced load from a postulated one foot side impact (20g):

Considering the mass of the neutron shield shell and NS-4-FR, the effective pressure load becomes:

$$\begin{aligned}M &= \left[(0.2885)(0.25) + (0.0607) \left[\frac{\frac{(99+98.2)}{2} - 86.7}{2} - 0.25 - 0.125 \right] \frac{12.1}{12.85} \right] \\ &= 0.392 \text{ pound}\end{aligned}$$

$$P = MA = (0.392)(20) \\ = 7.8 \text{ psi}$$

Service Level D

- 1) Service Level B loads plus dynamic induced load from a postulated 30-foot side impact (55g).

Considering the mass of the neutron shield shell and the NS-4-FR, the affective pressure load becomes:

$$P = (0.392)(55) \\ = 21.56 \text{ psi}$$

The following evaluation is presented for two different load orientations of the heat transfer fin welds. Case 1 represents the loads induced as a result of loading applied to the neutron shield shell and Case 2 represents loading applied to the radial heat transfer fin.

Case 1 - Neutron Shield Shell Loading

Implementing the design criteria for noncontainment support structures presented in NF-3250, normal operation load service level stress in the weld region connecting the neutron shield shell to the radial heat transfer fin is evaluated using a conservative simplification of the plate and shell structure to that of a uniformly loaded beam having unit depth.

The maximum tension stress from Service Level B is:

$$S = \frac{6q}{t^2} = 26,112 \text{ psi}$$

where:

$$q = \frac{wl^2}{12} = 272 \text{ lb}$$

$$w = 19.1 + 3 = 22.1 \text{ psi}$$

$$I = 12.85 \text{ inch}$$

$$t = 0.25 \text{ inch}$$

Allowable stress limits defined in NF-3256.2 for full penetration groove welds defines acceptable stress for this condition of load as:

$$S_{\text{allowable}} = 1.33 \times 1.5 \times 17,300 \\ = 34,514 \text{ psi}$$

$$\text{Margin of Safety} = \frac{34,514}{26,112} - 1 = +0.18$$

The maximum tension stress for Service Level C load is:

$$S = \frac{6q}{t^2} = 36,461 \text{ psi}$$

where:

$$q = \frac{wl^2}{12} = 379.8 \text{ lb}$$

$$w = 19.8 + 7.8 = 27.6 \text{ psi}$$

$$l = 12.85 \text{ inch}$$

$$t = 0.25$$

Allowable membrane plus bending stress limits defined in NF-3256.2 for Service Level C limits is:

$$S_{\text{allowable}} = 1.5 \times 1.5 \times 17,300 \\ = 38,925 \text{ psi}$$

The Margin of Safety is:

$$MS = \frac{38,925}{36,461} - 1 = +0.07$$

The maximum tension stress for Service Level D load is:

$$S = \frac{6q}{t^2} = 40,973 \text{ psi}$$

As directed by NE-3256.2 for Level D, qualification of the structure is based on ASME Code Section III, Appendix F, Paragraph F-1340, "Acceptance Criteria Using Plastic System Analysis".

Considering plastic failure of fixed-ended beams with uniformly distributed load, the plastic moment is (M.R. Horne, "Plastic Theory of Structures", 2nd Edition, Pergamon Press.):

$$M = \frac{wl^2}{16} = 426.8 \text{ lb}$$

where

$$w = 19.8 + 21.56 = 41.4 \text{ psi}$$

$$l = 12.85 \text{ inch}$$

$$t = 0.25 \text{ inch}$$

Paragraph F-1340 defines the allowable primary membrane plus primary bending stress intensity as the lesser of 1.5 (2.4S_m) and 1.5 (0.7S_u). Implementation of this criteria limits Service Level D stress to 69,300 psi. The resulting Margin of Safety is:

$$MS = \frac{69,300}{40,973} - 1 = +0.69$$

In addition to the evaluation of the maximum local bending stress in the weld region, shear stress is evaluated as:

$$S_s = \frac{wl}{2t}$$

where

$$l = 12.85$$

$$t = 0.25$$

Service Level	w (psi)	S _s (psi)	S _{Allowable} (psi)	Margin of Safety
B	19.8	509	1.33 (.4S _y)=11,790	Large
C	27.6	709	1.5(.4S _y)=13,500	Large
D	41.4	1,064	0.42S _u = 27,720	Large

Case 2 - Heat Transfer Fin Loading

Following a similar method as used in the evaluation of the neutron shield shell, the heat transfer fin is evaluated using a uniformly loaded beam with a fixed end at the cask outer shell surface and a simple support at the neutron shield shell. Since Level B load is developed from radial thermal growth of the NS-4-FR and postulated off gas pressure, service level B does not load the fin in the lateral direction. Tension stress developed in the fin from these radial loads is 70 psi and insignificant.

Lateral load from service level C produces the following stress:

$$S = \frac{6q}{t^2} = 4,481 \text{ psi}$$

where

$$q_{\text{Max}} = \frac{wl^2}{6} = 74.1 \text{ lb}$$

$$w = (0.0607)(12.1)(20) = 14.7 \text{ psi}$$

$$l = \frac{98.2 - 86.7}{2} - 0.25 = 5.5 \text{ inch}$$

$$t = 0.315 \text{ inch}$$

From the evaluation of the neutron shield shell above, the service level C allowable is 38.7 ksi, therefore, the Margin of Safety is:

$$MS = \frac{38,925}{4,481} - 1 = +7.7$$

Lateral load for Service Level D produces the following stress:

$$S = \frac{6q}{t^2} = 12,317 \text{ psi}$$

where

$$q_{\text{Max}} = \frac{wl^2}{6} = 203.7 \text{ inch lb}$$

$$w = (0.0607)(12.1)(55) = 40.4 \text{ psi}$$

$$l = 5.5 \text{ inch}$$

$$t = 0.315 \text{ inch}$$

Using the Acceptance Criteria for an elastic system analysis provided in ASME Section III, Appendix F, Paragraph F-1332.2, $(1.5 \times 1.2S_y \text{ or } 1.5 \times 1.55 S_m < 1.5 \times .7S_u)$.

$$S_{\text{Allowable}} = 46,500 \text{ psi}$$

$$MS = \frac{46,500}{12,317} - 1 = +2.8$$

In addition to the evaluation of the maximum local bending stress in the weld region, shear stress is evaluated as:

$$S_s = \frac{wl}{2t}$$

where

$$l = 5.5 \text{ inch}$$

$$t = 0.31 \text{ inch}$$

Service Level	w (psi)	S_s (psi)	$S_{\text{Allowable}}$ (psi)	Margin of Safety
C	14.7	130	$1.5(0.4S_y) = 13,500$	Large
D	40.4	358	$0.42(S_u) = 27,720$	Large

Therefore, the heat transfer load path through the welds connecting the neutron shield skin to the radial heat transfer fins is maintained for all transport package normal and accident condition loads.

2.6.7.6.3 Tiedown Bearing Analysis

The maximum vertical tiedown load applied to the cask during transport in a railcar is 4g (Section 2.5.2.2.1). Considering half of this tiedown load to be restrained by the tiedown strap (the other half of the load is carried by the rear support, through the rotation trunnion), the load on the tiedown strap is:

$$\begin{aligned} P &= 1/2 (4)(260,000) \\ &= 520,000 \text{ lb} \end{aligned}$$

The tiedown strap bears on the cask top forging between the lifting trunnion and the neutron shield endplates.

Bearing stress, S_s , of 5,091 psi is calculated by conservatively assuming 90° contact between the tiedown bar and the cask top forging.

Bearing stress:

$$\text{Bearing stress, } S_s = \frac{2P}{\pi R t} = 5,091 \text{ psi}$$

where:

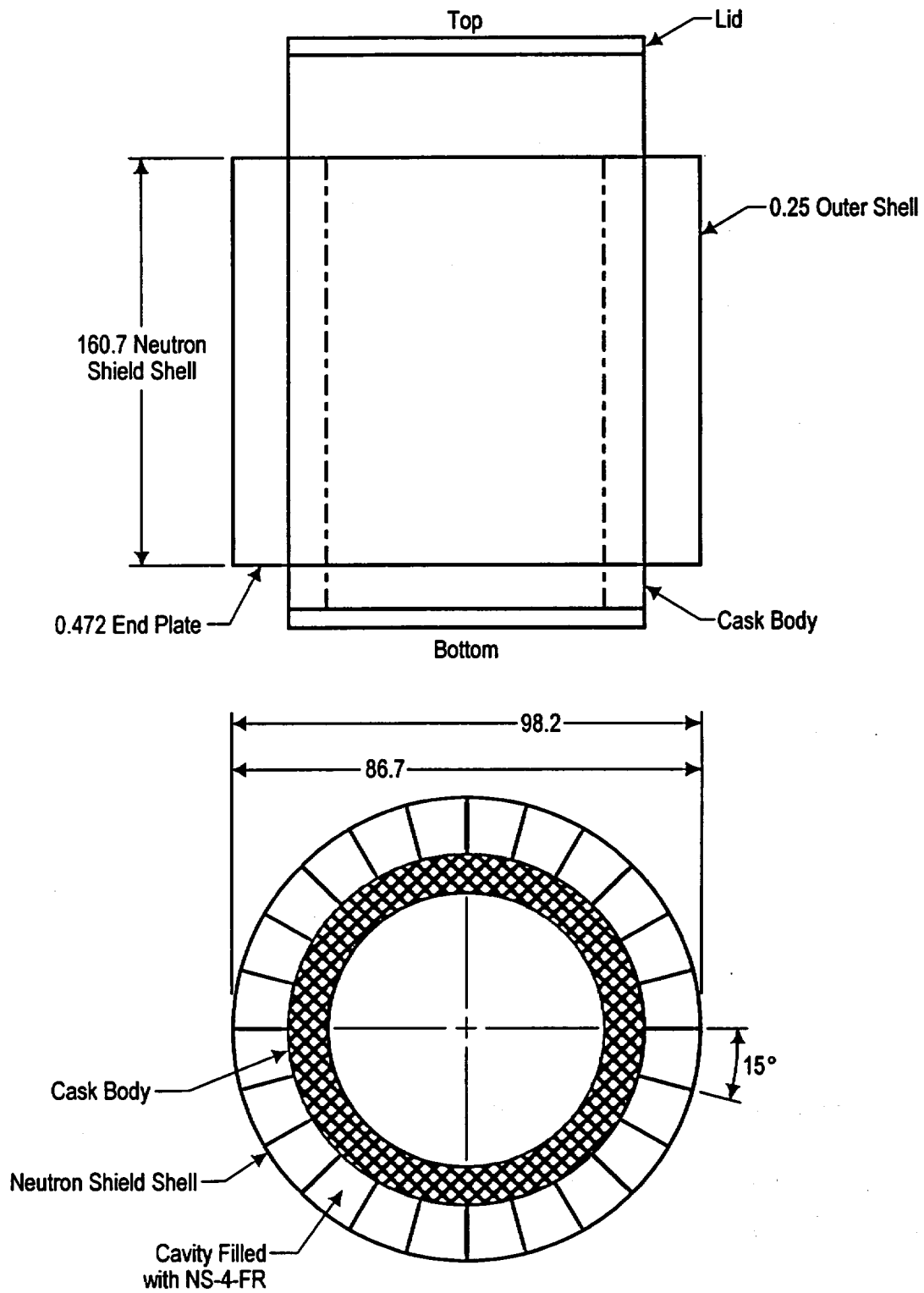
$t = 1.5$ inches, Thickness of tiedown bar

$R = 43.35$ inches, Cask surface radius

The temperature of the neutron shield shell during normal operation is 241°F with material yield stress, S_y , of 23,980 psi.

$$MS = \frac{S_y}{S_s} - 1 = +3.71$$

Figure 2.6.7.6-1 Neutron Shield Shell Geometry



(Dimensions in inches)

Table 2.6.7.6-1 Neutron Shield Expansion Foam - Manufacturer's Force-Deflection Data

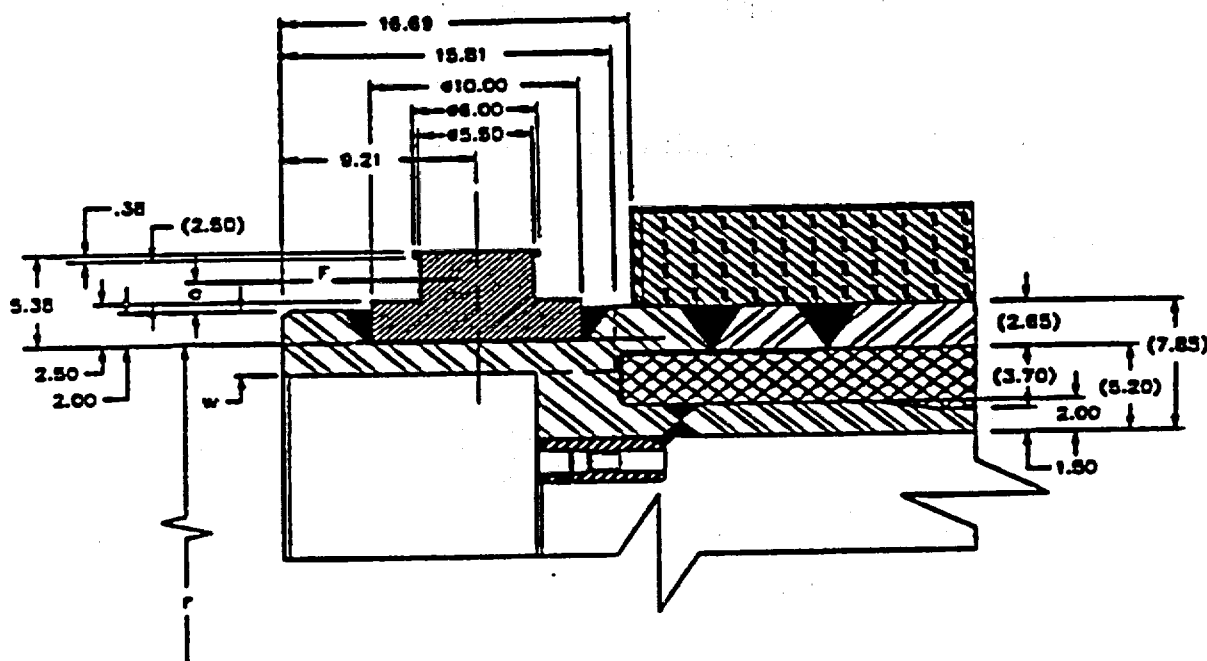
% COMPRESSED	HT800¹ DEFLECTION FORCE (psi)
10 %	3.6
25 %	8.3
40 %	13.7
55 %	24.9
70 %	60.9

1. Data provided by BISCO Products, Inc.

THIS PAGE INTENTIONALLY LEFT BLANK

2.6.7.7 Upper Ring/Outer Shell Intersection Analysis

A bounding analysis of the directly loaded fuel configuration and the canistered Yankee-MPC and CY-MPC configurations of the NAC-STC is presented in this section. A weight of 260,000 pounds (CY-MPC design weight) is used, which bounds the 250,000-pound design weight of the Yankee-MPC and directly loaded fuel configurations. Bending stresses are induced in the upper ring and outer shell intersection region of the cask body when the cask is lifted at the lifting trunnions. These stresses are evaluated via a closed form ring solution based on a method described in the paper, "How to Find Deflection and Moment of Rings and Arcuate Beams," (Blake). For the purpose of the calculation, this region is taken to be a ring (shown below). The support provided by the bolted inner and outer lids is conservatively neglected in this analysis.



(Dimensions in inches)

Forces Applied to Trunnion For Cask Lifting Analysis

The geometry and loading of the equivalent ring are defined as follows:

$$\begin{aligned} F &= \text{lifting force} = \frac{260,000}{2} \\ &= 130,000 \text{ lb} \end{aligned}$$

$$q = \text{dead weight load per unit length}$$

$$w = \text{width of equivalent ring} = 3.79 \text{ in}$$

$$\begin{aligned} r &= \text{mean radius of the equivalent ring} = \frac{43.35 + 39.56}{2} \\ &= 41.455 \text{ in} \end{aligned}$$

$$\begin{aligned} a &= \text{moment arm for the equivalent ring} = 45.1 - 41.455 \\ &= 3.645 \text{ in} \end{aligned}$$

Based on a total weight of 260,000 pounds, q is calculated as:

$$q (\pi)(41.455)(2) = 260,000$$

$$q = 998.2 \text{ lb/in}$$

The moment and torque on the equivalent ring are given by:

$$M = \frac{T_o \sin \theta}{2} - qr^2 \left(1 - \frac{\pi}{2} \sin \theta \right)$$

$$T = \frac{T_o \cos \theta}{2} + qr^2 \left(\theta + \frac{\pi}{2} \cos \theta - \frac{\pi}{2} \right)$$

where

θ is measured from the trunnion ($\theta = 0$) in plane perpendicular to the centerline of the cask ($0 \leq \theta \leq 180$)

$$T_o = (F)(a) = (130,000)(3.645) = 473,850 \text{ in-lb}$$

Substituting for T_o , q , r (Table 2.6.7.7-1)

$$M = 2.369 \times 10^5 \sin \theta - 1.715 \times 10^6 \left(1 - \frac{\pi}{2} \sin \theta\right)$$

$$T = 2.369 \times 10^5 \cos \theta + 1.715 \times 10^6 \left(\theta + \frac{\pi}{2} \cos \theta - \frac{\pi}{2}\right)$$

The normal stress is treated as bending, due to the moment acting over a cross section.

$$\sigma = \frac{M(h/2)}{I}$$

where

$$h = 15.81 \text{ in}$$

$$I = \frac{wh^3}{12}$$

$$= 1248.1 \text{ in}^4$$

so

$$\sigma = \frac{(15.81/2)}{1,248.1} (M)$$

$$= 0.00633 (M)$$

The shear stress is obtained from Roark and Young, 5th Edition, Table 20, Case 4:

$$\begin{aligned}\tau &= \frac{T \left[3 \left(\frac{h}{2} \right) + 1.8 \left(\frac{w}{2} \right) \right]}{8 \times \frac{h^2}{4} \times \frac{w^2}{4}} \\&= \frac{2T[(1.5)(h) + (0.9)(w)]}{(h)^2(w)^2} \\&= \frac{2T[(1.5)(15.85) + (0.9)(3.79)]}{(15.85)^2(3.79)^2} \\&= 0.151T\end{aligned}$$

The maximum stress intensity, where the moment and torque are functions of σ , is calculated as:

$$\begin{aligned}\text{S.I.} &= 2\sqrt{\sigma^2/4 + \tau^2} \\&= 2\sqrt{(10.017 \times 10^{-6})M^2 + (2.28 \times 10^{-4})T^2}\end{aligned}$$

Resultant values of the stress intensity are evaluated in Table 2.6.7.7-1.

The margin of safety is:

$$MS = \frac{30,000}{22,790} - 1 = \underline{+0.32}$$

where

$$S_m = 20,000 \text{ psi}$$

$$S_{\text{allow}} = 1.5 S_m = 30,000 \text{ psi}$$

Table 2.6.7.7-1 Resultant Stress Intensity Values in the Equivalent Ring

Angle (degrees)	Moment (E+6) (in-lbs)	Torque (E+5) (in-lbs)	S.I. (psi)
0.0	-1.715	2.369	13,000
5.0	-1.460	3.754	14,620
10.0	-1.206	4.917	16,700
15.0	-.956	5.860	18,700
20.0	-.713	6.588	20,400
25.0	-.476	7.106	21,670
30.0	-.249	7.422	22,470
35.0	-.034	7.545	22,790
40.0	.169	7.485	22,630
45.0	.357	7.254	22,020
50.0	.530	6.866	21,000
55.0	.686	6.334	19,620
60.0	.823	5.674	17,910
65.0	.941	4.903	15,960
70.0	1.039	4.038	13,850
75.0	1.116	3.096	11,720
80.0	1.171	2.096	9,749
85.0	1.205	1.058	8,268
90.0	1.216	0.000	7,696

THIS PAGE INTENTIONALLY LEFT BLANK

2.6.8 Corner Drop (1 Foot)

According to 10 CFR 71.71(c)(8), this test is not applicable to the NAC-STC because the cask is composed of materials other than fiberboard or wood and the cask weight exceeds 220 pounds (100 kg).

THIS PAGE INTENTIONALLY LEFT BLANK

2.6.9 Compression

According to 10 CFR 71.71(c)(9), this test is not applicable to the NAC-STC because the package weight is greater than 5,000 kilograms (11,023 lb).

THIS PAGE INTENTIONALLY LEFT BLANK

2.6.10 Penetration

This condition is defined in 10 CFR 71 as a 40-inch drop of a 13-pound, 1.25-inch diameter penetration cylinder with a hemispherical end onto any exposed surface of the cask. The acceptance criteria is that the drop will not adversely affect the ability of the cask to maintain containment of the contents or to survive a hypothetical accident. The impact limiters, the neutron shield, and the port covers could potentially be damaged by this penetration impact. An evaluation of a penetration impact on each of these components follows.

THIS PAGE INTENTIONALLY LEFT BLANK

2.6.10.1 Impact Limiter - Penetration

There are two NAC-STC cask impact limiter configurations. The first is constructed of redwood and balsa and may be used in the transport of directly loaded fuel or the Yankee-MPC canistered fuel or GTCC waste. This impact limiter configuration is referred to as the redwood impact limiter. The second is constructed of all balsa and must be used with the CY-MPC canistered fuel or GTCC waste configurations, but may be used with the directly loaded and Yankee-MPC configurations. Both impact limiter configurations have the impact absorbing wood enclosed in a stainless steel shell.

2.6.10.1.1 Redwood Impact Limiter Penetration

The 0.25-inch thick stainless steel outer shell of the impact limiter, backed by redwood and balsa wood, resists puncture by the penetration cylinder. However, the puncture resistance of the shell is conservatively not considered in this analysis. The 13.0-pound penetration cylinder drops 40.0 inches, producing $(13.0)(40.0) = 520$ inch-pounds of energy, which is assumed to be absorbed only by the redwood and balsa wood materials. The crush strength of the redwood material is about 500 psi for initial strain conditions, and the area of the penetration cylinder is 1.227 square inches. Therefore, using the redwood crush strength and the average impact area in the conservation of energy equation, the penetration cylinder might penetrate bare redwood material to a depth of $520/[(500)(1.227)/2] = 1.7$ inches. This depth of depression would not significantly affect the performance of the impact limiter.

2.6.10.1.2 Balsa Impact Limiter Penetration

Similar to the redwood impact limiter evaluation, the 0.25-inch thick stainless steel outer shell of the impact limiter, backed by balsa, resists puncture by the penetration cylinder. The dropped cylinder produces 520 inch-pounds of energy, which is absorbed by the balsa. The crush strength of the balsa is about 1,500 psi for initial strain conditions, and the area of the penetration cylinder is 1.227 square inches. Therefore, using the balsa crush strength and the average impact area in the conservation of energy equation, the penetration cylinder might penetrate bare redwood material to a depth of $520/[(1,500)(1.227)/2] = 0.57$ inches. This depth of depression would not significantly affect the performance of the impact limiter.

THIS PAGE INTENTIONALLY LEFT BLANK

2.6.10.2 Neutron Shield Shell - Penetration

The neutron shield shell, with NS-4-FR material backing it up, can be simulated as an infinitely large plate sitting on an elastic foundation. This simulation is conservative since the arch effect of the curved neutron shield shell and the fin stiffness are not included. The following formulas are from Theory of Plates and Shells, pages 267 through 269 (Timoshenko):

$$W = \frac{Pl^2}{8D}$$

$$M = \frac{(1+\nu)P}{4\pi} \left[\ln\left(\frac{1}{c}\right) + 0.616 \right]$$

$$\sigma = \frac{6M}{t^2}$$

$$D = \frac{E_{\text{sec}} t^3}{12(1-\nu^2)}$$

$$l^2 = \sqrt{\frac{D}{K}}$$

where

P = center concentrated load

C = radius of applied load, 0.625 in

ν = Poisson ratio, 0.275

t = neutron shield shell thickness, 0.236 in (6 mm)

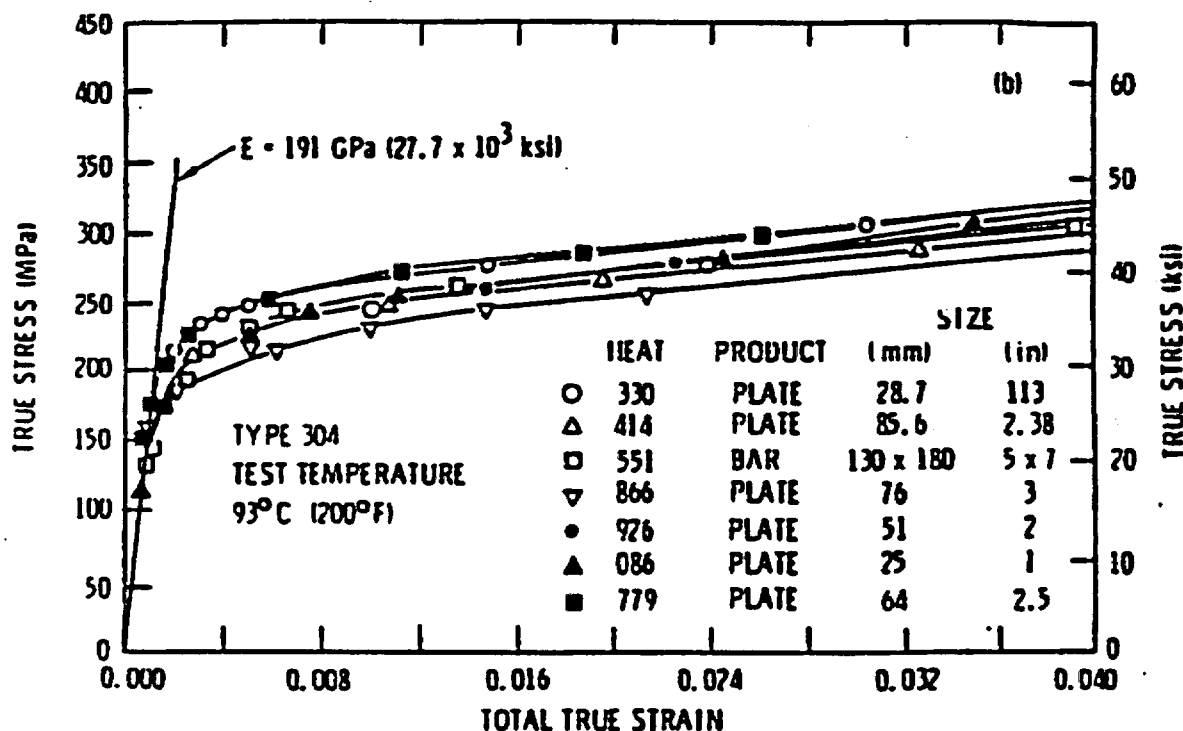
E = compressive modulus of elasticity for NS-4-FR

E_{sec} = the secant modulus (used in evaluating the plastic response of the neutron shield shell)

K = elastic foundation modulus for NS-4-FR, $\frac{561,000}{5.2}$ lb/in²/in

The material properties of the Type 304 stainless steel shell and fins and of NS-4-FR are presented in Section 2.3.

A conservative stress-strain diagram for Type 304 stainless steel is shown below. The stress-strain diagram is used to determine the secant modulus for use in the plastic analysis of the penetration event.



Stress-Strain Diagrams for Type 304 Stainless Steel

The plastic analysis is based on an iterative process. Figure 2.6.10.2-1 is a flow diagram of the plastic analysis. The calculation is shown in Table 2.6.10.2-1. The result shows that the true stress is approximately 41 ksi. Since the ultimate tensile strength of SA 240, Type 304 stainless steel is 71 ksi, the margin of safety is:

$$M.S. = \frac{71}{41} - 1 = +0.73$$

Thus, the neutron shield shell will not be penetrated.

Figure 2.6.10.2-1 Flow Diagram of the Plastic Analysis of Neutron Shield Shell

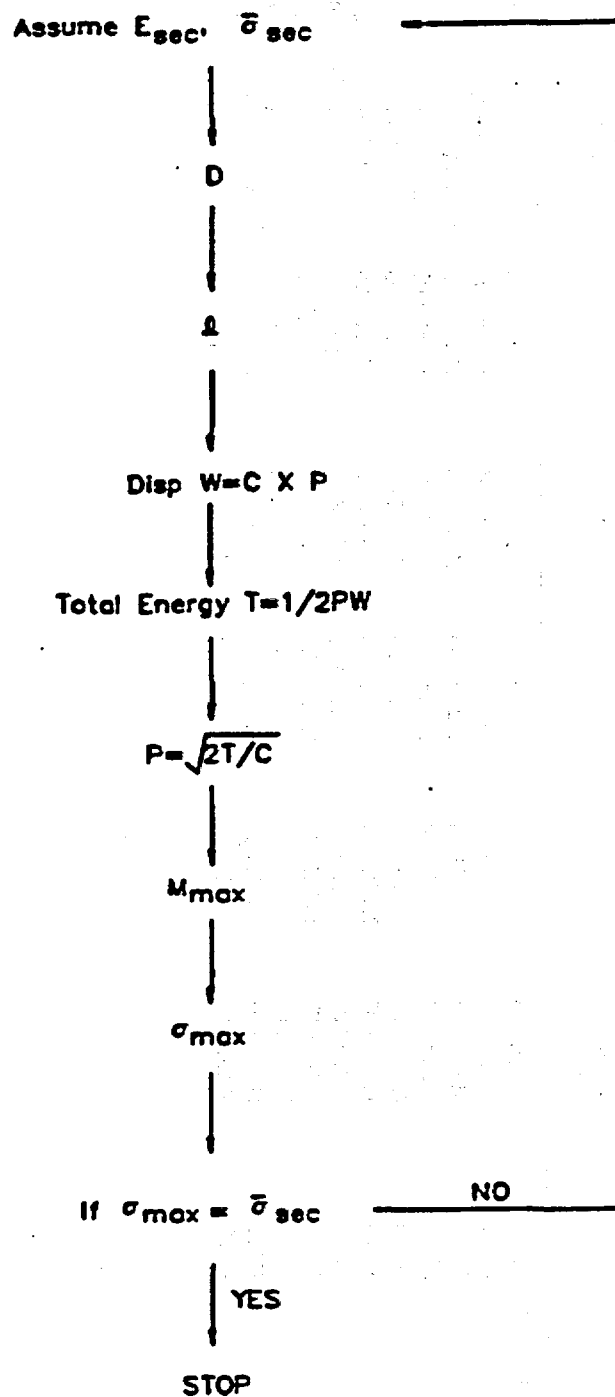


Table 2.6.10.2-1 Stress Iteration Table for the Penetration Analysis of the Neutron Shield Shell
(13-Pound Cylinder Drop From a 40-Inch Height)

Strain (in/in)	S ₁ (psi)	Secant Modulus (psi)	D	t ²	t ² /8D (E-05)	P (lb)	Moment (in-lb)	S ₂ (psi)	S ₂ -S ₁
.0009	25000	.2770E+08	.3282E+05	.5516E+00	.2101E-05	.2225E+05	.1780E+04	.1918E+06	> 0
.004	29500	.7375E+07	.8739E+04	.2846E+00	.4071E-05	.1598E+05	.7422E+03	.7996E+05	> 0
.008	33000	.4125E+07	.4888E+04	.2129E+00	.5443E-05	.1382E+05	.4382E+03	.4720E+05	> 0
.012	35100	.2925E+07	.3466E+04	.1792E+00	.6464E-05	.1268E+05	.2915E+03	.3140E+05	< 0
.016	36600	.2288E+07	.2711E+04	.1585E+00	.7309E-05	.1193E+05	.1998E+03	.2152E+05	< 0
.020	37500	.1875E+07	.2222E+04	.1435E+00	.8074E-05	.1135E+05	.1328E+03	.1431E+05	< 0
.024	38600	.1608E+07	.1905E+04	.1329E+00	.8718E-05	.1092E+05	.8523E+02	.9182E+04	< 0
.028	39600	.1414E+07	.1676E+04	.1246E+00	.9297E-05	.1058E+05	.4805E+02	.5176E+04	< 0
.032	40600	.1262E+07	.1495E+04	.1177E+00	.9841E-05	.1028E+05	.1704E+02	.1836E+04	< 0
.036	41500	.1153E+07	.1366E+04	.1125E+00	.1030E-04	.1005E+05	-.6364E+01	-.6856E+03	< 0
.040	42400	.1060E+07	.1256E+04	.1079E+00	.1074E-04	.9841E+04	-.2723E+02	-.2933E+04	< 0

2.6.10.3 Port Cover - Penetration

Two analyses are performed to demonstrate that the 10 CFR 71 penetration event will not cause loss of the cask containment capability by damaging a port cover. The first analysis uses classical methods; the second uses the ANSYS finite element structural analysis code. The port cover geometry and loading are shown in Figure 2.6.10.3-1.

$$\begin{aligned}\text{P.E.} &= \text{Projectile Potential Energy} \\ &= (W)(h) \\ &= 520 \text{ in-lb}\end{aligned}$$

where

$$\begin{aligned}W &= 13 \text{ lb} \\ h &= 40 \text{ in}\end{aligned}$$

The geometric properties of the port cover lid are:

$$\begin{aligned}t &= 1.01 \text{ in} \\ D &= 3.75 \text{ in (bolt circle)} \\ v &= 0.275 \\ m &= 1/v = 3.6364 \\ a &= 1.875 \text{ in} \\ r_o &= 0.625 \text{ in} \\ a/r_o &= 3.0 \\ \ln(a/r_o) &= 1.0986\end{aligned}$$

The material properties for SA-705, Type 630, H1150, 17-4 PH stainless steel at normal transport temperatures (200°F) are as follows:

$$\begin{aligned}S_y &= 97,100 \text{ psi} \\ S_u &= 135,000 \text{ psi} \\ E &= 27.6 \times 10^6 \text{ psi}\end{aligned}$$

2.6.10.3.1 Classical Analysis

For the deflection equations in the classical analysis (Roark, Case 2, pages 370 and 216), a thin plate formula is used as an approximation to obtain a conservative result, since no shear stiffness is considered.

$$\frac{d_i}{d} = 1 + \left(1 + \frac{2h}{d}\right)^{0.5}$$

where

d_i = vertical deformation due to an impact load from a moving body

d = vertical deformation due to the weight of the moving body
applied as a static load

h = height from which the body falls
= 40 in

For the static loading, the maximum displacement of the port cover is:

$$\begin{aligned} d_{\text{Maxy}} &= \frac{3W(m-1)(3m+1)a^2}{4\pi E m^2 t^3} \\ &= 9.11 \times 10^{-7} \text{ in} \end{aligned}$$

where

W = 13 lb

a = 1.875 in (radius of bolt circle)

v = 0.275

m = $1/v$ = 3.636

t = 1.01 in

E = 27.6×10^6 psi

then

$$d_i = d \left[1 + \left(1 + 2 \left[\frac{40}{d} \right] \right)^{0.5} \right]$$
$$= 0.00854 \text{ in}$$

For such a small displacement, the port cover is adequate to protect the port against the penetration event.

This analytical method is deemed reasonable for a "relatively heavy body moving at low velocity." The initial assumption of perfect elasticity of the plate and rigidity of the projectile leads to a conservative analysis. The following ANSYS analysis removes part of the conservatism by allowing plastic deformation of the plate.

2.6.10.3.2 ANSYS Finite Element Analysis

The penetration loading condition was evaluated using an ANSYS program solution for a finite element model of a similar port cover system. Figure 2.6.10.3-2 depicts the finite element model of the port cover. The impact of the 13-pound, 1.25-inch diameter projectile dropped from a height of 40 inches is assumed to occur at the center of the port cover. The bolt preload is 2557 pounds.

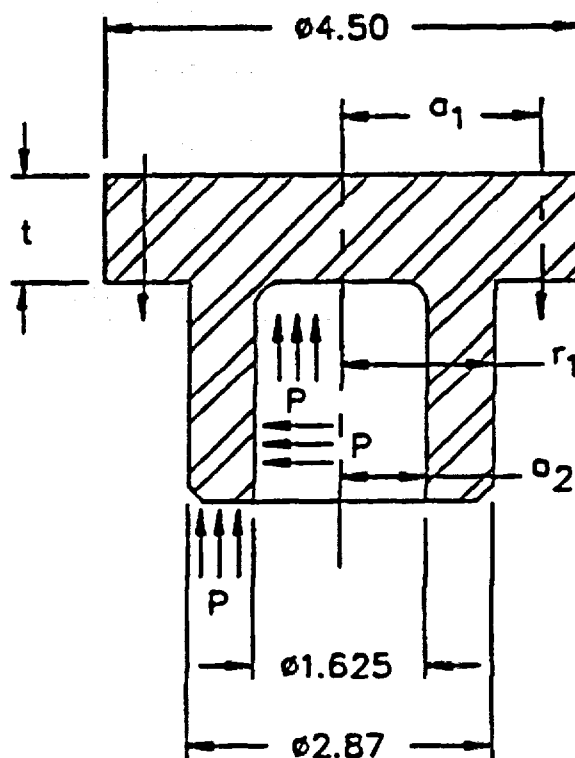
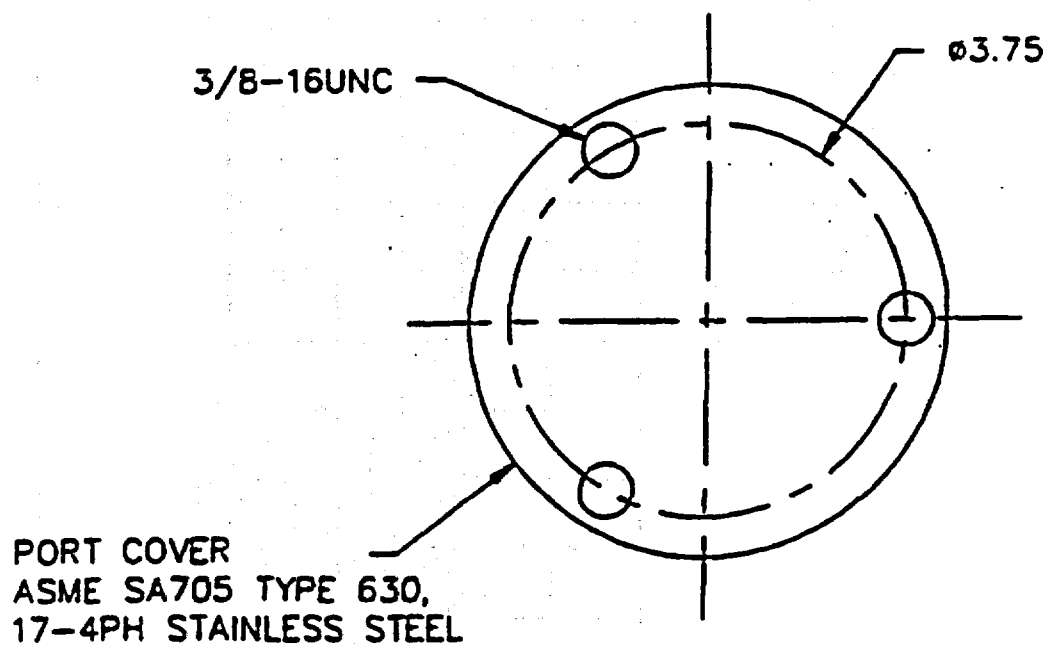
The dynamic impact load is applied as a center concentrated load, and elastic/plastic material property stress-strain curves are used. The analysis is based on the following two assumptions:

1. 100 percent of the projectile's momentum is absorbed by the cover.
2. The time of impact is 0.001 second. The load peaks at 0.0005 second, increasing and decreasing linearly.

Momentum calculations yield an average load of 5915 pounds over the 0.001-second impact time interval. Therefore, the peak loading is 11,830 pounds at 0.0005 second. This peak load is distributed over the impact area.

The ANSYS analysis results calculate a maximum port cover displacement of 0.00541 inch at 0.0005 second, which is less than the conservative 0.00854-inch displacement calculated by classical methods. Plasticity effects occur only very locally in the vicinity of the load application region. The plastic ratio of the cross-section at the port cover center is only 9.64×10^{-4} . The cover bolts are also shown to be preloaded sufficiently to maintain the gap elements closed between the port cover and the cask body during the impact. Figure 2.6.10.3-3 presents a plot of the cover displacement at the top of the plate versus time. The port cover is shown to be adequate to protect the valve against the 10 CFR 71 penetration event.

Figure 2.6.10.3-1 Port Cover Geometry and Loading



(DIMENSIONS IN INCHES)

Figure 2.6.10.3-2 Finite Element Model of Port Cover

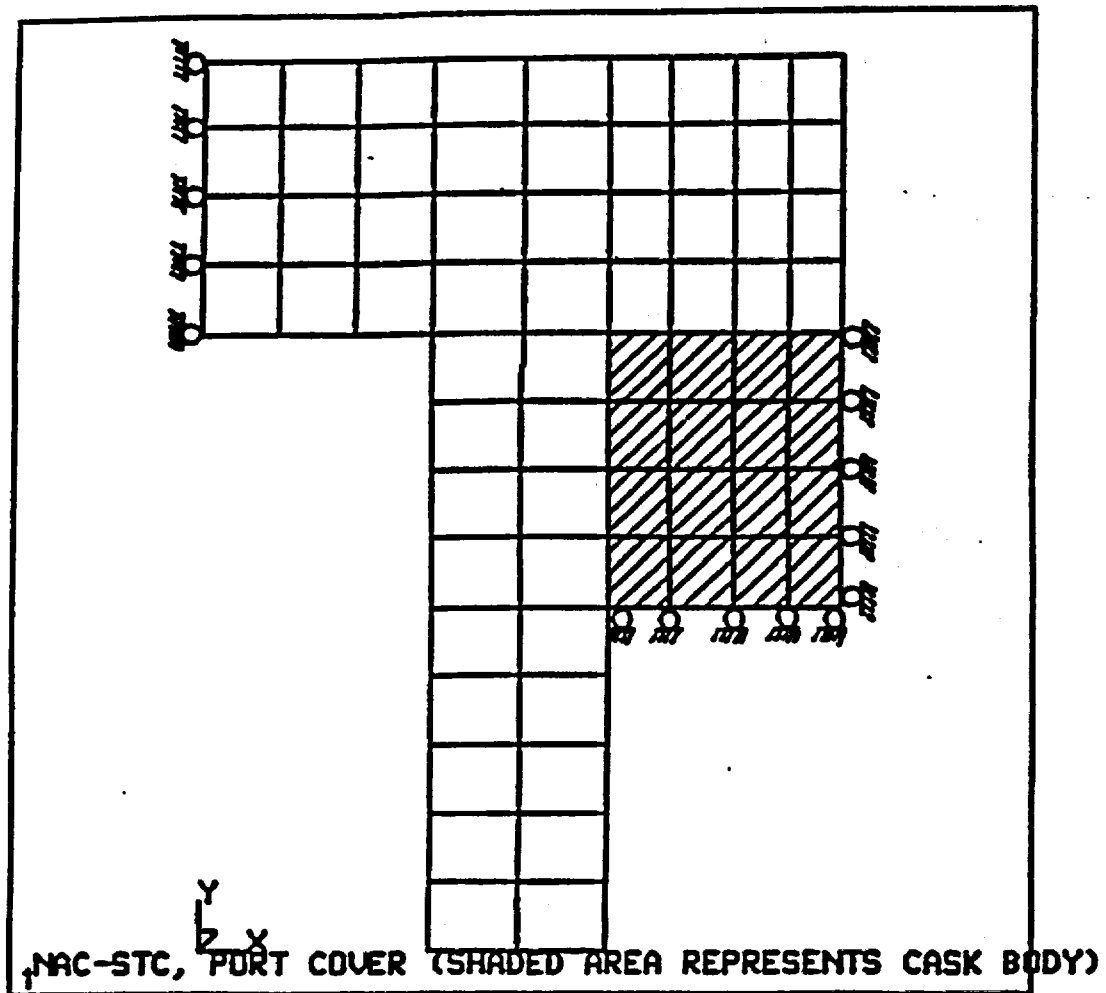
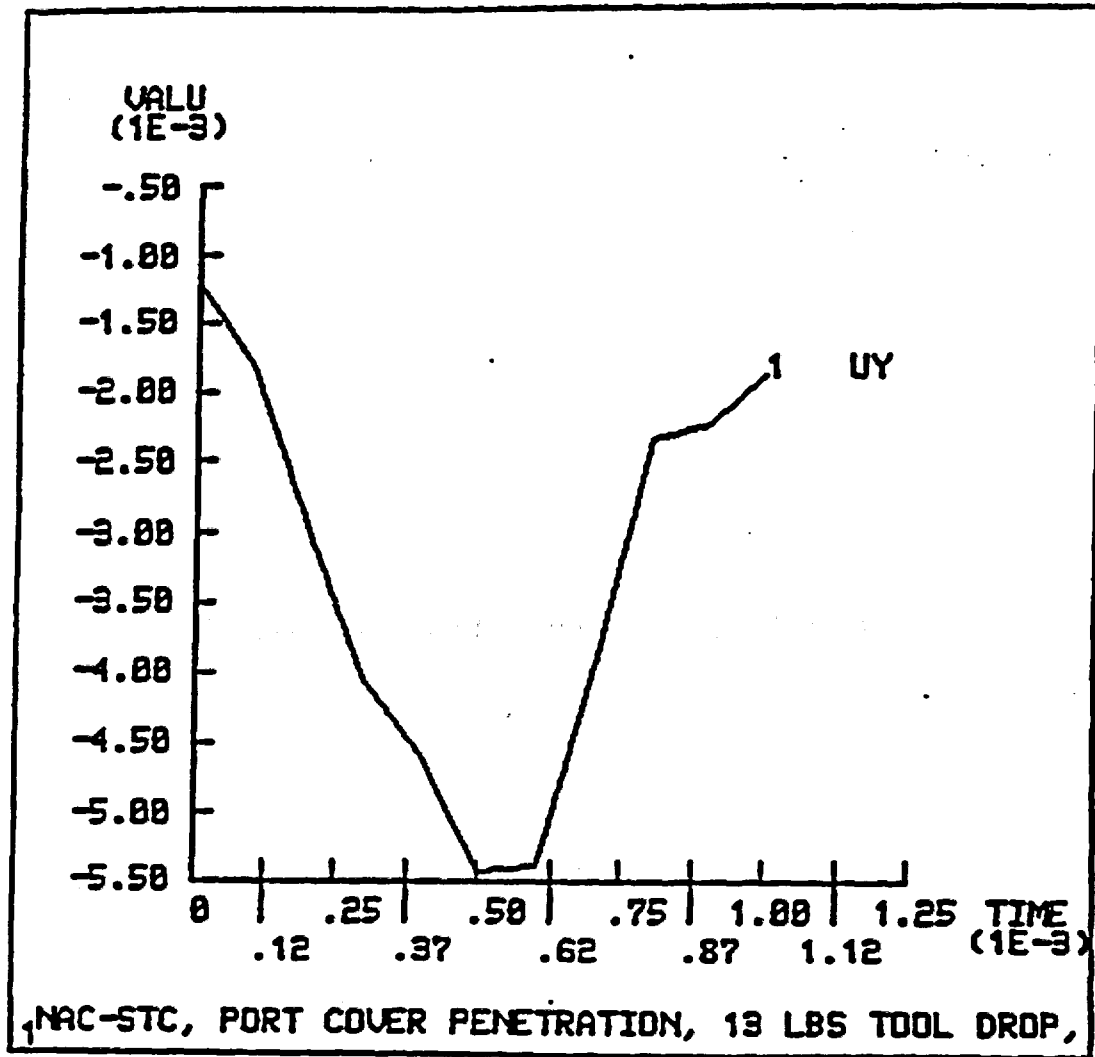


Figure 2.6.10.3-3 Port Cover Response to Penetration Event



THIS PAGE INTENTIONALLY LEFT BLANK

2.6.11 Fabrication Conditions

The process of manufacturing the NAC-STC can introduce thermal stresses in the inner and outer shells as a result of pouring molten lead between them. These thermal stresses are evaluated in this section to provide assurance that the manufacturing process does not adversely affect the normal operation of the cask or its ability to survive an accident. Any residual stresses in the containment vessel shell due to inelastic strain associated with the secondary local bending stresses, which result from the lead pour thermal gradient, must be considered in the total stress range for normal and accident load conditions according to Regulatory Position 7 of Regulatory Guide 7.6. Residual stresses in the containment vessel and the outer shell induced by shrinkage of the lead shielding after the lead pouring operation are relieved early in the life of the cask because of the low creep strength of lead.

For the lead pouring process, the temperatures of the cask shells are controlled between 640°F (338°C) and 740°F (393°C), and the lead temperature before pouring is between 650°F (343°C) and 750°F (399°C). Heating of the cask is performed using heaters inside the inner shell and heating rings around the outside of the outer shell. Heat up is time controlled, consistent with maintaining shell temperatures uniformly. The heating procedures ensure that the surface temperature of the cask does not exceed 800°F (427°C). The shell temperatures are measured by thermocouples attached to the shell surfaces. A portable thermometer is also used to measure temperature at any location. Cask heating is carried out after all of the preparations have been completed (including melting of the lead) in order to minimize the time that the cask is at elevated temperatures.

The lead is poured after the cask reaches the specified temperatures. Prior to lead pouring, the cask flange area is heated with hand-held burners to between 640°F (338°C) and 740°F (393°C). Pouring is carried out continuously using a filling tube with its open end maintained under the lead surface. The pouring time is kept as short as possible. During pouring, the interior heaters and exterior heating rings are continuously energized.

The cooling process consists of sequentially turning the exterior heating rings and interior heaters off, starting from the lowest point, and of spraying the cask with water from the outside. A layer of molten lead is maintained until the upper surface starts to solidify. This process allows the molten lead to fill the open space below it created by the lead shrinkage as it cools.

The basic requirements and procedures for the NAC-STC lead pour operations are described in Section 8.4.2.

2.6.11.1 Lead Pour

2.6.11.1.1 Cask Shell Geometry

At 70°F, the Type 304 stainless steel shell geometry is as follows:

Inner Shell

Inside Diameter (d_i)	= 71.0 in
Outside Diameter (d_o)	= 74.0 in
Shell Thickness (t_i)	= 1.5 in

Outer Shell

Inside Diameter (D_i)	= 81.4 in
Outside Diameter (D_o)	= 86.7 in
Shell Thickness (T_o)	= 2.65 in

2.6.11.1.2 Stresses Due to Lead Pour

As stated in Section 8.4.2, Description of Lead Pour Procedures, the maximum lead temperature during the pouring operations is 750°F. Assuming that the lead and the inner and outer shells are uniformly at 750°F, the hydrostatic pressure produced by the column of lead is:

$$p = \rho h$$

$$= 66 \text{ psi}$$

where

$$\rho = 0.41 \text{ lb/in}^3 \text{ (lead density)}$$

$$h = 161 \text{ in (maximum height of lead column)}$$

At 750°F, the shell geometric dimensions are:

$$d_o' = d_o (1 + \alpha \Delta T)$$

$$D_i' = D_i (1 + \alpha \Delta T)$$

$$d_m' = \left[\frac{d_i + d_o}{2} \right] (1 + \alpha \Delta T)$$

$$D_m' = \left[\frac{D_i + D_o}{2} \right] (1 + \alpha \Delta T)$$

$$t' = t (1 + \alpha \Delta T)$$

where

$$\alpha = 9.76 \times 10^{-6} \text{ in/in/}^\circ\text{F at } 750^\circ\text{F (stainless steel)}$$

$$\Delta T = 750 - 70 = 680^\circ\text{F}$$

$$\begin{aligned} d_o' &= (74.0) [1 + (9.76 \times 10^{-6})(680)] \\ &= 74.49 \text{ in} \end{aligned}$$

$$\begin{aligned} d_m' &= \left[\frac{71.0 + 74.0}{2} \right] [1 + (9.76 \times 10^{-6})(680)] \\ &= 72.98 \text{ in} \end{aligned}$$

$$\begin{aligned} d_i' &= (81.4) [1 + (9.76 \times 10^{-6})(680)] \\ &= 81.94 \text{ in} \end{aligned}$$

$$\begin{aligned} D_m' &= \left[\frac{81.4 + 86.7}{2} \right] [(1 + (9.76 \times 10^{-6})(680))] \\ &= 84.61 \text{ in} \end{aligned}$$

$$\begin{aligned}t_i' &= (1.50) [1 + (9.76 \times 10^{-6})(680)] \\&= 1.51 \text{ in}\end{aligned}$$

$$\begin{aligned}t_o' &= (2.65) [1 + (9.76 \times 10^{-6})(680)] \\&= 2.668 \text{ in}\end{aligned}$$

The inner shell is subjected to an external hydrostatic pressure, and the outer shell to an internal hydrostatic pressure, of 66 psi. This causes the inner shell to decrease in diameter and the outer shell to increase in diameter.

The inner shell decreases in size radially (Roark and Young, 5th ed., Case 1b, page 448):

$$\Delta r_o = \frac{q(d_o'/2)^2}{Et_i'} = \frac{(-66)(74.9/2)^2}{(24.4 \times 10^6)(1.51)} = -0.00248 \text{ in}$$

$$\Delta r_m = \frac{q(d_m'/2)^2}{Et_i'} = \frac{(-66)(72.98/2)^2}{(24.4 \times 10^6)(1.51)} = -0.00239 \text{ in}$$

where

$$E = 24.4 \times 10^6 \text{ psi at } 750^\circ\text{F.}$$

The outer shell increases in size radially:

$$\Delta R_i = \frac{q(d_i'/2)^2}{Et_o'} = \frac{(66)(81.94/2)^2}{(24.4 \times 10^6)(2.668)} = 0.00170 \text{ in}$$

$$\Delta R_m = \frac{q(D_m'/2)^2}{Et_o'} = \frac{(66)(84.61/2)^2}{(24.4 \times 10^6)(2.668)} = 0.00181 \text{ in}$$

The shell geometries at 750°F and 66 psi hydrostatic pressure are:

$$d_o'' = 74.49 - (2)(0.00248) = 74.485 \text{ in}$$

$$D_o'' = 81.94 + (2)(0.00170) = 81.943 \text{ in}$$

$$d_m'' = 72.98 - (2)(0.00239) = 72.975 \text{ in}$$

$$D_m'' = 84.61 + (2)(0.00181) = 84.614 \text{ in}$$

The hoop stresses are evaluated at the mean diameter of the inner and outer shells at 750°F:

$$\begin{aligned} S_{hi} &= \frac{Pd_m''}{2t_i} \\ &= \frac{(-66)(72.975)}{(2)(1.51)} = -1595 \text{ psi (inner shell)} \end{aligned}$$

$$\begin{aligned} S_{ho} &= \frac{PD_o''}{2t_o} \\ &= \frac{(66)(84.614)}{(2)(2.668)} = 1047 \text{ psi (outer shell)} \end{aligned}$$

These stresses are negligible.

2.6.11.2 Cooldown

2.6.11.2.1 Hoop Stresses

Lead decreases in volume during solidification. As the lower lead region solidifies, the molten lead above fills the shrinkage void between the solidifying lead and the inner and outer shells, thus, maintaining the 66 psi pressure on the shells.

The stress-free inner and outer radii of the solidified lead can be calculated (Roark and Young, 5th ed., Cases 1a and 1c, page 504) as:

$$\Delta a = \frac{q}{E} \left[\frac{2ab^2}{a^2 - b^2} \right] - \frac{qa}{E} \left[\frac{a^2 - b^2}{a^2 - b^2} - \nu \right] = \frac{q}{E} a(\nu - 1)$$
$$= -0.001104 \text{ in}$$

$$\Delta b = \frac{qb}{E} \left[\frac{a^2 + b^2}{a^2 - b^2} + \nu \right] - \frac{q}{E} \left[\frac{2a^2b}{a^2 - b^2} \right] = \frac{q}{E} b(\nu - 1)$$
$$= -0.001003 \text{ in}$$

where

$$q = 66 \text{ psi (pressure)}$$

$$E = 1.47 \times 10^6 \text{ psi at } 620^\circ\text{F (modulus of elasticity)}$$

$$\nu = 0.4 \text{ (Poisson's ratio)}$$

$$a = D''/2 = 81.943/2 = 40.9715$$

$$b = d''/2 = 74.485/2 = 37.2425$$

then

$$R_{ol} = 40.9715 - 0.001104 = 40.9704$$

$$R_{il} = 37.2425 - 0.001003 = 37.2415$$

When cooled to 70°F, the inside radius of the lead is such that:

$$\frac{R_{il}}{1 + \alpha \Delta T} = R'_{il}$$

where

R'_{il} = inside radius of the stress-free lead at 70°F

$$\alpha = 20.4 \times 10^{-6} \text{ in/in/}^{\circ}\text{F}$$

$$\Delta T = 550^{\circ}\text{F} \text{ (620-70)}$$

then

$$R'_{il} = 36.828 \text{ in}$$

likewise

$$\frac{R_{ol}}{1 + \alpha \Delta T} = R'_{ol}$$

$$R'_{ol} = 40.516 \text{ in}$$

The outside radius of the stress-free inner shell is $74.0/2 = 37.0$ inches, which is larger than the stress-free inner radius of the lead shell. Therefore, there exists an interface pressure between the lead and the inner shell after cooling to 70°F. The interface pressure, when acting on the lead cylinder and inner shell, is such that

the inner radius of the lead cylinder is the same as the outer radius of the inner shell (Roark and Young, 5th ed., Case 1a, page 504).

$$\begin{aligned} R'_{it} &= b + \Delta b \\ &= b + \frac{qb}{E} \left[\frac{a^2 + b^2}{a^2 - b^2} + \nu \right] \end{aligned}$$

where

R'_{it} = inside radius of lead cylinder at 70°F

$$\nu = 0.4$$

$$E = 2.28 \times 10^6 \text{ psi at } 70^\circ\text{F}$$

$$a = 40.516 \text{ in}$$

$$b = 36.828 \text{ in}$$

then

$$\begin{aligned} R'_{it} &= 36.828 + \left(\frac{36.828q}{2.28 \times 10^6} \right) \left(\frac{(40.516)^2 + (36.828)^2}{(40.516)^2 - (36.828)^2} + 0.4 \right) \\ &= 36.828 + 1.762 \times 10^{-4} q \end{aligned}$$

The outside radius of the inner shell at 70°F under the interface pressure, q , (Roark and Young, 5th ed., Case 1c, page 504) is:

$$\begin{aligned} r_o &= a_s - \Delta a_s \\ &= a_s - \frac{qa_s}{E} \left(\frac{a_s^2 + b_s^2}{a_s^2 - b_s^2} - \nu \right) \end{aligned}$$

where

$$r_o = \text{outside radius of inner shell at } 70^\circ\text{F}$$

$$a_s = 74.0/2 = 37.0 \text{ in}$$

$$b_s = 71.0/2 = 35.5 \text{ in}$$

$$E = 28.3 \times 10^6 \text{ psi at } 70^\circ\text{F}$$

$$\nu = 0.275$$

then

$$\begin{aligned} r_o &= 37.0 - \left(\frac{37.0q}{28.3 \times 10^6} \right) \left(\frac{(37.0)^2 + (35.5)^2}{(37.0)^2 - (35.5)^2} - 0.275 \right) \\ &= 37.0 - 3.125 \times 10^{-5} q \end{aligned}$$

Equating R'_{it} and r_o and solving for q :

$$q = 1187 \text{ psi interface pressure}$$

The lead shell geometry is:

$$\begin{aligned} R'_{it} &= 36.828 + \left(\frac{(36.828)(1187)}{2.28 \times 10^6} \right) \left(\frac{(40.516)^2 + (36.828)^2}{(40.516)^2 - (36.828)^2} - 0.4 \right) \\ &= 37.037 \text{ in} \end{aligned}$$

$$\begin{aligned} R'_{ot} &= R'_{ot} + \frac{q}{E} \left(\frac{2R'_{ot}R'_{it}{}^2}{R'_{ot}{}^2 - R'_{it}{}^2} \right) \\ &= 40.516 + \left(\frac{1187}{2.28 \times 10^6} \right) \left(\frac{(2)(40.516)(36.828)^2}{(40.516)^2 - (36.828)^2} \right) \\ &= 40.521 \text{ in} \end{aligned}$$

The interference between the lead shell and the inner shell is 0.172 inches (37.0 - 36.828). To fully accommodate this interference, the lead must undergo a strain of $0.172/36.828 = 0.0047$ or 0.47 percent. From Figure 24 of NUREG/CR-0481, the lead stress for the above strain is 800 psi. The corresponding interface pressure for this stress in the lead shell is:

$$\begin{aligned} q &= (S) \left(\frac{R_{ot}^2 - R_{it}^2}{R_{ot}^2 + R_{it}^2} \right) \\ &= (800) \left(\frac{(40.521)^2 - (37.037)^2}{(40.521)^2 + (37.037)^2} \right) \\ &= 72 \text{ psi interface pressure} \end{aligned}$$

The change in geometry of the inner shell for this interface pressure is:

$$\begin{aligned} \Delta a &= \left[\frac{-72}{28.3 \times 10^6} \right] \left[\frac{(2)(37.0)(35.5)^2}{(37.0)^2 - (35.5)^2} \right] \\ &= 0.0022 \text{ in} \end{aligned}$$

This can conservatively be neglected in the analysis. The inner shell hoop stress is:

$$\begin{aligned} S_{his} &= (-72) \left[\frac{(37.0)^2 + (35.5)^2}{(37.0)^2 - (35.5)^2} \right] \\ &= -1740 \text{ psi} \end{aligned}$$

This stress is negligible.

2.6.11.2.2 Axial Stresses

Axial stresses also develop in the lead shell and inner shell during fabrication as a result of the unequal shrinkage of the lead and steel shells. Assume bonding of the lead shell to the inner shell during the cooldown process after completion of lead pouring. The strain in the lead, when cooled to 70°F, is:

$$\begin{aligned}\epsilon_{\ell} &= (\alpha_{\ell} - \alpha_s)\Delta T \\ &= 0.0060 \text{ in/in or 0.60 percent}\end{aligned}$$

where

$$a_{\ell} = 20.4 \times 10^{-6} \text{ in/in/}^{\circ}\text{F}$$

$$a_s = 9.56 \times 10^{-6} \text{ in/in/}^{\circ}\text{F}$$

$$\Delta T = 620 - 70 = 550^{\circ}\text{F}$$

Extrapolating from Figure 24 of NUREG/CR-0481 for this strain, an axial stress of approximately 825 psi exists in the lead shell. The total force in the lead caused by assuming no deformation of the inner shell is:

$$\begin{aligned}P_{sPb} &= p_{\ell} A_{\ell} \\ &= 825\pi[(40.7)^2 - (37.0)^2] \\ &= 745,120 \text{ lb tensile force}\end{aligned}$$

The corresponding compression stress in the inner shell to maintain equilibrium is:

$$\begin{aligned}p_{sST} &= \frac{P_s}{A_s} \\ &= \frac{-745,120}{\pi[(37.0)^2 - (35.5)^2]} \\ &= -2180 \text{ psi}\end{aligned}$$

This stress is negligible.

This is a highly conservative estimate of the compressive stress that can develop in the inner shell for the following reasons:

1. It assumes no axial deformation of the inner shell and no load development in the outer shell.
2. Creep in the lead is neglected. This also reduces the stress and force in the lead (Section 2.6.11.3).
3. It assumes the strain is uniform through the thickness of the lead shell, i.e., no shear strain exists in the plane formed by the radial axis and the longitudinal axis. A particle away from the inner shell should develop less strain, consequently lower stress, than a particle adjacent to the inner shell; this also reduces the total force in the lead shell.

2.6.11.2.3 Effects of Temperature Differential During Cooldown

The preceding analyses assume that the inner and outer shells and the lead are always at the same temperature at any time during the cooldown process. This assumption may not be true under actual conditions. However, because of the high thermal conductivity of the stainless steel and the lead and because of the time-controlled cooldown process, the temperature differential between any two of the above shells is kept to a minimum. To determine the effect of temperature differential on the stresses in the shells, a temperature differential of 100°F is used (Ref. Section 8.4.2).

If the inner shell is cooler than the lead, the interference between them as well as the corresponding interface pressure and hoop stresses are less than for the case of equal temperatures. Hence, the preceding analysis is conservative.

If the inner shell is hotter than the lead shell, an analysis is required. Assume the temperature of the inner shell to be 170°F and that of the lead to be 70°F. The inner radius of the stress-free lead shell at 70°F is 36.828 inches (R_{iL}); the outer radius of the inner shell at 170°F is:

$$R = 37.0 [1 + (8.71 \times 10^{-6})(100)]$$
$$= 37.032 \text{ in}$$

The interference between the inner shell and the lead is $37.032 - 36.828 = 0.204$ inch. To fully accommodate this interference, the lead has to undergo a strain of $0.204/36.828 = 0.0055$ inch/inch or 0.55 percent. From Figure 24 of NUREG/CR-0481, the hoop stress in the lead is approximately 810 psi for a 0.0055 inch/inch strain. The interface pressure is:

$$q = (810) \left[\frac{(40.516)^2 - (36.828)^2}{(40.516)^2 + (36.828)^2} \right]$$
$$= 77 \text{ psi}$$

The hoop stress in the inner shell becomes:

$$S_{his} = (-77) \left[\frac{(37)^2 + (35.5)^2}{(37)^2 - (35.5)^2} \right]$$
$$= -1862 \text{ psi}$$

Note that the thermal expansion or contraction of a shell subjected to a constant pressure does not affect the hoop stress; i.e.,

$$S_h = q \left[\frac{(ka)^2 + (kb)^2}{(ka)^2 - (kb)^2} \right] = q \left[\frac{a^2 + b^2}{a^2 - b^2} \right]$$

where

$$k = 1 + \alpha \Delta T$$

This -1862 psi hoop stress (the inner shell is assumed to be 100°F hotter than the lead shell) reduces to the previously calculated hoop stress of -1837 psi as both the inner shell and lead reach an ambient temperature of 70°F. This does not take into account the beneficial effect of the creep properties of the lead.

The axial stress in the inner shell also increases when the inner shell is 100°F hotter than the lead shell. The axial stress of -2180 psi calculated when both the inner shell and lead shell are at 70°F is recalculated for the inner shell temperature of 170°F, $\alpha = 8.71 \times 10^{-6}$ inch/inch/°F (Type 304 stainless steel):

$$\begin{aligned}\epsilon_t &= (20.38 - 9.56)(10^{-6})(620 - 70) + (8.71 \times 10^{-6})(170 - 70) \\ &= 0.00595 \text{ in/in or } 0.595 \text{ percent}\end{aligned}$$

Referring to Figure 24 of NUREG/CR-0481, the axial stress in the lead is approximately 820 psi. The corresponding axial stress in the inner shell is -2167 psi. As before, cooling of the inner shell reduces this stress. The previous assumptions apply in arriving at this inner shell compressive stress.

Temperature differentials between the inner and outer shells are of no consequence, since the axial restraint between them is welded in place after cooldown, when the cask is at a uniform ambient temperature. Welding of the outer shell and the bottom inner forging to the bottom outer forging after cooldown is, therefore, a necessary fabrication step.

The question of buckling of the inner shell due to the combined effect of external pressure and fabrication inaccuracies must also be addressed. According to the "ASME Boiler and Pressure Vessel Code," Article NE-4221.1, the difference between the maximum and minimum inside diameters at any cross section shall not exceed 1 percent of the nominal diameter at the cross section under consideration. This amounts to $(0.01)(71.0) = 0.71$ inch. The relation between the initial radial deviation, ω_1 , and the maximum and minimum diameter (Timoshenko and Gere, Figure 7-10) is:

$$D_{\max} = D_{\text{nom}} + 2\omega_1$$

$$D_{\min} = D_{\text{nom}} - 2\omega_1$$

thus

$$D_{\max} - D_{\min} = 4\omega_1$$

or

$$\Delta D = 4\omega_1$$

Hence, the maximum initial radial deviation allowed is:

$$\omega_{\max} = \Delta D/4 = 0.71/4 = 0.1775 \text{ in}$$

From Timoshenko and Gere, equation (7-15), page 293:

$$\begin{aligned} S_{cr} &= \left[\frac{E}{1 - \nu^2} \right] \left[\frac{h}{2R} \right]^2 \\ &= 12,856 \text{ psi} \end{aligned}$$

where

$$E = 27.76 \times 10^6 \text{ psi at } 170^\circ\text{F}$$

$$\nu = 0.275$$

$$h = \text{shell thickness} = 1.50 \text{ in}$$

$$R = \text{shell radius} = 36.25 \text{ in}$$

Then from Timoshenko and Gere, equation (7-12), page 289:

$$\begin{aligned} q_{cr} &= \left[\frac{E}{4(1 - \nu^2)} \right] \left[\frac{h}{R} \right]^3 \\ &= S_{cr} \left[\frac{h}{r} \right] \\ &= 532 \text{ psi} \end{aligned}$$

When the cylinder has fabrication inaccuracies, the external pressure, q_{YP} , required to produce yielding in the extreme fibers can be solved in the following equation (Timoshenko and Gere, equation (e), page 296):

$$q_{YP}^2 - \left[\frac{S_{YP}}{m} + (1 + 6mn)q_{cr} \right] q_{YP} + \frac{S_{YP}}{m} q_{cr} = 0$$

where

$S_{YP} = 26,150$ psi at 170°F for Type 304 stainless steel

$$m = R/h = 36.25/1.50 = 24.1667$$

$$n = \omega_1/R = \omega_1/36.25$$

then

$$q_{YP}^2 - [1082 + (1 + 4\omega_1)(532)] q_{YP} + 575,660 = 0$$

The value of ω_1 can vary from 0.0 inches (perfect cylinder) up to 0.1775 inch (maximum allowed according to the "ASME Boiler and Pressure Vessel Code"). Solving q_{YP} for varying values of ω_1 gives the following:

Initial Radial Deviation ω_1 (in)	Yield Pressure q_{YP} (psi)
0.001	530
0.06	443
0.12	389
0.1775	351

Thus, the margin of safety against yielding for the inner shell with maximum allowed radial deviation subjected to 77 psi lead pressure (inner shell temperature is assumed to be 100°F higher than lead temperature) is:

$$MS = \frac{351}{77} - 1 = +3.55$$

Since the margin of safety for this conservative load case is positive, the inner shell does not buckle when subjected to the lead pressure produced during the cooling of the cask.

2.6.11.3 Lead Creep

As shown in Sections 2.6.11.2.1 and 2.6.11.2.2, cooling of the lead shell and inner shell introduces a hoop stress of -1837 psi and an axial stress of -2180 psi in the inner shell. However, the significant creep rate of lead at room, or elevated, temperatures causes the stresses to be relieved early in the life of the cask. From Figure 21 of Tietz, it can be seen that maintaining a constant strain of 0.59 percent at 250°F for only five hours reduces the lead stress to approximately 200 psi. For this stress in the lead, the corresponding hoop and axial stresses in the inner shell are:

$$\sigma_h = \frac{200}{800} (-1837) = -459 \text{ psi}$$

$$\sigma_a = \frac{200}{825} (-2180) = -528 \text{ psi}$$

During fabrication following the lead pour, the lead creep relieves the stresses in the lead shell, and the stresses in the inner shell, to a point that they become negligible.

THIS PAGE INTENTIONALLY LEFT BLANK

2.6.12 Fuel Basket Analysis (For Directly Loaded Fuel) - Normal Transport Conditions

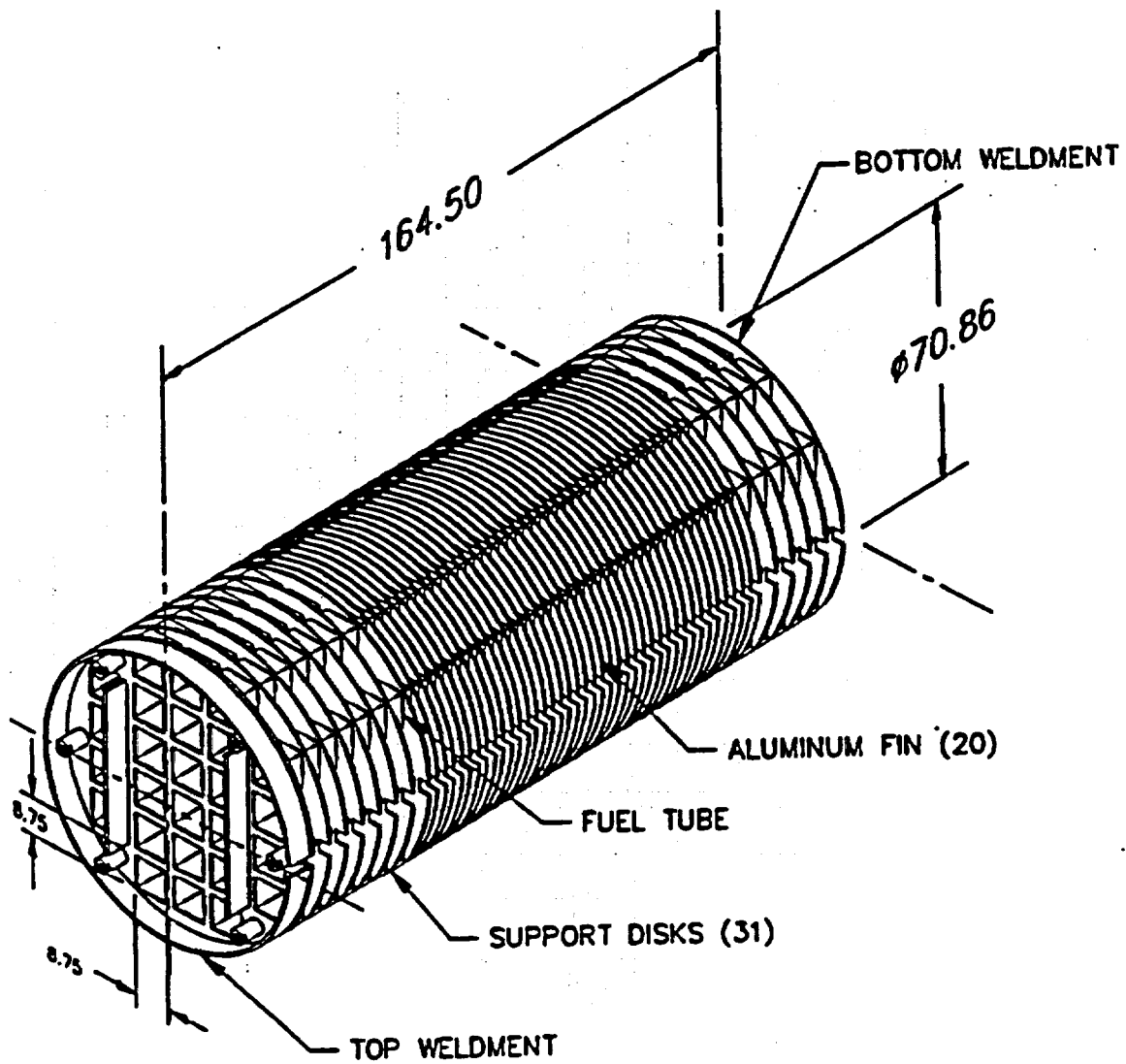
The NAC-STC fuel basket for directly loaded fuel is designed to accommodate 26 fuel assemblies. The basket is a right circular cylinder structure, and is fabricated with the following components: 26 square fuel tubes, 31 circular support disks equally spaced between top and bottom plates, 20 aluminum heat transfer disks, and 6 threaded rods with spacer nuts. The basket components and their geometry are illustrated in Figure 2.6.12-1 and 2.6.12-2. Each fuel tube has an 8.78-inch square inside dimension, a 0.142-inch thick composite wall (includes encased BORAL), and holds one design basis PWR fuel assembly. Figure 2.6.12-3 shows details of the stainless steel tube with the encased BORAL. The fuel tubes are open at each end; therefore, longitudinal fuel assembly loads are imparted to the cask body and not the fuel basket structure. The fuel assemblies, together with the tubes, are laterally supported in the holes in the stainless steel support disks. Each support disk is 0.5 inches thick, 70.86 inches in diameter, and has 26 holes that are each 9.234 inches square. There are two different web widths in the support disk. One web width is 1.47 inches between the holes and the other web width is 3.27 inches between the holes. The top and bottom plates are both 1.0 inch thick and have the same diameter as the support disks. The support disks are spaced at 4.87-inch center-to-center intervals and structurally connected by threaded spacer nuts located at six positions near the periphery of each disk. Aluminum heat transfer disks are located at the mid section of the cask cavity to fully optimize heat rejection from the package. Each heat transfer disk is 0.625 inch thick, 70.65 inches in diameter, and has 26 holes that are each 9.20 inches square. There are two different web widths, 1.50 inches and 3.3 inches. The dimensional difference between the heat transfer disk and the support disk accommodates the different rate of thermal growth between different materials preventing interference between the tube, support disk, and heat transfer disk. The heat transfer disks are supported by the six threaded rods and serve no structural function. The fuel basket contains the fuel and is laterally supported by the inner shell of the cask.

The 31 support disks and 2 end plates are fabricated from 17-4 PH and Type 304 stainless steel. The 20 heat transfer disks are fabricated from Type 6061-T651 aluminum alloy. The 26 fuel tubes are fabricated from Type 304 stainless steel. The threaded rods and spacer nuts are fabricated from 17-4 PH stainless steel. The stainless steel tubes are not structural components; therefore, they are not considered in the evaluation of the basket structural strength. The primary function of the threaded spacer nuts is to locate and structurally assemble the support disks, heat transfer disks and top and bottom weldment plates into an integral assembly. The threaded rod

carries the inertial weight of the spacer nuts, support disks, heat transfer disks, one end plate, and their own inertial weight for a normal transport conditions 1-foot end drop. The end drop loading of the spacer nuts and threaded rods represents a classical closed form structural analysis. Therefore, the only basket component that requires a detailed finite element structural evaluation is the support disk.

The fuel basket is evaluated for the normal transport condition loads in this section and is evaluated for the hypothetical accident condition loads in Section 2.7.8.

Figure 2.6.12-1 NAC-STC PWR Fuel Assembly Basket for Directly Loaded Fuel



(Dimension in inches)

Figure 2.6.12-2 Support Disk Cross-Section Configuration for Directly Loaded Fuel

**FIGURE WITHHELD AS SENSITIVE
UNCLASSIFIED INFORMATION**

Figure 2.6.12-3 Fuel Tube Configuration for Directly Loaded Fuel

**FIGURE WITHHELD AS SENSITIVE
UNCLASSIFIED INFORMATION**

THIS PAGE INTENTIONALLY LEFT BLANK

2.6.12.1 Detailed Analysis - PWR Basket For Directly Loaded Fuel

Based on criticality control requirements, the directly loaded fuel configuration fuel basket design criteria requires the maintenance of fuel support and control of spacing of the fuel assemblies for all load conditions. The structural design criteria for the structural components in the fuel basket is the ASME Boiler and Pressure Vessel Code, Section III, Division 1, Subsection NG, "Core Support Structures." Consistent with this criteria, the main structural component in the fuel basket, the stainless steel support disk, is shown to have a maximum stress intensity in any disk for any normal condition load and position orientation to be less than the design stress intensity value, S_m . The material design stress intensity used in this evaluation is based on the maximum material temperature of 650°F for all locations in the basket unless otherwise indicated. Using a stress allowable at 650°F is conservative since the material design stress intensity reduces with temperature and the hottest location in the basket structure during normal conditions is 498°F (Table 3.4-1). In the vertical orientation, the fuel basket components are loaded by their own inertial weight and do not experience load from the guided, but free standing fuel assemblies. Structural loads are experienced in the basket components from the fuel assemblies when the cask is in any orientation other than vertical. All possible orientations are evaluated. In addition to the load from inertial weight, the differential thermal expansion on the support disk is also evaluated.

THIS PAGE INTENTIONALLY LEFT BLANK

2.6.12.2 Finite Element Model Description - Directly Loaded PWR Fuel Basket

Three separate finite element analyses are performed for the directly loaded fuel configuration PWR basket support disk evaluations: One for the structural (stress) analysis of the normal transport conditions free thermal expansion, a second for the side drop impact condition, and a third for the evaluation of the end drop impact condition. These evaluations are performed using ANSYS, Revision 4.4.

The temperature distribution on the support disk is determined in a separate thermal analysis, which uses a three-dimensional finite element model representing one-quarter of the cask. The thermal analysis model, documented in Section 3.4, considers the fuel, fuel tubes, cavity gas, support disks, heat transfer disks, and basket end plates, lids, cask shells, neutron shield, and impact limiters.

The support disk and heat transfer disk nodes and elements at the axial location of maximum temperature in the thermal analysis model, Section 3.4, are extracted and converted into structural models. The temperature distribution determined from the thermal analysis is then respectively mapped to the thermal stress analysis models. An overall view of the finite element model for thermal stress analysis is shown in Figure 2.6.12.2-1. In the thermal stress analysis model, the support disk is modeled with ANSYS three-dimensional isoparametric solid elements (STIF45). The radius at the corners of the support disk holes is not modeled; thus, the corners of the holes in the support disk will behave as a notch in a uniaxial stress field. This finite element model is conservative for this analysis.

No displacement restraints are applied on the thermal expansion stress model. Thermal expansion stress is developed from the temperature gradient from the hot center of the disk to the cooler free edge. Since the center of the disk wants to expand faster than the edge, a tension stress is developed in the disk.

The finite element model for the side drop impact analysis uses (STIF42) ANSYS quadrilateral elements as shown in Figure 2.6.12.2-2, with ANSYS two-dimensional gap elements (STIF12) at all nodes on the periphery of the support disks. The gap elements are used to simulate the interface between the support disk and the inner shell of the cask. Each gap element contains two nodes; one, specified at the inner shell, is restrained. The gap size at each gap element is determined by the difference between the support disk diameter and the inside diameter of the

cask inner shell at the calculated normal transport conditions temperature. The stiffness of the gap elements is dependent upon the contact area between the disk and the inner shell.

A typical triangular element at the periphery of the support disk is shown in Figure A below in the cylindrical coordinate system R, θ , with respect to the support disk global cylindrical coordinate with its origin at the center of disk. The stiffness K of the gap element between the cask cavity and basket support disk is based on the stiffness of the adjacent isoparametric elements, in this case, ANSYS STIF42 triangular elements, as shown in Figure 2.6.12.2-2. Figures A through E depict the methodology used to calculate the stiffness for a typical element at the periphery of the support disk.

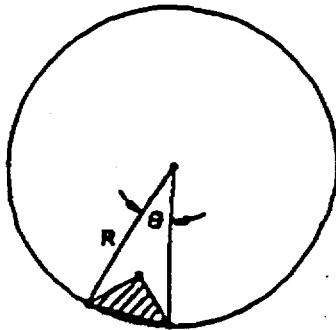


FIGURE A:
TYPICAL BOUNDARY ELEMENTS

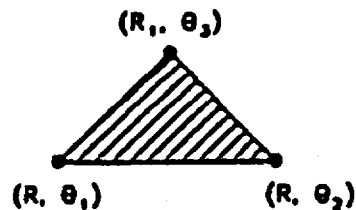


FIGURE B:
SPATIAL LOCATION OF NODE

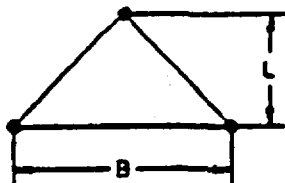


FIGURE C:

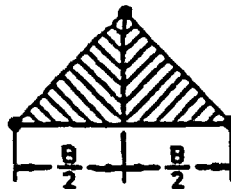


FIGURE D:

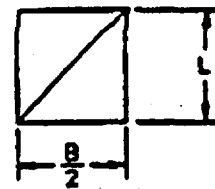


FIGURE E:

Basket/Cavity Gap Element Stiffness

Implementing this methodology, the gap element stiffness is calculated as follows:

$$K = \left(\frac{AE}{L} \right) = \left(\frac{BtE}{2L} \right) = 7.9E+6 \text{ pounds/in.}$$

where:

- t = Thickness of support, disk = 0.5 inch
E = Elastic modulus = 28.3E+6 psi at 70°F

L and B as shown in Figures C through E are calculated as follows:

$$\begin{aligned} R &= 35.41 \\ R_1 &= 34.594 \\ \theta_1 &= 56.744^\circ \\ \theta_2 &= 55.273^\circ \\ \theta_3 &= 56.016^\circ \\ B &= 2R \sin (\theta/2) \\ \theta &= 56.744 - 55.273 = 1.469^\circ \quad (\text{From coordinates shown in Figure B}) \\ R &= 35.41 \text{ in} \\ L &= R \cos (\theta/2) - R_1 = 0.8131 \\ R_1 &= 34.594 \text{ From coordinates shown in Figure B)} \\ \frac{\theta}{2} &= \frac{1.469^\circ}{2} = 0.7345^\circ \end{aligned}$$

The stiffness value used in all analyses is 1.0E+6 pounds per inch.

The analysis results are then examined to ensure that any overlapping between the loaded support disk and the cask inner shell in the ANSYS model is less than 1 percent of the thickness of the inner shell; the actual overlap is only 0.5 percent; therefore, the gap element stiffness of 1.0E+6 psi is appropriate for use in the basket support disk side drop evaluations.

The finite element model for the thermal stress conditions, ANSYS STIF45 (Figure 2.6.12.2-1), is used to evaluate the heat transfer disk and the support disk for the end impact condition. The gravity loading is applied in the cask longitudinal direction (lateral to the plane of the heat transfer disk and support disk). The support disks and the heat transfer disks are separated by spacer nuts on threaded rods at six locations near the periphery of the disks; therefore,

displacement restraints are applied at the nodes on the disk models where the six threaded rods are located.

Figure 2.6.12.2-1 Finite Element Model - Thermal Stress Analysis (NAC-STC PWR Basket Support Disk for Directly Loaded Fuel)

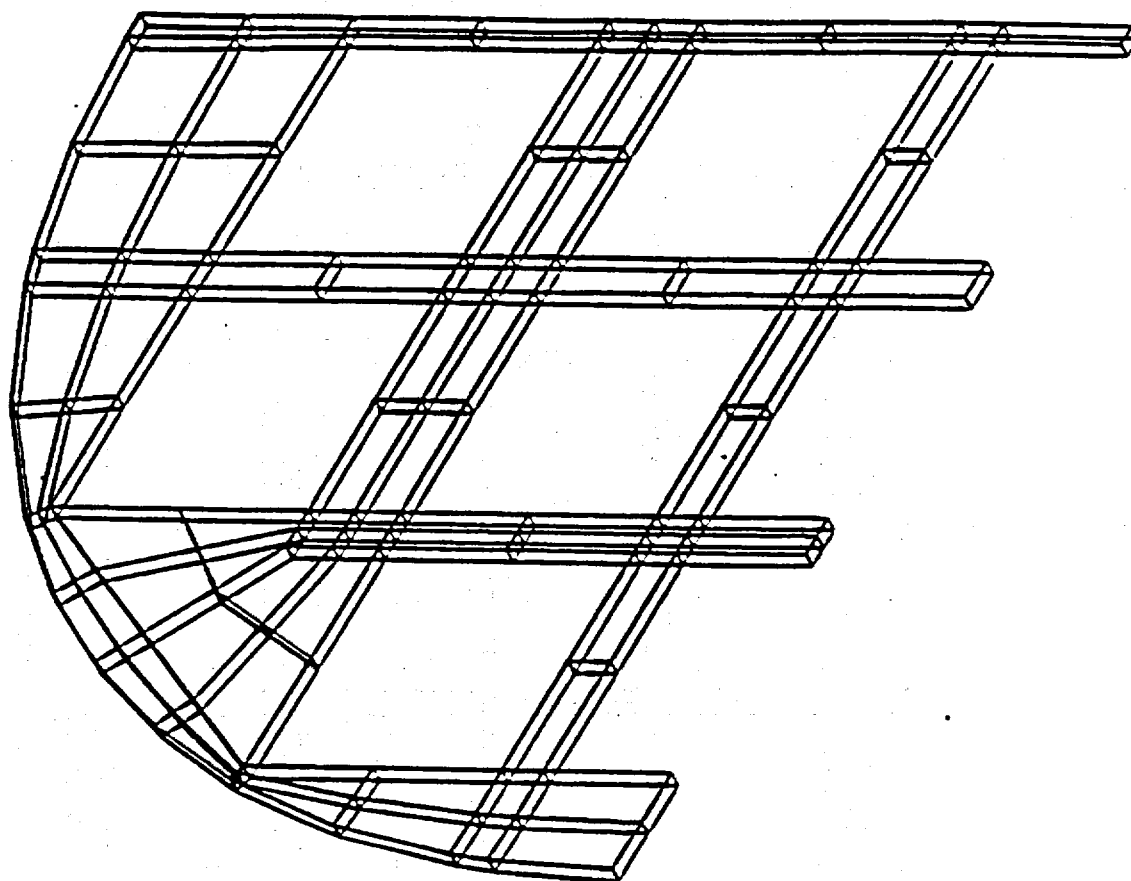
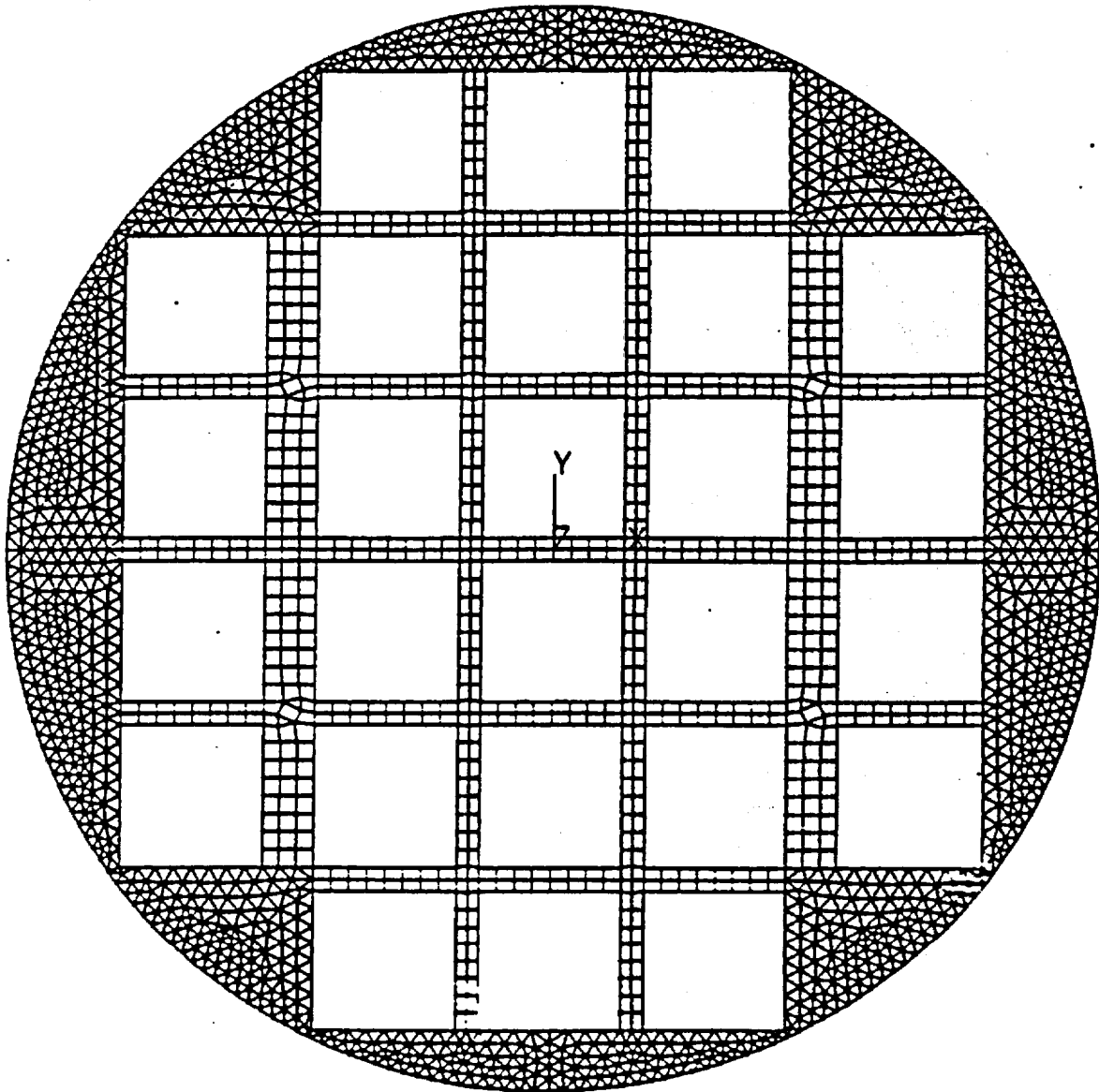


Figure 2.6.12.2-2 Finite Element Model - Side Impact Analysis (NAC-STC PWR Basket Support Disk for Directly Loaded Fuel)



2.6.12.3 Thermal Expansion Evaluation of Support Disk - Directly Loaded PWR Fuel Basket

A thermal stress analysis is performed, using ANSYS, to determine the differential thermal expansion and the associated thermal stresses in a support disk for the directly loaded fuel configuration that result from the heat load generated by the 26 fuel assemblies. The thermal stresses in the support disk are developed by differential thermal expansion resulting from a nonuniform temperature distribution, which is calculated using the ANSYS program for a heat load of 0.85 kilowatts per assembly in the thermal analysis (Section 3.4). The temperatures obtained from the thermal analysis are also used to determine the temperature-dependent material properties of the support disk and to evaluate the thermal strains in the support disk. No displacement restraints are imposed on the support disk for the free thermal stress analysis.

The stress summary for the 20 nodes with the maximum thermal stress intensity is shown in Table 2.6.12.3-1. The location of these nodes on the support disk is shown in Figure 2.6.12.3-1.

Evaluation of thermal expansion of the fuel basket relative to the inside surface of the inner shell of the cask has been performed for compatible sets of thermal data and transport package configurations.

The transport configuration with the cask in the horizontal position with impact limiters installed represents the normal transport configuration. Although the cask is backfilled with an inert atmosphere of helium at the time of fuel loading, in order to eliminate the need to disturb the containment boundary to perform tests to validate that helium remained in the cask cavity throughout an extended period of storage prior to package transport, heat transfer analysis has been performed considering the cask in a horizontal orientation, cavity filled with air, and fresh fuel decay heat of 0.85 kilowatts per assembly. Temperature data from this analysis is used to calculate the diametral thermal expansion of the inside diameter of the inner shell (0.134 inches), outer diameter of the steel support disk (0.148 inches) and the outer diameter of the aluminum heat transfer disk (0.336 inches). Considering maximum material conditions and the horizontal orientation as shown in Figure 2.6.12.3-2, the minimum gap between the basket steel support disk and the cask wall is 0.086 inches. For the heat transfer disk, the minimum gap is 0.108 inches.

Cask Horizontal With Air in Cavity (Directly Loaded Fuel Configuration)

	Hot Diameter (inches)	Tolerance (inches)	Gap (inches)
Inner Shell Surface	71.134	+0.06/-0.04	----
Steel Support Disk	71.008	+0.0/-0.02	0.086
Aluminum Heat Transfer Disk	70.986	+0.0/-0.02	0.108

Similar to the analysis performed for the cask in the horizontal configuration, temperatures throughout the cask and basket for the freshly loaded fuel backfilled with helium without impact limiters in the vertical configuration were calculated. This set of temperatures were then used to calculate the thermal expansion of the cask inside surface and the basket support disk and heat transfer disk. Considering maximum material conditions and manufacturing tolerances for the package in the vertical configuration, as shown in Figure 2.6.12.3-3, the minimum diametral gap between the steel support disk and cask wall is 0.084 inches, or 0.042 inches on the radius. The minimum diametral gap between the aluminum heat transfer disk and the cask wall is 0.062 inches, or 0.031 inches on the radius.

Cask Vertical With Helium In Cavity (Directly Loaded Fuel Configuration)

	Hot Diameter (inches)	Tolerance (inches)	Gap (inches)
Inner Shell Surface	71.1583	+0.06/-0.04	----
Steel Support Disk	71.0348	+0.0/-0.02	0.084
Aluminum Heat Transfer Disk	71.056	+0.0/-0.02	0.062

In addition to these steady state conditions, it has been postulated that the greatest difference in temperature of the basket relative to that of the cask body/inner shell is during the thermal transient created during the loading, and vacuum drying and heat-up process. This potential worst case condition is evaluated using component temperatures calculated as a function of time beginning from a 70°F material temperature condition through a steady state temperature profile for the design bases heat load. Considering maximum material conditions and manufacturing tolerances for the package in the vertical configuration as shown in Figure 2.6.12.3-3, the minimum gap between the basket and cask wall is 0.0778 inches over the diameter and 0.0389 inches on the radius for the steel support disk, and 0.0774 inches over the diameter and 0.0387 inches on the radius for the aluminum heat transfer disk. The results are summarized as:

Heat up Transient (Directly Loaded PWR Fuel Configuration)

	Hot Diameter (inches)	Tolerance (inches)	Gap (inches)
Inner Shell Surface	71.1378	+0.06/-0.04	----
Steel Support Disk	71.0200	+0.0/-0.02	0.0778
Aluminum Heat Transfer Disk	70.0204	+0.0/-0.02	0.0774

Based on these analyses for normal transport, vertical steady state, and heat-up transient, the basket assembly does not contact the cask inner shell wall and does not produce restrained thermal expansion loads on the steel support disks or aluminum heat transfer disks considering maximum design bases heat load, maximum material conditions, and worst case tolerance stack-up.

Figure 2.6.12.3-1 Location of the 20 Maximum SI Nodal Stresses in the NAC-STC Fuel Basket Support Disk for Directly Loaded Fuel - Thermal Condition

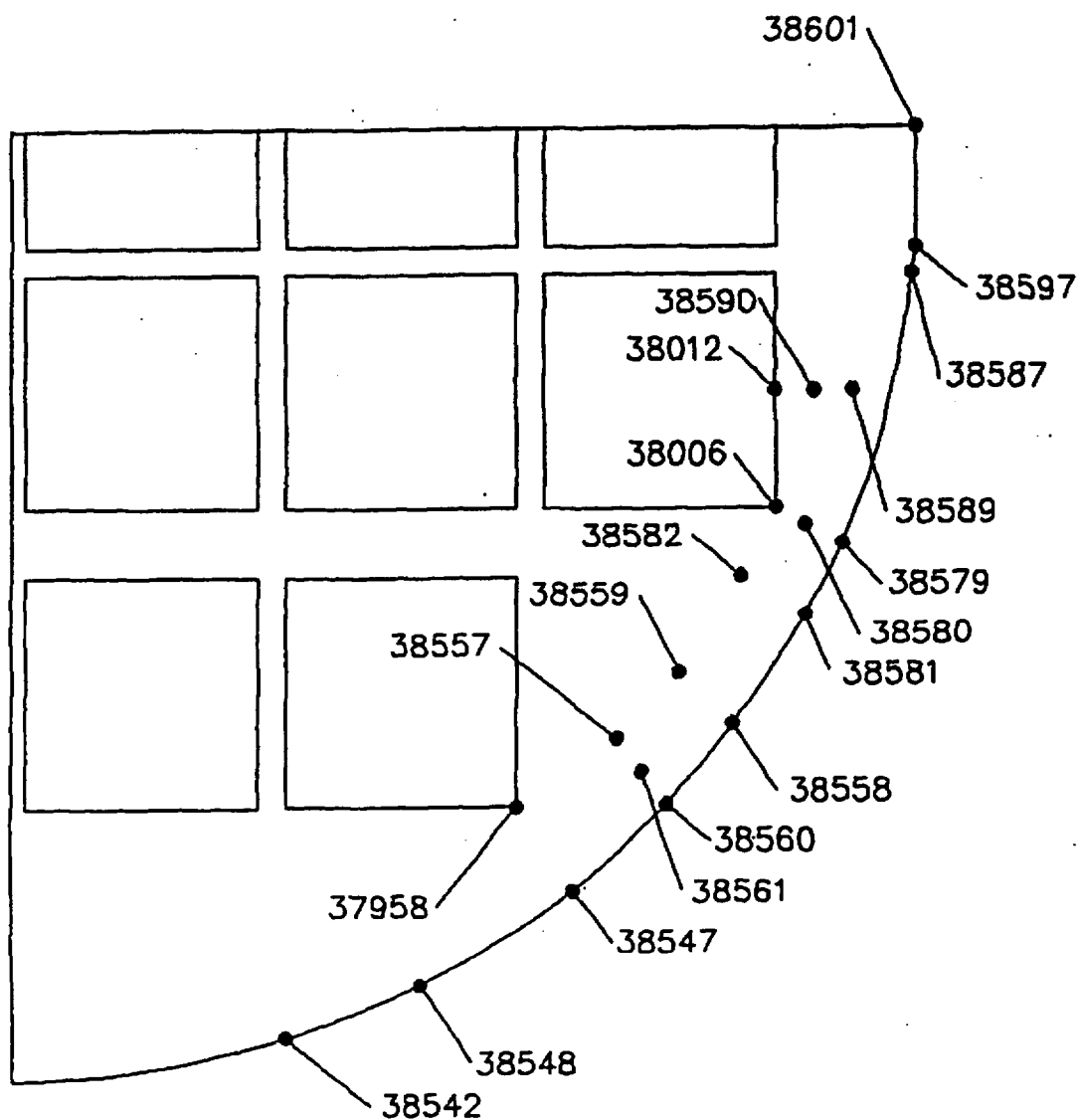


Figure 2.6.12.3-2 Basket Maximum Material Condition for the Directly Loaded Fuel Configuration in the Horizontal Orientation (inches)

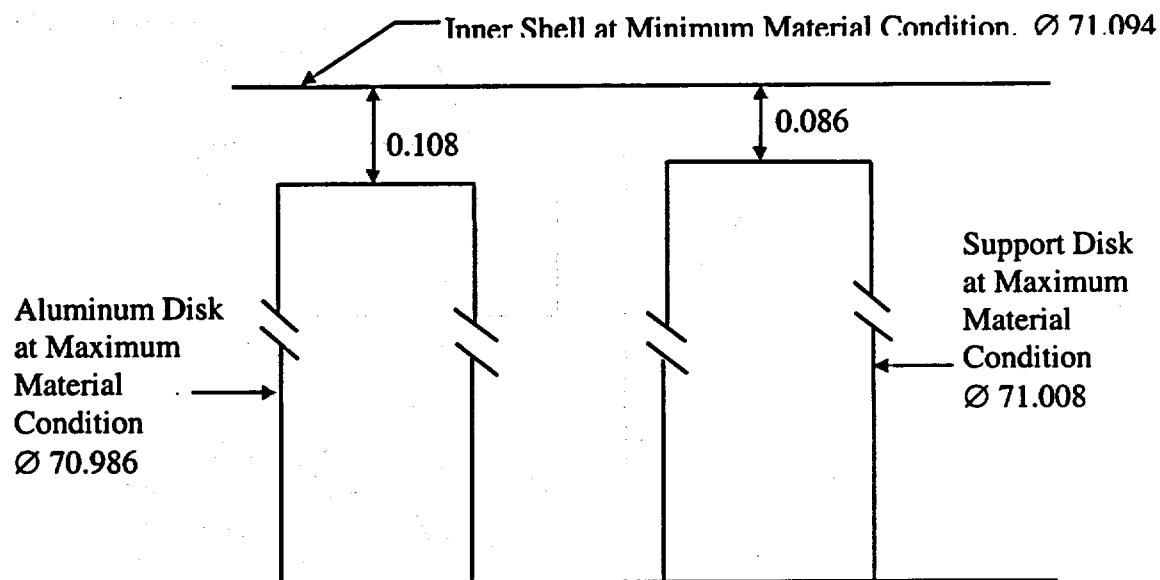
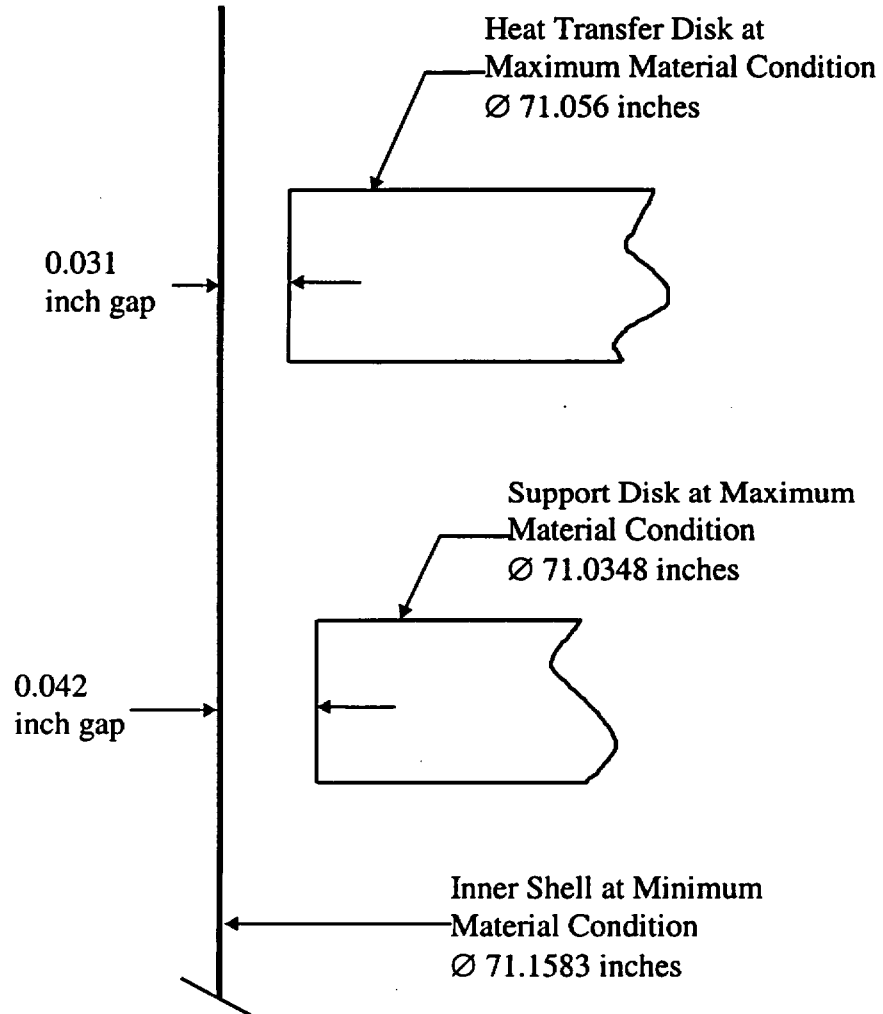


Figure 2.6.12.3-3 Basket Maximum Material Condition for Directly Loaded Fuel Configuration - Cask Vertical



The basket is assumed to be located at the center of the cask cavity.

Table 2.6.12.3-1 Thermal Stresses (NAC-STC PWR Basket - Directly Loaded Fuel Configuration)

Node No. ¹	S _x (ksi)	S _y (ksi)	S _z (ksi)	S _{xy} (ksi)	S _{yz} (ksi)	S _{xz} (ksi)	SI (ksi)
38006	2.3	23.6	0.8	10.1	0.0	-0.1	32.0
37958	19.6	8.2	-1.3	11.8	0.0	0.0	30.6
38558	12.2	17.8	-0.6	14.5	0.0	0.0	30.4
38580	4.7	18.7	-2.6	10.0	0.0	-0.1	29.4
38560	12.7	10.3	-0.7	12.6	-0.2	0.2	27.6
38581	8.2	18.3	0.3	11.4	0.0	0.2	26.4
38587	0.0	23.7	-0.3	3.9	0.0	0.0	25.4
38547	12.9	8.2	-2.3	9.5	0.2	-0.1	25.2
38589	0.6	20.3	0.1	6.7	0.0	0.0	24.0
38590	-1.1	19.8	0.0	5.3	0.0	-0.1	23.8
38561	12.3	8.6	0.9	10.9	-0.2	0.1	23.8
38579	4.7	15.6	-0.4	8.4	0.0	0.0	23.3
38559	8.9	13.6	-0.5	10.9	0.0	0.0	22.9
38597	0.1	22.8	0.4	1.2	0.0	0.0	22.8
38557	9.9	6.6	1.1	10.4	0.0	0.0	21.8
38582	7.6	16.3	1.4	9.2	0.0	0.0	21.5
38012	-3.3	15.6	-2.1	4.0	0.0	-0.1	20.7
38542	17.6	0.8	-0.5	5.6	0.0	0.0	20.5
38601	0.0	20.1	0.2	0.6	0.0	0.0	20.1
38548	13.3	2.5	-0.3	7.8	-0.1	0.0	19.4

¹ Stress components are listed for the nodes with the 20 highest thermal stresses (see Figure 2.6.12.3-1 for locations of these nodes). Note that S_x is the stress in the radial direction, S_y is the stress in the circumferential direction and S_{xy} is the shear stress.

THIS PAGE INTENTIONALLY LEFT BLANK

2.6.12.4 Stress Evaluation of Support Disk for a 1-Foot End Drop Load Condition
(Directly Loaded Fuel Configuration)

The support disks of the directly loaded fuel configuration of the NAC-STC fuel basket are located by threaded rods and spacer nuts positioned at six points on the circumference near the periphery of each disk. A structural analysis is performed, using ANSYS, to evaluate the effect of a 1-foot end drop impact (out-of-plane loading) on the support disks in the NAC-STC with the cask in the vertical position. The ANSYS STIF45 brick element as described in Section 2.6.12.2 is used in the model as shown in Figure 2.6.12-2. The end drop impact loading is applied in the cask longitudinal direction (perpendicular to the plane of the support disk). A load factor of 19.6 g is applied to the mass of the support disk. The value of 19.6 g is the maximum deceleration of the NAC-STC for the 1-foot end drop impact (Table 2.6.7.4.1-3). Displacement restraints are applied in the ANSYS model at the nodes where the six threaded rods with spacer nuts are located.

The stress summary for the locations of the 20 nodes with the highest stress intensity, SI, 1-foot end drop impact stresses shown in Figure 2.6.12.4-1 is provided in Table 2.6.12.4-1. The maximum SI nodal stress is 12.65 ksi. The minimum margin of safety calculated relative to the design stress intensity, S_m is +2.56. The margin of safety of +2.56 is conservative since further stress classification in accordance with ASME Code, Section III, Subsection NG criteria permits the membrane stress, P_m , which is lower than the total node point stress, SI, to reach S_m , or the primary membrane plus primary bending stress, $P_m + P_b$, to reach the value of $1.5S_m$.

Figure 2.6.12.4-1 Support Disk For the Directly Loaded Fuel Configuration - 19.6-g
End Drop

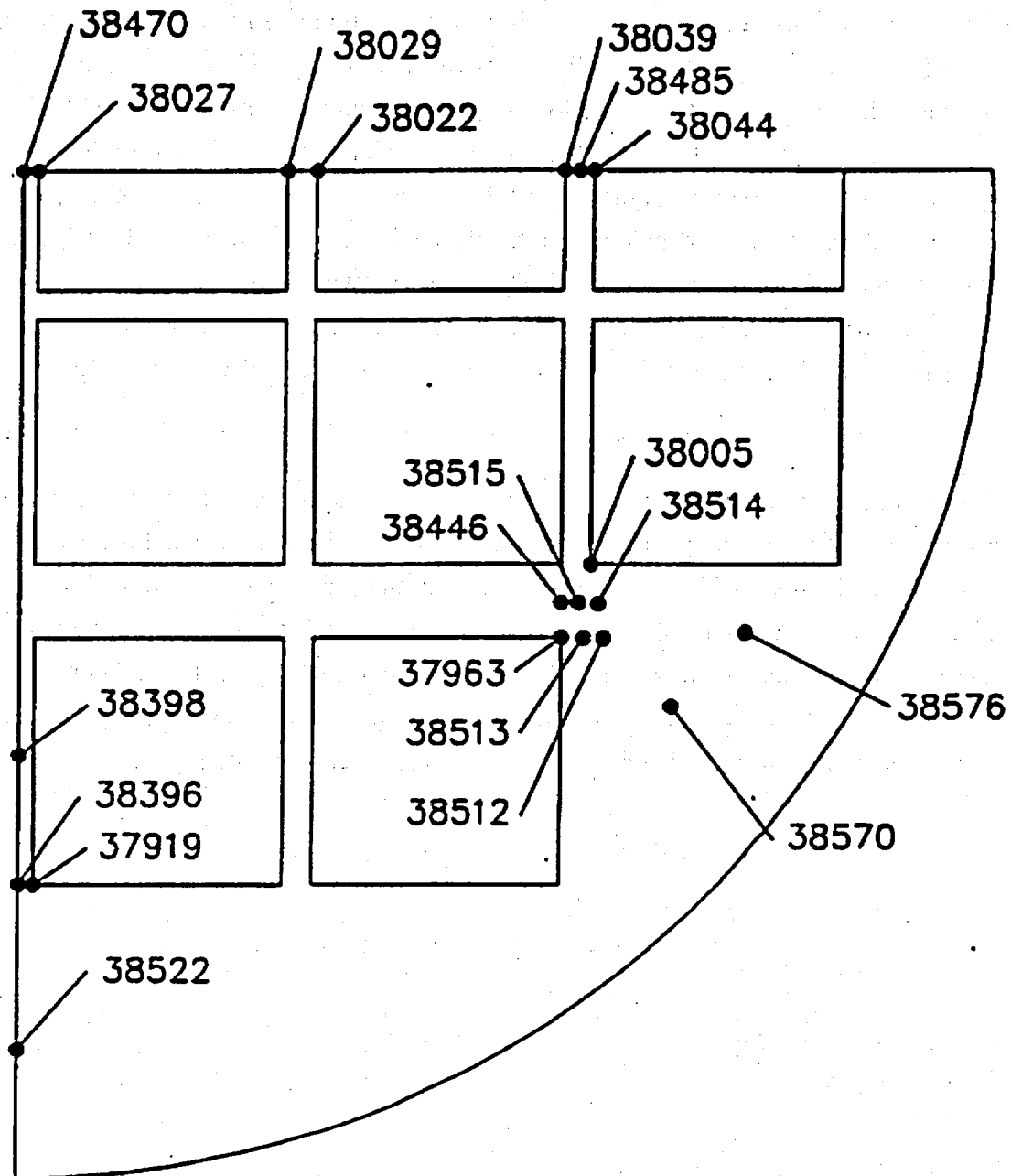


Table 2.6.12.4-1 Stresses for 1-Foot End Drop Impact with a 19.6-g Deceleration
(NAC-STC PWR Basket - Directly Loaded Fuel Configuration)

Node No. ¹	S _x (ksi)	S _y (ksi)	S _z (ksi)	S _{xy} (ksi)	S _{yz} (ksi)	S _{xz} (ksi)	SI (ksi)	MS ²
38512	-7.6	-8.3	1.8	0.7	1.7	0.0	12.7	2.6
38522	-3.2	-2.4	-0.4	-2.4	-4.6	-0.7	11.4	3.0
38513	-4.0	-4.9	1.2	1.4	-0.9	-0.7	10.9	3.1
38570	-3.6	-3.8	-0.5	0.5	0.0	1.2	10.4	3.3
38396	-3.3	-8.2	-0.2	2.0	2.4	-0.2	10.1	3.5
38514	-6.1	-5.5	0.5	0.6	0.9	0.8	10.0	3.5
37963	-2.8	-4.5	0.5	2.8	0.8	-1.0	9.7	3.6
37919	-2.7	-5.9	0.0	1.5	-1.6	-0.2	9.1	3.9
38515	-7.9	-7.0	-0.9	0.4	-0.8	1.4	8.4	4.3
38027	-0.7	6.5	-0.6	-0.2	-0.1	0.7	7.9	4.7
38576	-3.7	-5.7	-0.9	1.0	1.1	-0.5	7.9	4.7
38470	-0.8	6.3	-0.7	0.0	0.1	-0.8	7.8	4.7
38005	-5.0	-4.6	-0.4	1.5	0.7	-0.6	7.8	4.7
38029	0.1	7.1	-0.2	0.0	0.0	-0.5	7.6	4.9
38032	0.1	7.0	-0.2	0.0	0.0	0.0	7.6	4.9
38039	0.0	7.6	0.0	0.0	0.0	0.0	7.6	4.9
38044	0.0	7.4	0.0	0.0	0.0	0.0	7.4	5.0
38485	0.0	7.3	0.0	0.0	0.0	0.0	7.4	5.1
38446	-6.5	-5.0	-0.6	1.4	0.0	0.0	7.4	5.1
38398	0.8	-4.5	0.7	-0.6	-1.1	0.7	7.1	5.3

¹ Stress components are listed for the nodes with the 20 highest thermal stresses (see Figure 2.6.12.4-1 for locations of these nodes). Note that S_x is the stress in the radial direction, S_y is the stress in the circumferential direction and S_{xy} is the shear stress.

² The allowable stress is conservatively defined as S_m at the node point temperature defined by the quarter symmetry heat transfer analysis.

THIS PAGE INTENTIONALLY LEFT BLANK

2.6.12.5 Stress Evaluation of Support Disk (Directly Loaded Fuel Configuration) for Thermal Plus a 1-Foot End Drop Combined Load Condition

The thermal expansion loads in Section 2.6.12.3 are applied to the finite element model simultaneously with the 19.6 g end drop loads in Section 2.6.12.4 to produce a combined thermal expansion plus end impact loading. The stress evaluation is performed according to the ASME Code Section III, Division 1, Subsection NG. Table 2.6.12.5-1 documents the 20 highest total stresses (thermal expansion stresses plus 1-foot end drop impact stresses) at normal transport condition temperatures and the associated margins of safety. Figure 2.6.12.5-1 shows the locations for each of the 20 maximum stress intensity. Comparing these maximum nodal point primary plus secondary stress intensities to the material 3 S_m value validates the ASME Code elastic analysis methodology.

Figure 2.6.12.5-1 Location of the 20 Maximum SI Nodal Stresses in the NAC-STC Fuel Basket Support Disk (Directly Loaded Fuel Configuration) - Thermal + 19.6-g End Drop

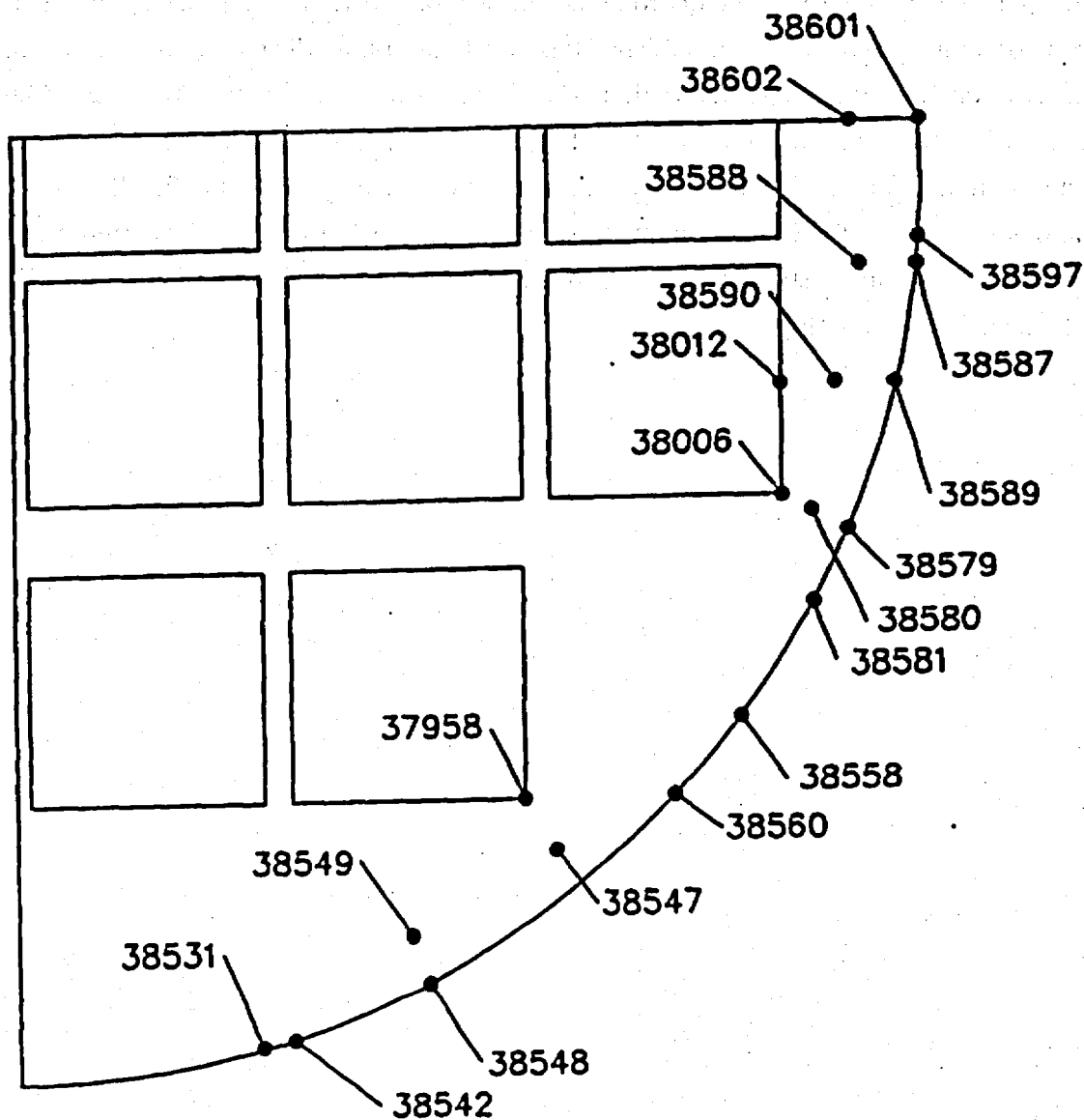


Table 2.6.12.5-1 Combined Stresses for Thermal + 19.6-g End Drop Impact (Directly Loaded Fuel Configuration - Support Disk)

Node No.	S _x (ksi)	S _y (ksi)	S _z (ksi)	S _{xy} (ksi)	S _{yz} (ksi)	S _{xz} (ksi)	SI (ksi)	3S _m ¹ (ksi)
38006	0.4	26.8	0.0	11.3	0.3	1.3	39.4	125.7
38587	0.4	35.9	0.3	4.2	-0.4	-0.2	38.2	125.7
38580	2.0	22.8	-5.4	11.1	0.2	-0.1	37.8	125.7
38590	-0.6	32.1	0.9	6.0	0.2	-0.6	36.5	125.7
38589	0.8	32.3	0.7	7.6	-0.9	0.2	35.9	125.7
38597	0.0	34.9	0.4	1.9	-0.9	0.3	35.6	125.7
37958	21.3	7.5	-1.8	12.7	0.8	0.0	35.3	125.7
38012	-2.9	28.4	-1.2	4.6	0.0	-1.4	35.0	125.7
38601	0.3	33.6	0.2	0.9	1.1	0.4	33.8	125.7
38542	26.6	1.8	0.0	6.4	0.4	0.5	30.4	125.7
38579	2.4	20.3	-0.9	9.5	0.0	-2.0	30.1	125.7
38547	15.3	7.1	-3.3	10.5	0.3	-0.5	29.9	125.7
38558	11.5	17.0	-0.6	13.7	0.0	0.0	28.7	125.7
38531	25.9	1.0	0.2	4.6	-0.1	1.0	27.4	125.7
38560	12.7	9.9	-0.7	12.1	-0.5	0.8	27.3	125.7
38549	19.4	0.5	0.4	7.7	0.6	-0.2	26.5	125.7
38548	19.5	2.6	-0.2	9.2	0.2	0.4	26.3	125.7
38581	8.0	18.4	0.5	10.8	-0.5	0.4	26.1	125.7
38588	-0.3	23.4	0.8	2.0	0.7	-0.3	25.3	125.7
38602	0.0	24.1	0.0	0.3	0.0	0.0	24.8	125.7

¹ S_m is conservatively defined for a temperature of 650°F.

THIS PAGE INTENTIONALLY LEFT BLANK

2.6.12.6 Stress Evaluation of Threaded Rods and Spacer Nuts for a 1-Foot End Drop Load Condition (Directly Loaded Fuel Configuration)

The deceleration for the NAC-STC for the normal conditions of transport 1-foot end drop is 19.6 g. During the 1-foot end drop, the threaded rods and spacer nuts in the directly loaded fuel configuration fuel basket are loaded with the weight of the 31 support disks, 20 aluminum heat transfer disks, one end plate and the weights of the threaded rods and spacer nuts. These loads are calculated as follows:

Total weight of basket	=	16,350 lbs
Less weight of bottom weldment	=	-645 lbs
Less weight of fuel tubes	=	-3,666 lbs
1-g load on the tie rods and spacer nuts	=	12,039 lbs
Normal conditions of transport load		
on tie rods and spacer nuts	=	(12,039)(19.6)
	=	235,964 lbs

The effective area of one threaded rod and spacer nut at each of the six locations supporting the weight of the support disks is equivalent to the gross area of the square spacer nut and is calculated as:

$$A = (2.5)(2.5) \\ = 6.25 \text{ in}^2$$

The average compressive stress in the threaded rods and spacer nuts is:

$$S_c = \frac{235,964}{(6)(6.25)} \\ = 6292 \text{ psi}$$

The allowable stress of the 17-4 PH stainless steel under normal conditions of transport is S_m .

Then, the margin of safety is:

$$MS = \frac{(S_m)}{S_c} - 1 = \underline{+Large}$$

where:

$$S_m = 43.8 \text{ ksi (17-4 PH stainless steel at 405°F)}$$

Therefore, the threaded rods and spacer nuts in the directly loaded fuel configuration of the fuel basket are structurally adequate for a 19.6-g end impact under normal conditions of transport.

2.6.12.7 Stress Evaluation of Support Disk (Directly Loaded Fuel Configuration) for a 1-Foot Side Drop Impact Load Condition

To determine the structural adequacy of the support disks in the 26 PWR fuel assembly basket (directly loaded fuel configuration) for the 1-foot side drop impact load condition, a quasi-static impact load equal to the weight of the fuel and tubes multiplied by an 18.1 g amplification factor is applied to the support disk structure. The 18.1 g inertial loading of the support disk is also included. Each support disk also carries the weight of a single aluminum heat transfer disk, which is applied through the six threaded rods. This additional load is applied to the support disk at the six threaded rod locations in the form of lumped masses. The value of 18.1 g is the NAC-STC impact limiter's design deceleration for a 1-foot side drop condition (Table 2.6.7.4.1-1). The fuel assembly loads are transmitted in direct compression through the tube wall to the web structure of each support disk. These loads are transmitted to the inner shell of the cask by the series of 31 support disks and the top and bottom plates.

The maximum loading occurs on a support disk during a side drop event. Thus, a detailed structural evaluation is required. Figure 2.6.12-2 shows a support disk cross-sectional configuration. A finite element analysis is performed, using the ANSYS computer code, to calculate the stresses in a support disk. The finite element model of the support disk for the side drop analysis is described in Section 2.6.12.2; the model is shown in Figure 2.6.12.2-2.

2.6.12.7.1 Drop Orientations

To bound all possible impact orientations, the support disk configuration (Figure 2.6.12-2) is analyzed for nine drop orientations: 0, 15, 30, 37, 45, 60, 64, 75, and 90 degrees. The drop orientations are identified in Figure 2.6.12.7-1. As shown in Figure 2.6.12.7-1, drop orientations 37 degrees and 64 degrees respectively put each of the support disk minimum ligaments in the direct load line. As discussed in Section 2.6.12.7, the maximum side impact force on the NAC-STC for normal conditions of transport is 18.1 g for a 1-foot side drop.

2.6.12.7.2 Analysis Results (1-Foot Side Drop)

Finite element stress analyses are performed for the 1-foot side impact load cases for the nine different impact orientations listed previously.

The allowable stress limit for the support disk primary membrane stress (P_m) is S_m , and primary membrane plus primary bending stress ($P_m + P_b$) is $1.5S_m$. The stress evaluation is performed in accordance with the ASME Code, Section III, Division 1, Subsection NG adopting the conservative methodology of evaluating nodal stress, $P_m + P_b$, at a maximum temperature of 650°F relative to the smaller P_m allowable of S_m . Implementing this method of structural evaluation is very conservative and demonstrates significant margins of safety.

The locations of the 20 highest nodal SI stresses in the support disk for each of the nine 1-foot side impact orientations evaluated are shown in Figures 2.6.12.7-2 through 2.6.12.7-10. Tables 2.6.12.7-1 through 2.6.12.7-9, respectively, provide tabulations of the nodal SI stresses at those 20 maximum stress locations in the support disk for each of the nine impact orientation. The tables also show the margin of safety for each analysis location for the 18.1 g side impact load condition. Table 2.6.12.7-10 presents a summary of the minimum margins of safety for the 18.1 g side impact analysis for the nine impact orientations.

The minimum conservatively calculated margin of safety for the support disk of the NAC-STC directly loaded fuel configuration basket for a 1-foot side drop is +1.52 which occurs at the 30 degree drop orientation. The margin of safety of +1.52 is conservative since further stress classification shows that the membrane stress, P_m and the membrane plus bending stress, $P_m + P_b$ is lower than the nodal stress intensity SI. The margin of safety of +1.52 is obtained by evaluating an allowable design stress, S_m relative to the total stress intensity, $P_m + P_b$ at a single node point. The ASME Code, Section III, Subsection NG, criteria permits this stress intensity to reach a level of $1.5 S_m$. Therefore, the support disks in the NAC-STC PWR fuel basket are structurally adequate for a 1-foot side drop load condition.

Figure 2.6.12.7-1 Support Disk Side Drop Orientations (Directly Loaded Fuel Configuration)

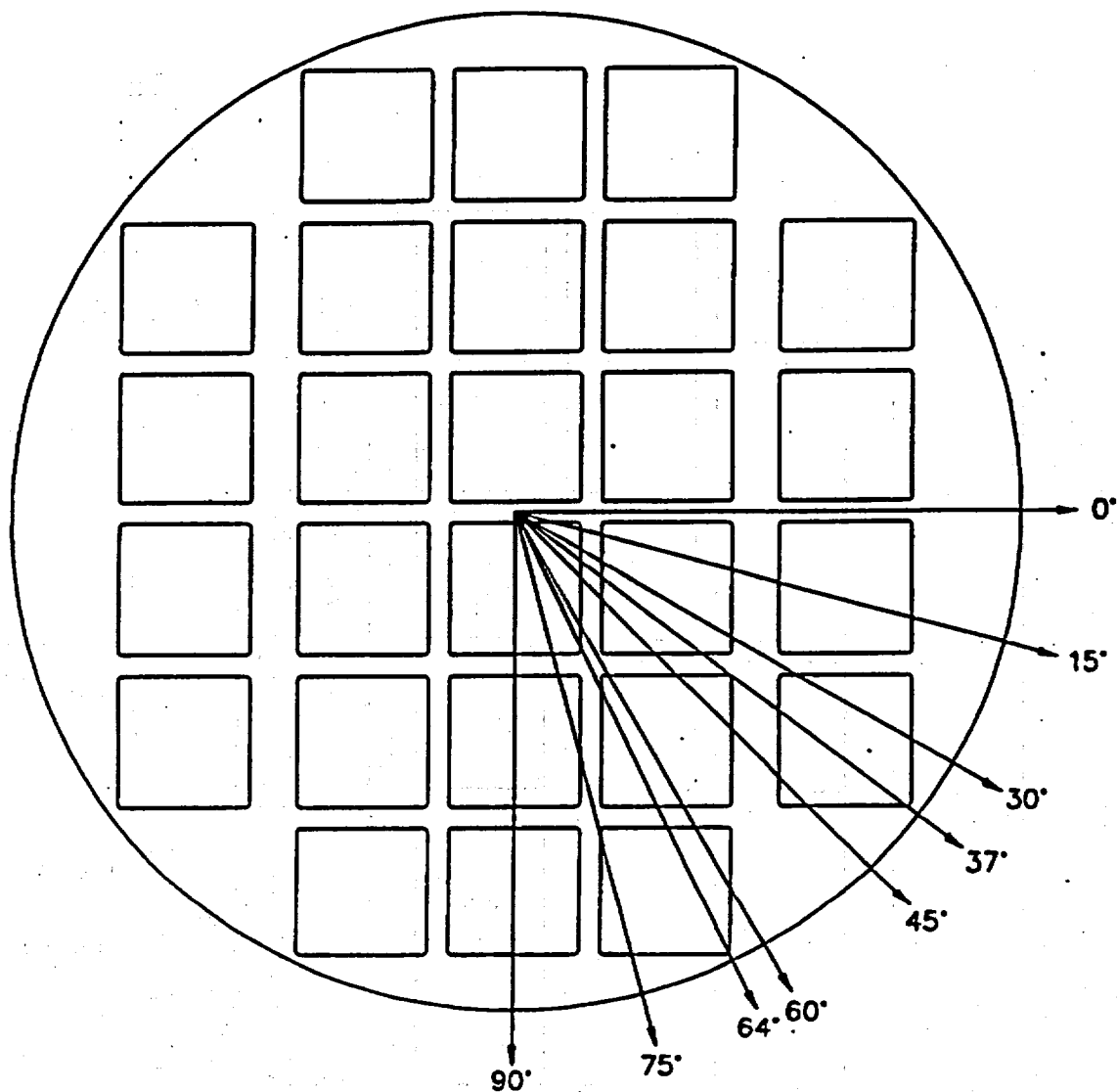


Figure 2.6.12.7-2 Locations of Maximum Nodal SI Stresses (Directly Loaded Fuel Configuration - Support Disk) - 18.1-g Side Impact Condition (0° Drop Orientation)

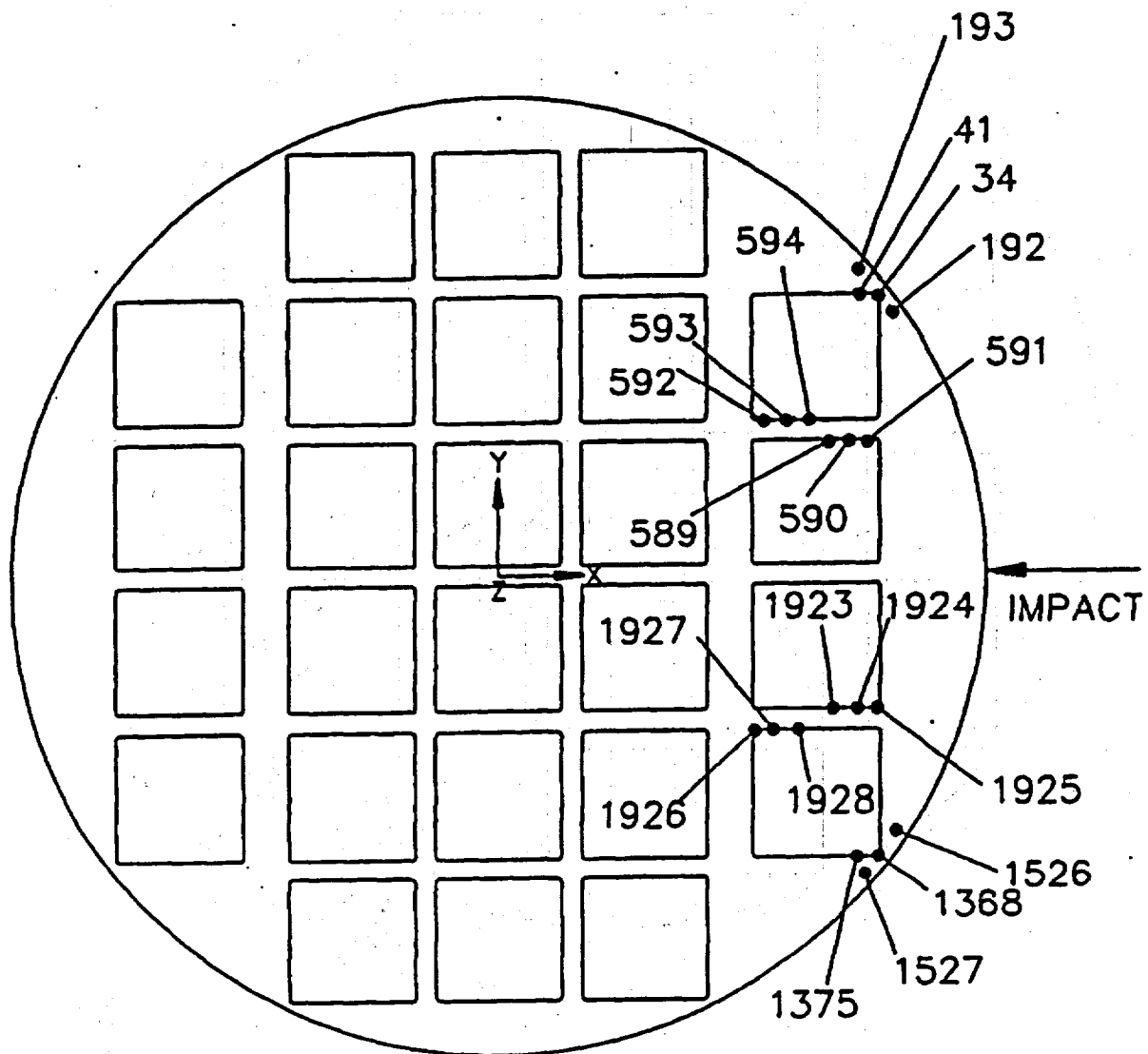


Figure 2.6.12.7-3 Location of Maximum Nodal SI Stresses (Directly Loaded Fuel Configuration - Support Disk) - 18.1-g Side Impact Condition (15° Drop Orientation)

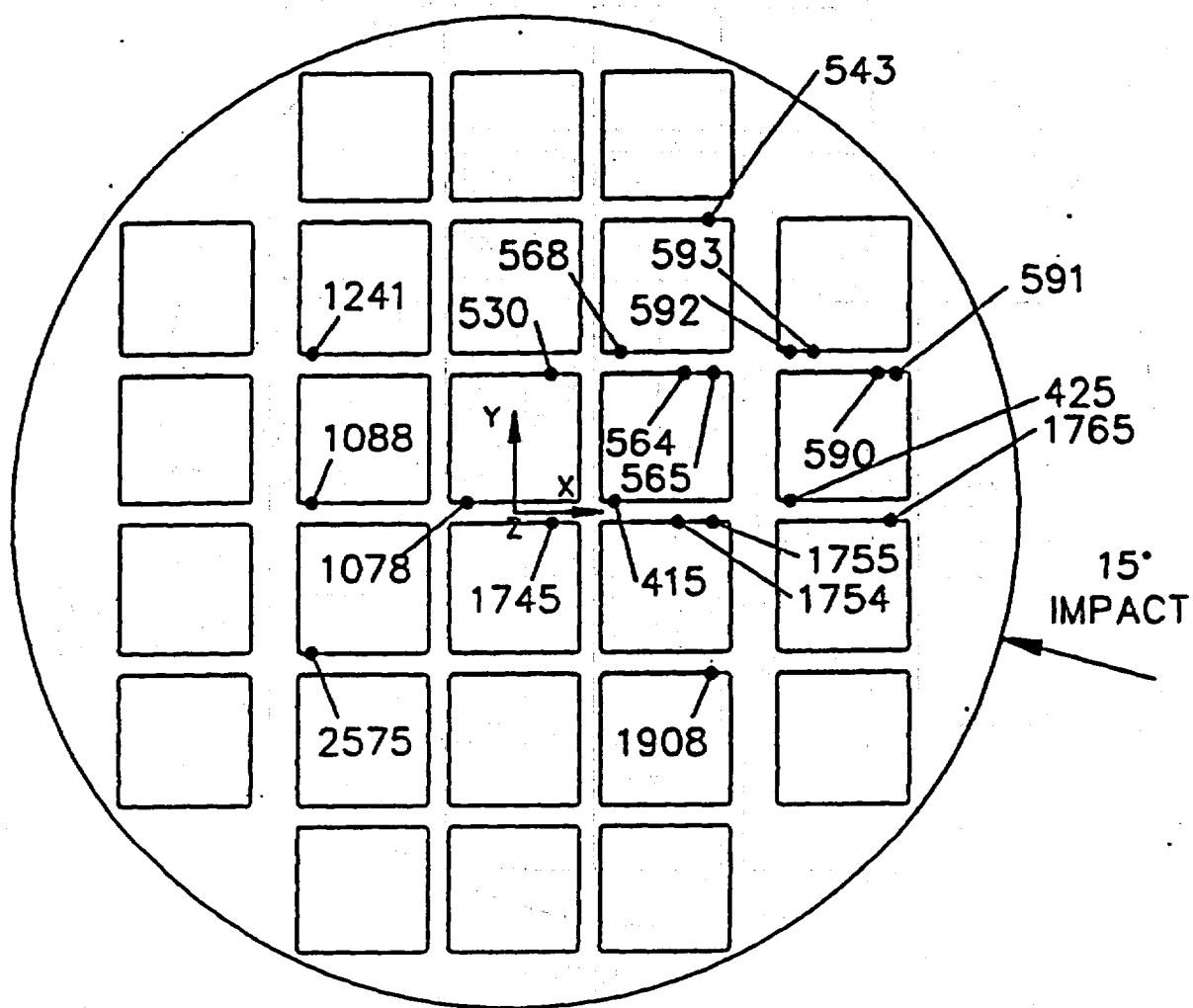


Figure 2.6.12.7-4 Location of Maximum Nodal SI Stresses (Directly Loaded Fuel Configuration - Support Disk) - 18.1-g Side Impact Condition (30° Drop Orientation)

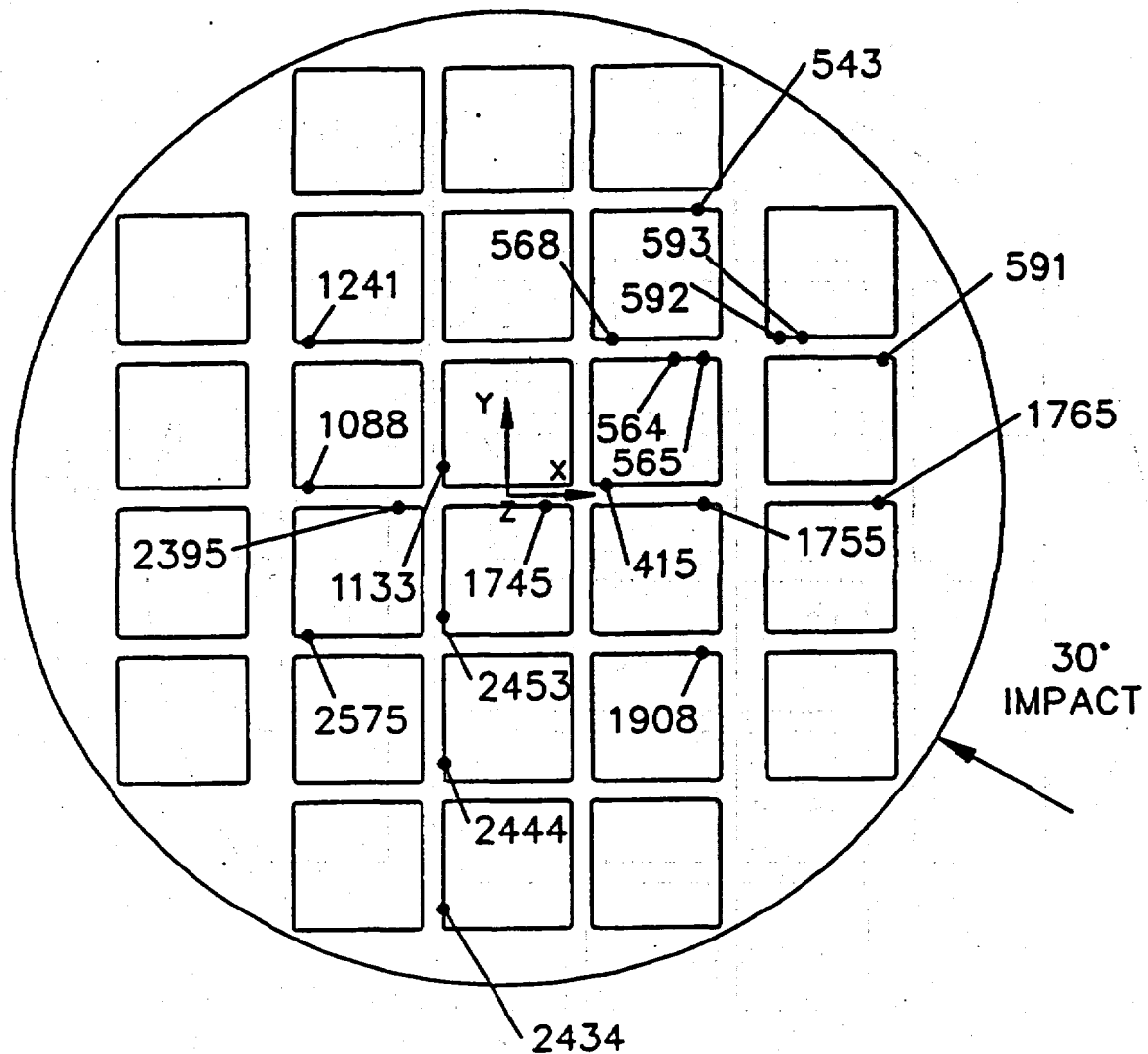


Figure 2.6.12.7-5 Location of Maximum Nodal SI Stresses (Directly Loaded Fuel Configuration - Support Disk) - 18.1-g Side Impact Condition (37° Drop Orientation)

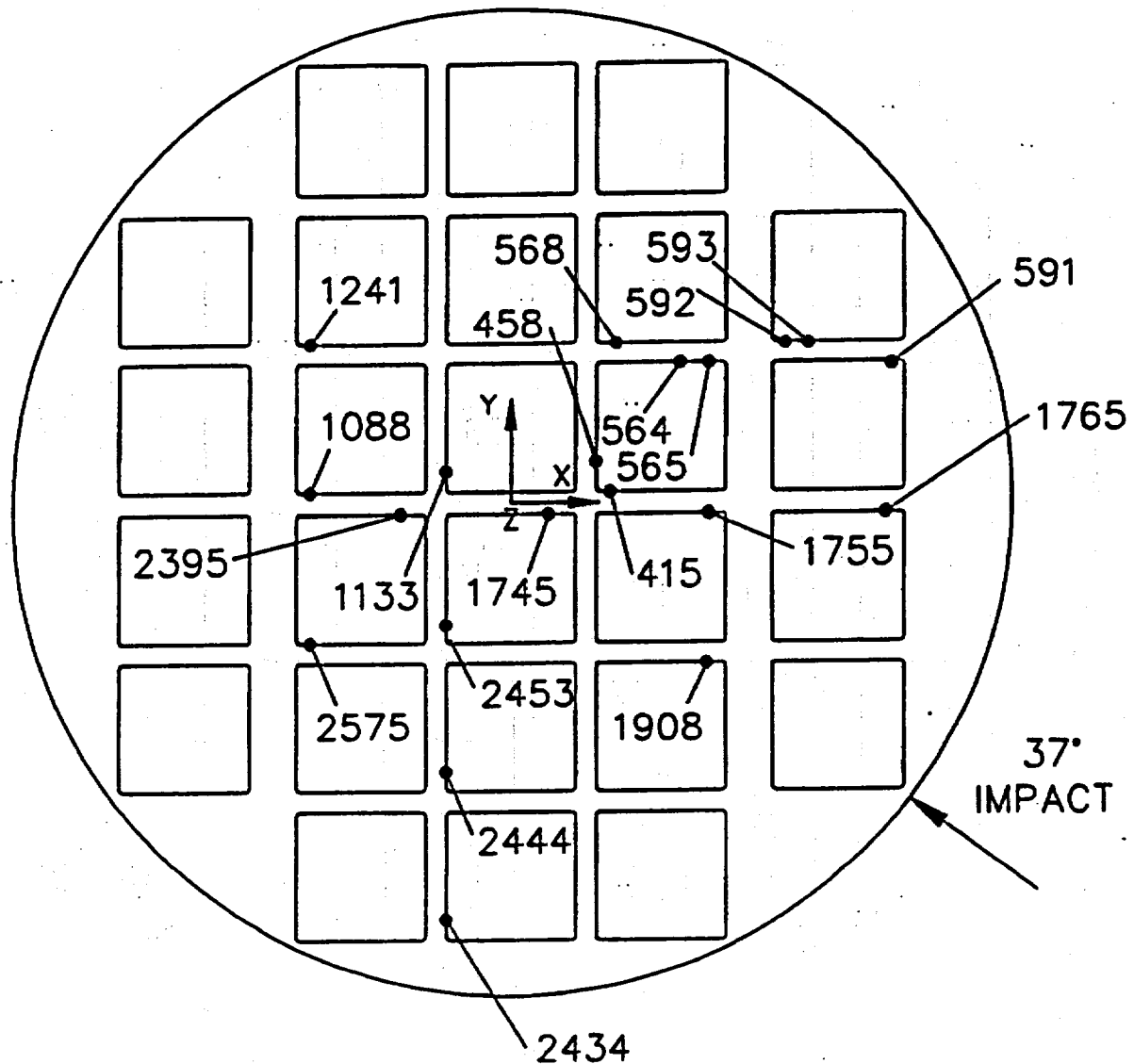


Figure 2.6.12.7-6 Location of Maximum Nodal SI Stresses (Directly Loaded Fuel Configuration - Support Disk) - 18.1-g Side Impact Condition (45° Drop Orientation)

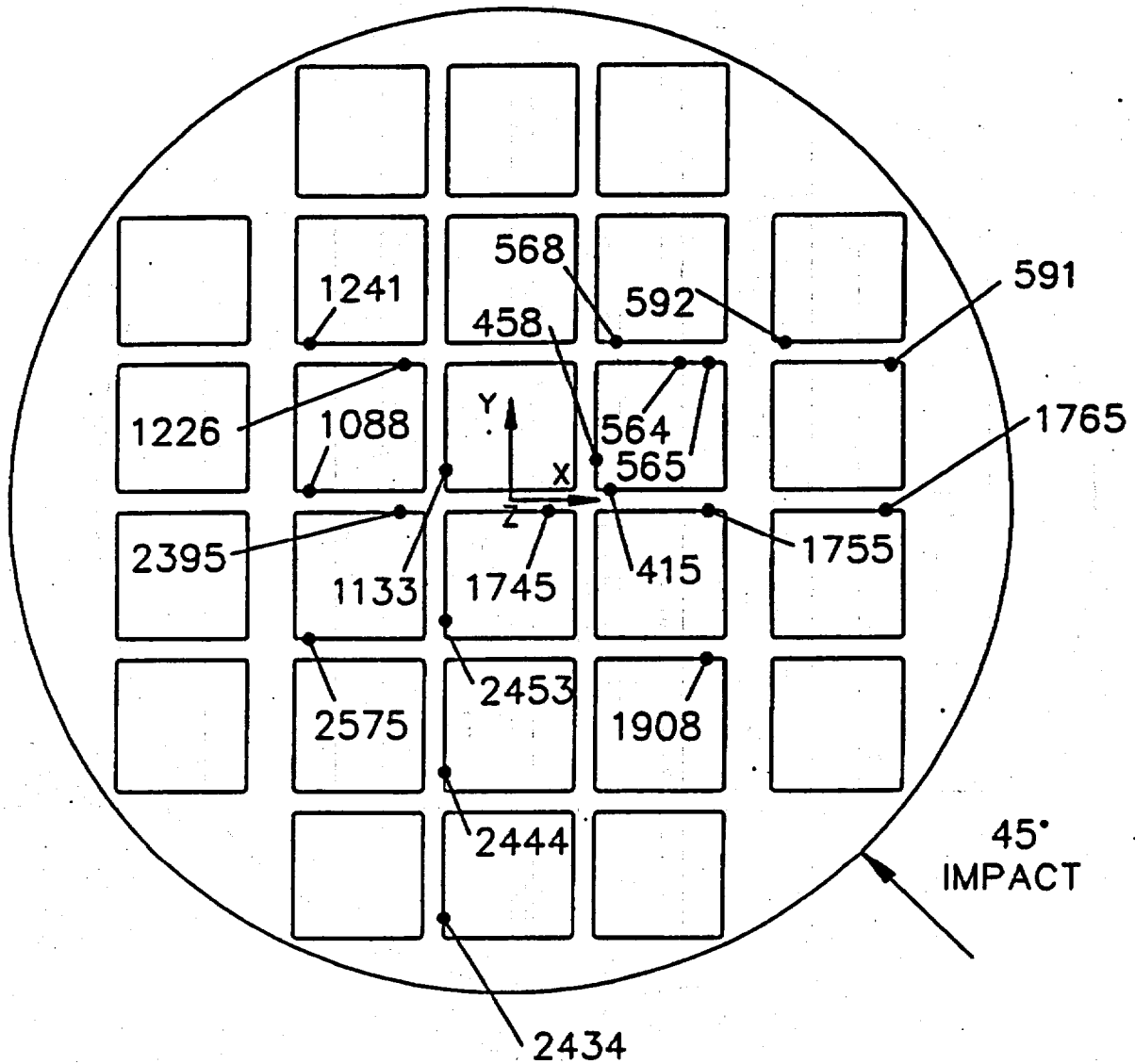


Figure 2.6.12.7-7 Location of Maximum Nodal SI Stresses (Directly Loaded Fuel Configuration - Support Disk) - 18.1-g Side Impact Condition (60° Drop Orientation)

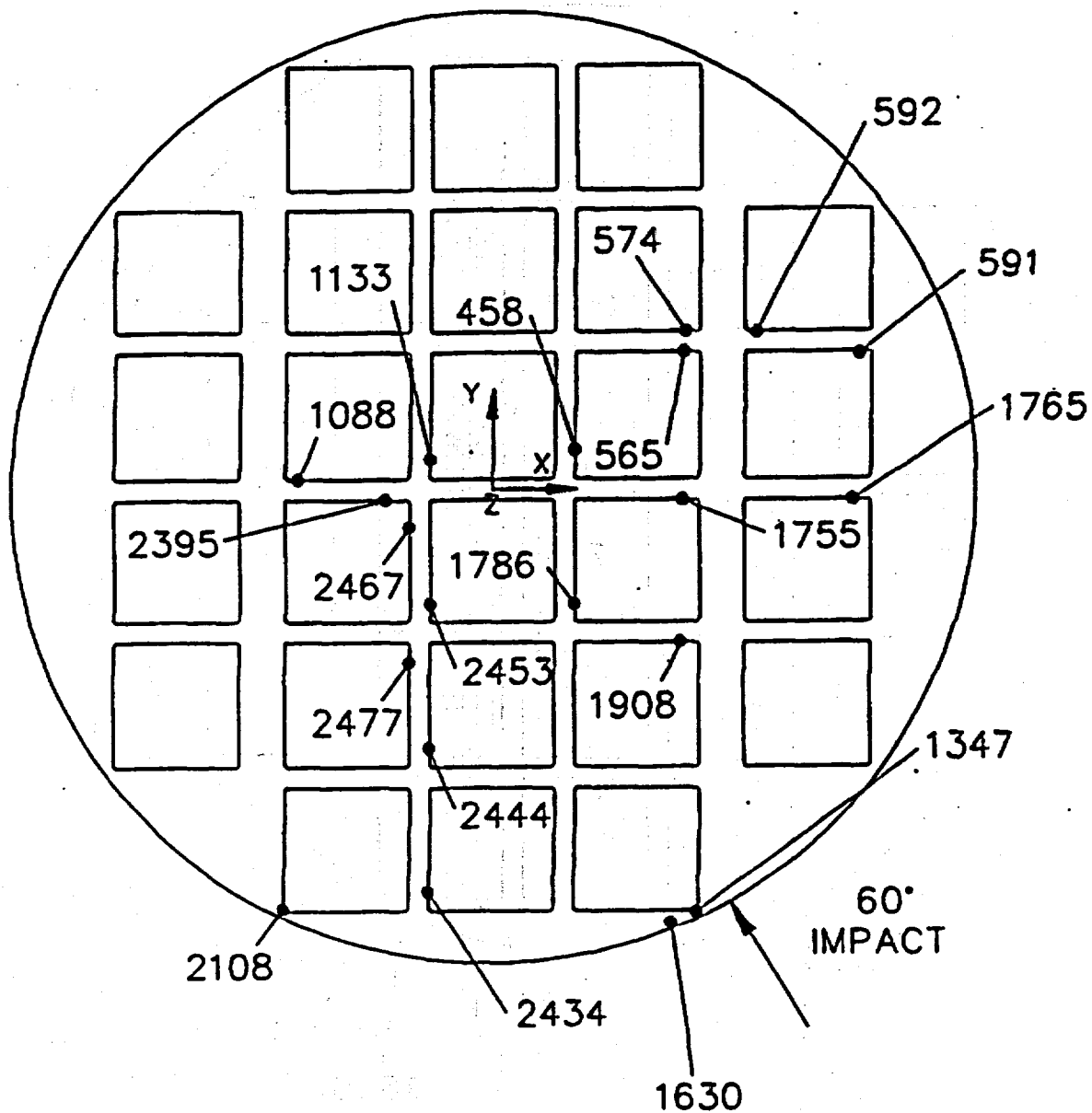


Figure 2.6.12.7-8 Location of Maximum Nodal SI Stresses (Directly Loaded Fuel Configuration - Support Disk) - 18.1g Side Impact Condition (64° Drop Orientation)

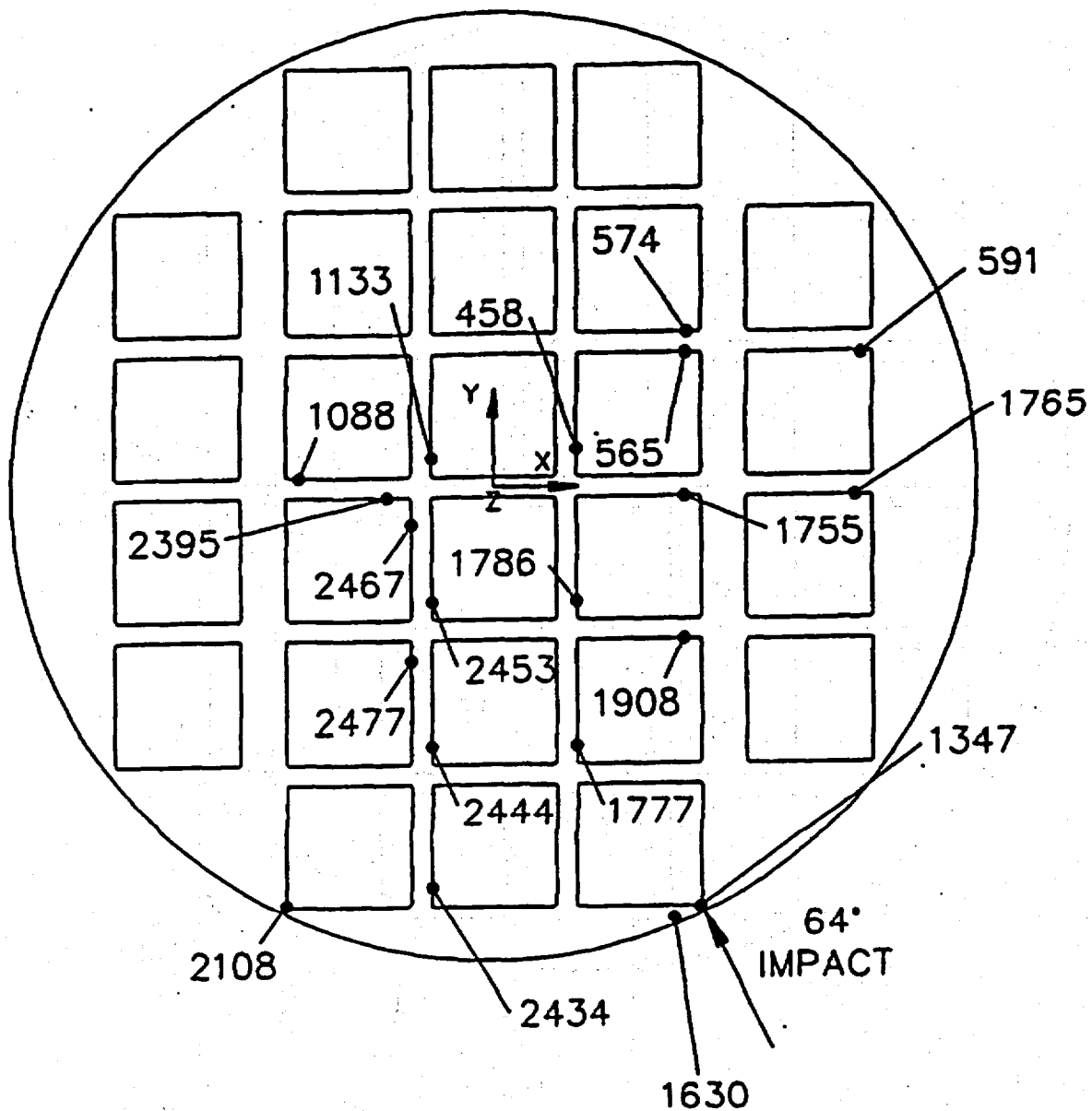


Figure 2.6.12.7-9 Location of Maximum Nodal SI Stresses (Directly Loaded Fuel Configuration - Support Disk) - 18.1-g Side Impact Condition (75° Drop Orientation)

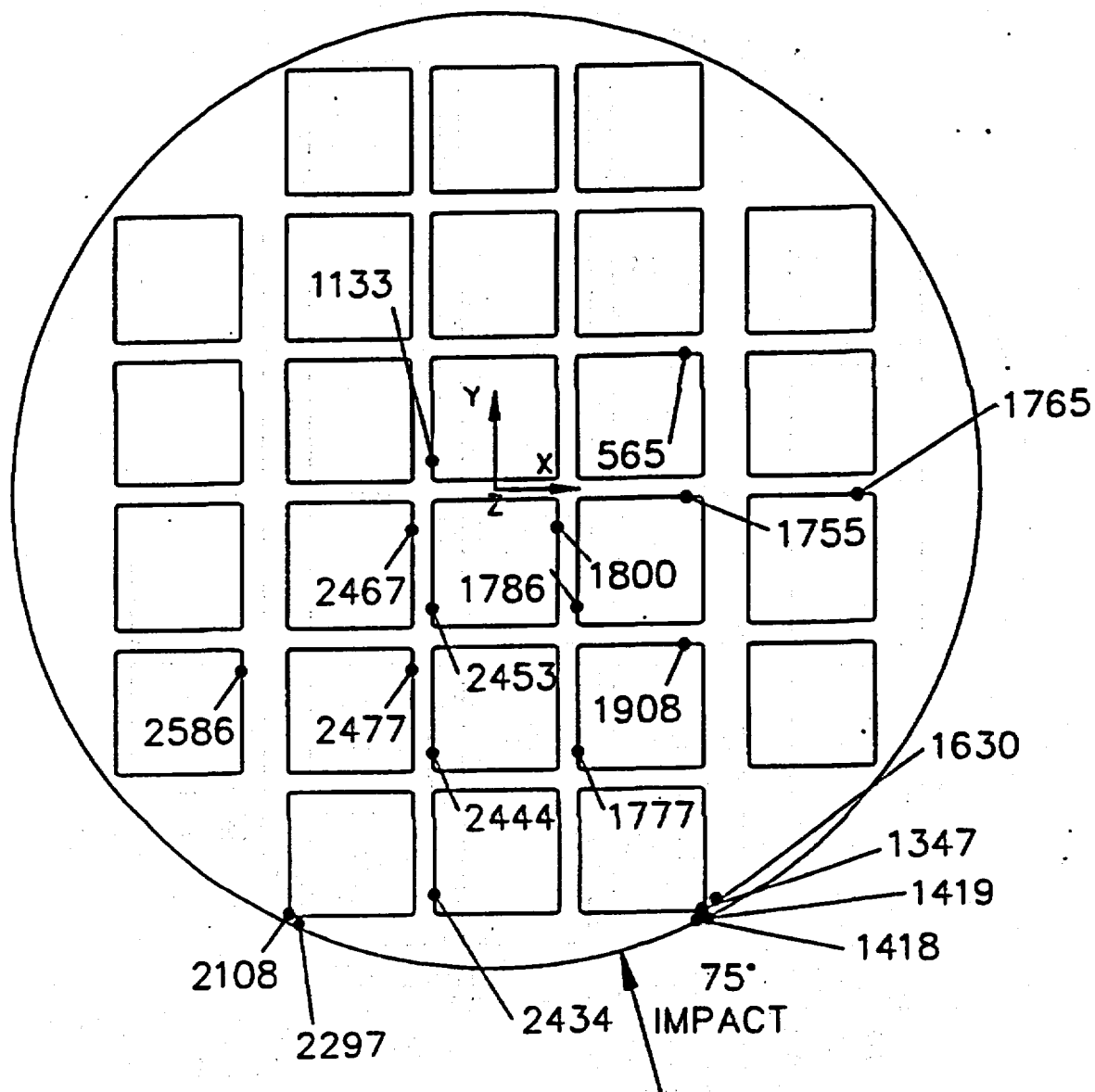


Figure 2.6.12.7-10 Location of Maximum Nodal SI Stresses (Directly Loaded Fuel Configuration - Support Disk) - 18.1-g Side Impact Condition (90° Drop Orientation)

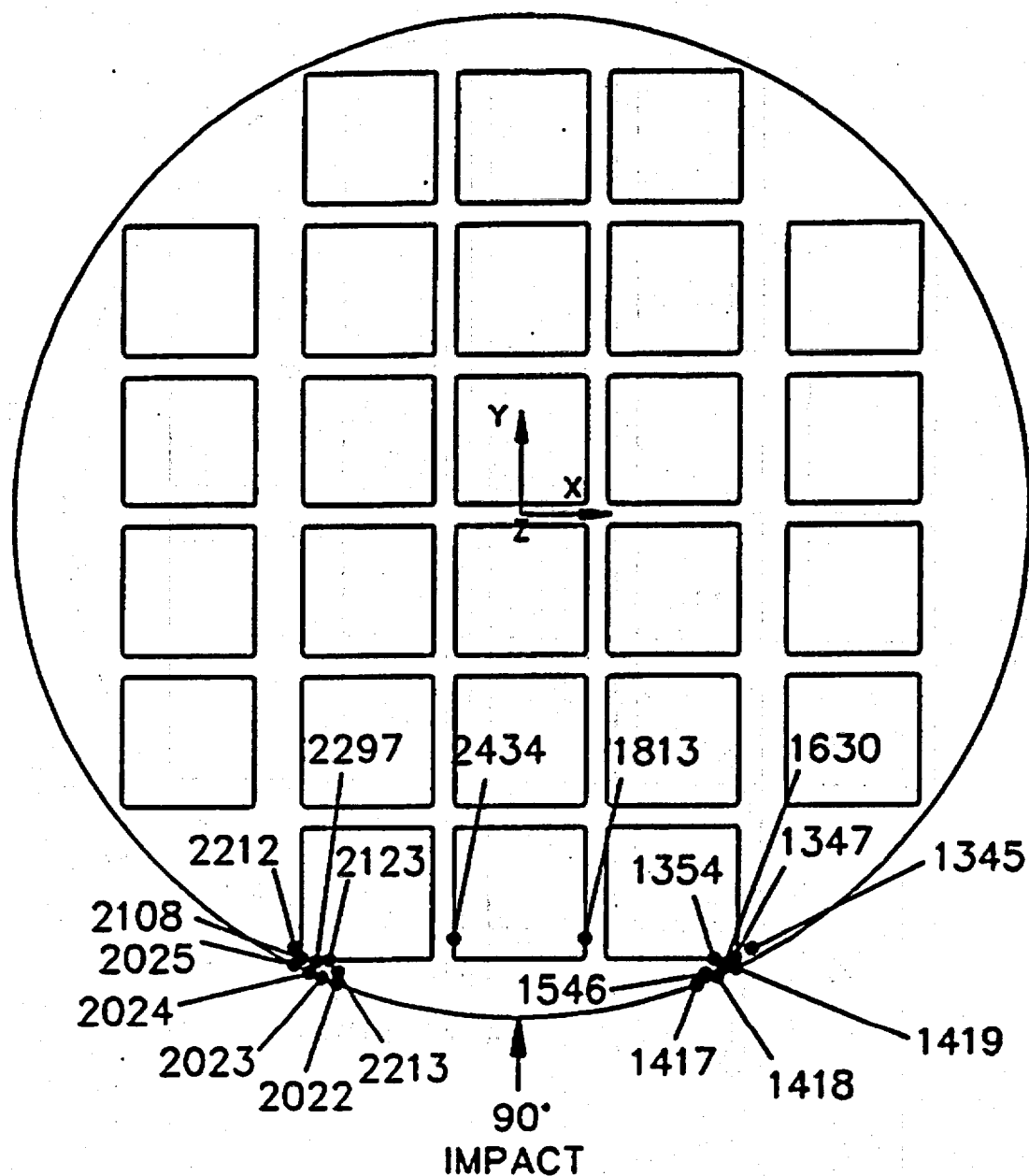


Table 2.6.12.7-1 18.1-g Side Impact Stresses for 0-Degree Drop Orientation (NAC-STC PWR Basket - Directly Loaded Fuel Configuration)

Node No. ¹	S _x (ksi)	S _y (ksi)	S _z (ksi)	S _{xy} (ksi)	SI (ksi)	MS ²
1368	-6.2	-6.0	0.0	-3.7	10.4	3.0
34	-6.2	-6.0	0.0	3.7	10.4	3.0
591	-9.6	0.3	0.0	0.3	10.0	3.2
1925	-9.6	0.3	0.0	-0.3	10.0	3.2
592	-9.7	0.2	0.0	0.4	10.0	3.2
1926	-9.7	0.2	0.0	-0.4	10.0	3.2
593	-8.4	0.0	0.0	0.0	8.4	4.0
1927	-8.4	0.0	0.0	0.0	8.4	4.0
590	-8.3	0.0	0.0	0.0	8.4	4.0
1924	-8.3	0.0	0.0	0.0	8.4	4.0
1527	-6.0	-4.2	0.0	-2.4	8.3	4.1
193	-6.0	-4.2	0.0	2.4	8.3	4.1
594	-8.0	0.0	0.0	0.2	8.0	4.3
1928	-8.0	0.0	0.0	-0.2	8.0	4.3
589	-7.9	0.0	0.0	0.2	8.0	4.3
1923	-7.9	0.0	0.0	-0.2	7.9	4.3
1526	-3.2	-5.3	0.0	-3.0	7.9	4.3
192	-3.2	-5.3	0.0	3.0	7.9	4.3
1375	-6.9	-1.6	0.0	-2.3	7.9	4.3
41	-6.9	-1.6	0.0	2.3	7.9	4.3

¹ Stress components are listed for the nodes with the 20 highest SI stresses (see Figure 2.6.12.7-2 for locations of these nodes). Note that S_x is the stress in the radial direction, S_y is the stress in the circumferential direction and S_{xy} is the shearing stress.

² The allowable stress is conservatively defined as S_m. S_m for 17-4 PH stainless steel at the conservative temperature of 650°F is 41.9 ksi.

Table 2.6.12.7-2 18.1-g Side Impact Stresses for 15-Degree Drop Orientation (NAC-STC PWR Basket - Directly Loaded Fuel Configuration)

Node No. ¹	S _x (ksi)	S _y (ksi)	S _z (ksi)	S _{xy} (ksi)	SI (ksi)	MS ²
565	-15.9	0.3	0.0	0.8	16.3	1.6
1755	-14.5	0.2	0.0	0.8	14.8	1.8
591	-14.0	0.5	0.0	0.8	14.6	1.9
592	-13.2	0.4	0.0	0.5	13.6	2.1
568	-11.9	0.8	0.0	0.7	12.8	2.3
1908	-12.4	0.2	0.0	0.7	12.7	2.3
1088	-11.9	0.5	0.0	0.5	12.4	2.4
415	-11.5	0.8	0.0	0.6	12.3	2.4
1241	-11.8	0.5	0.0	0.6	12.3	2.4
564	-12.1	0.1	0.0	0.7	12.3	2.4
1765	-11.5	0.4	0.0	0.6	12.0	2.5
2575	-10.7	0.5	0.0	0.5	11.3	2.7
1754	-11.1	0.0	0.0	0.6	11.2	2.7
543	-10.4	0.6	0.0	0.7	11.1	2.8
593	-11.0	0.0	0.0	0.3	11.1	2.8
1745	-10.7	0.3	0.0	0.6	11.1	2.8
590	-10.9	0.0	0.0	0.4	11.0	2.8
425	-10.6	0.2	0.0	0.4	10.9	2.9
1078	-9.8	0.8	0.0	0.5	10.7	2.9
530	-10.3	0.3	0.0	0.6	10.7	2.9

¹ Stress components are listed for the nodes with the 20 highest SI stresses (see Figure 2.6.12.7-3 for locations of these nodes). Note that S_x is the stress in the radial direction, S_y is the stress in the circumferential direction and S_{xy} is the shearing stress.

² The allowable stress is conservatively defined as S_m. S_m for 17-4 PH stainless steel at the conservative temperature of 650°F is 41.9 ksi.

Table 2.6.12.7-3 18.1-g Side Impact Stresses for 30-Degree Drop Orientation (NAC-STC PWR Basket - Directly Loaded Fuel Configuration)

Node No. ¹	S _x (ksi)	S _y (ksi)	S _z (ksi)	S _{xy} (ksi)	SI (ksi)	MS ²
565	-16.1	0.4	0.0	1.0	16.7	1.5
1755	-14.7	0.3	0.0	0.9	15.1	1.8
591	-14.5	0.5	0.0	0.9	15.1	1.8
592	-13.0	0.3	0.0	0.4	13.4	2.1
1908	-12.5	0.3	0.0	0.8	12.9	2.3
1765	-11.9	0.4	0.0	0.7	12.3	2.4
568	-11.4	0.8	0.0	0.6	12.3	2.4
1088	-11.7	0.5	0.0	0.5	12.2	2.4
1241	-11.5	0.5	0.0	0.5	12.0	2.5
564	-11.8	0.2	0.0	0.8	11.9	2.5
415	-11.0	0.8	0.0	0.5	11.9	2.5
1745	-10.7	0.5	0.0	0.7	11.3	2.7
2395	-10.4	0.7	0.0	0.9	10.2	2.7
1133	0.9	-10.2	0.0	0.9	11.2	2.7
2575	-10.6	0.5	0.0	0.4	11.2	2.8
593	-11.1	0.0	0.0	0.3	11.1	2.8
2453	0.4	-10.6	0.0	0.9	11.1	2.8
2444	0.2	-10.7	0.0	0.8	11.0	2.8
2434	0.5	-10.4	0.0	0.8	10.7	2.9
530	-10.3	0.3	0.0	0.6	11.0	2.8
543	-10.1	0.7	0.0	0.8	11.0	2.8

¹ Stress components are listed for the nodes with the 20 highest SI stresses (see Figure 2.6.12.7-4 for locations of these nodes). Note that S_x is the stress in the radial direction, S_y is the stress in the circumferential direction and S_{xy} is the shearing stress.

² The allowable stress is conservatively defined as S_m. S_m for 17-4 PH stainless steel at the conservative temperature of 650°F is 41.9 ksi.

Table 2.6.12.7-4 18.1-g Side Impact Stresses for 37-Degree Drop Orientation (NAC-STC PWR Basket - Directly Loaded Fuel Configuration)

Node No. ¹	S _x (ksi)	S _y (ksi)	S _z (ksi)	S _{xy} (ksi)	SI (ksi)	MS ²
565	-16.0	0.4	0.0	1.0	16.6	1.5
591	-14.5	0.5	0.0	1.0	15.2	1.8
1755	-14.7	0.4	0.0	1.0	15.2	1.8
592	-12.8	0.3	0.0	0.4	13.1	2.2
1908	-13.3	0.4	0.0	0.9	12.8	2.3
1765	-11.9	0.4	0.0	0.8	12.4	2.4
1088	-11.6	0.5	0.0	0.4	12.1	2.5
568	-11.1	0.8	0.0	0.5	11.9	2.5
1241	-11.3	0.5	0.0	0.4	11.8	2.7
2444	-0.2	-11.4	0.0	0.8	11.7	2.6
564	-11.5	0.2	0.0	0.9	11.6	2.6
2453	0.3	-11.1	0.0	0.9	11.6	2.6
415	-10.7	0.8	0.0	0.4	11.5	2.6
2395	-10.5	0.8	0.0	0.9	11.5	2.7
1133	0.8	-10.5	0.0	0.9	11.5	2.7
2434	0.5	-10.7	0.0	0.8	11.3	2.7
1745	-10.6	0.6	0.0	0.8	11.3	2.7
2575	-10.5	0.6	0.0	0.4	11.1	2.8
458	1.0	-9.8	0.0	1.0	11.0	2.8
593	-11.0	0.0	0.0	0.3	11.0	2.8

¹ Stress components are listed for the nodes with the 20 highest SI stresses (see Figure 2.6.12.7-5 for locations of these nodes). Note that S_x is the stress in the radial direction, S_y is the stress in the circumferential direction and S_{xy} is the shearing stress.

² The allowable stress is conservatively defined as S_m. S_m for 17-4 PH stainless steel at the conservative temperature of 650°F is 41.9 ksi.

Table 2.6.12.7-5 18.1-g Side Impact Stresses for 45-Degree Drop Orientation (NAC-STC PWR Basket - Directly Loaded Fuel Configuration)

Node No. ¹	S _x (ksi)	S _y (ksi)	S _z (ksi)	S _{xy} (ksi)	SI (ksi)	MS ²
565	-15.7	0.5	0.0	1.1	16.3	1.6
591	-14.5	0.5	0.0	1.0	15.1	1.8
1755	-14.4	0.4	0.0	1.0	15.0	1.8
1908	-12.1	0.5	0.0	0.9	12.7	2.3
592	-12.3	0.3	0.0	0.4	12.7	2.3
1765	-11.8	0.4	0.0	0.8	12.4	2.4
2444	0.1	-12.0	0.0	0.8	12.2	2.4
2453	0.3	-11.6	0.0	0.8	12.0	2.5
1088	-11.3	0.5	0.0	0.4	11.9	2.5
1133	0.7	-10.7	0.0	0.9	11.3	2.6
2395	-10.6	0.8	0.0	1.0	11.6	2.6
2434	0.6	-10.9	0.0	0.7	11.6	2.6
1241	-10.9	0.4	0.0	0.4	11.4	2.7
458	1.0	-10.1	0.0	0.9	11.2	2.7
568	-10.5	0.7	0.0	0.5	10.2	2.7
564	-11.0	-0.2	0.0	0.9	11.1	2.8
1745	-10.4	0.6	0.0	0.8	11.1	2.8
415	-10.2	0.8	0.0	0.4	11.0	2.8
1226	-9.9	0.8	0.0	1.0	10.9	2.9
593	-11.0	0.0	0.0	0.3	11.0	2.8
2575	-10.3	0.6	0.0	0.3	10.9	2.9

¹ Stress components are listed for the nodes with the 20 highest SI stresses (see Figure 2.6.12.7-6 for locations of these nodes). Note that S_x is the stress in the radial direction, S_y is the stress in the circumferential direction and S_{xy} is the shearing stress.

² The allowable stress is conservatively defined as S_m. S_m for 17-4 PH stainless steel at the conservative temperature of 650°F is 41.9 ksi.

Table 2.6.12.7-6 18.1-g Side Impact Stresses for 60-Degree Drop Orientation (NAC-STC PWR Basket - Directly Loaded Fuel Configuration)

Node No. ¹	S _x (ksi)	S _y (ksi)	S _z (ksi)	S _{xy} (ksi)	SI (ksi)	MS ²
565	-14.0	0.6	0.0	1.1	14.9	1.8
1755	-13.5	0.5	0.0	1.1	14.2	1.9
591	-13.3	0.5	0.0	1.1	14.0	2.0
2444	0.0	-12.7	0.0	0.7	12.8	2.3
2453	0.2	-12.1	0.0	0.8	12.3	2.4
2108	-7.1	-6.6	0.0	4.0	12.2	2.5
1908	-11.3	0.6	0.0	1.8	12.0	2.5
1765	-11.5	0.4	0.0	0.9	12.0	2.5
2434	0.6	-11.0	0.0	0.6	11.7	2.6
1133	0.6	-10.8	0.0	0.7	11.4	2.7
1347	-8.9	-3.6	0.0	-3.9	11.4	2.7
2395	-10.1	1.0	0.0	1.1	11.3	2.7
458	0.8	-10.3	0.0	0.8	11.2	2.7
2467	0.9	-10.3	0.0	0.4	11.2	2.7
1630	-9.3	-2.5	0.0	-3.5	11.0	2.8
2477	0.6	-10.5	0.0	0.3	11.0	2.8
1088	-10.4	0.5	0.0	0.3	10.9	2.8
1786	0.3	-10.5	0.0	0.7	10.9	2.8
574	9.7	-0.9	0.0	1.0	10.8	2.9
592	-10.5	0.2	0.0	0.3	10.8	2.9

¹ Stress components are listed for the nodes with the 20 highest SI stresses (see Figure 2.6.12.7-7 for locations of these nodes). Note that S_x is the stress in the radial direction, S_y is the stress in the circumferential direction and S_{xy} is the shearing stress.

² The allowable stress is conservatively defined as S_m. S_m for 17-4 PH stainless steel at the conservative temperature of 650°F is 41.9 ksi.

Table 2.6.12.7-7 18.1-g Side Impact Stresses for 64-Degree Drop Orientation (NAC-STC PWR Basket - Directly Loaded Fuel Configuration)

Node No. ¹	S _x (ksi)	S _y (ksi)	S _z (ksi)	S _{xy} (ksi)	SI (ksi)	MS ²
565	-13.3	0.7	0.0	1.1	14.1	2.0
1755	-13.1	0.6	0.0	1.1	13.9	2.0
591	-12.5	0.5	0.0	1.1	13.2	2.2
2444	0.0	-12.7	0.0	0.7	12.8	2.3
2108	-7.4	-6.7	0.0	4.1	12.5	2.4
2453	0.1	-12.1	0.0	0.7	12.3	2.4
1765	-11.3	0.4	0.0	1.0	11.8	2.5
1908	-11.0	0.6	0.0	1.0	11.8	2.6
1347	-9.1	-3.8	0.0	-4.0	11.7	2.6
2434	0.6	-10.9	0.0	0.6	11.6	2.6
2467	0.9	-10.4	0.0	0.5	11.4	2.7
1630	-9.5	-2.6	0.0	-3.6	11.3	2.7
1133	0.5	-10.6	0.0	0.7	11.3	2.7
2477	0.6	-10.7	0.0	0.3	11.3	2.7
2395	-9.9	1.0	0.0	1.1	11.1	2.8
458	0.7	-10.2	0.0	0.8	11.1	2.8
1786	0.3	10.6	0.0	0.7	10.9	2.8
574	9.8	-0.8	0.0	1.1	10.8	2.9
1777	0.0	-10.4	0.0	0.6	10.6	3.0
1088	-10.1	0.5	0.0	0.2	10.5	3.0

¹ Stress components are listed for the nodes with the 20 highest SI stresses (see Figure 2.6.12.7-8 for locations of these nodes). Note that S_x is the stress in the radial direction, S_y is the stress in the circumferential direction and S_{xy} is the shearing stress.

² The allowable stress is conservatively defined as S_m. S_m for 17-4 PH stainless steel at the conservative temperature of 650°F is 41.9 ksi.

Table 2.6.12.7-8 18.1-g Side Impact Stresses for 75-Degree Drop Orientation (NAC-STC PWR Basket - Directly Loaded Fuel Configuration)

Node No. ¹	S _x (ksi)	S _y (ksi)	S _z (ksi)	S _{xy} (ksi)	SI (ksi)	MS ²
2108	-8.4	-6.9	0.0	4.4	13.3	2.1
2444	0.0	-12.7	0.0	0.6	12.7	2.3
1347	-9.6	-4.2	0.0	-4.3	12.4	2.4
1755	-11.1	0.7	0.0	1.0	12.0	2.5
1630	-10.0	-2.8	0.0	-3.8	11.9	2.5
2453	0.0	-11.8	0.0	0.6	11.9	2.5
2477	0.5	-11.1	0.0	0.4	11.7	2.6
2467	0.8	-10.7	0.0	0.5	11.6	2.6
565	-10.4	0.8	0.0	1.0	11.4	2.7
2434	0.6	-10.6	0.0	0.5	11.3	2.7
2297	-8.3	-3.6	0.0	4.0	11.2	2.7
1908	-9.9	0.7	0.0	1.0	10.8	2.9
1786	0.2	-10.5	0.0	0.6	10.7	2.9
1777	0.0	-10.5	0.0	0.5	10.6	3.0
1800	0.7	-9.7	0.0	0.4	10.4	3.0
1419	-8.3	-3.7	0.0	-3.5	10.4	3.0
2586	-9.4	0.8	0.0	1.0	10.3	3.1
1765	-9.5	0.5	0.0	1.0	10.2	3.1
1418	-8.5	-2.7	0.0	-3.6	10.2	3.1
1133	0.3	-9.7	0.0	0.6	10.2	3.1

¹ Stress components are listed for the nodes with the 20 highest SI stresses (see Figure 2.6.12.7-9 for locations of these nodes). Note that S_x is the stress in the radial direction, S_y is the stress in the circumferential direction and S_{xy} is the shearing stress.

² The allowable stress is conservatively defined as S_m. S_m for 17-4 PH stainless steel at the conservative temperature of 650°F is 41.9 ksi.

Table 2.6.12.7-9 18.1-g Side Impact Stresses for 90-Degree Drop Orientation (NAC-STC PWR Basket - Directly Loaded Fuel Configuration)

Node No. ¹	S _x (ksi)	S _y (ksi)	S _z (ksi)	S _{xy} (ksi)	SI (ksi)	MS ²
2108	-10.7	5.9	0.0	5.0	14.7	1.9
1347	-10.7	-5.9	0.0	-5.0	14.7	1.9
2297	-11.1	-3.6	0.0	4.5	13.7	2.1
1630	-11.1	-3.6	0.0	-4.5	13.7	2.1
2024	-9.7	-3.3	0.0	4.2	11.8	2.5
1418	-9.7	-3.3	0.0	-4.2	11.8	2.5
2025	-9.1	-4.9	0.0	3.9	11.6	2.6
1419	-9.1	-4.9	0.0	-3.9	11.6	2.6
2123	-10.2	-1.2	0.0	2.6	11.2	2.8
1354	-10.2	-1.2	0.0	-2.6	11.2	2.8
2023	-9.3	-1.8	0.0	3.2	10.5	3.0
1417	-9.3	-1.8	0.0	-3.2	11.5	3.0
2212	-6.9	-5.7	0.0	3.4	10.3	3.1
1545	-6.9	-5.7	0.0	3.4	10.3	3.1
2213	-8.5	-1.7	0.0	2.7	9.7	3.3
1546	-8.5	-1.7	0.0	-2.7	9.7	3.3
2022	-8.2	-1.2	0.0	2.3	9.0	3.7
1416	-8.2	-1.2	0.0	-2.3	9.0	3.7
1813	0.5	-8.3	0.0	-0.3	8.9	3.7
1088	-10.1	0.5	0.0	0.2	10.5	3.0
2434	0.5	-8.3	0.0	0.3	8.9	3.7

¹ Stress components are listed for the nodes with the 20 highest SI stresses (see Figure 2.6.12.7-10 for locations of these nodes). Note that S_x is the stress in the radial direction, S_y is the stress in the circumferential direction and S_{xy} is the shearing stress.

² The allowable stress is conservatively defined as S_m. S_m for 17-4 PH stainless steel at the conservative temperature of 650°F is 41.9 ksi.

Table 2.6.12.7-10 18.1-g Side Impact Analysis Results (NAC-STC PWR Basket - Directly Loaded Fuel Configuration)

Drop Orientation (deg)	Maximum Nodal SI Stress (ksi)	Operating Temperature (°F)	Allow. Stress (ksi)	Margin of Safety
0	10.4	650	41.9	+3.03
15	16.3	650	41.9	+1.57
30	16.65	650	41.9	+1.52
37	16.61	650	41.9	+1.52
45	16.33	650	41.9	+1.57
60	14.86	650	41.9	+1.82
64	14.14	650	41.9	+1.96
75	13.33	650	41.9	+2.14
90	11.67	650	41.9	+1.86

2.6.12.8 Stress Evaluation of Support Disk (Directly Loaded Fuel Configuration) for Thermal Plus a 1-Foot Side Drop Combined Load Condition

The highest nodal stresses in the support disk from the thermal expansion analysis (Table 2.6.12.3-1) and the 1-foot side drop at the 30 degree drop orientation (Table 2.6.12.7-3) (since the minimum safety margin occurs at this drop orientation) are conservatively used as a basis to determine the maximum primary plus secondary stress for normal operations. The maximum stress intensity, SI, for thermal expansion and 1-foot side drop for the 30 degree drop orientation are respectively 32.2 ksi and 16.65 ksi. Using the conservative absolute summation method, the maximum bounding combined stress is 48.85 ksi.

The combined thermal plus impact stress of 48.85 ksi is very conservative since the dominant principal stresses for thermal expansion and the side impact analyses are respectively tensile and compressive in nature. Therefore, the stresses from the combination of thermal expansion and impact loads will tend to negate one another with the maximum combined stress located opposite to the region of impact and exactly at the same point of maximum thermal expansion stress. The magnitude of the maximum combined stress must therefore be equal to or slightly less than the maximum thermal expansion stress because the contribution of stress from inertial loads in this region is negligible.

Evaluation of peak stress and the fatigue mode of failure for normal operation events is conservatively performed by using the highest primary plus secondary stress calculated for the steel support disk in combination with a stress concentration factor of 3.0 to establish a stress range. Since the side drop analysis produced a conservative primary plus secondary stress of 48.9 ksi, which is higher than 39.4 ksi, that produced from the end drop (Section 2.6.12.5), the maximum peak stress intensity range is conservatively defined as twice the defined primary plus secondary stress times the stress concentration factor of 3.0. The maximum alternating stress intensity then becomes

$$S_{alt} = \frac{3(2)(48.9)}{2} = 146.7 \text{ ksi}$$

The allowable number of cycles for an alternating stress intensity range of 146.7 ksi at the conservative temperature of 500°F is approximately 1000 cycles. This number of allowable cycles considerably exceeds the number of normal operating cycles that the NAC-STC will meet during its lifetime.

2.6.12.9 Support Disk Web Stresses for a 1-Foot Side Drop Condition (Directly Loaded Fuel Configuration)

The support disk is analyzed for nine drop orientations in Section 2.6.12.7. The 20 maximum stress intensities for each drop orientation are listed in Tables 2.6.12.7-1 through 2.6.12.7-9. In this section, a supplementary stress summary of the support disk webs are presented for the same drop orientations.

The locations of the nodes in the ANSYS model of the support disk webs for each of the nine 1-foot side impact orientations evaluated are shown in Figure 2.6.12.9-1. Tables 2.6.12.9-1 through 2.6.12.9-9 summarize the nodal stress intensities at the defined locations on the web for each of the nine impact orientation. The tables also show the margin of safety for each node location for the 18.1 g side impact load condition using the conservative design stress intensity, S_m , at a maximum enveloping temperature of 650°F.

The conservative minimum margin of safety relative to the design strength, S_m at 650°F, for the support disk web of the NAC-STC PWR basket (directly loaded fuel configuration) for a 1-foot side drop is +4.52 for the 90 degree drop orientation.

Figure 2.6.12.9-1 Node Point Locations for Basket Web Stress Summaries (Directly Loaded Fuel Configuration)

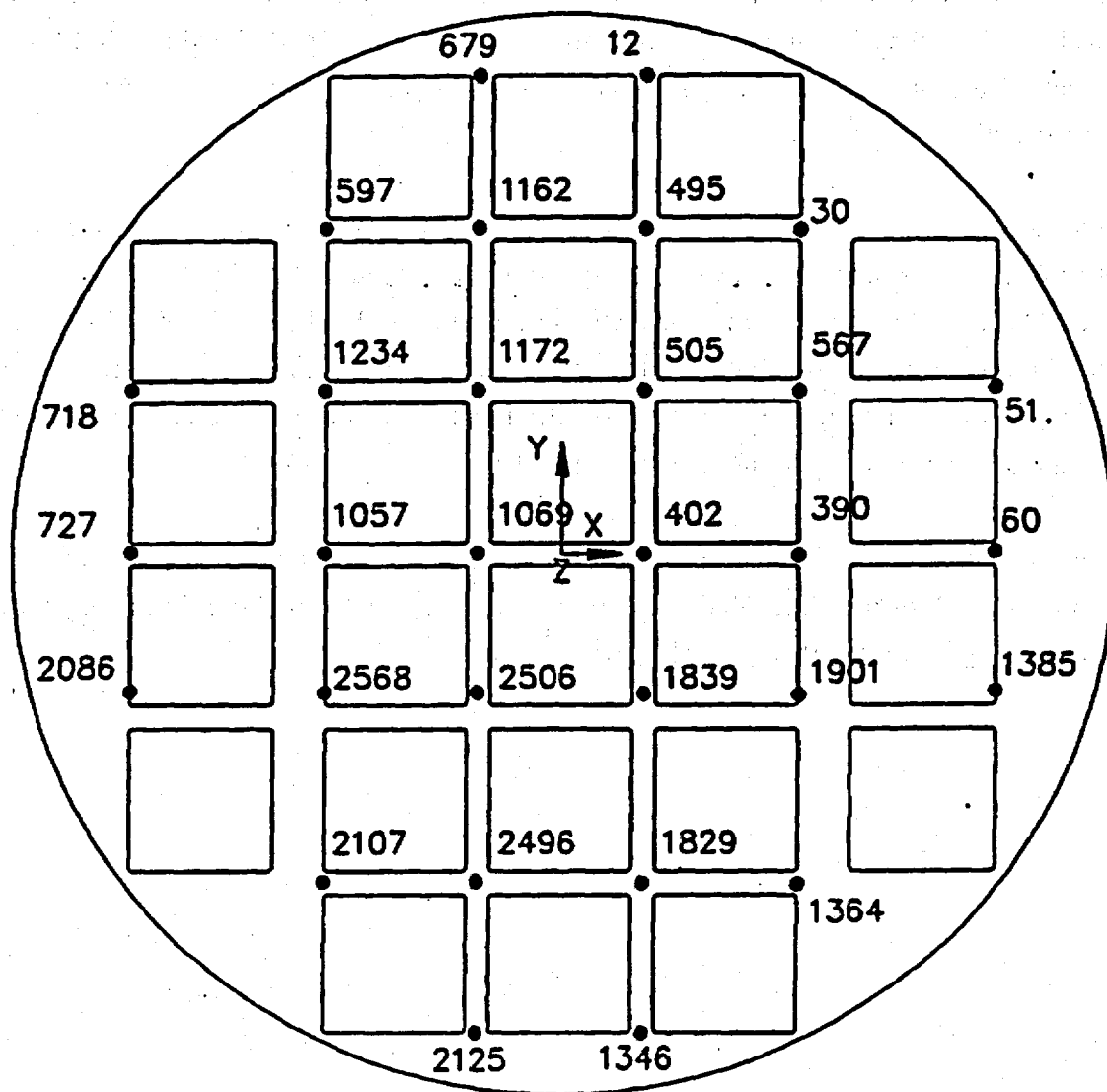


Table 2.6.12.9-1 18.1-g Side Impact Web Stresses for 0-Degree Drop Orientation (NAC-STC PWR Basket - Directly Loaded Fuel Configuration)

Node No. ¹	S _x (ksi)	S _y (ksi)	S _z (ksi)	S _{xy} (ksi)	SI (ksi)	MS ²
402	-4.7	1.3	0.0	0.0	6.0	6.0
390	-4.7	0.8	0.0	0.0	5.6	6.5
1901	-4.5	1.0	0.0	0.0	5.6	6.5
567	-4.5	1.0	0.0	0.0	5.6	6.5
60	-5.3	-1.5	0.0	0.0	5.4	6.7
1839	-4.1	1.2	0.0	0.4	5.4	6.8
505	-4.1	1.2	0.0	-0.4	5.4	6.8
51	-4.9	-1.9	0.0	0.0	5.1	7.2
1385	-4.9	-1.9	0.0	0.0	5.2	7.2
1829	-2.7	-0.9	0.0	0.4	3.7	10.2
495	-2.7	0.9	0.0	-0.5	3.7	10.2
1069	-3.3	0.4	0.0	-0.4	3.7	10.4
2506	-2.7	0.2	0.0	0.3	3.0	12.9
1172	-2.7	0.2	0.0	-0.3	3.0	12.9
1364	-2.4	-0.1	0.0	0.3	2.8	14.2
30	-2.4	-0.1	0.0	-0.3	2.8	14.2
1057	-2.0	-1.2	0.0	0.0	2.1	19.1
2568	-1.6	-1.2	0.0	0.0	1.7	23.0
1234	-1.6	-1.2	0.0	0.0	1.7	23.1
2496	-1.4	0.0	0.0	0.3	1.5	26.3
1162	-1.4	0.0	0.0	-0.3	1.5	26.3
727	-0.9	-0.6	0.0	0.0	1.0	41.8
697	-0.6	0.2	0.0	-0.1	0.8	53.5
2107	-0.6	0.2	0.0	0.1	0.8	53.5
1346	0.0	0.3	0.0	0.2	0.7	58.4
12	0.0	0.3	0.0	-0.2	0.7	58.4
2125	-0.1	-0.1	0.0	0.1	0.7	62.5
679	-0.1	0.1	0.0	-0.1	0.7	62.5
718	-0.3	-0.4	0.0	0.0	0.5	88.6
2086	-0.3	-0.4	0.0	0.0	0.5	88.6

¹ Stress components are listed for the nodes noted on Figure 2.6.12.9-1. Note that S_x is the stress in the radial direction, S_y is the stress in the circumferential direction and S_{xy} is the shearing stress.

² The allowable stress is conservatively defined as S_m. S_m for 17-4 PH stainless steel at the conservative temperature of 650°F is 41.9 ksi.

Table 2.6.12.9-2 18.1-g Side Impact Web Stresses for 15-Degree Drop Orientation (NAC-STC PWR Basket - Directly Loaded Fuel Configuration)

Node No. ¹	S _x (ksi)	S _y (ksi)	S _z (ksi)	S _{xy} (ksi)	SI (ksi)	MS ²
402	-4.3	0.2	0.0	-2.4	6.5	5.4
505	-3.6	0.3	0.0	-2.6	6.5	5.4
567	-4.2	0.8	0.0	0.3	5.7	6.3
1069	-2.9	-0.5	0.0	-2.5	5.5	6.6
390	-4.5	0.4	0.0	-0.3	5.5	6.6
1172	-2.3	-0.3	0.0	-2.6	5.5	6.6
1839	-3.8	-0.1	0.0	-1.9	5.3	6.9
60	-5.0	-1.4	0.0	-0.1	5.3	6.9
51	-4.9	-1.6	0.0	-0.2	52.2	7.0
1901	-4.1	0.1	0.0	-0.2	4.9	7.5
495	-1.7	0.2	0.0	-2.2	4.8	7.8
2506	-2.4	-1.2	0.0	-2.1	4.5	8.3
1385	-4.3	-1.6	0.0	-0.1	4.5	8.4
1162	-0.6	-0.1	0.0	-2.1	4.3	8.8
1364	-2.9	0.8	0.0	-0.1	3.9	9.8
2496	-1.5	-1.8	0.0	-1.8	3.8	9.9
1829	-3.0	-0.5	0.0	-1.3	3.8	10.0
30	-1.6	-1.7	0.0	-0.7	3.2	12.0
2125	-0.1	-1.7	0.0	-0.3	2.9	13.3
1057	-1.8	-1.1	0.0	-0.4	2.7	14.5
1234	-1.2	-0.8	0.0	0.4	2.6	15.4
2568	-1.6	-1.2	0.0	-0.4	2.4	16.2
697	-0.1	1.2	0.0	-0.6	2.3	17.5
2107	-0.8	-0.9	0.0	-0.5	2.1	19.1
1346	-0.3	-1.0	0.0	-0.1	1.9	20.9
12	-0.3	0.1	0.0	-0.4	1.1	37.1
727	-0.8	-0.5	0.0	-0.2	1.1	38.2
679	0.0	0.0	0.0	-0.4	1.0	39.8
718	0.0	0.0	0.0	-0.2	0.8	51.5
2086	-0.4	-0.6	0.0	-0.1	0.8	52.3

¹ Stress components are listed for the nodes noted on Figure 2.6.12.9-1. Note that S_x is the stress in the radial direction, S_y is the stress in the circumferential direction and S_{xy} is the shearing stress.

² The allowable stress is conservatively defined as S_m. S_m for 17-4 PH stainless steel at the conservative temperature of 650°F is 41.9 ksi.

Table 2.6.12.9-3 18.1-g Side Impact Web Stresses for 30-Degree Drop Orientation (NAC-STC PWR Basket - Directly Loaded Fuel Configuration)

Node No. ¹	S _x (ksi)	S _y (ksi)	S _z (ksi)	S _{xy} (ksi)	SI (ksi)	MS ²
505	-3.1	-0.2	0.0	-2.7	6.1	5.9
402	-3.7	-0.7	0.0	-2.5	5.8	6.2
1172	-2.0	-0.8	0.0	-2.6	5.4	6.8
1069	-2.5	-1.4	0.0	-2.6	5.3	6.9
567	-3.8	0.6	0.0	-0.2	5.3	6.9
390	-4.0	0.1	0.0	-0.2	5.1	7.3
51	-4.5	-1.3	0.0	-0.2	5.0	7.4
60	-4.6	-1.1	0.0	-0.1	4.9	7.6
2506	-1.8	-2.4	0.0	-2.2	4.8	7.8
1839	-3.1	-1.2	0.0	-2.0	4.6	8.0
495	-1.3	-0.1	0.0	-2.1	4.5	8.4
2496	-0.6	-3.3	0.0	-1.7	4.5	8.4
1901	-3.6	-0.2	0.0	-0.2	4.4	8.5
1162	-0.4	-0.3	0.0	-2.0	4.1	9.2
1385	-3.7	-1.4	0.0	-0.1	4.0	9.6
2125	-1.5	-2.8	0.0	-0.1	3.4	11.3
1829	-2.3	-1.9	0.0	-1.2	3.4	11.4
30	-1.2	-2.0	0.0	-0.7	3.4	11.4
1364	-2.5	0.3	0.0	-0.1	3.3	11.8
2107	-0.4	-2.3	0.0	-0.5	2.8	14.0
1057	-1.6	-1.3	0.0	-0.5	2.6	15.0
1346	-1.3	-2.0	0.0	-0.1	2.5	15.6
1234	-1.1	-0.9	0.0	-0.5	2.5	16.1
2568	-1.4	-1.5	0.0	-0.4	2.4	16.6
697	-0.1	1.4	0.0	-0.6	2.3	17.5
727	-0.7	-0.4	0.0	-0.3	1.2	33.9
12	-0.2	0.0	0.0	-0.4	1.0	40.4
2086	-0.4	-0.7	0.0	-0.3	1.0	41.2
718	0.0	0.1	0.0	-0.3	1.0	42.6
679	0.1	0.0	0.0	-0.4	1.0	43.5

¹ Stress components are listed for the nodes noted on Figure 2.6.12.9-1. Note that S_x is the stress in the radial direction, S_y is the stress in the circumferential direction and S_{xy} is the shearing stress.

² The allowable stress is conservatively defined as S_m. S_m is for 17-4 PH stainless steel at the conservative temperature of 650°F is 41.9 ksi.

Table 2.6.12.9-4 18.1-g Side Impact Web Stresses for 37-Degree Drop Orientation (NAC-STC PWR Basket - Directly Loaded Fuel Configuration)

Node No. ¹	S _x (ksi)	S _y (ksi)	S _z (ksi)	S _{xy} (ksi)	SI (ksi)	MS ²
505	-2.8	-0.5	0.0	-2.7	5.9	6.1
402	-3.4	-1.1	0.0	-2.5	5.5	6.6
1069	-2.2	-1.8	0.0	-2.6	5.3	6.9
1172	-1.7	-1.0	0.0	-2.6	5.3	6.9
567	-3.5	0.5	0.0	-0.2	5.1	7.3
2506	-1.5	-2.9	0.0	-2.3	5.0	7.4
2496	-0.6	-4.0	0.0	-1.7	5.0	7.5
391	-3.7	-0.0	0.0	-0.2	4.8	7.7
51	-4.2	-1.1	0.0	-0.2	4.8	7.7
60	-4.3	-0.9	0.0	0.1	4.7	8.0
1839	-2.7	-1.7	0.0	-2.0	4.5	8.3
495	-1.1	-0.2	0.0	-2.1	4.3	8.7
1901	-3.2	-0.3	0.0	-0.2	4.1	9.1
1162	-0.3	-0.4	0.0	-2.0	4.0	9.4
2125	-1.9	-3.3	0.0	-0.1	3.8	10.1
1385	-3.4	-1.2	0.0	-0.1	3.7	10.3
1829	-2.0	-2.5	0.0	-1.2	3.5	10.9
30	-1.0	-2.2	0.0	-0.7	3.5	11.1
2107	-0.3	-2.8	0.0	-0.5	3.3	11.9
1364	-2.3	0.2	0.0	-0.1	3.0	13.2
1346	-1.7	-2.5	0.0	-0.1	2.9	13.5
1057	-1.5	-1.4	0.0	-0.5	2.6	15.1
1234	-1.0	-0.9	0.0	-0.5	2.4	16.5
2568	-1.2	-1.7	0.0	-0.5	2.4	16.5
697	-0.1	1.5	0.0	-0.6	2.3	17.4
727	-0.7	-0.4	0.0	-0.3	1.3	31.7
2086	-0.4	-0.7	0.0	-0.3	1.1	37.7
718	0.0	0.1	0.0	-0.3	1.0	39.5
12	-0.2	0.0	0.0	-0.4	1.0	42.3
679	0.1	0.0	0.0	-0.4	0.9	45.4

¹ Stress components are listed for the nodes noted on Figure 2.6.12.9-1. Note that S_x is the stress in the radial direction, S_y is the stress in the circumferential direction and S_{xy} is the shearing stress.

² The allowable stress is conservatively defined as S_m. S_m for 17-4 PH stainless steel at the conservative temperature of 650°F is 41.9 ksi.

Table 2.6.12.9-5 18.1-g Side Impact Web Stresses for 45-Degree Drop Orientation (NAC-STC PWR Basket - Directly Loaded Fuel Configuration)

Node No. ¹	S _x (ksi)	S _y (ksi)	S _z (ksi)	S _{xy} (ksi)	SI (ksi)	MS ²
505	-2.4	-0.8	0.0	-2.7	5.7	6.5
2496	-0.3	-4.7	0.0	-1.6	5.5	6.6
1069	-1.9	-2.2	0.0	-2.7	5.4	6.8
402	-2.9	-1.5	0.0	-2.5	5.3	6.9
2506	-1.2	-3.4	0.0	-2.3	5.3	6.9
1172	-1.5	-1.3	0.0	-2.6	5.2	7.0
567	-3.1	0.3	0.0	-0.2	4.7	8.0
51	-3.8	-0.9	0.0	-0.3	4.5	8.2
390	-3.3	-0.1	0.0	-0.2	4.5	8.3
1839	-2.3	-2.3	0.0	-2.0	4.5	8.4
60	-3.8	-0.7	0.0	-0.1	4.4	8.4
2125	-2.4	-3.8	0.0	-0.1	4.2	8.9
495	-0.8	-0.4	0.0	-2.0	4.1	9.2
1162	-0.1	-0.5	0.0	-1.9	3.9	9.8
1829	-1.6	-3.2	0.0	-1.2	3.8	10.0
1901	-2.8	-0.5	0.0	-0.1	3.8	10.0
2107	-0.1	-3.4	0.0	-0.5	3.8	10.0
30	-0.7	-2.4	0.0	-0.7	3.5	10.9
1385	-3.0	-1.0	0.0	-0.1	3.4	11.4
1346	-2.1	-3.0	0.0	-0.1	3.3	11.6
1364	-2.1	0.0	0.0	-0.2	2.7	14.8
1057	-1.3	-1.5	0.0	-0.6	2.6	15.4
2568	-1.0	-1.8	0.0	-0.5	2.4	16.4
1234	-0.9	-0.9	0.0	-0.6	2.3	17.0
697	0.0	1.5	0.0	-0.6	2.3	17.5
727	-0.6	-0.4	0.0	-0.4	1.4	30.0
2086	-0.4	-0.7	0.0	-0.3	1.2	34.6
718	0.1	0.2	0.0	-0.4	1.1	36.8
12	-0.1	0.0	0.0	-0.4	0.9	44.6
679	0.1	0.0	0.0	-0.4	0.9	47.9

¹ Stress components are listed for the nodes noted on Figure 2.6.12.9-1. Note that S_x is the stress in the radial direction, S_y is the stress in the circumferential direction and S_{xy} is the shearing stress.

² The allowable stress is conservatively defined as S_m. S_m for 17-4 PH stainless steel at the conservative temperature of 650°F is 41.9 ksi.

Table 2.6.12.9-6 18.1-g Side Impact Web Stresses for 60-Degree Drop Orientation (NAC-STC PWR Basket - Directly Loaded Fuel Configuration)

Node No. ¹	S _x (ksi)	S _y (ksi)	S _z (ksi)	S _{xy} (ksi)	SI (ksi)	MS ²
2496	0.1	-5.6	0.0	-1.5	6.5	5.4
2506	-0.5	-4.2	0.0	-2.3	5.9	6.1
1069	-1.2	-2.8	0.0	-2.6	5.5	6.6
505	-1.4	-1.4	0.0	-2.6	5.1	7.2
402	-1.9	-2.2	0.0	-2.5	5.1	7.2
1172	-0.8	-1.7	0.0	-2.5	5.0	7.3
2125	-3.0	-4.5	0.0	-0.1	4.9	7.5
1839	-1.4	-3.2	0.0	-2.0	4.7	7.9
2107	0.1	-4.3	0.0	-0.5	4.7	8.0
1829	-0.9	-4.2	0.0	-1.1	4.6	8.2
1346	-2.6	-3.7	0.0	-0.1	4.1	9.3
60	-2.9	-0.2	0.0	-0.1	3.9	9.7
390	-2.4	-0.4	0.0	-0.2	3.8	10.0
51	-2.5	-0.5	0.0	-0.2	3.7	10.3
567	-2.0	-0.3	0.0	-0.2	3.7	10.4
495	-0.2	-0.7	0.0	-1.8	3.7	10.4
1162	0.2	-0.6	0.0	-1.7	3.5	10.8
30	-0.2	-2.4	0.0	-0.6	3.5	11.0
1901	-2.0	-0.7	0.0	-0.1	3.2	12.1
1385	2.1	-0.4	0.0	-0.1	2.8	14.2
2568	-0.7	-2.0	0.0	-0.6	2.4	16.2
1057	-0.9	-1.5	0.0	-0.6	2.4	16.6
1364	-1.6	-0.4	0.0	-0.2	2.2	17.8
697	0.0	1.6	0.0	-0.6	2.1	18.7
1234	-0.5	-0.8	0.0	-0.6	2.1	19.0
727	-0.5	-0.3	0.0	-0.4	1.5	27.5
2086	-0.4	-0.7	0.0	-0.4	1.3	30.7
718	0.2	0.4	0.0	-0.4	1.2	33.8
12	0.1	0.1	0.0	-0.3	0.8	49.3
679	0.2	0.0	0.0	-0.3	0.8	53.0

¹ Stress components are listed for the nodes noted on Figure 2.6.12.9-1. Note that S_x is the stress in the radial direction, S_y is the stress in the circumferential direction and S_{xy} is the shearing stress.

² The allowable stress is conservatively defined as S_m. S_m for 17-4 PH stainless steel at the conservative temperature of 650°F is 41.9 ksi.

Table 2.6.12.9-7 18.1-g Side Impact Web Stresses for 64-Degree Drop Orientation (NAC-STC PWR Basket - Directly Loaded Fuel Configuration)

Node No. ¹	S _x (ksi)	S _y (ksi)	S _z (ksi)	S _{xy} (ksi)	SI (ksi)	MS ²
2496	0.2	-5.8	0.0	-1.4	6.7	5.2
2506	-0.3	-4.4	0.0	-2.3	6.1	5.9
1069	-0.9	-3.0	0.0	-2.6	5.6	6.5
2125	-3.1	-4.7	0.0	-0.1	5.1	7.2
402	-1.6	-2.4	0.0	-2.5	5.1	7.3
505	-1.1	-1.5	0.0	-2.5	5.0	7.4
1172	-0.5	-1.8	0.0	-2.4	5.0	7.4
2107	0.2	-4.4	0.0	-0.5	4.9	7.6
1839	-1.1	-3.4	0.0	-2.0	4.8	7.7
1829	-0.7	-4.5	0.0	-1.0	4.8	7.8
1346	-2.8	-3.9	0.0	-0.1	4.2	8.9
60	-2.5	-0.1	0.0	-0.1	3.7	10.3
390	-2.1	-0.4	0.0	-0.2	3.6	10.8
495	-0.1	-0.7	0.0	-1.7	3.5	10.9
1162	0.2	-0.6	0.0	-1.7	3.4	11.4
567	-1.6	-0.5	0.0	-0.1	3.4	11.4
30	-0.1	-2.3	0.0	-0.5	3.4	11.4
51	-2.1	-0.7	0.0	-0.2	3.3	11.6
1901	-1.7	-0.8	0.0	-0.1	3.0	12.7
1385	-1.8	-0.3	0.0	-0.1	2.6	15.1
2568	-0.6	-2.0	0.0	-0.6	2.5	16.0
1157	-0.8	-1.5	0.0	-0.6	2.3	17.0
1364	-1.4	-0.5	0.0	-0.2	2.1	18.5
697	0.0	1.5	0.0	-0.6	2.0	19.5
1234	-0.3	-0.7	0.0	-0.6	2.0	20.0
727	-0.4	-0.3	0.0	-0.4	1.5	27.4
2086	-0.4	-0.7	0.0	-0.4	1.3	30.1
718	0.2	0.4	0.0	-0.4	1.2	33.6
12	0.0	-0.1	0.0	-0.3	0.8	50.5
679	0.2	0.1	0.0	-0.3	0.8	54.7

¹ Stress components are listed for the nodes noted on Figure 2.6.12.9-1. Note that S_x is the stress in the radial direction, S_y is the stress in the circumferential direction and S_{xy} is the shearing stress.

² The allowable stress is conservatively defined as S_m. S_m for 17-4 PH stainless steel at the conservative temperature of 650°F is 41.9 ksi.

Table 2.6.12.9-8 18.1-g Side Impact Web Stresses for 75-Degree Drop Orientation (NAC-STC PWR Basket - Directly Loaded Fuel Configuration)

Node No. ¹	S _x (ksi)	S _y (ksi)	S _z (ksi)	S _{xy} (ksi)	SI (ksi)	MS ²
2496	0.5	-6.2	0.0	-1.3	7.2	4.8
2506	0.2	-4.7	0.0	-2.2	6.6	5.4
1069	0.1	-3.3	0.0	-2.4	5.8	6.3
2125	-3.4	-4.9	0.0	0.0	5.4	6.8
1829	-0.2	-5.0	0.0	-0.9	5.4	6.8
1839	-0.3	-3.9	0.0	-1.9	5.3	6.9
2107	0.3	-4.8	0.0	-0.5	5.3	3.9
402	-0.5	-2.9	0.0	-2.3	5.2	7.0
1346	-3.1	-4.3	0.0	-0.1	4.6	8.1
1172	0.1	-2.0	0.0	-2.1	4.6	8.1
505	-0.2	-1.9	0.0	-2.1	4.5	8.3
495	0.0	-0.8	0.0	-1.4	3.0	13.1
390	-1.0	-1.0	0.0	-0.1	2.9	13.6
1162	0.2	-0.7	0.0	-1.4	2.8	13.7
30	0.0	-1.7	0.0	-0.4	2.8	13.8
567	-0.6	-1.1	0.0	-0.1	2.8	14.2
60	-1.3	-0.3	0.0	0.0	2.7	14.5
1901	-0.9	-1.0	0.0	-0.1	2.7	14.7
2568	-0.2	-1.9	0.0	-0.6	2.4	16.2
51	-0.8	-1.0	0.0	-0.2	2.4	16.5
1385	-1.0	0.1	0.0	-0.1	2.2	18.2
1057	-0.3	-1.2	0.0	-0.6	2.0	19.6
1364	-1.0	-0.8	0.0	-0.2	2.0	20.1
697	0.0	1.2	0.0	-0.5	1.7	23.7
1234	0.0	-0.4	0.0	-0.6	1.6	29.1
2086	-0.3	-0.6	0.0	-0.5	1.4	29.1
727	0.0	0.0	0.0	-0.4	1.4	19.1
718	0.2	0.6	0.0	-0.4	1.2	35.4
12	0.0	0.1	0.0	-0.2	0.8	53.4
679	0.2	0.0	0.0	-0.2	0.7	59.9

¹ Stress components are listed for the nodes noted on Figure 2.6.12.9-1. Note that S_x is the stress in the radial direction, S_y is the stress in the circumferential direction and S_{xy} is the shearing stress.

² The allowable stress is conservatively defined as S_m. S_m for 17-4 PH stainless steel at the conservative temperature of 650°F is 41.9 ksi.

Table 2.6.12.9-9 18.1-g Side Impact Web Stresses for 90-Degree Drop Orientation (NAC-STC PWR Basket - Directly Loaded Fuel Configuration)

Node No. ¹	S _x (ksi)	S _y (ksi)	S _z (ksi)	S _{xy} (ksi)	SI (ksi)	MS ²
1829	1.4	-6.2	0.0	0.2	7.6	4.5
2496	1.4	-6.2	0.0	-0.2	7.6	4.5
1839	1.6	-4.9	0.0	0.2	6.5	5.4
2506	1.6	-4.9	0.0	-0.2	6.5	5.4
1346	-3.7	-4.9	0.0	0.0	5.3	6.9
2125	-3.7	-4.9	0.0	0.0	5.3	6.9
402	0.7	-3.6	0.0	0.1	4.3	8.8
1069	0.7	-3.5	0.0	-0.1	4.3	8.8
1364	0.6	-3.6	0.0	0.1	4.2	8.9
2107	0.6	-3.6	0.0	-0.1	4.2	8.9
2568	0.8	-1.6	0.0	-0.3	2.5	15.6
1901	0.8	-1.6	0.0	0.3	2.5	15.6
1172	0.0	-2.1	0.0	0.0	2.2	18.0
505	0.0	-2.1	0.0	0.0	2.2	18.0
1057	0.2	-1.2	0.0	-0.3	1.6	24.8
390	0.2	-1.2	0.0	0.3	1.6	24.8
1234	-0.3	-0.9	0.0	-0.3	-1.1	36.8
567	-0.3	-0.9	0.0	0.3	1.1	36.8
697	-0.4	-0.1	0.0	0.0	0.9	45.0
30	-0.4	-0.1	0.0	0.0	0.9	45.0
1162	-0.3	-0.9	0.0	0.0	0.9	47.0
495	-0.3	-0.9	0.0	0.0	0.9	47.0
2086	0.4	-0.1	0.0	-0.3	0.8	50.7
1385	0.4	-0.1	0.0	0.3	0.8	50.7
727	0.0	0.0	0.0	-0.3	0.6	72.3
60	0.0	0.0	0.0	0.3	0.6	72.3
51	-0.3	0.0	0.0	0.2	0.6	72.9
718	-0.3	0.0	0.0	-0.2	0.6	72.9
679	0.0	-0.2	0.0	0.0	0.3	138.9
12	0.0	-0.2	0.0	0.0	0.3	139.0

¹ Stress components are listed for the nodes noted on Figure 2.6.12.9-1. Note that S_x is the stress in the radial direction, S_y is the stress in the circumferential direction and S_{xy} is the shearing stress.

² The allowable stress is conservatively defined as S_m. S_m for 17-4 PH stainless steel at the conservative temperature of 650°F is 41.9 ksi.

THIS PAGE INTENTIONALLY LEFT BLANK

2.6.12.10 Support Disk Shear Stresses for a 1-Foot Side Drop and a 1-Foot End Drop Conditions (Directly Loaded Fuel Configuration)

The maximum stress intensity for the 1-foot side drop is reported in Table 2.6.12.7-3 as 16.65 ksi, (30 degree drop orientation). Similarly, the maximum stress intensity for the 1-foot end drop is reported in Table 2.6.12.4-1 as 12.65 ksi. Therefore, the maximum enveloping shear stress anywhere for either of the two loading conditions mentioned above is 16.65/2 or 8.325 ksi.

ASME Code, Section III, Division 1, Subdivision NG, criteria defines the allowable for shear stress to be 0.6 S_m . The design stress intensity, S_m , for 17-4 PH at a bounding temperature of 650°F is 41.9 ksi.

Minimum Margin of Safety for Shear

$$\begin{aligned} MS &= \frac{(2)(0.6)S_m}{SI} - 1 \\ &= \frac{(2)(0.6)(41.9)}{16.65} - 1 = +2.02 \end{aligned}$$

Therefore, structural adequacy of the NAC-STC fuel basket support disk directly loaded fuel configuration design for the normal conditions of transport, 1-foot side drop and 1-foot end drop, is demonstrated for shear stress criteria.

THIS PAGE INTENTIONALLY LEFT BLANK

2.6.12.11 Bearing Stress - Basket Contact with Inner Shell (Directly Loaded Fuel Configuration)

During the 1-foot side drop the bearing load on the outer edge of the support disk is a maximum for the normal condition loads. Considering the total cavity design weight of 56,000 pounds being supported by the 31 stainless steel support disks and the contact area being limited to a 90 degree arch length the bearing stress is:

$$S_{br-1g} = 56,000 / (0.5 \times 31 \times 3.14 \times 71.0 \times 0.25) \\ = 64.8 \text{ psi}$$

For the 18.1 g 1-foot drop the maximum bearing stress in the support disk is:

$$S_{br-18.1g} = 18.1 \times 64.8 = 1170 \text{ psi}$$

Using a material allowable stress based on the conservative support disk temperature on the outer bearing surface, $1.0 S_y = 89.5 \text{ ksi}$ at 400°F (Table 3.4-1), the margin of safety is:

$$MS = 89.5 / 1.17 - 1 = \underline{+Large}$$

Therefore, the NAC-STC basket directly loaded fuel configuration design is acceptable relative to bearing stress limits for the basket cavity wall interface.

THIS PAGE INTENTIONALLY LEFT BLANK

2.6.12.12 Evaluation of Triaxial Stress for the Fuel Basket Support Disk (Directly Loaded Fuel Configuration)

The ASME Code Section III, Division 1, Subsection NG criteria requires that the combination of all stress components be limited to a value of $4S_m$. Since the structural analysis of the fuel basket is conservatively performed by calculating the stress intensity values at specific node point for all membrane and bending stress components acting at the node and the value compared to S_m to evaluate acceptance, previously summarized stress results will have a minimum margin of safety of four times the reported value for this specific evaluation criteria.

Therefore, the NAC-STC stainless steel fuel basket (directly loaded fuel configuration) satisfies ASME Code structural criteria for Core Support Structures and basket design normal condition loading.

THIS PAGE INTENTIONALLY LEFT BLANK

2.6.12.13 Fuel Basket (Directly Loaded Fuel Configuration) Weldment Analysis for 1-Foot End Drop

The responses of the top and the bottom weldment plates of the fuel basket assembly to a 19.6g normal operation deceleration load are examined. The top and the bottom weldment plates are both 1-inch thick and fabricated from SA 240, Type 304 stainless steel. The top weldment supports its own weight and 26 fuel tubes (without the fuel assemblies) during a 1-foot top end drop. Similarly the bottom weldment supports its own weight and 26 fuel tubes (without the fuel assemblies) during a 1-foot bottom end drop. The responses of the end plates to the 1-foot end drop are analyzed using ANSYS STIF63 three-dimensional, six degrees-of-freedom, elastic quadrilateral shell elements. The finite element model for both plates is shown in Figure 2.6.12.13-1. Figure 2.6.12.13-2 and 2.6.12.13-3 display the boundary conditions for the top weldment plate and the bottom weldment plate respectively. The evaluation is based on material properties of SA 240, Type 304 at a conservative temperature of 500°F. The hottest steel support disk during normal transport conditions is 498°F, see Table 3.4-1.

The primary membrane plus primary bending stress in the top weldment plate for the 1-foot top end drop is 21.5 ksi. The primary membrane plus primary bending stress in the bottom weldment plate for the 1-foot bottom end drop is 17.9 ksi. At 500°F, the normal condition stress allowable, $1.5 S_m$, is 26.25 ksi. The minimum margin of safety for the top weldment plate and the bottom weldment plate are +0.22 and +0.47 respectively. Therefore, the structural adequacy of the NAC-STC fuel basket weldment end plates (directly loaded fuel configuration) for the normal condition of transport is demonstrated.

Figure 2.6.12.13-1 Fuel Basket Weldment Model (Directly Loaded Fuel Configuration)

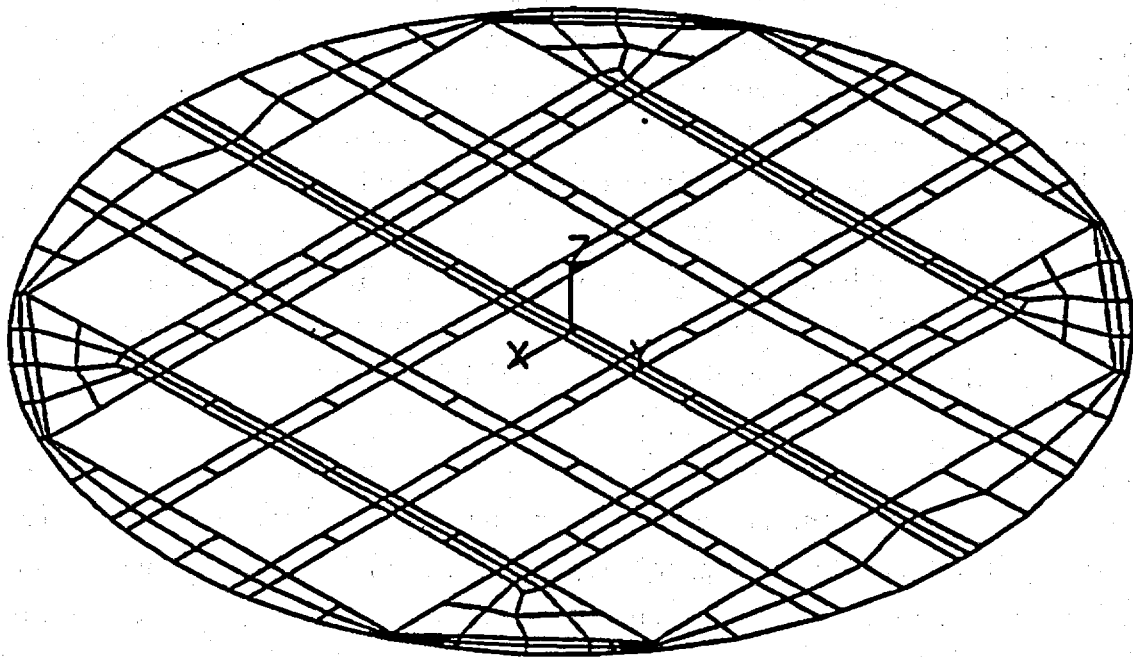


Figure 2.6.12.13-2 Fuel Basket Top Weldment Boundary Conditions (Directly Loaded Fuel Configuration)

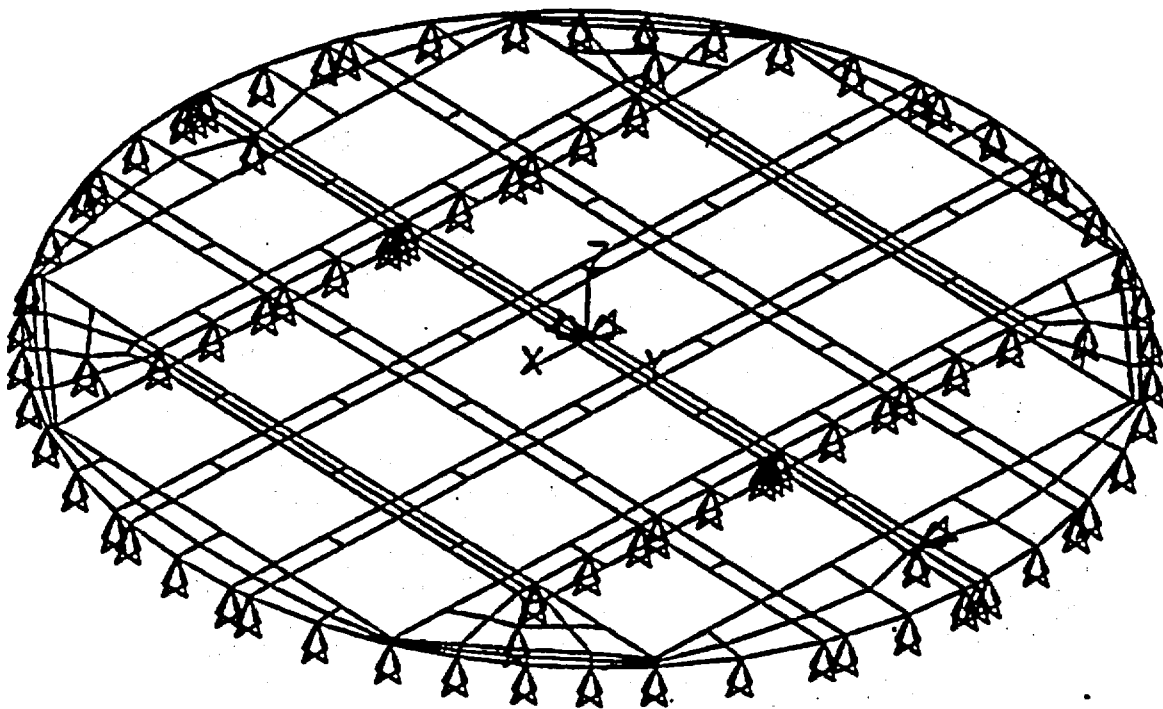
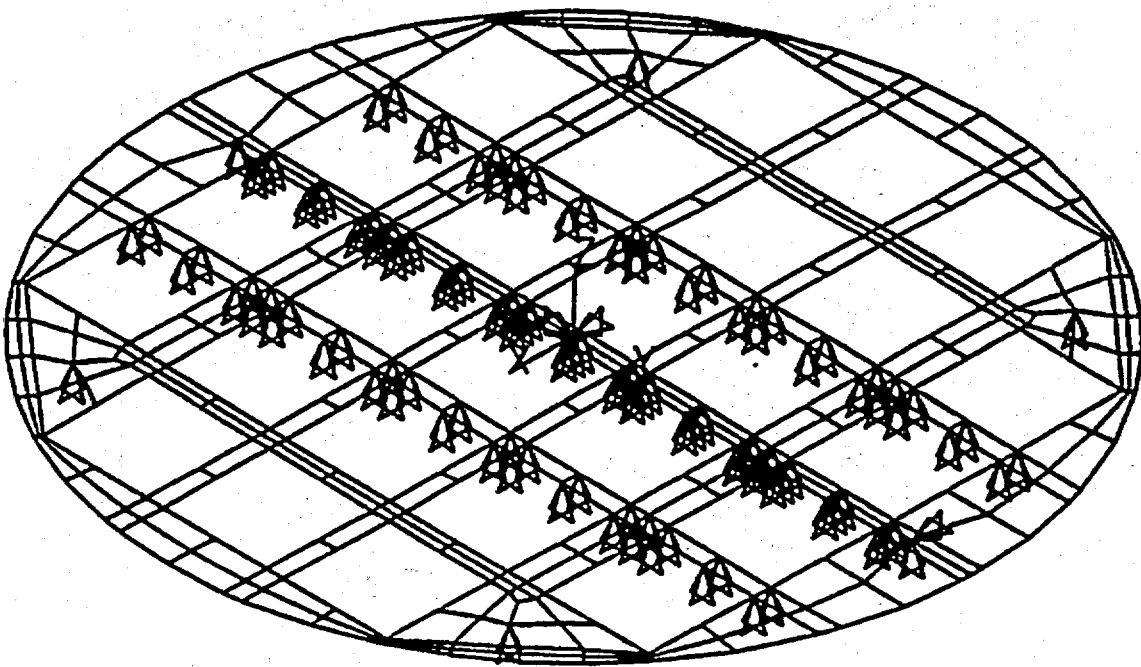


Figure 2.6.12.13-3 Fuel Basket Bottom Weldment Boundary Conditions (Directly Loaded Fuel Configuration)



2.6.13 Yankee-MPC Transportable Storage Canister Analysis - Normal Transport Condition

The NAC-STC has three contents configurations - uncanistered (directly loaded fuel); canistered Yankee Class spent fuel or Greater Than Class C (GTCC) waste; and, canistered Connecticut Yankee spent fuel or GTCC. The canistered Yankee Class spent fuel or GTCC waste is referred to as the Yankee-MPC configuration. The Yankee-MPC canister is evaluated for the Normal Conditions of Transport in this section and for the Hypothetical Accident Conditions in Section 2.7.11. The Normal Conditions of Transport analysis of the Yankee-MPC canistered fuel basket is presented in Section 2.6.14, and that of the canistered Yankee-MPC GTCC basket is presented in Section 2.6.19.1.

The canistered fuel configuration consists of a transportable storage canister with top and bottom spacers to properly locate the canister in the NAC-STC cask cavity. The analysis of the top and bottom spacers is presented in Section 2.6.15. The principal components of the transportable storage canister are the canister, the canister fuel basket, the shield lid, and the structural lid. In an alternate configuration, the transportable storage canister may include the Yankee-MPC GTCC basket instead of the canister fuel basket. Detailed descriptions of the geometries and materials of construction of the canister, baskets, and spacers are provided in Sections 1.2.1.2.8, 1.2.1.2.8.1, 1.2.1.2.8.2, and 1.2.1.2.8.3, respectively.

The Yankee-MPC transportable storage canister and the canister shell, bottom, and lids are shown in Figures 2.6.13-1 and 2.6.13-2, respectively.

Figure 2.6.13-1 Yankee-MPC Transportable Storage Canister

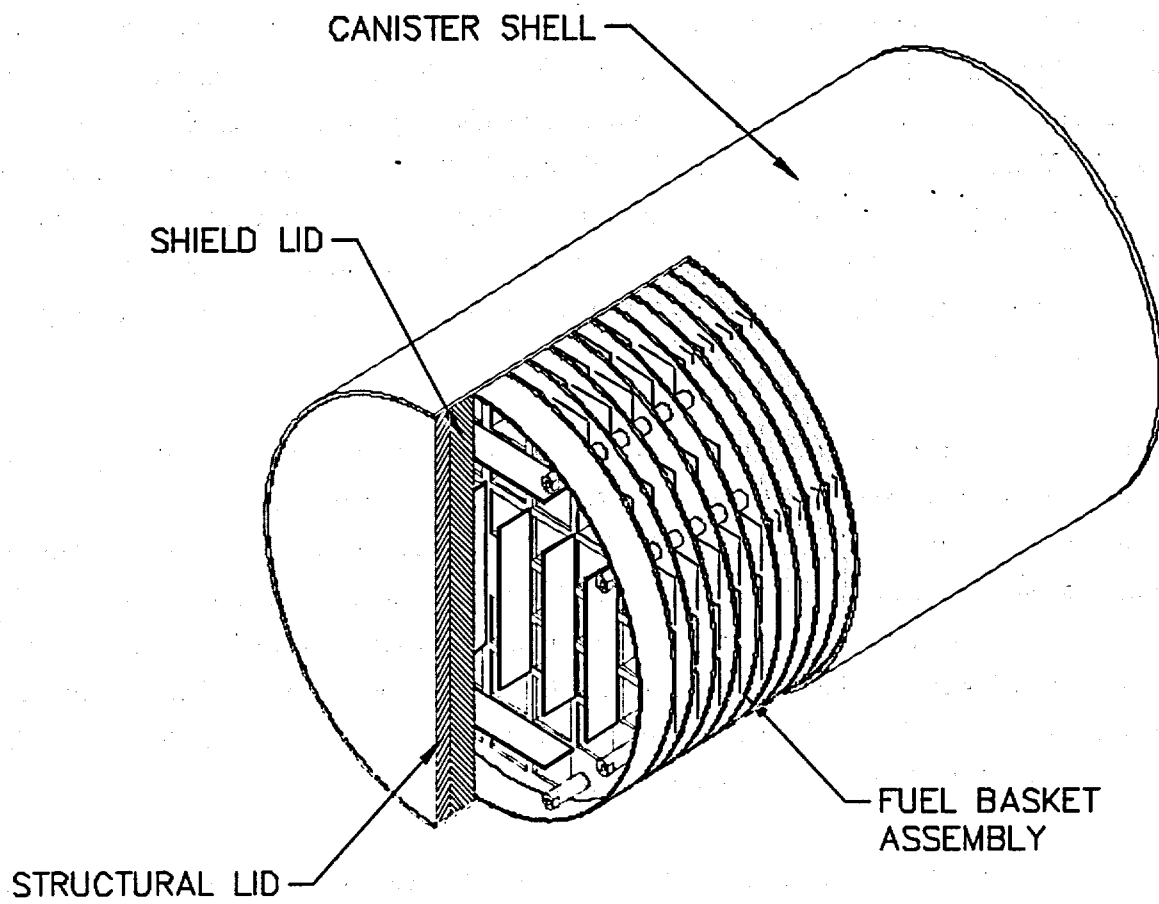
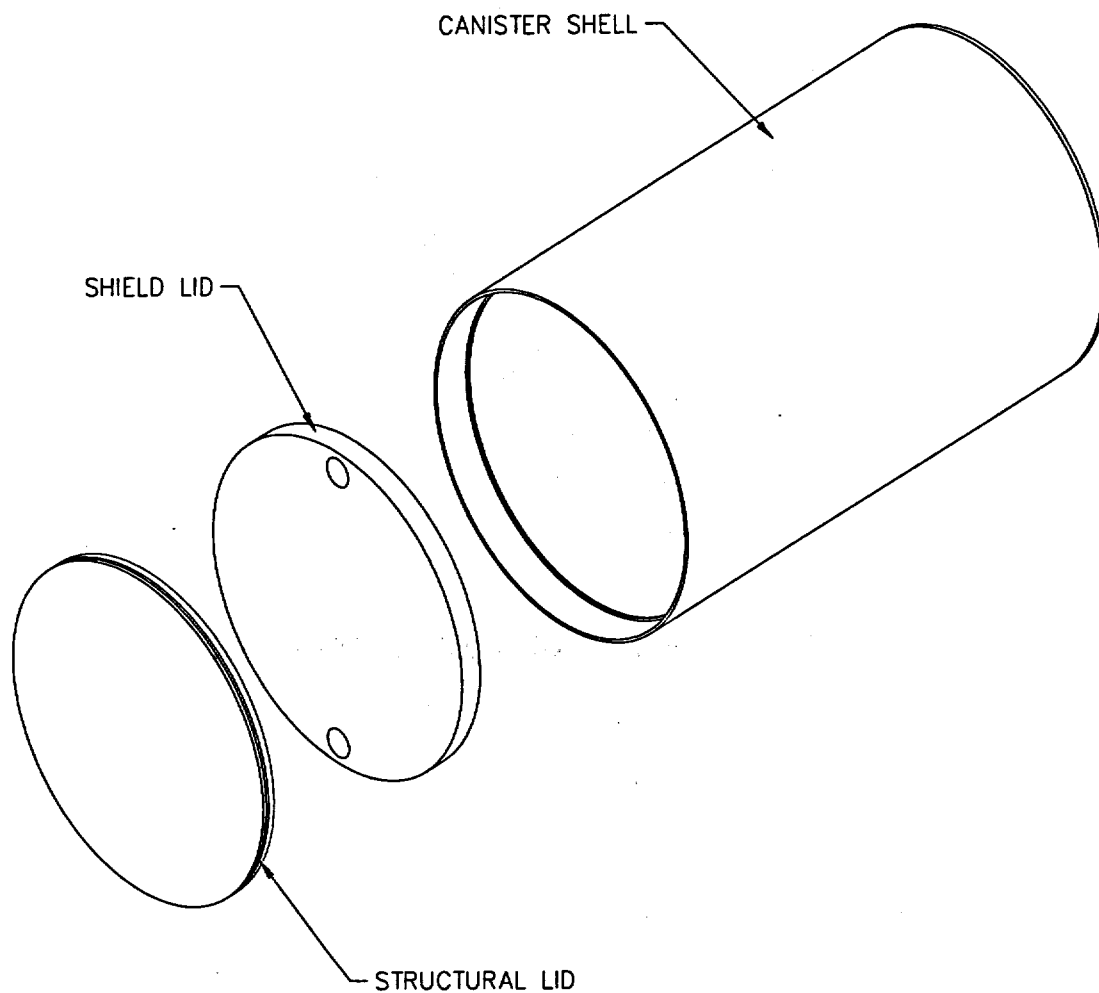


Figure 2.6.13-2 Yankee-MPC Canister for Fuel Basket or GTCC Basket



THIS PAGE INTENTIONALLY LEFT BLANK

2.6.13.1 Yankee-MPC Canister Description and Analysis

The transportable storage canister contains/confines the spent fuel in the canister fuel basket or the waste in the canister GTCC basket. The canister is the defined confinement boundary for its contents during storage operation, but the canister is not considered for containment during transport operation; the NAC-STC provides the containment boundary for transport. The canister in the transfer cask serves as the handling component for its basket and contents during loading, closure, and transfer from the pool to storage and/or transport.

The canister is a right-circular shell fabricated from rolled 5/8-inch thick, Type 304L stainless steel plate and closed by a circular 1-inch thick, Type 304L stainless steel plate that is welded to one end of the shell. The canister is closed at the top end by the installation and welding of the 5-inch thick, Type 304 stainless steel shield lid and the 3-inch thick, Type 304L stainless steel structural lid. The canister may enclose either the canister fuel basket and contents or the canister GTCC basket and contents. The empty canister with basket is handled using lifting rings located on the top end of the basket. The loaded canister is lifted using 6 hoist rings threaded into the top of the structural lid. Type 304L stainless steel was selected for the canister's exterior components based on its enhanced corrosion resistance, especially in the weld regions (refer to Section 2.5.1.3).

The structural design criteria for the canister is the ASME Code Section III, Subsection NB, "Class 1 Components." Consistent with this criteria, the structural components of the canister are shown to satisfy the allowable stress limits presented in Tables 2.1.2-1 and 2.1.2-2 as applicable. The allowable stresses used in this analysis are based on a maximum material temperature of 350°F for all locations in the canister, unless otherwise indicated. These allowables are conservative because the maximum calculated canister material temperature is 338°F.

The canister is analyzed using the ANSYS finite element computer program for the 1-foot drop condition in the end and side impact orientations.

The canister structural lid closure weld is specifically evaluated for the normal conditions of transport. The lid weld is identified as Section 8 in Figure 2.6.13.3-1. Either a progressive liquid penetrant examination is performed on the root, each successive 3/8-inch layer, and the final surface of the weld in accordance with the ASME Code, Section V, Article 6, or an ultrasonic examination of the weld is performed in accordance with Section V, Article 5. In accordance with NRC guidance, if a multi-pass liquid penetrant examination is performed on the structural

lid closure weld, two separate weld stress reduction factors are applied to the structural lid canister shell weld – a 0.8 factor to conservatively consider the weld configuration and a 0.8 factor per NRC ISG-4, Item 5. Thus, a total weld stress reduction factor of 0.64 (0.8×0.8) is applied to the stress allowable for the structural lid weld. The canister closure weld evaluation for normal conditions is presented in Section 2.6.13.12. The evaluation, which is based on the finite element analysis stress result as shown in Sections 2.6.13.4 through 2.6.13.7, shows a minimum margin of safety of +0.17 for the weld.

2.6.13.2 Yankee-MPC Canister Finite Element Model

A finite element model of the Yankee-MPC canister was constructed using ANSYS solid (SOLID45) elements. The model represents a one-half (180°) section of the canister and basket. The basket support discs were modeled with three-dimensional shell (SHELL63) elements. The model uses gap-spring elements to simulate contact between adjacent components. Interaction between the basket and canister were accomplished using three-dimensional gap elements (CONTAC52) along the periphery of the support disks. Contact between the canister and the cask inner shell is also modeled using CONTAC52 gap elements. Contact between the canister structural lid and shield lid is modeled using COMBIN40 combination elements in the axial degree of freedom. Simulation of the backing ring is accomplished using a ring of COMBIN40 spring gap elements connecting the shield lid and the canister in the axial direction at the lid lower outside radius. In addition, CONTAC52 elements are used to model interaction between the structural lid and canister shell and the shield lid and canister shell just below the respective lid weld joints. The size of the CONTAC52 gaps were determined from the nominal dimensions of contacting components. The COMBIN40 elements used between the structural and shield lids and for the backing ring are assigned gap sizes of 1E-8 inches. The maximum gap size is 0.08 inches. However, use of the small gap size results in the highest stresses at critical sections, resulting in the lowest margin of safety. All gap-spring elements are assigned a stiffness of 1E8 lb/in.

A central hole was modeled in the bottom, shield and structural lids. These holes were then filled with solid elements. This technique was used to avoid a small hole (which can cause a stress concentration) or a series of degenerate solid elements (which can produce a region of excessive stiffness).

Spring elements were inserted over the gap elements located on the model symmetry plane to help stabilize the model during solutions phases. The springs were given a low stiffness of 10 lb/in so their presence would not adversely affect the accuracy of the solutions.

Boundary conditions were applied to enforce symmetry at the cut boundary of the model. All nodes on the cask shell side of the canister to cask spring gap elements were fixed in all degrees of freedom. In addition, the axial and inplane rotational degrees of freedom of the basket nodes were fixed.

Additionally, the structural analyses of the canister were performed with temperature distributions corresponding to the hot (100°F ambient with solar heat load) and cold (-40°F ambient) external conditions.

Table 2.6.13.2-1 lists the real constants assigned to specific components of the model. Table 2.6.13.2-2 lists the material properties used for the model.

Figure 2.6.13.2-1 is a plot of the entire canister finite element model. An isolated view of the canister shield and structural lids portion of the model is presented in Figure 2.6.13.2-2 and an enlarged view of the model in the structural lid and shield lid weld regions is shown in Figure 2.6.13.2-3. The canister bottom plate portion of the model is shown in Figure 2.6.13.2-4.

The loading for the normal operating condition is based on 1-foot drops in conjunction with the internal pressure loading (to the canister). Drop orientations considered are the end and side drops. In the end drop orientation, the fuel contents load is transferred to the canister end and directly to the transport cask end through the cavity spacer. This corresponds to a compressive stress in the canister ends which is present in the finite element model. For the side drop condition, the loads from the canister contents weight is transferred through the support disks into the canister wall, which is backed by the NAC-STC inner shell. Since the canister wall and the inner shell have different radii, a gap exists between the two surfaces. This results in the load passing only through regions in which the canister shell deflects to contact the inner shell. This load pattern is reflected in the side drop analysis. The operational conditions also contain loads developed from the temperature distribution in the canister. These are included in the canister model analyses.

Figure 2.6.13.2-1 Yankee-MPC Canister Finite Element Model

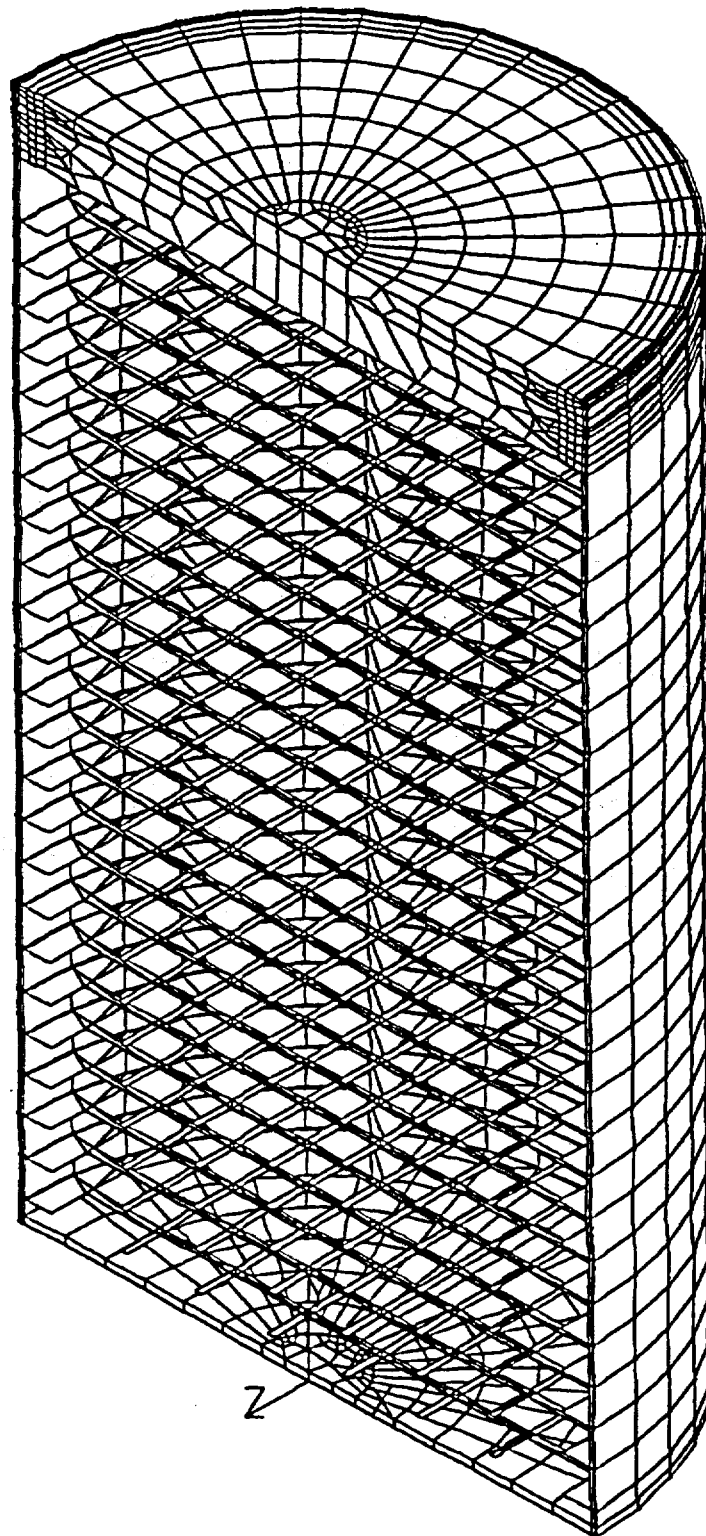


Figure 2.6.13.2-2 Yankee-MPC Canister Structural and Shield Lid Finite Element Mesh

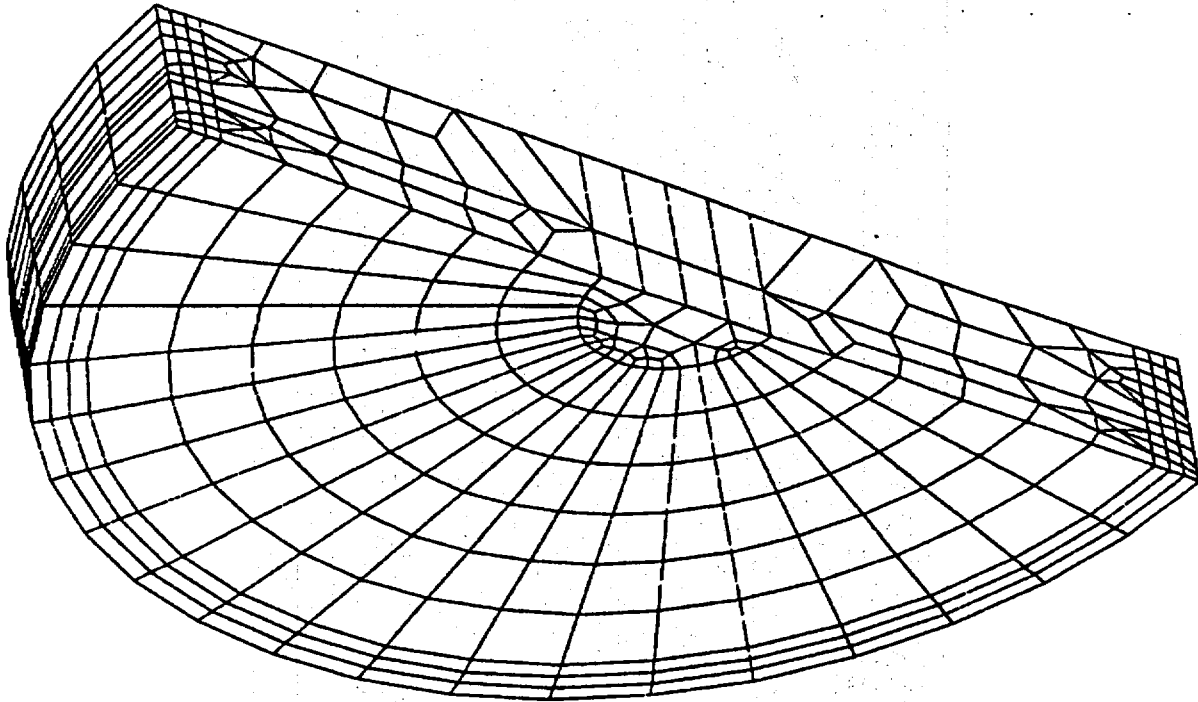


Figure 2.6.13.2-3 Yankee-MPC Structural and Shield Lid Weld Regions Finite Element Mesh

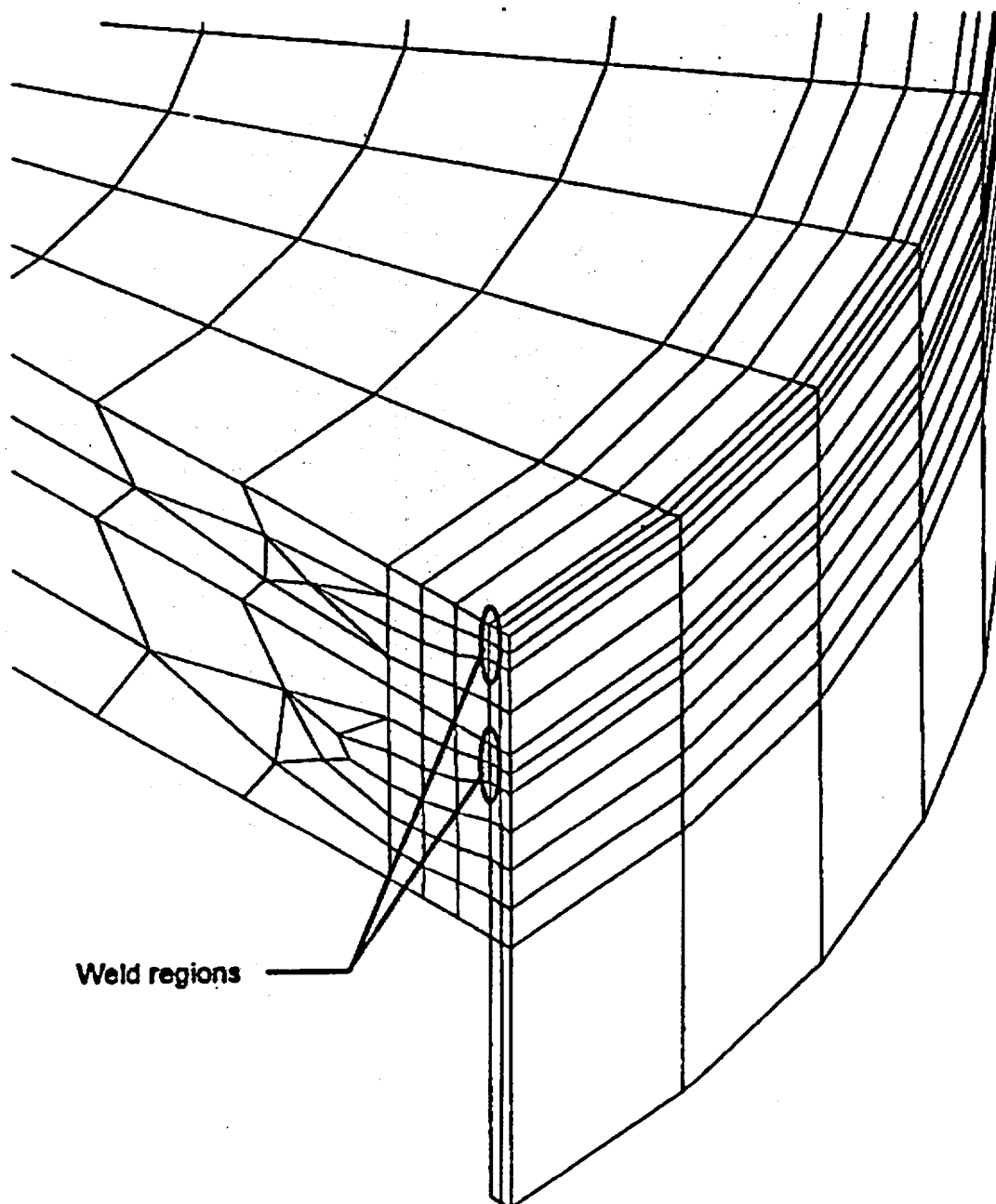


Figure 2.6.13.2-4 Yankee-MPC Canister Bottom Plate Finite Element Mesh

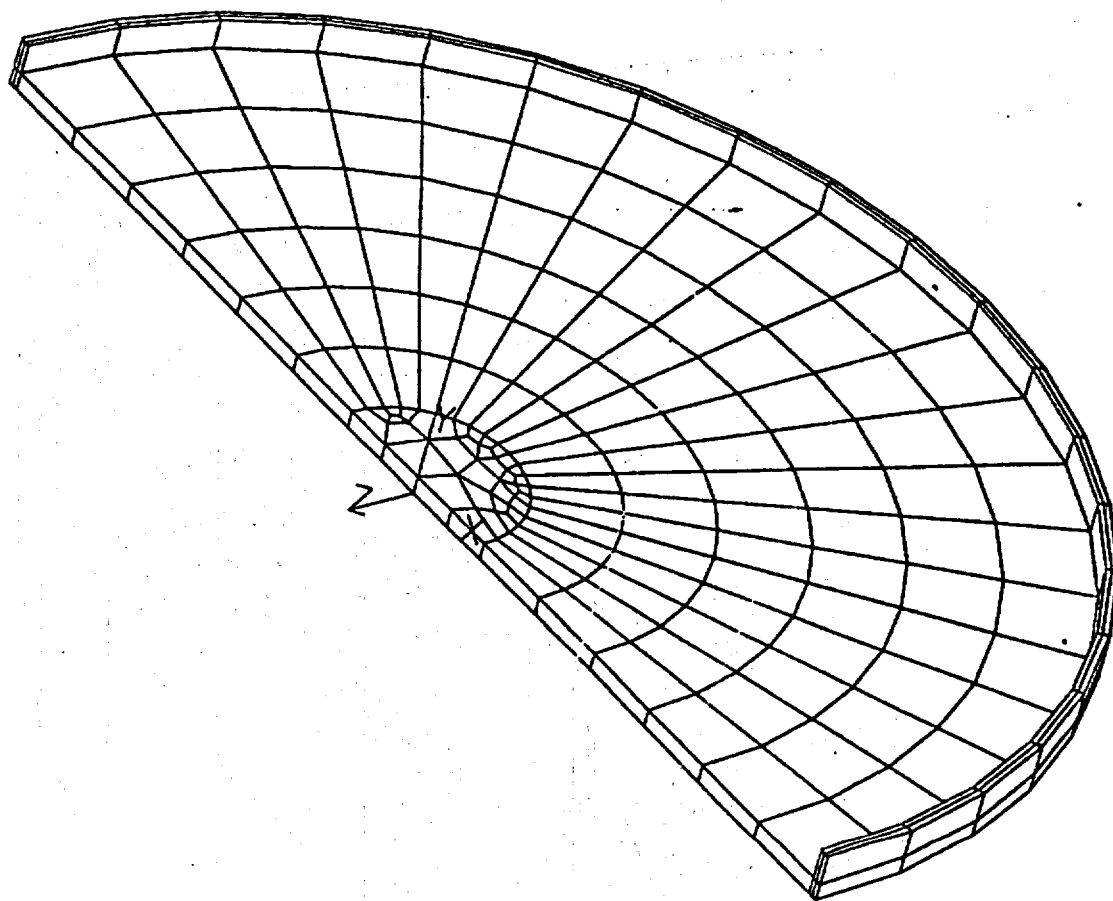


Table 2.6.13.2-1 Real Constant Sets Defined in Yankee-MPC Canister Model

Real Constant Set	Component
1	Canister Bottom Plate (SOLID45)
2-9	Canister Shell (SOLID45)
10-11	Shield Lid (SOLID45)
12-13	Structural Lid (SOLID45)
100	Axial Gaps from Canister Bottom Plate to Cask Shell (CONTAC52)
200	Radial Gaps from Canister Side to Cask Shell (CONTAC52)
300	Axial Gaps from Structural Lid Top to Cask Shell (CONTAC52)
400	Axial Gaps Between Structural and Shield Lid (COMBIN40)
500	Radial Gaps Between Shield Lid and Canister Inner Surface (CONTAC40)
600	Radial Gaps Between Shield Lid and Canister Inner Radius (CONTAC52)
700	Axial Gaps Between Shield Lid and Canister Wall to Simulate Backing Ring (COMBIN40)
800	Radial Gaps Between Basket and Canister Inner Surface (CONTAC52)
1000	Intermediate Basket Thickness Real Constant
1100	End Basket Thickness Real Constant
1200	Weak Spring Real Constant

Table 2.6.13.2-2 Material Sets Defined in Yankee-MPC Canister Model

Material Property Set	Component	Material
1	Canister Shell and Structural Lid	304L Stainless Steel; ASME SA240
2	Top and Bottom End Basket Disk	304 Stainless Steel; ASME SA240
3	Shield Lid	304 Stainless Steel; ASME SA240
4	Intermediate Basket Disk (support disk)	ASME SA693 Type 630

THIS PAGE INTENTIONALLY LEFT BLANK

2.6.13.3 Thermal Expansion Evaluation of Yankee-MPC Canister with Spent Fuel

A thermal stress evaluation is performed using ANSYS to determine the differential thermal expansion and the associated thermal stresses that result from a heat load of 12.5 kW. In assessing the thermal stresses, three extreme conditions are considered:

Condition	Ambient Temperature	Solar Insolance Applied to Cask Surface	12.5 kW Fuel Load
1	100°F	Yes	Yes
2	-40°F	No	Yes
3	-40°F	No	No

The following temperatures are obtained from the Yankee-MPC thermal analysis:

Location	Temperature (°F)		
	Condition 1	Condition 2	Condition 3
Structural Lid (center, top)	206	67	-40
Structural Lid (outer, top)	192	55	-40
Shield Lid (center, bottom)	209	71	-40
Bottom Plate (center, bottom)	255	121	-40
Bottom Plate (outer radius, bottom)	225	92	-40
Lateral Shell (mid-height)	338	215	-40

While most of the temperature gradients between the different locations are very close for condition 3, no thermal gradient exists, so there are no thermal stresses. The most significant gradient is between the lateral shell mid-height and the outer surface of the structural lid. The ΔT values are 132°F and 148°F for conditions 1 and 2, respectively (the change in temperature for condition 2 is 12% larger than that of condition 1). Thermal stresses are also increased because the modulus of elasticity and the coefficient of thermal expansion increase with temperature. The values of the coefficient of thermal expansion and the modulus of elasticity are obtained from Table 2.3.2-4. For condition 1, the product of the coefficient of thermal expansion and the modulus of elasticity at an average temperature of 272°F $((338+206)/2)$ is 242.9 psi/°F; whereas for condition 2, the corresponding value is 241.2 psi/°F. The effect of the temperature is,

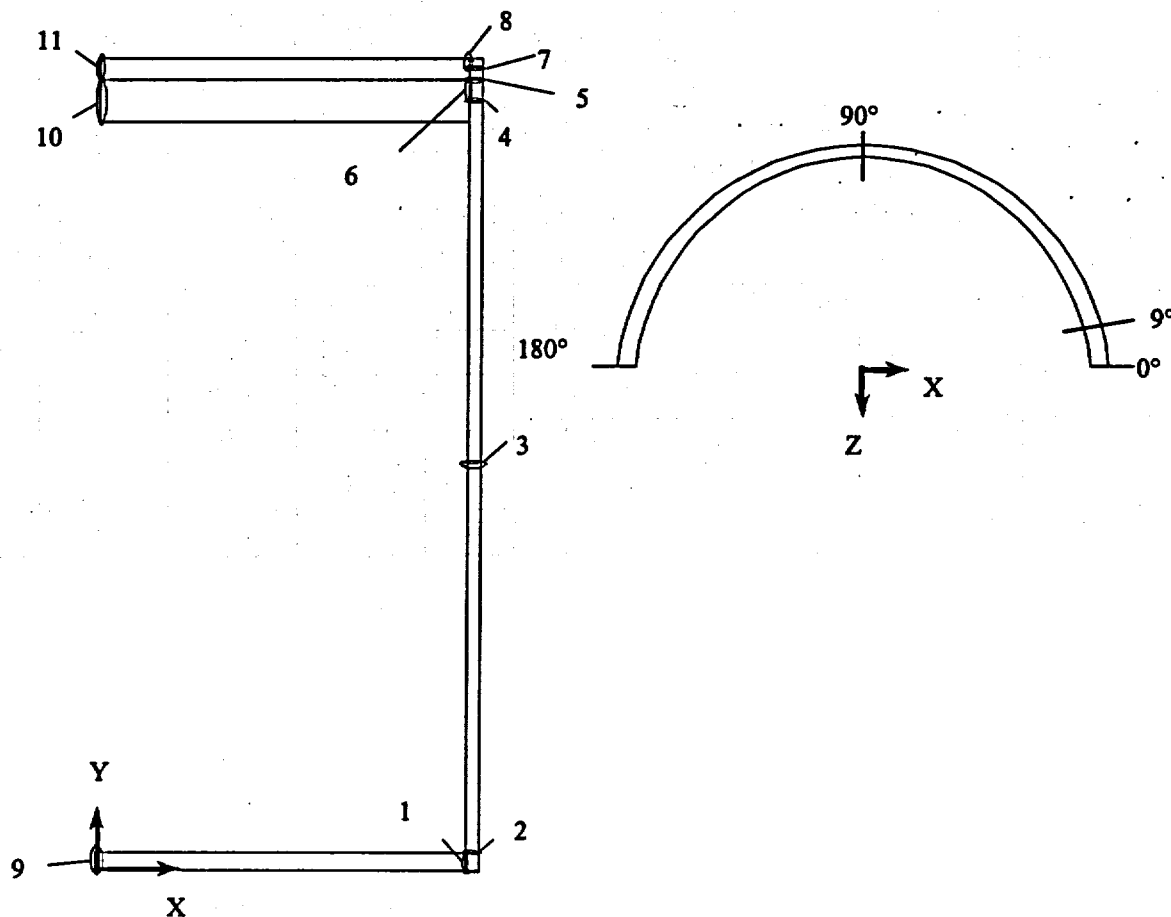
therefore, considered to be negligible. For normal condition thermal stresses, $3 S_m$ is the allowable stress criteria. Below 300°F, the value of S_m (16.7 ksi) does not change for SA-240, Type 304L stainless steel. For heat condition 1, the maximum temperature is 338°F and $S_m = 16.35$ ksi. This results in a 2% decrease in the allowable stress for condition 1, which is offset by the 12% increase in the temperature gradient for condition 2. For this reason, only condition 2 thermal stresses are included in the canister evaluations. In the three conditions considered above, the cask is assumed to be in the horizontal position and both the canister cavity and the cask cavity are assumed to be backfilled with helium.

The temperatures employed in the thermal stress analysis were obtained by applying the above temperatures as thermal boundary conditions to the thermal equivalent model of the structural canister model. The structural finite element model is described in Section 2.6.13.2. The equivalent thermal model is obtained by changing the structural element (SOLID45, which has three global displacements for degrees of freedom) to a SOLID70, which has temperature degrees of freedom at the individual nodes. The temperature dependent thermal conductivity for the canister material was employed in the thermal conduction analysis. The temperatures generated in this analysis were used in the thermal stress analysis to evaluate the properties at temperature, as well as the stresses due to thermal expansion.

According to ASME Code, Section III, Subsection NB, the allowable stress criteria is based on the evaluation of linearized stresses across critical cross sections through the canister wall. For the evaluation of the thermal stresses, the criteria for the stresses is based on peak stresses. The stress values taken from the analyses are the nodal stresses at the surface. The sections used in this evaluation are shown in Figure 2.6.13.3-1. For the sections identified, the thermal stresses are reported in Table 2.6.13.3-1. The thermal stresses reported in Table 2.6.13.3-1 correspond to the maximum stresses for any circumferential section, for the location shown in Figure 2.6.13.3-1.

For condition 1 or 2, the canister is hotter than the cask body and will undergo more thermal expansion than the cask body. To conservatively determine the minimum gap between the canister and the cask body due to thermal expansion, only expansion of the canister will be considered. The canister is considered to be at 338°F (shell temperature for condition 1) and the cask inner shell temperature is assumed to be 70°F. Using the outer radius of the canister of 35.32 inches and the coefficient of expansion for Type 304L stainless steel of $9.0722E-6$, the canister inner shell gap is reduced by $(9.0722E-6)(35.32)(268) = 0.086$ inches. Since the nominal radial canister-inner shell gap is 0.18 inches, the canister shell does not bind with the inner shell due to thermal expansion.

Figure 2.6.13.3-1 Identification of the Sections for Evaluating the Linearized Stresses in the Yankee-MPC Canister



Section	Node 1		Node 2	
	X	Y	X	Y
1	34.695	0.000	34.695	1.000
2	34.695	1.000	35.320	1.000
3	34.695	57.269	35.320	57.269
4	34.695	118.000	35.320	118.000
5	34.695	119.000	35.320	119.000
6	34.695	118.000	34.695	119.000
7	34.695	121.120	35.320	121.120
8	34.695	121.120	34.695	122.000
9	0.000	0.000	0.000	1.000
10	0.000	114.000	0.000	119.000
11	0.000	119.000	0.000	122.000

Table 2.6.13.3-1 Linearized Stresses in the Yankee-MPC Canister - Thermal Only (Condition 2)

Section No.	Q Stresses (psi)						Principal Stresses (psi)			S.I. (psi)
	SX	SY	SZ	SXY	SYZ	SXZ	S1	S2	S3	
1	89.9	278.7	782.4	22.8	13.7	-52.3	786.6	281.3	83.1	703.5
2	-76.6	-485.6	376.6	35.1	2.8	-35.5	379.4	-76.4	-488.6	868.0
3	-76.6	1374.0	-532.6	0.1	-0.3	13.7	1374.0	-76.2	-533.0	1907.0
4	254.4	-1722.0	-1224.0	-174.8	-19.8	111.8	278.3	-1232.0	-1738.0	2016.0
5	-339.4	102.5	-818.1	-27.0	11.5	-34.3	104.4	-338.7	-820.7	925.0
6	386.1	1361.0	-178.7	-81.8	1.7	38.1	1368.0	381.8	-181.3	1549.0
7	-652.7	1073.0	-18.4	0.0	62.9	0.0	1077.0	-22.0	-652.7	1730.0
8	-568.3	156.3	84.5	89.8	-6.6	47.3	167.3	87.9	-582.7	750.0
9	-5120.0	-2081.0	-5059.0	6.5	-210.8	62.4	-2066.0	-5030.0	-5164.0	3097.0
10	-9.6	1020.0	-211.7	-3.9	30.1	21.0	1021.0	-7.4	-214.6	1235.0
11	435.2	1412.0	226.1	23.1	-65.6	26.7	1416.0	438.3	218.8	1197.0

2.6.13.4 Stress Evaluation of the Yankee-MPC Canister for 1-Foot End Drop Load Condition

A structural analysis is performed using ANSYS to evaluate the effect of a 1-foot end drop impact for both the bottom and top end orientations of the Yankee-MPC canister. The ASME Code, Section III, NB requires the stresses arising from operational loads be assessed based on the primary loads. The primary loads for the 1-foot drop are due to the deceleration of the canister and its contents (56,000 pounds) and the conservatively assumed 20 psig pressure load internal to the canister. The applied deceleration is 20g for both orientations. The inertial load of the canister is addressed by the deceleration factor applied to the canister density. The fuel weight (30,600 pounds) is represented by a pressure load on the inner end surface of the canister. Displacement constraints are applied to the plane of symmetry and the gap elements attached at the canister end to represent the top or bottom of the transport cask.

To determine the effect of the 20 psig pressure load, the top end and bottom end orientations with and without the pressure load were analyzed. The maximum stresses are summarized below:

Drop Orientation	Internal Pressure (psi)	Maximum Stress Intensity (ksi)
Bottom End Drop	0	4.6
Bottom End Drop	20	3.0
Top End Drop	0	7.6
Top End Drop	20	12.5

It is concluded that the bottom end drop without pressure is limiting for the bottom end drop orientation. For the top end drop, the addition of pressure is limiting.

The location of the linearized stresses is shown in Figure 2.6.13.3-1. The maximum stresses for P_m and $P_m + P_b$ are tabulated in Tables 2.6.13.4-2 through 2.6.13.4-7. The critical sections for the pressure and the pressure plus the deceleration load, with reference to the section and the appropriate tables, are shown in Table 2.6.13.4-1.

Additional analysis is performed for the bottom end drop conditions assuming a maximum gap size of 0.08 inch between the structural lid and shield lid (see Section 2.6.13.2). The minimum margins of safety for P_m and $P_m + P_b$ (see Table 2.6.13.4-1) are +4.93 (at Section No. 8) and +3.84 (at Section No. 7), respectively. The margins of safety in these tables are calculated as: $M.S. = (\text{allowable stress}/S.I.) - 1$.

Table 2.6.13.4-1 Summary of Critical Sections of the Yankee-MPC Canister for the 1-Foot End Drop Condition

Condition	Stress	Critical Section	Table	Minimum Margin of Safety
Pressure (only)	P_m	1	2.6.13.4-2	+ 1.43
Pressure (only)	$P_m + P_b$	2	2.6.13.4-3	+ 0.39
Top End Drop Pressure + Inertia	P_m	1	2.6.13.4-4	+ 2.95
Top End Drop Pressure + Inertia	$P_m + P_b$	2	2.6.13.4-5	+ 1.25
Bottom End Drop Inertia	P_m	8	See Note 1	+ 4.53
Bottom End Drop + Inertia	$P_m + P_b$	7	See Note 1	+ 3.84

Note:

1. The minimum margin of safety for the bottom end drop condition is based on the analysis considering the maximum gap of 0.08 inch between the structural lid and shield lid.

Table 2.6.13.4-2 Internal Pressure Only (20 psi) – Yankee-MPC Canister Primary Membrane Stresses (psi)

Section No.	P _m Stresses						Principal Stresses			S.I.	S _m Allow. Stress	Margin of Safety
	SX	SY	SZ	SXY	SYZ	SXZ	S1	S2	S3			
1	-1104.0	5051.0	1657.0	1170.0	533.2	-168.1	5333.0	1613.0	-1342.0	6675.0	16250.0	1.43
2	2664.0	-2093.0	-1670.0	-1001.0	165.0	-258.0	2884.0	-1668.0	-2314.0	5198.0	16250.0	2.13
3	4.9	550.0	1106.0	0.0	0.0	87.4	1113.0	550.0	-2.0	1115.0	16250.0	13.57
4	209.6	379.2	383.3	-142.6	-12.2	-17.0	460.4	385.0	126.8	333.6	16250.0	47.71
5	-437.2	327.2	269.9	-19.3	-2.5	48.4	327.9	272.9	-441.0	768.9	16250.0	20.13
6	-84.6	-378.3	118.7	-11.7	-14.6	18.0	120.7	-85.8	-379.1	499.9	16250.0	31.51
7	426.5	-125.8	146.4	-22.9	-2.9	13.1	428.1	145.8	-126.8	554.9	16250.0	28.28
8	-68.5	420.6	135.7	62.7	-7.7	16.8	428.6	137.1	-77.8	506.4	10400.0*	19.54
9	677.2	-15.6	676.7	189.9	-981.0	-0.2	1388.0	677.1	-726.9	2115.0	16250.0	6.68
10	-26.2	8.7	-22.9	-8.4	13.8	-1.2	15.5	-26.1	-29.8	45.3	19350.0	426.25
11	73.0	0.6	72.9	0.2	-0.3	0.0	73.0	72.9	0.6	72.3	16250.0	223.63

* Includes two stress reduction factors for weld: $0.8 \times 0.8 = 0.64$ (See Section 2.6.13.12).

Table 2.6.13.4-3 Internal Pressure Only (20 psi) – Yankee-MPC Canister Primary Membrane Plus Primary Bending Stresses (psi)

Section No.	P _m + P _b Stresses						Principal Stresses			S.I.	1.5 S _m Allow. Stress	Margin of Safety
	SX	SY	SZ	SXY	SYZ	SXZ	S1	S2	S3			
1	-7041.0	331.6	676.6	1704.0	661.0	-357.5	1274.0	138.7	-7446.0	8720.0	24375.0	1.80
2	1390.0	-15890.0	-6275.0	1254.0	7.0	559.8	1521.0	-6315.0	-15980.0	17500.0	24375.0	0.39
3	0.0	551.5	1118.0	-2.6	-0.2	-88.7	1125.0	551.5	-7.0	1132.0	24375.0	20.53
4	154.5	213.3	312.5	-193.2	-14.1	-15.4	379.3	313.8	-12.9	392.2	24375.0	61.15
5	-251.0	2063.0	855.3	-105.9	-4.7	-78.9	2068.0	860.9	-261.5	2330.0	24375.0	9.46
6	-569.9	-1205.0	-233.8	-131.7	-10.5	23.1	-231.8	-545.6	-1231.0	999.0	24375.0	23.40
7	650.3	1548.0	-52.3	0.1	-34.6	0.0	1549.0	650.3	-53.0	1602.0	24375.0	14.22
8	-587.5	235.5	-104.6	80.7	-9.9	32.8	243.5	-102.4	-597.6	841.1	15600.0*	17.55
9	16730.0	1006.0	16720.0	189.9	-980.7	222.1	16970.0	16540.0	942.3	16030.0	24375.0	0.52
10	-1202.0	-48.9	-1194.0	-5.3	14.4	-5.7	-48.7	-1191.0	-1205.0	1156.0	29025.0	24.11
11	130.7	3.9	130.6	-0.2	0.1	0.2	130.8	130.4	3.9	126.9	24375.0	191.08

* Includes two stress reduction factors for weld: $0.8 \times 0.8 = 0.64$ (See Section 2.6.13.12).

Table 2.6.13.4-4 Top End Drop: 1-ft. Drop + Internal Pressure (20 psi) - Yankee-MPC Canister Primary Membrane Stresses (psi)

Section No.	P _m Stresses						Principal Stresses			S.I.	S _m	
	SX	SY	SZ	SXY	SYZ	SXZ	S1	S2	S3		Allow. Stress	Margin of Safety
1	-683.1	3107.0	1031.0	723.2	334.6	-105.1	3283.0	1003.0	-831.1	4114.0	16250.0	2.95
2	1662.0	-1303.0	-973.3	615.2	102.9	155.2	1795.0	-973.1	-1436.0	3231.0	16250.0	4.03
3	1.9	7.3	1105.0	0.0	0.0	-87.5	1112.0	7.3	-5.0	1117.0	16250.0	13.55
4	98.4	-443.9	-17.7	46.0	-9.1	-6.0	102.7	-17.9	-448.0	550.7	16250.0	28.51
5	-44.0	-400.2	-36.0	0.0	-23.4	0.0	-34.5	-44.0	-401.7	367.2	16250.0	43.25
6	23.0	-201.0	-14.8	0.0	-15.7	0.0	23.0	-13.5	-202.3	225.3	16250.0	71.13
7	10.2	-357.3	-25.4	11.0	-7.1	1.5	10.5	-25.3	-357.8	368.3	16250.0	43.12
8	5.0	-257.4	-7.8	0.0	-11.0	0.0	5.0	-7.3	-257.9	262.9	10400.0*	38.56
9	431.4	-17.3	432.2	199.8	-597.3	-0.2	876.2	431.3	-461.3	1337.0	16250.0	11.15
10	0.7	-233.0	3.2	-1.0	2.1	-0.2	3.3	0.7	-233.0	236.3	19350.0	80.89
11	-9.8	-263.2	0.8	-0.8	-2.0	-0.7	0.9	-9.8	-263.2	264.1	16250.0	60.53

* Includes two stress reduction factors for weld: $0.8 \times 0.8 = 0.64$ (See Section 2.6.13.12).

Table 2.6.13.4-5 Top End Drop: 1-ft. Drop + Internal Pressure (20 psi) - Yankee-MPC Canister Primary Membrane Plus Primary Bending Stresses (psi)

Section No.	P _m + P _b Stresses						Principal Stresses			S.I.	1.5 S _m	
	SX	SY	SZ	SXY	SYZ	SXZ	S1	S2	S3		Allow. Stress	Margin of Safety
1	-4384.0	198.5	371.7	1057.0	415.0	-220.7	768.3	52.5	-4635.0	5403.0	24375.0	3.51
2	861.9	-9812.0	-3818.0	770.9	3.2	340.4	941.6	-3842.0	-9867.0	10810.0	24375.0	1.25
3	-3.0	8.7	1117.0	-1.6	-0.2	-88.8	1124.0	8.8	-10.1	1134.0	24375.0	20.49
4	72.0	-940.5	-176.8	57.7	-9.0	-17.0	76.5	-177.9	-943.8	1020.0	24375.0	22.90
5	-11.9	-443.8	-59.4	33.0	-10.1	-5.0	-8.7	-59.9	-446.5	437.8	24375.0	54.68
6	-56.8	-370.6	-104.1	0.0	-12.3	0.0	-56.8	-103.6	-371.2	314.3	24375.0	76.55
7	-1.2	-394.9	-43.9	-4.6	-6.9	-0.5	-1.2	-43.8	-395.1	394.0	24375.0	60.87
8	-5.3	-295.0	-1.0	0.0	-17.5	0.0	0.0	-5.3	-296.0	296.0	15600.0*	51.70
9	10210.0	608.9	0.1	200.1	-597.1	100.1	10300.0	10130.0	567.4	9736.0	24375.0	1.50
10	35.9	-233.3	39.3	-0.3	4.3	0.2	39.3	35.9	-233.4	272.7	29025.0	105.44
11	-4.3	-263.5	3.6	1.3	3.7	0.0	3.7	-4.3	-263.5	267.2	24375.0	90.22

* Includes two stress reduction factors for weld: $0.8 \times 0.8 = 0.64$ (See Section 2.6.13.12).

Table 2.6.13.4-6 Bottom End Drop: 1-ft. Drop + Internal Pressure (0 psi) - Yankee-MPC Canister Primary Membrane Stresses (psi)

Section No.	P _m Stresses						Principal Stresses			S.I.	S _m Allow. Stress	Margin of Safety
	SX	SY	SZ	SXY	SYZ	SXZ	S1	S2	S3			
1	-25.3	-704.5	-129.2	63.1	25.1	8.0	-18.5	-129.1	-711.3	692.8	16250.0	22.46
2	103.7	-1854.0	-422.7	32.7	19.4	33.8	106.4	-424.7	-1855.0	1961.0	16250.0	7.29
3	0.8	-1740.0	0.3	0.0	0.1	0.0	0.8	0.3	-1740.0	1741.0	16250.0	8.33
4	-760.4	-800.7	-389.0	0.0	263.2	0.0	-260.7	-760.4	-929.1	668.4	16250.0	23.31
5	905.9	-756.4	-546.9	-107.1	0.2	99.9	919.5	-553.5	-763.5	1683.0	16250.0	8.66
6	196.5	704.2	-233.2	5.1	30.5	-37.5	705.2	199.7	-237.4	942.6	16250.0	16.24
7	-1072.0	339.2	-546.8	-127.7	13.9	19.5	350.9	-546.2	-1084.0	1435.0	16250.0	10.32
8	207.7	-1240.0	-718.6	162.8	42.2	74.7	232.4	-723.0	-1260.0	1493.0	10400.0*	5.97
9	29.5	-243.2	33.7	2.3	20.8	-0.2	35.3	29.5	-244.7	280.0	16250.0	57.04
10	70.7	23.7	69.5	16.0	-20.2	0.7	80.9	71.0	12.1	68.8	19350.0	280.17
11	-161.1	50.4	-157.0	16.1	-39.4	-1.4	58.9	-161.5	-165.1	223.9	16250.0	71.58

* Includes two stress reduction factors for weld: $0.8 \times 0.8 = 0.64$ (See Section 2.6.13.12).

Table 2.6.13.4-7 Bottom End Drop: 1-ft. Drop + Internal Pressure (0 psi) - Yankee-MPC Canister Primary Membrane Plus Primary Bending Stresses (psi)

Section No.	P _m + P _b Stresses						Principal Stresses			S.I.	1.5 S _m Allow. Stress	Margin of Safety
	SX	SY	SZ	SXY	SYZ	SXZ	S1	S2	S3			
1	142.5	-957.2	-136.2	45.1	24.2	13.3	145.1	-136.2	-959.7	1105.0	24375.0	21.06
2	-711.1	-2701.0	30.4	0.0	-11.5	0.0	30.5	-711.1	-2701.0	2731.0	24375.0	7.93
3	0.8	-1741.0	1.0	0.4	0.1	0.0	1.053	0.8	-1741.0	1742.0	24375.0	12.99
4	-808.8	-1111.0	-254.6	0.0	290.6	0.0	-165.3	-808.8	-1200.0	1035.0	24375.0	22.55
5	522.1	-3735.0	-1569.0	111.2	1.6	147.5	535.4	-1580.0	-3738.0	4273.0	24375.0	4.70
6	1194.0	1910.0	344.1	288.9	19.6	-60.7	2012.0	1097.0	338.7	1674.0	24375.0	13.56
7	-838.6	2970.0	331.1	-166.6	14.8	69.5	2977.0	335.2	-850.0	3827.0	24375.0	5.37
8	1555.0	-560.8	-178.8	213.3	56.8	122.6	1586.0	-183.1	-587.0	2173.0	15600.0*	6.18
9	37.6	-244.7	35.9	2.9	21.5	-0.6	38.0	37.2	-246.4	284.4	24375.0	84.71
10	2529.0	140.9	2515.0	13.6	-17.2	12.0	2536.0	2508.0	140.7	2395.0	29025.0	11.12
11	-1383.0	-19.4	-1389.0	14.6	-41.9	-6.1	-17.9	-1380.0	-1393.0	1375.0	24375.0	16.73

* Includes two stress reduction factors for weld: $0.8 \times 0.8 = 0.64$ (See Section 2.6.13.12).

THIS PAGE INTENTIONALLY LEFT BLANK

2.6.13.5 Stress Evaluation of the Yankee-MPC Canister for Thermal Plus a 1-Foot End Drop Load Condition

The thermal expansion loads described in Section 2.6.13.3 are applied in conjunction with the primary loads in Section 2.6.13.4 to produce a combined thermal expansion plus end impact loading. The stress evaluation is performed according to the ASME Code, Section III, Subsection NB. Based on the results in Section 2.6.13.4, the pressure is included with the inertia loading for the top end drop. For the bottom end drop, the pressure is not considered in order to produce the smallest margins. The most critical sections are listed in Table 2.6.13.5-1 and 2.6.13.5-2. The stresses reported in this table correspond to the nodal stress at the surface. The minimum margin of safety is +3.33 when $3 S_m$ is used as the stress criteria. It is clear from the table that all of the stress intensities are less than $1.5 S_m$, so the stress intensity range criterion of $3.0 S_m$ is satisfied. The margins of safety are calculated as: $M.S. = (\text{allowable stress}/S.I.) - 1$.

Table 2.6.13.5-1 Yankee-MPC Canister Bottom End Drop: 1-ft. Drop + Internal Pressure (0 psi) + Thermal (cold) (psi)

Section No.	$P_m + P_b + Q$ Stresses						Principal Stresses			S.I.	3 S_m Allow. Stress	Margin of Safety
	SX	SY	SZ	SXY	SYZ	SXZ	S1	S2	S3			
1	-362.7	-390.4	485.1	-110.5	35.3	57.0	489.9	-265.7	-492.1	982.0	48750.0	48.64
2	93.2	-4076.0	-653.9	85.0	22.6	49.6	98.2	-657.1	-4078.0	4176.0	48750.0	10.67
3	112.2	-3128.0	-1243.0	0.1	0.3	-81.8	117.2	-1248.0	-3128.0	3245.0	48750.0	14.02
4	118.2	-3626.0	-2174.0	-66.7	-5.4	-177.6	133.1	-2188.0	-3628.0	3761.0	48750.0	11.96
5	468.8	-3854.0	-2210.0	41.3	-18.6	-194.2	483.2	-2224.0	-3855.0	4338.0	48750.0	10.24
6	344.6	1651.0	-694.2	-282.5	27.6	84.3	1709.0	293.9	-702.1	2411.0	48750.0	19.22
7	-665.0	2034.0	25.0	96.2	3.6	-33.3	2038.0	26.6	-670.0	2708.0	48750.0	17.00
8	1029.0	-397.2	-362.8	-120.6	66.4	-97.5	1046.0	-328.1	-449.6	1496.0	31200.0*	19.86
9	-5218.0	-2696.0	-5209.0	-3.2	51.1	68.6	-2695.0	-5145.0	-5283.0	2588.0	48750.0	17.84
10	-2483.0	718.4	-2668.0	20.5	-52.6	10.8	719.3	-2482.0	-2670.0	3389.0	58050.0	16.13
11	-3704.0	-1983.0	-3642.0	22.9	96.4	19.7	-1977.0	-3643.0	-3710.0	1733.0	48750.0	27.13

* Includes two stress reduction factors for weld: $0.8 \times 0.8 = 0.64$ (See Section 2.6.13.12).

Table 2.6.13.5-2 Yankee-MPC Canister Top End Drop: 1-ft. Drop + Internal Pressure (20 psi) + Thermal (cold) (psi)

Section No.	$P_m + P_b + Q$ Stresses						Principal Stresses			S.I.	3 S_m Allow. Stress	Margin of Safety
	SX	SY	SZ	SXY	SYZ	SXZ	S1	S2	S3			
1	-4572.0	171.1	793.8	1088.0	436.4	-269.6	1033.0	191.8	-4832.0	5865.0	48750.0	7.31
2	783.6	-10270.0	-3431.0	804.1	6.1	304.0	863.2	-3452.0	-0.1	11190.0	48750.0	3.36
3	112.9	-1374.0	-146.4	-1.7	0.1	-6.8	113.1	-146.5	-1374.0	1488.0	48750.0	31.76
4	485.2	-2765.0	-1075.0	474.6	-48.6	-114.3	561.8	-1083.0	-2834.0	3395.0	48750.0	13.36
5	-1740.0	-3805.0	-1358.0	0.0	382.8	0.0	-1299.0	-1740.0	-3864.0	2565.0	48750.0	18.01
6	-1420.0	-3327.0	-1626.0	407.6	0.9	28.4	-1334.0	-1628.0	-3411.0	2077.0	48750.0	22.47
7	775.6	-5663.0	-1230.0	31.3	-27.1	-138.2	785.3	-1240.0	-5663.0	6449.0	48750.0	6.56
8	51.3	-132.1	-1047.0	0.0	-148.5	0.0	51.3	-108.6	-1071.0	1122.0	31200.0*	26.81
9	-10390.0	832.9	-10350.0	182.6	-460.5	-32.7	854.9	-10350.0	-10410.0	11260.0	48750.0	3.33
10	305.0	478.7	120.0	-8.3	-55.5	20.9	487.8	306.2	109.7	378.2	58050.0	152.49
11	-2044.0	-2872.0	-1970.0	0.3	-13.0	28.9	-1960.0	-2054.0	-2872.0	912.2	48750.0	52.44

* Includes two stress reduction factors for weld: $0.8 \times 0.8 = 0.64$ (See Section 2.6.13.12).

2.6.13.6 Stress Evaluation of the Yankee-MPC Canister for a 1-Foot Side Drop Load Condition

The determination of the stresses in the canister due to a 1-foot side drop is accomplished using ANSYS. In the local regions of the lids and bottom plate, the loads are transmitted through the canister shell into the cask body inner shell. Outside of the lid and bottom plate regions, stress develops in the canister shell as a result of the basket loading the canister wall. The basket, canister and cask body have different radii which implies that the contact angle between the components is dependent on the loading. For this reason, the finite element model described in Section 2.6.13.2 contains a half model of the basket. Gap elements between the basket and the canister allow the interface to be dependent on the loading. The interface between the canister and the cask body inner shell is also represented by gap elements.

The load due to the contents is applied to the basket via pressure acting in the plane of the disks. The weight is assumed to act over the effective width of 8.254 inches in which the disk is .5 inches thick. The content weight includes the 900 pounds per fuel assembly (for 36 fuel assemblies) plus the fuel tube weight (58.6 pounds). This weight is distributed over the 22 support disks plus two end weldments. A deceleration factor of 20g is applied to the load and the pressure per slot is computed as:

$$(900+58.6)(20) / [(8.254)(.5)(24)] \text{ psi} = 193.6 \text{ psi}$$

The 45° circumferential orientation of the basket is the configuration that results in the greatest distortion of the canister. This requires that both sides of the slots be loaded and factored by .707. This loading differs from the loading used in the basket analysis since the purpose of this loading in the canister model is to obtain the overall deflection of the basket. In addition to the contents load, a 20 psig pressure is conservatively applied to the inner surface of the canister.

The methodology used to evaluate the stresses for this condition is taken from Section 2.6.13.4 and the location of the sections are identified in Figure 2.6.13.3-1. The critical section stresses are reported in Table 2.6.13.6-1 and Table 2.6.13.6-2 for P_m and $P_m + P_b$ stresses, respectively. The minimum margin of safety for the canister in the side drop, assuming the minimum gap size, (Section 2.6.13.2) is +0.04, which occurs at Section 1 in Figure 2.6.13.3-1.

The minimum margin of safety for P_m assuming a maximum gap of 0.08 inches, is +0.16, at Section 6, and for $P_m + P_b$ it is +0.12 at Section 1. The margins of safety are calculated as: $M.S. = (\text{allowable stress}/S.I.) - 1$.

Table 2.6.13.6-1 Yankee-MPC Canister Side Drop: 1-ft. Drop + Internal Pressure (20 psi) - Primary Membrane Stresses (psi)

Section No.	P _m Stresses						Principal Stresses			S.I.	S _m	
	SX	SY	SZ	SXY	SYZ	SXZ	S1	S2	S3		Allow. Stress	Margin of Safety
1(0°)	-10227.0	856.0	-4685.1	375.9	199.7	-908.3	873.9	-4543.6	-10386.4	11262.0	16250	0.44
2(0°)	5431.7	1884.3	-732.0	-276.8	-292.7	-442.5	5481.0	1902.2	-800.0	6281.1	16250	1.59
3(0°)	-692.7	765.9	1360.0	4.7	-5.3	114.9	1367.4	765.9	-699.1	2065.7	16250	6.87
4(9°)*	-292.6	2090.9	659.1	159.2	1019.3	427.2	2660.3	279.9	-482.3	3142.7	16250	4.17
5(0°)	-9019.0	-32.9	-3701.6	-1049.6	954.2	-599.5	345.1	-3914.4	-9184.7	9529.7	16250	0.71
6(0°)	-15561.2	-2614.2	-4803.6	-1996.5	811.3	-748.8	-2010.2	-5071.0	-15896.8	13883.5	16250	0.17
7(9°)*	1925.2	1097.9	814.8	69.9	485.8	-45.5	1931.5	1460.7	446.1	1484.8	16250	9.94
8(0°-4.5°)	-10240.0	-2130.0	-3090.0	-490.0	750.0	-1260.0	-1574.5	-3351.3	-10544.7	8880.0	10400**	0.17
9	-478.9	-198.6	806.7	71.4	22.0	-22.2	807.5	-181.7	-496.6	1304.5	16250	11.46
10	-425.3	-1.7	78.9	-25.7	6.7	-10.9	79.7	-0.7	-427.1	506.8	19350	37.18
11	-382.5	-2.7	174.5	-16.4	2.8	-13.3	174.9	-2.1	-383.6	558.5	16250	28.10

* See bearing stress calculation for section stress at 0°.

** Includes two stress reduction factors for weld: $0.8 \times 0.8 = 0.64$ (See Section 2.6.13.12).

Table 2.6.13.6-2 Yankee-MPC Canister Side Drop: 1-ft. Drop + Internal Pressure (20 psi) - Primary Membrane Plus Primary Bending Stresses (psi)

Section No.	P _m + P _b Stresses						Principal Stresses			S.I.	1.5 S _m	
	SX	SY	SZ	SXY	SYZ	SXZ	S1	S2	S3		Allow. Stress	Margin of Safety
1(0°)	-26047.2	-2107.7	-10104.3	413.8	217.7	-1116.8	-2095.1	-10030.9	-26131.1	24044.4	25000**	0.04
2(90°)	-4429.3	-11241.0	1092.6	364.4	886.8	-75.4	1156.6	-4409.4	-11324.9	12478.3	24375	0.95
3(0°)	-759.6	1198.5	2829.1	7.8	-5.9	227.3	2842.8	1198.5	-774.0	3617.7	24375	5.74
4(9°)*	599.0	4274.1	2236.7	208.0	755.2	1088.4	4603.4	2456.9	50.1	4553.0	24375	4.35
5(0°)	-11146.6	26.7	-3044.1	-1644.2	728.4	-827.9	466.5	-3185.6	-11450.7	11912.1	24375	1.05
6(0°)	-19996.8	-4548.8	-6797.0	-2643.5	1026.7	-594.2	-3707.8	-7185.0	-20447.7	16735.7	24375	0.46
7(9°)*	2385.6	321.5	419.3	86.5	664.6	-648.9	1677.8	651.1	-962.1	2639.3	24375	8.24
8(0°-4.5°)	-13310.0	-3190.0	-4740.0	-1000.0	1090.0	980.0	-2460.0	-5252.4	-13526.9	10930.0	15600***	0.43
9	-956.6	-172.7	869.4	75.4	9.5	10.3	869.6	-165.6	-963.9	1833.0	24375	12.30
10	-1095.8	-29.5	-493.6	-25.3	7.2	-18.4	-28.7	-493.2	-1096.8	1068.5	29025	26.16
11	-814.4	-19.7	-190.1	-16.0	3.0	-15.9	-19.4	-189.8	-815.2	795.8	24375	29.63

* See bearing stress calculation for section stress at 0°.

** Allowable stress taken at 225°. Refer to page 2.6.13.3-1

*** Includes two stress reduction factors for weld: $0.8 \times 0.8 = 0.64$ (See Section 2.6.13.12).

2.6.13.7 Stress Evaluation of the Yankee-MPC Canister for Thermal Plus a 1-Foot Side Drop Load Condition

The thermal expansion loads described in Section 2.6.13.3 are applied in conjunction with the primary loads in Section 2.6.13.6 to produce a combined thermal expansion plus 1-foot side drop loading. The stress evaluation is performed according to the ASME Code, Section III, Subsection NB. The most critical sections are listed in Table 2.6.13.7-1. The stresses reported in this table correspond to the nodal stress at the surface. The minimum margin is +0.75 at location 4 (see Figure 2.6.13.3-1) when $3 S_m$ is used as the stress criteria. The calculated stress intensity for each section location except No. 4 is less than $1.5 S_m$, so the P+Q stress limit is satisfied as discussed in Section 2.6.7.1. For section no. 4, the P+Q stress intensity is calculated conservatively by combining the bottom end drop condition stress intensity with that of the side drop as: $|3761.0 + 27892.8| = 31,653.8$ psi, which is less than $3 S_m = 48750$ psi, so the criteria is satisfied. The margins of safety are calculated as: $M.S. = (\text{allowable stress}/S.I.) - 1$.

Table 2.6.13.7-1 Yankee-MPC Canister Side Drop: 1-ft. Drop + Internal Pressure (20 psi) + Thermal (cold) (psi)

Section No.	P _m + P _b + Q Stresses						Principal Stresses			S.I.	3 S _m Allow. Stress	Margin of Safety
	SX	SY	SZ	SXY	SYZ	SXZ	S1	S2	S3			
1(0°)	-23971.0	-2690.7	-6679.6	65.7	335.6	-1001.4	-2663.4	-6650.2	-24033.9	21370.5	48750	1.28
2(90°)	-4942.1	-12352.5	1044.5	-93.3	972.2	-35.4	1114.7	-4941.0	-12415.4	13537.4	48750	2.60
3(0°)	-621.9	-4204.9	-6819.0	-1.4	-7.2	-449.7	-589.4	-4204.9	-6851.6	6262.2	48750	6.78
4(0°)	-21999.6	5747.4	-7234.3	-184.1	1304.5	322.8	5877.4	-7357.0	-22010.1	27892.8	48750	0.75
5(0°)	-11241.0	-904.7	-3601.9	-1774.2	672.4	-1122.0	-379.1	-3707.8	-11660.4	11282.9	48750	3.32
6(0°)	-20269.4	-4268.9	-6936.5	-2993.8	1044.4	-800.3	-3344.0	-7294.1	-20846.2	17501.1	48750	1.79
7(0°)	-15403.9	619.3	-5682.4	82.0	1114.7	47.0	811.0	-5873.2	-15403.9	16211.4	48750	2.01
8(0°)	-14690.9	-3475.1	-4428.2	-1008.3	1114.7	-834.8	-2599.5	-5162.3	-14837.7	12237.2	31200*	1.55
9	-5518.8	-2656.1	-4895.9	-42.9	60.8	77.8	-2653.0	-4888.6	-5529.3	2876.3	48750	15.95
10	-2743.1	-1511.0	-1608.6	-20.3	-62.2	-6.1	-1480.6	-1639.0	-2743.1	1262.5	58050	44.98
11	153.9	1367.4	576.6	10.5	-29.2	15.3	1368.4	576.1	153.3	1215.3	48750	39.11

* Includes two stress reduction factors for weld: $0.8 \times 0.8 = 0.64$ (See Section 2.6.13.12).

2.6.13.8 Yankee-MPC Canister Shear Stresses for a 1-Foot Side Drop and a 1-Foot End Drop Condition

The evaluation of the maximum shear stress utilizes the membrane values of the stress intensity due to primary loading which were evaluated for the pressure, end drops and side drop loading. The maximum membrane stress intensity is 13.88 ksi for location 6 (Table 2.6.13.6-1). Using a bounding temperature of 338°F, the S_m for Type 304L stainless steel is 16.36 ksi, the margin of safety is determined by:

$$M.S. = (0.6)(16.36)/(13.88/2) - 1$$

$$M.S. = +.41$$

THIS PAGE INTENTIONALLY LEFT BLANK

2.6.13.9 Yankee-MPC Canister Bearing Stresses for a 1-Foot Side Drop

The bearing stress of the canister on the cask inner shell is evaluated in the region of the canister lids and over the length of the canister shell. The bearing stress associated with the lids is calculated using the membrane S_x stress at Section 7 (see Figure 2.6.13.3-1). The S_x stress component, associated with the radial direction at the plane of symmetry of the canister, is 20.3 ksi based on the finite element evaluation (Section 2.6.13.6). The bearing stress allowable is S_y for the operational condition. Using a bounding temperature of 206°F, $S_y=21.5$ ksi. The margin of safety is:

$$M.S. = (21.5/20.3)-1$$

$$M.S. = + 0.06$$

For the bearing stress acting along the inner shell, an angular contact of 18 degrees is assumed (at a radius of 35.5 inches). In this bearing stress, the lids are not considered to be a contributor. This reduces the contents weight to 56,000-10,000 = 46,000 pounds = 46 kips. For a basket length of 98 inches (removing the lengths of both weldments and the first spacer), the margin for the bearing stress is computed as:

$$S_{br} = (46.0)(20)/[(98)(35.5)(18/57.2958)]$$
$$= 1.09 \text{ ksi}$$

$$M.S. = (18.55/S_{br}) - 1 = +21$$

$$M.S. = + \text{Large}$$

THIS PAGE INTENTIONALLY LEFT BLANK

2.6.13.10 Yankee-MPC Canister Buckling Evaluation for 1-Foot End Drop

The Yankee-MPC canister shell is axially loaded by the weights of the structural lid, the shield lid, and the inertial weight of the shell during a 1-foot end drop impact. The impact load amplification factor is 20g. The shell is evaluated as an unsupported, right circular cylinder using a critical buckling load per Blake, 2nd Edition, "Practical Stress Analysis in Engineering Design":

$$S_{cr} = \frac{E(0.605 - 10^{-7} M^2)}{M(1 + 0.004\phi)}$$
$$= 40.3 \text{ ksi}$$

Where the canister material is Type 304L stainless steel, conservatively assumed to be at 400°F for normal operation, and:

$$E = 26.5 \text{ E03 ksi} \quad R = (69.39 + 0.625)/z = 35.01 \text{ in.}$$
$$S_y = 17.5 \text{ ksi} \quad t = 0.625 \text{ in.}$$

$$\phi = \frac{E}{S_y} = 1514.3 \quad M = \frac{R}{t} = 56.0$$

The axial compression load in the canister shell is:

$$P_A = \left[\left(\frac{\pi}{4} \right) (69.03)^2 (0.291)(8) + \left(\frac{\pi}{4} \right) (70.64^2 - 69.39^2) (121.5)(0.291) \right] (20)$$
$$= 271,464 \text{ pounds}$$

and the axial compression stress is:

$$S_A = \frac{P_A}{\left(\frac{\pi}{4} \right) (70.64^2 - 69.39^2)} = 1,975 \text{ psi}$$

Then, the margin of safety for canister shell buckling is:

$$M.S. = \frac{S_{cr}}{S_A} - 1 = +19.4$$

Page 10

1. The first of these is the fact that the

the second of these is the fact that the

the third of these is the fact that the

the fourth of these is the fact that the

the fifth of these is the fact that the

the sixth of these is the fact that the

the seventh of these is the fact that the

the eighth of these is the fact that the

the ninth of these is the fact that the

the tenth of these is the fact that the

the eleventh of these is the fact that the

the twelfth of these is the fact that the

the thirteenth of these is the fact that the

the fourteenth of these is the fact that the

the fifteenth of these is the fact that the

the sixteenth of these is the fact that the

the seventeenth of these is the fact that the

the eighteenth of these is the fact that the

the nineteenth of these is the fact that the

the twentieth of these is the fact that the

THIS PAGE INTENTIONALLY LEFT BLANK

2.6.13.11 Yankee-MPC Canister Lifting Evaluation

The lifting of the Yankee-MPC canister is accomplished by attaching vendor qualified eyehooks to six locations in the structural lid. During the lifting of the canister, the contents weight of 40,130 pounds is transmitted to the canister bottom and up through the canister 0.625-inch thick shell. A pressure load of 11.3 psig is also applied to the canister during normal operations. The evaluation of this load configuration of the canister is accomplished by a three-dimensional finite element model, as shown in Figure 2.6.13.11-1. This model is essentially the same model presented in Section 2.6.13.2, with the elements for the basket removed. The model is used to evaluate the lower portion of the canister, especially the bottom plate and the junction of the bottom plate and the canister shell. Since the canister is in a vertical position under a lift condition, the model is only restrained at the lift locations at the structural lid. The loads considered in the analysis are internal pressure, dead load with a dynamic load factor of 1.1, and the thermal load. A pressure of 11.5 psig is conservatively applied to represent the operating pressure (the calculated internal pressure is 11.3 psig). The weight of the contents is applied to the bottom plate as a uniform pressure. The 1.1 dynamic load factor is also applied to the contents weight. The thermal stress analysis is performed using the methodology described in Section 2.6.13.3. The temperatures of the key locations considered in the analysis are:

Top center of the structural lid	=	140°F
Top outer diameter of the structural lid	=	100°F
Bottom center of the bottom plate	=	250°F
Bottom outer diameter of the bottom plate	=	130°F
Mid-elevation of the canister shell	=	500°F

The table below shows the temperature differences (ΔT) in the radial and axial directions applied in the model and those calculated by thermal analysis for normal conditions of transport.

	Applied in Model ($\Delta^\circ\text{F}$)	Thermal Analysis Calculation	
		Heat Condition ($\Delta^\circ\text{F}$)	Cold Condition ($\Delta^\circ\text{F}$)
Lid (Radial)	40	14	12
Bottom Plate (Radial)	120	30	29
Shell (Axial)	400	146	160

As shown in the table, the temperature differences in the model envelope the calculated values. Therefore, the thermal stress analysis is conservative.

Allowable stresses at a temperature of 250°F for the lid region, 550°F for the canister shell and 250°F for the bottom plate region, are applied. These temperatures envelope the calculated maximum temperatures of the canister components (see Tables 3.4-1 and 3.4-2) except for the bottom plate, which has a calculated maximum temperature of 255°F for the heat condition of transport. Since the value of design stress intensity (S_m) for SA 240 Type 304L does not change for temperatures below 300°F, the allowable stresses used in this evaluation remain bounding.

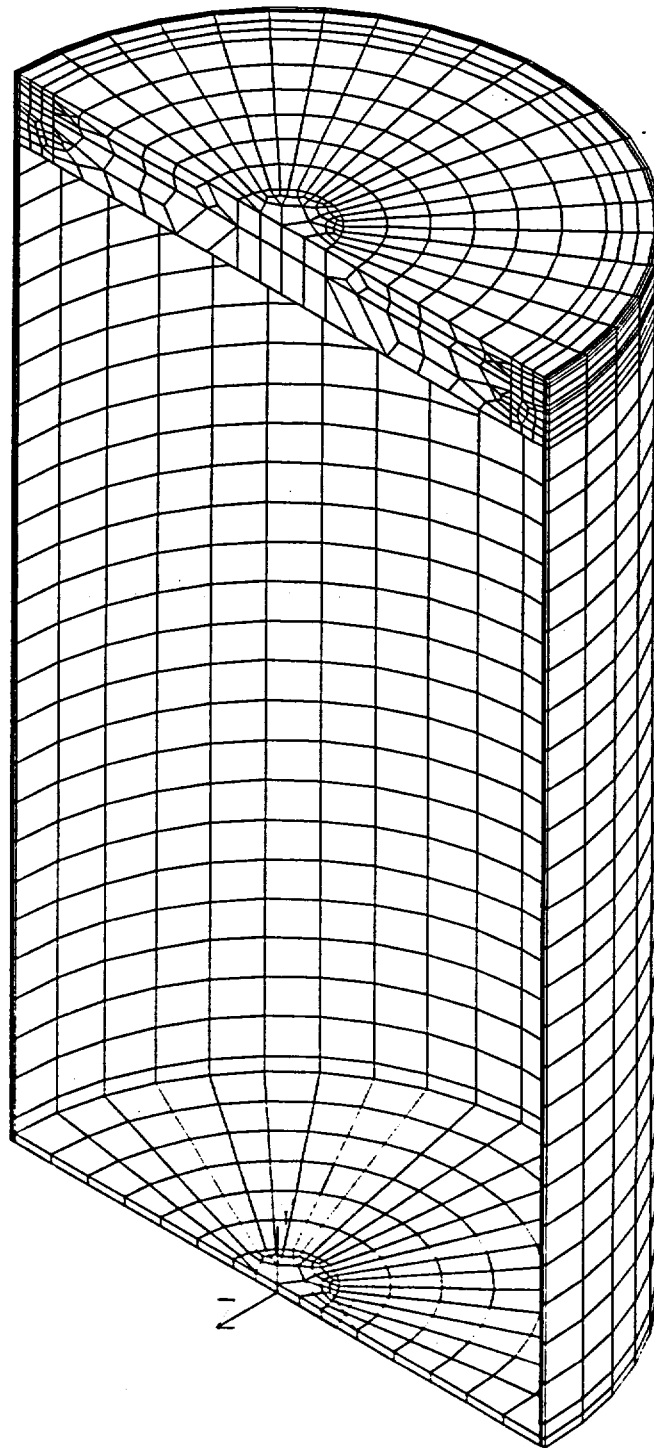
Based on the stress allowables required by the ASME Code, Section III, Subsection NB, the minimum margins of safety are:

Stress Category	Max. Stress (ksi)	Allowable Stress (ksi)	Margin of Safety
P_m	9.47 ¹	16.7	0.76
$P_m + P_b$	20.5 ²	25.05	0.22
$P + Q$	27.74 ¹	50.1	0.81

¹ Maximum stress occurs at the center of bottom plate.

² Maximum stress occurs at junction of the bottom plate and the canister shell.

Figure 2.6.13.11-1 Finite Element Model for Yankee-MPC Canister Lift Evaluation



THIS PAGE INTENTIONALLY LEFT BLANK

2.6.13.12 Yankee-MPC Canister Closure Weld Evaluation – Normal Conditions

2.6.13.12.1 Stress Evaluation for the Yankee-MPC Canister Closure Weld

The closure weld for the Yankee-MPC canister is a partial penetration weld with a thickness of 0.9 inches. The evaluation of this weld, in accordance with NRC guidance, is to incorporate two separate weld stress reduction factors: a 0.8 factor per NRC ISG-4, Item 5, and an additional 0.8 factor to provide conservative consideration of the weld configuration. These two stress reduction factors are incorporated by applying a factor of 0.64 (0.8 x 0.8) to the stress allowable for this weld.

The stresses for the canister are evaluated using sectional stresses as permitted by Subsection NB using the finite element model as described in Section 2.6.13.2. The location of the section for the canister weld evaluation is shown in Figure 2.6.13.3-1 and corresponds to Section 8. The governing P_m , $P_m + P_b$, and $P + Q$ stress intensity for Section 8 for all normal conditions of transport and the associated allowables are listed below. The factored allowables, incorporating a 0.64 stress reduction factor, and the resulting margin of safety are:

Stress Type	Analysis Stress Intensity (ksi)	0.64 x Allowable Stress (ksi)	Margin of Safety
P_m	8.88	10.40	0.17
$P_m + P_b$	10.93	15.60	0.43
$P + Q$	12.24	31.20	1.55

This confirms that the canister closure weld is acceptable for normal conditions of transport.

2.6.13.12.2 Critical Flaw Size for the Yankee-MPC Canister Closure Weld

The closure weld for the Yankee-MPC canister is comprised of multiple weld beads using a compatible weld material for Type 304L stainless steel. An allowable (critical) flaw evaluation has been performed to determine the critical flaw size in the weld region. The result of the flaw evaluation is used to define the minimum flaw size, which must be identifiable in the nondestructive examination of the weld. Due to the inherent toughness associated with Type

304L stainless steel, a limit load analysis is used in conjunction with a J-integral/tearing modulus approach.

The safety margins used in this evaluation correspond to the stress limits contained in Section XI of the ASME Code.

One of the stress components used in the evaluation for the critical flaw size is the radial stress component in the weld region of the structural lid. For the normal operation condition, in accordance with ASME Code Section XI, a safety factor of 3 is required. For the purpose of identifying the stress for the flaw evaluation, the weld region corresponding to Section 8 of Figure 2.6.13.3-1 is considered. The maximum radial tensile stress is 2.2 ksi. To perform the flaw evaluation, a 10 ksi stress is conservatively used, resulting in a significantly larger safety factor than the required safety factor of 3. Using 10 ksi as the basis for the evaluation, the critical flaw size is 0.52 inch for a flaw that extends 360 degrees around the circumference of the canister. Stress components for the circumferential and axial directions are associated with flaws oriented in the radial and horizontal directions, respectively. The maximum stress reported for these components is 1.1 ksi, which is also enveloped by the stress value of 10 ksi for radial stresses. The 360-degree flaw employed for the circumferential direction is considered to be bounding with respect to any partial flaw in the weld, which could occur in the radial and horizontal directions. Therefore, using a minimum detectable flaw size of 3/8 inch is acceptable, since it is less than the very conservatively determined 0.52-inch critical flaw size.

2.6.14 Yankee-MPC Fuel Basket Analysis - Normal Conditions of Transport

The NAC-STC canistered fuel basket for Yankee class fuel is designed to accommodate up to 36 fuel assemblies. The basket is a right cylinder structure and is fabricated with the following components: 36 square fuel tubes, 22 circular support disks, 14 heat transfer disks, 8 tie rods with split spacers, and two end weldment plates. The basket components and their geometry are illustrated in Figure 2.6.14-1 and Figure 2.6.14-2. Each fuel tube has a 7.80-inch square inside dimension, 0.141-inch thick composite wall, and holds the design basis Yankee Class fuel assembly. Figure 2.6.14-3 shows the details of the stainless steel tube with the encased BORAL. The fuel tubes are open at each end; therefore, longitudinal fuel assembly loads are imparted to the cask body and not the fuel basket structure. The fuel assemblies, together with the tubes are laterally supported in the holes in the stainless steel support disks. Each support disk is 0.5 inches thick, 69.15 inches in diameter and has 37 holes that are each 8.254 inches square. There are three web thicknesses in the support disks; 0.875 inch, 0.810 inch, and 0.75 inch. The widest web is nearest the center of the basket, the web decreases in width towards the outer radius of the basket. The support disks are equally spaced at 4.41 inches except for the disk nearest the bottom weldment, which is spaced 6.50 inches from the bottom weldment plate. The weldments are geometrically similar to the support disks and are 1-inch thick and 68.98 inches in diameter. The tie rod has 3.0 inches of 1 1/8-8 UN-2B threads at the upper end of the rod, which corresponds to the top of the basket. Fourteen (14) aluminum heat transfer disks are located at the mid-section of the cavity to fully optimize the passive heat rejection from the package. Each heat transfer disk is 0.50-inch thick, 68.87 inches in diameter, and has 37 holes that are 8.224 inches square. There are three different web widths, 0.905 inches, 0.84 inches and 0.78 inches. The widest aluminum web is nearest the center of the basket to optimize passive heat rejection. The dimensional differences between the heat transfer disk and the support disk accommodates the different rate of thermal growth between aluminum and stainless steel preventing interference between the tube, the support disk, and heat transfer disks. The heat transfer disks, which serve no structural function, are supported by the eight tie rods with split spacers. The center hole of the support and heat transfer disks is not accessible as it is blocked by the top end weldment plate, which has only 36 fuel tube positions.

The fuel basket contains the fuel and is laterally supported by the canister shell. The 22 support disks and two (2) end plates are fabricated from 17-4 PH and Type 304 stainless steels, respectively. The 14 heat transfer disks are fabricated from Type 6061-T651 aluminum alloy. The 36 fuel tubes are fabricated from Type 304 stainless steel. The tie rods and spacers are fabricated from Type 304 stainless steel. The stainless steel tubes are not considered to be a

structural component with respect to the disks and are not included in the basket or weldment analyses. The primary function of the split spacers and the threaded top nut is to locate and structurally assemble the support disks, heat transfer disks and the top and bottom weldment plates into an integral assembly. The spacers carry the inertial weight of the support disks, heat transfer disks, one end plate, and their own inertial weight for a normal transport condition 1-foot end drop. The end drop loading of the split spacers and tie rods represent a classical closed form structural analysis. Therefore the only component that requires a detailed finite element analysis is the support disk.

The fuel basket is evaluated for the normal transport loads in this section and is evaluated for the hypothetical accident condition in Section 2.7.9

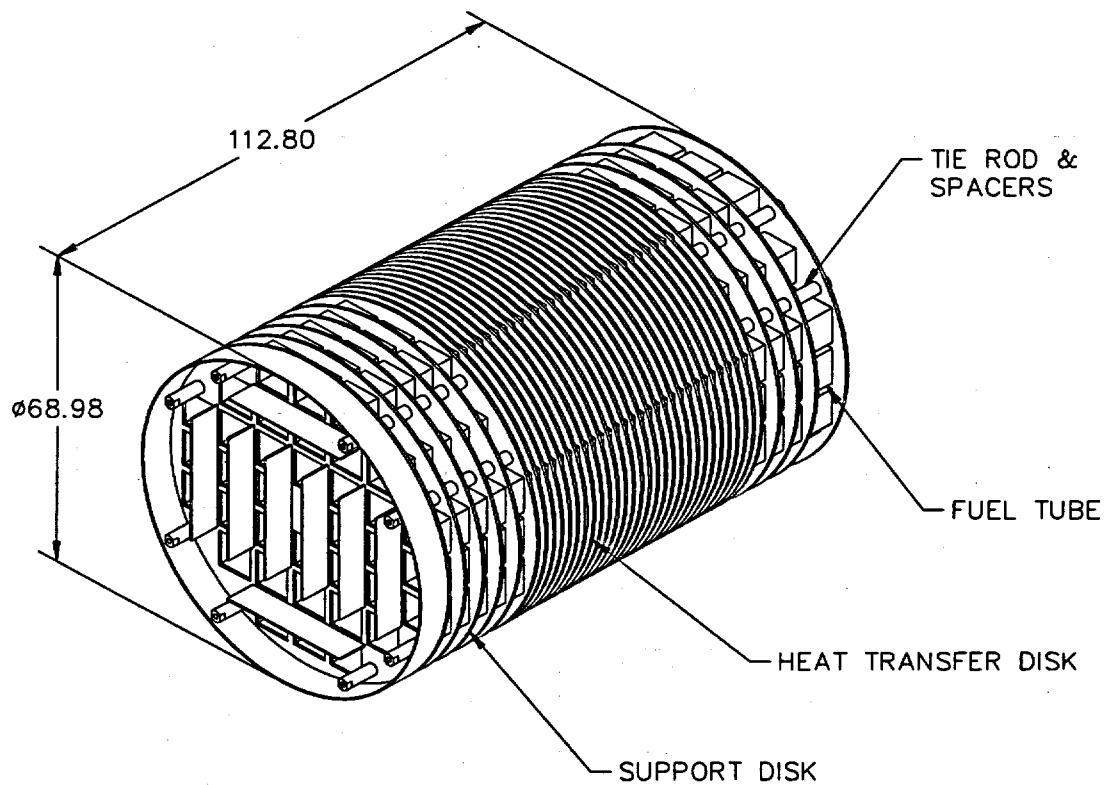
The canistered fuel basket may contain one or more Reconfigured Fuel Assemblies which are designed to confine Yankee Class spent fuel rods, or portions thereof, which are classified as failed, and to maintain the geometry of the rods. The total number of full length rods that can be placed in the Reconfigured Fuel Assembly is less than that in a standard Yankee class fuel assembly (64 rods versus 256 rods). Consequently, the effects of a Reconfigured Fuel Assembly placed in a canister (e.g. criticality, weight, thermal output, source term) are significantly less than the effects of a design basis (standard) Yankee Class fuel assembly. Consequently, Reconfigured Fuel Assemblies may replace standard Yankee class fuel assemblies on a one-for-one basis in any Yankee-MPC spent fuel canister.

The Reconfigured Fuel Assembly is designed to the requirements of the ASME Code, Section III, Article NG-3000, to NUREG/CR-6322, "Buckling Analysis of Spent Fuel Baskets," and to the additional guidance contained in ASME Section III, Article NF-3000, and Appendix F.

The Reconfigured Fuel Assembly has been evaluated for normal conditions of transport and is structurally adequate for a postulated end drop resulting in a deceleration of 20g. It is also structurally adequate for a postulated side drop resulting in a deceleration of 20 g.

The Reconfigured Fuel Assembly has also been evaluated for accident conditions in Section 2.7.9.

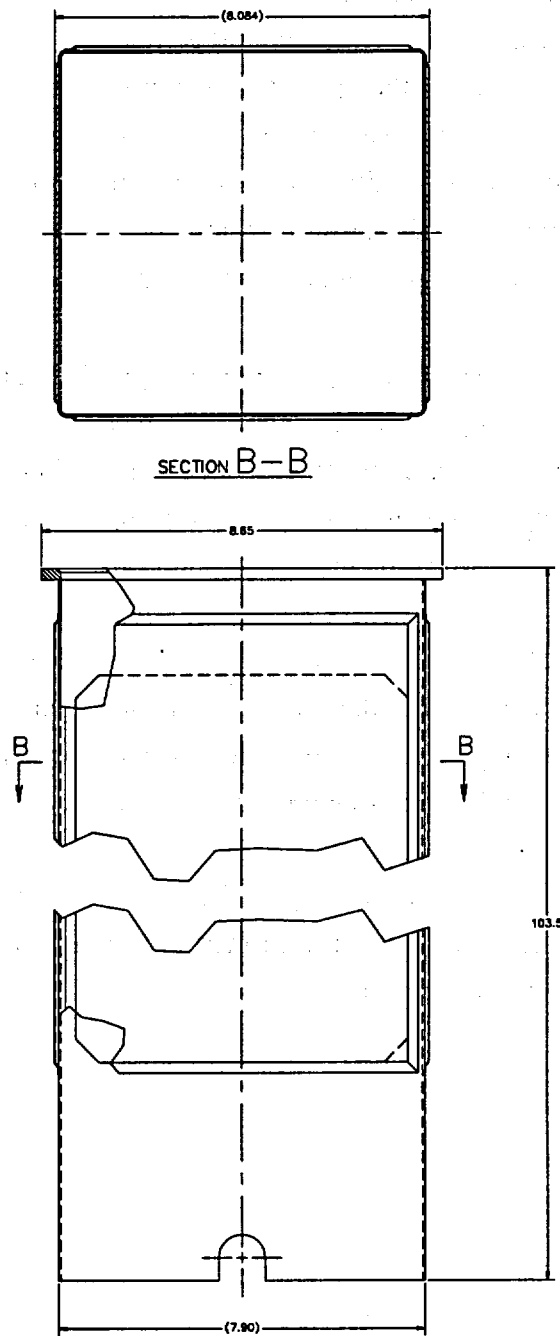
Figure 2.6.14-1 Yankee MPC Fuel Basket



I Figure 2.6.14-2 Support Disk Cross Section Configuration - Yankee-MPC Fuel Basket

**FIGURE WITHHELD AS SENSITIVE
UNCLASSIFIED INFORMATION**

Figure 2.6.14-3 Fuel Tube Configuration – Yankee-MPC Fuel Basket



2.6.14.1 Detailed Analysis – Yankee-MPC Fuel Basket

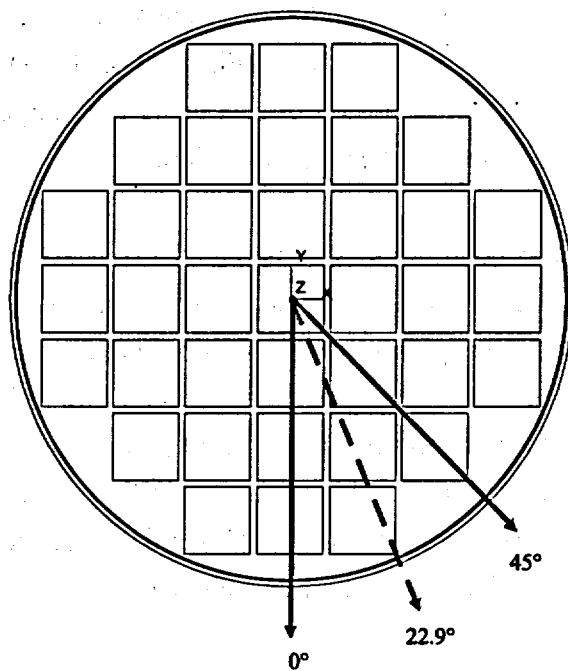
Based on criticality control requirements, the canistered fuel basket design criteria requires the maintenance of fuel support and control of spacing of the fuel assemblies for all load conditions. The structural design criteria for the fuel basket is the ASME Boiler and Pressure Vessel Code, Section III, Division 1, Subsection NG, "Core Support Structures." Consistent with this criteria, the main structural component in the fuel basket, the stainless steel support disk, is shown to have a maximum primary membrane stress intensity and primary membrane + bending stress intensity in any disk for any normal condition load and position orientation that is less than the design stress intensity value S_m and $1.5S_m$ respectively. The value of S_m is defined at conservative temperatures for the component being analyzed.

For the side drop conditions, three basket drop orientations (0° , 22.9° , and 45°) are considered, as shown in Figure 2.6.14.1-1. Angles of 22.9° and 45° were selected because minimal web thickness occurs at these orientations. A parametric study in Section 2.10.11.1 indicates that the 22.9° drop case is bounded by the 45° drop case. Therefore, detailed analysis is performed for the 0 and 45-degree basket orientations for side drop conditions.

In the side drop, the loads of the fuel assemblies are transferred into the plane of the support disks, from which they are transmitted to the canister shell, and then to the cask body (cask inner shell). In the end drop, the support disks are loaded by their own inertial weight and do not experience load from the guided, but free standing fuel assemblies.

Finite element models are used to perform analyses for end drop and side drop conditions using the ANSYS program. In addition to the load from inertial weight, the analyses also consider the stresses due to differential thermal expansion.

Figure 2.6.14.1-1 Yankee-MPC Fuel Basket Drop Orientations



2.6.14.2 Finite Element Model Description – Yankee-MPC Fuel Basket

Three finite element models were generated to analyze the canistered Yankee class fuel basket for the normal operating conditions; one for the end drop (Figure 2.6.14.2-1), in which the loads are perpendicular to the plane of the disk and two for the side drop, in which the loads act in the plane of the disk, for two basket orientations, 0° (Figure 2.6.14.2-2) and 45° (Figure 2.6.14.2-3). All models accommodate thermal expansion effects using the temperature distribution from the thermal analysis and the coefficient of thermal expansion.

The model for the end drop conditions is constructed using ANSYS SHELL63 elements. It consists of a single support disk with a thickness of 0.5 inch. The shell elements accommodate the out-of-plane bending, which is present in the end-drop condition. The support disk in the end drop orientation is restrained by the split spacers on the eight tie rods. The nodes corresponding to the location of the tie rods are restrained in the out of plane direction (the cask axial direction). Four additional in-plane transitional restraints are specified at the outer edge of the model (located 90° apart from each other) in the tangential direction to prohibit rigid body displacements. The only loading is the inertial weight of the support disk in the out-of-plane direction.

The finite element models for the side drop evaluation of the support disks are three dimensional models and include the lower section of the canister and cask as well as 14 of the support disks. The two models are identical except for the orientation of the support disks. The canister and cask body are included in the model to more accurately simulate the boundary conditions for the support disks. Although the top and bottom portions of the canister and transport cask are not symmetric, the asymmetry is expected to have negligible impact on the support disk stress results because the canister bottom plate is less rigid than the canister lids. This allows slightly more deformation of the canister shell and the support disks. The interface between the support disks and the canister elements is modeled using the ANSYS CONTAC52 element (Figure 2.6.14.2-4), which acts as a compression only element, connecting adjacent nodes across the interface. To prevent rigid body motion of the support disks, two BEAM4 elements are defined at the centerline of the model for each disk. These beam elements have very small properties, e.g. $\text{area}=0.5\text{E-}3 \text{ inch}^2$, and, therefore, have negligible contribution to the contact stiffness (Figure 2.6.14.2-4). The interface between the canister shell and the cask inner shell is modeled as CONTAC49 elements, which permit compression and sliding to occur. The CONTAC49 is a five node element which defines a target surface and a contact node. This negates the need to have nodes adjacent to one another on either side of the interface (Figure 2.6.14.2-5). Both

interface elements employ a stiffness (1.0×10^6 lbf/in) to avoid excessive overlap of the two adjacent surfaces, similar to those employed for the NAC-STC. A study (Section 2.10.11.2) indicates that the stress results of the support disk are not sensitive to the value of the gap stiffness used in the analysis.

In the support disk side drop models, the canister bottom is comprised of SHELL63 elements, which support out of plane bending, and the canister shell is constituted of SOLID45 elements. The cask body is modeled with SOLID45 elements. The support disk is modeled entirely with SHELL63 elements. Since fourteen disks are involved in the side drop model, critical disks are modeled with a more refined mesh in the ligaments (Figure 2.6.14.2-6) while remaining ones are meshed coarser (Figure 2.6.14.2-7). To increase the accuracy of the analysis, the element size is reduced towards the intersections of the ligaments. Mesh sensitivity studies were performed to assure sufficient precision (Section 2.10.11.3). Five of the fourteen disks are defined as critical and are post-processed accordingly by their disk number (Figure 2.6.14.2-8). The contact angle is bounded at the two ends of the model where the canister and cask flexure are at extremes. For this reason, two disks at each end are considered. An additional disk, near the midpoint of the modeled disk assembly, is also defined. Since this disk is not truly mid-span, the disk chosen is alternated to either side of the line of symmetry between the 0 and 45 degree analysis to assure the design is encompassed.

While the cask, canister and support disks are modeled explicitly, the impact limiters are represented by CONTAC52 elements. Cask and impact limiter modeling reflect the same approach as described in Section 2.6.7.2. The load from the fuel and fuel tube assembly is modeled as a single point force (acting at a node) at the inner surface of each support disk opening. The Yankee class fuel differs from standard PWR fuel in that it does not have a uniform surface, so the fuel assembly may not have a single surface of contact. While the load from the fuel assembly is a distributed load, it was modeled conservatively as a point force acting mid span of the disk ligaments (Figure 2.6.14.2-6).

To determine the most critical regions, a series of cross sections are considered. To aid in the identification of these sections, Figures 2.6.14.2-9 and 2.6.14.2-10 show the section locations on a support disk for the 0° and 45° basket drop cases, respectively. Tables 2.6.14.2-1 and 2.6.14.2-2 list the geometric locations of the end points of the cross sections.

Figure 2.6.14.2-1 Yankee-MPC Basket Support Disk End Drop Model

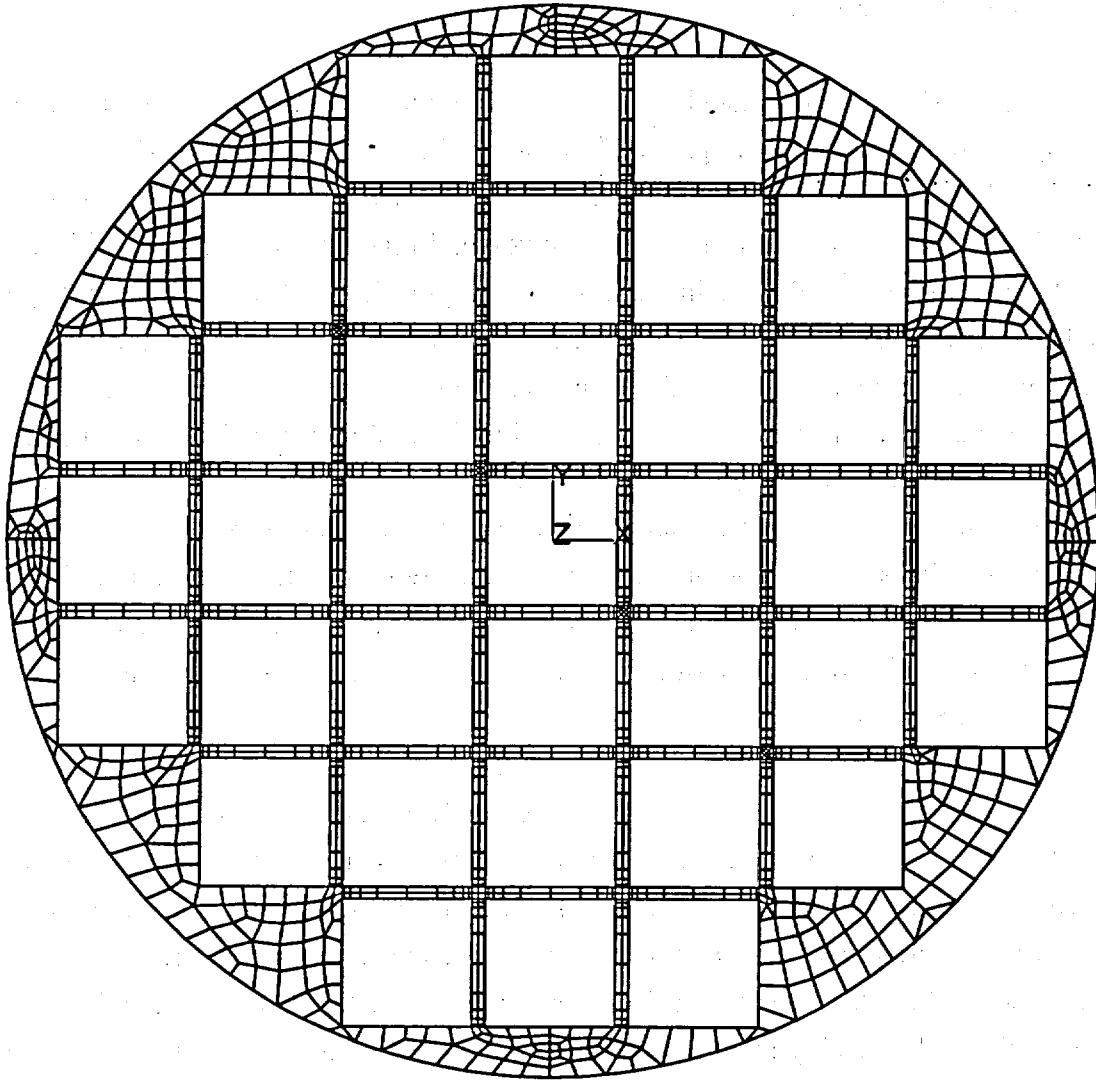


Figure 2.6.14.2-2 Yankee-MPC Basket Support Disk Side Drop Model - 0° Orientation

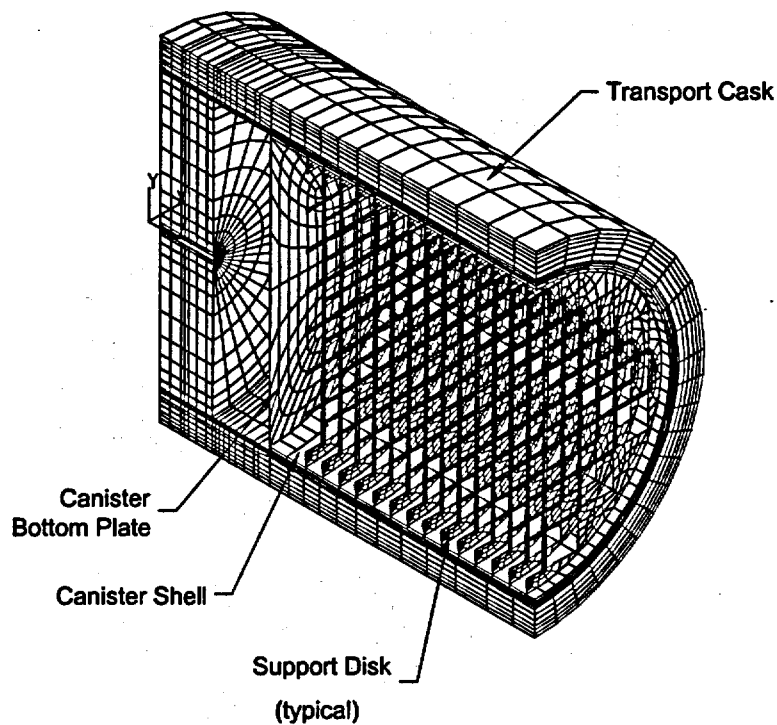


Figure 2.6.14.2-3 Yankee-MPC Basket Support Disk Side Drop Model - 45° Orientation

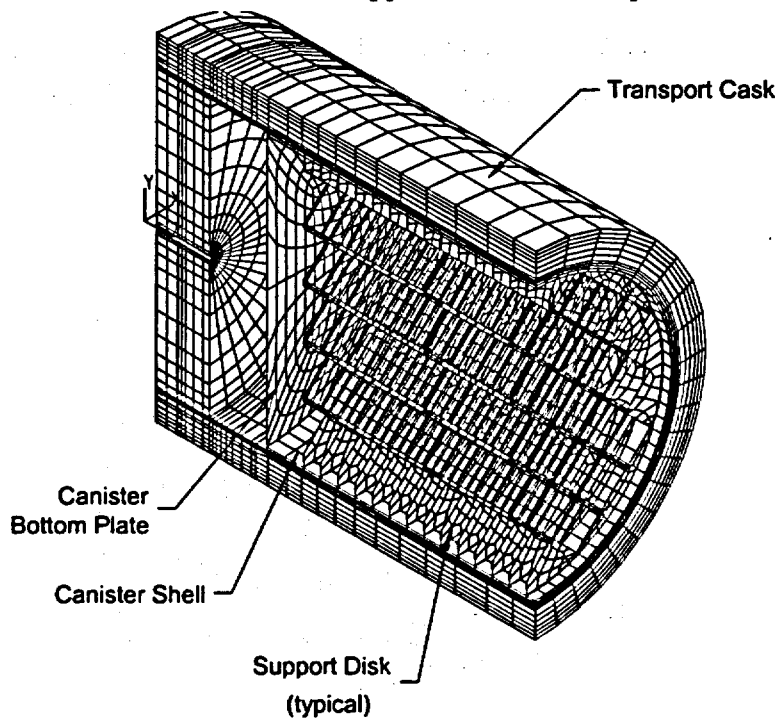


Figure 2.6.14.2-4 **CONTAC52 Elements in the Yankee-MPC Basket Support Disk Side Drop Model (Interface between Disks and Canister Shell)**

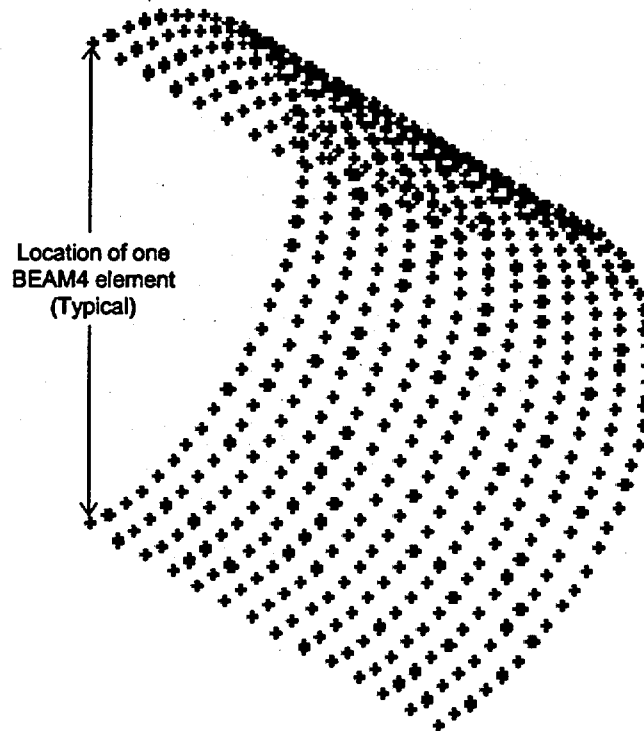


Figure 2.6.14.2-5 **CONTAC49 Elements in the Yankee-MPC Basket Support Disk Side Drop Model (Interface between Canister Shell and Cask Inner Shell)**

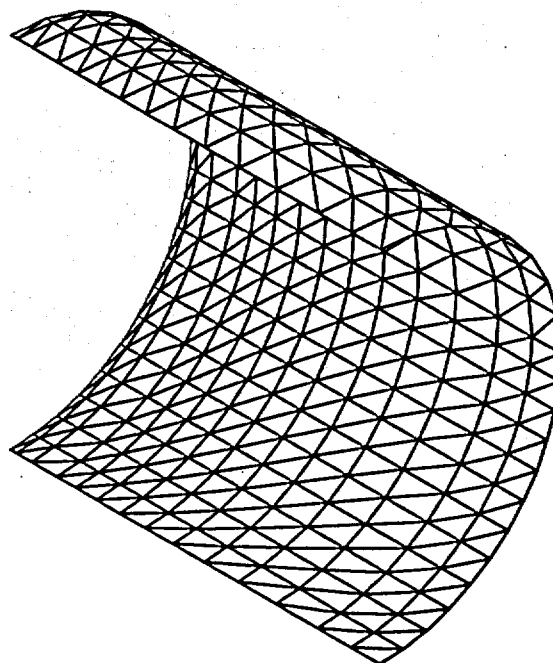


Figure 2.6.14.2-6 Yankee-MPC Basket Support Disk Side Drop Model - Refined Mesh Disk

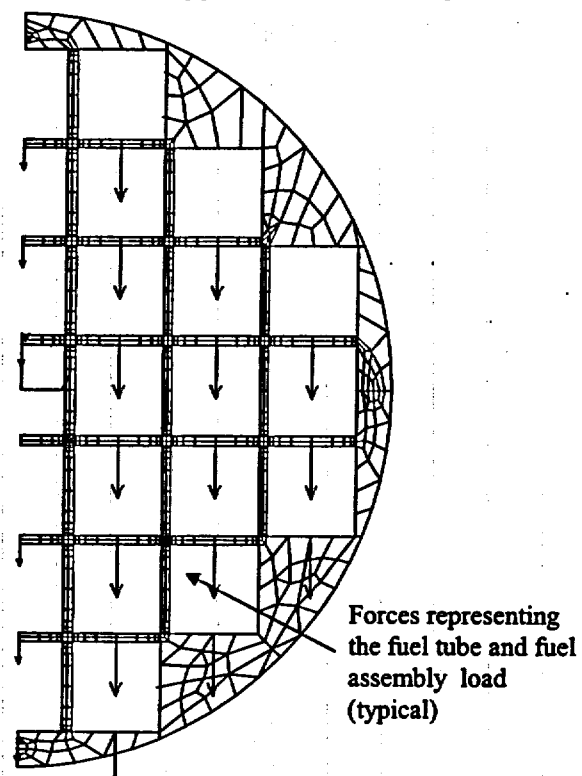


Figure 2.6.14.2-7 Yankee-MPC Basket Support Disk Side Drop Model - Coarse Mesh Disk

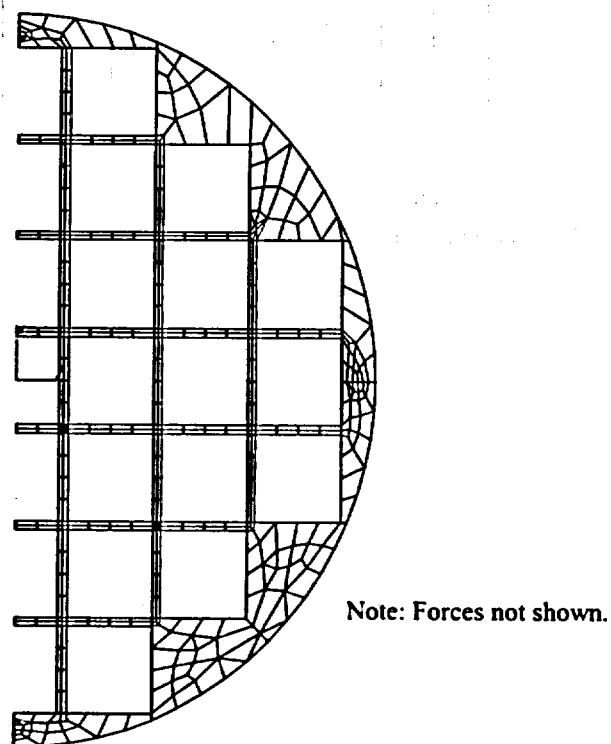
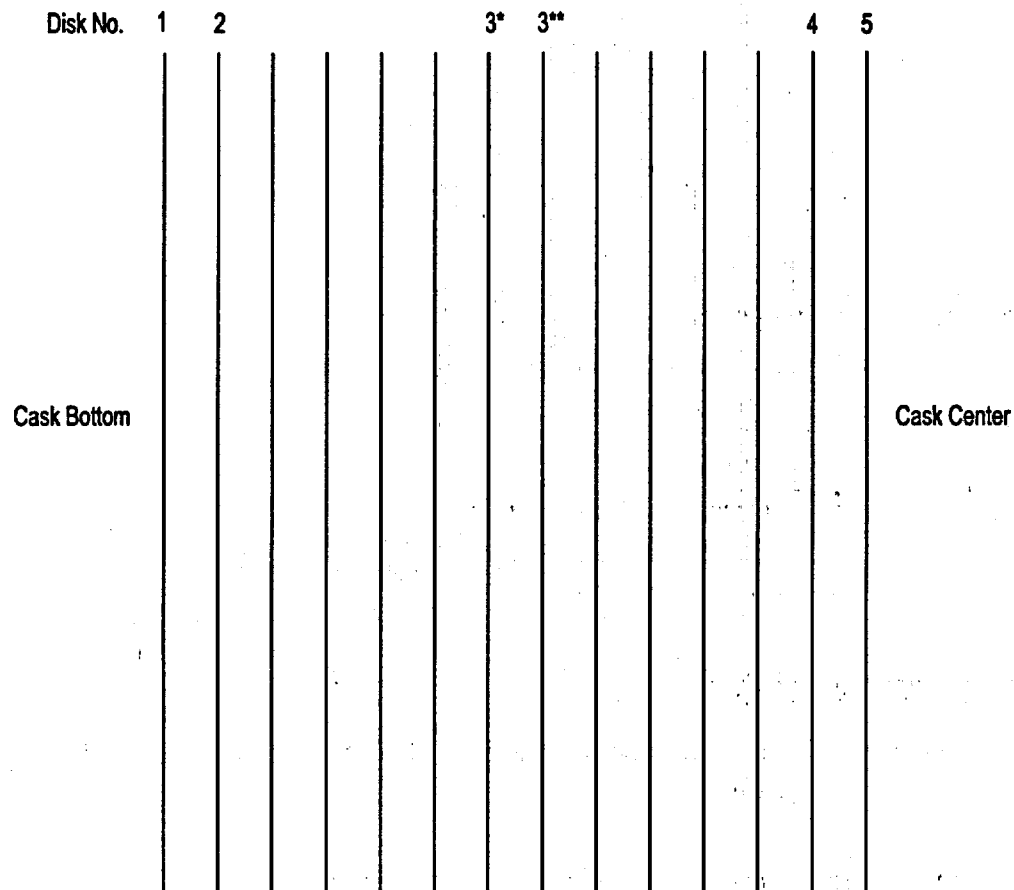


Figure 2.6.14.2-8 Yankee-MPC Basket Support Disk Side Drop Model - Support Disks Side View (Disk Number)



*for model with 0° basket orientation
**for model with 45° basket orientation

Figure 2.6.14.2-9 Location of the Sections to Obtain Linearized Stresses for
0° Yankee-MPC Basket Orientation

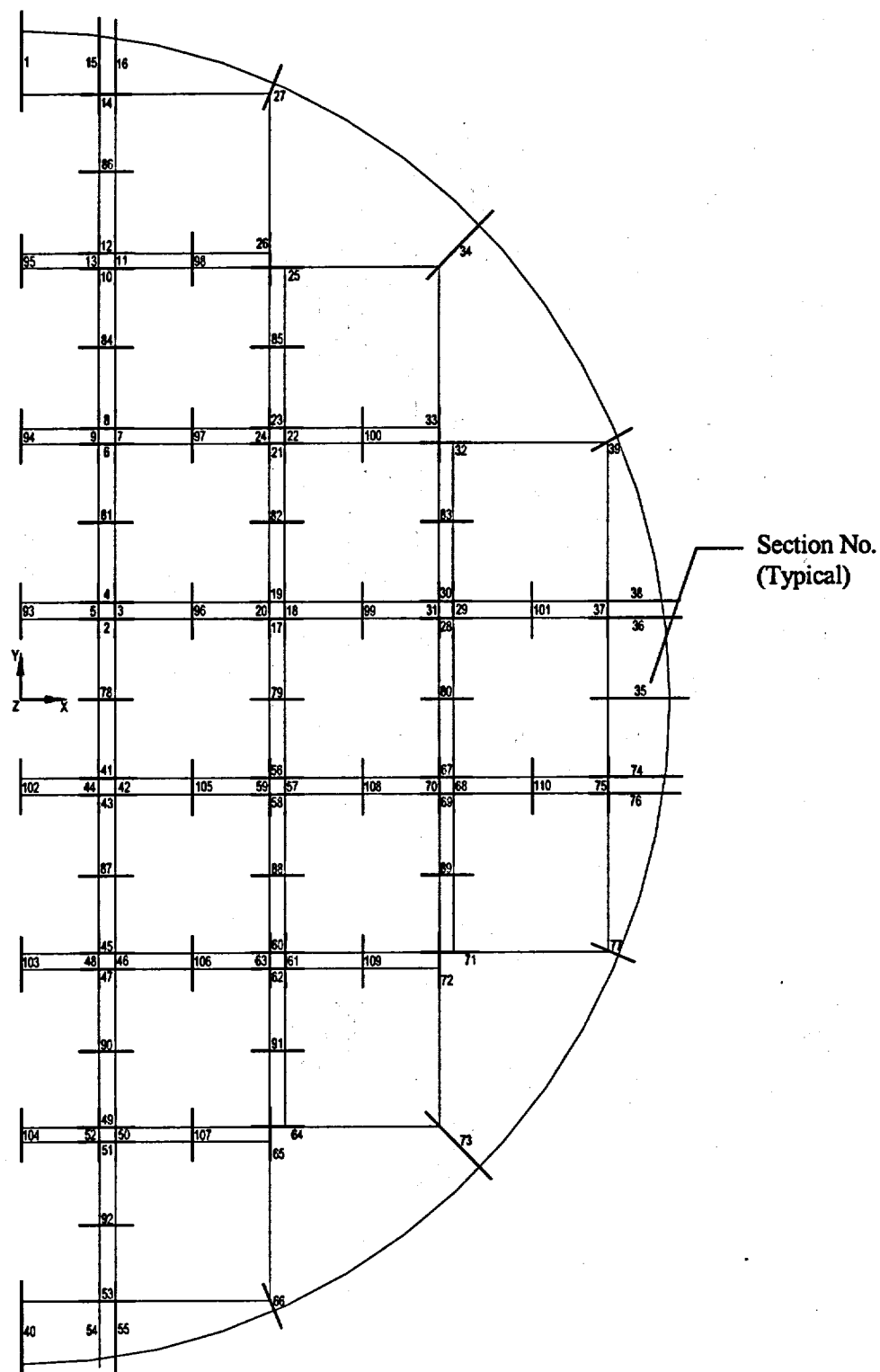


Figure 2.6.14.2-10 Location of the Sections to Obtain Linearized Stresses for
45° Yankee-MPC Basket Orientation

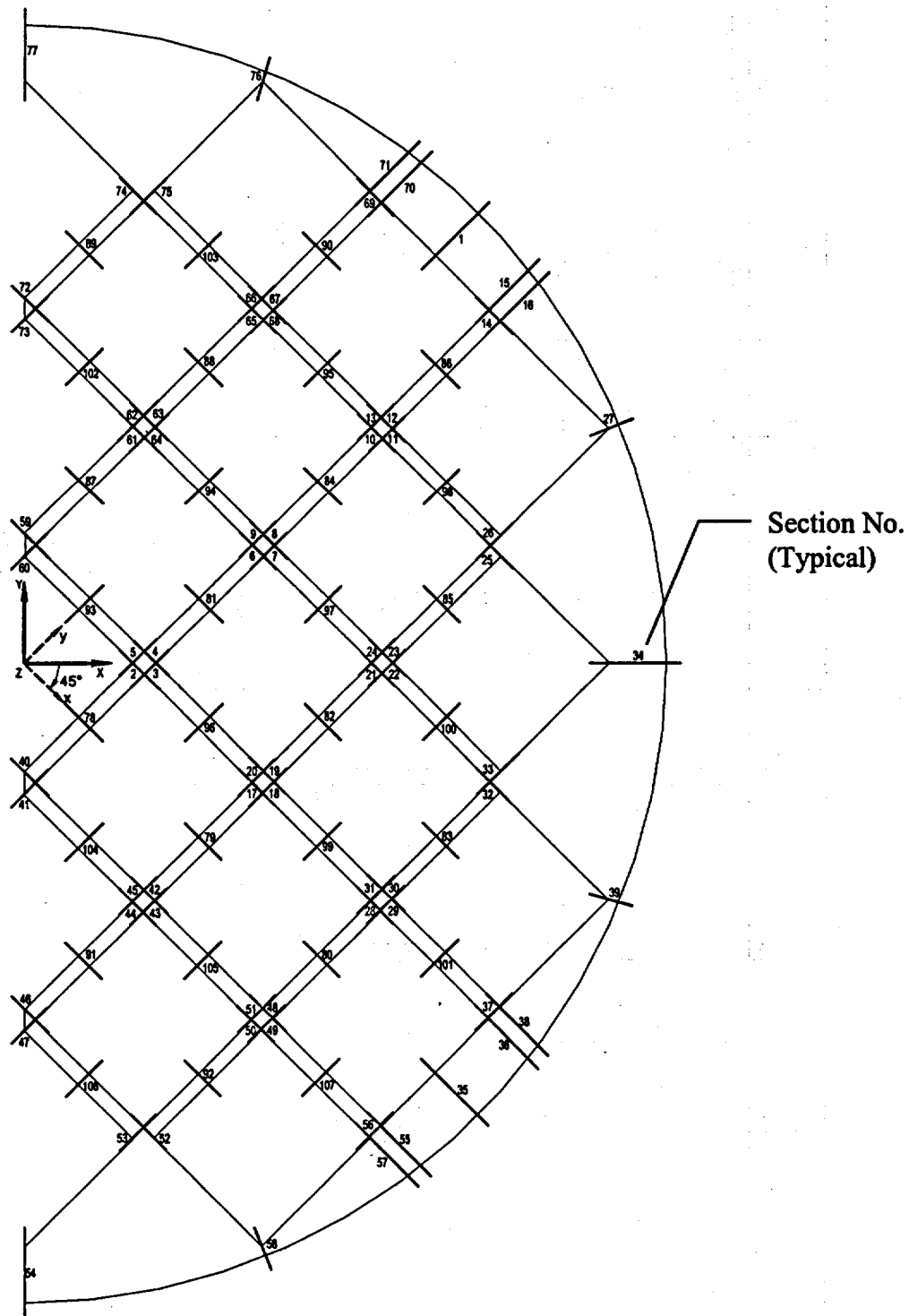


Table 2.6.14.2-1 Listing of Cross Sections for Stress Evaluation of Yankee-MPC
Basket Support Disk (0° Basket Drop Orientation)

Section Number	Point 1	Point 2	Coordinates (in.)			
			Point 1		Point 2	
			X	Y	X	Y
1	1	2	0.00	31.32	0.00	34.49
2	3	4	4.13	4.13	5.00	4.13
3	5	6	5.00	4.13	5.00	5.00
4	7	8	5.00	5.00	4.13	5.00
5	9	10	4.13	5.00	4.13	4.13
6	11	12	4.13	13.26	5.00	13.26
7	13	14	5.00	13.26	5.00	14.07
8	15	16	5.00	14.07	4.13	14.07
9	17	18	4.13	14.07	4.13	13.26
10	19	20	4.13	22.32	5.00	22.32
11	21	22	5.00	22.32	5.00	23.07
12	23	24	5.00	23.07	4.13	23.07
13	25	26	4.13	23.07	4.13	22.32
14	27	28	4.13	31.32	5.00	31.32
15	29	30	4.13	31.32	4.13	34.24
16	31	32	5.00	31.32	5.00	34.13
17	33	34	13.26	4.13	14.07	4.13
18	35	36	14.07	4.13	14.07	5.00
19	37	38	14.07	5.00	13.26	5.00
20	39	40	13.26	5.00	13.26	4.13
21	41	42	13.26	13.26	14.07	13.26
22	43	44	14.07	13.26	14.07	14.07
23	45	46	14.07	14.07	13.26	14.07
24	47	48	13.26	14.07	13.26	13.26
25	49	50	13.26	22.32	14.07	22.32
26	51	52	13.26	22.32	13.26	23.07
27	53	54	13.26	31.32	13.44	31.76
28	55	56	22.32	4.13	23.07	4.13
29	57	58	23.07	4.13	23.07	5.00
30	59	60	23.07	5.00	22.32	5.00
31	61	62	22.32	5.00	22.32	4.13
32	63	64	22.32	13.26	23.07	13.26
33	65	66	22.32	13.26	22.32	14.07
34	67	68	22.32	22.32	24.39	24.39
35	69	70	31.32	0.00	34.49	0.00

Table 2.6.14.2-1 Listing of Cross Sections for Stress Evaluation of Yankee-MPC
Basket Support Disk (0° Basket Drop Orientation) (Continued)

Section Number	Point 1	Point 2	Coordinates (in.)			
			Point 1		Point 2	
			X	Y	X	Y
36	71	72	31.32	4.13	34.24	4.13
37	73	74	31.32	4.13	31.32	5.00
38	75	76	31.32	5.00	34.13	5.00
39	77	78	31.32	13.26	31.71	13.47
40	79	80	0.00	-31.32	0.00	-34.49
41	81	82	4.13	-4.13	5.00	-4.13
42	83	84	5.00	-4.13	5.00	-5.00
43	85	86	5.00	-5.00	4.13	-5.00
44	87	88	4.13	-5.00	4.13	-4.13
45	89	90	4.13	-13.26	5.00	-13.26
46	91	92	5.00	-13.26	5.00	-14.07
47	93	94	5.00	-14.07	4.13	-14.07
48	95	96	4.13	-14.07	4.13	-13.26
49	97	98	4.13	-22.32	5.00	-22.32
50	99	100	5.00	-22.32	5.00	-23.07
51	101	102	5.00	-23.07	4.13	-23.07
52	103	104	4.13	-23.07	4.13	-22.32
53	105	106	4.13	-31.32	5.00	-31.32
54	107	108	4.13	-31.32	4.13	-34.24
55	109	110	5.00	-31.32	5.00	-34.13
56	111	112	13.26	-4.13	14.07	-4.13
57	113	114	14.07	-4.13	14.07	-5.00
58	115	116	14.07	-5.00	13.26	-5.00
59	117	118	13.26	-5.00	13.26	-4.13
60	119	120	13.26	-13.26	14.07	-13.26
61	121	122	14.07	-13.26	14.07	-14.07
62	123	124	14.07	-14.07	13.26	-14.07
63	125	126	13.26	-14.07	13.26	-13.26
64	127	128	13.26	-22.32	14.07	-22.32
65	129	130	13.26	-22.32	13.26	-23.07
66	131	132	13.26	-31.32	13.44	-31.76
67	133	134	22.32	-4.13	23.07	-4.13
68	135	136	23.07	-4.13	23.07	-5.00
69	137	138	23.07	-5.00	22.32	-5.00
70	139	140	22.32	-5.00	22.32	-4.13

Table 2.6.14.2-1 Listing of Cross Sections for Stress Evaluation of Yankee-MPC
Basket Support Disk (0° Basket Drop Orientation) (Continued)

Section Number	Point 1	Point 2	Coordinates (in.)			
			Point 1		Point 2	
			X	Y	X	Y
71	141	142	22.32	-13.26	23.07	-13.26
72	143	144	22.32	-13.26	22.32	-14.07
73	145	146	22.32	-22.32	24.39	-24.39
74	147	148	31.32	-4.13	34.24	-4.13
75	149	150	31.32	-4.13	31.32	-5.00
76	151	152	31.32	-5.00	34.13	-5.00
77	153	154	31.32	-13.26	31.76	-13.44
78	155	156	4.13	0.00	5.00	0.00
79	157	158	13.26	0.00	14.07	0.00
80	159	160	22.32	0.00	23.07	0.00
81	161	162	4.13	9.13	5.00	9.13
82	163	164	13.26	9.13	14.07	9.13
83	165	166	22.32	9.13	23.07	9.13
84	167	168	4.13	18.19	5.00	18.19
85	169	170	13.26	18.19	14.07	18.19
86	171	172	4.13	27.20	5.00	27.20
87	173	174	4.13	-9.13	5.00	-9.13
88	175	176	13.26	-9.13	14.07	-9.13
89	177	178	22.32	-9.13	23.07	-9.13
90	179	180	4.13	-18.19	5.00	-18.19
91	181	182	13.26	-18.19	14.07	-18.19
92	183	184	4.13	-27.20	5.00	-27.20
93	185	186	0.00	4.13	0.00	5.00
94	187	188	0.00	13.26	0.00	14.07
95	189	190	0.00	22.32	0.00	23.07
96	191	192	9.13	4.13	9.13	5.00
97	193	194	9.13	13.26	9.13	14.07
98	195	196	9.13	22.32	9.13	23.07
99	197	198	18.19	4.13	18.19	5.00
100	199	200	18.19	13.26	18.19	14.07
101	201	202	27.20	4.13	27.20	5.00
102	203	204	0.00	-4.13	0.00	-5.00
103	205	206	0.00	-13.26	0.00	-14.07
104	207	208	0.00	-22.32	0.00	-23.07
105	209	210	9.13	-4.13	9.13	-5.00
106	211	212	9.13	-13.26	9.13	-14.07
107	213	214	9.13	-22.32	9.13	-23.07

Table 2.6.14.2-1 Listing of Cross Sections for Stress Evaluation of Yankee-MPC
Basket Support Disk (0° Basket Drop Orientation) (Continued)

Section Number	Point 1	Point 2	Coordinates (in.)			
			Point 1		Point 2	
			X	Y	X	Y
108	215	216	18.19	-4.13	18.19	-5.00
109	217	218	18.19	-13.26	18.19	-14.07
110	219	220	27.20	-4.13	27.20	-5.00
105	209	210	-10.02	-16.16	-11.52	-16.16
106	211	212	-20.29	-10.02	-20.29	-11.52
107	213	214	-10.02	-31.18	-10.02	-30.44
108	215	216	-31.18	-10.02	-30.44	-10.02
109	217	218	5.39	-11.02	5.39	-10.02
110	219	220	5.39	-20.29	5.39	-21.17

Table 2.6.14.2-2 Listing of Cross Sections for Stress Evaluation of Yankee-MPC
Basket Support Disk (45° Basket Drop Orientation)

Section Number	Point 1	Point 2	Coordinates (in.)			
			Point 1		Point 2	
			X	Y	X	Y
1	1	2	22.15	22.15	24.39	24.39
2	3	4	5.84	0	6.46	-0.62
3	5	6	6.46	-0.62	7.07	0
4	7	8	7.07	0	6.46	0.62
5	9	10	6.46	0.62	5.84	0
6	11	12	12.29	6.46	12.91	5.84
7	13	14	12.91	5.84	13.48	6.41
8	15	16	13.48	6.41	12.86	7.03
9	17	18	12.86	7.03	12.29	6.46
10	19	20	18.7	12.86	19.32	12.25
11	21	22	19.32	12.25	19.85	12.78
12	23	24	19.85	12.78	19.23	13.4
13	25	26	19.23	13.4	18.7	12.86
14	27	28	25.07	19.23	25.69	18.61
15	29	30	25.07	19.23	27.13	21.3
16	31	32	25.69	18.61	27.67	20.59
17	33	34	12.29	-6.46	12.86	-7.03
18	35	36	12.86	-7.03	13.48	-6.41
19	37	38	13.48	-6.41	12.91	-5.84
20	39	40	12.91	-5.84	12.29	-6.46
21	41	42	18.75	0	19.32	-0.57
22	43	44	19.32	-0.57	19.89	0
23	45	46	19.89	0	19.32	0.57
24	47	48	19.32	0.57	18.75	0
25	49	50	25.16	6.41	25.73	5.84
26	51	52	25.16	6.41	25.69	6.94
27	53	54	31.52	12.78	31.97	12.96
28	55	56	18.7	-12.86	19.23	-13.4
29	57	58	19.23	-13.4	19.85	-12.78
30	59	60	19.85	-12.78	19.32	-12.25
31	61	62	19.32	-12.25	18.7	-12.86
32	63	64	25.16	-6.41	25.69	-6.94
33	65	66	25.16	-6.41	25.73	-5.84
34	67	68	31.57	0	34.49	0
35	69	70	22.15	-22.15	24.39	-24.39

Table 2.6.14.2-2 Listing of Cross Sections for Stress Evaluation of Yankee-MPC
Basket Support Disk (45° Basket Drop Orientation) (Continued)

Section Number	Point 1	Point 2	Coordinates (in.)			
			Point 1		Point 2	
			X	Y	X	Y
36	71	72	25.07	-19.23	27.13	-21.3
37	73	74	25.07	-19.23	25.69	-18.61
38	75	76	25.69	-18.61	27.67	-20.59
39	77	78	31.52	-12.78	31.95	-12.9
40	79	80	0	-5.84	0.62	-6.46
41	81	82	0.62	-6.46	0	-7.07
42	83	84	6.46	-12.29	7.03	-12.86
43	85	86	7.03	-12.86	6.41	-13.48
44	87	88	6.41	-13.48	5.84	-12.91
45	89	90	5.84	-12.91	6.46	-12.29
46	91	92	0	-18.75	0.57	-19.32
47	93	94	0.57	-19.32	0	-19.89
48	95	96	12.86	-18.7	13.4	-19.23
49	97	98	13.4	-19.23	12.78	-19.85
50	99	100	12.78	-19.85	12.25	-19.32
51	101	102	12.25	-19.32	12.86	-18.7
52	103	104	6.41	-25.16	6.94	-25.69
53	105	106	6.41	-25.16	5.84	-25.73
54	107	108	0	-31.57	0	-34.49
55	109	110	19.23	-25.07	21.3	-27.13
56	111	112	19.23	-25.07	18.61	-25.69
57	113	114	18.61	-25.69	20.59	-27.67
58	115	116	12.78	-31.52	12.96	-31.97
59	117	118	0	7.07	0.62	6.46
60	119	120	0.62	6.46	0	5.84
61	121	122	6.46	12.29	5.84	12.91
62	123	124	5.84	12.91	6.41	13.48
63	125	126	6.41	13.48	7.03	12.86
64	127	128	7.03	12.86	6.46	12.29
65	129	130	12.86	18.7	12.25	19.32
66	131	132	12.25	19.32	12.78	19.85
67	133	134	12.78	19.85	13.4	19.23
68	135	136	13.4	19.23	12.86	18.7
69	137	138	19.23	25.07	18.61	25.69
70	139	140	19.23	25.07	21.3	27.13

Table 2.6.14.2-2 Listing of Cross Sections for Stress Evaluation of Yankee-MPC
Basket Support Disk (45° Basket Drop Orientation) (Continued)

Point 2 Number	Point 1	Point 2	Coordinates (in.)			
			Point 1		Point 2	
			X	Y	X	Y
71	141	142	18.61	25.69	20.59	27.67
72	143	144	0	19.89	0.57	19.32
73	145	146	0.57	19.32	0	18.75
74	147	148	6.41	25.16	5.84	25.73
75	149	150	6.41	25.16	6.94	25.69
76	151	152	12.78	31.52	12.9	31.95
77	153	154	0	31.57	0	34.49
78	155	156	2.92	-2.92	3.54	-3.54
79	157	158	9.37	-9.37	9.95	-9.95
80	159	160	15.78	-15.78	16.31	-16.31
81	161	162	9.37	3.54	9.99	2.92
82	163	164	15.83	-2.92	16.4	-3.49
83	165	166	22.24	-9.33	22.77	-9.86
84	167	168	15.78	9.95	16.4	9.33
85	169	170	22.24	3.49	22.81	2.92
86	171	172	22.15	16.31	22.77	15.69
87	173	174	3.54	9.37	2.92	9.99
88	175	176	9.95	15.78	9.33	16.4
89	177	178	3.49	22.24	2.92	22.81
90	179	180	16.31	22.15	15.69	22.77
91	181	182	2.92	-15.83	3.49	-16.4
92	183	184	9.33	-22.24	9.86	-22.77
93	185	186	2.92	2.92	3.54	3.54
94	187	188	9.37	9.37	9.95	9.95
95	189	190	15.78	15.78	16.31	16.31
96	191	192	9.37	-3.54	9.99	-2.92
97	193	194	15.83	2.92	16.4	3.49
98	195	196	22.24	9.33	22.77	9.86
99	197	198	15.78	-9.95	16.4	-9.33
100	199	200	22.24	-3.49	22.81	-2.92
101	201	202	22.15	-16.31	22.77	-15.69
102	203	204	2.92	15.83	3.49	16.4
103	205	206	9.33	22.24	9.86	22.77
104	207	208	3.54	-9.37	2.92	-9.99
105	209	210	9.95	-15.78	9.33	-16.4
106	211	212	3.49	-22.24	2.92	-22.81
107	213	214	16.31	-22.15	15.69	-22.77

2.6.14.3 Thermal Expansion Evaluation of Yankee-MPC Fuel Basket Support Disk

A thermal stress analysis of the Yankee-MPC fuel basket support disk is performed using ANSYS to determine the differential thermal expansion and the associated thermal stresses. Three thermal conditions are considered and the associated thermal stresses that result from a heat load of 12.5 kW are evaluated.

<u>Thermal Condition</u>	<u>Ambient Temperature</u>	<u>Solar Insolence Applied to Cask Surface</u>	<u>12.5 kW Fuel Load</u>
1	100°F	yes	yes
2	-40°F	no	yes
3	-40°F	no	no

The temperature distribution of the support disk for Thermal Conditions 1 and 2 are determined in Chapter 3. Temperature data from the thermal analysis is used to calculate the radial thermal expansion of the inside surface of the canister, outer surface of the steel support disk and outer surface of the aluminum heat transfer disk. Considering the maximum material conditions that contribute to creating the minimum gap, the gaps between the basket disks and the canister wall are shown in the following table.

	Nominal Diameter At 70°F (inches)	Machining Tolerance (inches)	Max./Min. Material Diameter At Max. Temp. (inches)	Minimum Radial Gap (inches)
Canister Shell Inner Surface	69.39	+0.12/-0.16	69.376 (Min)	-----
Steel Support Disk	69.15	+0.00/-0.02	69.281 (Max)	0.048
Aluminum Heat Transfer Disk	68.87	+0.00/-0.02	69.188 (Max)	0.094

The amount of diametral thermal expansion of the canister shell (0.146 inches), the steel support disk (0.131 inches) and the aluminum heat transfer disk (0.318 inches) is obtained from the finite element model results described in Section 3.4.1.2.1.

The minimum gap size between the steel support disk and the canister inner surface is 0.048 inches. The gap size between the aluminum heat transfer disk and the canister inner surface is 0.094 inches. Therefore, there is no interference between the disks and the canister shell.

The thermal stresses arise from the hotter interior of the support disk expanding against the cooler outer region of the support disk. The results of the thermal analysis for the above thermal conditions are summarized below.

Thermal Condition	Disk Maximum Temperature (°F)	Disk Outer Temperature (°F)	ΔT (°F)
1	539	244	295
2	431	115	316
3	-40	-40	0

The thermal stress is governed by the temperature difference, ΔT , the modulus of elasticity, E , and the coefficient of thermal expansion, α , and their product, $E\alpha$, for Thermal Conditions 1 and 2 are shown below:

Thermal Condition	E (ksi)*	α (in/in-°F)*	$E\alpha$
1	26.54E3	5.909E-6	0.157
2	27.16E3	5.90E-6	0.160

*Properties taken at $T_{avg} = (T_{max} + T_{min})/2$

Since the values of ΔT and $E\alpha$ for Thermal Condition 1 are lower than those for Thermal Condition 2, Thermal Condition 1 is bounded by Thermal Condition 2 for thermal stress calculations. Therefore, Thermal Conditions 2 and 3 are used in the finite element analyses. Since the allowable stresses decrease as the temperature increases, the allowable stresses for the Thermal Condition 2 evaluation are conservatively based on the maximum disk temperature of Thermal Condition 1 (539°F). Thermal Condition 3 allowable stresses are based on a temperature of -40°F.

Temperatures are applied to the support disk models to simulate worst-case temperature conditions. As discussed, Thermal Conditions 2 and 3 are used in the analysis. For Thermal Condition 2, the maximum disk temperature (431°F) is applied to the center of the support disk and the minimum temperature (115°F) is applied to the outer edge of the disk. For the side drop evaluation, constant temperatures of 215°F and 188°F are applied to the canister shell and the cask inner shell, respectively. Note that they are the maximum temperatures of canister shell and the cask inner shell for Thermal Condition 2 based on thermal analysis results (Section 3.0). Use

of these temperatures for the canister and cask body results in the largest gap between the disks and the canister shell and between the canister shell and the cask inner shell. A steady state thermal conduction analysis (with all planar structural elements temporarily changed to ANSYS SHELL57 thermal elements and solid structural elements changed to SOLID70 thermal elements) is performed to determine the temperature distribution across the disk. The temperature data is then read back into the structural model so that material properties can be taken at temperature. For Thermal Condition 3, a constant temperature of -40°F is applied throughout the model.

For each thermal condition and basket drop orientation, two analyses are performed. The first analysis is for the support disk without thermal stresses (impact load only) and the second accounts for thermal stresses (impact plus thermal).

2.6.14.4 Stress Evaluation of Yankee-MPC Fuel Basket Support Disk for a 1-Foot End Drop Condition

The support disks of the Yankee-MPC fuel basket are located by 8 tie rods with spacers. A structural analysis is performed using ANSYS to evaluate the effect of a 1-foot end drop impact, which corresponds to the most severe out-of-plane loading. The model described in Section 2.6.14.2 is used in conjunction with a 20g deceleration. Linearized stresses at the cross sections identified in Figure 2.6.14.2-9 are compared to stress allowables in accordance with the ASME Code, Section III, Subsection NG.

The stress evaluation results for the 1-foot end drop condition are summarized as.

Thermal Condition	P _m		P _m +P _b	
	Stress Intensity (ksi)	M.S.	Stress Intensity (ksi)	M.S.
2	0	N/A	18.93	2.39
3	0	N/A	19.20	2.51

The margin of safety (M.S.) is calculated as:

$$\text{M.S.} = (\text{Stress Allowable}/\text{Stress Intensity}) - 1$$

The allowable stress intensity for $P_m + P_b$ is $1.5 S_m$. At 539°F, for 17-4PH material, this value is equal to 63.8 ksi and at -40°F this value is equal to 67.5 ksi.

The minimum margin of safety is +2.39. The P_m stresses in the support disk for end drop conditions are essentially zero because there is no in-plane loading. Tables 2.6.14.4-1 and 2.6.14.4-2 list the 40 highest $P_m + P_b$ stress intensities for thermal conditions 2 and 3 respectively. Locations of the 10 highest $P_m + P_b$ stress intensities for Thermal Condition 2 are shown in Figure 2.6.14.4-1. Note that the locations are not exactly symmetric because the locations of the restraints (8 tie-rod spacers) in the model are not symmetric due to the finite element mesh not being symmetric (Figure 2.6.14.2-1).

Figure 2.6.14.4-1 Locations of Maximum $P_m + P_b$ Stresses in the Yankee-MPC Fuel Basket,
1-Foot End Drop, Thermal Condition 2

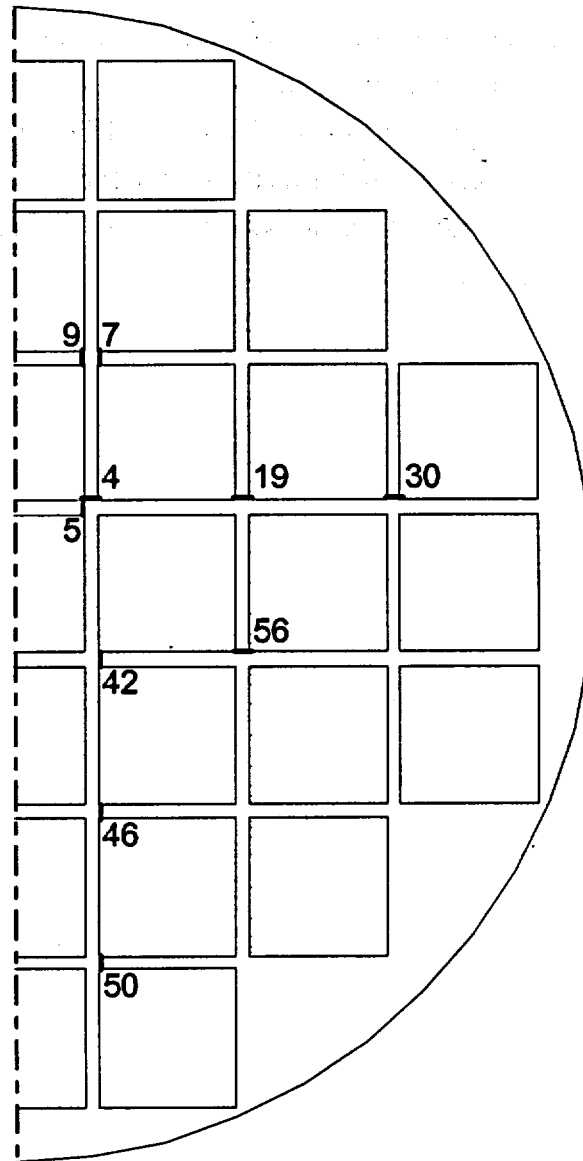


Table 2.6.14.4-1 P_m+P_b Stresses for Yankee-MPC Basket Support Disk—1-Foot
End Drop Thermal Condition 2

Section	Sx (ksi)	Sy (ksi)	Sxy (ksi)	Stress Intensity (ksi)	Allowable Stress (ksi)	Margin of Safety
50	-18.8	-2.0	-1.2	18.9	63.8	2.39
46	-18.8	-6.4	0.5	18.8	63.8	2.40
19	-6.5	-18.7	-0.1	18.7	63.8	2.41
5	-18.7	-9.9	0.0	18.7	63.8	2.42
30	-2.2	-18.4	1.0	18.4	63.8	2.46
56	-6.5	-18.4	0.2	18.4	63.8	2.47
9	-18.3	-6.8	0.0	18.3	63.8	2.49
7	-18.3	-6.7	-0.2	18.3	63.8	2.49
4	-9.8	-18.3	-0.1	18.3	63.8	2.50
42	-18.1	-9.8	0.4	18.1	63.8	2.52
11	-18.1	-2.1	1.0	18.1	63.8	2.53
3	-17.9	-9.9	-0.1	17.9	63.8	2.56
67	-2.3	-16.6	-0.6	16.7	63.8	2.83
79	0.0	-16.6	0.1	16.6	63.8	2.85
103	-16.6	0.0	0.1	16.6	63.8	2.86
13	-16.3	-2.4	0.5	16.3	63.8	2.91
94	-16.3	0.0	0.0	16.3	63.8	2.93
80	0.0	-16.2	-0.1	16.2	63.8	2.93
104	-16.2	0.0	-0.1	16.2	63.8	2.93
95	-15.9	0.0	-0.1	15.9	63.8	3.03
78	0.0	-15.7	0.1	15.7	63.8	3.07
102	-15.7	0.0	0.1	15.7	63.8	3.07
93	-15.6	0.0	0.0	15.6	63.8	3.09
77	-2.2	-12.5	-3.6	13.7	63.8	3.68
66	-12.5	-2.2	-3.6	13.7	63.8	3.68
89	-0.2	-13.5	-1.2	13.6	63.8	3.71
88	-0.2	-13.4	0.5	13.4	63.8	3.77
20	-13.3	-10.1	0.0	13.3	63.8	3.81
45	-10.0	-13.2	0.3	13.2	63.8	3.84
87	-0.1	-12.8	0.3	12.9	63.8	3.97
82	0.1	-12.7	-0.2	12.8	63.8	3.97
37	3.2	-9.2	1.4	12.7	63.8	4.04
53	-9.4	2.9	-1.5	12.6	63.8	4.06
81	0.1	-12.6	-0.1	12.6	63.8	4.06
106	-12.4	0.1	0.5	12.6	63.8	4.07
107	-12.1	0.2	-1.2	12.5	63.8	4.10
83	0.2	-12.1	1.0	12.4	63.8	4.14
97	-12.3	0.1	-0.2	12.4	63.8	4.15
96	-12.3	0.1	-0.1	12.4	63.8	4.17
105	-12.3	0.1	0.3	12.4	63.8	4.17

Note: See Figure 2.6.14.2-9 for section locations and definition of coordinate system.

Table 2.6.14.4-2 $P_m + P_b$ Stresses for Yankee-MPC Basket Support Disk—1-Foot
End Drop Thermal Condition 3

Section	Sx (ksi)	Sy (ksi)	Sxy (ksi)	Stress Intensity (ksi)	Allowable Stress (ksi)	Margin of Safety
5	-19.2	-10.2	0.0	19.2	67.5	2.51
46	-18.9	-6.5	0.6	18.9	67.5	2.56
19	-6.7	-18.9	-0.2	18.9	67.5	2.58
50	-18.7	-2.1	-1.1	18.8	67.5	2.59
4	-10.0	-18.7	-0.1	18.7	67.5	2.61
42	-18.5	-10.1	0.4	18.6	67.5	2.64
56	-6.7	-18.5	0.2	18.5	67.5	2.64
9	-18.4	-6.9	-0.1	18.4	67.5	2.66
7	-18.4	-6.8	-0.3	18.4	67.5	2.66
30	-2.2	-18.3	1.0	18.4	67.5	2.67
3	-18.3	-10.2	-0.1	18.3	67.5	2.68
11	-18.0	-2.2	0.9	18.1	67.5	2.74
79	0.0	-16.7	0.1	16.7	67.5	3.05
103	-16.6	0.0	0.1	16.6	67.5	3.06
67	-2.4	-16.6	-0.6	16.6	67.5	3.06
94	-16.3	0.0	0.0	16.3	67.5	3.13
13	-16.3	-2.4	0.4	16.3	67.5	3.15
80	0.0	-16.1	-0.1	16.1	67.5	3.18
102	-16.1	0.0	0.1	16.1	67.5	3.18
78	0.0	-16.1	0.1	16.1	67.5	3.18
104	-16.1	0.0	-0.1	16.1	67.5	3.18
93	-16.0	0.0	0.0	16.0	67.5	3.21
95	-15.8	0.0	-0.1	15.8	67.5	3.28
20	-13.6	-10.1	-0.1	13.6	67.5	3.96
45	-10.1	-13.5	0.4	13.6	67.5	3.98
88	-0.2	-13.5	0.6	13.5	67.5	4.01
89	-0.2	-13.4	-1.1	13.5	67.5	4.01
77	-2.2	-12.2	-3.5	13.3	67.5	4.06
66	-12.2	-2.2	-3.5	13.3	67.5	4.06
87	-0.1	-13.2	0.4	13.2	67.5	4.13
81	0.1	-12.9	-0.2	13.0	67.5	4.21
82	0.1	-12.8	-0.3	12.9	67.5	4.22
106	-12.5	0.1	0.6	12.7	67.5	4.31
105	-12.6	0.1	0.4	12.7	67.5	4.33
96	-12.6	0.1	-0.1	12.7	67.5	4.33
37	3.1	-9.1	1.3	12.5	67.5	4.40
8	-9.8	-12.5	-0.1	12.5	67.5	4.40
97	-12.4	0.1	-0.3	12.5	67.5	4.41
53	-9.3	2.8	-1.5	12.5	67.5	4.41
107	-12.1	0.2	-1.1	12.4	67.5	4.43

Note: See Figure 2.6.14.2-9 for section locations and definition of coordinate system.

2.6.14.5 Stress Evaluation of Yankee-MPC Fuel Basket Support Disk for Thermal Plus a 1-Foot End Drop Combined Condition

The thermal expansion loads described in Section 2.6.14.3 are applied to the finite element model simultaneously with the 20g end drop loads described in Section 2.6.14.4 to produce a combined thermal expansion plus end impact loading. The stress evaluation results for thermal plus the 1-foot end drop conditions are summarized below. The allowable stress is $3.0 S_m$ in accordance with the ASME Code, Section III, Subsection NG for primary plus secondary (P+Q) stress intensity range. The minimum margin of safety is +3.57. Thermal Condition 2 is the governing case. Note that the thermal stress (Q) is essentially zero for Thermal Condition 3, since there is no temperature gradient in the disk. Table 2.6.14.5-1 shows the 40 highest P+Q stress intensities for Thermal Condition 2. Locations of the 10 highest P+Q stress intensities for Thermal Condition 2 are shown in Figure 2.6.14.5-1.

<u>Thermal</u> <u>Condition</u>	<u>P + Q</u> <u>Stress Intensity (ksi)</u>	<u>Margin of Safety</u>
2	27.9	3.57
3	19.2	6.03

Figure 2.6.14.5-1 Locations of Maximum P+Q Stresses in the Yankee-MPC Basket Support Disk for the 1-Foot End Drop, Thermal Condition 2

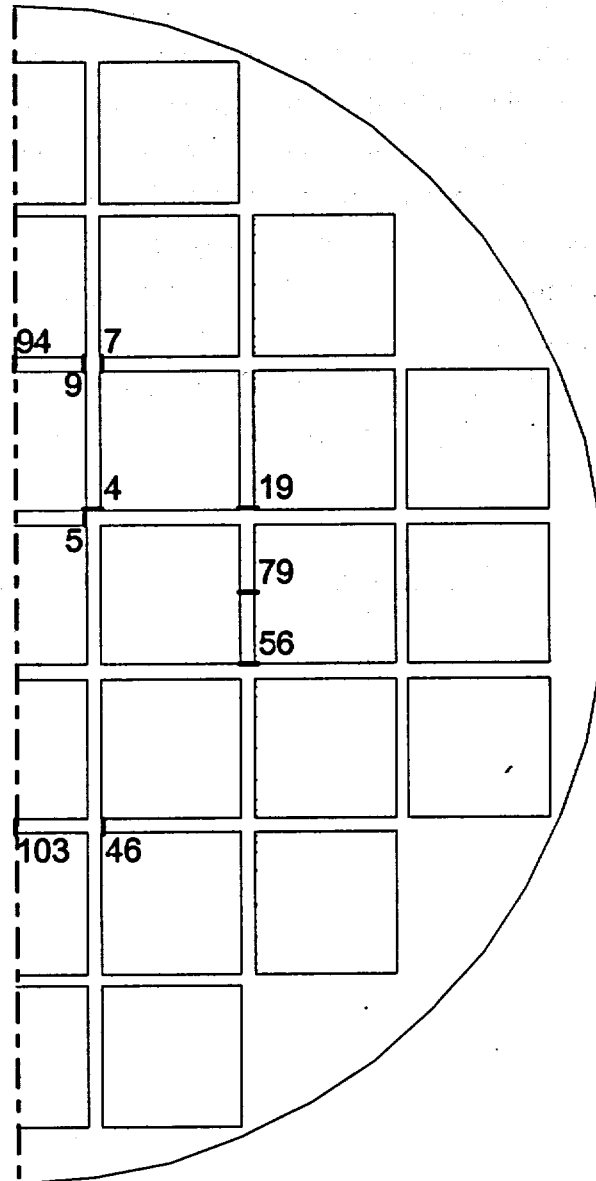


Table 2.6.14.5-1 P+Q Stresses for Yankee-MPC Basket Support Disk—1-Foot
End Drop Thermal Condition 2

Section	Sx (ksi)	Sy (ksi)	Sxy (ksi)	Stress Intensity (ksi)	Allowable Stress (ksi)	Margin of Safety
46	-27.9	-12.3	0.8	27.9	127.7	3.57
19	-12.3	-27.9	-0.4	27.9	127.7	3.58
7	-27.4	-12.5	-0.5	27.5	127.7	3.65
56	-11.0	-27.4	0.2	27.4	127.7	3.65
9	-27.4	-11.3	0.0	27.4	127.7	3.66
79	0.0	-25.6	0.1	25.6	127.7	3.98
103	-25.6	0.0	0.1	25.6	127.7	3.99
94	-25.3	0.0	0.0	25.3	127.7	4.04
5	-25.0	-16.0	0.0	25.0	127.7	4.11
4	-13.4	-24.5	-0.3	24.5	127.7	4.22
42	-24.3	-13.5	0.5	24.4	127.7	4.24
3	-24.1	-13.6	-0.2	24.1	127.7	4.31
88	-0.2	-22.5	0.8	22.5	127.7	4.67
102	-22.1	0.0	0.1	22.1	127.7	4.78
78	0.0	-22.1	0.1	22.1	127.7	4.78
82	0.1	-21.9	-0.5	22.0	127.7	4.80
93	-21.9	0.0	0.0	21.9	127.7	4.83
106	-21.6	0.1	0.8	21.8	127.7	4.87
97	-21.4	0.1	-0.5	21.6	127.7	4.91
23	-14.0	-20.9	0.2	20.9	127.7	5.12
50	-20.7	-5.4	-0.8	20.7	127.7	5.17
22	-20.5	-14.3	0.2	20.5	127.7	5.23
30	-5.6	-20.3	0.7	20.3	127.7	5.29
24	-20.0	-12.2	-0.2	20.0	127.7	5.38
61	-20.0	-13.9	0.2	20.0	127.7	5.38
11	-20.0	-5.6	0.7	20.0	127.7	5.38
45	-18.9	-19.4	0.5	19.7	127.7	5.49
20	-19.4	-18.9	-0.2	19.5	127.7	5.56
87	-0.1	-19.1	0.5	19.1	127.7	5.70
81	0.1	-18.8	-0.3	18.9	127.7	5.77
67	-7.4	-18.7	-0.6	18.8	127.7	5.81
105	-18.5	0.1	0.5	18.6	127.7	5.87
96	-18.4	0.1	-0.2	18.5	127.7	5.90
13	-18.4	-7.4	0.4	18.4	127.7	5.93
80	0.0	-18.3	-0.1	18.3	127.7	5.98
104	-18.3	0.0	-0.1	18.3	127.7	5.98
8	-14.2	-18.2	-0.1	18.2	127.7	6.00
95	-18.0	0.0	-0.1	18.0	127.7	6.11
18	-17.9	-14.4	0.0	17.9	127.7	6.14
57	-17.6	-14.4	0.2	17.7	127.7	6.24

Note: See Figure 2.6.14.2-9 for section locations and definition of coordinate system.

2.6.14.6 Stress Evaluation of Yankee-MPC Basket Tie Rods and Spacers for a 1-Foot End Drop Load Condition

The Yankee-MPC basket support disks are connected by eight tie rods with spacers to maintain the spacing of the support disks. The tie rods and spacers are constructed from Type 304 stainless steel. The tie rods are only threaded at the upper end for the top nut to provide rigidity of the basket assembly. The tie rods do not transmit any load other than their own weight. In a side drop the load due to the disks and the fuel are transmitted directly into the canister wall by the support disks. In an end drop the spacers and split-spacers transmit the load due to the weight of the support disks, aluminum heat transfer disks, one end weldment, and the spacers. The weight of the fuel assemblies is transmitted directly into the canister lid or bottom, since the fuel tubes in the basket are open at both ends. In drop orientations other than on the end, the spacers only experience that component of the weight of the support disks, heat transfer disks, one end weldment, and the spacers that act along the axis of the cask. Thus, the end drop is the critical loading condition.

During an end drop, the weight of the 22 support disks, 1 weldment, 14 aluminum heat transfer disks, and the spacers and end nuts will be supported by the spacers on the 8 tie rods. This results in compressive stress over the cross-sectional area of the spacers. The total weight of the basket is 9,530 pounds. Since the weight of 1 end weldment weighing 438 pounds (the one nearest the plane of impact) and the fuel tubes weighing 2,164 pounds are transmitted directly into the end of the canister, the remaining load acting over the area of the spacers is 6,928 pounds. For the 1-foot end drop, the deceleration is 20g, which results in a total end drop load of 138,560 pounds. The area in compression is $3.68 \text{ inch}^2 (= \pi(2.5^2 - 1.25^2)/4)$. The compressive stress is $138,560/(8 \times 3.68) = 4.7 \text{ ksi}$ and is considered to be a membrane stress. The allowable membrane stress, based on ASME Code, Section III, Subsection NG is $1.0 S_m$. Using a material temperature of 500°F, $S_m = 17.5 \text{ ksi}$ and the corresponding margin of safety is:

$$\begin{aligned} \text{M.S.} &= (17.5/4.7) - 1 \\ &= +2.72 \end{aligned}$$

Therefore, structural adequacy of the tie rod/spacer assemblies is demonstrated.

2.6.14.7 Stress Evaluation of Yankee-MPC Basket Support Disk for a 1-Foot Side Drop Load Condition

To determine the structural adequacy of the support disk in the 1-foot side drop impact load condition, a quasi-static impact load equal to the weight of the fuel and tubes multiplied by a 20g amplification factor is applied to the support disk structure. The inertial loading of the support disk is included via the density input for the 17-4 PH stainless steel. The value of 20g is conservative since the impact limiter design deceleration for a 1-foot side drop is 18.1g. The fuel assembly load is transmitted by direct compression through the tube wall to the web structure of the support disk. While there are 24 total disks (22 support disks plus two end weldments), only 22 of the disks are assumed to transmit the load to the canister shell. The maximum in-plane loading occurs in the side drop, which is evaluated using a finite element analysis. The analysis is performed using the three-dimensional support disk side drop model described in Section 2.6.14.2. As discussed in Section 2.6.14.1, two bounding cases of basket orientation (0° and 45°) are considered in the analysis.

The material properties are evaluated at two thermal conditions: Thermal Condition 2, the cold condition (-40°F with 12.5 kW heat load) which has the largest change in temperature from the center of the basket to the outer edge and Thermal Condition 3, extreme cold (-40°F ambient with no heat load). Linearized stresses at the cross-sections (Figures 2.6.14.2-9 and 2.6.14.2-10) for the five critical disks (Figure 2.6.14.2-8) are compared to the stress allowable per the ASME Code, Section III, Subsection NG.

Primary membrane stress intensity is compared to $1.0 S_m$ and primary membrane plus bending stress intensity is compared to $1.5 S_m$ for the material at 539°F and -40°F for Thermal Conditions 2 and 3 (Section 2.6.14.3), respectively. The stress evaluation results for the 1-foot side drop condition are summarized in Table 2.6.14.7-1. The minimum margin of safety is +0.09, which occurs in disk No. 5 for the 45° basket drop orientation (Thermal Condition 2). For the 0° basket orientation, the highest P_m and P_m+P_b stresses occur in Disk No. 1 (Thermal Condition 2). Tables 2.6.14.7-2 through 2.6.14.7-5 list the 40 highest P_m and P_m+P_b stress intensities for Disk No. 1. For the 45° basket orientation, the highest P_m and P_m+P_b stresses occur in Disk No. 5 (Thermal Condition 2). Tables 2.6.14.7-6 through 2.6.14.7-9 list the 40 highest P_m and P_m+P_b stress intensities for Disk No. 5. Locations of the 10 highest P_m and P_m+P_b stress intensities for Disk No. 1 (0° basket orientation, Thermal Condition 2) are shown in Figures 2.6.14.7-1 and 2.6.14.7-2, respectively. Locations of the 10 highest P_m and P_m+P_b stress intensities for disk No. 5 (45° basket orientation, Thermal Condition 2) are shown in Figures 2.6.14.7-3 and 2.6.14.7-4, respectively.

Figure 2.6.14.7-1 Locations of Maximum P_m Stresses, Yankee-MPC Basket, Disk 1,
1-Foot Side Drop, 0° Orientation, Thermal Condition 2

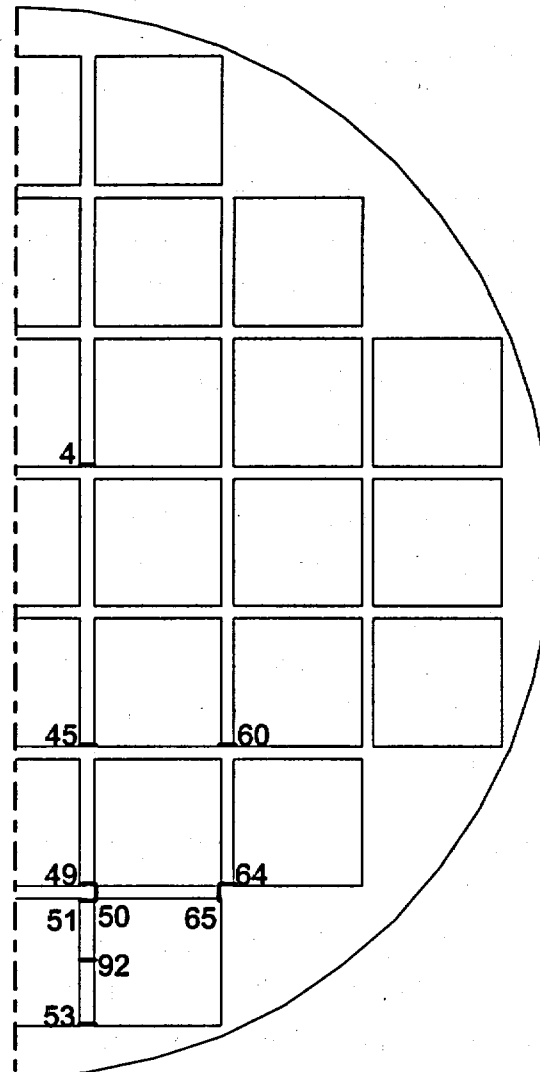


Figure 2.6.14.7-2 Locations of Maximum P_m+P_b Stresses, Yankee-MPC Basket, Disk 1,
1-Foot Side Drop, 0° Orientation, Thermal Condition 2

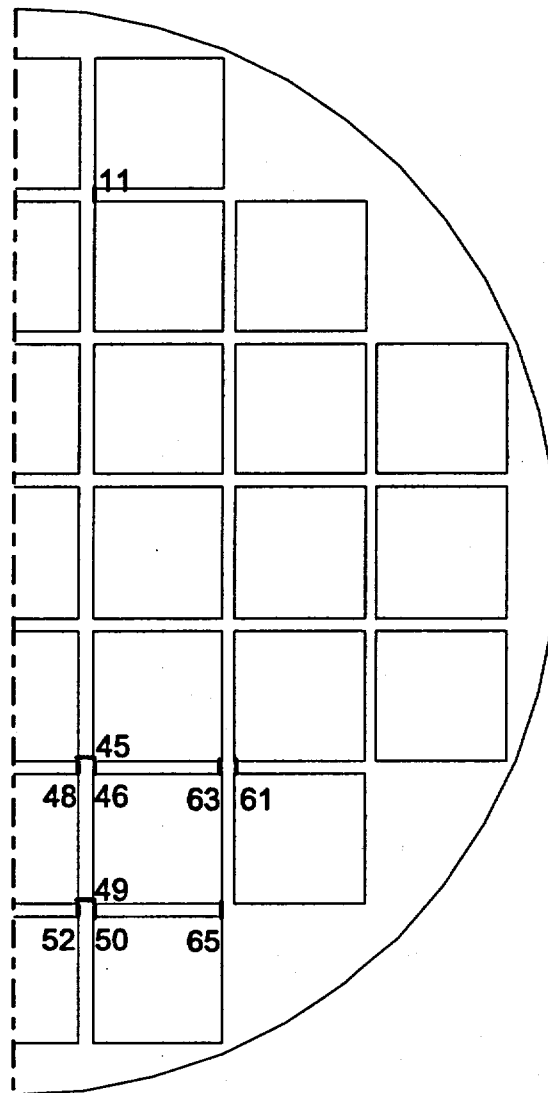


Figure 2.6.14.7-3 Locations of Maximum P_m Stresses, Yankee-MPC Basket, Disk 5,
1-Foot Side Drop, 45° Orientation, Thermal Condition 2

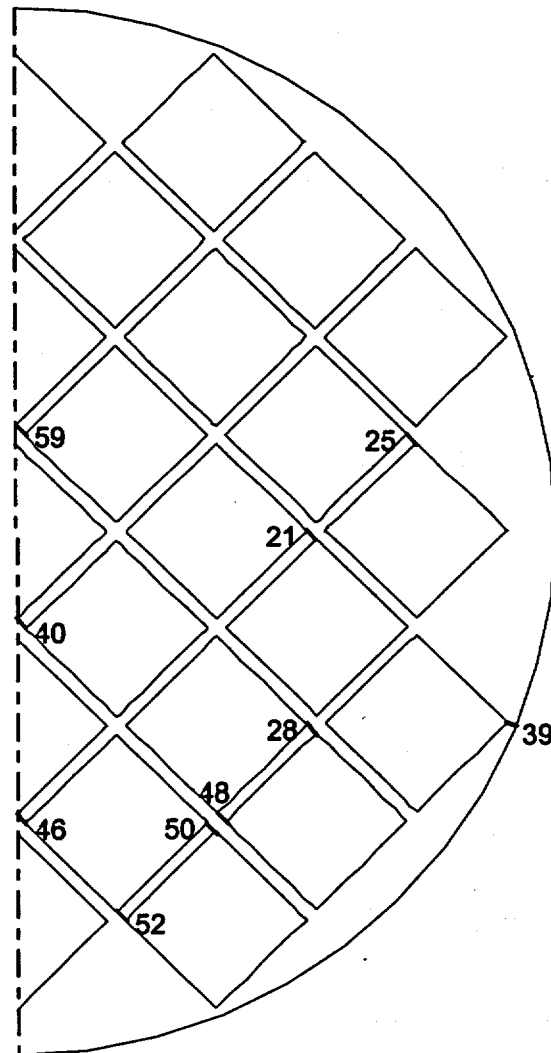


Figure 2.6.14.7-4 Locations of Maximum $P_m + P_b$ Stresses, Yankee-MPC Basket, Disk 5,
1-Foot Side Drop, 45° Orientation, Thermal Condition 2

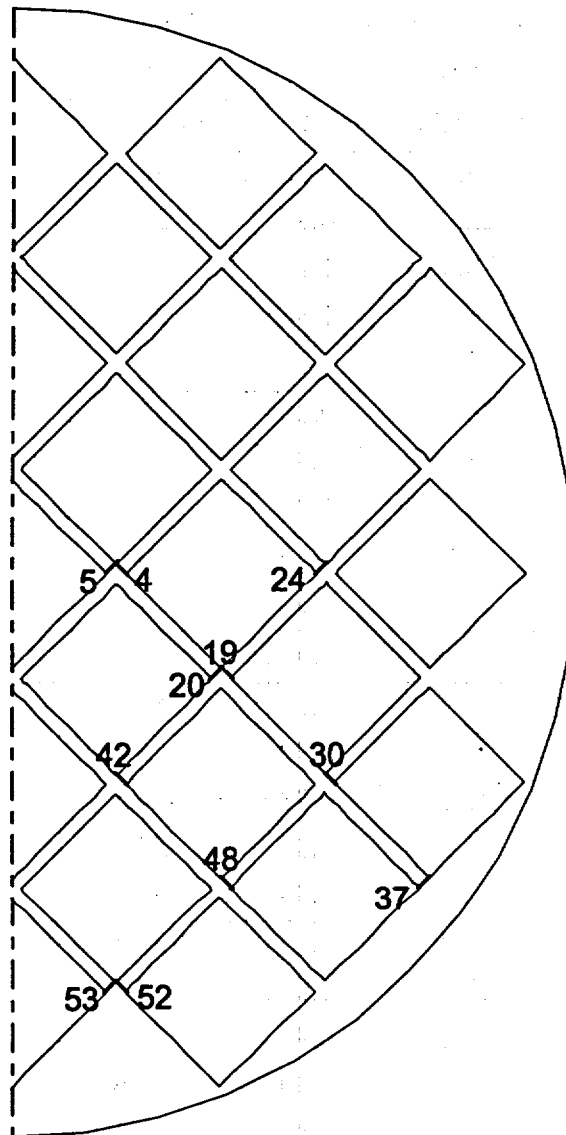


Table 2.6.14.7-1 Summary of Maximum Yankee-MPC Basket Support Disk Stresses for
1-Foot Side Drop

Thermal Condition	Disk Number	P_m		P_m+P_b	
		Stress Intensity (ksi)	Margin of Safety	Stress Intensity (ksi)	Margin of Safety
0° Basket Drop Orientation					
2	1	23.7	0.80	32.3	0.98
	2	22.9	0.86	30.9	1.06
	3	20.0	1.13	26.5	1.41
	4	18.0	1.36	23.5	1.71
	5	18.6	1.29	24.3	1.63
3	1	23.9	0.88	32.6	1.07
	2	23.1	0.95	31.2	1.16
	3	20.4	1.21	27.0	1.50
	4	18.0	1.46	24.0	1.82
	5	18.6	1.37	24.8	1.72
45° Basket Drop Orientation					
2	1	19.9	1.13	54.0	0.18
	2	21.4	0.99	56.1	0.14
	3	22.1	0.92	57.5	0.11
	4	22.5	0.89	58.2	0.10
	5	22.7	0.88	58.8	0.09
3	1	21.0	1.15	55.5	0.22
	2	22.1	1.04	57.7	0.17
	3	23.4	0.93	59.0	0.14
	4	23.7	0.90	59.6	0.13
	5	23.9	0.88	60.1	0.12

Table 2.6.14.7-2 P_m Stresses for Yankee-MPC Basket Support Disk—1-Foot Side Drop, 0° Basket Orientation, Thermal Condition 2, Disk Number 1

Section	Sx (ksi)	Sy (ksi)	Sxy (ksi)	Stress	Allowable	Margin of Safety
				Intensity (ksi)	Stress (ksi)	
49	12.2	-11.5	0.0	23.7	42.6	0.80
45	11.1	-9.2	-0.2	20.3	42.6	1.10
64	8.0	-10.4	-0.1	18.4	42.6	1.32
60	9.3	-8.2	-0.1	17.4	42.6	1.44
65	4.9	-10.3	1.0	15.3	42.6	1.78
53	-7.3	-13.8	-0.1	13.8	42.6	2.08
92	0.0	-13.8	-0.1	13.8	42.6	2.08
51	-7.7	-13.8	-0.1	13.8	42.6	2.09
50	4.9	-8.5	-1.4	13.7	42.6	2.11
4	7.5	-5.7	0.0	13.3	42.6	2.21
66	-9.9	-7.8	-4.1	13.1	42.6	2.25
71	8.2	-4.9	0.0	13.1	42.6	2.26
52	5.0	-7.9	1.2	13.1	42.6	2.26
56	6.9	-5.9	-0.1	12.8	42.6	2.33
41	4.3	-8.0	-0.2	12.4	42.6	2.44
48	4.3	-7.4	1.1	11.9	42.6	2.57
8	8.2	-3.5	-0.1	11.7	42.6	2.64
90	0.0	-11.5	0.0	11.5	42.6	2.70
47	-7.0	-11.5	0.0	11.5	42.6	2.71
63	4.5	-6.3	0.9	10.9	42.6	2.90
46	4.5	-5.9	-1.3	10.7	42.6	2.98
10	-10.6	-3.4	-0.1	10.6	42.6	3.00
72	4.5	-5.7	1.0	10.5	42.6	3.07
91	0.0	-10.4	-0.1	10.4	42.6	3.10
62	-4.9	-10.4	-0.1	10.4	42.6	3.11
61	4.5	-5.4	-1.2	10.3	42.6	3.14
67	7.5	-2.5	0.0	10.0	42.6	3.25
12	8.4	-1.2	-0.1	9.7	42.6	3.41
87	0.0	-9.2	-0.2	9.2	42.6	3.62
6	-9.2	-5.7	0.0	9.2	42.6	3.63
43	-4.2	-9.2	-0.2	9.2	42.6	3.63
19	5.4	-3.7	-0.1	9.1	42.6	3.66
2	-9.0	-8.0	-0.2	9.0	42.6	3.72
23	6.6	-1.6	0.0	8.2	42.6	4.21
88	0.0	-8.1	-0.1	8.1	42.6	4.23
58	-6.7	-8.1	-0.1	8.1	42.6	4.24
78	0.0	-8.0	-0.2	8.0	42.6	4.30
42	1.3	-5.8	-1.1	7.5	42.6	4.71
28	-7.4	-2.4	0.0	7.4	42.6	4.73
21	-7.3	-3.7	-0.1	7.3	42.6	4.80

Note: See Figure 2.6.14.2-9 for section locations and definition of coordinate system.

Table 2.6.14.7-3 $P_m + P_b$ Stresses for Yankee-MPC Basket Support Disk—1-Foot Side Drop, 0° Basket Orientation, Thermal Condition 2, Disk Number 1

Section	Sx (ksi)	Sy (ksi)	Sxy (ksi)	Stress	Allowable	Margin of Safety
				Intensity (ksi)	Stress (ksi)	
50	28.9	-3.4	0.0	32.3	63.8	0.98
52	23.4	-4.6	-0.1	28.1	63.8	1.27
46	25.5	-1.2	-0.3	26.7	63.8	1.39
49	11.2	-13.0	3.0	24.9	63.8	1.56
48	19.7	-4.8	-0.3	24.5	63.8	1.61
11	-23.9	-6.4	-1.8	24.1	63.8	1.65
45	9.7	-12.9	2.6	23.1	63.8	1.76
61	21.8	-0.8	-0.3	22.6	63.8	1.83
65	15.7	-5.5	-1.1	21.3	63.8	2.00
63	15.3	-5.1	-0.2	20.4	63.8	2.13
60	7.3	-12.5	2.0	20.2	63.8	2.17
13	-19.6	-5.1	1.7	19.8	63.8	2.22
7	-19.4	-7.3	-1.9	19.7	63.8	2.24
64	9.7	-9.7	-1.3	19.5	63.8	2.28
53	-8.2	-18.0	-3.9	19.3	63.8	2.31
3	18.0	-1.1	0.1	19.1	63.8	2.34
107	18.2	-0.5	1.0	18.8	63.8	2.39
51	-8.9	-16.4	-3.6	17.9	63.8	2.58
57	16.0	-1.1	0.0	17.1	63.8	2.73
109	16.4	-0.6	1.0	17.1	63.8	2.74
72	15.3	-1.5	-0.3	16.8	63.8	2.81
104	15.8	-0.8	1.2	16.7	63.8	2.82
9	-16.0	-6.1	1.9	16.3	63.8	2.92
43	-7.5	-15.7	-2.1	16.2	63.8	2.94
66	-11.7	-9.3	-5.3	15.9	63.8	3.01
41	1.1	-14.4	0.7	15.6	63.8	3.10
42	14.9	-0.6	0.2	15.6	63.8	3.11
106	14.9	-0.5	0.9	15.5	63.8	3.11
22	-15.2	-5.5	-1.6	15.4	63.8	3.14
5	13.3	-1.8	0.1	15.1	63.8	3.23
40	-14.9	-3.6	-0.5	15.0	63.8	3.27
103	14.1	-0.7	1.1	14.9	63.8	3.27
33	-14.8	-0.4	0.7	14.9	63.8	3.29
68	14.6	0.8	-0.6	14.6	63.8	3.38
71	9.2	-5.0	-1.6	14.5	63.8	3.40
98	-14.4	-1.1	1.1	14.5	63.8	3.40
2	-10.3	-11.6	-3.5	14.5	63.8	3.41
56	5.9	-8.1	1.5	14.4	63.8	3.44
4	6.8	-6.7	2.0	14.1	63.8	3.54
47	-7.9	-12.4	-3.2	14.0	63.8	3.56

Note: See Figure 2.6.14.2-9 for section locations and definition of coordinate system.

Table 2.6.14.7-4 P_m Stresses for Yankee-MPC Basket Support Disk—1-Foot Side
Drop, 0° Basket Orientation, Thermal Condition 3, Disk Number 1

Section	Sx (ksi)	Sy (ksi)	Sxy (ksi)	Stress	Allowable	Margin of Safety
				Intensity (ksi)	Stress (ksi)	
49	12.3	-11.7	-0.1	23.9	45.0	0.88
45	11.1	-9.3	-0.2	20.5	45.0	1.20
64	7.9	-10.4	-0.1	18.3	45.0	1.46
60	9.2	-8.1	-0.1	17.3	45.0	1.60
65	4.9	-10.2	1.0	15.3	45.0	1.94
53	-7.2	-14.0	-0.1	14.0	45.0	2.22
92	0.0	-13.9	-0.1	13.9	45.0	2.23
51	-7.7	-13.9	-0.1	13.9	45.0	2.23
50	4.9	-8.6	-1.4	13.8	45.0	2.26
4	7.6	-5.8	-0.1	13.5	45.0	2.35
52	5.0	-8.0	1.2	13.2	45.0	2.41
66	-9.8	-7.8	-4.1	13.0	45.0	2.45
71	8.1	-4.9	0.0	13.0	45.0	2.47
56	6.8	-5.9	-0.1	12.6	45.0	2.56
41	4.4	-8.1	-0.2	12.6	45.0	2.57
48	4.3	-7.5	1.1	12.0	45.0	2.76
8	8.3	-3.5	-0.1	11.8	45.0	2.81
90	0.0	-11.6	0.0	11.6	45.0	2.87
47	-7.1	-11.6	0.0	11.6	45.0	2.88
63	4.5	-6.3	0.9	10.9	45.0	3.14
10	-10.8	-3.5	-0.1	10.8	45.0	3.17
46	4.5	-6.0	-1.3	10.8	45.0	3.18
72	4.5	-5.6	1.0	10.4	45.0	3.34
91	0.0	-10.3	-0.1	10.3	45.0	3.36
62	-4.9	-10.3	-0.1	10.3	45.0	3.37
61	4.5	-5.4	-1.2	10.2	45.0	3.39
67	7.5	-2.4	0.0	9.9	45.0	3.53
12	8.5	-1.3	-0.1	9.7	45.0	3.62
87	0.0	-9.3	-0.2	9.3	45.0	3.83
6	-9.3	-5.8	-0.1	9.3	45.0	3.83
43	-4.4	-9.3	-0.2	9.3	45.0	3.83
2	-9.2	-8.1	-0.2	9.2	45.0	3.90
19	5.3	-3.7	-0.1	9.0	45.0	4.00
78	0.0	-8.1	-0.2	8.1	45.0	4.54
88	0.0	-8.1	-0.1	8.1	45.0	4.55
58	-6.5	-8.1	-0.1	8.1	45.0	4.56
23	6.5	-1.6	0.0	8.1	45.0	4.57
42	1.3	-5.9	-1.1	7.5	45.0	4.99
28	-7.4	-2.4	0.0	7.4	45.0	5.06
21	-7.3	-3.7	-0.1	7.3	45.0	5.18

Note: See Figure 2.6.14.2-9 for section locations and definition of coordinate system.

Table 2.6.14.7-5 P_m+P_b Stresses for Yankee-MPC Basket Support Disk—1-Foot Side Drop, 0° Basket Orientation, Thermal Condition 3, Disk Number 1

Section	Sx (ksi)	Sy (ksi)	Sxy (ksi)	Stress	Allowable	Margin of Safety
				Intensity (ksi)	Stress (ksi)	
50	29.2	-3.4	0.0	32.6	67.5	1.07
52	23.5	-4.7	-0.1	28.3	67.5	1.39
46	25.8	-1.2	-0.3	27.0	67.5	1.50
49	11.3	-13.3	3.0	25.2	67.5	1.68
48	19.7	-4.9	-0.3	24.6	67.5	1.75
11	-24.3	-6.6	-1.9	24.5	67.5	1.76
45	9.7	-13.1	2.6	23.4	67.5	1.89
61	21.8	-0.7	-0.4	22.5	67.5	2.01
65	15.5	-5.5	-1.1	21.1	67.5	2.21
63	15.0	-5.2	-0.2	20.2	67.5	2.34
60	7.1	-12.6	2.0	20.1	67.5	2.36
7	-19.8	-7.4	-2.0	20.1	67.5	2.36
13	-19.7	-5.1	1.7	19.9	67.5	2.39
3	18.5	-1.1	0.1	19.5	67.5	2.45
53	-8.2	-18.2	-3.9	19.5	67.5	2.46
64	9.7	-9.6	-1.3	19.4	67.5	2.48
107	18.3	-0.5	1.0	18.9	67.5	2.56
51	-9.0	-16.6	-3.6	18.1	67.5	2.74
109	16.4	-0.6	1.0	17.1	67.5	2.95
57	16.0	-1.1	0.0	17.0	67.5	2.97
104	15.8	-0.8	1.2	16.8	67.5	3.03
72	15.2	-1.4	-0.2	16.6	67.5	3.06
43	-7.8	-16.0	-2.2	16.5	67.5	3.09
9	-16.0	-6.1	1.9	16.4	67.5	3.12
66	-11.7	-9.4	-5.3	16.0	67.5	3.23
41	1.2	-14.7	0.7	15.9	67.5	3.23
42	15.4	-0.5	0.2	15.9	67.5	3.24
106	14.9	-0.5	0.9	15.6	67.5	3.34
22	-15.2	-5.6	-1.6	15.5	67.5	3.37
5	13.4	-1.9	0.1	15.2	67.5	3.43
40	-15.0	-3.6	-0.5	15.1	67.5	3.48
103	14.0	-0.7	1.1	14.9	67.5	3.54
2	-10.5	-12.0	-3.5	14.9	67.5	3.54
33	-14.8	-0.3	0.7	14.8	67.5	3.55
98	-14.6	-1.1	1.0	14.7	67.5	3.61
68	14.5	0.8	-0.6	14.6	67.5	3.64
71	9.1	-4.9	-1.6	14.4	67.5	3.68
56	5.7	-8.3	1.5	14.4	67.5	3.70
4	6.8	-7.0	2.0	14.4	67.5	3.70
47	-8.0	-12.6	-3.2	14.3	67.5	3.73

Note: See Figure 2.6.14.2-9 for section locations and definition of coordinate system.

Table 2.6.14.7-6 P_m Stresses for Yankee-MPC Basket Support Disk—1-Foot Side
Drop, 45° Basket Orientation, Thermal Condition 2, Disk Number 5

Section	Sx (ksi)	Sy (ksi)	Sxy (ksi)	Stress	Allowable	Margin of Safety
				Intensity (ksi)	Stress (ksi)	
39	-11.4	-19.7	-5.8	22.7	42.6	0.88
59	-14.7	3.9	-6.5	22.7	42.6	0.88
52	11.8	-8.5	1.6	20.6	42.6	1.07
40	-11.9	3.3	-5.7	19.0	42.6	1.24
46	-11.7	3.2	-5.2	18.2	42.6	1.34
25	-10.5	5.7	-0.2	16.3	42.6	1.62
50	-14.7	-8.5	-0.1	14.7	42.6	1.90
21	-10.6	3.6	0.7	14.3	42.6	1.97
28	-13.9	-6.2	0.1	13.9	42.6	2.06
48	7.1	-6.2	1.8	13.8	42.6	2.08
49	-5.0	-12.9	-0.2	12.9	42.6	2.31
32	-12.8	-4.1	0.4	12.8	42.6	2.32
17	-10.9	1.5	0.7	12.5	42.6	2.40
45	-1.2	9.9	2.1	11.9	42.6	2.59
20	-3.2	7.4	2.3	11.6	42.6	2.67
58	-0.8	-8.3	-4.3	11.4	42.6	2.74
29	-6.5	-11.4	0.2	11.4	42.6	2.74
60	-1.9	-11.0	0.9	11.1	42.6	2.82
30	4.9	-4.1	2.1	10.0	42.6	3.27
43	-3.4	-9.6	0.3	9.6	42.6	3.41
44	-9.4	-0.5	-0.1	9.4	42.6	3.52
31	-4.8	3.7	1.9	9.3	42.6	3.59
41	-1.2	-9.2	0.7	9.3	42.6	3.60
72	-6.0	1.7	-2.4	9.1	42.6	3.66
23	8.0	5.7	1.3	8.6	42.6	3.95
22	-2.9	5.6	0.0	8.5	42.6	3.98
47	-1.5	-8.5	0.5	8.5	42.6	4.00
92	-0.6	-8.5	-0.1	8.5	42.6	4.03
5	-1.9	5.0	2.4	8.4	42.6	4.09
27	-3.7	-0.5	3.8	8.2	42.6	4.19
33	-3.0	-7.7	1.6	8.2	42.6	4.21
37	-6.5	0.9	1.7	8.1	42.6	4.28
10	-5.5	2.2	-0.2	7.7	42.6	4.55
54	0.3	-2.1	-3.6	7.5	42.6	4.65
19	6.0	3.6	2.3	7.4	42.6	4.74
7	-2.3	5.1	0.5	7.4	42.6	4.74
42	6.4	1.5	2.3	7.3	42.6	4.84
51	-3.4	2.5	1.8	6.9	42.6	5.21
26	-2.2	3.9	1.4	6.7	42.6	5.37
101	-6.5	-0.6	0.2	6.5	42.6	5.57

Note:1. See Figure 2.6.14.2-10 for section locations.

2. Stress components are based on the coordinate system shown in Figure 2.6.14.2-10, rotated 45°.

Table 2.6.14.7-7 $P_m + P_b$ Stresses for Yankee-MPC Basket Support Disk—1-Foot Side Drop, 45° Basket Orientation, Thermal Condition 2, Disk Number 5

Section	Sx (ksi)	Sy (ksi)	Sxy (ksi)	Stress	Allowable	Margin of Safety
				Intensity (ksi)	Stress (ksi)	
19	24.4	58.2	4.5	58.8	63.8	0.09
42	23.4	56.9	4.3	57.5	63.8	0.11
20	-55.3	-13.0	0.3	55.3	63.8	0.16
30	-9.5	-54.4	0.8	54.4	63.8	0.17
4	22.9	53.0	3.4	53.4	63.8	0.20
5	-53.0	-14.9	0.9	53.0	63.8	0.21
48	-5.1	-49.9	0.1	49.9	63.8	0.28
53	-49.4	-11.2	2.9	49.6	63.8	0.29
24	-49.4	-15.4	2.3	49.5	63.8	0.29
37	-47.8	-8.8	2.7	48.0	63.8	0.33
52	-0.4	-46.7	-0.1	46.7	63.8	0.37
31	-46.5	-12.8	0.7	46.5	63.8	0.37
45	-45.6	-7.4	-0.9	45.6	63.8	0.40
60	-38.7	-30.3	8.2	43.7	63.8	0.46
51	-42.9	-11.8	0.7	42.9	63.8	0.49
9	-42.1	-17.3	2.9	42.5	63.8	0.50
59	-38.0	-20.5	3.6	38.7	63.8	0.65
21	2.2	38.5	-2.1	38.6	63.8	0.65
33	-37.6	-16.5	2.9	38.0	63.8	0.68
3	-37.5	-21.6	2.7	37.9	63.8	0.68
6	9.7	37.6	-0.5	37.6	63.8	0.70
41	-31.3	-25.2	6.7	35.7	63.8	0.79
62	-35.0	-14.1	2.4	35.3	63.8	0.81
56	-34.5	-6.4	3.0	34.8	63.8	0.83
47	-30.9	-23.2	6.1	34.3	63.8	0.86
2	-22.4	-32.9	3.0	33.7	63.8	0.90
40	7.2	23.7	-14.2	32.8	63.8	0.95
32	-21.9	-31.5	3.5	32.7	63.8	0.95
26	-32.2	-1.6	-0.2	32.2	63.8	0.99
17	2.6	31.8	-2.2	31.9	63.8	1.00
46	6.3	22.0	-12.9	30.3	63.8	1.11
23	19.4	28.6	4.2	30.2	63.8	1.12
61	-16.2	-28.5	1.9	28.8	63.8	1.22
7	-27.9	-5.7	-0.8	27.9	63.8	1.29
28	-22.0	-24.2	4.1	27.4	63.8	1.33
39	-11.4	-20.2	-10.5	27.2	63.8	1.35
18	-25.6	-19.0	2.3	26.3	63.8	1.43
13	-26.1	-3.1	0.3	26.1	63.8	1.45
50	-20.5	-19.2	4.3	24.2	63.8	1.64
43	-18.6	-21.3	3.6	23.7	63.8	1.69

- Note: 1. See Figure 2.6.14.2-10 for section locations.
2. Stress components are based on the coordinate system shown in Figure 2.6.14.2-10, rotated 45°.

Table 2.6.14.7-8 P_m Stresses for Yankee-MPC Basket Support Disk—1-Foot Side Drop,
45° Basket Orientation, Thermal Condition 3, Disk Number 5

Section	Sx (ksi)	Sy (ksi)	Sxy (ksi)	Stress Intensity (ksi)	Allowable Stress (ksi)	Margin of Safety
59	-15.5	4.0	-6.9	23.9	45.0	0.88
39	-11.4	-19.7	-6.0	22.8	45.0	0.98
52	12.0	-8.6	1.7	20.9	45.0	1.16
40	-12.7	3.5	-6.0	20.2	45.0	1.23
46	-12.0	3.3	-5.3	18.7	45.0	1.41
25	-10.4	5.8	-0.2	16.2	45.0	1.78
50	-14.9	-8.6	-0.1	14.9	45.0	2.02
21	-10.6	3.7	0.8	14.3	45.0	2.14
28	-14.1	-6.3	0.2	14.1	45.0	2.20
48	7.2	-6.3	1.9	14.0	45.0	2.21
49	-5.1	-13.0	-0.2	13.0	45.0	2.45
32	-12.8	-4.2	0.4	12.9	45.0	2.50
17	-11.1	1.5	0.7	12.7	45.0	2.54
45	-1.3	10.1	2.2	12.1	45.0	2.71
60	-1.9	-11.7	1.0	11.8	45.0	2.81
20	-3.3	7.3	2.4	11.7	45.0	2.86
29	-6.5	-11.4	0.2	11.4	45.0	2.94
58	-0.7	-8.2	-4.2	11.3	45.0	2.98
30	5.0	-4.2	2.1	10.1	45.0	3.44
41	-1.2	-9.8	0.7	9.9	45.0	3.56
43	-3.5	-9.8	0.3	9.8	45.0	3.57
44	-9.6	-0.5	0.0	9.6	45.0	3.70
72	-6.2	1.8	-2.5	9.5	45.0	3.76
31	-4.8	3.5	1.9	9.2	45.0	3.88
47	-1.5	-8.7	0.6	8.7	45.0	4.15
23	8.1	5.7	1.4	8.7	45.0	4.16
22	-2.8	5.9	0.0	8.7	45.0	4.18
92	-0.6	-8.6	0.0	8.6	45.0	4.23
5	-2.0	4.9	2.4	8.5	45.0	4.32
33	-2.8	-7.9	1.6	8.4	45.0	4.38
37	-6.5	0.9	1.7	8.2	45.0	4.51
27	-3.6	-0.5	3.7	8.1	45.0	4.59
7	-2.2	5.5	0.5	7.7	45.0	4.82
10	-5.5	2.2	-0.2	7.7	45.0	4.86
19	6.1	3.6	2.4	7.5	45.0	4.97
54	0.3	-2.1	-3.5	7.5	45.0	5.03
42	6.4	1.5	2.3	7.4	45.0	5.11
51	-3.5	2.5	1.8	7.0	45.0	5.47
26	-2.2	3.8	1.4	6.6	45.0	5.80
2	-6.3	-0.7	1.2	6.5	45.0	5.89

Note: 1. See Figure 2.6.14.2-10 for section locations.
2. Stress components are based on the coordinate system shown in Figure 2.6.14.2-10, rotated 45°.

Table 2.6.14.7-9 $P_m + P_b$ Stresses for Yankee-MPC Basket Support Disk—1-Foot Side Drop, 45° Basket Orientation, Thermal Condition 3, Disk Number 5

Section	Sx (ksi)	Sy (ksi)	Sxy (ksi)	Stress Intensity (ksi)	Allowable Stress (ksi)	Margin of Safety
19	25.0	59.5	4.6	60.1	67.5	0.12
42	24.0	58.6	4.4	59.2	67.5	0.14
20	-56.8	-13.7	0.4	56.8	67.5	0.19
4	23.8	55.0	3.5	55.4	67.5	0.22
30	-9.7	-55.2	0.8	55.3	67.5	0.22
5	-55.2	-15.9	1.0	55.2	67.5	0.22
48	-5.3	-51.0	0.1	51.0	67.5	0.32
53	-50.0	-11.3	2.9	50.3	67.5	0.34
24	-50.0	-15.9	2.4	50.1	67.5	0.35
37	-48.6	-8.9	2.8	48.8	67.5	0.38
52	-0.5	-47.5	0.0	47.5	67.5	0.42
31	-47.4	-13.3	0.8	47.4	67.5	0.42
45	-47.0	-7.9	-0.9	47.0	67.5	0.44
60	-40.8	-32.0	8.7	46.2	67.5	0.46
51	-43.8	-12.2	0.8	43.8	67.5	0.54
9	-43.2	-18.2	3.1	43.6	67.5	0.55
59	-40.1	-21.7	3.8	40.8	67.5	0.65
3	-39.6	-22.4	2.8	40.0	67.5	0.69
21	2.7	39.7	-2.0	39.8	67.5	0.70
6	10.3	39.3	-0.5	39.3	67.5	0.72
33	-37.9	-16.9	3.0	38.3	67.5	0.76
41	-33.3	-26.8	7.2	38.0	67.5	0.78
62	-36.0	-15.0	2.5	36.3	67.5	0.86
2	-23.4	-35.1	3.1	35.9	67.5	0.88
56	-35.1	-6.4	3.1	35.5	67.5	0.90
47	-31.7	-23.8	6.3	35.1	67.5	0.92
40	7.7	25.2	-15.1	34.9	67.5	0.94
17	3.0	33.5	-2.2	33.6	67.5	1.01
32	-22.1	-32.3	3.5	33.4	67.5	1.02
26	-31.9	-1.7	-0.1	31.9	67.5	1.11
46	6.5	22.6	-13.3	31.1	67.5	1.17
61	-16.7	-30.3	2.0	30.6	67.5	1.21
23	19.7	28.7	4.2	30.4	67.5	1.22
7	-28.7	-5.6	-0.9	28.7	67.5	1.35
28	-22.5	-25.3	4.2	28.3	67.5	1.39
39	-11.5	-20.2	-10.7	27.4	67.5	1.47
18	-26.6	-19.4	2.3	27.3	67.5	1.47
13	-26.1	-3.3	0.3	26.1	67.5	1.58
50	-21.0	-19.9	4.4	24.9	67.5	1.71
43	-19.7	-21.9	3.6	24.6	67.5	1.74

- Note: 1. See Figure 2.6.14.2-10 for section locations.
2. Stress components are based on the coordinate system shown in Figure 2.6.14.2-10, rotated 45°.

2.6.14.8 Stress Evaluation of Yankee-MPC Fuel Basket Support Disk for Thermal Plus a 1-Foot Side Drop Combined Condition

The loading for the 1-foot side drop (Section 2.6.14.7) is combined with the thermal loading (Section 2.6.14.3) to produce a combined thermal plus impact loading condition. The allowable P + Q stress intensity range is $3 S_m$.

The stress evaluation results for thermal plus 1-foot side drop condition are summarized in Table 2.6.14.8-1. Thermal condition 2 is the governing case. The minimum margin of safety is +0.78, which occurs in disk No. 5 for 45° basket drop orientation (Thermal Condition 2). For 0° basket drop orientation, the highest P+Q stress occurs in Disk No. 1 (Thermal Condition 2). Table 2.6.14.8-2 lists the 40 highest P+Q stress intensities for Disk No. 1. For 45° basket drop orientation, the highest P+Q stress occurs in Disk No. 5 (Thermal Condition 2). Table 2.6.14.8-3 lists the 40 highest P+Q stress intensities for Disk No. 5. Locations of the 10 highest P+Q stress intensities for Disk No. 1 (0° basket drop orientation, Thermal Condition 2) are shown in Figure 2.6.14.8-1. Locations of the 10 highest P+Q stress intensities for Disk No. 5 (45° basket drop orientation, Thermal Condition 2) are shown in Figure 2.6.14.8-2.

Figure 2.6.14.8-1 Locations of Maximum P+Q Stresses, Yankee-MPC Basket, Disk 1,
1-Foot Side Drop, 0° Orientation, Thermal Condition 2

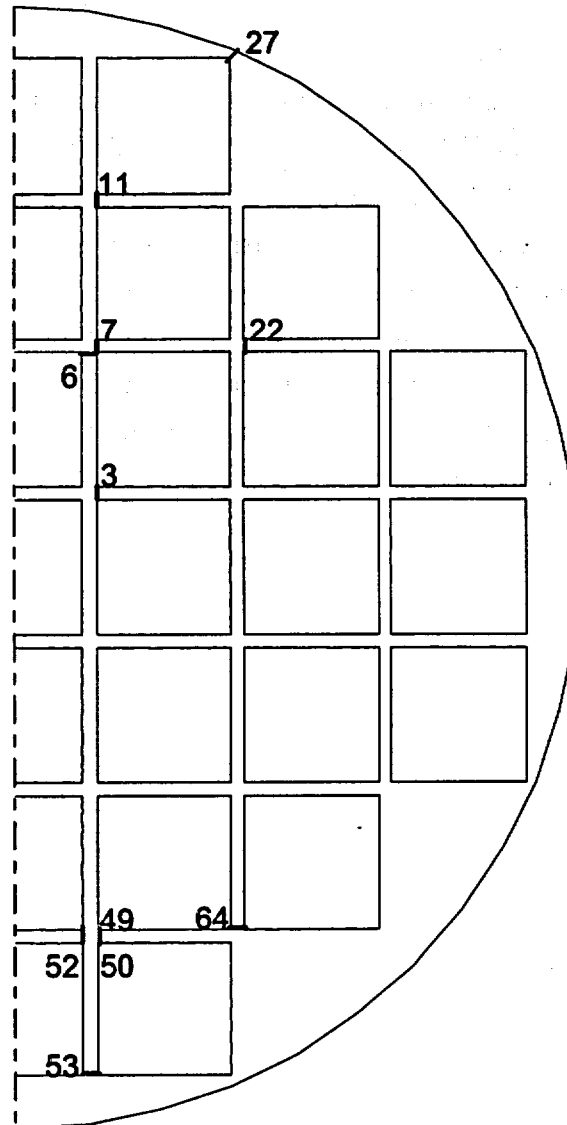


Figure 2.6.14.8-2 Locations of Maximum P+Q Stresses, Yankee-MPC Basket, Disk 5,
1-Foot Side Drop, 45° Orientation, Thermal Condition 2

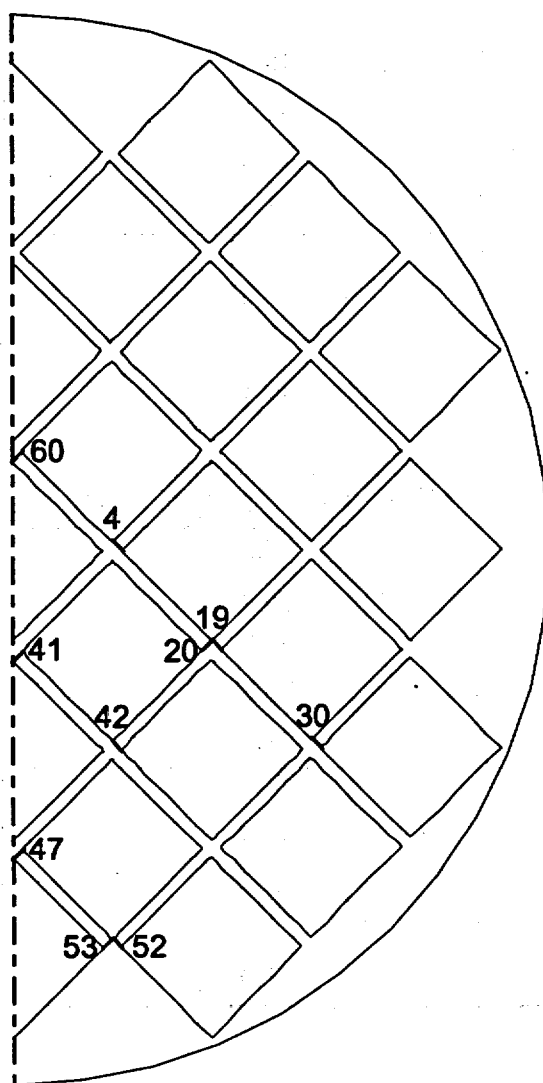


Table 2.6.14.8-1 Summary of Maximum Yankee-MPC Basket Support Disk Stresses for Thermal Plus 1-Foot Side Drop

Thermal Condition	Disk Number	P+Q Stress Intensity (ksi)	Margin of Safety
0° Basket Drop Orientation			
2	1	46.9	1.72
	2	46.0	1.77
	3	44.1	1.90
	4	42.8	1.98
	5	43.3	1.95
3	1	32.2	3.20
	2	30.9	3.38
	3	25.2	4.35
	4	22.3	5.06
	5	22.8	4.93
45° Basket Drop Orientation			
2	1	67.2	0.90
	2	68.9	0.85
	3	69.9	0.83
	4	70.9	0.80
	5	71.7	0.78
3	1	56.1	1.41
	2	57.9	1.33
	3	59.7	1.26
	4	60.4	1.23
	5	61.0	1.21

Table 2.6.14.8-2 P+Q Stresses for Yankee-MPC Basket Support Disk—1-Foot Side Drop, 0° Basket Orientation, Thermal Condition 2, Disk Number 1

Section	Sx (ksi)	Sy (ksi)	Sxy (ksi)	Stress Intensity (ksi)	Allowable Stress (ksi)	Margin of Safety
7	-46.2	-18.2	-4.6	46.9	127.7	1.72
11	-43.9	-14.8	-3.3	44.3	127.7	1.89
3	-36.8	-17.7	-4.3	37.7	127.7	2.39
50	26.8	-9.3	1.1	36.2	127.7	2.52
64	10.2	-25.5	-0.4	35.7	127.7	2.57
53	-9.5	-34.6	-5.2	35.6	127.7	2.59
52	23.8	-10.3	-1.3	34.1	127.7	2.74
6	-22.8	-28.1	-6.8	32.7	127.7	2.90
22	-30.4	-16.6	-4.3	31.7	127.7	3.03
49	10.5	-20.7	2.2	31.5	127.7	3.06
51	-8.6	-30.5	-4.0	31.2	127.7	3.09
2	-18.5	-28.2	-6.1	31.1	127.7	3.10
21	-16.0	-29.8	-4.2	31.0	127.7	3.12
9	-29.2	-10.5	3.6	29.9	127.7	3.27
47	-14.2	-27.6	-5.2	29.4	127.7	3.34
19	-6.8	-28.5	-1.5	28.6	127.7	3.46
43	-12.2	-27.1	-3.9	28.1	127.7	3.55
46	-25.6	-16.5	-4.5	27.4	127.7	3.66
14	-11.2	-26.0	-4.5	27.3	127.7	3.68
41	-4.6	-27.2	-1.0	27.2	127.7	3.69
10	-20.0	-22.3	-5.9	27.2	127.7	3.70
27	23.2	6.3	-9.1	27.2	127.7	3.70
62	-11.3	-25.9	-4.3	27.0	127.7	3.72
58	-11.1	-25.9	3.9	26.9	127.7	3.75
75	-25.2	-8.7	2.9	25.7	127.7	3.98
97	-25.6	-2.1	0.5	25.6	127.7	3.99
13	-24.9	-10.1	3.2	25.5	127.7	4.00
72	-25.1	-7.9	2.8	25.5	127.7	4.01
65	16.0	-9.1	-2.2	25.5	127.7	4.01
48	-22.8	-15.6	4.4	24.9	127.7	4.13
29	-24.3	-4.8	-1.4	24.4	127.7	4.24
5	-22.8	-13.0	4.1	24.3	127.7	4.26
17	-11.1	-23.0	-3.4	23.9	127.7	4.34
100	-23.6	-1.6	1.0	23.7	127.7	4.39
4	1.6	-21.5	0.9	23.2	127.7	4.50
33	-21.3	1.6	1.1	23.0	127.7	4.55
42	-20.8	-15.6	-3.9	22.9	127.7	4.58
63	-20.1	-14.3	3.9	22.1	127.7	4.78
98	-22.0	-2.0	0.5	22.0	127.7	4.81
45	3.0	-18.9	0.3	21.9	127.7	4.84

Note: See Figure 2.6.14.2-9 for section locations and definition of coordinate system.

Table 2.6.14.8-3 P+Q Stresses for Yankee-MPC Basket Support Disk—1-Foot Side Drop, 45° Basket Orientation, Thermal Condition 2, Disk Number 5

Section	Sx (ksi)	Sy (ksi)	Sxy (ksi)	Stress Intensity (ksi)	Allowable Stress (ksi)	Margin of Safety
60	-68.6	-37.4	10.4	71.7	127.7	0.78
42	27.6	70.4	4.8	70.9	127.7	0.80
19	27.8	69.4	4.9	70.0	127.7	0.83
53	-67.9	-15.5	4.1	68.2	127.7	0.87
41	-60.8	-34.3	9.2	63.6	127.7	1.01
20	-63.6	-17.6	0.9	63.6	127.7	1.01
4	25.0	62.7	3.4	63.0	127.7	1.03
47	-59.2	-32.0	8.6	61.7	127.7	1.07
30	-9.3	-60.6	0.6	60.6	127.7	1.11
52	0.5	-60.1	-0.4	60.6	127.7	1.11
48	-5.2	-59.5	0.0	59.5	127.7	1.15
5	-59.0	-18.4	1.2	59.1	127.7	1.16
24	-57.9	-19.2	2.9	58.1	127.7	1.20
45	56.8	32.1	5.5	57.9	127.7	1.20
37	-54.7	-9.4	2.9	54.9	127.7	1.32
31	-53.3	-18.3	1.7	53.4	127.7	1.39
9	-52.5	-22.1	3.6	52.9	127.7	1.41
51	-51.4	-17.5	1.7	51.5	127.7	1.48
3	-51.1	-26.2	3.3	51.5	127.7	1.48
59	-48.0	-31.3	4.3	49.1	127.7	1.60
6	-23.3	-46.2	2.7	46.5	127.7	1.75
62	-44.1	-19.1	3.1	44.5	127.7	1.87
21	4.9	44.3	-2.0	44.4	127.7	1.88
56	-43.6	-6.5	3.1	43.8	127.7	1.91
17	-29.4	-42.0	4.3	43.3	127.7	1.95
2	-25.5	-42.6	3.1	43.1	127.7	1.96
40	-42.0	-28.7	3.7	43.0	127.7	1.97
33	-42.3	-20.3	3.6	42.9	127.7	1.98
32	-25.4	-40.8	4.3	41.9	127.7	2.05
28	-26.9	-39.8	5.3	41.7	127.7	2.06
46	-40.9	-26.7	3.5	41.7	127.7	2.06
61	-19.3	-39.5	2.2	39.8	127.7	2.21
50	-26.4	-36.7	5.7	39.2	127.7	2.26
23	21.9	36.6	4.5	37.9	127.7	2.37
18	-35.6	-22.5	2.5	36.1	127.7	2.54
7	-35.2	-7.7	-0.8	35.2	127.7	2.62
26	33.7	9.2	2.7	34.0	127.7	2.75
43	-31.4	-26.3	4.1	33.6	127.7	2.80
73	-32.4	-16.4	4.3	33.5	127.7	2.82
44	-24.1	-30.0	3.3	31.4	127.7	3.06

Note: 1. See Figure 2.6.14.2-10 for section locations.
2. Stress components are based on the coordinate system shown in Figure 2.6.14.2-10, rotated 45°.

2.6.14.9 Yankee-MPC Fuel Basket Support Disk Shear Stresses for 1-Foot Drops

The evaluation of the maximum shear stress in the Yankee-MPC fuel basket support disk utilizes the membrane values of the stress intensity due to primary loading, which were evaluated for end and side drop conditions. The maximum membrane stress intensity is 23.7 ksi for section 49 (see Tables 2.6.14.7-1 and 2.6.14.7-2). Therefore, the maximum shear stress is $23.7/2$ or 11.85 ksi. In accordance with ASME Code, Section III, Division 1, Subsection NG, the Level A allowable for shear stress is $0.6 S_m$. Using the bounding temperature of 539°F, S_m for Type 17-4 PH stainless steel is 42.6 ksi, the margin of safety is:

$$M.S. = (0.6)(42.6)/11.85 - 1$$

$$= +1.16$$

2.6.14.10 Bearing Stress - Basket Contact with Canister Shell

For the bearing stress (S_{br}) acting along the basket disk-canister shell interface, an angular contact of 18 degrees is conservatively considered based on ANSYS gap element status (at a diameter of 69.15 inches). The load considered to be acting on the disk is the total contents weight (56,000 pounds = 56 kips, which is conservative) times the deceleration (20 g) divided between 22 disks. The bearing area is considered to be the 0.5-inch thick disk and the contact area corresponding to an 18 degree angular contact.

$$S_{br} = (56/22)(20)/[(.5)(\pi)(69.15)(18/360)] = 9.4 \text{ ksi}$$

The allowable bearing stress is the yield stress, which for 17-4 PH at a temperature of 400°F, is 89.6 ksi (The maximum canister shell temperature for transport conditions is 338°F). The margin of safety is:

$$M.S. = 89.6/S_{br} - 1$$

$$M.S. = + 8.5$$

2.6.14.11 Yankee-MPC Fuel Basket Weldment Analysis for 1-Foot End Drop

The responses of the top and bottom weldment plates of the fuel basket assembly to a 1-foot end drop in conjunction with the thermal expansion stress are also evaluated. The top and bottom weldment plates are 0.5-inch thick plates of Type 304 stainless steel. The weldments support their own weight plus the weight of 36 fuel assembly tubes. A finite element analysis is performed for both plates, since the support for each weldment is different due to the location of the welded ribs for each. Both models use the SHELL63 element, which permits out of plane loading. Figures 2.6.14.11-1 and 2.6.14.11-2 show the finite element models for the weldments. The ribs supporting the disk were represented by axial translational restraints. The load from the fuel tubes (2,108 pounds) is represented as point force applied to the nodes at the periphery of the fuel assembly slots. An average point force is applied. For a total of 695 nodes around the slots, the nodal force is $2,108/695 = 3.033$ pounds per node. The application of the nodal loads at the slot periphery is accurate since the tube weight is transmitted to the edge of the slot, which provides support to the fuel tubes in the end drop condition.

The analysis using the applied nodal forces demonstrates that the weldment design satisfies the primary membrane (P_m) and the primary membrane plus bending ($P_m + P_b$) stress criteria. An analysis including the thermal expansion stresses is also performed. The determination of the weldment temperatures is discussed in Chapter 3.

The margins of safety are calculated as:

$$M.S. = [(P_m + P_b) / 1.5 S_m] - 1$$

or

$$M.S. = [(P_m + P_b + Q) / 3 S_m] - 1$$

The margins of safety evaluated at the weldment temperatures are shown in Table 2.6.14.11-1. The weldments are shown to satisfy the stress criteria in ASME Code, Section III Division I, Subsection NG.

Figure 2.6.14.11-1 Finite Element Model of the Yankee-MPC Fuel Basket Top Weldment Plate

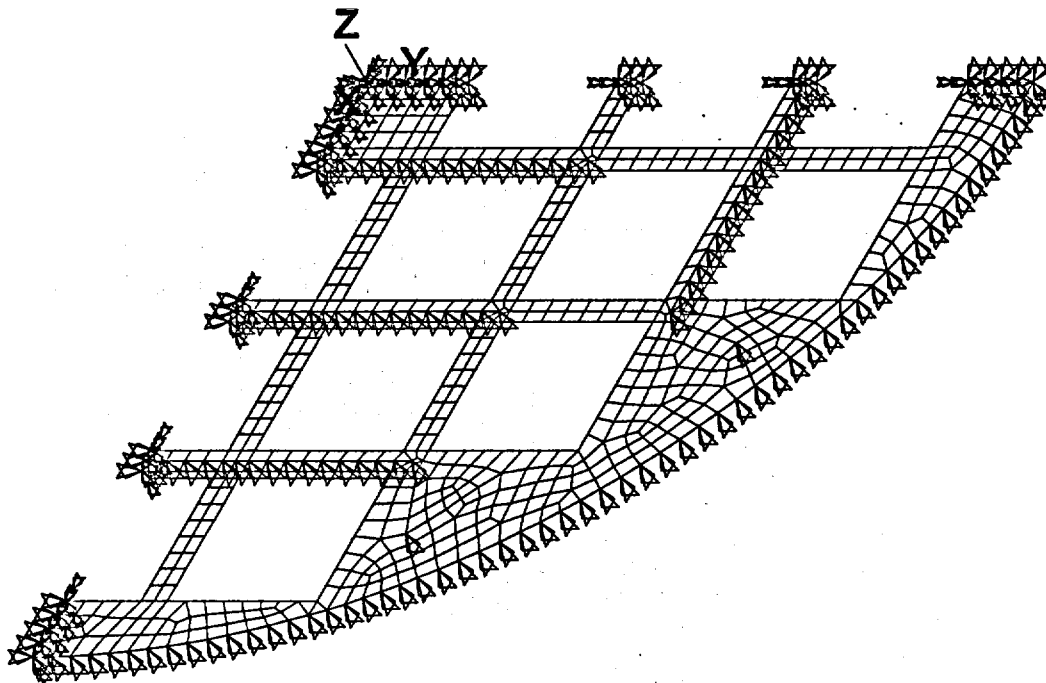


Figure 2.6.14.11-2 Finite Element Model of the Yankee-MPC Fuel Basket Bottom Weldment Plate

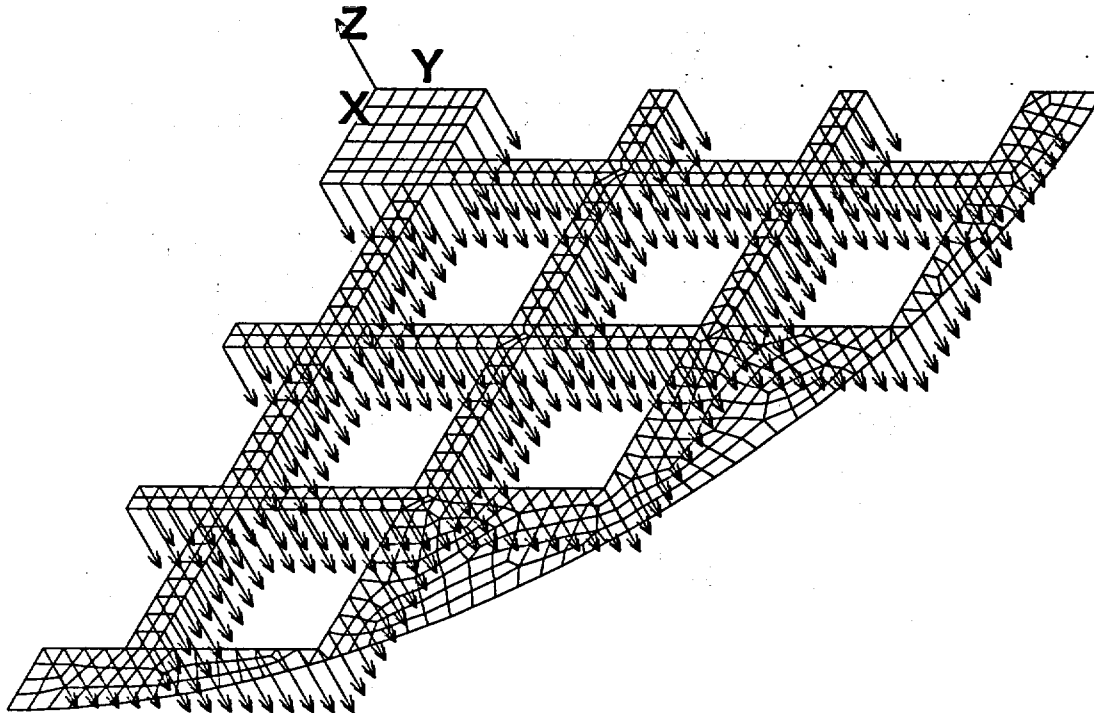


Table 2.6.14.11-1 Minimum Margins of Safety for the Yankee-MPC Fuel Basket Top/Bottom Weldments for 1-Foot End Drop With and Without Thermal Stresses

Component/Condition	$P_m + P_b$ (ksi)	Nodal Temp. (°F)	$1.5S_m$ (ksi)	M.S.
Top Weldment/1-ft. End Drop	20.6	223	30.0	+0.45
Bottom Weldment/1-ft. End Drop	17.1	257	30.0	+0.75
Component/Condition	$P_m + P_b + Q$ (ksi)	Nodal Temp. (°F)	$3S_m$ (ksi)	M.S.
Top Weldment/1-ft. End Drop	46.5	205	60.0	+0.29
Bottom Weldment/1-ft. End Drop	35.7	254	60.0	+0.68

2.6.14.12 Yankee-MPC Fuel Basket Support Disk - Buckling Evaluation (Normal Conditions of Transport)

The canistered fuel basket support disk is subjected to compressive and/or inertia loads during a 1-foot drop of the NAC-STC cask onto an unyielding surface. Depending on the cask orientation for the 1-foot drop impact, the support disk may have both in-plane and out-of-plane loads applied to it. The in-plane loads (basket side impact component) apply compressive forces and in-plane (strong axis) bending moments on the support disk and the out-of-plane inertial loads (basket end-impact component) produce out-of-plane (weak axis) bending moments on the support disk. Buckling of the support disk is evaluated in accordance with the methods and acceptance criteria of NUREG/CR-6322.

The buckling evaluation of the support disk web is based on the Interaction Equations 31 and 32 in NUREG/CR-6322. These two equations adopt the "Limit Analysis Design" approach for structural members subjected to stresses beyond the yield limit of the material, i.e., for members deformed elastically as a result of axial load or bending moment. Other equations applicable to the calculations are listed later in this section.

The maximum forces and moments are determined from the finite element analysis stress results for the Support Disk End-Drop Model as well as the Support Disk Side Drop Models (two different basket orientations, 0° and 45°). The buckling evaluations account for both in-plane (about the strong axis of the web) and out-of-plane (about the weak axis of the web) buckling modes.

The methodology and equations used for the buckling evaluation are summarized as follows:

Symbols and Units

- P = applied axial compressive loads, kips
- M = applied bending moment, kips-inch
- P_a = allowable axial compressive load, kips
- P_{cr} = critical axial compression load, kips
- P_e = Euler buckling loads, kips
- P_y = average yield load, equal to profile area times specified minimum yield stress, kips
- C_c = column slenderness ratio separating elastic and inelastic buckling

- C_m = coefficient applied to bending term in interaction equation
 M_m = critical moment that can be resisted by a plastically designed member in the absence of axial load, kip-in.
 M_p = plastic moment, kip-in.
 F_a = axial compressive stress permitted in the absence of bending moment, ksi
 F_e = Euler stress for a prismatic member divided by factor of safety, ksi
 k = ratio of effective column length to actual unsupported length
 l = unsupported length of member, in.
 r = radius of gyration, in.
 S_y = yield strength, ksi
 A = cross sectional area of member, in²
 Z_x = plastic section modulus, in³
 λ = allowable reduction factor, dimensionless.

From NUREG/CR-6322, the following equations are used to evaluate the support disk for normal condition of transport:

$$\frac{P}{P_{cr}} + \frac{C_m M}{\left[1 - \frac{P}{P_e}\right] M_m} \leq 1.0 \quad (\text{Eq. 31, NUREG/CR-6322})$$

$$\frac{P}{P_y} + \frac{M}{1.18 M_p} \leq 1.0 \quad (\text{Eq. 32, NUREG/CR-6322})$$

where: $P_{cr} = 1.7 \times A \times F_a$

$$F_a = \frac{\left[1 - \frac{1}{2} \left(\frac{k \cdot l}{r \cdot C_c}\right)^2\right] \cdot S_y}{\frac{5}{3} + \frac{3}{8} \left(\frac{k \cdot l}{r \cdot C_c}\right) - \frac{1}{8} \left(\frac{k \cdot l}{r \cdot C_c}\right)^3} \quad \text{for } \frac{k \cdot l}{r} < C_c = \sqrt{2 \cdot \pi^2 \frac{E}{S_y}}$$

$$P_e = 1.92 \times A \times F_e$$

$$F_e = \frac{\pi^2 \cdot E}{1.92 \left(\frac{k \cdot l}{r} \right)^2} \text{ (non-austenitic)}$$

$$P_y = S_y \times A$$

$$C_m = 0.85 \text{ for members with joint translation (sideways).}$$

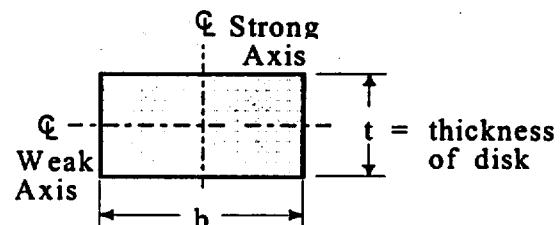
$$M_p = S_y \times Z_x$$

$$M_m = M_p \cdot \left(1.07 - \frac{\left(\frac{1}{r} \right) \cdot \sqrt{S_y}}{3160} \right) \leq M_p$$

Buckling evaluation is performed on all sections in the disk ligaments defined in Figures 2.6.14.2-9 and 2.6.14.2-10. Using the cross-sectional stresses calculated at each of the sections for each loading condition the maximum corresponding compressive forces (P) and bending moment are determined as follows,

$$P = \sigma_m A,$$

$$M = \sigma_b A,$$



where, σ_m is the membrane stress, σ_b is the strong axis bending stress or weak axis bending stress, A is the area ($b \times t$), and S is the section modulus ($tb^2/6$ for strong axis bending and $bt^2/6$ for weak axis bending).

To determine the margin of safety:

$$P_1 = P/P_{cr} \quad M_1 = \frac{C_m M}{(1 - P/P_{cr}) M_p} \quad (P_1 + M_1 \leq 1) \quad (\text{Eq. 31, NUREG/CR-6322})$$

$$\text{and} \quad P_2 = P/P_y \quad M_2 = \frac{M}{1.18 M_p} \quad (P_1 + M_1 \leq 1) \quad (\text{Eq. 32, NUREG/CR-6322})$$

The margins of safety are:

$$MS1 = \frac{1}{P_1 + M_1} - 1$$

$$MS2 = \frac{1}{P_2 + M_2} - 1$$

The side drop conditions are the governing conditions for strong axis buckling evaluation since the axial compressive force (P) and the strong axis bending moment (M) decrease with the drop angle. Therefore, evaluation of strong axis buckling is performed for side drop conditions only.

The results of the strong axis buckling evaluations for the support disks, normal condition, are summarized in the following table. The minimum margin of safety is +0.98. As the tables demonstrate, the support disks meet the requirements of NUREG/CR-6322.

Loading Condition	Stress State	Thermal Condition	Section Number	Disk Number	P (kip)	P _{cr} (kip)	M (in-kip)	M _p (in-kip)	M _m (in-kip)	MS1	MS2
Strong Axis, 1-Foot Drop, 0° Basket Drop Orientation											
Normal	P	2	53	1	6.05	33.71	0.26	8.24	8.03	3.80	4.33
	P+Q	2	7	1	3.93	30.73	1.83	7.06	6.82	1.75	2.01
	P	3	53	1	6.11	40.76	0.27	10.05	9.69	4.74	5.42
	P+Q	3	53	1	5.99	40.76	0.23	10.05	9.69	4.95	5.66
Strong Axis, 1-Foot Drop, 45° Basket Drop Orientation											
Normal	P	2	30	5	1.55	27.94	2.35	6.05	5.79	1.46	1.65
	P+Q	2	52	3	4.63	27.97	2.22	6.06	5.80	0.98	1.20
	P	3	30	5	1.59	33.70	2.39	7.37	6.98	1.92	2.18
	P+Q	3	30	5	1.54	33.70	2.31	7.37	6.98	2.03	2.29

Notes:

1. P = Primary Stress, P+Q = Primary + Secondary Stresses.
2. See Figures 2.6.14.2-9 and 2.6.14.2-10 for section location.
3. See Figure 2.6.14.2-8 for disk number.

The weak axis buckling evaluation is not required for the side drop condition since there is no out-of-plane (weak axis) bending moment in the support disk for the side drop condition. The maximum out-of-plane moment occurs in the end drop condition. Since there is no in-plane force in the disk for the end drop condition, it is not required to evaluate the weak axis buckling

for the end drop condition either. Therefore, the weak axis buckling is only considered for the 1-foot corner drop condition. The cask drop angle is 24° from the cask centerline for the corner drop condition and the corresponding calculated g load factor is only 5.3 g (Table 2.6.7.4.1-3). The following discussion demonstrates that the weak axis buckling evaluation for the 1-foot corner drop condition is bounded by the worst case weak axis buckling evaluation for the 30-foot drop conditions (Section 2.7.9.3). 56.1 g and 55 g are used for the evaluation of 30-foot end drop and 30-foot side drop conditions, respectively.

As presented in Section 2.7.9.3, the minimum margin of safety (+0.78) for weak axis buckling evaluation for the 30-foot drop conditions occurs at Section 56, Disk No. 1 for cask drop angle of 30 degree (thermal condition 2 and primary plus secondary stress state). As shown in the table below, the margin of safety remains positive (+0.63) when the evaluation is performed using the equations for the normal condition (as presented in this Section) with the accident loads (axial force of 4.9 kips and bending moment of 1.8 in-kip) as input. Since the gravitational loading for the 30-foot drop condition is approximately 10 times ($55g/5.3g=10.3$) greater than that for the 1-foot corner drop condition, it is concluded that the weak axis evaluation for the 30-foot drop conditions bounds that for the 1-foot corner drop condition. Therefore, no further evaluation is required for the weak axis buckling of the support disks for the normal conditions of transport.

Case	Stress State	Thermal Condition	Section Number	Drop Angle	Disk Number	P (kip)	P_{cr} (kip)	M (in-kip)	M_p (in-kip)	M_m (in-kip)	MS1	MS2
Accident*	P+Q	2	56	30	1	4.90	32.80	1.80	4.40	3.90	0.78	1.06
Normal	P+Q	2	56	30	1	4.90	26.14	1.80	4.40	3.90	0.63	1.06

* From Section 2.7.9.3

2.6.15 CY-MPC Transportable Storage Canister Analysis - Normal Conditions of Transport

The NAC-STC has two contents configurations - uncanistered (directly loaded fuel), and canistered (fuel or Greater Than Class C (GTCC) waste). This section describes the evaluation of the CY-MPC canister configuration. The canister is evaluated for the Normal Conditions of Transport in this section and for the Hypothetical Accident Conditions in Section 2.7.12. The Normal Conditions of Transport analysis of the CY-MPC canistered fuel basket is presented in Section 2.6.16.

The CY canistered fuel configuration consists of a transportable storage canister with a bottom spacer to properly locate the canister in the NAC-STC cask cavity. The analysis of the bottom spacers is presented in Section 2.6.17. The principal components of the transportable storage canister are the canister, the canister fuel basket, the shield lid, and the structural lid. In an alternate configuration the transportable storage canister may include the CY canister GTCC waste basket instead of the CY canister fuel basket. Detailed descriptions of the geometries and materials of construction of the canister, baskets, and spacers are provided in Sections 1.2.1.2.8, 1.2.1.2.8.1, 1.2.1.2.8.2, and 1.2.1.2.8.3, respectively.

The transportable storage canister and the canister shell, bottom, and lids are shown in Figures 2.6.13-1 and 2.6.13-2, respectively.

THIS PAGE INTENTIONALLY LEFT BLANK

2.6.15.1 Analysis Description – CY-MPC Canister

The CY-MPC canister contains/confines the spent fuel in the canister fuel basket or the waste in the canister GTCC basket. The canister is the defined confinement boundary for its contents during storage operation and is considered the separate inner container for containment during transport operation; the NAC-STC provides the primary containment boundary for transport. The canister in the transfer cask serves as the handling component for its basket and contents during loading, closure, and transfer from the pool to storage and/or transport.

The canister is a right-circular shell fabricated from rolled 5/8-inch thick, Type 304L stainless steel plate and closed by a circular 1.75-inch thick, Type 304L stainless steel plate that is welded to one end of the shell. The canister is closed at the top end by the installation and welding of the 5-inch thick, Type 304 stainless steel shield lid and the 3-inch thick, Type 304L stainless steel structural lid. The CY-MPC canister encloses the CY basket and contents. The empty canister with basket is handled using lifting rings located on the top end of the basket. The loaded canister is lifted using 6 hoist rings threaded into the top of the structural lid. Type 304L stainless steel was selected for the canister's exterior components based on its enhanced corrosion resistance, especially in the weld regions (refer to Section 2.5.1.3).

The structural design criteria for the canister is the ASME Code Section III, Subsection NB, "Class 1 Components." Consistent with this criteria, the structural components of the canister are shown to satisfy the allowable stress limits presented in Tables 2.1.2-1 and 2.1.2-2 as applicable. The allowable stresses used in this analysis are based on a maximum material temperature of 350°F for all locations in the canister, unless otherwise indicated.

The canister is analyzed using the ANSYS finite element computer program for the 1-foot drop condition in the end and side impact orientations.

The canister structural lid closure weld is specifically evaluated for the normal conditions of transport. The lid weld is identified as Section 8 in Figure 2.6.15.3-1. Either a progressive liquid penetrant examination is performed on the root, each successive 3/8-inch layer, and the final surface of the weld in accordance with the ASME Code, Section V, Article 6, or an ultrasonic examination of the weld is performed in accordance with Section V, Article 5. In accordance with NRC guidance, if a multi-pass liquid penetrant examination is performed on the structural lid closure weld, a weld stress reduction factor is applied to the structural lid to canister shell

weld —a 0.8 factor per NRC ISG-4, Item 5. The canister closure weld evaluation for normal conditions is presented in Section 2.6.15.12. The evaluation, which is based on the finite element analysis stress result as shown in Sections 2.6.15.4 through 2.6.15.7, shows a minimum margin of safety of +0.58 for the weld.

2.6.15.2 Finite Element Model Description – CY-MPC Canister

A finite element model of the Connecticut Yankee canister was constructed using ANSYS solid (SOLID45) elements similar to that for described in this section for the canistered fuel and GTCC waste. The model represents a one-half (180°) section of the Connecticut Yankee canister and basket. The basket support discs were modeled with three-dimensional shell (SHELL63) elements. The model uses gap-spring elements to simulate contact between adjacent components. Interaction between the basket and canister were accomplished using three-dimensional gap elements (CONTAC52) along the periphery of the support disks. Contact between the canister and the cask inner shell is also modeled using CONTAC52 gap elements. Contact between the canister structural lid and shield lid is modeled using COMBIN40 combination elements in the axial degree of freedom. Simulation of the backing ring is accomplished using a ring of COMBIN40 spring gap elements connecting the shield lid and the canister in the axial direction at the lid lower outside radius. In addition, CONTAC52 elements are used to model interaction between the structural lid and canister shell and the shield lid and canister shell just below the respective lid weld joints. The size of the CONTAC52 gaps were determined from the nominal dimensions of contacting components. The COMBIN40 elements used between the structural and shield lids and for the backing ring are assigned gap sizes of 1E-8 inches. The maximum gap size is 0.08 inches. However, use of the small gap size results in the highest stresses at critical sections, resulting in the lowest margin of safety. All gap-spring elements are assigned a stiffness of 1E8 lb/in.

Spring elements were inserted over the gap elements located on the model symmetry plane to help stabilize the model during solutions phases. The springs were given a low stiffness of 10 lb/in so their presence would not adversely affect the accuracy of the solutions.

Boundary conditions were applied to enforce symmetry at the cut boundary of the model. All nodes on the cask shell side of the canister to cask spring gap elements were fixed in all degrees of freedom. In addition, the axial and inplane rotational degrees of freedom of the basket nodes were fixed.

Additionally, the thermal structural analyses of the canister were performed with temperature distributions corresponding to the hot (100°F ambient with solar heat load) and cold (-40°F ambient) external conditions.

Table 2.6.15.2-1 lists the real constants assigned to specific components of the model. Table 2.6.15.2-2 lists the material properties used for the model.

Figure 2.6.15.2-1 is a plot of the entire canister finite element model. An isolated view of the canister shield and structural lids portion of the model is presented in Figure 2.6.15.2-2 and an enlarged view of the model in the structural lid and shield lid weld regions is shown in Figure 2.6.15.2-3. The canister bottom plate portion of the model is shown in Figure 2.6.15.2-4.

The loading for the normal operating condition is based on 1-foot drops in conjunction with the internal pressure loading (to the canister). Drop orientations considered are the end and side drops. In the end drop orientation, the fuel contents load is transferred to the canister end and directly to the transport cask end through the cavity spacer. This corresponds to a compressive stress in the canister ends which is present in the finite element model. For the side drop condition, the loads from the canister contents weight is transferred through the support disks into the canister wall, which is backed by the NAC-STC inner shell. Since the canister wall and the inner shell have different radii, a gap exists between the two surfaces. This results in the load passing only through regions in which the canister shell deflects to contact the inner shell. This load pattern is reflected in the side drop analysis. The operational conditions also contain loads developed from the temperature distribution in the canister. These are included in the canister model analyses.

Figure 2.6.15.2-1 CY-MPC Canister Assembly Finite Element Model

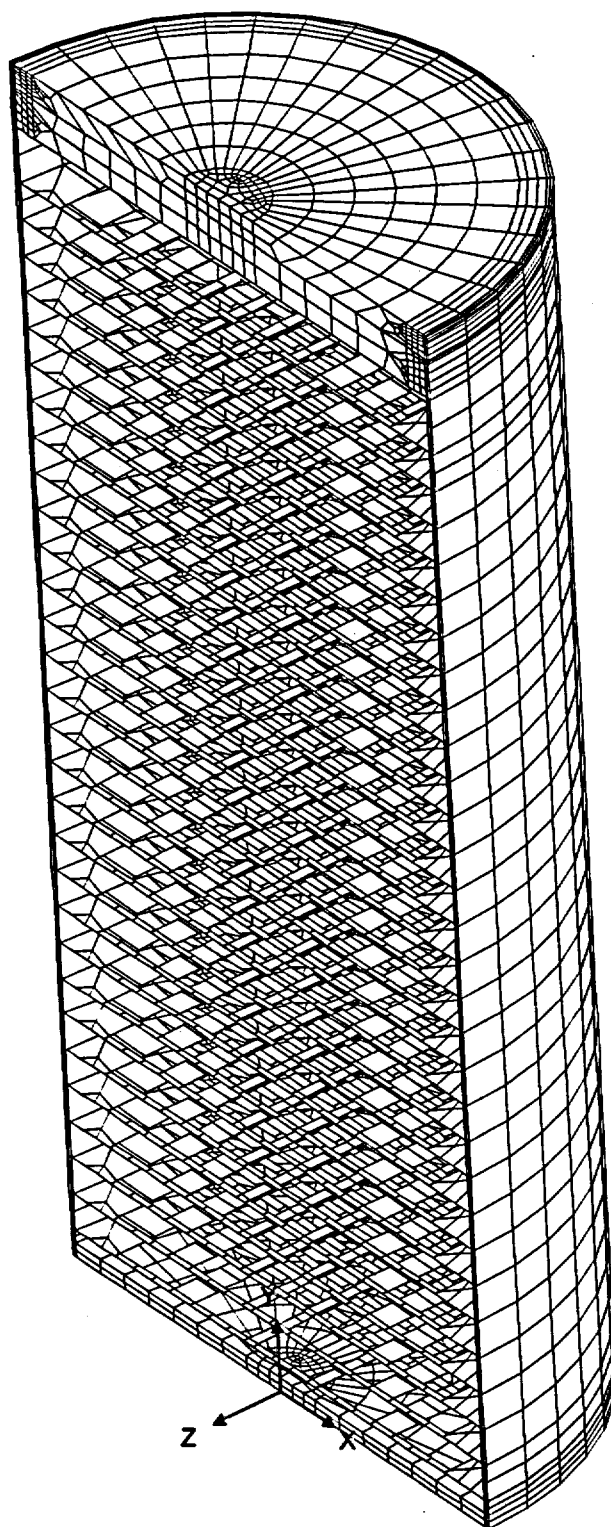


Figure 2.6.15.2-2 CY-MPC Canister Structural and Shield Lid Finite Element Mesh

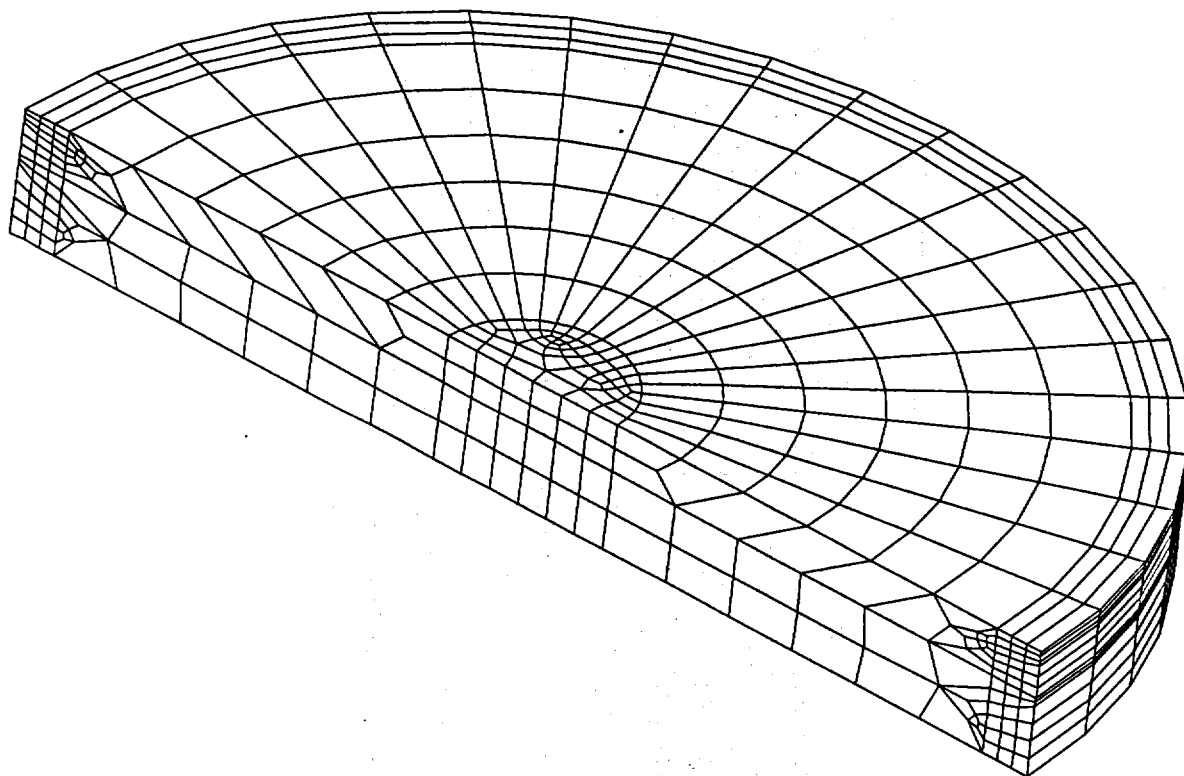


Figure 2.6.15.2-3 CY-MPC Canister Structural and Shield Lid Weld Region Finite Element Mesh

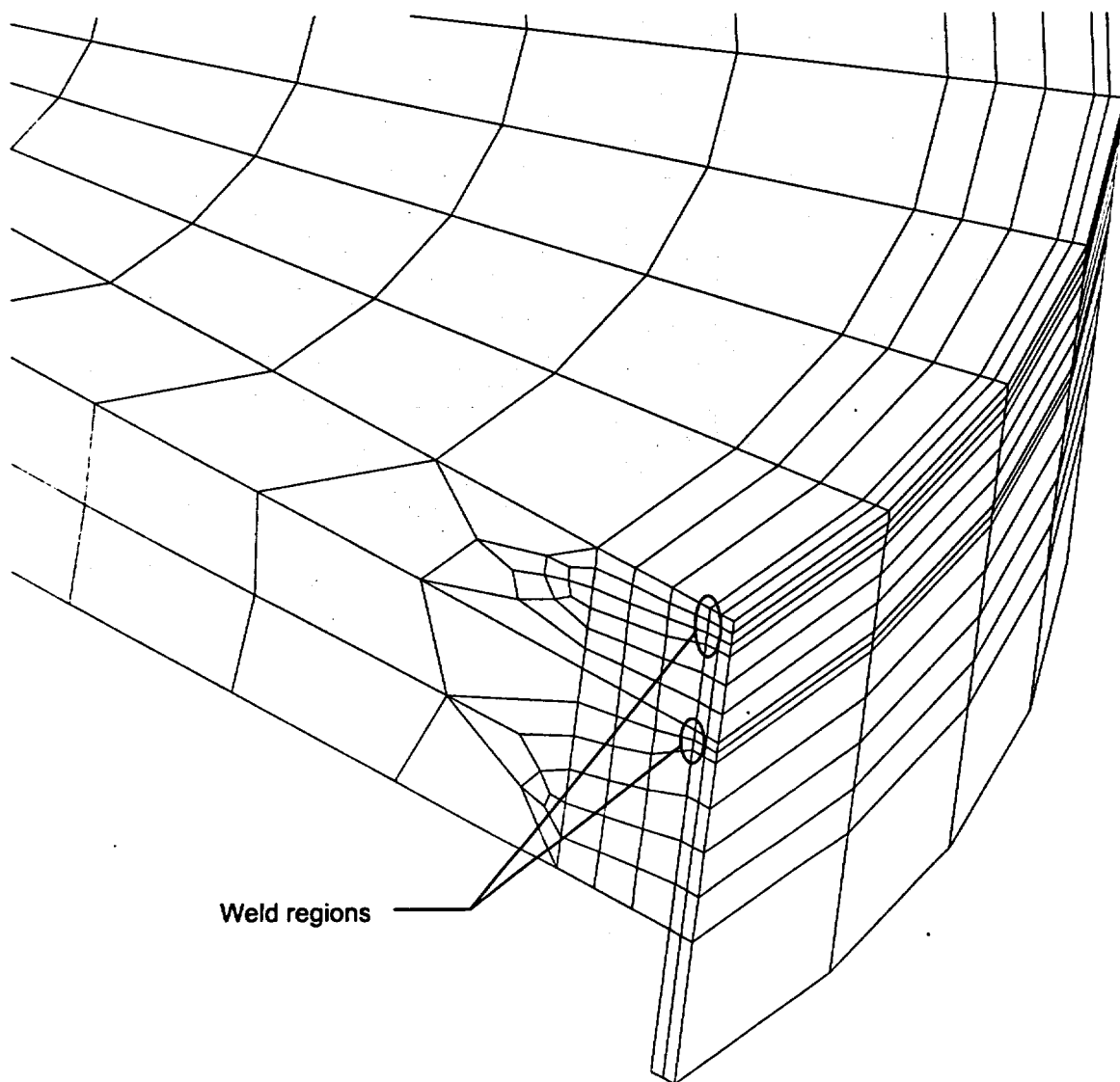


Figure 2.6.15.2-4 CY-MPC Canister Bottom Plate Finite Element Mesh

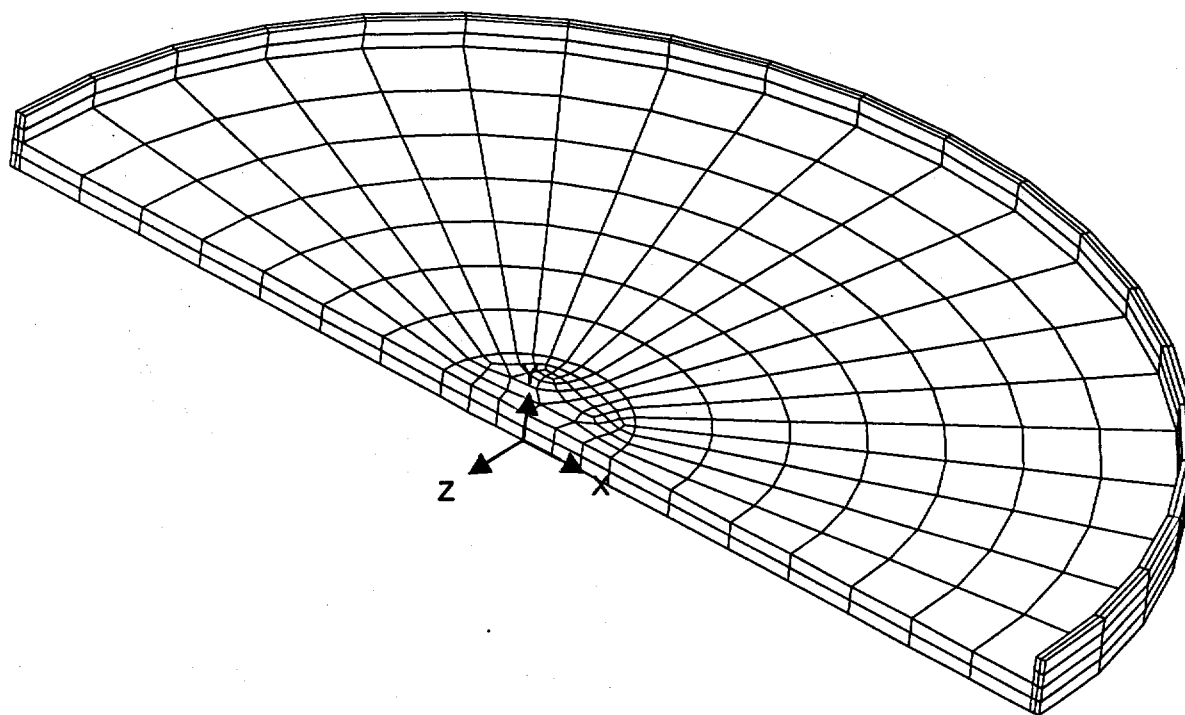


Table 2.6.15.2-1 Real Constant Sets Defined in CY-MPC Canister Model

Real Constant Set	Component
1	Canister Bottom Plate (SOLID45)
2-9	Canister Shell (SOLID45)
10-11	Shield Lid (SOLID45)
12-13	Structural Lid (SOLID45)
100	Axial Gaps from Canister Bottom Plate to Cask Shell (CONTAC52)
200	Radial Gaps from Canister Side to Cask Shell (CONTAC52)
300	Axial Gaps from Structural Lid Top to Cask Shell (CONTAC52)
400	Axial Gaps Between Structural and Shield Lid (COMBIN40)
500	Radial Gaps Between Shield Lid and Canister Inner Surface (CONTAC40)
600	Radial Gaps Between Shield Lid and Canister Inner Radius (CONTAC52)
700	Axial Gaps Between Shield Lid and Canister Wall to Simulate Backing Ring (COMBIN40)
800	Radial Gaps Between Basket and Canister Inner Surface (CONTAC52)
1000	Intermediate Basket Thickness Real Constant
1100	End Basket Thickness Real Constant
1200	Weak Spring Real Constant

Table 2.6.15.2-2 Material Sets Defined in CY-MPC Canister Model

Material Property Set	Component	Material
1	Canister Shell and Structural Lid	304L Stainless Steel; ASME SA240
2	Top and Bottom End Basket Disk	304 Stainless Steel; ASME SA240
3	Shield Lid	304 Stainless Steel; ASME SA240
4	Intermediate Basket Disk (support disk)	ASME SA693 Type 630

THIS PAGE INTENTIONALLY LEFT BLANK

2.6.15.3 Thermal Expansion Evaluation of CY-MPC Canister Containing Fuel

A thermal stress evaluation is performed using ANSYS to determine the differential thermal expansion and the associated thermal stresses that result from a heat load of 17.0 kW for the Connecticut Yankee system. In assessing the thermal stresses, three extreme conditions are possible:

Condition	Ambient Temperature	Solar Insolation Applied to Cask Surface	17 kW Fuel Load
1	100°F	Yes	Yes
2	-40°F	No	Yes
3	-40°F	No	No

The following temperatures are obtained from the thermal analysis for Connecticut Yankee Canister with a 0-degree basket orientation:

Location	Temperature (°F)		
	Condition 1	Condition 2	Condition 3
Structural Lid (center, top)	220	89	-40
Structural Lid (outer, top)	217	87	-40
Shield Lid (center, bottom)	221	91	-40
Bottom Plate (center, bottom)	346	226	-40
Bottom Plate (outer radius, bottom)	277	151	-40
Lateral Shell (mid-height)	348	228	-40

While most of the temperature gradients between the different locations are very close for condition 3, no thermal gradient exists, so there are no thermal stresses. Thermal stresses were calculated for both conditions 1 and 2. Condition 2 resulted in the largest thermal stress (6.31 ksi at section 9 versus 5.91 ksi for condition 1), a 6.8% increase in thermal stress.

For normal condition thermal stresses, 3 S_m is the allowable stress criteria. Below 300°F, the value of S_m (16.7 ksi) does not change for SA-240, Type 304L stainless steel. For heat condition 1, the maximum temperature is 349°F and S_m = 16.3 ksi. This results in a 2.4% decrease in the

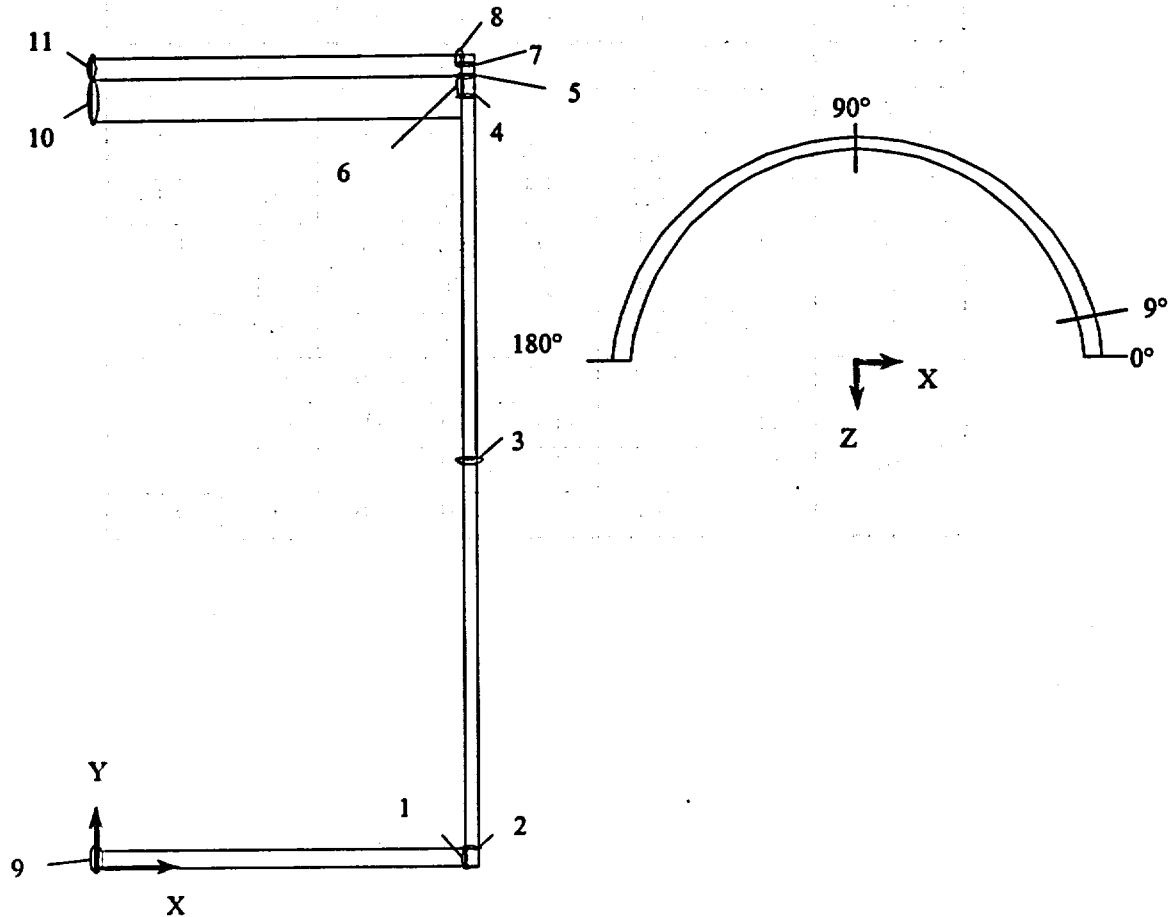
allowable stress for condition 1, which is offset by the 6.8% increase in the thermal stress for condition 2. For this reason, only condition 2 thermal stresses are included in the canister evaluations. In the three conditions considered above, the cask is assumed to be in the horizontal position and both the canister cavity and the cask cavity are assumed to be backfilled with helium.

The temperatures employed in the thermal stress analysis were obtained by applying the above temperatures as thermal boundary conditions to the thermal equivalent model of the structural canister model. The structural finite element model is described in Section 2.6.15.2. The equivalent thermal model is obtained by changing the structural element (SOLID45, which has three global displacements for degrees of freedom) to a SOLID70, which has temperature degrees of freedom at the individual nodes. The temperature dependent thermal conductivity for the canister material was employed in the thermal conduction analysis. The temperatures generated in this analysis were used in the thermal stress analysis to evaluate the properties at temperature, as well as the stresses due to thermal expansion.

According to ASME Code, Section III, Subsection NB, the allowable stress criteria is based on the evaluation of linearized stresses across critical cross sections through the canister wall. For the evaluation of the thermal stresses, the criteria for the stresses is based on peak stresses. The stress values taken from the analyses are the nodal stresses at the surface. The sections used in this evaluation are shown in Figure 2.6.15.3-1. For the sections identified, the thermal stresses are reported in Table 2.6.15.3-1. The thermal stresses reported in Table 2.6.15.3-1 correspond to the maximum stresses for any circumferential section, for the location shown in Figure 2.6.15.3-1.

For condition 1 or 2, the canister is hotter than the cask body and will undergo more thermal expansion than the cask body. To conservatively determine the minimum gap between the canister and the cask body due to thermal expansion, only expansion of the canister will be considered. The canister is considered to be at 349°F (shell temperature for condition 1) and the cask inner shell temperature is assumed to be 70°F. Using the outer radius of the canister of 35.32 inches and the coefficient of expansion for Type 304L stainless steel of $9.095\text{E-}6$, the canister inner shell gap is reduced by $(9.095\text{E-}6)(35.32)(349-70) = 0.090$ inches. Since the nominal radial canister-inner shell gap is 0.18 inches, the canister shell does not bind with the inner shell due to thermal expansion.

Figure 2.6.15.3-1 Identification of the Sections for Evaluating the Linearized Stresses in the CY-MPC Canister



Section	Node 1		Node 2	
	X (inch)	Y (inch)	X (inch)	Y (inch)
1	34.695	0.00	34.695	1.75
2	34.695	1.75	35.32	1.75
3	34.695	72.75	35.32	75.75
4	34.695	148.25	35.320	148.25
5	34.695	148.75	35.320	148.75
6	34.695	148.25	34.695	148.75
7	34.695	150.87	35.320	150.87
8	34.695	150.87	34.695	151.75
9	0.10	0.00	0.10	1.75
10	0.10	143.75	0.10	148.73
11	0.10	148.77	0.10	151.75

Table 2.6.15.3-1 CY-MPC Linearized Stresses - Thermal Only (Condition 2)

Section No.	Q Stresses (ksi)						S.I. (ksi)
	SX	SY	SZ	SXY	SYZ	SXZ	
1	0	0	1	0	0	0.1	1.1
2	0	-0.2	0.8	0	0	-0.1	1
3	0	0.8	-0.3	0	0	0	1.1
4	0.3	-0.7	-0.3	0.3	0	0	1.19
5	-0.5	1.1	0	0.2	0	0	1.63
6	-1.8	-0.6	-0.9	-0.2	0	0.1	1.29
7	0.4	-2.4	-0.6	0.1	0	-0.1	2.84
8	-0.9	0.2	-0.2	0.1	0	0.1	1.14
9	-15.1	-9	-14.6	0	-1.1	-0.1	6.31
10	0.7	0.5	0.6	0	0	0	0.2
11	0.4	0.1	0.4	0	0	0	0.22

2.6.15.4 Stress Evaluation of the CY-MPC Canister for 1-Foot End Drop Load Condition

A structural analysis is performed using ANSYS to evaluate the effect of a 1-foot end drop impact for both the bottom and top end orientations of the canister. The ASME Code, Section III, NB requires the stresses arising from operational loads be assessed based on the primary loads. The primary loads for the 1-foot drop are due to the deceleration of the canister and its contents (65,821 pounds - fuel) and the conservatively assumed 20 psig pressure load internal to the canister. The applied deceleration is 20g for both orientations. The inertial load of the canister was addressed by the deceleration factor applied to the canister density, while the fuel and basket weight (49,155 pounds) was represented by a pressure load on the inner end surface of the canister. Displacement constraints are applied to the plane of symmetry and the gap elements attached at the canister end to represent the top or bottom of the transport cask.

To determine the effect of the 20 psig pressure load, the top end and bottom end orientations with and without the pressure load were analyzed. The maximum stresses are summarized below:

Drop Orientation	Internal Pressure (psi)	Maximum Stress Intensity (ksi)
Bottom End Drop	0	4.6
Bottom End Drop	20	3.0
Top End Drop	0	5.3
Top End Drop	20	5.8

It is concluded that the bottom end drop without pressure is limiting for the bottom end drop orientation. For the top end drop, the addition of pressure is limiting.

The location of the linearized stresses is shown in Figure 2.6.15.3-1. The maximum stresses for P_m and $P_m + P_b$ are tabulated in Tables 2.6.15.4-2 through 2.6.15.4-7. The critical sections for the pressure and the pressure plus the deceleration load, with reference to the section and the appropriate tables, are shown in Table 2.6.15.4-1.

Table 2.6.15.4-1 Summary of Critical Sections of the Canister for the 1-Foot End Drop Condition

Condition	Stress	Critical Section	Table	Minimum Margin of Safety
Pressure (only)	P_m	2	2.6.15.4-2	+3.88
Pressure (only)	$P_m + P_b$	2	2.6.15.4-3	+ 1.2
Top End Drop Pressure + Inertia	P_m	2	2.6.15.4-4	+ 8.9
Top End Drop Pressure + Inertia	$P_m + P_b$	2	2.6.15.4-5	+ 3.22
Bottom End Drop Inertia	P_m	2	See Note 1	+ 8.63
Bottom End Drop +Inertia	$P_m + P_b$	5	2.6.15.4-7	+ 4.35

Note:

1. The minimum margin of safety for the bottom end drop condition is based on the analysis considering the maximum gap of 0.08 inch between the structural lid and shield lid.

Table 2.6.15.4-2 Internal Pressure Only (20 psi) – Primary Membrane Stresses (ksi)

Section No.	P _m Stresses						S.I.	S _m Allow. Stress	Margin of Safety
	SX	SY	SZ	SXY	SYZ	SXZ			
1	0.1	2.1	0.8	-0.3	0	0.1	2.16	16.25	6.53
2	1.4	-1.5	-1.9	-0.3	0	-0.2	3.33	16.25	3.88
3	0	0.6	1.1	0	0	0.1	1.12	16.25	13.5
4	0.3	0.4	0.5	0.2	0	0	0.47	16.25	33.89
5	-0.7	0.3	0.2	0	0	0.1	1	16.25	15.32
6	-0.3	-0.5	0.1	0	0	0	0.66	16.25	23.47
7	0.5	-0.2	0.1	0	0	0	0.64	16.25	24.46
8	0	0.4	0.1	0.1	0	0	0.48	13.0*	26.1
9	0.2	0	0.2	0	-0.1	0	0.33	16.25	48.79
10	0	0	0	0	0	0	0.03	16.25	463.95
11	0.1	0	0.1	0	0	0	0.06	16.25	291.42

* Includes a stress reduction factors for the weld of 0.8 (See Section 2.6.15.12).

Table 2.6.15.4-3 Internal Pressure Only (20 psi) - Primary Membrane Plus Primary Bending Stresses (ksi)

Section No.	P _m + P _b Stresses						S.I.	1.5 S _m Allow. Stress	Margin of Safety
	SX	SY	SZ	SXY	SYZ	SXZ			
1	1.5	5.2	-0.1	-0.1	0	-0.1	5.28	24.38	3.62
2	0.7	-10.2	-4.4	-0.7	0	-0.4	11.08	24.38	1.2
3	0	0.6	1.1	0	0	0.1	1.14	24.38	20.44
4	0.2	0.7	0.6	0.3	0	0	0.76	24.38	31.19
5	-0.3	2.1	0.8	0.2	0	0.1	2.41	24.38	9.14
6	-1.1	-1.3	-0.3	-0.2	0	0.1	1.13	24.38	20.63
7	0.3	-1.2	-0.2	0	0	0	1.43	24.38	16.11
8	-0.6	0.1	-0.1	0.1	0	0	0.69	19.5*	27.27
9	6.9	-0.1	6.9	-0.1	-0.1	0	7	24.38	2.48
10	-1.1	0	-1.1	0	0	0	1.06	24.38	21.93
11	0.1	0	0.1	0	0	0	0.08	24.38	296.55

* Includes a stress reduction factors for the weld of 0.8 (See Section 2.6.15.12).

Table 2.6.15.4-4 Top End Drop: 1-ft. Drop + Internal Pressure (20 psi) - Primary Membrane Stresses (ksi)

Section No.	P_m Stresses						S.I.	S_m Allow. Stress	Margin of Safety
	SX	SY	SZ	SXY	SYZ	SXZ			
1	0.1	1.1	0.4	-0.2	0	0	1.12	16.25	13.47
2	0.7	-0.8	-0.9	-0.2	0	-0.1	1.64	16.25	8.9
3	0	-0.1	1.1	0	0	-0.1	1.26	16.25	11.94
4	0.1	-0.6	0	0	0	0	0.72	16.25	21.51
5	-0.1	-0.6	-0.1	0	0	0	0.51	16.25	30.73
6	0	-0.3	0	0	0	0	0.32	16.25	49.97
7	0	-0.6	-0.1	0	0	0	0.58	16.25	27.24
8	0	-0.4	0	0	0	0	0.42	13.0*	29.95
9	0.1	0	0.1	0	0	0	0.18	16.25	91.65
10	0	-0.3	0	0	0	0	0.29	16.25	55.15
11	0	-0.3	0	0	0	0	0.29	16.25	56

* Includes a stress reduction factors for the weld of 0.8 (See Section 2.6.15.12).

Table 2.6.15.4-5 Top End Drop: 1-ft. Drop + Internal Pressure (20 psi) - Primary Membrane Plus Primary Bending Stresses (ksi)

Section No.	$P_m + P_b$ Stresses						S.I.	1.5 S_m Allow. Stress	Margin of Safety
	SX	SY	SZ	SXY	SYZ	SXZ			
1	0.8	2.7	0.1	0	0	0	2.64	24.38	8.25
2	0.3	-5.3	-2.1	-0.4	0.1	-0.4	5.77	24.38	3.22
3	0	-0.1	1.1	0	0	-0.1	1.27	24.38	18.25
4	0.1	-1.1	-0.2	-0.1	0	0	1.16	24.38	20.09
5	0	-0.8	-0.1	-0.1	0	0	0.75	24.38	31.31
6	-0.2	-0.4	-0.1	0	0	0	0.36	24.38	66.33
7	0	-0.7	-0.1	0	0	0	0.68	24.38	34.98
8	0	-0.4	0	0	0	0	0.43	19.5*	44.35
9	3.4	0	3.4	0	0	0	3.46	24.38	6.04
10	0.1	-0.3	0.1	0	0	0	0.35	24.38	67.78
11	0	-0.3	0	0	0	0	0.3	24.38	80.33

* Includes a stress reduction factors for the weld of 0.8 (See Section 2.6.15.12).

Table 2.6.15.4-6 Bottom End Drop: 1-ft. Drop + Internal Pressure (0 psi) - Primary Membrane Stresses (ksi)

Section No.	P _m Stresses						S.I.	S _m Allow. Stress	Margin of Safety
	SX	SY	SZ	SXY	SYZ	SXZ			
1	0	-0.7	-0.1	0	0	0	0.73	16.25	21.4
2	0.2	-1.8	-0.3	-0.1	0	0	1.98	16.25	7.23
3	0	-1.7	0	0	0	0	1.72	16.25	8.44
4	-0.4	-1.1	-1	-0.3	0	-0.1	0.94	16.25	16.29
5	1.1	-0.8	-0.5	0.2	0	-0.1	1.95	16.25	7.32
6	0.5	1.1	-0.2	0.1	0.1	-0.1	1.31	16.25	11.41
7	-1.2	0.4	-0.6	-0.1	0	0	1.64	16.25	8.93
8	0.1	-1.2	-0.7	-0.2	0	-0.1	1.35	13.0*	8.63
9	0	-0.3	0	0	0	0	0.3	16.25	53.59
10	0.1	0	0.1	0	0	0	0.13	16.25	128.28
11	-0.1	0	-0.1	0	0	0	0.11	16.25	147

* Includes a stress reduction factors for the weld of 0.8 (See Section 2.6.15.12).

Table 2.6.15.4-7 Bottom End Drop: 1-ft. Drop + Internal Pressure (0 psi) - Primary Membrane Plus Primary Bending Stresses (ksi)

Section No.	P _m + P _b Stresses						S.I.	1.5 S _m Allow. Stress	Margin of Safety
	SX	SY	SZ	SXY	SYZ	SXZ			
1	0	-0.9	-0.1	-0.1	0	0	1	24.38	23.3
2	0.1	-2.5	-0.6	0	0	0	2.6	24.38	8.39
3	0	-1.7	0	0	0	0	1.72	24.38	13.16
4	-0.3	-2.4	-1.3	-0.4	0	-0.1	2.24	24.38	9.87
5	0.4	-4.1	-1.6	-0.1	0	-0.1	4.55	24.38	4.35
6	1.8	2.2	0.4	0.5	0	-0.1	2.08	24.38	10.7
7	-0.7	3.5	0.4	-0.2	0	0.1	4.2	24.38	4.81
8	1.5	-0.1	-0.1	-0.2	0.1	-0.1	1.76	19.5*	10.08
9	0	-0.3	0	0	0	0	0.33	24.38	72.35
10	2.1	0	2.1	0	0	0	2.09	24.38	10.69
11	-1.4	0	-1.4	0	0	0	1.39	24.38	16.56

* Includes a stress reduction factors for the weld of 0.8 (See Section 2.6.15.12).

THIS PAGE INTENTIONALLY LEFT BLANK

2.6.15.5 Stress Evaluation of the Canister for Thermal Plus a 1-Foot End Drop Load Condition

The thermal expansion loads described in Section 2.6.15.3 are added to the canister primary loads in Section 2.6.15.4 to produce a combined thermal expansion plus end impact loading. The stress evaluation is performed according to the ASME Code, Section III, Subsection NB. Based on the results in Section 2.6.15.4, the pressure is included with the inertia loading for the top end drop, but for the bottom end drop, the pressure is not considered. These combinations produce the most critical (smallest) margins of safety. The most critical sections are listed in Table 2.6.15.4-1 for the end drops. The smallest margin of safety reported is 3.22 at section 2. The stress is 5.77 ksi. Conservatively adding the largest thermal stress from Table 2.6.15.3-1 of 6.31 ksi at section 9 results in a total stress of 12.1 ksi. The minimum margin of safety is +3.03 when $3 S_m$ is used as the stress criteria. It is clear from the table that all of the stress intensities are less than $1.5 S_m$, so the stress intensity range criterion of $3.0 S_m$ is satisfied. The margins of safety are calculated as:

$$MS = (\text{allowable stress}/S.I.) - 1.$$

THIS PAGE INTENTIONALLY LEFT BLANK

2.6.15.6 Stress Evaluation of the Canister for a 1-Foot Side Drop Load Condition

The determination of the stresses in the canister due to a 1-foot side drop is accomplished using ANSYS. In the local regions of the lids and bottom plate, the loads are transmitted through the canister shell into the cask body inner shell. Outside of the lid and bottom plate regions, stress develops in the canister shell as a result of the basket loading the canister wall. The basket, canister and cask body have different radii which implies that the contact angle between the components is dependent on the loading. For this reason, the finite element model described in Section 2.6.15.2 contains a half model of the basket. Gap elements between the basket and the canister allow the interface to be dependent on the loading. The interface between the canister and the cask body inner shell is also represented by gap elements.

The load due to the contents is applied to the basket via pressure acting in the plane of the disks. The weight is assumed to act over the effective width of 9.17 inches for the normal slot or 9.57 inches for the oversized slot in which the disk is .5 inches thick. The content weight includes the heat transfer disks (1998 lbs), regular fuel tube (117 lbs.), oversize fuel tube (122.3 lbs), standard fuel weight per tube (1500 lbs.), and the oversized fuel weight per tube (1600 lbs). The actual fuel weight is bounded since the total fuel weight is 35,100 lbs versus 39,400 lbs ($1600 \times 4 + 1500 \times 22 = 39,400$ lbs) used in the model. This weight is distributed over the 28 support disks, excluding the two end weldments. A deceleration factor of 20g is applied to the load and the force per unit length for the regular size slot is computed as:

$$(1998/26 + 1500 + 117)(20) / [(9.17)(28)] \text{ psi} = 131.94 \text{ lb/in.}$$

For the oversized slot the force per unit length is:

$$(1998/26 + 1600 + 122)(20) / [(9.57)(28)] \text{ psi} = 134.3 \text{ lb/in.}$$

The 0-degree circumferential orientation of the basket is the configuration that results in the least amount of contact between the canister and cask inner shell and is considered bounding for the side drop. In addition to the contents load, a 20 psig pressure is conservatively applied to the inner surface of the canister.

The methodology used to evaluate the stresses for this condition is taken from Section 2.6.15.4 and the location of the sections are identified in Figure 2.6.15.3-1. The critical section stresses are reported in Table 2.6.15.6-1 and Table 2.6.15.6-2 for P_m and $P_m + P_b$ stresses, respectively. The minimum margin of safety for P_m is +0.03, at Section 6, and for $P_m + P_b$ it is +0.26 at Section 1. The margins of safety are calculated as: $M.S. = (\text{allowable stress}/S.I.) - 1$.

Table 2.6.15.6-1 Side Drop: 1-ft. Drop + Internal Pressure (20 psi) - Primary Membrane Stresses (ksi)

Section No.	P _m Stresses						S.I.	S _m	Margin of Safety
	SX	SY	SZ	SXY	SYZ	SXZ		Allow. Stress	
1(0°)	-8.3	1.4	-2.9	1.3	-0.1	-0.9	10.15	16.25	0.6
2(0°)	3.9	2.5	-1	0.3	-0.6	-0.6	5.24	16.25	2.1
3(0°)	-1	1.2	1.2	0	0	0.2	2.26	16.25	6.19
4(9°)	-3.2	1.9	-2.0	-0.1	1.1	-0.3	5.5	16.25	1.95
5(0°)	-12.6	0.8	-4.4	-2.7	0.9	-0.1	14.58	16.25	0.11
6(0°)	-17.8	-4.3	-5.4	-3.8	0.7	-0.3	15.79	16.25	0.03
7(9°)	0.3	0.8	-1.5	0.4	0.9	-0.8	3.3	16.25	3.92
8(0-4.5°)	-7.5	-1.7	-2.8	-0.4	0.6	-1.3	6.6	13.0*	0.97
9	-0.6	0	0.3	0	0	0	0.93	16.25	16.45
10	-0.4	0	0.1	0	0	0	0.47	16.25	33.41
11	-0.4	0	0.2	0	0	0	0.59	16.25	26.58

* Includes a stress reduction factors for the weld of 0.8 (See Section 2.6.15.12).

Table 2.6.15.6-2 Side Drop: 1-ft. Drop + Internal Pressure (20 psi) - Primary Membrane Plus Primary Bending Stresses (ksi)

Section No.	P _m + P _b Stresses						S.I.	1.5 S _m	Margin of Safety
	SX	SY	SZ	SXY	SYZ	SXZ		Allow. Stress	
1(0°)	-20.1	-1	-5.7	1.2	0	-0.9	19.31	24.38	0.26
2(18°)	0.6	-7.1	-2.3	-0.5	-0.1	-1	8.11	24.38	2.01
3(0°)	-1	1.6	2.6	0	0	0.3	3.69	24.38	5.61
4(9°)	-2.5	4.0	-1.4	0.2	1.2	0.3	6.8	24.38	2.6
5(0°)	-11.3	3.3	-4.8	-1.2	1.2	0.1	15.03	24.38	0.62
6(0°)	-20.6*	-5.1	-6.5	-3.5	1	-0.3	17.33	24.38	0.41
7(9°)	-0.4	0.2	-1.9	0.3	0.9	-1.4	3.6	24.38	5.8
8(0-4.5°)	-8.6	-2.9	-3.8	-0.9	0.6	-1.2	6.9	19.5**	1.85
9	-0.6	0	0.3	0	0	0	0.94	24.38	24.97
10	-1	0	-0.4	0	0	0	1	24.38	23.45
11	-0.8	0	-0.2	0	0	0	0.82	24.38	28.62

* See bearing stress calculation for section stress at 0° (See Section 2.6.15.9).

** Includes a stress reduction factors for the weld of 0.8 (See Section 2.6.15.12).

THIS PAGE INTENTIONALLY LEFT BLANK

2.6.15.7 Stress Evaluation of the CY-MPC Canister for Thermal Plus a 1-Foot Side Drop Load Condition

The thermal expansion loads described in Section 2.6.15.3 are added to the canister primary loads in Section 2.6.15.4 to produce a combined thermal expansion plus side impact loading. The stress evaluation is performed according to the ASME Code, Section III, Subsection NB. The most critical sections are listed in Table 2.6.15.6-2 for the side drop. Conservatively adding the thermal stress intensity at each section to the corresponding membrane plus bending stress intensity results in a peak stress of 20.4 ksi at section 1. The minimum margin of safety is +1.39 when $3 S_m$ is used as the stress criteria. At section 8 with the reduced allowable, the total stress is 8.0 ksi and the margin of safety is +2.9. It is clear from these results that all of the stress intensities are less than $1.5 S_m$, so the stress intensity range criterion of $3.0 S_m$ is satisfied in Section 2.6.7.1. The margins of safety are calculated as: $M.S. = (\text{allowable stress}/S.I.) - 1$.

1. The first part of the report is a summary of the work done during the year.

2. The second part is a detailed account of the work done during the year.

3. The third part is a summary of the work done during the year.

4. The fourth part is a detailed account of the work done during the year.

5. The fifth part is a summary of the work done during the year.

6. The sixth part is a detailed account of the work done during the year.

7. The seventh part is a summary of the work done during the year.

8. The eighth part is a detailed account of the work done during the year.

9. The ninth part is a summary of the work done during the year.

10. The tenth part is a detailed account of the work done during the year.

THIS PAGE INTENTIONALLY LEFT BLANK

2.6.15.8 CY-MPC Canister Shear Stresses for a 1-Foot Side Drop and a 1-Foot End Drop Condition

The evaluation of the maximum shear stress utilizes the membrane values of the stress intensity due to primary loading which were evaluated for the pressure, end drops and side drop loading. The maximum membrane stress intensity is 15.8 ksi for location 6 (Table 2.6.15.6-1). Using a bounding temperature of 350°F, the S_m for Type 304L stainless steel is 16.25 ksi, the margin of safety is determined by:

$$M.S. = (0.6)(16.25)/(15.8/2) - 1$$

$$M.S. = +0.23$$

THIS PAGE INTENTIONALLY LEFT BLANK

2.6.15.9 CY-MPC Canister Bearing Stresses for a 1-Foot Side Drop

The bearing stress of the canister on the cask inner shell is evaluated in the region of the canister lids and over the length of the canister shell. The bearing stress associated with the lids is calculated using the membrane S_x stress at Section 7 (see Figure 2.6.15.3-1). The S_x stress component, associated with the radial direction at the plane of symmetry of the canister, is 19.5 ksi based on the finite element evaluation (Section 2.6.15.6). The bearing stress allowable is S_y for the operational condition, and using a bounding temperature of 220°F, $S_y=21.0$ ksi, the margin of safety is computed as:

$$M.S. = (21.0/19.5)-1$$

$$M.S. = + 0.08$$

For the bearing stress acting along the inner shell, an angular contact of 18 degrees is assumed (at a radius of 35.5 inches). In this bearing stress, the lids are not considered to be a contributor. This reduces the contents weight to $65,821-8,663 = 57,158$ pounds = 57.2 kips. For a basket length of 124 inches (removing the lengths of both weldments and the first spacer), the margin for the bearing stress is computed as:

$$S_{br} = (57.2)(20)/[(124)(35.5)(18/57.2958)]$$
$$= 0.83 \text{ ksi}$$

$$M.S. = (18.35/S_{br}) - 1 = +21$$

$$M.S. = + \text{Large}$$

THIS PAGE INTENTIONALLY LEFT BLANK

2.6.15.10 CY-MPC Canister Buckling Evaluation for 1-Foot End Drop

The canister shell is axially loaded by the weights of the structural lid, the shield lid, and the inertial weight of the shell during a 1-foot end drop impact. The impact load amplification factor is 20g. The shell is evaluated as an unsupported, right circular cylinder using a critical buckling load per Blake, 2nd Edition, "Practical Stress Analysis in Engineering Design":

$$S_{cr} = \frac{E(0.605 - 10^{-7} M^2)}{M(1 + 0.004\phi)}$$
$$= 40.3 \text{ ksi}$$

Where the canister material is Type 304L stainless steel, conservatively assumed to be at 400°F for normal operation, and:

$$E = 26.5 \text{ E03 ksi} \quad R = (69.39 + 0.625)/2 = 35.01 \text{ in.}$$
$$S_y = 17.5 \text{ ksi} \quad t = 0.625 \text{ in.}$$

$$\phi = \frac{E}{S_y} = 1514.3 \quad M = \frac{R}{t} = 56.0$$

The axial compression load in the canister shell is:

$$P_a = [(\pi/4)(69.03)^2(0.291)(8) + (\pi/4)(70.64^2 - 69.39^2)(151.75)(0.291)]20$$
$$= 295,680 \text{ pounds}$$

and the axial compression stress is:

$$S_A = \frac{P_A}{(\pi/4)(70.64^2 - 69.39^2)} = 2,151 \text{ psi}$$

Then, the margin of safety for canister shell buckling is:

$$\text{M.S.} = (40.3 / 2.15) - 1 = +17.7$$

THIS PAGE INTENTIONALLY LEFT BLANK

2.6.15.11 CY-MPC Canister Lifting Evaluation

The lifting of the canister is accomplished by attaching vendor qualified eyehooks to six locations in the structural lid. During the lifting of the canister, the contents weight of 40,130 pounds is transmitted to the canister bottom and up through the canister 0.625-inch thick shell. The calculated canister internal pressure is 11.3 psig during normal operations. The evaluation of this load configuration of the canister is accomplished by a three-dimensional finite element model, as shown in Figure 2.6.15.11-1. This model is essentially the same model presented in Section 2.6.15.2, with the elements for the basket removed. The model is used to evaluate the lower portion of the canister, especially the bottom plate and the junction of the bottom plate and the canister shell. Since the canister is in a vertical position under a lift condition, the model is only restrained at the lift locations at the structural lid. The loads considered in the analysis are internal pressure, dead load with a dynamic load factor of 1.1, and the thermal load. A pressure of 11.5 psig is conservatively applied to represent the operating pressure (the calculated internal pressure is 11.3 psig). The weight of the contents is applied to the bottom plate as a uniform pressure. The 1.1 dynamic load factor is also applied to the contents weight. The thermal stress analysis is performed using the methodology described in Section 2.6.15.3. The temperatures of the key locations considered in the analysis are:

Top center of the structural lid	=	140°F
Top outer diameter of the structural lid	=	100°F
Bottom center of the bottom plate	=	250°F
Bottom outer diameter of the bottom plate	=	130°F
Mid-elevation of the canister shell	=	500°F

The table below shows the temperature differences (ΔT) in the radial and axial directions applied in the model and those calculated by thermal analysis for normal conditions of transport.

	Applied in Model ($\Delta^\circ\text{F}$)	Thermal Analysis Calculation	
		Heat Condition ($\Delta^\circ\text{F}$)	Cold Condition ($\Delta^\circ\text{F}$)
Lid (Radial)	40	14	12
Bottom Plate (Radial)	120	30	29
Shell (Axial)	400	146	160

As shown in the table, the temperature differences in the model envelope the calculated values. Therefore, the thermal stress analysis is conservative.

Allowable stresses at a temperature of 250°F for the lid region, 550°F for the canister shell and 250°F for the bottom plate region, are applied. These temperatures envelope the calculated maximum temperatures of the canister components (see Tables 3.4-1 and 3.4-2) except for the bottom plate, which has a calculated maximum temperature of 255°F for the heat condition of transport. Since the value of design stress intensity (S_m) for SA 240 Type 304L does not change for temperatures below 300°F, the allowable stresses used in this evaluation remain bounding.

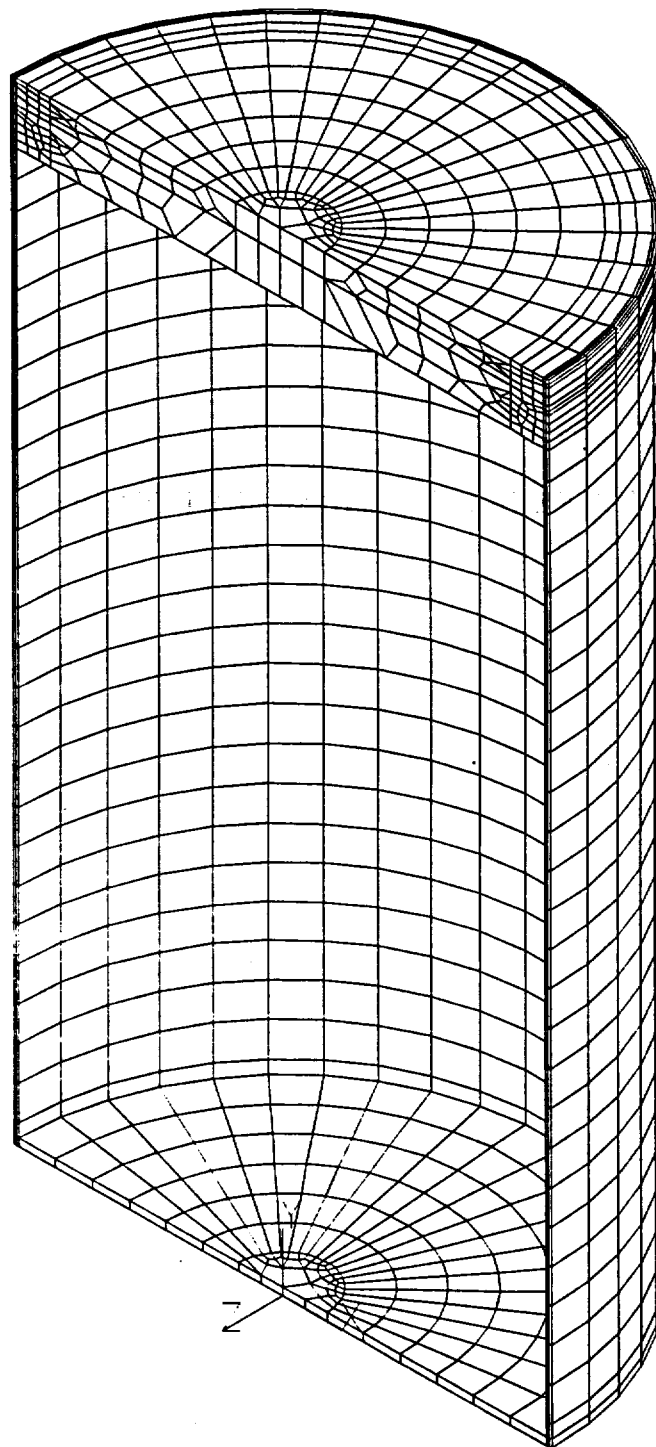
Based on the stress allowables required by the ASME Code, Section III, Subsection NB, the minimum margins of safety are:

Stress Category	Max. Stress (ksi)	Allowable Stress (ksi)	Margin of Safety
P_m	9.47 ¹	16.7	0.76
$P_m + P_b$	20.5 ²	25.05	0.22
$P + Q$	27.74 ¹	50.1	0.81

¹ Maximum stress occurs at the center of bottom plate.

² Maximum stress occurs at junction of the bottom plate and the canister shell.

Figure 2.6.15.11-1 Finite Element Model for CY-MPC Canister Lift Evaluation



THIS PAGE INTENTIONALLY LEFT BLANK

2.6.15.12 CY-MPC Canister Closure Weld Evaluation – Normal Conditions of Transport

2.6.15.12.1 Stress Evaluation for the CY-MPC Canister Closure Weld

The closure weld for the canister is a partial penetration weld with a leg length of 1.13 inches. The evaluation of this weld, in accordance with NRC guidance, is to incorporate a weld stress reduction factor of 0.8 in accordance with NRC ISG-4, Item 5, to provide conservative consideration of the weld configuration. This stress reduction factor is incorporated by applying a factor of 0.8 to the stress allowable for this weld.

The stresses for the canister are evaluated using sectional stresses as permitted by Subsection NB using the finite element model as described in Section 2.6.15.2. The location of the section for the canister weld evaluation is shown in Figure 2.6.15.3-1 and corresponds to Section 8. The governing P_m , $P_m + P_b$, and $P + Q$ stress intensity for Section 8 for all normal conditions of transport and the associated allowables are listed below. The factored allowables, incorporating a 0.8 stress reduction factor, and the resulting margin of safety are:

Stress Type	Analysis Stress Intensity (ksi)	0.8 x Allowable Stress (ksi)	Margin of Safety
P_m	6.6	13.0	0.97
$P_m + P_b$	6.9	19.5	1.83
$P + Q$	8.0	39.0	3.88

This confirms that the canister closure weld is acceptable for normal conditions of transport.

2.6.15.12.2 Critical Flaw Size for the Canister Closure Weld

The closure weld for the canister is comprised of multiple weld beads using a compatible weld material for Type 304L stainless steel. An allowable (critical) flaw evaluation has been performed to determine the critical flaw size in the weld region. The result of the flaw evaluation is used to define the minimum flaw size, which must be identifiable in the nondestructive examination of the weld. Due to the inherent toughness associated with Type 304L stainless steel, a limit load analysis is used in conjunction with a J-integral/tearing modulus approach.

The safety margins used in this evaluation correspond to the stress limits contained in Section XI of the ASME Code.

One of the stress components used in the evaluation for the critical flaw size is the radial stress component in the weld region of the structural lid. For the normal operation condition, in accordance with ASME Code Section XI, a safety factor of 3 is required. For the purpose of identifying the stress for the flaw evaluation, the weld region corresponding to Section 8 of Figure 2.6.15.3-1 is considered. The maximum radial tensile stress is 1.0 ksi. To perform the flaw evaluation, a 10 ksi stress is conservatively used, resulting in a significantly larger safety factor than the required safety factor of 3. Using 10 ksi as the basis for the evaluation, the critical flaw size is 0.52 inch for a flaw that extends 360 degrees around the circumference of the canister. Stress components for the circumferential and axial directions are associated with flaws oriented in the radial and horizontal directions, respectively. The maximum stress reported for these components is 0.5 ksi, which is also enveloped by the stress value of 10 ksi for radial stresses. The 360-degree flaw employed for the circumferential direction is considered to be bounding with respect to any partial flaw in the weld, which could occur in the radial and horizontal directions. Therefore, using a minimum detectable flaw size of 3/8 inch is acceptable, since it is less than the very conservatively determined 0.52-inch critical flaw size.

2.6.16 CY-MPC Fuel Basket Analysis - Normal Conditions of Transport

There are two different fuel basket assemblies for Connecticut Yankee class fuel. The first fuel basket is designed to accommodate up to 24 fuel assemblies. The second fuel basket is designed to accommodate up to 26 fuel assemblies. The 26-fuel assembly basket supports the maximum load with the minimum structure. Therefore, only the 26-fuel assembly basket is considered in this analysis.

The fuel basket assembly is a right cylinder structure and is fabricated using 26 square fuel tubes, 28 circular support disks, 27 heat transfer disks, 6 tie rods with split spacers, and two end weldment plates.

The basket components and their geometry are illustrated in Figures 2.6.16-1 and 2.6.16-2. The basket contains two sizes of fuel tubes. There are 22 standard and 4 oversized fuel tubes. Figures 2.6.16-3 and 2.6.16-4 show the details of the stainless steel tubes with the encased BORAL. The standard fuel tube has a 8.72-inch square inside dimension, 0.141-inch thick composite wall. The oversized fuel tube has a 9.12-inch square inside dimension, a 0.141-inch thick composite wall. Both fuel tubes hold the design basis Connecticut Yankee Class fuel assembly. The fuel tubes are open at each end. Therefore, longitudinal fuel assembly loads are imparted to the canister body and not the fuel basket structure.

The fuel assemblies, together with the tubes are laterally supported in the holes in the stainless steel support disks. Each support disk is 0.5 inches thick, 69.15 inches in diameter and has 26 holes. There are 22 holes that are each 9.17 inches square and 4 holes that are 9.57 inches square. There are four web thicknesses in the support disks; 1.50 inch, 1.25 inch, 1.10 inch, and 1.00 inch. The widest web is nearest the center of the basket, the web decreases in width towards the outer radius of the basket. The support disks are equally spaced at 4.09 inches.

The weldments are geometrically similar to the support disks and are 68.98 inches in diameter and .50 in thick. The top weldment includes support ribs and an outer ring. The bottom weldment includes support ribs and tie rod support bosses. The total heights of the top and bottom weldments are 6.8 and 2.0 inches, respectively.

Twenty-seven (27) aluminum heat transfer disks are interleaved with the support disks to fully optimize the passive heat rejection from the package. Each heat transfer disk is .50-inch thick, 68.9 inches in diameter, and has 26 holes for the fuel tubes. There are 22 standard holes that are

9.14 inches square and 4 oversized holes that are 9.54 inches square. There are five different web widths, 1.56 inches, 1.46 inches, 1.26 inches, 1.16 inches, and 1.06 inches. The widest aluminum web is nearest the center of the basket to optimize passive heat rejection. The dimensional differences between the heat transfer disk and the support disk accommodates the different rate of thermal growth between aluminum and stainless steel preventing interference between the tube, the support disk, and heat transfer disks. The heat transfer disks, which serve no structural function, are supported by the six (6) tie rods with split spacers. Each tie rod has 3.0 inches of 1 5/8-8 UN-2A threads at the upper end of the rod, which thread into the top nuts that clamp against the top weldment. The fuel basket contains the fuel and is laterally supported by the canister shell.

The 28 support disks and 2 end weldments are fabricated from 17-4 PH and Type 304 stainless steels, respectively. The 27 heat transfer disks are fabricated from Type 6061-T651 aluminum alloy. The 26 fuel tubes are fabricated from Type 304 stainless steel. The tie rods and spacers are fabricated from Type 304 stainless steel. The stainless steel tubes are not considered to be a structural component with respect to the disks and are not included in the basket or weldment analyses. The primary function of the split spacers and the threaded top nut is to locate and structurally assemble the support disks, heat transfer disks and the top and bottom weldment plates into an integral assembly. The spacers carry the inertial weight of the support disks, heat transfer disks, one end plate, and their own inertial weight for a normal transport condition 1-foot end drop. The end drop loading of the split spacers and tie rods represent a classical closed form structural analysis. Therefore the only component that requires a detailed finite element analysis is the support disk.

The fuel basket is evaluated for the normal transport loads in this section and is evaluated for the hypothetical accident condition in Section 2.7.13.

Figure 2.6.16-1 CY-MPC Fuel Assembly Basket

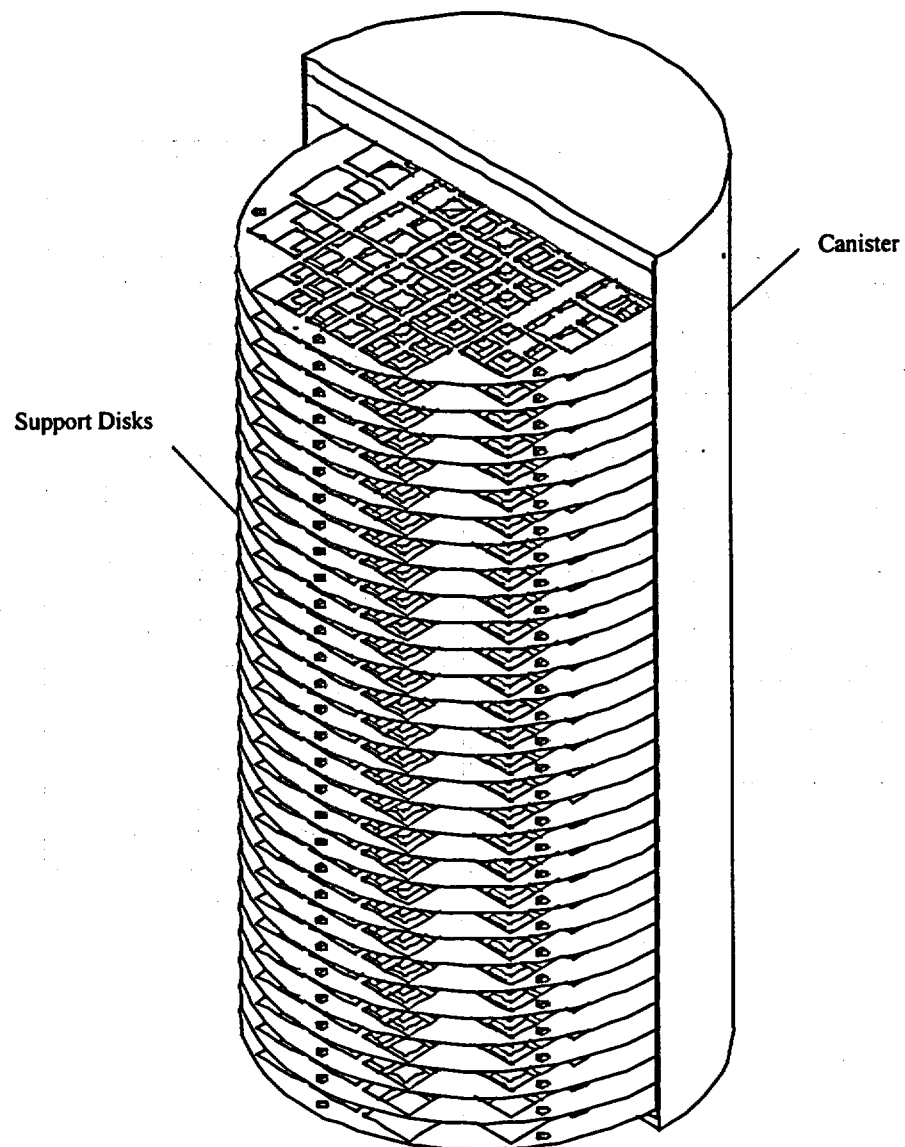


Figure 2.6.16-2 CY-MPC Support Disk Configuration - Canistered Fuel Basket

**FIGURE WITHHELD AS
SENSITIVE UNCLASSIFIED
INFORMATION**

Figure 2.6.16-3 CY-MPC Basket Standard Fuel Tube

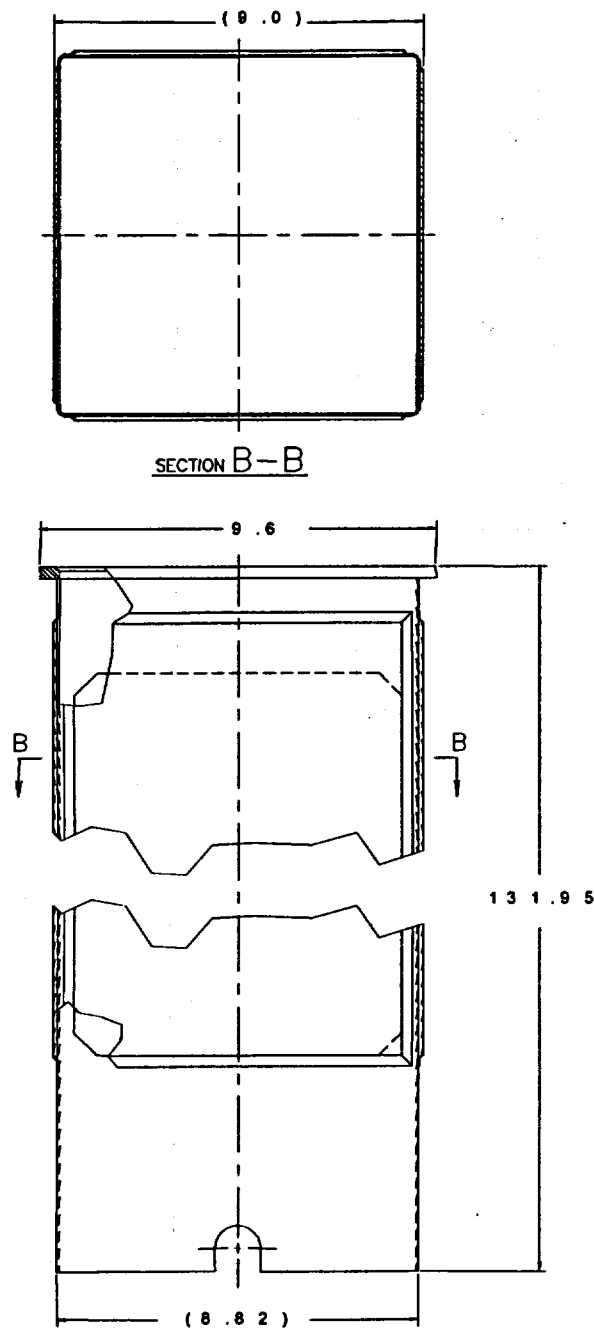
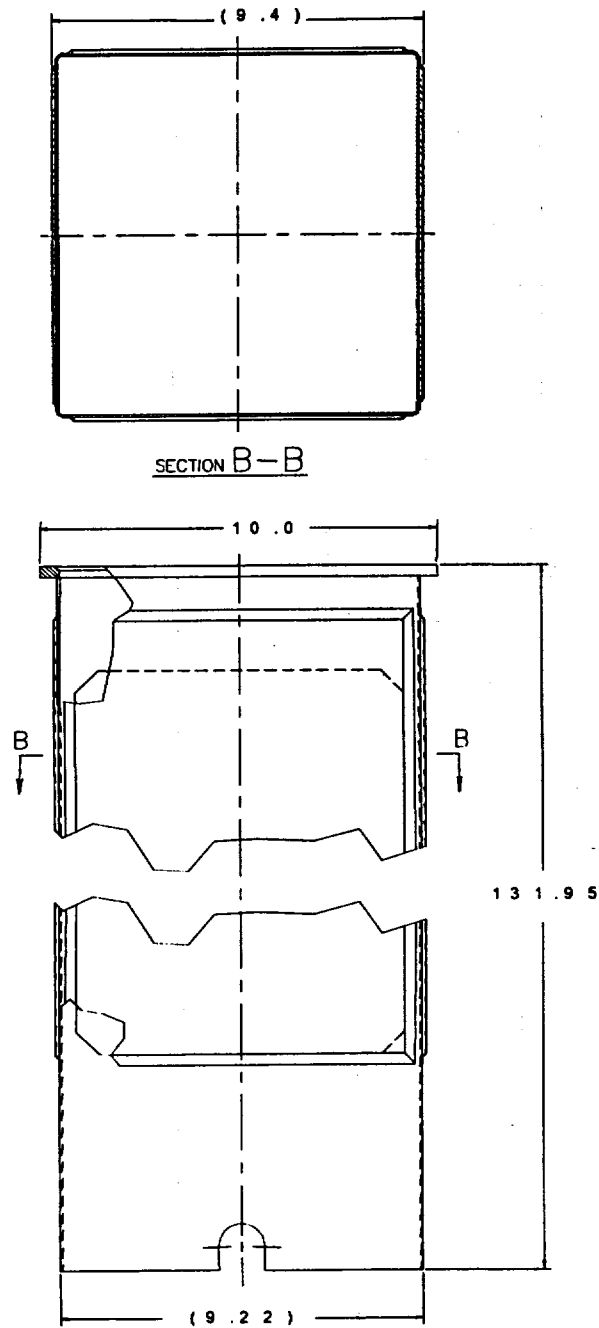


Figure 2.6.16-4 CY-MPC Basket Oversize Fuel Tube



2.6.16.1 Detailed Analysis of the CY-MPC Fuel Basket

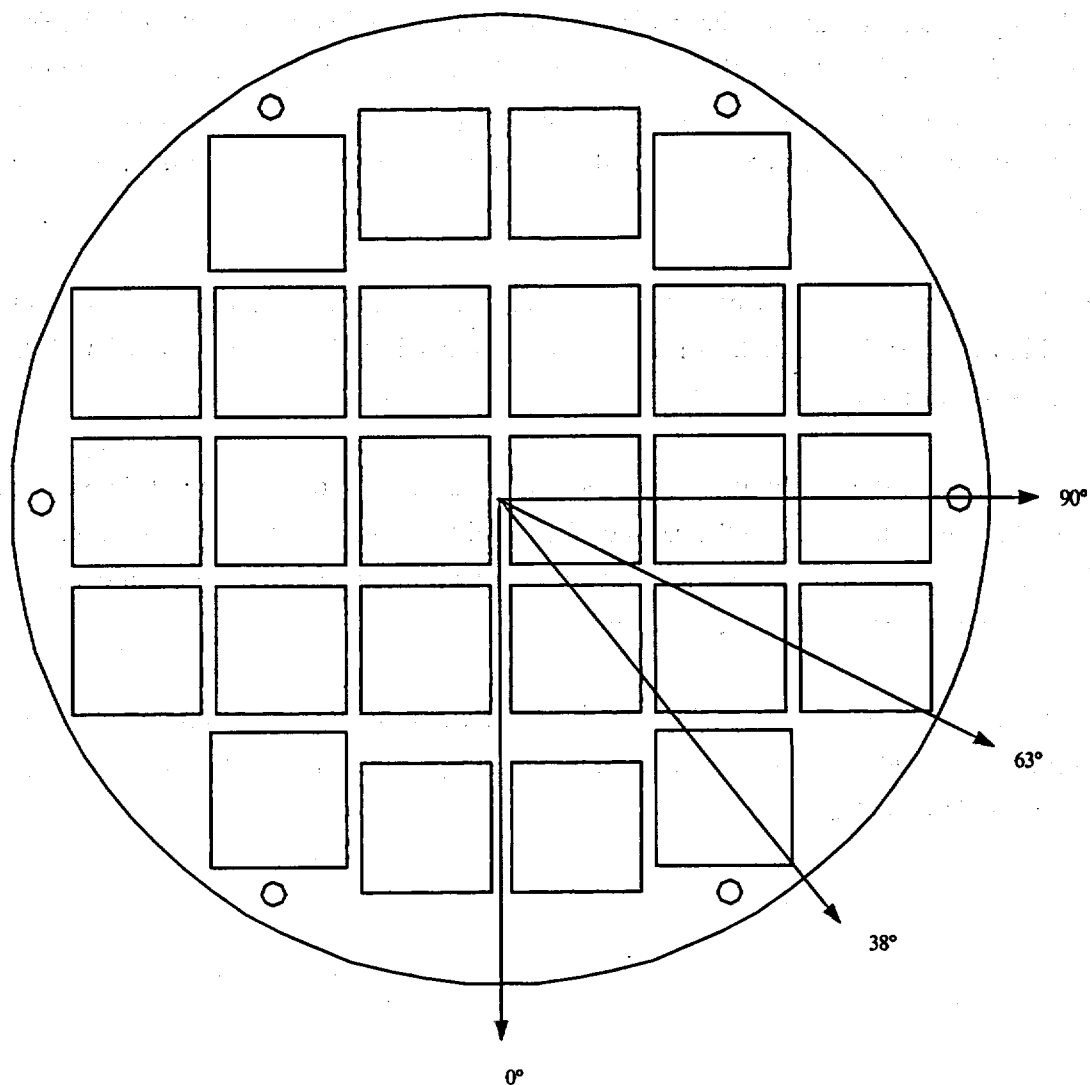
Based on criticality control requirements, the canistered fuel basket design criteria requires the maintenance of fuel support and control of spacing of the fuel assemblies for all load conditions. The structural design criteria for the fuel basket is the ASME Boiler and Pressure Vessel Code, Section III, Division 1, Subsection NG, "Core Support Structures." Consistent with these criteria, the fuel basket is shown to have a maximum P_m and $(P_m + P_b)$ under normal loading conditions that is less than S_m and $1.5S_m$, respectively. The value of S_m is defined at conservative temperatures for the component being analyzed.

For the side drop conditions, four basket drop orientations (0° , 38° , 63° , and 90°) are considered, as shown in Figure 2.6.16.1-1. Angles of 38° and 63° were selected because minimal web thickness occurs at these orientations.

In the side drop, the loads of the fuel assemblies are transferred into the plane of the support disks, from which they are transmitted to the canister shell, and then to the cask body (cask inner shell). In the end drop, the support disks are loaded only by their own inertial mass and do not experience load from the guided, but free standing fuel assemblies.

Finite element models are used to perform analyses for end drop and side drop conditions using the ANSYS program. In addition to the load from inertial weight, the analyses also consider the stresses due to differential thermal expansion.

Figure 2.6.16.1-1 CY-MPC Basket Drop Orientations



2.6.16.2 CY-MPC Fuel Basket Finite Element Model Description

Two finite element models were generated to analyze the canistered Connecticut Yankee class fuel basket for the normal operating conditions. The first model simulates the side drop (Figure 2.6.16.2-1) at the basket orientations shown in Figure 2.6.16.1-1. The second model simulates the end drop (Figure 2.6.16.2-2). These results are then combined to simulate various oblique drops as shown in Figure 2.6.16.2-3. All calculations accommodate thermal expansion effects using the temperature distribution from the thermal analysis and the coefficient of thermal expansion.

The model for the end drop simulation is constructed using ANSYS SHELL63 elements. It consists of a single support disk with a thickness of 0.5 inch. The shell elements accommodate the out-of-plane bending, which is present in the end-drop condition. The support disk is restrained in the direction of the drop by the split spacers on the six tie rods. Therefore, the nodes corresponding to the location of the tie rods are restrained in the out of plane direction (the cask axial direction) as well as all 5 remaining DOF to stabilize the model. The only loading is the inertial weight of the support disk in the out-of-plane direction.

The finite element model for the side drop evaluation of the support disk is a three-dimensional model and includes a slice, or section of the canister and cask as well as a single support disk. The canister and the cask body are included in the model to more accurately simulate the boundary conditions for the support disk. The top and bottom portions of the canister and transport cask are not considered in this analysis. Neglecting these end effects is conservative because it allows slightly more deformation of the canister shell and the support disks. The interface between the support disks and the canister element and the interface between the canister shell and the cask inner shell are modeled using ANSYS CONTAC52 elements (Figure 2.6.16.2-4). These elements act in compression only, connecting adjacent nodes across the interface. To prevent rigid body motion of the support disks, two BEAM4 elements are defined at the centerline of the model for each disk. These beam elements have very small properties, e.g. $\text{area} = 0.5 \times 10^{-3} \text{ in.}^2$, and, therefore, have negligible contribution to the contact stiffness.

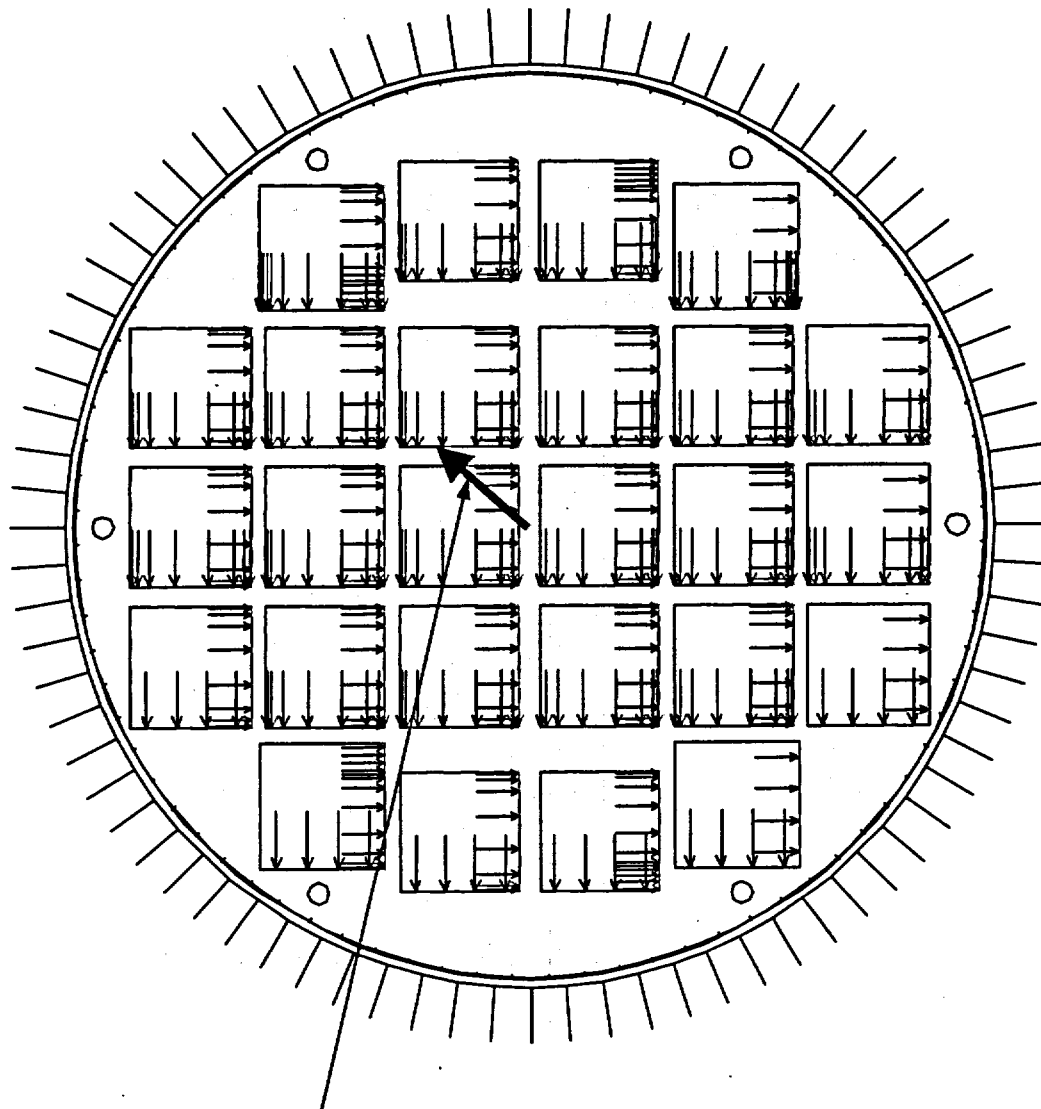
In the support disk side drop models, the canister shell and the cask body are modeled with SOLID45 elements. To increase the accuracy of the analysis, the element size is reduced towards the intersections of the ligaments.

While the cask, canister and support disk are modeled explicitly, the impact limiters are represented by CONTAC52 elements. Cask and impact limiter modeling reflect the same approach as described in

Section 2.6.7.4. The load from each fuel assembly is modeled as a line-pressure on the inner surfaces of each support disk opening.

To determine the most critical regions, a series of 131 cross sections are considered. To aid in the identification of these sections, Figure 2.6.16.2-5 shows the section locations on a support disk for the all of the side drop cases. Table 2.6.16.2-1 lists the geometric locations of the end points for each cross section.

Figure 2.6.16.2-1 CY-MPC Support Disk Side Drop Model



Acceleration Vector
(38° basket orientation shown)

Note: mesh is omitted for clarity.

Figure 2.6.16.2-2 CY-MPC Support Disk End Drop Model

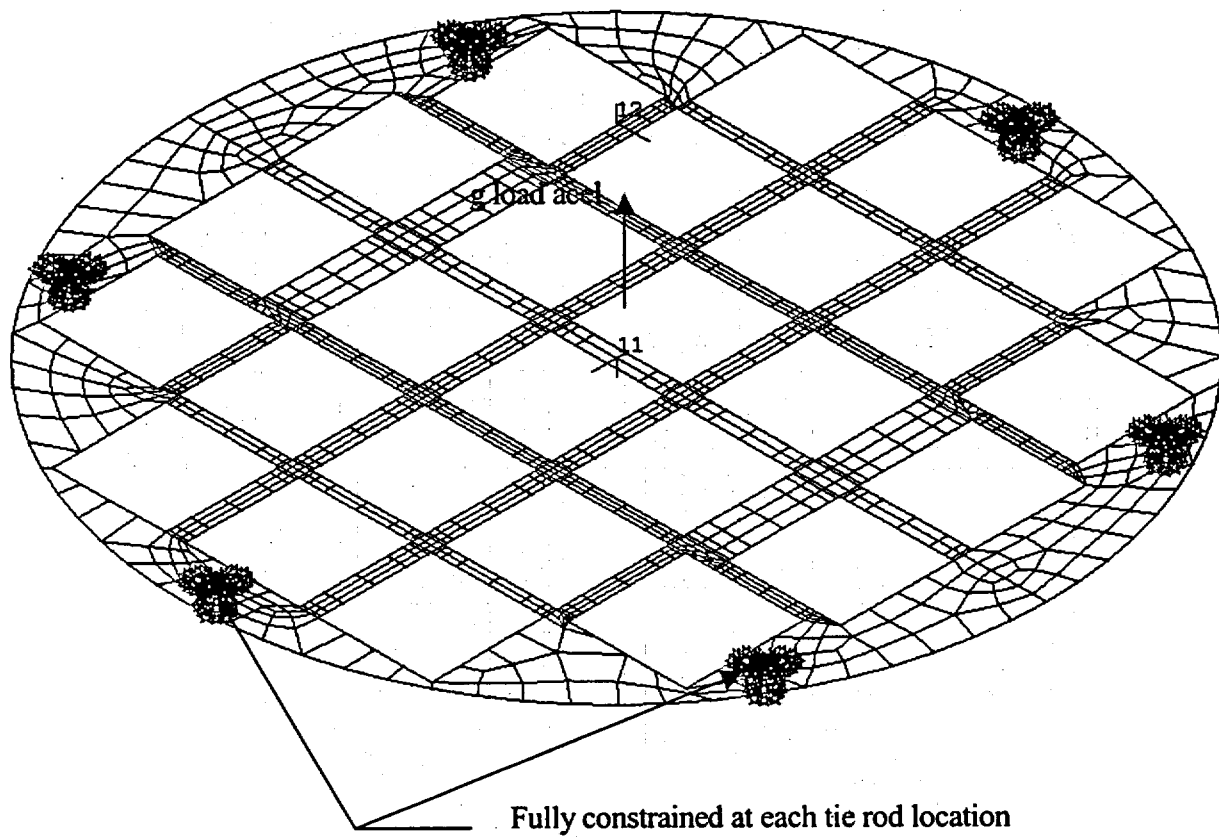


Figure 2.6.16.2-3 Cask Orientation

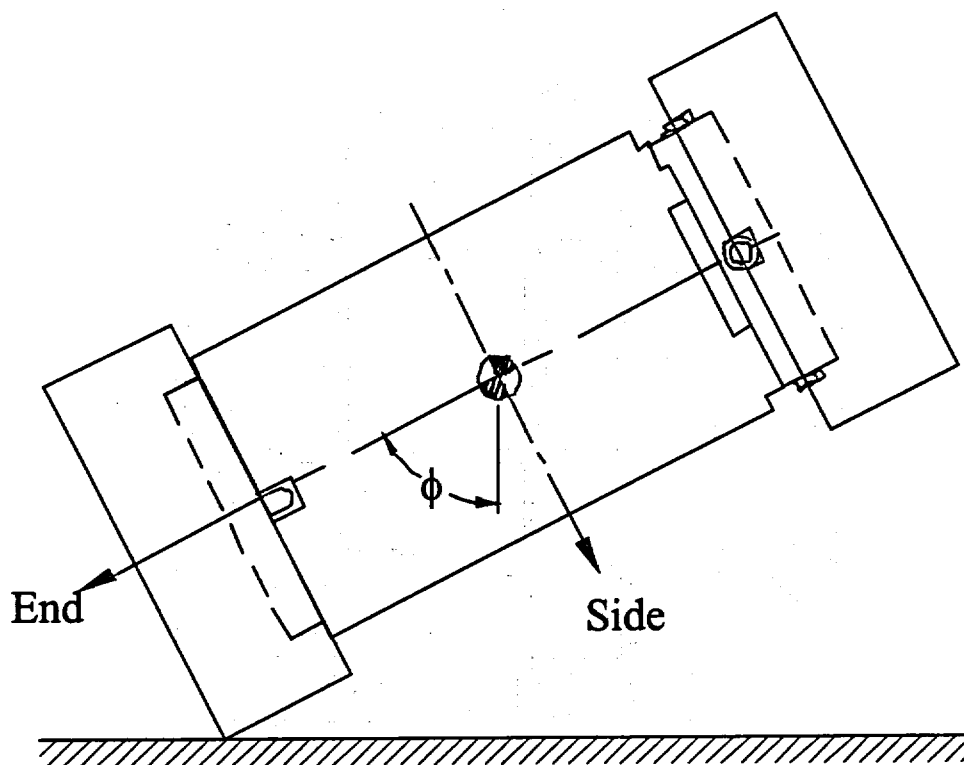


Figure 2.6.16.2-4 CONTAC52 Elements in the CY-MPC Support Disk Side Drop Model

(Interface between Disks & Canister Shell and between Canister Shell and Cask)

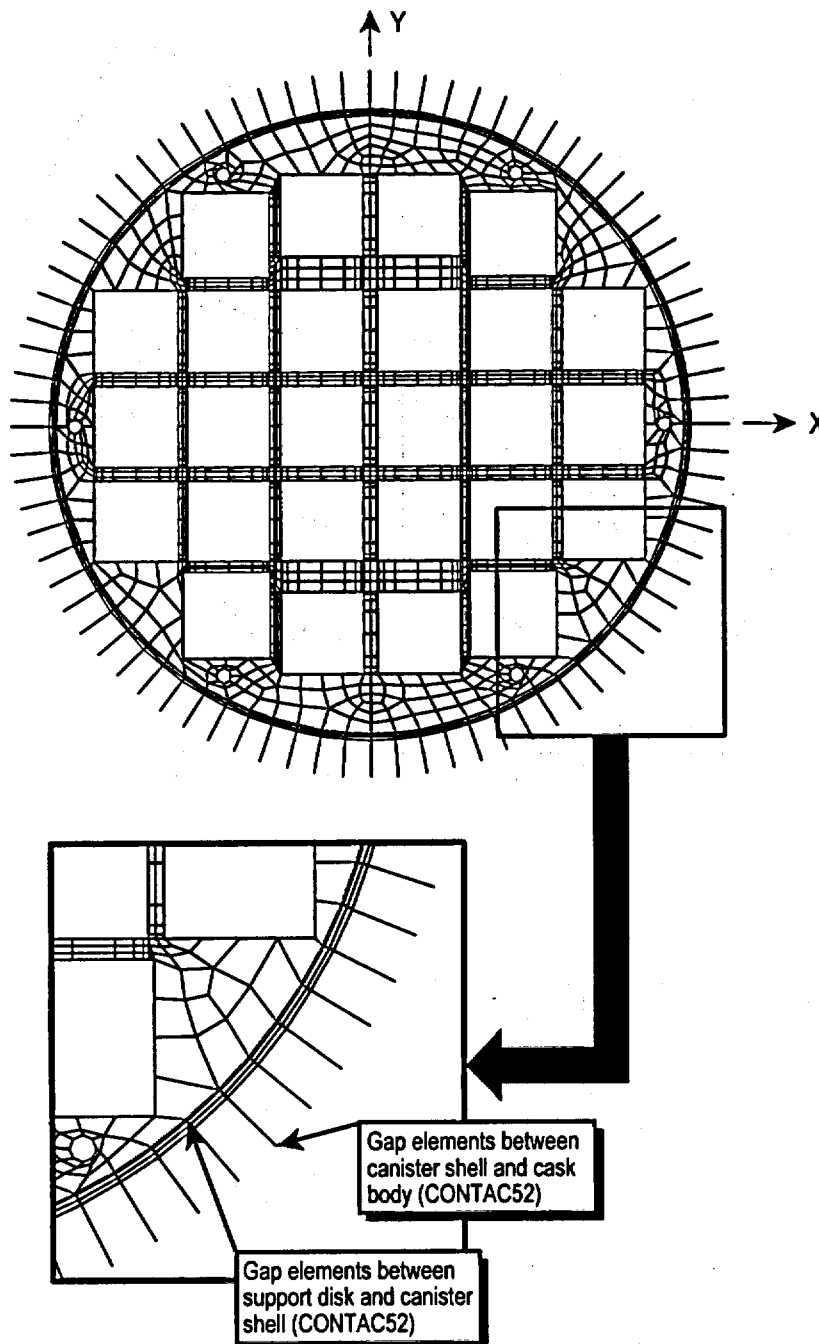


Figure 2.6.16.2-5 Location of the Sections to Obtain Linearized Stresses – CY-MPC Basket Support Disk

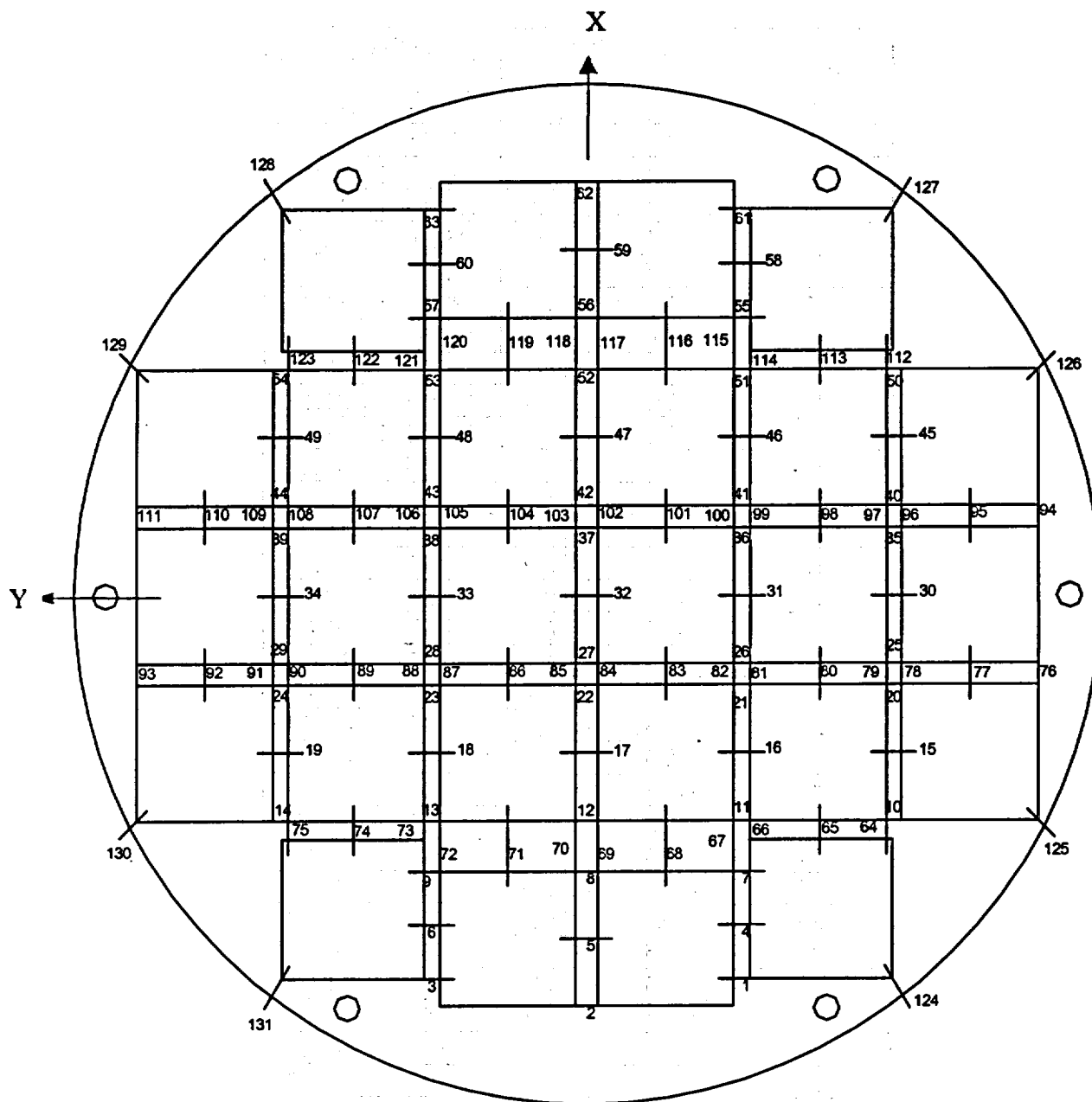


Table 2.6.16.2-1

Cross Sections for Stress Evaluation of CY-MPC Support Disk

SECTION	POINT 1		POINT 2	
	X	Y	X	Y
1	26.075	-9.92	26.075	-11.02
2	27.925	0.75	27.925	-0.75
3	26.075	9.92	26.075	11.02
4	22.415	-9.92	22.415	-11.02
5	23.34	0.75	23.34	-0.75
6	22.415	9.92	22.415	11.02
7	18.755	-9.92	18.755	-11.02
8	18.755	0.75	18.755	-0.75
9	18.755	9.92	18.755	11.02
10	15.255	-20.19	15.255	-21.19
11	15.255	-9.92	15.255	-11.02
12	15.255	0.75	15.255	-0.75
13	15.255	9.92	15.255	11.02
14	15.255	20.19	15.255	21.19
15	10.67	-20.19	10.67	-21.19
16	10.67	-9.92	10.67	-11.02
17	10.67	0.75	10.67	-0.75
18	10.67	9.92	10.67	11.02
19	10.67	20.19	10.67	21.19
20	6.085	-20.19	6.085	-21.19
21	6.085	-9.92	6.085	-11.02
22	6.085	0.75	6.085	-0.75
23	6.085	9.92	6.085	11.02
24	6.085	20.19	6.085	21.19
25	4.585	-20.19	4.585	-21.19
26	4.585	-9.92	4.585	-11.02
27	4.585	0.75	4.585	-0.75
28	4.585	9.92	4.585	11.02
29	4.585	20.19	4.585	21.19
30	0	-20.19	0	-21.19
31	0	-9.92	0	-11.02
32	0	0.75	0	-0.75
33	0	9.92	0	11.02
34	0	20.19	0	21.19
35	-4.585	-20.19	-4.585	-21.19
36	-4.585	-9.92	-4.585	-11.02
37	-4.585	0.75	-4.585	-0.75
38	-4.585	9.92	-4.585	11.02

Table 2.6.16.2-1 Cross Sections for Stress Evaluation of CY-MPC Support Disk (Continued)

SECTION	POINT 1		POINT 2	
	X	Y	X	Y
39	-4.585	20.19	-4.585	21.19
40	-6.085	-20.19	-6.085	-21.19
41	-6.085	-9.92	-6.085	-11.02
42	-6.085	0.75	-6.085	-0.75
43	-6.085	9.92	-6.085	11.02
44	-6.085	20.19	-6.085	21.19
45	-10.67	-20.19	-10.67	-21.19
46	-10.67	-9.92	-10.67	-11.02
47	-10.67	0.75	-10.67	-0.75
48	-10.67	9.92	-10.67	11.02
49	-10.67	20.19	-10.67	21.19
50	-15.255	-20.19	-15.255	-21.19
51	-15.255	-9.92	-15.255	-11.02
52	-15.255	0.75	-15.255	-0.75
53	-15.255	9.92	-15.255	11.02
54	-15.255	20.19	-15.255	21.19
55	-18.755	-9.92	-18.755	-11.02
56	-18.755	0.75	-18.755	-0.75
57	-18.755	9.92	-18.755	11.02
58	-22.415	-9.92	-22.415	-11.02
59	-23.34	0.75	-23.34	-0.75
60	-22.415	9.92	-22.415	11.02
61	-26.075	-9.92	-26.075	-11.02
62	-27.925	0.75	-27.925	-0.75
63	-26.075	9.92	-26.075	11.02
64	16.505	-20.19	15.255	-20.19
65	16.505	-15.755	15.255	-15.755
66	16.505	-11.02	15.255	-11.02
67	18.755	-9.92	15.255	-9.92
68	18.755	-5.335	15.255	-5.335
69	18.755	-0.75	15.255	-0.75
70	18.755	0.75	15.255	0.75
71	18.755	5.335	15.255	5.335
72	18.755	9.92	15.255	9.92
73	16.505	11.02	15.255	11.02
74	16.505	15.755	15.255	15.755
75	16.505	20.19	15.255	20.19

Table 2.6.16.2-1 Cross Sections for Stress Evaluation of CY-MPC Support Disk (Continued)

SECTION	POINT 1		POINT 2	
	X	Y	X	Y
76	6.085	-30.36	4.585	-30.36
77	6.085	-25.775	4.585	-25.775
78	6.085	-21.19	4.585	-21.19
79	6.085	-20.19	4.585	-20.19
80	6.085	-15.755	4.585	-15.755
81	6.085	-11.02	4.585	-11.02
82	6.085	-9.92	4.585	-9.92
83	6.085	-5.335	4.585	-5.335
84	6.085	-0.75	4.585	-0.75
85	6.085	0.75	4.585	0.75
86	6.085	5.335	4.585	5.335
87	6.085	9.92	4.585	9.92
88	6.085	11.02	4.585	11.02
89	6.085	15.755	4.585	15.755
90	6.085	20.19	4.585	20.19
91	6.085	21.19	4.585	21.19
92	6.085	25.775	4.585	25.775
93	6.085	30.36	4.585	30.36
94	-6.085	-30.36	-4.585	-30.36
95	-6.085	-25.775	-4.585	-25.775
96	-6.085	-21.19	-4.585	-21.19
97	-6.085	-20.19	-4.585	-20.19
98	-6.085	-15.755	-4.585	-15.755
99	-6.085	-11.02	-4.585	-11.02
100	-6.085	-9.92	-4.585	-9.92
101	-6.085	-5.335	-4.585	-5.335
102	-6.085	-0.75	-4.585	-0.75
103	-6.085	0.75	-4.585	0.75
104	-6.085	5.335	-4.585	5.335
105	-6.085	9.92	-4.585	9.92
106	-6.085	11.02	-4.585	11.02
107	-6.085	15.755	-4.585	15.755
108	-6.085	20.19	-4.585	20.19
109	-6.085	21.19	-4.585	21.19
110	-6.085	25.775	-4.585	25.775
111	-6.085	30.36	-4.585	30.36
112	-16.505	-20.19	-15.255	-20.19

Table 2.6.16.2-1 Cross Sections for Stress Evaluation of CY-MPC Support Disk (Continued)

SECTION	POINT 1		POINT 2	
	X	Y	X	Y
113	-16.505	-15.755	-15.255	-15.75
114	-16.505	-11.02	-15.255	-11.02
115	-18.755	-9.92	-15.255	-9.92
116	-18.755	-5.335	-15.255	-5.335
117	-18.755	-0.75	-15.255	-0.75
118	-18.755	0.75	-15.255	0.75
119	-18.755	5.335	-15.255	5.335
120	-18.755	9.92	-15.255	9.92
121	-16.505	11.02	-15.255	11.02
122	-16.505	15.755	-15.255	15.755
123	-16.505	20.19	-15.255	20.19
124	26.075	-20.59	27.225	-21.265
125	15.255	-30.36	15.685	-30.795
126	-15.255	-30.36	-15.685	-30.795
127	-26.075	-20.59	-27.225	-21.265
128	-26.075	20.59	-27.225	21.265
129	-15.255	30.36	-15.685	30.795
130	15.255	30.36	15.685	30.795
131	26.075	20.59	27.225	21.265

2.6.16.3 Thermal Expansion Evaluation of the CY-MPC Support Disk

A thermal stress analysis of the support disk is performed using ANSYS to determine the differential thermal expansion and the associated thermal stresses. Three thermal conditions are considered and the associated thermal stresses that result from a heat load of 17 kW are evaluated.

Thermal Condition	Ambient Temperature	Solar Insolance Applied to Cask Surface	17 kW Fuel Load
1	100°F	yes	yes
2	-40°F	no	yes
3	-40°F	no	no

Temperature data from the thermal analysis is used to calculate the radial thermal expansion of the canister, the steel support disk and the aluminum heat transfer disk. Considering the maximum material conditions, the minimum gaps between the basket disks and the canister wall are shown in the following table. A maximum disk temperature of 550°F was used. This bounds the maximum of 536°F from Thermal Condition 1. For simplicity, the radial expansion of each component is conservatively based on each component at a uniform temperature equal to its maximum calculated temperature. The spreadsheet used for this calculation is shown below.

Component	Nom. Dia.		MMC		T max (°F)	Tmax - T ₀ (°F)	α (in/in/°F)	Δr (inches)	Radius at Temp. (inches)	Min. Gap (inches)
	At 70°F (inches)	Tolerance (inches)	Dia (inches)	Radius (inches)						
Canister Shell	69.39	+0.12/-0.16	69.23	34.615	351	281	9.08E-06	0.088	34.703	-
Support Disk	69.15	+0.00/-0.02	69.15	34.575	536	466	5.91E-06	0.095	34.670	0.033
Heat Transfer Disk	68.9	0	68.9	34.45	534	464	1.30E-05	0.208	34.658	0.046

The minimum gap size between the steel support disk and the canister inner surface is 0.033 inches. The gap size between the aluminum heat transfer disk and the canister inner surface is 0.046 inches. Therefore, there is no interference between the disks and the canister shell.

The thermal stresses arise from the hotter interior of the support disk expanding against the cooler outer region of the support disk. The results of the thermal analysis for the above thermal conditions are summarized below.

Thermal Condition	Disk Maximum Temperature (°F)	Disk Outer Temperature (°F)	ΔT (°F)
1	536	324	212
2	428	203	225
3	-40	-40	0

The thermal stress is governed by the temperature difference, ΔT , the modulus of elasticity, E , and the coefficient of thermal expansion, α , and their product, $E\alpha$. These values are shown below for Thermal Conditions 1 and 2.

Thermal Condition	ΔT (°F)	E (ksi)*	α (in/in-°F) *	$E\alpha$
1	212	26300	5.91 E-6	.155
2	225	26900	5.91 E-6	.159

*Properties taken at $T_{avg} = (T_{max} + T_{min})/2$

Since the values of ΔT and $E\alpha$ for Thermal Condition 1 are lower than those for Thermal Condition 2, Thermal Condition 1 is bounded by Thermal Condition 2 for thermal stress calculations. Therefore, Thermal Conditions 2 and 3 are used in the thermal expansion analyses. Since the allowable stresses decrease as the temperature increases, the allowable stresses for the Thermal Condition 2 evaluation are conservatively based on 550°F, which bounds the maximum disk temperature of Thermal Condition 1 (536°F).

Temperatures are applied to the support disk models to simulate worst-case temperature conditions. Conditions 1 and 2 were combined for the side- and end- drop evaluations. A maximum disk temperature of 550°F, which bounds the maximum of 536°F from Thermal Condition 1 was used with the maximum ΔT 225°F from Thermal Condition 2. A constant temperature of 460°F was applied to the canister shell and the cask inner shell in the side drop evaluation. This bounds the actual maximum temperatures (351°F and 232°F) determined in Chapter 3. Use of these temperatures for the canister and cask body results in the largest gap between the disks and the canister shell and between the canister shell and the cask inner shell.

A steady-state thermal conduction analysis (with all planar structural elements temporarily changed to ANSYS SHELL57 thermal elements) is performed to determine the temperature distribution across the disk. The temperature data is then read back into the structural model so that material properties can be taken at temperature. The side and end drop evaluations considered only the high temperature case described above.

For each basket drop orientation, two analyses are performed. The first analysis is for the support disk without thermal stresses (impact load only) and the second accounts for thermal stresses (impact plus thermal).

2.6.16.4 Stress Evaluation of the CY-MPC Support Disk for a 1-Foot End Drop

Six (6) tie rods locate the support disks of the canistered fuel basket with spacers. A structural analysis is performed using ANSYS to evaluate the effect of a 1-foot end drop impact, which corresponds to the most severe out-of-plane loading under normal conditions. The model described in Section 2.6.16.2 is used with a 20g deceleration. Linearized stresses at the cross sections identified in Figure 2.6.16.2-5 are compared to stress allowables in accordance with the ASME Code, Section III, Subsection NG.

The allowable stress intensity for P_m is S_m . For 17-4PH material, this value is equal to 42.5 ksi at 650°F and 45.0 ksi at -40°F. The allowable stress intensity for $P_m + P_b$ is $1.5 S_m$. For 17-4PH material, this value is equal to 63.8 ksi at 650°F and 67.5 ksi at -40°F.

The minimum margin of safety is 0.64 for P_m stresses and 0.73 for $P_m + P_b$ stresses. Tables 2.6.16.4-1 and 2.6.16.4-2 list the 10 highest P_m and $P_m + P_b$ stress intensities, respectively. Locations of the 10 highest P_m and $P_m + P_b$ stress intensities are shown in Figures 2.6.16.4-1 and 2.6.16.4-2, respectively.

Figure 2.6.16.4-1 Locations of CY-MPC Support Disk Maximum P_m Stresses, 1-Foot End Drop

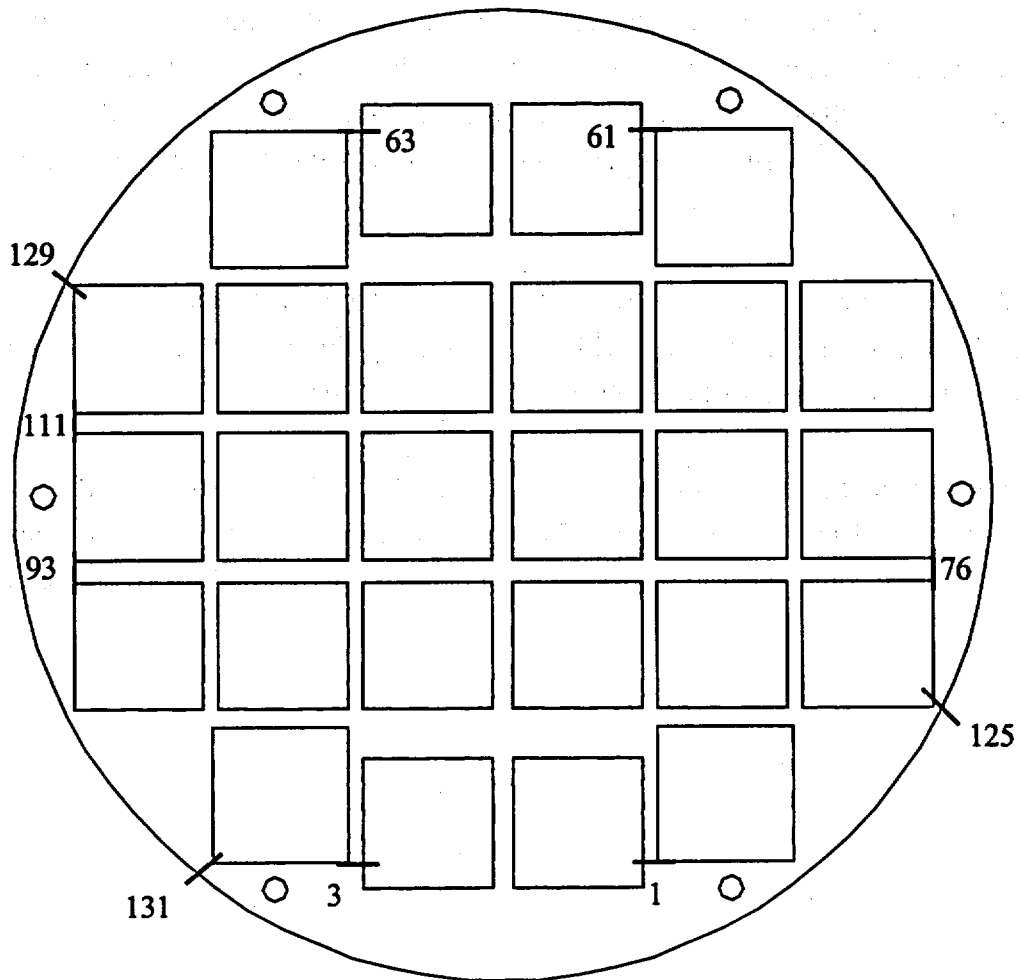


Figure 2.6.16.4-2 Locations of CY-MPC Support Disk Maximum $P_m + P_b$ Stresses, 1-Foot End Drop

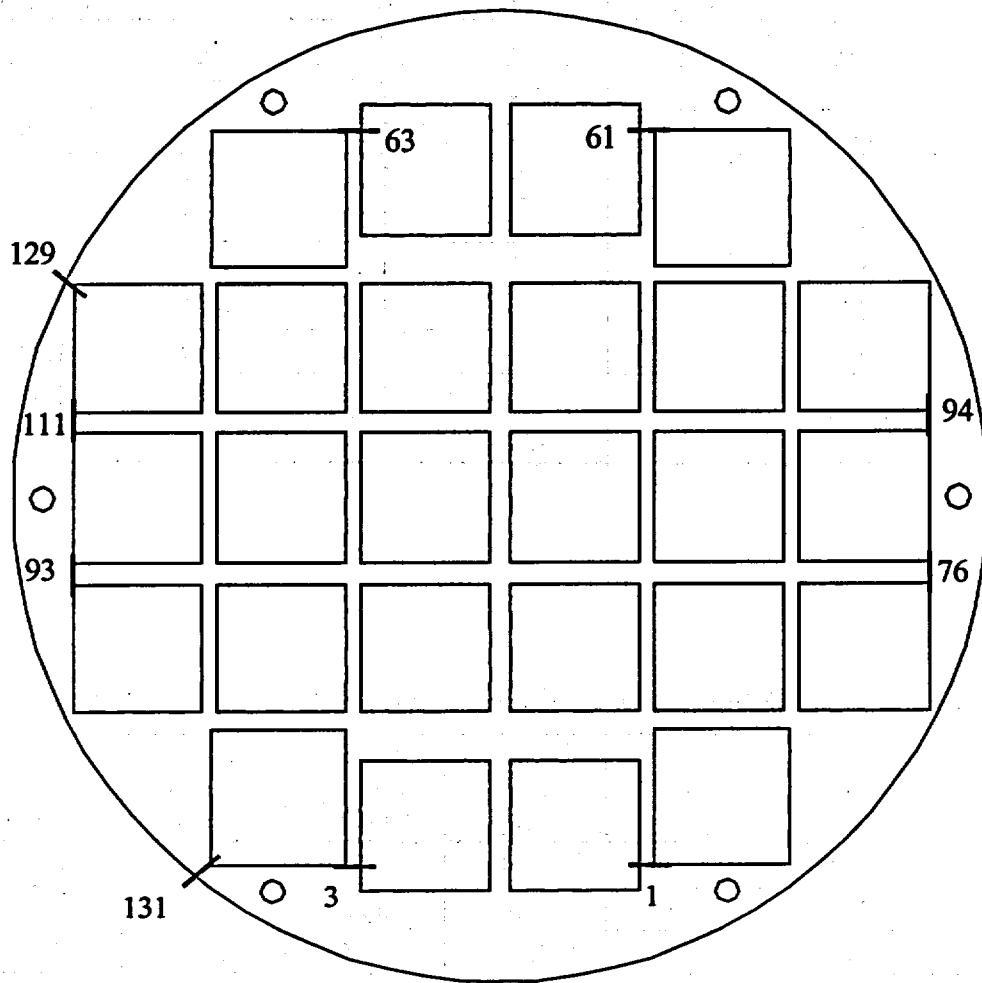


Table 2.6.16.4-1 P_m Stresses for CY-MPC Support Disk, 1-Foot End Drop

Section	Sx (ksi)	Sy (ksi)	Sxy (ksi)	Stress Intensity (ksi)	Allowable Stress (ksi)	Margin of Safety
61	23.8	-1.9	6.9	25.9	42.5	0.64
63	24.0	-1.9	-6.5	25.7	42.5	0.65
1	24.0	-1.7	-6.7	26.0	43.7	0.68
3	23.8	-1.8	6.9	25.9	43.7	0.68
131	6.3	7.4	-5.8	18.0	43.4	1.41
111	0.9	-15.7	1.1	15.8	42.5	1.69
129	-14.1	2.2	-4.8	15.8	42.5	1.69
125	-14.1	2.2	-4.8	15.8	42.9	1.72
62	10.0	5.0	-0.1	15.0	42.5	1.83
93	0.4	-14.8	-1.2	14.9	42.6	1.87

Table 2.6.16.4-2 $P_m + P_b$ Stresses for CY-MPC Support Disk, 1-Foot End Drop

Section	Sx (ksi)	Sy (ksi)	Sxy (ksi)	Stress Intensity (ksi)	Allowable Stress (ksi)	Margin of Safety
61	31.8	-6.7	12.4	36.8	63.8	0.73
63	31.8	-6.8	-11.4	36.2	63.8	0.76
3	31.7	-6.6	12.1	36.6	65.5	0.79
1	31.9	-6.4	-11.5	36.3	65.5	0.81
76	2.3	-18.8	6.1	23.3	63.9	1.74
93	1.7	-18.9	-6.0	23.2	63.9	1.75
94	2.3	-18.8	-6.0	23.1	63.8	1.76
111	1.7	-19.9	5.5	22.7	63.8	1.81
131	7.5	9.0	-6.3	18.8	65.1	2.45
129	-16.1	3.6	-5.0	17.8	63.8	2.58

Note: See Figure 2.6.16.2-5 for section locations and definition of coordinate system.

2.6.16.5 Stress Evaluation of the CY-MPC Support Disk for a Combined Thermal and 1-Foot End Drop Load Condition

The thermal expansion loads described in Section 2.6.16.3 are applied to the finite element model simultaneously with the 20g end drop loads described in Section 2.6.16.4 to produce a combined thermal expansion plus end impact loading. The stress evaluation results for thermal plus the 1-foot end drop conditions are summarized below. The allowable stress is $3.0 S_m$ in accordance with the ASME Code, Section III, Subsection NG for primary plus secondary (P+Q) stress intensity range. The minimum margin of safety is +0.16. The thermal condition used bounds both the maximum support disk temperature ($T_{max} = 550^{\circ}F$) and the maximum thermal gradient across the disk ($\Delta T = 225^{\circ}F$). Table 2.6.16.5-1 shows the 10 highest $P_m + P_b + Q$ stress intensities for a 1 ft end drop. Figure 2.6.16.5-1 shows the locations of the 10 highest stress intensities for this case.

<u>$P_m + P_b + Q$</u>	
<u>Stress Intensity (ksi)</u>	<u>Margin of Safety</u>
110.4	0.16

Figure 2.6.16.5-1 Locations of Maximum $P_m + P_b + Q$ Stresses for CY-MPC Support Disk for a 1-Foot End Drop, $T_{max} = 550^\circ\text{F}$ and $T_{min} = 325^\circ\text{F}$

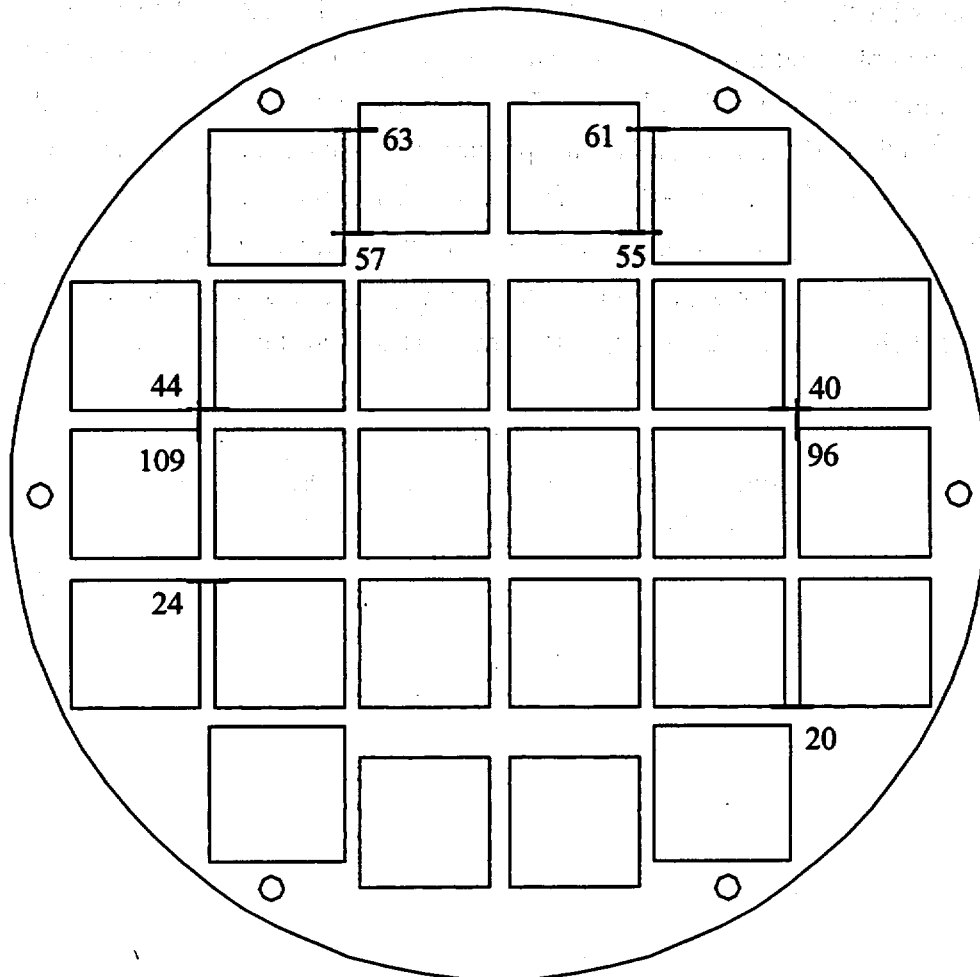


Table 2.6.16.5-1 P + Q Stresses for CY-MPC Support Disk—1-Foot End Drop

$T_{\max} = 550^{\circ}\text{F}$ and $T_{\min} = 325^{\circ}\text{F}$

Section	Sx (ksi)	Sy (ksi)	Sxy (ksi)	Stress Intensity (ksi)	Allowable Stress (ksi)	Margin of Safety
57	-108.4	38.7	12.0	110.4	127.5	0.16
63	-109.9	39.1	-13.1	109.9	127.5	0.16
44	-86.1	89.7	-19.8	107.8	127.5	0.18
55	-105.9	36.5	9.1	106.8	127.5	0.19
40	-84.7	89.3	19.5	106.6	127.5	0.20
61	-103.7	43.7	19.3	103.9	127.5	0.23
24	-82.6	82.6	19.4	102.0	127.9	0.25
109	-79.5	84.5	-19.1	101.2	127.5	0.26
96	-78.0	84.2	18.9	100.2	127.5	0.27
20	-79.4	81.1	-18.9	99.2	127.9	0.29

Note: See Figures 2.6.16.5-1 and 2.6.16.2-5 for section locations and definition of the coordinate system.

2.6.16.6 Stress Evaluation of CY-MPC Tie Rods and Spacers for 1-Foot End Drop

Tie Rods

The tie rods serve basket assembly purposes and are not part of the load path for the conditions evaluated. The tie rods are pre-loaded in tension during basket assembly by an initial applied torque (T) of 50 ± 10 ft-lb. The resulting initial tension (P_b) in each tie rod is:

$$P_b = \frac{T}{0.159L + 1.156\mu d} = \frac{60(12)}{0.159(0.125) + 1.156(0.18)(1.625)} = 2,011 \text{ lbs. (Machinery's)}$$

where:

- T = 60 ft-lb (maximum wrench torque)
- μ = 0.18, (for lubricated threads)
- d = 1.625 in. (tie rod nominal diameter)
- L = 1/n = 1/8 (n = number of threads)

The tie rods are not loaded during drop conditions; therefore, no structural analysis is required.

Spacers

Six tie rods and cylindrical spacers, to maintain disk spacing, connect the basket support disks and heat transfer disks. In a side drop, the load path is through the support disks into the canister wall. In an end drop, the load path is through the spacers to either the canister lid or bottom depending on the drop orientation. The load comprises the weight of the top or bottom weldment (depending on the drop orientation), the weight of the support and heat transfer disks, and the weight of the spacers and washers. The weight of the fuel assemblies is transmitted directly into the canister lid or bottom because the fuel tubes in the basket are open at both ends. In drop orientations between a side drop and an end drop, only a portion of the load acts along the tie rod axis. Thus, the end drop is the critical loading condition for the spacers. The bottom-end drop is the governing case because the top weldment is heavier than the bottom weldment.

During an end drop, the 6 split spacers at the bottom of the heat transfer disk array are loaded by the top weldment, the 27 heat transfer disks, the spacers and washers above, and the 28 support disks. The total weight on the split spacers is 8,225 pounds.

The initial tie rod pre-load, tension, will be diminished by the compressive effect of the end drop. However, for conservatism, the total compression (2,011 lbs) induced by the 50 ± 10 ft-lb bolt torque will be included in the load on the split spacers.

The maximum total load (P_{ssp}) on the split spacer is, for normal conditions:

$$P_{ssp} = 2,011 + (8,225) \times 20/6 = 33,847 \text{ lb, use } 29,428 \text{ lb}$$

The stress (σ_{ssp}) is determined by applying the total load to the cross-sectional area (A_{ssp}) of the split spacer. A_{ssp} is conservatively taken as the area of the decreased diameter section.

$$\sigma_{ssp} = \frac{P_{ssp}}{A_{ssp}} = \frac{35,000 \text{ lb}}{2.45 \text{ in.}^2} = 14,286 \text{ psi}$$

Where

$$A_{ssp} = \frac{\pi}{4} (2.50^2 - 1.77^2) = 2.45 \text{ in}^2$$

The margin of safety (MS) is:

$$MS = \frac{1.0S_m}{\sigma_{ssp}} - 1 = \frac{18,700}{14,286} - 1 = +0.31 \text{ (Normal condition, } 400^\circ\text{F)}$$

The load on the bottom spacers comprises the weight of the top weldment, the weight of the support and heat transfer disks, and the weight of the spacers and washers.

During a bottom end drop, the 6 bottom spacers support the top weldment, the 27 heat transfer disks, the spacers and washers above, and the 28 support disks. The total weight on the spacers is 9,874 lbs.

The initial tie-rod pre-load tension will be diminished by the compressive effect of the end drop. However, for conservatism, the total compression (2,011 lbs) induced by the 50 ± 10 ft-lb bolt torque will be included in the load on the bottom spacers.

The maximum total load (P_{bsp}) on the bottom spacer is:

$$P_{bsp} = 2,011 + (9,874) \times 20/6 = 34,924 \text{ lbs. (use } 35,000 \text{ lbs)}$$

The stress (σ_{bsp}) is determined by applying the total load to the cross-sectional area (A_{bsp}) of the bottom spacer.

$$\sigma_{bsp} = \frac{P_{bsp}}{A_{bsp}} = \frac{35,000 \text{ lbs}}{4.03 \text{ in.}^2} = 8,685 \text{ psi}$$

Where

$$A_{bsp} = \frac{\pi}{4} (2.875^2 - 1.77^2) = 4.03 \text{ in}^2$$

The margin of safety (MS) is:

$$MS = \frac{1.0S_m}{\sigma_{bsp}} - 1 = \frac{17,400}{8,685} - 1 = +1.00 \text{ (Normal condition, 400°F)}$$

2.6.16.7 Stress Evaluation of CY-MPC Support Disk for a 1-Foot Side Drop

To determine the structural adequacy of the support disk in the 1-foot side drop impact load condition, a quasi-static impact load equal to the weight of the fuel and tubes multiplied by a 20g amplification factor is applied to the support disk structure. The inertial loading of the support disk is included via the density input for the 17-4 PH stainless steel. The value of 20g is conservative since the impact limiter design deceleration for a 1-foot side drop is 18.1g. The fuel assembly load is transmitted by direct compression through the tube wall to the web structure of the support disk. The maximum in-plane loading occurs in the side drop, which is evaluated using a finite element analysis. The analysis is performed using the three-dimensional support disk side drop model described in Section 2.6.16.2. As discussed in Section 2.6.16.1, four bounding cases of basket orientation (0°, 38°, 63°, and 90°) are considered in the analysis.

As described in Section 2.6.16.5, the material properties are evaluated at a bounding thermal condition which bounds both the maximum disk temperature combined with the maximum thermal gradient across the disk. Specifically, the maximum disk temperature is equal to 550°F and the minimum disk temperature is equal to 325°F. Linearized stresses at the cross-sections (Figures 2.6.16.2-5) are compared to the stress allowable per the ASME Code, Section III, Subsection NG.

Primary membrane (P_m) stress intensity is compared to $1.0 S_m$ and primary membrane plus bending ($P_m + P_b$) stress intensity is compared to $1.5 S_m$ for the material at the temperature corresponding to each section location. The stress evaluation results for the 1-foot side-drop condition are summarized in Table 2.6.16.7-1. The minimum margin of safety is +0.15, which occurs for a 38° basket orientation. Tables 2.6.16.7-2 through 2.6.16.7-9 list the 30 highest P_m and $P_m + P_b$ stress intensities at each basket orientation considered. Locations of the 10 highest P_m and $P_m + P_b$ stresses are shown in Figures 2.6.16.7-1 and 2.6.16.7-2 at the worst case drop angle of 38°.

Figure 2.6.16.7-1 Locations of CY-MPC Support Disk Maximum P_m Stresses, 1-Foot Side Drop, 38° Orientation

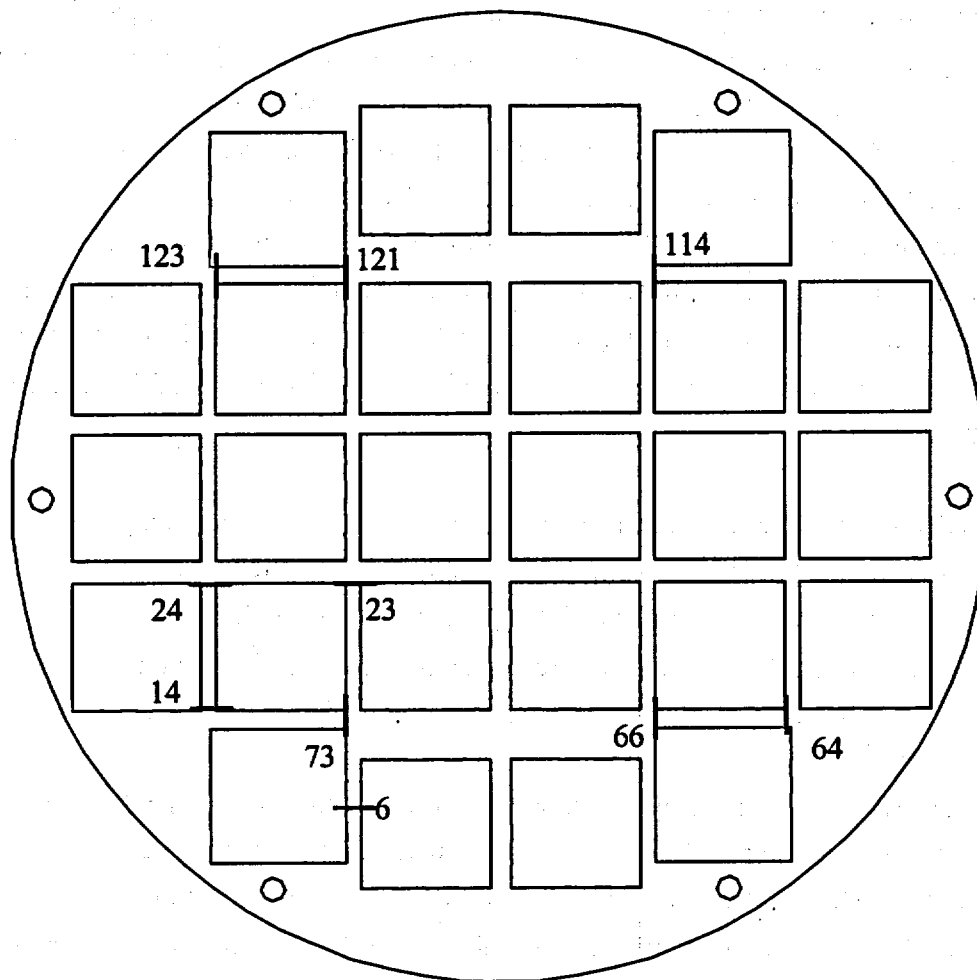


Figure 2.6.16.7-2 Locations of CY-MPC Support Disk Maximum $P_m + P_b$ Stresses, 1-Foot Side Drop, 38° Orientation

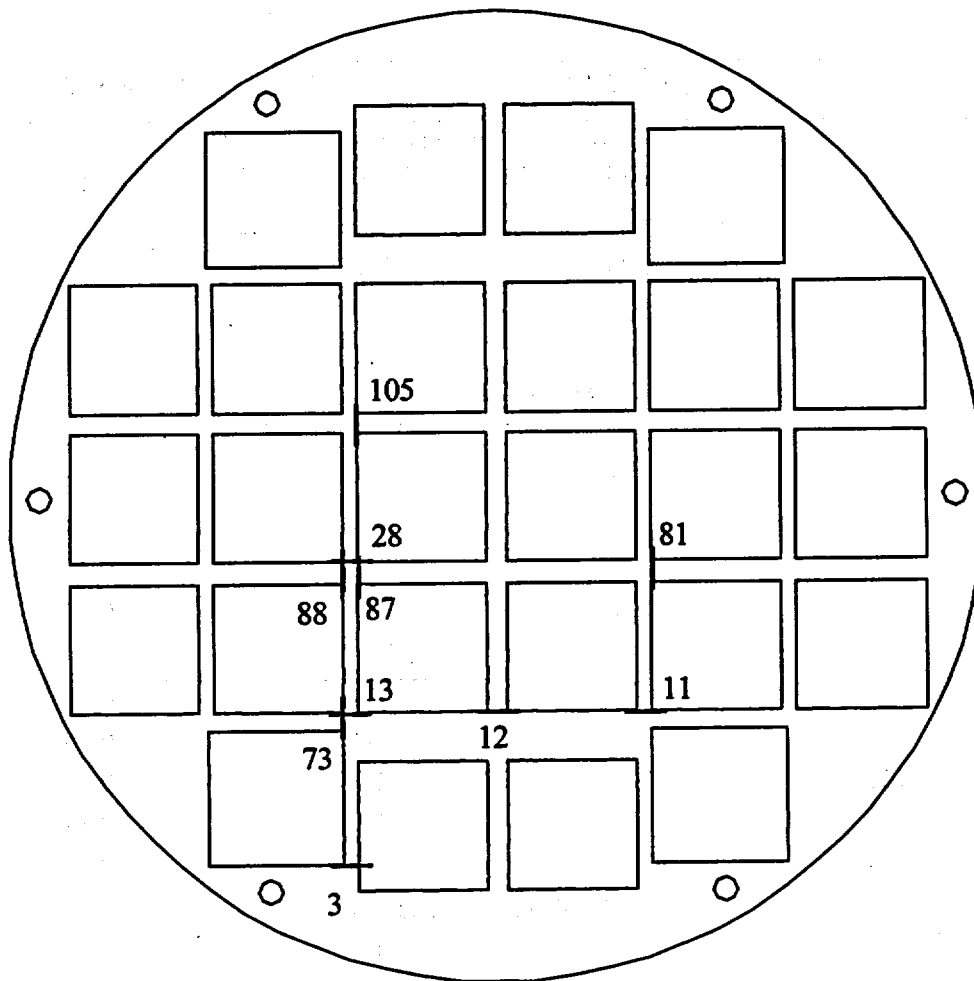


Table 2.6.16.7-1 Summary of Maximum CY-MPC Support Disk Stresses for 1-Foot Side Drop

P_m		P_m+P_b	
Section	Margin of Safety	Section	Margin of Safety
0° Basket Orientation			
2	1.34	1	1.10
11	1.43	3	1.14
13	1.45	9	1.43
12	1.52	7	1.44
1	1.58	11	2.02
38° Basket Orientation			
73	0.36	13	0.15
66	0.96	3	0.18
6	1.40	28	0.23
14	1.45	88	0.29
114	1.58	87	0.30
63° Basket Orientation			
73	0.82	28	0.35
66	1.14	43	0.36
121	1.35	106	0.38
24	1.37	105	0.38
114	1.45	88	0.39
90° Basket Orientation			
108	0.88	129	0.99
90	0.88	108	1.41
105	1.57	90	1.44
87	1.57	44	1.55
44	2.04	24	1.59

Table 2.6.16.7-2 P_m Stresses for CY-MPC Support Disk 1-Foot Side Drop, 0° Basket Orientation

Section	Sx (ksi)	Sy (ksi)	Sxy (ksi)	Stress Intensity (ksi)	Allowable Stress (ksi)	Margin of Safety
2	-12.6	-6.2	0.0	18.8	44.0	1.34
11	-8.4	-9.3	1.1	17.8	43.1	1.43
13	-8.3	-9.1	-1.0	17.6	43.1	1.45
12	-9.9	-7.2	0.0	17.2	43.2	1.52
1	-12.7	-4.2	0.3	16.9	43.7	1.58
3	-12.7	-4.0	-0.3	16.6	43.7	1.62
5	-16.5	0.0	0.0	16.5	43.6	1.64
9	-12.8	-3.2	-0.3	16.0	43.2	1.70
7	-12.5	-2.8	-0.1	15.3	43.2	1.82
27	-8.7	-5.5	0.0	14.2	42.7	2.01
8	-12.8	9.9	0.0	12.8	43.3	2.38
131	-11.5	5.5	2.4	12.3	43.4	2.51
26	-6.2	-5.8	0.7	12.1	42.6	2.53
28	-6.2	-5.7	-0.7	12.0	42.6	2.56
17	-11.6	0.0	0.0	11.6	42.9	2.68
69	-9.3	-1.7	-0.8	11.2	43.2	2.87
4	-10.9	0.0	-1.1	11.2	43.5	2.89
70	-9.2	-1.7	0.8	11.1	43.2	2.90
6	-10.9	0.0	1.1	11.1	43.5	2.91
42	-6.9	-3.9	0.0	10.8	42.5	2.95
22	-10.0	5.5	0.0	10.0	42.7	3.29
16	-9.7	0.0	-0.6	9.8	42.9	3.38
18	-9.7	0.0	0.5	9.7	42.9	3.40
32	-9.6	0.0	0.0	9.6	42.5	3.44
73	-6.1	-3.4	0.3	9.5	43.1	3.54
66	-6.1	-3.3	-0.3	9.5	43.1	3.54
85	-7.8	-1.3	0.5	9.2	42.7	3.64
84	-7.8	-1.3	-0.5	9.2	42.7	3.65
21	-8.0	6.0	0.6	8.2	42.7	4.21
41	-3.6	-4.5	0.5	8.1	42.5	4.22

Note: See Figure 2.6.16.2-5 for section locations and definition of coordinate system.

Table 2.6.16.7-3 P_m Stresses for CY-MPC Support Disk 1-Foot Side Drop, 38° Basket Orientation

Section	Sx (ksi)	Sy (ksi)	Sxy (ksi)	Stress Intensity (ksi)	Allowable Stress (ksi)	Margin of Safety
73	-31.6	2.1	2.5	31.8	43.1	0.36
66	21.5	0.3	1.5	22.0	43.1	0.96
6	-17.2	0.2	-3.1	18.1	43.5	1.40
14	-8.4	-8.8	1.8	17.6	43.0	1.45
114	-14.5	-1.8	1.0	16.4	42.5	1.58
24	-8.4	14.6	2.7	15.6	42.6	1.74
121	14.8	-0.2	2.1	15.2	42.5	1.80
123	-10.5	-3.3	0.9	13.8	42.5	2.07
23	-9.0	9.5	4.2	13.5	42.7	2.16
64	-10.0	-2.9	2.1	13.6	43.0	2.17
91	-11.4	4.3	4.3	13.4	42.6	2.19
13	-11.8	-0.8	1.6	13.0	43.1	2.32
39	-6.2	11.5	2.5	12.5	42.5	2.40
29	-6.9	-5.2	1.7	12.5	42.6	2.40
88	-9.8	3.2	4.6	12.2	42.6	2.50
1	-3.4	-9.0	-0.3	12.5	43.7	2.51
18	-11.0	0.1	-2.7	12.2	42.9	2.52
85	-2.4	2.4	6.0	12.1	42.7	2.53
103	-4.2	1.1	5.7	11.9	42.5	2.57
28	-7.1	-2.4	3.6	11.9	42.6	2.58
55	5.0	6.8	0.7	11.9	42.5	2.59
38	-6.4	7.7	4.2	11.2	42.5	2.79
75	5.0	6.2	0.3	11.2	43.0	2.83
19	-10.6	0.1	-1.7	11.0	42.8	2.88
44	-4.9	-5.4	1.8	10.9	42.5	2.89
7	-3.3	-7.6	0.6	10.9	43.2	2.96
54	-2.9	10.2	1.9	10.7	42.5	2.98
84	-4.0	2.4	5.3	10.7	42.7	2.99
10	3.6	7.0	0.3	10.7	43.0	3.03
57	-4.1	-6.3	-0.1	10.4	42.5	3.09

Note: See Figure 2.6.16.2-5 for section locations and definition of coordinate system.

Table 2.6.16.7-4 P_m Stresses for CY-MPC Support Disk 1-Foot Side Drop, 63° Basket Orientation

Section	Sx (ksi)	Sy (ksi)	Sxy (ksi)	Stress Intensity (ksi)	Allowable Stress (ksi)	Margin of Safety
73	-23.5	6.4	2	23.7	43.1	0.82
66	18.1	1.9	1.2	20.2	43.1	1.14
121	17.9	-1	1.9	18.1	42.5	1.35
24	-4.9	17.4	2.8	18	42.6	1.37
114	-14.7	-2.4	1.2	17.3	42.5	1.45
75	5.9	11.1	0.6	17	43	1.53
123	-11.8	-4.2	1.4	16.3	42.5	1.61
91	-11.7	9.1	4	14.6	42.6	1.92
90	3.7	8	3.2	13.3	42.6	2.21
39	-3.3	12.2	3.1	13.2	42.5	2.23
102	5.3	2.3	4.9	12.5	42.5	2.41
88	-8.8	7.4	3.9	12.1	42.6	2.54
81	5.9	3.9	3.1	11.6	42.6	2.68
84	2	5.1	4.5	11.4	42.7	2.73
64	-10.6	-0.3	1.9	11.5	43	2.73
109	-6.6	6.9	4.4	11.2	42.5	2.8
87	2.9	6.4	3.1	11.2	42.7	2.82
103	-5.4	3.8	5.3	10.8	42.5	2.94
108	1	6.1	4	10.7	42.5	2.98
92	-0.1	10.5	-1.2	10.7	42.6	2.98
78	6.7	2.2	3	10.7	42.6	2.99
23	-3.6	8.1	4.1	10.5	42.7	3.07
38	-2.2	7.1	4.4	10.2	42.5	3.18
14	-4.8	-4.7	1.8	10.2	43	3.24
112	9.4	-1.1	2.2	10	42.5	3.25
85	-3.5	5.7	4.9	10	42.7	3.25
106	-5.6	5.6	4.3	9.9	42.5	3.28
105	2.4	4.6	3.4	9.7	42.5	3.38
89	-0.1	8.5	-1.8	9.2	42.7	3.63
6	-8.1	0.2	-2.5	9.3	43.5	3.67

Note: See Figure 2.6.16.2-5 for section locations and definition of coordinate system.

Table 2.6.16.7-5 P_m Stresses for CY-MPC Support Disk 1-Foot Side Drop, 90° Basket Orientation

Section	Sx (ksi)	Sy (ksi)	Sxy (ksi)	Stress Intensity (ksi)	Allowable Stress (ksi)	Margin of Safety
108	12	10.6	0.8	22.7	42.5	0.88
90	11.9	10.7	-0.7	22.7	42.6	0.88
105	8	8.5	0.4	16.5	42.5	1.57
87	8.1	8.5	-0.4	16.6	42.7	1.57
44	4.5	9.5	-0.4	14	42.5	2.04
24	4.5	9.4	0.4	13.9	42.6	2.06
110	0	13.4	-0.4	13.4	42.5	2.17
92	0	13.4	0.4	13.4	42.6	2.18
102	7.4	5.9	0.7	13.4	42.5	2.18
84	7.4	5.9	-0.6	13.4	42.7	2.19
29	4.7	8.2	-1.2	13.2	42.6	2.24
39	4.7	8.1	1.2	13	42.5	2.26
109	-5.2	11.8	0.7	11.9	42.5	2.58
91	-5.2	11.8	-0.6	11.9	42.6	2.58
107	0	11.1	-0.2	11.1	42.5	2.81
89	0	11.2	0.2	11.2	42.7	2.82
129	-6.2	9	-3.1	11	42.5	2.87
81	6.7	4.1	-0.4	10.9	42.6	2.92
99	6.7	4.1	0.4	10.8	42.5	2.92
111	-1.3	10.8	-0.1	10.8	42.5	2.94
93	-0.9	10.8	0.3	10.8	42.6	2.95
106	-7.6	9.7	0.5	9.8	42.5	3.32
88	-7.6	9.8	-0.5	9.9	42.6	3.33
130	-3.7	8.9	1.1	9.1	42.9	3.7
104	0	8.9	-0.3	8.9	42.5	3.77
38	1	7.6	1.1	8.9	42.5	3.77
86	0	8.9	0.3	8.9	42.7	3.77
28	1	7.6	-1.1	8.9	42.6	3.79
14	4.4	4.2	-0.6	8.6	43	3.98
97	-8.3	3.3	0.5	8.3	42.5	4.1

Note: See Figure 2.6.16.2-5 for section locations and definition of coordinate system.

Table 2.6.16.7-6 $P_m + P_b$ Stresses for CY-MPC Support Disk 1-Foot Side Drop, 0°
Basket Orientation

Section	Sx (ksi)	Sy (ksi)	Sxy (ksi)	Stress Intensity (ksi)	Allowable Stress (ksi)	Margin of Safety
1	-31.2	-9.4	0.9	31.2	65.5	1.10
3	-30.5	-8.9	-0.9	30.6	65.5	1.14
9	-26.7	-6.5	-0.8	26.7	64.9	1.43
7	-26.6	-7.1	-0.9	26.6	64.9	1.44
11	-16.3	-13.7	1.6	21.4	64.7	2.02
13	-16.2	-13.4	-1.6	21.2	64.7	2.05
2	-12.7	-6.4	0.8	19.0	66.0	2.47
70	-12.2	-10.7	3.2	17.3	64.8	2.74
69	-12.5	-10.8	-3.2	17.3	64.8	2.75
12	-9.9	-7.3	0.7	17.2	64.8	2.76
81	-16.3	-12.0	-1.4	16.5	64.0	2.87
131	-14.8	8.5	3.9	16.7	65.1	2.89
88	-16.1	-11.8	1.4	16.4	64.0	2.91
21	-15.7	11.1	3.0	16.3	64.0	2.92
66	-16.0	-14.8	-2.0	16.5	64.7	2.92
5	-16.6	0.0	0.0	16.6	65.4	2.95
23	-15.6	11.0	-2.9	16.2	64.0	2.95
73	-15.9	-14.6	1.9	16.3	64.7	2.97
64	-1.8	-16.1	1.1	16.1	64.5	3.00
67	-12.8	-2.9	0.9	15.8	64.7	3.09
72	-12.5	-3.1	-0.8	15.7	64.7	3.11
8	-13.0	10.0	-3.6	15.4	64.9	3.21
75	-1.9	-14.8	-1.0	14.8	64.5	3.35
124	-8.1	-10.4	-5.5	14.7	65.2	3.42
27	-8.7	-5.5	0.1	14.2	64.0	3.51
82	-9.4	-4.4	2.3	13.8	64.0	3.64
87	-9.2	-4.4	-2.3	13.6	64.0	3.70
26	-11.9	-10.3	1.0	13.4	64.0	3.78
28	-11.8	-10.1	-0.9	13.2	64.0	3.84
85	-10.3	-7.4	1.8	12.9	64.0	3.97

Note: See Figure 2.6.16.2-5 for section locations and definition of coordinate system.

Table 2.6.16.7-7 $P_m + P_b$ Stresses for CY-MPC Support Disk 1-Foot Side Drop, 38°
Basket Orientation

Section	Sx (ksi)	Sy (ksi)	Sxy (ksi)	Stress Intensity (ksi)	Allowable Stress (ksi)	Margin of Safety
13	-56.2	-21.1	1.9	56.3	64.7	0.15
3	-54.4	19.8	-6.3	55.5	65.5	0.18
28	-51.5	-33.2	3.9	52.0	64.0	0.23
88	-49.4	19.3	7.1	49.5	64.0	0.29
87	-48.8	32.8	4.1	49.1	64.0	0.30
12	-49.1	18.7	1.2	49.1	64.8	0.32
73	-48.5	9.4	8.6	48.9	64.7	0.32
105	-47.2	30.3	3.8	47.5	63.7	0.34
11	47.8	-23.0	2.9	48.2	64.7	0.34
81	45.2	23.6	4.2	45.6	64.0	0.40
82	-45.0	27.4	4.8	45.6	64.0	0.40
26	44.4	33.7	3.9	45.2	64.0	0.41
23	-44.9	36.8	7.3	45.1	64.0	0.42
2	-46.4	14.0	-1.5	46.5	66.0	0.42
43	-44.1	-32.2	3.6	44.8	63.7	0.42
38	-44.2	34.9	6.5	44.5	63.7	0.43
1	-44.9	-20.0	-4.5	45.3	65.5	0.45
29	-43.9	-24.3	1.9	44.0	63.9	0.45
106	-43.5	17.8	6.0	43.8	63.7	0.45
70	-44.2	9.5	4.5	44.3	64.8	0.46
66	44.0	14.5	4.7	44.1	64.7	0.47
84	-40.4	36.7	6.2	43.3	64.0	0.48
99	42.4	-21.8	4.2	42.8	63.7	0.49
9	-42.6	18.1	4.9	42.7	64.9	0.52
22	-39.2	41.2	4.1	42.1	64.0	0.52
41	40.8	29.1	3.7	41.6	63.7	0.53
100	-40.6	-23.7	4.1	41.4	63.7	0.54
72	-41.8	11.2	2.0	41.8	64.7	0.55
85	-36.3	32.2	6.8	39.9	64.0	0.60
36	38.0	-28.5	4.3	39.4	63.7	0.62

Note: See Figure 2.6.16.2-5 for section locations and definition of coordinate system.

Table 2.6.16.7-8 $P_m + P_b$ Stresses for CY-MPC Support Disk 1-Foot Side Drop, 63°
Basket Orientation

Section	Sx (ksi)	Sy (ksi)	Sxy (ksi)	Stress Intensity (ksi)	Allowable Stress (ksi)	Margin of Safety
28	-47.2	33.6	2.3	47.5	64	0.35
43	-46	32.8	3.2	46.8	63.7	0.36
106	-45.9	25.2	2.5	46.2	63.7	0.38
105	45.7	-21.6	3.2	46.1	63.7	0.38
88	-46	26	1.3	46.1	64	0.39
13	-45.3	24.7	1	45.4	64.7	0.43
29	-44	18.5	1.1	44.1	63.9	0.45
44	-42.9	21.3	1.6	43	63.7	0.48
87	42.5	-17	3.1	42.9	64	0.49
41	41.1	-24.9	3.2	41.7	63.7	0.53
26	41	-21.5	3.2	41.5	64	0.54
100	-40.7	24.7	2.4	41.1	63.7	0.55
99	40.8	-16.9	2.4	41	63.7	0.55
73	-41.2	17.7	-2.9	41.6	64.7	0.56
109	-40	15	2.5	40.3	63.7	0.58
3	-40.5	18.2	-4.7	41.4	65.5	0.58
111	-13	39.9	-2.5	40.2	63.7	0.59
81	39.8	-12.8	2.2	39.9	64	0.6
82	-39.5	25.7	1.7	39.7	64	0.61
42	-37.2	38.1	1.5	39.3	63.7	0.62
53	38.8	-17.8	3.2	39.3	63.7	0.62
52	39.1	-15.4	0.4	39.1	63.7	0.63
103	-36.8	32.6	3.7	39	63.7	0.64
102	37.6	-27.2	4	38.9	63.7	0.64
91	-38.4	11.3	1.3	38.5	63.9	0.66
108	37.4	-15.9	4.2	38.2	63.7	0.67
38	-36.4	33.5	2.8	38.2	63.7	0.67
11	38.3	-15.8	2.3	38.6	64.7	0.68
75	-5.9	36.7	-0.2	36.7	64.5	0.76
25	36	-12.5	1.4	36.1	63.9	0.77

Note: See Figure 2.6.16.2-5 for section locations and definition of coordinate system.

Table 2.6.16.7-9 $P_m + P_b$ Stresses for CY-MPC Support Disk 1-Foot Side Drop, 90°
Basket Orientation

Section	Sx (ksi)	Sy (ksi)	Sxy (ksi)	Stress Intensity (ksi)	Allowable Stress (ksi)	Margin of Safety
129	-18.1	21.2	-12.2	32	63.7	0.99
108	17.7	8.8	-0.5	26.5	63.7	1.41
90	17.3	8.8	0.6	26.2	63.9	1.44
44	22.8	2.1	-0.1	25	63.7	1.55
24	22.4	2.3	0.1	24.7	64	1.59
29	11.5	7.4	-1.1	19.1	63.9	2.35
39	11.2	7.5	1.1	18.8	63.7	2.39
105	13.5	5.1	-0.5	18.6	63.7	2.42
130	-12.4	13.5	5.8	18.7	64.3	2.43
87	13.2	5.3	0.5	18.6	64	2.45
43	17	-1	0.7	17	63.7	2.75
23	16.7	-0.7	-0.7	16.7	64	2.82
111	-3.8	15.8	-2.3	16.2	63.7	2.93
93	-3	15.5	2.7	16	63.9	2.99
109	-11.5	15.2	-0.9	15.4	63.7	3.15
110	0	15.3	-0.4	15.4	63.7	3.15
40	-15.2	7.6	-0.9	15.3	63.7	3.18
92	0	15.2	0.4	15.2	63.9	3.2
91	-11	14.9	0.9	15.1	63.9	3.23
20	-14.9	7.5	0.9	15	64	3.26
42	-13	13.8	-1.4	14.8	63.7	3.3
22	-12.8	13.6	1.4	14.6	64	3.38
14	10.8	3.8	-0.6	14.7	64.6	3.39
54	11	3.5	0.3	14.4	63.7	3.42
106	-12.6	12.2	-2	14.4	63.7	3.44
88	-12.4	12.1	2	14.2	64	3.5
41	-13.9	11.3	-0.9	14.2	63.7	3.5
28	7.2	6.9	-0.1	14.1	64	3.55
38	6.9	7.1	0.1	14	63.7	3.56
21	-13.6	11.1	1	13.9	64	3.59

Note: See Figure 2.6.16.2-5 for section locations and definition of coordinate system.

2.6.16.8 Stress Evaluation of the CY-MPC Support Disk for a Combined Thermal and 1-Foot Side Drop Load Condition

The loading for the 1-foot side drop (Section 2.6.16.7) is combined with the thermal loading (Section 2.6.16.3) to produce a combined thermal plus impact loading condition. The allowable P + Q stress intensity range is $3S_m$.

The stress evaluation results for thermal plus 1-foot side drop condition are summarized in Table 2.6.16.8-1. The thermal condition is identical to that used in Section 2.6.16.7, except that the thermal expansion stresses are included in this calculation. The minimum margin of safety is +1.95, which occurs at the 38° basket drop orientation. Tables 2.6.16.8-2 through 2.6.16.8-5 list the 30 highest P+Q stress intensities for each basket orientation considered. Locations of the 10 highest P+Q stress intensities at the worst-case 38° basket orientation are shown in Figure 2.6.16.8-1.

Figure 2.6.16.8-1 Locations of CY-MPC Support Disk Maximum P + Q Stresses, 1-Foot Side Drop, 38° Orientation

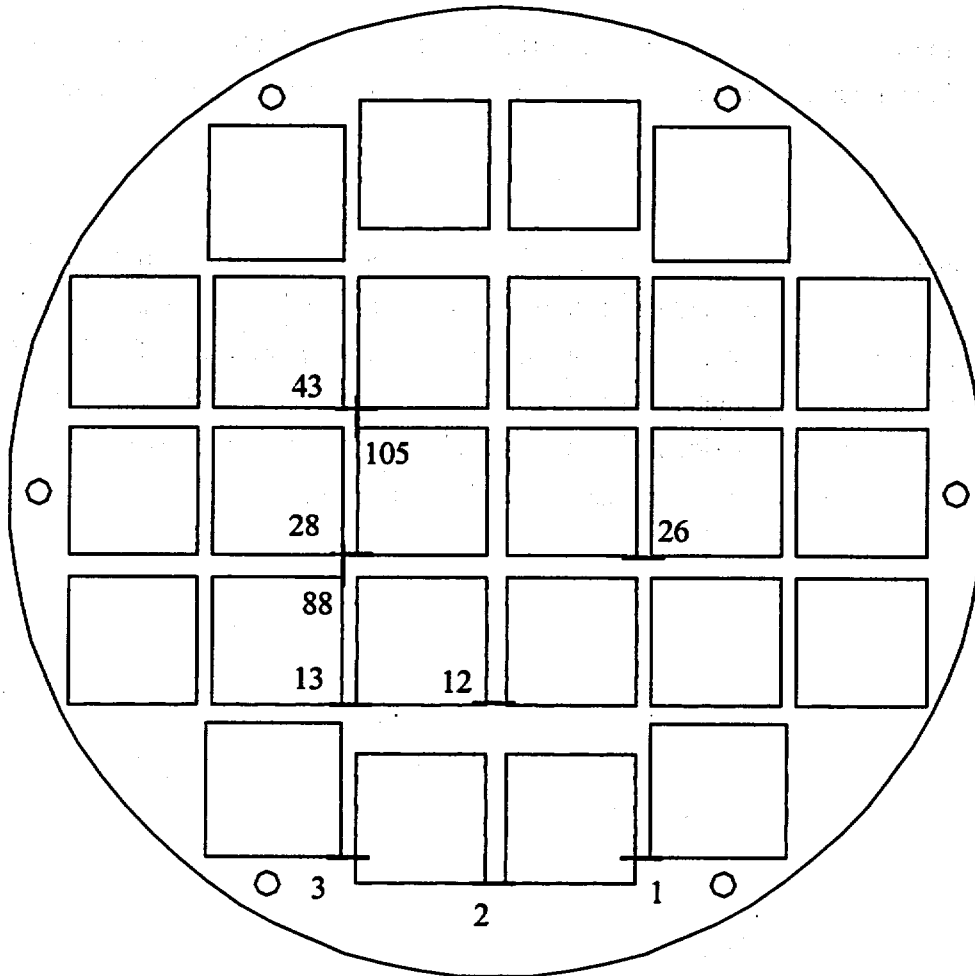


Table 2.6.16.8-1 Summary of Maximum CY-MPC Support Disk P + Q Stresses for 1-Foot Side Drop

Section	Margin of Safety
0° Basket Orientation	
1	4.10
3	4.20
9	4.89
7	4.90
11	5.52
38° Basket Orientation	
3	1.95
13	1.95
28	2.04
1	2.15
2	2.21
63° Basket Orientation	
43	2.11
106	2.22
28	2.27
13	2.39
3	2.40
90° Basket Orientation	
129	3.82
108	4.47
90	4.52
24	4.85
44	4.87

Table 2.6.16.8-2 P + Q Stresses for CY-MPC Support Disk 1-Foot Side Drop, 0°
Basket Orientation

Section	Sx (ksi)	Sy (ksi)	Sxy (ksi)	Stress Intensity (ksi)	Allowable Stress (ksi)	Margin of Safety
1	-25.7	-6.9	0.5	25.7	131.1	4.10
3	-25.2	-6.5	-0.5	25.2	131.1	4.20
9	-22.0	-4.1	-0.3	22.0	129.7	4.89
7	-22.0	-4.5	-0.3	22.0	129.7	4.90
11	-14.5	-11.4	1.2	19.8	129.4	5.52
13	-14.4	-11.2	-1.2	19.7	129.4	5.58
66	-16.1	-13.0	-2.4	16.7	129.4	6.73
73	-15.9	-12.8	2.3	16.5	129.4	6.83
2	-11.6	-4.1	1.1	15.7	132.1	7.40
81	-14.4	-9.8	-1.6	14.8	127.9	7.62
69	-11.2	-8.4	-2.9	15.0	129.5	7.63
70	-11.0	-8.3	2.9	15.0	129.5	7.64
5	-15.2	0.0	0.0	15.2	130.9	7.64
21	-13.9	10.1	2.9	14.8	128.0	7.66
88	-14.3	-9.6	1.6	14.7	127.9	7.69
131	-13.5	5.9	3.6	14.9	130.1	7.71
23	-13.8	10.0	-2.9	14.7	128.0	7.72
12	-9.5	-5.1	0.9	14.7	129.5	7.78
4	-13.8	0.0	-0.7	13.9	130.4	8.41
67	-10.6	-3.1	0.4	13.7	129.4	8.42
72	-10.5	-3.3	-0.4	13.7	129.4	8.42
8	-11.9	8.2	-3.2	13.7	129.8	8.47
6	-13.7	0.0	0.7	13.8	130.4	8.47
82	-8.6	-4.2	2.4	12.8	128.0	8.99
26	-11.4	-8.1	0.5	12.8	127.9	9.03
87	-8.5	-4.1	-2.4	12.6	128.0	9.13
28	-11.3	-8.0	-0.5	12.6	127.9	9.16
27	-8.4	-3.9	-0.2	12.4	128.0	9.35
99	-11.5	9.8	-1.2	12.1	127.5	9.52
124	-7.8	-7.8	-4.9	12.3	130.3	9.63

Note: See Figure 2.6.16.2-5 for section locations and definition of coordinate system.

Table 2.6.16.8-3 P + Q Stresses for CY-MPC Support Disk 1-Foot Side Drop, 38°
Basket Orientation

Section	Sx (ksi)	Sy (ksi)	Sxy (ksi)	Stress Intensity (ksi)	Allowable Stress (ksi)	Margin of Safety
3	-43.5	14.9	-5.2	44.4	131.1	1.95
13	-43.8	-16.6	1.1	43.8	129.4	1.95
28	-41.9	-24.2	3.2	42.1	127.9	2.04
1	-41.4	-17.6	-3.6	41.6	131.1	2.15
2	-41.1	8.4	-1.2	41.1	132.1	2.21
88	-39.2	15.2	6.3	39.2	127.9	2.26
43	-38.3	-25.2	2.8	38.6	127.5	2.30
12	-38.8	-13.7	1.1	38.8	129.5	2.34
105	-37.7	28.0	3.1	37.9	127.5	2.37
26	-37.0	27.2	3.1	37.6	127.9	2.41
82	-37.3	21.5	4.6	37.5	128.0	2.41
100	-36.8	20.4	4.3	37.2	127.5	2.43
87	-37.1	27.7	3.3	37.3	128.0	2.43
73	-37.2	5.5	7.2	37.6	129.4	2.44
99	36.5	19.6	3.3	36.8	127.5	2.46
41	-36.1	26.2	2.8	36.8	127.5	2.46
106	-36.7	15.3	5.7	36.8	127.5	2.47
81	35.4	20.8	3.0	35.7	127.9	2.58
52	-35.2	14.4	1.5	35.2	127.5	2.62
42	-34.5	30.4	1.8	34.9	127.5	2.65
11	-35.2	-18.8	2.3	35.2	129.4	2.67
29	-34.7	-16.8	1.5	34.7	127.9	2.68
38	-34.3	30.5	6.1	34.4	127.5	2.70
70	-34.7	5.0	4.2	34.7	129.5	2.73
103	-33.0	25.2	6.6	34.0	127.5	2.74
9	-34.5	13.4	3.9	34.6	129.7	2.75
84	-31.7	30.4	4.9	34.0	128.0	2.76
23	-33.6	29.7	6.4	33.6	128.0	2.81
22	-30.3	33.3	4.0	33.4	128.1	2.83
102	28.9	29.8	4.0	33.3	127.5	2.83

Note: See Figure 2.6.16.2-5 for section locations and definition of coordinate system.

Table 2.6.16.8-4 P + Q Stresses for CY-MPC Support Disk 1-Foot Side Drop, 63°
Basket Orientation

Section	Sx (ksi)	Sy (ksi)	Sxy (ksi)	Stress Intensity (ksi)	Allowable Stress (ksi)	Margin of Safety
43	-40.8	28.7	1.9	41.1	127.5	2.11
106	-39.5	22.0	1.0	39.5	127.5	2.22
28	-38.9	26.9	1.2	39.1	127.9	2.27
13	-38.1	18.2	0.6	38.1	129.4	2.39
3	-37.5	15.7	-4.6	38.5	131.1	2.40
105	37.0	-15.5	2.7	37.3	127.5	2.42
88	-37.2	20.5	0.3	37.2	127.9	2.44
41	36.1	-20.2	2.8	36.6	127.5	2.48
100	-36.1	22.2	1.4	36.3	127.5	2.52
44	-35.5	19.0	0.8	35.5	127.5	2.59
99	35.3	-12.5	1.9	35.4	127.5	2.60
42	-34.2	33.9	0.7	34.8	127.5	2.67
103	-33.1	28.8	2.3	34.1	127.5	2.74
73	-33.9	12.1	-2.9	34.3	129.4	2.77
29	-33.8	14.9	0.4	33.8	127.9	2.78
52	-33.4	11.7	0.5	33.4	127.5	2.82
26	32.6	-16.4	2.6	33.0	127.9	2.88
102	31.9	-20.7	3.3	32.8	127.5	2.89
111	-10.7	32.1	-2.7	32.4	127.5	2.93
109	-32.2	13.8	1.3	32.3	127.5	2.94
82	-32.2	20.8	0.8	32.3	128.0	2.96
87	31.8	-12.4	2.6	32.1	128.0	2.98
81	31.3	-9.0	1.6	31.4	127.9	3.07
129	-19.2	19.6	-11.9	31.3	127.5	3.08
53	-31.0	14.1	0.4	31.0	127.5	3.11
108	30.2	-9.9	3.1	30.7	127.5	3.16
38	-28.3	29.5	1.5	30.6	127.5	3.17
51	-29.4	12.8	2.5	29.8	127.5	3.28
37	-18.6	29.3	2.1	29.7	127.5	3.29
40	29.4	-11.2	1.2	29.5	127.5	3.32

Note: See Figure 2.6.16.2-5 for section locations and definition of coordinate system.

Table 2.6.16.8-5 P + Q Stresses for CY-MPC Support Disk 1-Foot Side Drop, 90° Basket Orientation

Section	Sx (ksi)	Sy (ksi)	Sxy (ksi)	Stress Intensity (ksi)	Allowable Stress (ksi)	Margin of Safety
129	-13.8	18.9	-9.8	26.5	127.5	3.82
108	15.0	8.3	-0.3	23.3	127.5	4.47
90	12.8	10.4	0.6	23.2	127.9	4.52
24	17.3	4.6	0.1	21.9	127.9	4.85
44	19.2	2.5	0.0	21.7	127.5	4.87
29	11.2	7.1	-0.6	18.4	127.9	5.96
105	12.0	5.7	-0.2	17.7	127.5	6.22
39	8.7	8.8	0.7	17.6	127.5	6.24
87	9.8	7.2	0.4	17.0	128.0	6.54
20	-16.7	9.0	1.2	16.9	127.9	6.56
40	-16.4	7.8	-1.1	16.6	127.5	6.70
111	-5.7	14.8	-3.0	15.7	127.5	7.10
43	-13.9	14.6	-1.2	15.5	127.5	7.24
110	-0.1	15.3	-0.3	15.3	127.5	7.32
125	9.6	-8.7	5.9	15.1	128.7	7.52
130	-8.9	12.6	3.9	15.0	128.7	7.57
23	13.0	1.7	-0.6	14.8	128.0	7.67
91	-8.5	14.2	1.3	14.5	127.9	7.79
21	-14.1	11.6	1.1	14.5	128.0	7.80
42	-12.0	13.6	-1.4	14.4	127.5	7.84
109	-10.4	14.1	-1.0	14.4	127.5	7.85
41	-13.8	11.4	-1.1	14.3	127.5	7.93
106	-12.1	12.5	-2.0	14.3	127.5	7.94
92	-0.1	14.2	0.2	14.2	127.8	7.97
126	9.3	-7.8	-5.5	14.1	127.5	8.07
93	-4.7	12.8	3.3	14.0	127.7	8.12
28	7.4	6.4	0.3	13.8	127.9	8.26
79	-13.4	5.7	1.5	13.7	127.9	8.37
22	-11.2	12.7	1.5	13.6	128.1	8.42
54	7.5	5.8	0.9	13.4	127.5	8.49

Note: See Figure 2.6.16.2-5 for section locations and definition of coordinate system.

2.6.16.9 CY-MPC Support Disk Shear Stresses for 1-Foot Drop

The evaluation of the maximum shear stress in the support disk utilizes the membrane values of the stress intensity due to primary loading, which were evaluated for end and side drop conditions. The maximum membrane stress intensity is 31.8 ksi for section 73 (see Tables 2.6.16.7-1 and 2.6.16.7-3). Therefore, the maximum shear stress is $31.8/2$ or 15.9 ksi. In accordance with ASME Code, Section III, Division 1, Subsection NG, the Level A allowable for shear stress is $0.6 S_m$. Using the bounding temperature of 650°F, S_m for Type 17-4 PH stainless steel is 41.9 ksi, the margin of safety is:

$$M.S. = 25.14/15.9 - 1 = .58$$

2.6.16.10 Bearing Stress - Basket Contact with Canister Shell - CY-MPC

For the bearing stress (S_{br}) acting along the basket disk-canister shell interface, an angular contact of 30 degrees is conservatively considered based on ANSYS gap element status (at a diameter of 69.15 inches). The load considered to be acting on the disk is the total contents weight (70 kips, which is conservative) times the deceleration (20 g) divided between 28 disks. The bearing area is considered to be the 0.5-inch thick disk and the contact area corresponding to a 30 degree angular contact.

$$S_{br} = (70/28)(20)/[(.5)(\pi)(69.15)(30/360)] = 5.5 \text{ ksi}$$

The allowable bearing stress is the yield stress, which for 304L stainless steel at a temperature of 400°F, is 17.5 ksi. The maximum canister shell temperature for transport conditions is 351°F. The margin of safety is:

$$M.S. = 17.5/5.5 - 1 = 2.18$$

2.6.16.11 CY-MPC Fuel Basket Weldment Analysis for 1-Foot End Drop

The responses of the top and bottom weldment plates of the fuel basket assembly to a 1-foot end drop in conjunction with the thermal expansion stress are also evaluated. The top and bottom weldment plates are 0.5-inch thick plates of Type 304 stainless steel. The weldments support their own weight plus the weight of 26 fuel assembly tubes. A finite element analysis is performed for both plates, since the support for each weldment is different due to the location of the support ribs for each. Both models use the SHELL63 element, which permits out of plane loading. Figures 2.6.16.11-1 and 2.6.16.11-2 show the finite element models for the weldments. The ribs supporting the disk were also represented by SHELL63. Evenly distributed nodal forces around the periphery of the fuel assembly slot represent the force on the weldment from each fuel tube. The application of the nodal loads at the slot periphery is accurate since the tube weight is transmitted to the edge of the slot, which provides support to the fuel tubes in the end drop condition.

This analysis demonstrates that the weldment design satisfies the primary membrane plus bending ($P_m + P_b$) and the primary and secondary ($P + Q$) stress criteria. For the end drop, the primary membrane stresses in the weldments are small. An analysis including the thermal expansion stresses is also performed using a bounding temperature distribution throughout the weldment. The determination of the weldment temperatures is discussed in Chapter 3.

The margins of safety are calculated as:

$$M.S. = [(P_m + P_b) / 1.5 S_m] - 1$$

or

$$M.S. = [(P_m + P_b + Q) / 3 S_m] - 1$$

The margins of safety are conservatively evaluated at the maximum temperature of 500°F. The calculated temperatures are shown in Table 2.6.16.11-1. The weldments are shown to satisfy the stress criteria in ASME Code, Section III Division I, Subsection NG.

Figure 2.6.16.11-1 Finite Element Model of the CY-MPC Top Weldment Plate

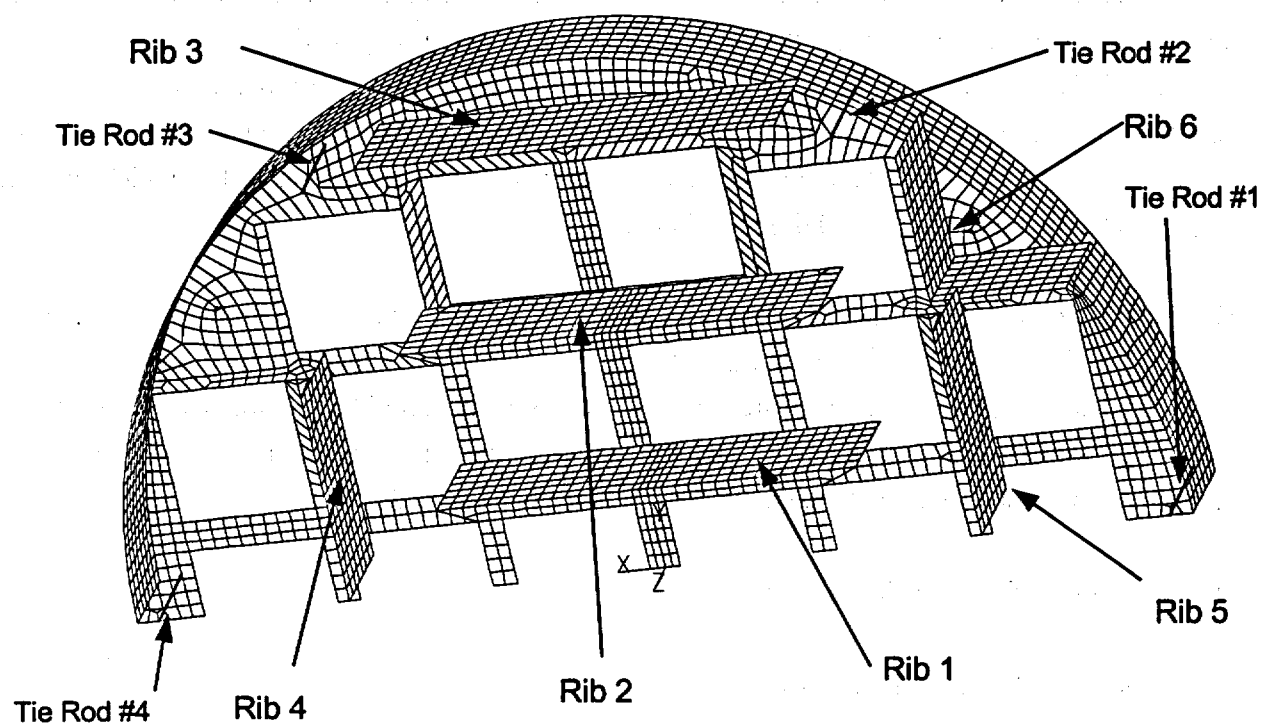


Figure 2.6.16.11-2 Finite Element Model of the CY-MPC Bottom Weldment Plate

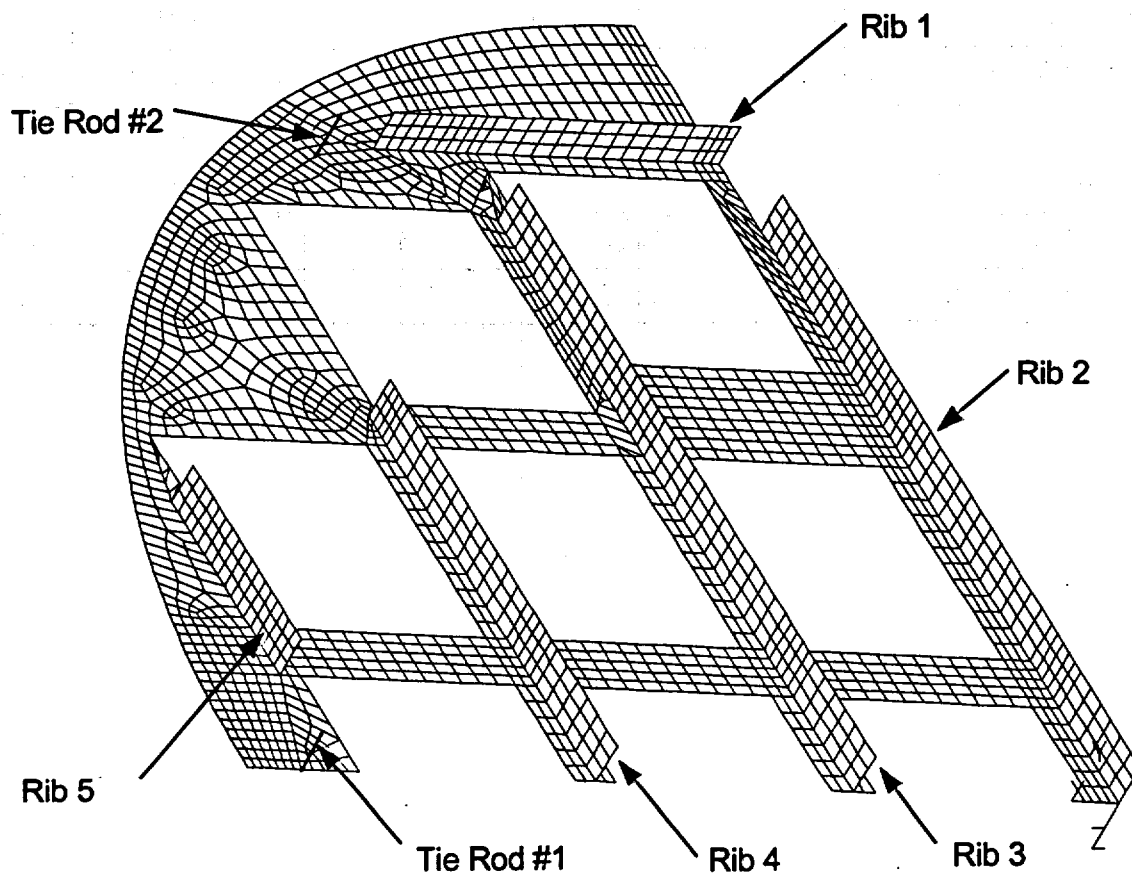


Table 2.6.16.11-1 Minimum Margins of Safety for the CY-MPC Top/Bottom Weldments for a 1-Foot End Drop With and Without Thermal Stresses

Component/Condition	$P_m + P_b$ (ksi)	Nodal Temp. (°F)	$1.5S_m@500°F$ (ksi)	M.S.
Top Weldment/1-ft. End Drop	19.21	247	26.25	+0.37
Bottom Weldment/1-ft. End Drop	15.73	221	26.25	+0.67
Component/Condition	$P_m + P_b + Q$ (ksi)	Nodal Temp. (°F)	$3S_m$ (ksi)	M.S.
Top Weldment/1-ft. End Drop	34.26	235	52.50	+0.53
Bottom Weldment/1-ft. End Drop	22.83	200	52.50	+1.3

2.6.16.12 CY-MPC Fuel Basket Support Disk - Buckling Evaluation

The CY-MPC fuel basket support disk is subjected to compressive and/or inertia loads during a 1-foot drop of the NAC-STC cask onto an unyielding surface. Depending on the cask orientation for the 1-foot drop impact, the support disk may have both in-plane and out-of-plane loads applied to it. The in-plane loads (basket side impact component) apply compressive forces and in-plane (strong axis) bending moments on the support disk and the out-of-plane inertial loads (basket end-impact component) produce out-of-plane (weak axis) bending moments on the support disk. Buckling of the support disk is evaluated in accordance with the methods and acceptance criteria of NUREG/CR-6322.

Buckling analysis was completed only for the 38° basket orientation because this is the worst case angle (see Section 2.6.16.7). The minimum margin of safety is +1.23, which occurs at section number 13. The results for the 20 worst-case sections are summarized in Table 2.6.16.12-1.

Table 2.6.16.12-1 NUREG/CR 6322 Buckling Analysis for the CY-MPC Support Disk
1-Foot Side Drop, 38° Basket Orientation

Sect.	P (kip)	Per (kip)	Py (kip)	M (in-kip)	Mp (in-kip)	Mm (in-kip)	MS1	MS2
13	6.47	43.81	48.30	4.48	13.28	13.02	1.23	1.38
3	5.55	44.51	49.07	4.47	13.49	13.22	1.39	1.54
28	3.91	43.13	47.54	4.48	13.07	12.83	1.55	1.68
23	4.94	43.18	47.59	3.62	13.09	12.84	1.78	1.95
29	3.46	38.51	43.17	3.09	10.79	10.50	1.90	2.10
12	2.96	62.28	65.94	8.47	24.73	24.73	1.94	1.98
38	3.50	42.86	47.23	3.82	12.99	12.75	1.94	2.09
9	4.64	43.97	48.47	3.44	13.33	13.07	2.00	2.18
43	2.49	42.86	47.23	4.00	12.99	12.75	2.06	2.19
2	3.47	63.85	67.61	7.84	25.36	25.36	2.14	2.19
1	1.89	44.51	49.07	4.18	13.49	13.22	2.19	2.32
14	4.21	39.06	43.80	2.28	10.95	10.64	2.40	2.66
39	3.09	38.31	42.93	2.50	10.73	10.44	2.48	2.71
22	2.99	61.33	64.93	6.60	24.35	24.35	2.57	2.63
44	2.43	38.31	42.93	2.56	10.73	10.44	2.64	2.87
24	4.21	38.55	43.21	1.94	10.80	10.51	2.71	3.01
52	1.13	60.84	64.40	7.08	24.15	24.15	2.73	2.76
53	1.17	42.86	47.23	3.57	12.99	12.75	2.75	2.88
27	2.33	61.26	64.85	6.21	24.32	24.32	2.91	2.96
42	1.45	60.84	64.40	6.56	24.15	24.15	2.92	2.96

2.6.16.13 Stress Evaluation of the CY-MPC Support Disk for 1-Foot Oblique Drop

This section documents the methodology used to calculate the stresses due to oblique impacts of the transport cask. The results show that the stress criteria are met for all oblique conditions. Note that the methodology used for the oblique drop evaluation is very conservative since the g loads decrease significantly for oblique drops (see Section 2.6.7.4).

To evaluate oblique impacts, the stress components (i.e., S_x , S_y , S_{xy}) are combined from the side drop and end drop cases for both the 0° and 38° basket drop orientations (Figure 2.6.16.1-1). The stresses are combined according to the following cask drop angles: $\phi = 0^\circ, 24^\circ, 30^\circ, 45^\circ, 60^\circ, 73^\circ, 75^\circ, 77^\circ, 80^\circ, 83^\circ, 85^\circ, 88^\circ$ and 90° . Note that the 0° and 90° cask drop angles are equivalent to the end- and side- drop cases, respectively. The normal stresses (S_x and S_y) and the shear stress (S_{xy}) for a drop with an angle of ϕ (Figure 2.6.16.2-3) are calculated using the following equations:

$$S_{x(\phi)} = S_{x(\text{end})}\cos\phi + S_{x(\text{side})}\sin\phi,$$

$$S_{y(\phi)} = S_{y(\text{end})}\cos\phi + S_{y(\text{side})}\sin\phi,$$

$$S_{xy(\phi)} = S_{xy(\text{end})}\cos\phi + S_{xy(\text{side})}\sin\phi,$$

where:

$S_{x(\text{end})}$, $S_{y(\text{end})}$, and $S_{xy(\text{end})}$ are the sectional stresses resulting from the Support Disk End Drop Model, and $S_{x(\text{side})}$, $S_{y(\text{side})}$, and $S_{xy(\text{side})}$ are the section stresses resulting from the Support Disk Side Drop Model.

Oblique principal stresses (i.e., S_1 , S_2) are calculated by using the following equation:

$$S_1, S_2 = \frac{S_{x(\phi)} + S_{y(\phi)}}{2} \pm \sqrt{\left(\frac{S_{x(\phi)} - S_{y(\phi)}}{2}\right)^2 + S_{xy(\phi)}^2}$$

Once the oblique principle stresses are calculated, new stress intensities (SI) and margins of safety can be calculated. A summary of the maximum stress intensities in the 1-foot oblique drop conditions is shown below. Note that the 0° and 90° cask drop angles, equivalent to the end

drop and side drop, are the worst case conditions for the 0° and 38° basket orientations, respectively.

Stress State ¹	Section ²	Cask Drop Angle (°) ³	S _x (ksi)	S _y (ksi)	S _{xy} (ksi)	Stress Intensity (ksi)	Allowable Stress (ksi)	Margin of Safety
0° BASKET DROP ORIENTATION ⁴								
P _m	61	0	23.8	-1.9	6.9	29.8	42.5	0.43
P _m +P _b	61	0	31.8	-6.7	12.4	41.6	63.8	0.53
38° BASKET DROP ORIENTATION ⁴								
P _m	73	90	-31.6	2.1	2.5	35.6	43.1	0.21
P _m +P _b	13	90	-56.2	19.5	1.9	57.1	64.7	0.13

Notes:

1. P_m = Primary Membrane Stress, P_m + P_b = Primary Membrane + Bending Stress.
2. See Figure 2.6.16.2-5 for section locations.
3. See Figure 2.6.16.2-3 for definition of cask drop angle.
4. See Figure 2.6.16.1-1 for definition of basket drop orientation.

2.6.16.14 Stress Evaluation of the CY-MPC Support Disk for a Combined Thermal and 1-Foot Oblique Drop Load Condition

The thermal expansion loads described in Section 2.6.16.3 are applied to the finite element model simultaneously with the 20g oblique drop loads described in Section 2.6.16.13 to produce a combined thermal expansion plus oblique impact loading. A summary of the maximum stress intensities in the thermal plus 1-foot oblique drop conditions is shown below. Note that the 0° cask drop angle, equivalent to the end drop, is the worst case condition for both basket orientations considered.

Basket Drop Orientation Angle (°) ⁴	Stress State ¹	Section ²	Cask Drop Angle (°) ³	Sx (ksi)	Sy (ksi)	Sxy (ksi)	Stress Intensity (ksi)	Allowable Stress (ksi)	Margin of Safety
0	P + Q	57	0	-108.4	38.7	12.0	112.4	127.5	0.13
38	P + Q	57	0	-108.4	38.7	12.0	112.4	127.5	0.13

Notes:

1. P_m = Primary Membrane Stress, $P_m + P_b$ = Primary Membrane + Bending Stress.
2. See Figure 2.6.16.2-5 for section locations.
3. See Figure 2.6.16.2-3 for definition of cask drop angle.
4. See Figure 2.6.16.1-1 for definition of basket drop orientation.

THIS PAGE INTENTIONALLY LEFT BLANK

2.6.17 CY-MPC Reconfigured Fuel Assembly and Damaged Fuel Can Analysis- Normal Conditions of Transport

The CY-MPC reconfigured fuel assembly and damaged fuel can are evaluated for normal conditions of transport for a 20g end-drop and 20g side-drop. Material properties for the reconfigured fuel assembly evaluation are taken at 750°F. The material properties for the damaged fuel can are taken at 600°F. These temperatures envelope all operating condition temperatures.

2.6.17.1 CY-MPC Reconfigured Fuel Assembly Evaluation

The CY-MPC reconfigured fuel assembly weldment is evaluated for end, corner and side impacts.

End Impact

For the end impact, the corner angles are evaluated to the criteria specified in NUREG/CR-6322, "Buckling Analysis of Spent Fuel Basket." Length (L) for both corner angles and tubes is conservatively taken as the length of the tube divided into five equal spans by the tube support grids, $L = 135.09/5 = 27.02$ inches.

Corner Angle

For the corner angle,

$$\frac{KL}{r} = \frac{1.0(27.02)}{0.6168} = 43.8$$

where

$$r = \sqrt{\frac{I}{A}} = \sqrt{\frac{0.272}{0.715}} = 0.6168 \text{ in.}$$

$A = 0.715 \text{ in}^2$, corner angle cross-sectional area

$I = 0.272 \text{ in}^4$, corner angle moment of inertia

The width-thickness ratio is:

$$\frac{b}{t} = \frac{2.0}{0.1875} = 10.67$$

Applying the NUREG/CR-6322 criteria, (for $S_y = 17.3 \text{ ksi}$)

$\frac{KL}{r} = 43.8 \leq 120$, and $\frac{b}{t} = 10.67 \leq \frac{76}{\sqrt{S_y}} = 18.27$, therefore the allowable stress (F_a) is:

$$F_a = S_y \left(0.47 - \frac{\frac{KL}{r}}{444} \right) = 17.3 \left(0.47 - \frac{43.8}{444} \right) = 6.42 \text{ ksi.}$$

The total load on the angles includes the weights of the top housing, the guide plate, the lid weldment, 4 corner angles, and 4 tube support grids:

Total load = 32 + 7 + 32 + 112 + 32 = 215 lb; use 225 lb for the analysis.

The load on each angle (P_{20g}) for the off-normal condition is:

$$P_{20g} = \frac{225(20g)}{4} = 1,125 \text{ lb, and the compressive stress } (\sigma_c) \text{ in the angle is:}$$

$$\sigma_c = \frac{1,125 \text{ lb}}{0.715 \text{ in.}^2} = 1,574 \text{ psi}$$

The margin of safety (MS) for the off-normal condition is:

$$MS = \frac{F_a}{\sigma_c} - 1 = \frac{6.42}{1.57} - 1 = +3.08$$

2.6.17.1.1 CY-MPC Reconfigured Fuel Assembly Fuel Tube Evaluation

End Impact

In the end-drop scenario, the tubes are loaded by their self-weight \times the appropriate acceleration factor for the condition being evaluated.

For the tube,

$$\frac{KL}{r} = \frac{1.0(27.02)}{0.1869} = 144.57$$

where

$$r = \sqrt{\frac{I}{A}} = \sqrt{\frac{0.002026}{0.0580}} = 0.1869 \text{ in.}$$

$$A = \frac{\pi}{4}(0.5625^2 - 0.4925^2) = 0.058 \text{ in.}^2$$

$$I = \frac{\pi}{64}(0.5625^4 - 0.4925^4) = 0.002026 \text{ in.}^4$$

The width-thickness ratio is:

$$\frac{b}{t} = \frac{0.5625}{0.035} = 16.1.$$

Applying the NUREG/CR-6322 criteria,

$\frac{KL}{r} = 144.57 > 120$, and $\frac{b}{t} = 16.1 \leq \frac{76}{\sqrt{S_y}} = 18.27$. Therefore, the allowable stress (F_a) is:

$$F_a = S_y \left(0.40 - \frac{\frac{KL}{r}}{600} \right) = 17.3 \left(0.40 - \frac{144.57}{600} \right) = 2.75 \text{ ksi.}$$

The axial compressive load (P) on each tube is the tube weight ($2.27 \text{ lb} \times 20g$, the off-normal condition acceleration factor) = 45.4 lb ; use 50 lb for the analysis. The compressive stress (σ_c) is:

$$\sigma_c = \frac{P_{20g}}{A} = \frac{50 \text{ lb}}{0.0580 \text{ in.}^2} = 862 \text{ psi}$$

The margin of safety (MS) for the off-normal condition is:

$$MS = \frac{F_a}{\sigma_c} - 1 = \frac{2.75 \text{ ksi}}{0.862 \text{ ksi}} - 1 = +2.19$$

Side Impact

The reconfigured fuel assembly corner angles and tubes are each evaluated as a continuous beam supported at 6 places – the top and bottom housings and 4 intermediate tube support grids. The beam model for the corner angle is analyzed with a uniformly distributed load that is the self-weight of the angle multiplied by the acceleration factor (20g). The beam model for the tube is analyzed with a uniformly distributed load comprising the weight of the fuel rods and the self weight of the tube multiplied by an acceleration factor (20g).

Corner Angle Impact

The corner angle length between the top and bottom housing is approximately 135.09 inches. The four intermediate tube support grids divide the corner angle into five equal spans approximately 27.02 inches long.

The maximum moment (M_{max}) in the corner angle is:

$$M_{max} = 0.0779wl^2 = 0.0779(0.2033)(27.02^2)(20g) = 232 \text{ lb-in.}$$

The maximum shear force (V) in the corner angle is:

$$V = \frac{23}{38}(wl) = \frac{23}{38}(0.2033)(27.02)(20g) = 67 \text{ lb}$$

The maximum bending stress (σ_b) is:

$$\sigma_b = \frac{M_{max} \times c}{I} = \frac{232(1.431)}{0.272} = 1,221 \text{ psi}$$

The maximum shear stress (τ) is:

$$\tau = \frac{V}{A} = \frac{67}{0.715} = 94 \text{ psi}$$

The combined stress is:

$$\sigma_{1,2} = \frac{\sigma_b}{2} \pm \sqrt{\left(\frac{\sigma_b}{2}\right)^2 + \tau^2} = \frac{1,221}{2} \pm \sqrt{\left(\frac{1,221}{2}\right)^2 + (94)^2} = 611 \pm 618 \text{ psi}$$

$$\sigma_1 = 1,229 \text{ psi}$$

$$\sigma_2 = -7 \text{ psi}$$

The maximum combined stress (σ_{\max}) is:

$$\sigma_{\max} = |\sigma_1 - \sigma_2| = 1,236 \text{ psi}$$

The margin of safety, MS, is:

$$MS = \frac{3S_m}{\sigma_{\max}} - 1 = \frac{3(15,600)}{1,236} - 1 = +36.8$$

Fuel Tube Support

The tube length between the top and bottom housing is approximately 135.09 inches. The four intermediate tube support grids divide the tube into five equal spans approximately 27.02 inches long.

The maximum moment (M_{\max}) in the tube is:

$$M_{\max} = 0.0779wl^2 = 0.0779(0.076)(27.02^2)(20g) = 87 \text{ lb-in.}$$

The maximum shear force (V) in the tube is:

$$V = \frac{23}{38}(wl) = \frac{23}{38}(0.076)(27.02)(20g) = 25 \text{ lb}$$

The maximum bending stress (σ_b) is:

$$\sigma_b = \frac{M_{\max} \times c}{I} = \frac{87(0.28125)}{.002026} = 12,077 \text{ psi}$$

The maximum shear stress (τ) is:

$$\tau = \frac{V}{A} = \frac{25}{0.0580} = 431 \text{ psi}$$

The combined stress is:

$$\sigma_{1,2} = \frac{\sigma_b}{2} \pm \sqrt{\left(\frac{\sigma_b}{2}\right)^2 + \tau^2} = \frac{12,077}{2} \pm \sqrt{\left(\frac{12,077}{2}\right)^2 + (431)^2} = 6039 \pm 6054 \text{ psi}$$

$$\sigma_1 = 12,093 \text{ psi}$$

$$\sigma_2 = -15 \text{ psi}$$

The maximum combined stress is:

$$\sigma_{\max} = |\sigma_1 - \sigma_2| = 12108 \text{ psi}$$

The margin of safety MS is:

$$MS = \frac{3S_m}{\sigma_{\max}} - 1 = \frac{3(15,600)}{12,108} - 1 = +2.87$$

2.6.17.1.1 CY-MPC Reconfigured Fuel Assembly Tube Support Grid

Analysis of the reconfigured fuel assembly support grid uses an ANSYS finite element model to evaluate the stresses during impact conditions. The model consists of 1/2 of the support grid and is used to evaluate both side and end impacts. The support grid plate is 0.5 inches thick and constructed of Type 304 stainless steel. Figure 2.6.17-1 shows a plot of the finite element model. The regions where the support grid is welded to the corner angles are shown on the figure as heavy lines. These weld regions are fixed in the appropriate directions to represent the fixity of the angles. A plane of symmetry also exists and is appropriately constrained.

End Drop

During the end drop, the model is loaded using a static gravity load of 20g. Thermal stresses are also considered in the model by first performing a steady-state thermal solution. This thermal solution is obtained using a peak temperature of 750°F at the center of the support grid and 650°F (100°F delta)

at the perimeter of the support grid. The intermediate support grid temperatures are then calculated and applied in the structural solution.

The maximum nodal stress calculated for the 20g end impact load is 1.8 ksi. The allowable stress is conservatively determined using the allowable for P_m stress ($1.0S_m$). For Type 304 stainless steel at 750°F, the allowable stress is 15.6 ksi and the resulting margin of safety is $15.6/1.8 - 1 = +7.6$.

The peak nodal stress calculated for the 20g loading plus thermal is 9.17 psi. The normal condition allowable stress at 750°F is $3.0 \times 15.6 = 46.8$ ksi and the resulting margin of safety is +4.1.

Side Drop

During the side-drop, the model (same as used in end-drop) is loaded using a static gravity load of 20g.

The maximum nodal stress calculated for the 20g side impact load is 14.6 ksi. The allowable stress is conservatively determined using the allowable for P_m stress ($1.0S_m$). For Type 304 stainless steel at 750°F, the allowable stress is 15.6 ksi and the resulting margin of safety is $15.6/14.6 - 1 = +0.07$.

The peak nodal stress calculated for the 20g loading plus thermal is 18.8 ksi. The normal condition allowable stress at 750°F is $3.0 \times 15.6 = 46.8$ ksi and the resulting margin of safety is +1.49.

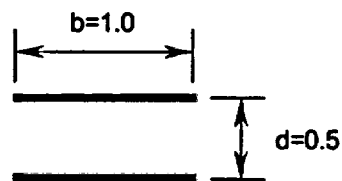
2.6.17.1.3 CY-MPC Reconfigured Fuel Assembly Weld Analysis

Maximum forces and moments for analysis of the welds joining the tube support grids to the corner angles are taken from the finite element analysis output. Each support grid is welded to the four corner angles with 1/8-in. fillet welds one inch in length both top and bottom. Using Blodgett's (R1) method of considering the weld as a line, the bending force (F_b) on the weld per inch of length is determined as follows:

$$F_b = \frac{M}{S_w} = \frac{15.3 \text{ lb} \cdot \text{in.}}{0.5 \text{ in.}^2} = 30.6 \text{ lb/in.}$$

The shear force (F_v) is:

$$F_v = \frac{V}{A_w} = \frac{17.1 \text{ lb}}{2.0 \text{ in.}} = 8.6 \text{ lb/in.}$$



where

$$S_w = b \times d$$

$$A_w = 2 \times b$$

The resultant force (F) on the weld is:

$$F = \sqrt{F_h^2 + F_v^2} = 31.8 \text{ lb}$$

The effective throat thickness of the 1/8-in. fillet weld is $0.707(0.125 \text{ in.}) = 0.088 \text{ in.}$, the effective throat area is $0.088 \text{ in.}^2/\text{in.}$, and the stress (f) in the weld is:

$$f = \frac{F}{nA} = \frac{31.8 \text{ lb/in.}}{0.4(0.088 \text{ in.}^2/\text{in.})} = 903.4 \text{ psi}$$

where

$n = 0.4$ is the minimum quality factor for a Category E Type V weld per ASME Section III-NG.

The margin of safety (MS) is determined on the basis of the parent metal yield strength:

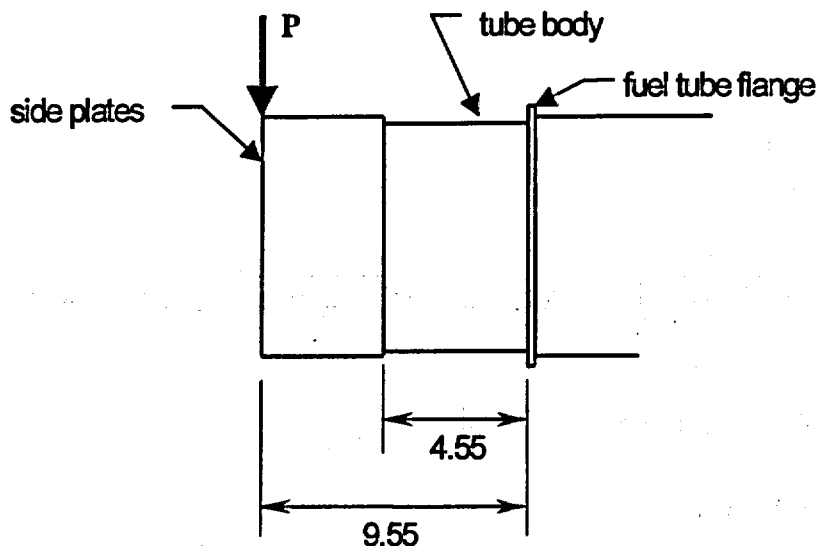
$$MS = \frac{3S_m}{f} - 1 = \frac{3(15,600) \text{ psi}}{(361.4 \text{ psi})} - 1 = + \text{ Large}$$

2.6.17.2 CY-MPC Damaged Fuel Can Evaluation

This section evaluates the CY-MPC damaged fuel can for normal transport conditions. The cask 1-foot drop is evaluated considering a 20g end-impact and a 20g side-impact.

Material properties for ASME SA 240/SA479 Type 304 stainless steel, ASME Code Section III, Subsection NG, are determined at a bounding temperature of 600°F.

S_u	63.3 ksi
S_y	18.6 ksi
S_m	16.7 ksi
E	25.2×10^3 ksi



The weight of the damaged fuel can top assembly (lid) is 19.46 lbs, and the weight of the can weldment is 91.6 pounds. Twenty-five pounds and 95 pounds are used in the analysis for the top assembly and can weldment, respectively.

2.6.17.2.1 CY-MPC Damaged Fuel Can Tube Body Evaluation – Side Impact

The majority of the tube body is contained within the fuel tube in the basket assembly. Because both the tube body and the fuel tube have square cross sections, they will be in full contact (for 131.95 in. longitudinally) during the side impact and no significant bending stress will be introduced into the tube body. The last 4.55 in. of the body tube and the 5.0-in. length of the side plates will be unsupported past the fuel tube flange in the side impact configuration.

The tube body will be evaluated as a cantilevered beam with the combined weight (P) of the overhanging tube body, side plates and lid assembly multiplied by a deceleration factor of 20g. The maximum bending stress (f_b) is:

$$f_b = \frac{M_{\max} c}{I} = \frac{6,685(4.44)}{22.95} \approx 1,293 \text{ psi}$$

where:

$$M_{\max} = P g \times L = 35(20)(9.55) = 6,685 \text{ lb-in.}$$

$$g = 20$$

The shear stress (τ) is:

$$\tau = \frac{Pg}{A} = \frac{35(20)}{1.766} \cong 396 \text{ psi}$$

$$\sigma_1, \sigma_2 = \frac{1}{2} \left(f_b \pm \sqrt{f_b^2 + 4\tau^2} \right) = \frac{1}{2} \left(1,293 \pm \sqrt{1,293^2 + 4(396)^2} \right) \cong 1,405 \text{ psi and } -112 \text{ psi}$$

The stress intensity (σ_{\max}) = $|\sigma_1 - \sigma_2| = 1,517 \text{ psi}$

The Margin of Safety (MS) is:

$$MS = \frac{1.5 S_m}{\sigma_{\max}} - 1 = \frac{1.5(16,700)}{1,517} - 1 = +16.5$$

2.6.13.2.2 CY-MPC Damaged Fuel Can Weld Evaluation

The welds joining the tube body to the side plates are full penetration welds (Type III, ASME Code Section III, Subsection NG paragraph NG-3352.3). Per Table NG-3352-1 (ASME Code Section III, Subsection NG), the weld quality factor (n) for a Type III weld with visual surface inspection is 0.5.

The margin of safety (MS) for the weld is:

$$MS = \frac{(1.5)n \cdot S_m}{\sigma_{\max}} - 1 = \frac{(1.5)(0.5)(16,700 \text{ psi})}{1,517 \text{ psi}} - 1 = +7.3$$

2.6.17.2.3 CY-MPC Damaged Fuel Can Tube Body Evaluation – End Impact

For the bottom end drop, the top assembly (lid), the side plates, and the tube body act against the bottom assembly. For the top end drop, the bottom assembly, tube body, and side plates act against the top assembly. Because the top assembly is heavier, the bottom end drop is the governing case for the tube body compression. The can contents bear against the bottom assembly through which the loads are transferred to the bottom plate. The compressive load (P) on the tube is the combined mass of the lid, side plates and tube body multiplied by the 20g deceleration.

$P = 1,994.2 \text{ lb}$; use 3,000 lb for evaluation.

The compressive stress (S_c) in the tube body is:

$$S_c = \frac{P}{A} = \frac{3,000 \text{ lb}}{1.766 \text{ in.}^2} \cong 1,699 \text{ psi}$$

where:

$$A = 8.88^2 - 8.78^2 = 1.766 \text{ in}^2$$

The margin of safety (MS) is then:

$$MS = \frac{S_m}{S_c} - 1 = \frac{16,700}{1,699} - 1 = +8.8$$

2.6.17.2.4 CY-MPC Damaged Fuel Can Tube Body Buckling Evaluation – End Impact

The tube is evaluated, using the Euler formula, to determine the critical buckling load (P_{cr}):

$$P_{cr} = \frac{\pi^2 EI}{L_c^2} = \frac{\pi^2 (25.2 \times 10^6) (22.95)}{2(136.5)^2} = 76,587 \text{ lb}$$

where:

$$E = 25.2 \times 10^6 \text{ psi}$$

$$I = \frac{8.88^4 - 8.78^4}{12} = 22.95 \text{ in}^4$$

$$L_c = 2L \text{ (worst case condition)}$$

$$L = \text{unsupported tube body length (136.5 in.)}$$

Because the maximum compressive load (3,000 lb) is much less than the critical buckling load (76,587 lb) the tube has adequate resistance to buckling.

2.6.17.2.5 CY-MPC Damaged Fuel Can Lid Evaluation – End Impact

During a bottom end impact, the top lid will be subjected to bending stresses caused by the weight of the top lid. The top lid assembly conservatively weighs 25 lbs. Under a 20g load, the load on the plate is 500 lbs or $(500/8.77^2) \cong 6.5$ psi. The maximum stress for the lid is calculated by conservatively assuming a unit width simply supported beam 8.77-inches long with a thickness of 0.75-inches.

$$M = \frac{6.5(8.77^2)}{8} = 62.5 \text{ in} \cdot \text{lbs}$$

$$S_b = \frac{6(62.5)}{1.0(0.75^2)} = 667 \text{ psi}$$

The Margin of Safety is:

$$MS = \frac{16,700}{667} - 1 = + \text{Large}$$

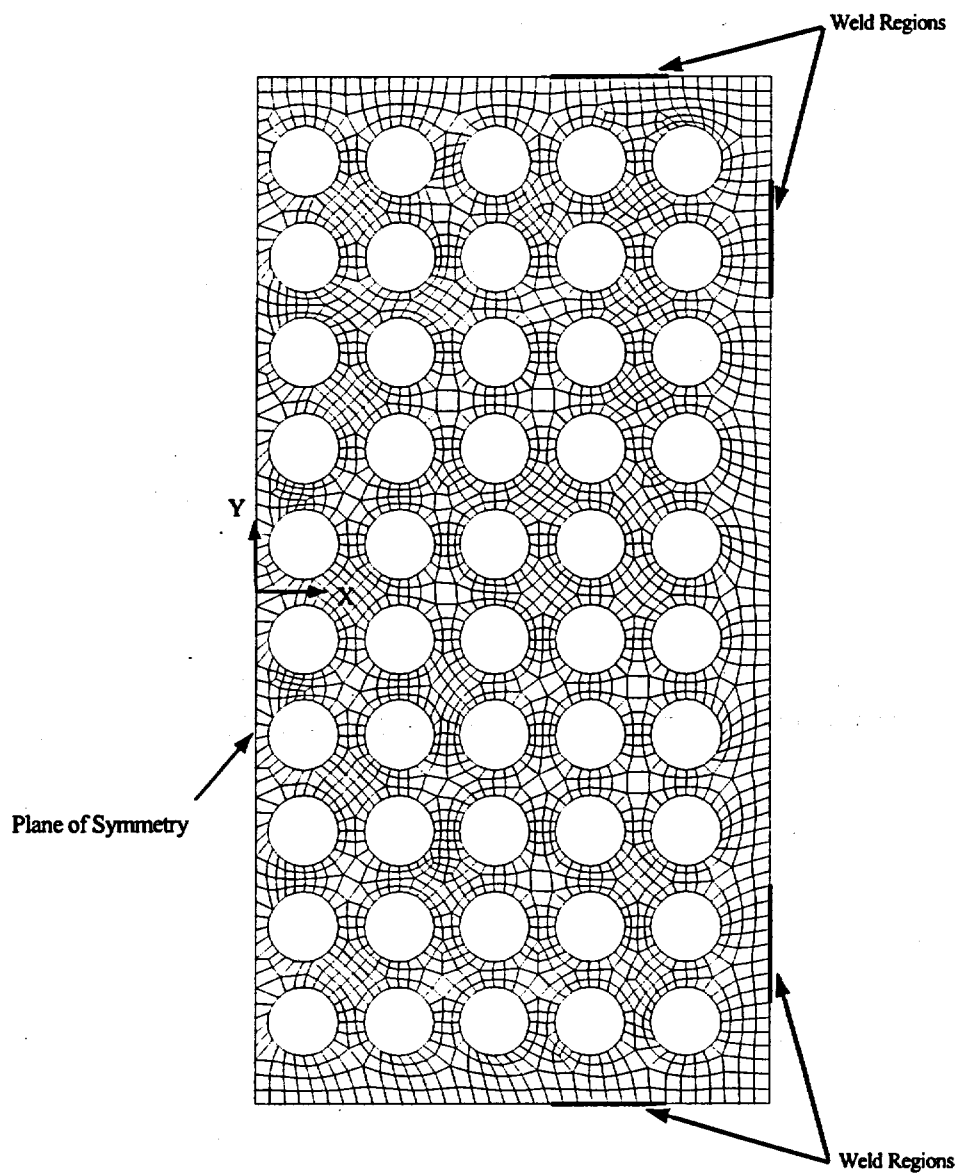
2.6.17.2.6 CY-MPC Damaged Fuel Can Thermal Considerations

The coefficient of thermal expansion for SA240 Type 304 stainless steel is 9.0×10^{-6} in./in./°F. Both the CY-MPC damaged fuel can and the CY-MPC canister in which it is contained are made of 304 stainless steel having the same coefficient of thermal expansion (α) $\cong 9.0 \times 10^{-6}$ in./in./°F. The damaged fuel can outside height is initially 0.75 in. shorter than the canister internal height. For interference to occur because of differential thermal expansion, a ΔT of approximately 589°F between the damaged fuel can and the canister must exist.

$$\Delta T = \frac{\Delta L}{\alpha \cdot L} = \frac{0.75}{9.0 \times 10^{-6} (141.5)} \cong 589^\circ \text{F}$$

The close proximity of the damaged fuel can and the canister, and the design temperature limits, preclude such a temperature differential because the differential thermal expansion causes no interference or binding, no further thermal stress evaluation is required.

Figure 2.6.17-1 CY-MPC Reconfigured Fuel Assembly Tube Support Grid Finite Element Model



THIS PAGE INTENTIONALLY LEFT BLANK

2.6.18 Spacer Design for Canistered Fuel - Normal Conditions of Transport

This section presents the design analyses for the spacers used to position the spent fuel or GTCC waste canister in the NAC-STC. The following requirements bound the spacer design:

1. The spacer must meet the normal conditions of transport requirements detailed in 10 CFR 71.43(f) when subjected to the free drop (10 CFR 71.71).
2. The spacer must provide spacing of the canister so that the center of gravity of the cask and contents is maintained.

For impact loading conditions, the spacer was designed to meet the requirements of 10 CFR 71.43(f) for the 1-foot drop condition (10 CFR 71.71). 10 CFR 71.43(f) requires that no substantial reduction in the effectiveness of the package will be experienced in normal conditions of transport. Classical analysis is used to demonstrate compliance with these requirements.

The dimensions of the spacer must be selected to maintain the center of gravity at a distance of 96.01 inches from the bottom of the cask (see Table 2.2-1), which is the center of gravity for the NAC-STC for directly loaded PWR fuel.

2.6.18.1 Spacer Evaluation for Yankee-MPC Canister Fuel and GTCC Waste

Aluminum honeycomb manufactured by Hexcel Corporation was selected as the spacer material for the Yankee-MPC canister as it has the combination of low weight, good thermal conductivity, and strength needed to meet the design requirements. The properties of the aluminum honeycomb are:

Nominal Density (pcf)	Crush Strength (psi)	Compressive Strength	
		Typical (psi)	Minimum (psi)
4.5	320	700	500

For the normal conditions of transport, the stabilized compressive strength of the aluminum honeycomb is used. The compressive strength represents the strength of the material prior to yield, whereas, the crush strength is the strength of the material after yield. The crush strength is

used for evaluating g-loads experienced during the 30-foot drop prior to compressing the material to "stack height." In order to maintain the compressive strength during the normal conditions of transport, the aluminum honeycomb is assumed not to be precrushed.

The Yankee-MPC canister has an overall length of 122.5 inches while the length of the NAC-STC cask cavity is 165 inches. The bottom of the canister must be 14.0 inches from the bottom of the cask cavity. To maintain this location of the canister, a top and a bottom spacer are used. Both spacers are comprised of aluminum honeycomb material. While both spacers are of the same construction, the top spacer is 28.0 inches long while the bottom spacer is 14.0 inches long. These are free standing components that are confined by the canister ends and the transport cask cavity surfaces. The top and bottom of each spacer consists of a 0.38-inch thick and a 0.13-inch thick Type 6061-T6 aluminum plate, respectively. Inserted into the top of the aluminum plate are three threaded inserts to facilitate lifting of the spacers. The aluminum honeycomb material is enclosed by a 0.0625-inch thick 6061-T6 aluminum alloy outer shell.

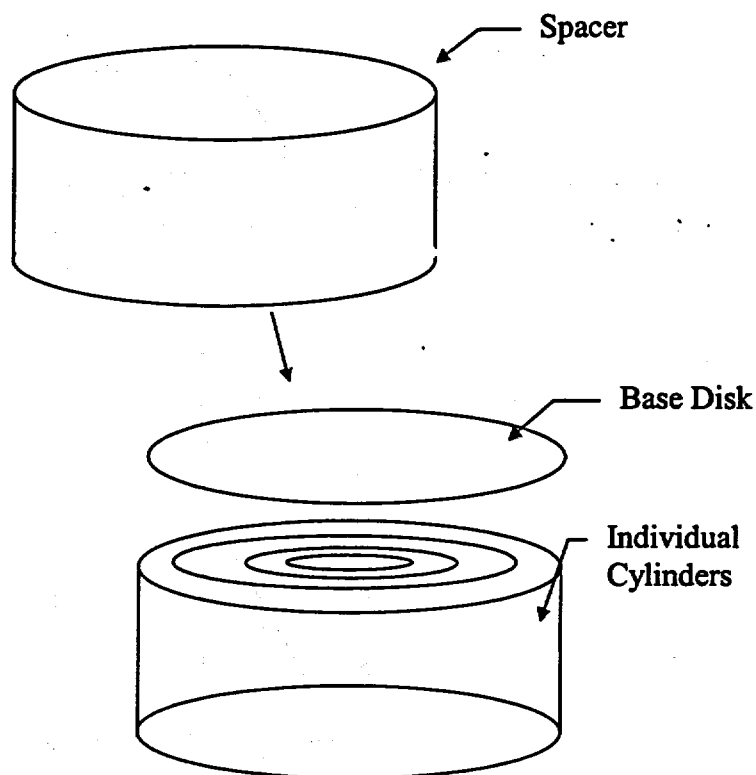
To apply a 1-foot end drop load to the spacer, a total load of 56,000 lbs x 20g (conservative canister weight plus spacer weight) was applied. The diameter of the crushable material in the spacer is taken to be 68.9 inches in diameter. This results in a crushing pressure (P_{cr}) of:

$$P_{cr} = (56,000)(20)/(3.1415 \times 68.9^2 / 4) = 300 \text{ psi}$$

The compressive strength of 5056 Alloy aluminum honeycomb is a minimum of 500 psi to a typical 700 psi. At a maximum normal operating temperature of 250°F, the compressive strength drops to approximately 80% of the nominal values ($500 \times 0.8 = 400$ psi). The maximum pressure load during the 1-foot drop is 300 psi. Since the pressure load is less than the nominal compressive strength, the spacer will not permanently deform during the 1-foot drop. The margin of safety is $M.S. = (400/300) - 1 = +0.33$. This compressive evaluation is valid for both the top and bottom spacers.

2.6.18.2 Spacer Evaluation for CY-MPC Canister Fuel and GTCC Waste

The canister spacer is a weldment made of Type 304 stainless steel, ASTM A 240, 3/8-in. plate. The weldment consists of a circular base with 6 concentric cylinders welded to it. A sketch of the spacer is provided below.



The spacer is analyzed for a 1-foot end drop (20g) normal transport condition.

A total load of $(65,821 \text{ lb} + 1,800 \text{ lb}) \times 20 \text{ g}$ (heaviest canister weighs 65,821; 1,800 lb represents a conservative value for the spacer self-weight) is applied as a uniform pressure to the base plate of the spacer.

The total force exerted on each cylinder is obtained from the finite element model:

$$F_1 = 80,250 \text{ lb.}$$

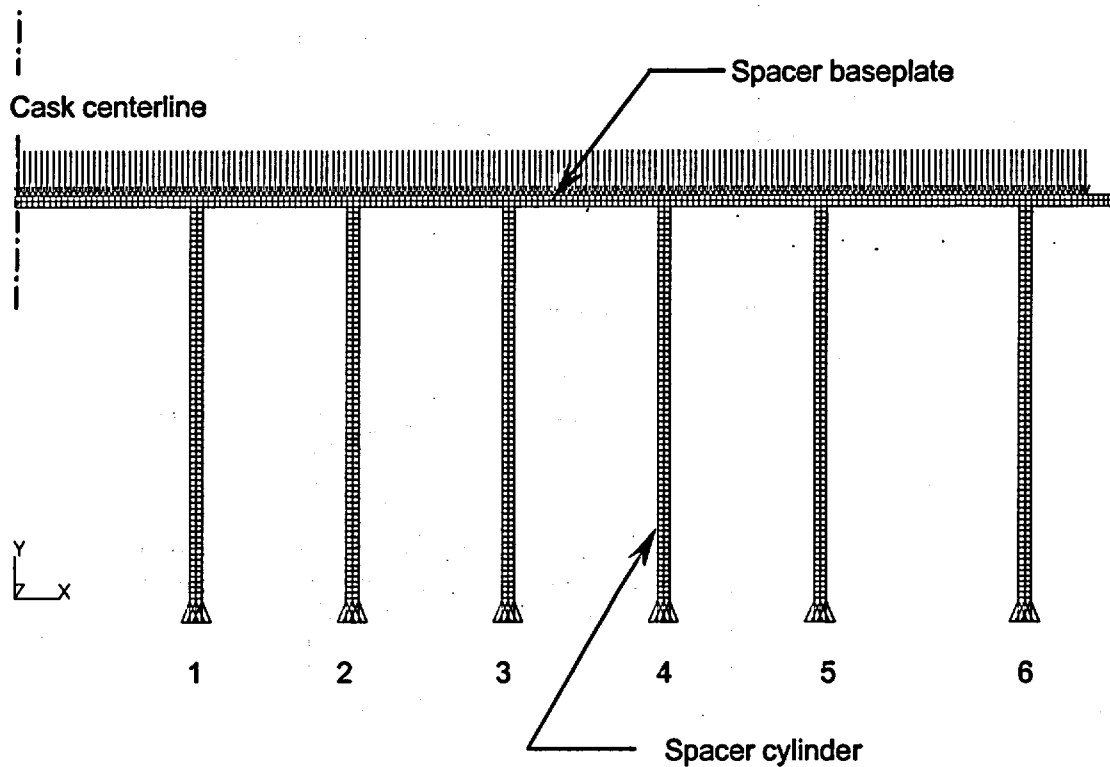
$$F_2 = 121,000 \text{ lb.}$$

$$F_3 = 183,184 \text{ lb.}$$

$$F_4 = 228,402 \text{ lb.}$$

$$F_5 = 358,767 \text{ lb.}$$

$$F_6 = 380,817 \text{ lb.}$$



The membrane stress in each cylinder is:

$$\sigma_{\text{membrane}} = F/A$$

where

$$A = \pi/4(D_o^2 - D_i^2)$$

$$\sigma_1 = 80,250 \text{ lb} / 13.7 \text{ in}^2 = 5,858 \text{ psi}$$

$$\sigma_2 = 121,000 \text{ lb} / 25.5 \text{ in}^2 = 4,745 \text{ psi}$$

$$\sigma_3 = 183,184 \text{ lb} / 37.3 \text{ in}^2 = 4,811 \text{ psi}$$

$$\sigma_4 = 228,402 \text{ lb} / 49.0 \text{ in}^2 = 4,661 \text{ psi}$$

$$\sigma_5 = 358,767 \text{ lb} / 60.8 \text{ in}^2 = 5,901 \text{ psi}$$

$$\sigma_6 = 380,817 \text{ lb} / 76.1 \text{ in}^2 = 5,004 \text{ psi}$$

Based on the allowable membrane stress at 400° ($F = S_m = 18,700$ psi), the lowest margin of safety is:

$$MS = (18,700/5,901) - 1 = +2.16$$

To evaluate the buckling, the critical stress is determined and compared to the actual stress:

$$\sigma_{\text{critical}} = E \frac{0.605 \cdot 10^{-7} \text{ m}^2}{m(1 + 0.004\phi)}$$

where

E = modulus of elasticity (26.5×10^6 psi for Type 304 SS at 400°F)

m = R/T = radius/thickness

ϕ = E/S_y (for 304 SS = $26.5 \times 10^6 / 20,700$ psi = 1,280.2)

$$\sigma_{\text{critical-1}} = 163,702 \text{ psi}$$

$$\sigma_{\text{critical-2}} = 89,293 \text{ psi}$$

$$\sigma_{\text{critical-3}} = 61,368 \text{ psi}$$

$$\sigma_{\text{critical-4}} = 46,750 \text{ psi}$$

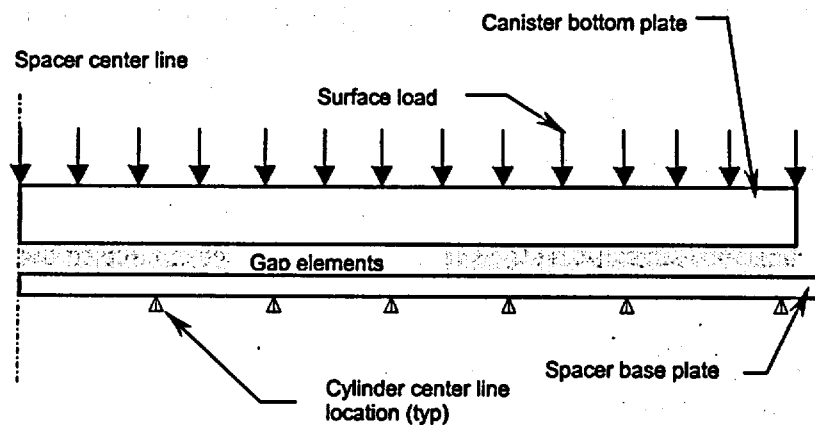
$$\sigma_{\text{critical-5}} = 37,751 \text{ psi}$$

$$\sigma_{\text{critical-6}} = 30,185 \text{ psi}$$

The buckling evaluation demonstrates a minimum margin of safety as follows:

$$MS = (30,185/5,004) - 1 = +5.03$$

The base disk of the canister spacer is evaluated to determine its ability to carry the loading of the canister. ANSYS version 5.5 is used to construct a finite element model of the canister bottom and the spacer base plate (shown in Figure 3). PLANE42 elements are used to represent the canister and the spacer base plate. The model is conservatively restrained at the center point of each cylinder wall. CONTAC52 elements are used to transmit the load from the canister bottom to the base disk. A maximum nodal stress of 13,431 psi is calculated by ANSYS.



Conservatively comparing the maximum nodal stress to the allowable membrane stress at 400°F ($S_m = 18,700$ psi), the margin of safety is:

$$MS = (18,700/13,431) - 1 = +0.39$$

2.6.19 Greater Than Class C (GTCC) Basket Analysis - Normal Conditions of Transport

The Greater Than Class C baskets for Yankee-MPC and CY-MPC configurations are evaluated against the requirements of the ASME Code, Section III, Subsection NF (component supports). This ensures that the basket components are structurally adequate for loads imposed during normal conditions of transport (presented in this Section) and hypothetical accident conditions (presented in Section 2.7.10).

2.6.19.1 Yankee-MPC GTCC Basket Analysis

The Yankee-MPC GTCC basket is designed to transport up to 24 containers of GTCC waste. The basket is constructed with 2.5-inch thick, SA240, Type 304 stainless steel plates that form walls in the general shape of a cross. A total of 8 circular disks, also of Type 304 stainless steel material with 68.98-inch diameter and 1-inch thickness, provide support to the basket wall structure. The disks are spaced 15.6 inches center-to-center and are welded to the wall structure with a circumferential fillet weld. The GTCC waste containers are positioned and supported using 24 stainless steel tubes that are located within the welded wall structure.

Each stainless steel tube has a 7.82-inch square inside dimension, a 0.25-inch thick wall, and holds one waste container. The tubes inside the basket are stacked together with a maximum of 6 tubes in a row. The basket wall and circular disks support the tubes when the canister is in the horizontal position. In the vertical orientation, the canister encloses and provides end support to the tubes.

The configuration of the Yankee-MPC GTCC basket is shown in Figure 2.6.19-1.

2.6.19.1.1 Method of Analysis of the Yankee-MPC GTCC Basket

The adequacy of the Yankee-MPC GTCC basket is evaluated in accordance with the ASME Code Section III, Subsection NF (component supports) for 1-ft side and end drops (Normal Conditions of Transport) and 30-ft side and end drops (Accident Conditions). Since the total weight of the contents of the GTCC basket configuration is less than that of the directly loaded fuel basket configuration, the decelerations (g-loads) developed in Section 2.6.7.4 are applicable to the structural evaluation. A load amplification factor of 20 g is used for the 1-ft side and end

drop analyses. Load amplification factors of 55 g and 56.1 g are used for the 30-ft side drop and 30-ft end drop accident analyses, respectively.

The minimum ratio of loads for the 30-ft and 1-ft drops is $55/20 = 2.75$. In comparing the allowables for accident condition stresses to the allowables for normal conditions of transport stresses, the maximum increase of allowable is 1.7 (NF-3341.1). Therefore, the 30-ft drop load conditions are the limiting conditions and are considered in the evaluation of the support disk and support wall of the GTCC basket in Section 2.7.10. Thus, no further evaluation of the GTCC basket support disk and support wall for normal conditions of transport is required. However, the tubes of the GTCC basket are evaluated for the 1-ft drop conditions (Normal Conditions of Transport) and presented in Sections 2.6.19.2 and 2.6.19.3. For accident conditions, the tubes are not required to remain intact since the GTCC waste will be contained within the support wall of the basket.

Based on the thermal analysis results for the Yankee-MPC GTCC basket, the ΔT across the support wall thickness is less than 2°F and the ΔT between the inner and outer surfaces of the support disk is less than 11°F . The support disk is free to expand radially and the tubes are also free to expand without any thermal restraint. Therefore, the evaluations for the GTCC basket consider impact loads only, since the thermal loads are negligible (Note that consideration for thermal effect is not required for Accident Conditions).

Conservatively, the material allowable stress values were taken at 500°F for this evaluation of the support disks and the wall structure, while stress allowables at 550°F are used for the tubes. Note that the calculated maximum component temperatures based on the thermal analysis for the GTCC basket are:

Tubes - 529°F

Support Wall Structures - 391°F

Support Disk - 389°F

The yield stress (S_y) for Type 304 stainless steel is 19.4 ksi at 500°F and 19.0 ksi at 550°F .

2.6.19.1.2 Yankee-MPC GTCC Basket Tube - End Drop Evaluation

For the end drop condition, the tubes are considered to be free standing, and the only loading is that of the tube ($5934.9/24 = 247.3$ pounds). The tubes are evaluated for a 20-g impact loading.

The tube is considered to be loaded by an axial compressive force (P):

$$P = 20(247.3) = 4,946 \text{ pounds}$$

The length of the tube is 109.8 inches and the cross sectional area of the tube is computed to be

$$A = (8.32^2 - 7.82^2) = 8.07 \text{ in}^2$$

The allowable stress, F_a , for an axially loaded compression member is given by NF-3322.1(c)(2).

$$F_a = S_y \left(0.47 - \frac{Kl/r}{444} \right) = 7,662 \text{ psi},$$

where,

$$K = 1.0 \text{ for the end conditions,}$$

$$l = 109.8 \text{ in., length of disk to shell,}$$

$$r = \sqrt{\frac{8.32^4 - 7.82^4}{12 \times 8.07}} = 3.296 \text{ (Ref. 8).}$$

Therefore, $Kl/r = 33.07 < 120$.

The allowable axial load on a tube is calculated to be

$$P_y = A F_a = (8.07)(7662) = 61,832 \text{ lb}$$

The margin of safety is computed to be

$$M.S. = \left(\frac{61,832}{4,946} \right) - 1 = +11.5$$

2.6.19.1.3 Yankee-MPC GTCC Basket Tube - Side Drop Evaluation

Similar to the end drop condition, the tubes are evaluated for a 20g side impact load. During the drop condition, the weight from the baffles and tubes is transmitted via the tube walls. Since the GTCC basket has a stack of six tubes (maximum), five tubes and their contents can be accumulated to a single tube and result in maximum compressive stresses on the tube wall. As shown in the following figure, a 1-inch section of the tube wall is considered in the structural evaluation. Knowing that the total tube length is 109.8 inches, the applied load during a 20 g normal conditions of transport impact is

$$P = \frac{(P_1 + P_2)20}{109.8} = 369 \text{ lb/in}$$

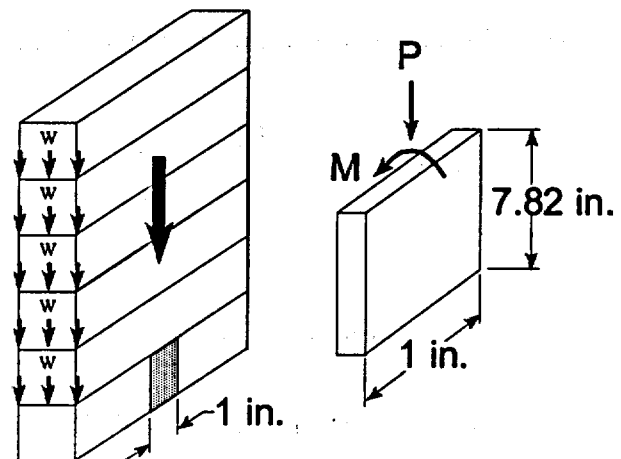
where,

$$P_1 = 12,341/24 \times 5 \times 0.5 = 1,286 \text{ lb,}$$

weight of the waste

$$P_2 = 5,935/24 \times 6 \times 0.5 = 742 \text{ lb}$$

weight of the tubes



The out-of-plane moment is considered to be ½ of the fix-end moment due to the waste weight

$$M = \left(\frac{1}{12} wL^2 \right) 0.5 = 31 \text{ in.-lb,}$$

where,

$$w = \left(\frac{12,341}{24} \right) \left(\frac{1}{109.8} \right) \left(\frac{1}{7.82} \right) 20 = 12 \text{ lb / in., the distributed load across the tube}$$

$$L = 7.82 \text{ in., tube inside width}$$

The cross-sectional area of the tube is:

$$A = (1/4)(1) = 0.25 \text{ in}^2,$$

The section modulus is:

$$S = \frac{bt^2}{6} = \frac{(1/4)^2}{6} = 0.01 \text{ in}^3.$$

The axial compressive stress due to the load P is calculated to be:

$$f_a = \frac{P}{A} = \frac{369}{0.25} = 1,476 \text{ psi},$$

and the bending stress is

$$f_b = \frac{M}{S} = \frac{31}{0.01} = 3,100 \text{ psi}.$$

From NF-3322.1(e)(1), the Euler stress divided by factor of safety is

$$F'_e = \frac{\pi^2 E}{2.15(Kl/r)^2} = \frac{\pi^2(25,800)}{2.15(108.4)^2} = 10.08 \text{ ksi}.$$

where,

K = 1.0 for the end conditions,

l = 7.82 inch, inside dimension of tube

$$r = \frac{d}{\sqrt{12}} = 0.072$$

d = 1/4 inch, thickness of tube

Therefore, $Kl/r = 108.4 < 120$.

The allowable axial compressive stress is

$$F_a = S_y \left(0.47 - \frac{KI/r}{444} \right) = 4,291 \text{ psi},$$

and the allowable bending stress is

$$F_b = 0.75 S_y = 0.75 (19,000) = 14,250$$

The combined stresses from NF-3222.1 calculated by equations (20) and (21) must be less than 1.0 to provide an adequate margin of safety.

From Equation (20):

$$\frac{f_a}{F_a} + \frac{C_m f_b}{(1 - f_a/F_a) F_b} = \frac{1,476}{4,291} + \frac{0.85(3,100)}{\left(1 - \frac{1,476}{10,080}\right) 14,250} = 0.56 < 1$$

The margin of safety is

From Equation (21):

$$\frac{f_a}{0.6 S_y} + \frac{f_b}{F_b} = \frac{1,476}{0.6(19,000)} + \frac{3,100}{14,250} = 0.35 < 1.$$

The margin of safety is:

$$M.S. = \left(\frac{1}{0.35} \right) - 1 = +1.88$$

2.6.19.2 CY-MPC GTCC Basket Analysis

The CY-MPC GTCC basket is evaluated against the requirements of the ASME Code, Section III, Subsection NF (component supports), to ensure that the basket components are structurally adequate for loads imposed during normal conditions of transport (presented in this Section) and hypothetical accident conditions (presented in Section 2.7.10).

The GTCC basket is designed to transport up to 24 containers of GTCC waste. The basket (shield shell weldment) is constructed with 2.25-inch thick SA240 Type 304 stainless steel plates that form walls in an octagon configuration. A total of 9 circular disks, also of Type 304 stainless steel material with 69.15-inch diameter and 1-inch thickness provide support to the basket wall structure. The disks are spaced 17.0 inches center-to-center and are welded to the wall structure with a circumferential fillet welds. The GTCC waste containers (tube array weldment) are positioned and supported using 24 stainless steel tubes that are located within the welded wall structure.

Each stainless steel tube has an 8.72-inch square inside dimension, a 0.25-inch thick wall, and can hold one waste container. The tubes inside the basket are stacked together with a maximum of 6 tubes in a row and are welded together around at the 12 perimeter locations. The basket wall and circular disks support the tubes when in a horizontal position. The ends of the basket are enclosed by the canister, which provides end support to tubes in case of non-horizontal configurations.

Tube Array Weldment

The tube array weldment is required to maintain structural integrity during normal conditions of transport. The tube array weldment is analyzed for 20g end drop and 20g side drop conditions.

End Drop Analysis:

The maximum compressive load for a tube weldment is the weight of the tube multiplied by 20g.

Tube weight (single tube):

$$W = (9.22^2 - 8.72^2) \times 141.5 \times 0.288 \times 20 = 7,311 \text{ lbs use } 7,500 \text{ lbs}$$

where:

9.22 inch	tube outside width
8.72 inch	tube inside width
141.5 inch	tube length
0.288 lbs/in ³	density stainless steel

The maximum compressive stress occurs at the bottom end of the tube.

Cross sectional area at the bottom of the tube:

$$A = (9.22^2 - 8.72^2) - 4 \times 3.00 \times 0.25 = 5.97 \text{ in}^2$$

where:

3.00 inch slot lengths in bottom of weldment
4 quantity of slots
0.25 tube wall thickness

Stress:

$$S = \frac{P}{A} = \frac{7,500}{5.97} \approx 1,300 \text{ psi}$$

The maximum tube weldment temperature is 595°F. Using a bounding temperature of 600°F the margin of safety for the tube weldment is:

$$MS = \frac{S_m}{S} - 1 = \frac{16,700}{1,300} - 1 = +\text{large}$$

Using NUREG/CR-6322, the buckling load for a single tube weldment is calculated. Assuming a pinned-free column ($K=2.0$), the critical buckling stress is:

$$r = \sqrt{\frac{I}{A}} = \sqrt{\frac{120.38}{8.97}} = 3.66 \text{ in.}$$

$$I = \frac{9.22^4 - 8.72^4}{12} = 120.38 \text{ in}^4$$

$$A = 9.22^2 - 8.72^2 = 8.97 \text{ in}^2$$

$$\frac{KI}{r} = \frac{2.0 \times 141.5}{3.66} = 77.32$$

$l = 141.5$ inch tube length

$$C_c = \sqrt{\frac{2\pi^2 E}{S_y}} = \sqrt{\frac{2\pi^2 24.87E6}{18,600}} = 162.6$$

$E = 24.87E6$ at $600^\circ F$

$$S_{cr} = S_y \left[1 - \frac{\left(\frac{Kl}{r} \right)^2}{2 \times C_c^2} \right] = 18,600 \left[1 - \frac{77.32^2}{2 \times 162.6^2} \right] = 16,497 \text{ psi}$$

Critical buckling load is:

$$P_{cr} = 16,497 \text{ psi} \times 8.97 \approx 148,000 \text{ lbs}$$

Factor of Safety for buckling is

$$FS = \frac{P_{cr}}{P} = \frac{148,000}{7,500} = +\text{large}$$

Note, the buckling analysis of a single tube weldment is conservative because the tube array weldment is welded together and a single tube is supported by the surrounding tubes and structure.

Side Drop Analysis

For a side-drop scenario, a three-dimensional periodic finite element model of the tube array weldment is used, Figure 2.6.19-2. The model represents an 8.50-inch segment of the weldment. The tube assemblies are constructed of SOLID45 elements. Only the outer tubes are welded together using a full-length quarter-inch v-groove weld, 12 locations. These weld joints are modeled using BEAM4 and CONTAC52 elements. The interior tubes are not welded together and are modeled with gaps between them using CONTAC52 elements and soft BEAM4 elements to prevent the BEAM4 elements from carrying load. Load is transferred by the gaps closing

between tubes. The exterior BEAM4 elements are modeled to allow load to be carried by the welded joints (Figure 2.6.19-4). The CONTAC52 elements have a stiffness, $K = 0.1E9$ lbs/in.

Boundary conditions for the finite element model are shown in Figure 2.6.19-3. Pressure loads are applied to the slots to represent the mass of the GTCC waste. For 20g, the pressure loads applied are:

$$P = \frac{1000}{8.72 \times 141.5} \times 20 = 16.2 \text{ psi for slots containing 1,000 lbs of waste}$$

$$P = 16.2 \times 1.5 = 24.3 \text{ psi for slots containing 1,500 lbs of waste}$$

Using the temperature distribution obtained from the CY-MPC GTCC thermal analysis, the tube array weldment model thermal stresses are calculated for two thermal conditions (ambient temperatures of 100°F and -40°F). Stress results are presented for primary stresses and for primary plus secondary (thermal) stresses. Four drop orientations of 45°, 60°, 75°, and 90° are considered. Stress allowables are based on the actual nodal temperature.

The minimum margins of safety for the CY-MPC GTCC are 0.37 (Table 2.6.19-1) for primary stresses and 0.10 (Table 2.6.19-2) for primary plus secondary (thermal) stresses. This worst case condition occurs at a drop angle of 90° and an ambient temperature of 100°F.

Weld Analysis

The tube array weldment tubes are welded together, structurally, around the outer perimeter only; the outer welds are quarter-inch full length fillet weld. The interior joints may be tack welded only for assembly purposes. See Figure 2.6.19-4 for typical weld locations. These tack welds are not considered in this model. Weld loads, presented in Tables 2.6.19-3 and 2.6.19-4, are obtained from the basket periodic model by obtaining the sum of the forces carried by the BEAM4 elements at each of the 12 exterior weld locations. The maximum weld load over the 8.5 in segment modeled is 14,285 lbs. The weld stress due to this loading is:

$$S_w = \frac{14,285}{(.7071 \times 0.25) \times 8.50} = 9,506 \text{ psi}$$

Assuming a bounding temperature of 600°F, the allowable weld stress for normal conditions is:

$$S_{w \text{ allow}} = 0.6 \times S_m = 0.6 \times 16,700 = 10,020 \text{ psi}$$

The margin of safety is:

$$MS = \frac{10,020}{9,506} - 1 = 0.05$$

Shield Shell Weldment

The shield shell weldment is required to maintain structural integrity during normal conditions of transport.

End Drop Analysis

During an end drop the entire weight of the shield shell weldment applies a compressive load at the base of the shell weldment. The shield shell weldment consists of the octagon shell and the nine support disks. The weight of the assembly is, conservatively:

$$W = 19,500 + 9 \times 250 = 21,750 \text{ lbs}$$

where

19,500 lbs = weight of octagon shell (19,047 lbs actual)

250 lbs = weight of support disk (222 lbs actual)

The cross sectional area of the shell weldment at the base is:

$$A = 2.25 \times [4 \times (18.28 + 22.66 - 8)] = 296 \text{ in}^2$$

The stress at the base of the assembly is:

$$S_s = \frac{20 \times 21,750}{296} = 1,470 \text{ psi}$$

For a bounding temperature of 400°F where S_m is 18,700 psi. The margin of safety is:

$$MS = \frac{18700}{1470} - 1 = +\text{large}$$

Side Drop Analysis

For a side-drop scenario, a three-dimensional periodic finite element model of the shell assembly is used, Figure 2.6.19-5. The model represents an 8.50-inch segment of the assembly. The model is constructed of SOLID45 elements. CONTAC52 elements at the periphery of the support disk are used to represent the gap between the basket and canister and the gap between the canister shell and the transport cask inner liner. The canister is conservatively not modeled.

Boundary conditions for the finite element model are shown in Figure 2.6.19-6. Pressure loads are applied as shown in Figure 2.6.19-6 to represent the weight of the loaded tube weldment (the tube array weldment weight is 11,353 lbs. and the GTCC waste weight is 20,230 lbs.). The pressure load is applied as a triangular distribution for a 45° basket orientation. The 45° basket orientation is used to maximize the bending in the shell. A triangular load distribution is used to represent the loading of the tube array on the shell.

Using the temperature distribution obtained from the CY-GTCC thermal analysis, the shell assembly model is analyzed for two thermal conditions, using ambient temperatures of 100°F and -40°F. Primary and secondary (thermal) stresses are calculated using the finite element model with a 20g acceleration for the normal condition.

The maximum primary membrane sectional stress in the shell assembly is 18.6 ksi. The allowable stress is 19.7 ksi (S_m), resulting in a margin of safety of +0.06. The maximum primary membrane plus bending sectional stress in the shell assembly is 29.4 ksi. The allowable stress is 29.5 ksi ($1.5S_m$). The margin of safety is +0.01. The maximum primary plus secondary (thermal) stress is 36.8 ksi, with an allowable stress of 59.1 ksi ($3S_m$). The margin of safety is +0.60. The allowable stresses are based on a temperature of 325°F, which is conservative with respect to the calculated maximum temperature of 318°F. The maximum stresses occur in the shell support disk.

Basket / Canister Bearing Analysis for Side Drop

The weight of a loaded CY-MPC GTCC basket is conservatively assumed to be 50,000 lbs. Using a 20g acceleration, the load on each disk is:

$$P_{\text{disk}} = \frac{50,000(20)}{9} = 111,111 \text{ lbs/disk}$$

The contact between the basket and canister is conservatively taken to be 10° (12.0 inches). The bearing stress is then:

$$S_{\text{brg}} = \frac{111,111}{12.0 \times 1.00} = 9,300 \text{ psi}$$

The margin of safety is calculated using SA-240 304L stainless steel properties at 350°F. The yield stress, at 350°F, is 18.4 ksi. Therefore, the margin of safety is:

$$MS = \frac{18.4}{9.3} - 1 = 0.98$$

No additional analysis of the CY-GTCC canister is required since the analysis of GTCC canister is bounded by the loaded fuel canister for both normal and accident conditions.

Figure 2.6.19-1 Yankee-MPC GTCC Basket Assembly

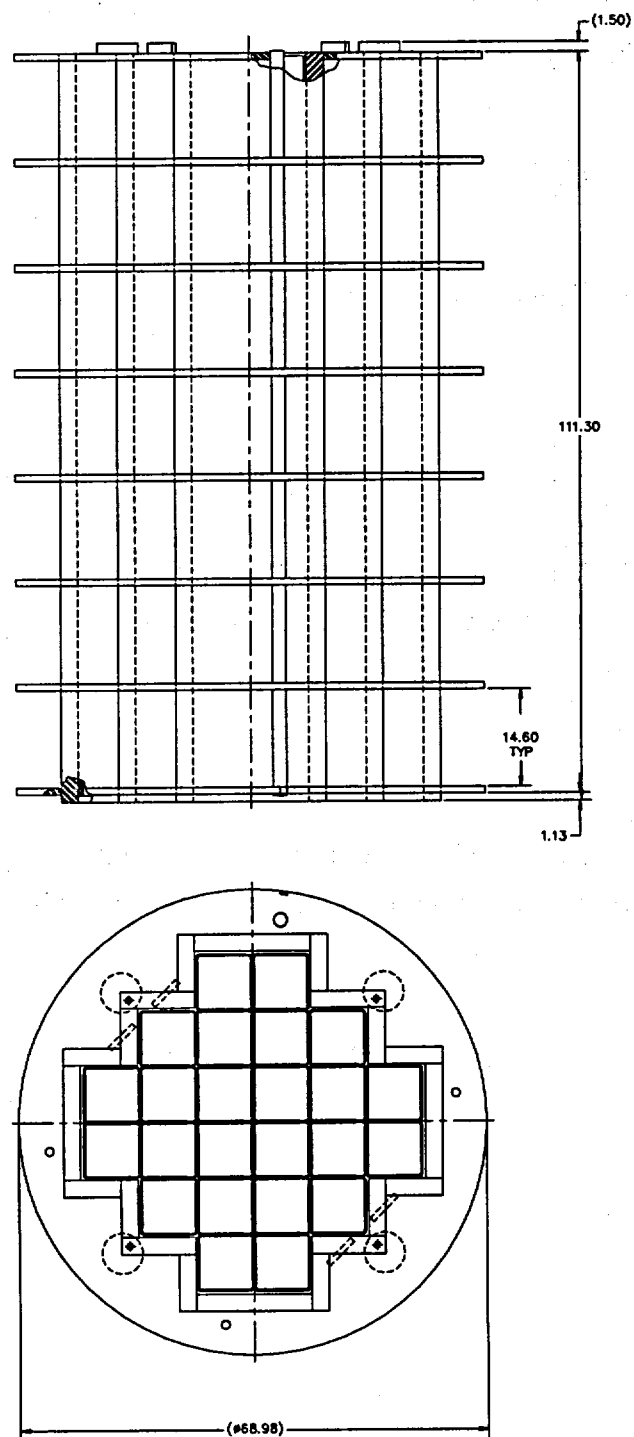


Figure 2.6.19-2 CY-MPC GTCC Basket Tube Array Weldment Finite Element Model

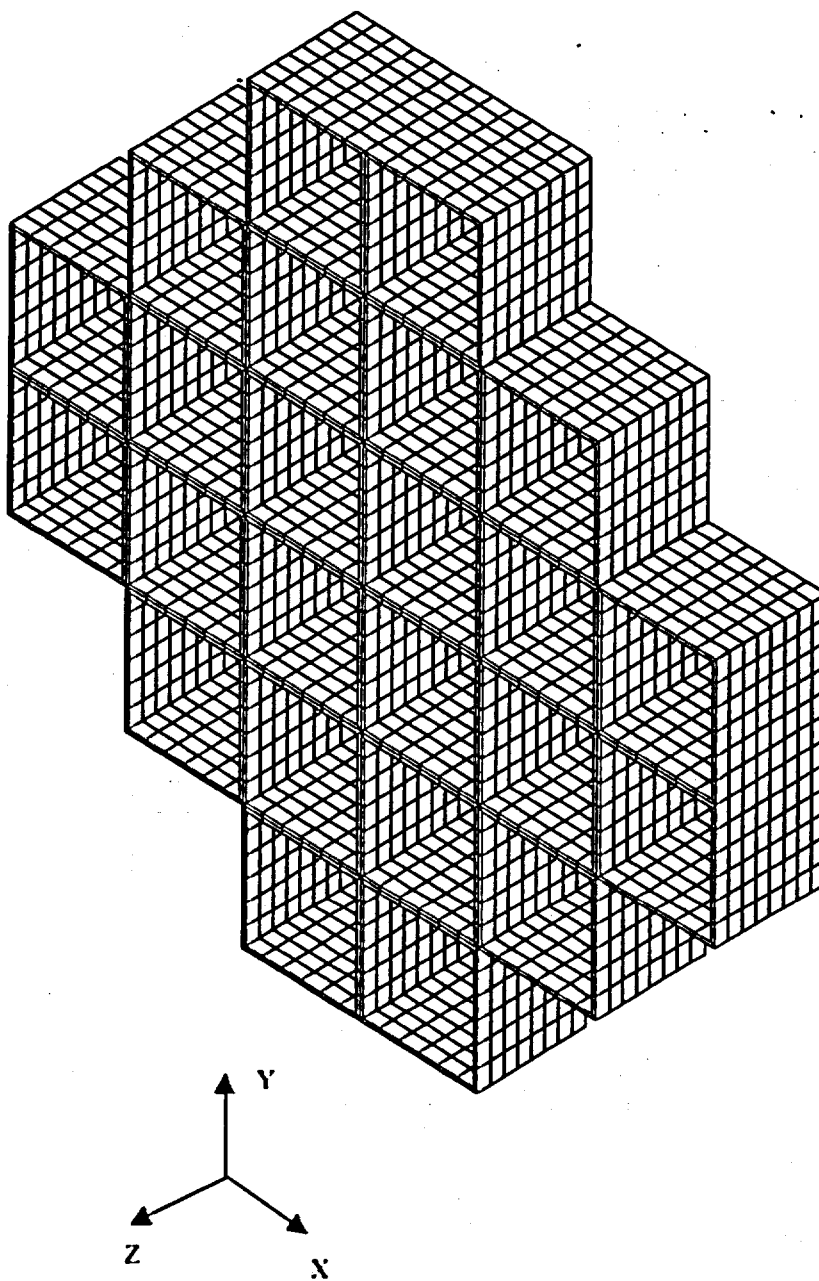
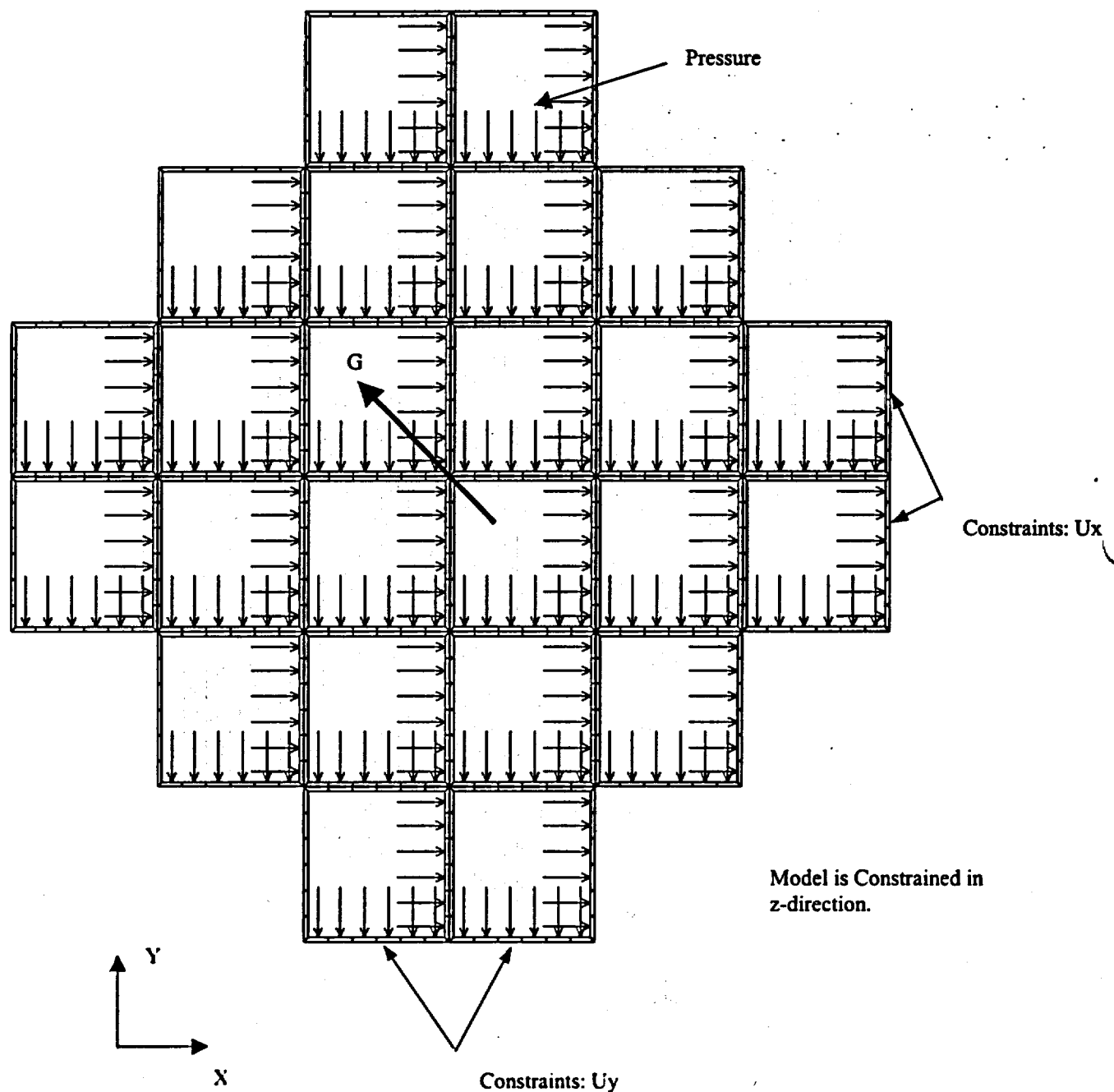
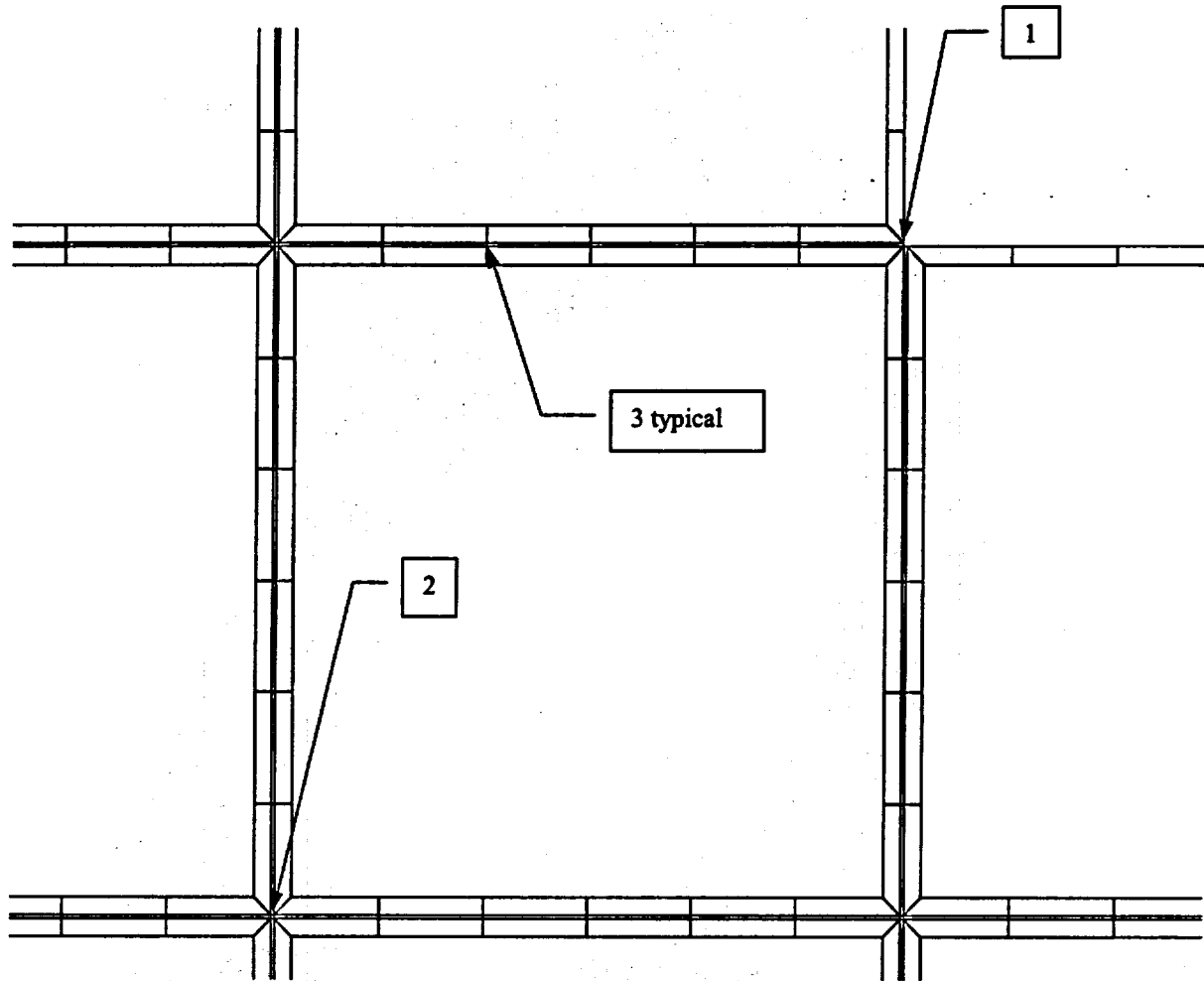


Figure 2.6.19-3 CY-MPC GTCC Tube Array Weldment Boundary Conditions (45° Impact Orientation)



Note: The vector labeled "g" corresponds to the direction of acceleration. The corresponding load is in the opposite direction, which is the direction of impact.

Figure 2.6.19-4 CY-MPC GTCC Tube Array – Typical Weldment Welds



1. Typical welded exterior joint modeled with BEAM4 and CONTAC52 elements.
2. Typical interior corner intersection modeled with soft BEAM4 and CONTAC52 elements.
3. Typical interior tube face intersection modeled with soft BEAM4 and CONTAC53 elements.

Figure 2.6.19-5 CY-MPC GTCC Basket Shield Shell Assembly Finite Element Model

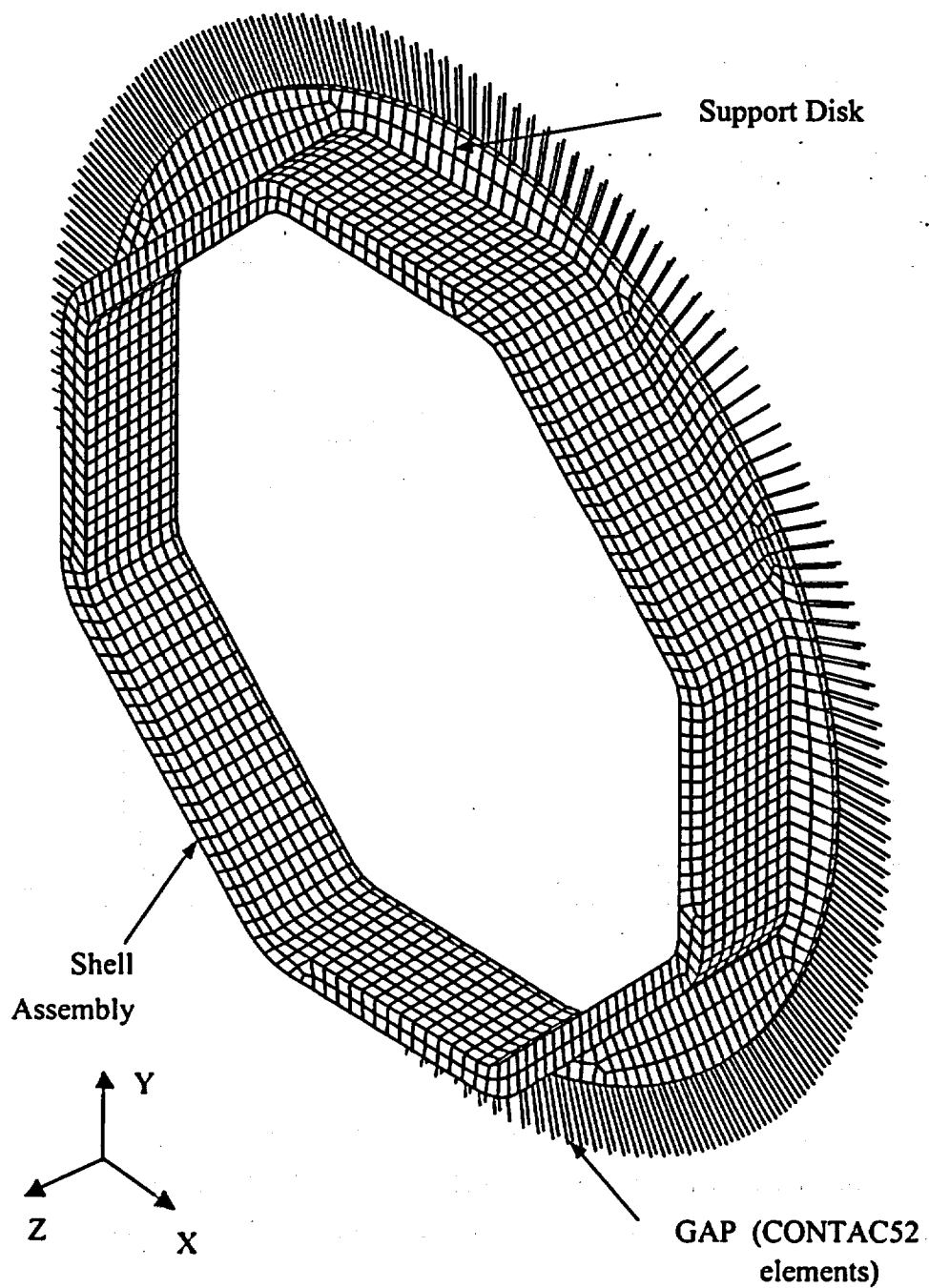


Figure 2.6.19-6 CY-MPC GTCC Basket Shield Shell Assembly Loading and Boundary Conditions

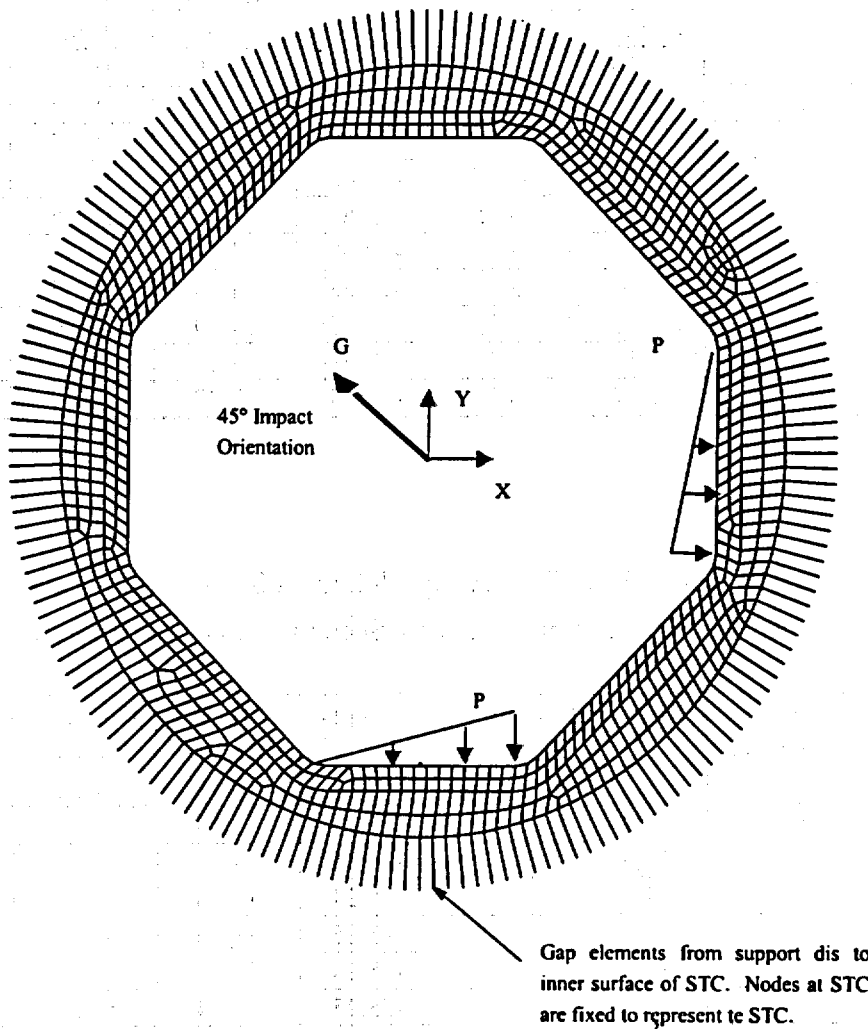


Table 2.6.19-1 CY-MPC GTCC Tube Array Weldment Stress Summary – 100°F
Ambient, Side Drop Primary Stresses

Node Number	Node Temperature (°F)	Principal Stress Components (ksi)			Stress Intensity (ksi)	Allowable Stress (ksi)	Margin of Safety
		S1	S2	S3			
21210	343.0	1.50	-3.35	-12.68	14.19	19.45	0.37
4290	341.1	1.50	-3.35	-12.68	14.19	19.47	0.37
24030	343.1	1.50	-3.35	-12.68	14.19	19.45	0.37
1470	340.9	1.50	-3.35	-12.68	14.19	19.47	0.37
18390	342.8	1.50	-3.35	-12.68	14.19	19.45	0.37
7110	341.4	1.50	-3.35	-12.68	14.19	19.47	0.37
15570	342.6	1.50	-3.35	-12.68	14.19	19.45	0.37
9930	341.8	1.50	-3.35	-12.68	14.19	19.46	0.37
12750	342.2	1.50	-3.35	-12.68	14.19	19.46	0.37
4995	341.1	1.47	-3.31	-12.49	13.97	19.47	0.39

Table 2.6.19-2 CY-MPC GTCC Tube Array Weldment Stress Summary – 100°F
Ambient, Side Drop Primary + Secondary (Thermal) Stresses

Node Number	Node Temperature (°F)	Principal Stress Components (ksi)			Stress Intensity (ksi)	Allowable Stress (ksi)	Margin of Safety
		S1	S2	S3			
18390	342.8	37.91	1.87	-15.25	53.16	58.34	0.10
21210	343.0	37.91	1.87	-15.25	53.16	58.34	0.10
15570	342.6	37.91	1.87	-15.24	53.16	58.35	0.10
24030	343.1	37.91	1.87	-15.25	53.16	58.34	0.10
12750	342.2	37.92	1.87	-15.24	53.15	58.37	0.10
9930	341.8	37.91	1.87	-15.23	53.14	58.38	0.10
7110	341.4	37.91	1.87	-15.21	53.12	58.40	0.10
4290	341.1	37.91	1.87	-15.18	53.09	58.41	0.10
1470	340.9	37.91	1.87	-15.15	53.06	58.42	0.10
24735	343.1	37.93	1.84	-15.11	53.04	58.33	0.10

Table 2.6.19-3 CY-MPC GTCC Tube Array Weld Loads (lbs), Normal Conditions - 100°F
Ambient Temperature

Structural Weld Load												
	Weld Number											
Drop	1	2	3	4	5	6	7	8	9	10	11	12
45	1684	10733	2696	1743	2055	2046	1724	2698	10987	5317	8638	8485
60	1609	8074	2366	1226	2056	1937	2099	2877	12992	5482	11282	5681
75	1429	4825	1915	611	1912	1743	2351	2860	14115	5215	13232	3161
90	984	1453	1544	127	1545	1470	2430	2652	14211	4628	14285	2559
Structural + Thermal Weld Load												
	Weld Number											
Drop	1	2	3	4	5	6	7	8	9	10	11	12
45	1296	9227	3958	1641	2471	2804	1634	4156	8841	5287	7271	7473
60	1220	6580	3724	1183	2552	2681	1986	4250	10836	5460	9428	5369
75	1041	4036	3345	754	2471	2512	2228	4238	11954	5203	11074	3269
90	596	2304	2872	736	2860	2320	2304	4120	12047	4631	12120	3915

Table 2.6.19-4 CY-MPC GTCC Tube Array Weld Loads (lbs), Normal Conditions - -40°F
Ambient Temperature

Structural Weld Load												
	Weld Number											
Drop	1	2	3	4	5	6	7	8	9	10	11	12
45	1684	10733	2696	1743	2055	2046	1724	2698	10987	5317	8638	8485
60	1609	8074	2366	1226	2056	1937	2099	2877	12992	5482	11282	5681
75	1429	4825	1915	611	1912	1743	2351	2860	14115	5215	13232	3161
90	984	1453	1544	127	1545	1470	2430	2652	14211	4628	14285	2559
Structural + Thermal Weld Load												
	Weld Number											
Drop	1	2	3	4	5	6	7	8	9	10	11	12
45	1243	9053	4156	1641	2558	2925	1631	4368	8610	5284	7242	7489
60	1168	6466	3916	1194	2642	2802	1976	4461	10601	5459	9258	5377
75	987	4043	3540	799	2628	2645	2217	4454	11717	5203	10900	3274
90	543	2453	3071	806	3058	2466	2292	4336	11808	4632	11880	4131

THIS PAGE INTENTIONALLY LEFT BLANK

2.7 Hypothetical Accident Conditions

The NAC-STC is required to be structurally adequate for the free drop, puncture, fire, crush, and water immersion hypothetical accident scenario in accordance with 10 CFR 71.73. In the free drop analyses, the cask impact orientation evaluated must be that which inflicts the maximum damage to the cask. The cask accident assessment must also be at the most unfavorable ambient temperature in the range from -20°F to 100°F. Likewise, for the Yankee-MPC and CY-MPC canistered fuel or GTCC waste configurations, the NAC-STC has been evaluated for structural adequacy, considering the inclusion of the transportable storage canister in the free drop, puncture, fire, crush, and water immersion hypothetical accident scenario in accordance with 10 CFR 71.73. Where bounded by the directly loaded fuel (uncanistered) configuration analyses, the analyses sections are so noted. The following subsections contain the evaluation of the NAC-STC for structural integrity under hypothetical accident conditions.

NAC-STC Directly Loaded Fuel and Yankee-MPC

After the NAC-STC cask body structural analyses were completed, the cask closure geometry, the fuel basket design and the heat transfer analyses were subsequently reanalyzed. Two- and three-dimensional structural analyses of the cask discussed in this section and summarized in the tables presented in Section 2.10.4 are not influenced by the localized changes to the closure system, the basket design, or the heat transfer analysis and thus, have not been revised to incorporate these design and analyses enhancements.

The revised heat transfer analyses are presented in Chapter 3 for the NAC-STC. Section 2.10.10 presents a comparison of temperature gradients obtained from the original and the revised heat transfer analyses for the NAC-STC and an evaluation of conservative margins of safety identified using original temperature distributions in the cask structural qualification. It has been concluded from the evaluation in Section 2.10.10 that the detailed finite element analyses performed for normal and accident condition loads using the original temperature distribution are conservative. Therefore, the detailed finite element analyses for the NAC-STC have not been changed to incorporate the revised temperature distribution.

Temperature distributions for both normal and accident conditions were recalculated as a result of improvements in the modeling of the boundary conditions used in the heat transfer analyses and design changes made to the fuel basket. These boundary condition improvements better reflect actual conditions than those originally modelled in the cask thermal analyses. The most

significant revisions to the boundary conditions included modeling the gap between the basket and inner shell, and consideration of an adiabatic surface for the area of the cask covered by the impact limiter.

The revised thermal analysis resulted in reduced thermal gradients and the associated secondary stresses applicable to the normal condition structural qualification throughout the cask, and increased the maximum component temperature in the regions of the cask influenced by the insulating effect of the impact limiter (Section 2.10.10). Based on the fact that accident condition structural criteria are based on primary membrane and primary bending stresses, changes in temperature do not create higher stresses in the cask for structural evaluation accident condition loads. Therefore, the resulting influence of the increase in component temperature on the stress qualification is limited to reducing the temperature dependent material allowable stresses. Revisions to the hypothetical accident conditions structural qualification of the cask that result from the newly calculated temperatures are presented as changes in the allowable stresses and the margins of safety in the stress summary tables in Section 2.10.4.

Impact Limiters

As described in Sections 2.3.7 and 2.6.7.4, two impact limiter designs are used with the NAC-STC cask. The redwood impact limiters described in License Drawings 423-209 and 423-210 may be used with the directly loaded fuel and the Yankee-MPC canistered fuel and GTCC waste configurations. The balsa impact limiters described in License Drawings 423-257 and 423-258 must be used with the NAC-STC cask transporting the CY-MPC canistered fuel and GTCC waste configurations, but may also be used in the transport of directly loaded fuel and the Yankee-MPC canistered fuel and GTCC waste configurations.

2.7.1 Free Drop (30 Feet)

The NAC-STC is required by 10 CFR 71.73(c)(1) to demonstrate structural adequacy for a free drop through a distance of 30 feet onto a flat, unyielding, horizontal surface. The cask strikes the surface in an orientation that inflicts maximum damage. In determining which orientation produces the maximum damage, the NAC-STC is evaluated for impact orientations in which the cask strikes the impact surface on its top end, top end oblique, side, bottom end, and bottom end oblique. The redwood and balsa impact limiters and the impact limiter attachments are evaluated in Section 2.6.7.4 for all loading conditions.

Impacts with the maximum and minimum weights of contents are considered. The environmental temperature for the drop is between -20°F and 100°F. Internal heat generation from the contents and solar heating are also considered. Regarding internal pressure, the maximum or minimum normal transport pressure is applied to produce the critical stress condition in conjunction with the other loads previously discussed. Closure lid bolt preload and fabrication stresses are also considered.

The following method and assumptions are adopted in all of the drop analyses:

1. The finite element method is utilized to do the impact analyses. The analyses are performed using the ANSYS computer program.
2. The analyses assume linearly elastic behavior of the cask.
3. The impact loads calculated in Section 2.6.7.4 are statically applied to the impact surface of the cask. The dynamic wave propagation produced by the impact is assumed to spread throughout the cask body simultaneously.
4. The finite element model of the NAC-STC includes only the major structural components of the cask body; thus, the weight of the modeled cask body does not include the weight of the neutron shield material, the neutron shield shell, nor the cavity contents. However, the applied loads on the cask model are based on a cask design weight of 250,000 pounds for the directly loaded and Yankee-MPC configurations, and of 260,000 pounds for the CY-MPC configurations.

5. To account for the lead slump during the drops, and for the differential thermal expansion between the cask stainless steel shells and lead shell, gap elements are used in the finite element model.
6. For the Yankee-MPC and CY-MPC designs, which include a transportable storage canister in the NAC-STC, the same load scenarios, methods and assumptions have been considered.
7. The drop scenarios for the canistered Yankee-MPC class design with spent fuel bound the canistered Yankee-MPC with GTCC contents, as the latter configuration has a lower weight.
8. The redwood impact limiters and the balsa impact limiters are designed to limit the g-loads applied to the NAC-STC to the same values.

The types of loading considered in the accident condition analyses include: (1) thermal, (2) internal pressure, (3) closure lid bolt preload, and (4) impact and inertial loads resulting from the impact event. These loadings and the boundary conditions, used in the finite element analyses, are discussed in Sections 2.7.1.1 through 2.7.1.4. Section 2.10 documents the procedures, analysis and stress results for the 30-foot drop accident conditions.

Note that the fabrication stresses are considered negligible as explained in Section 2.6.11. The puncture analysis is performed using classical hand calculations, as shown in Section 2.7.2.

2.7.1.1 Thirty-Foot End Drop

The NAC-STC is structurally evaluated for the hypothetical accident 30-foot end drop condition in accordance with the requirements of 10 CFR 71.73(c)(1). In this evaluation, the directly loaded NAC-STC (equipped with an impact limiter over each end) falls through a distance of 30 feet onto a flat, unyielding, horizontal surface. The cask strikes the surface in a vertical position; consequently, an end impact on the bottom end or top end of the cask occurs. The types of loading involved in an end drop accident are closure lid bolt preload, internal pressure, thermal, impact load, and inertial body load. There are six credible end impact conditions to be considered, according to Regulatory Guide 7.8:

1. Top end drop with 100°F ambient temperature, maximum decay heat load, and maximum solar insolation.
2. Top end drop with -20°F ambient temperature, maximum decay heat load, and no solar insolation.
3. Top end drop with -20°F ambient temperature, no decay heat load, and no solar insolation.
4. Bottom end drop with 100°F ambient temperature, maximum decay heat load, and maximum solar insolation.
5. Bottom end drop with -20°F ambient temperature, maximum decay heat load, and no solar insolation.
6. Bottom end drop with -20°F ambient temperature, no decay heat load, and no solar insolation.

2.7.1.1.1 Thirty-Foot End Drop—NAC STC Directly Loaded and Yankee-MPC Configurations

The finite element analysis method is utilized to perform the end drop stress evaluations for the NAC-STC. The end drop accident condition can be analyzed using a two-dimensional axisymmetric model, because of the symmetry of both the cask structure and the loads involved in the end drop case. The cask is modeled as an axisymmetric structure using ANSYS STIF42

isoparametric elements. A detailed description of the two-dimensional finite element model of the NAC-STC is provided in Section 2.10.2.1.1.

During an impact event, the cask body will experience a vertical deceleration. Considering the cask as a free body, the impact limiter will apply the load to the cask end to produce the deceleration. Since the deceleration represents an amplification factor for the inertial loading of the cask, the equivalent static method is adopted to perform the impact evaluations. The analyses consider the behavior of the cask to be linearly elastic. Additionally, the fabrication stresses are considered to be negligible (Section 2.6.11).

Five categories of load--closure lid bolt preload, internal pressure, thermal, impact, and inertial body loads--are considered on the cask:

1. Closure lid bolt preload - The required total bolt preload on the inner lid bolts is 4.51×10^6 pounds. For the outer lid bolts, the total bolt preload is 6.02×10^5 pounds. Individual bolt preload is applied to the model by imposing initial strains to the bolt shafts, as explained in Section 2.10.2.2.3. The bolts are modeled as beam (ANSYS STIF3) elements.
2. Internal pressure - The cask internal pressure is temperature dependent and is evaluated in Section 3.4.4. Pressures of 50 psig and 12 psig are applied on the interior surfaces of the cask cavity for the hot ambient and cold ambient cases, respectively. These pressures envelope the calculated pressures for cask configurations - directly loaded fuel (12 psig), Yankee-MPC canistered fuel (11.3 psig), and Yankee-MPC canistered GTCC waste (<11.3 psig).
3. Thermal - The heat transfer analyses performed in Sections 3.4.2 and 3.4.3 determine the cask temperature distributions for the following three combinations of ambient temperature, heat load, and solar insolation for directly loaded fuel.

Condition 1. 100°F ambient temperature, with maximum decay heat load, and maximum solar insolation.

Condition 2. -20°F ambient temperature, with maximum decay heat load, and no solar insolation.

Condition 3. -20°F ambient temperature, with no decay heat load, and no solar insolation.

The cask temperatures calculated for each of the three thermal conditions discussed above are used in the ANSYS structural analyses to determine the values of the temperature-dependent material properties.

Additional heat transfer analyses were performed for the Yankee-MPC canistered fuel configuration as described in Section 2.6.7.1.

4. Impact loads - The impact loads are induced by the impact limiter acting on the cask end during an end drop condition. The impact loads are determined from the energy absorbing characteristics of the impact limiters, as described in Section 2.6.7.4. The impact load is expressed in terms of the design cask weight (loaded or empty), multiplied by appropriate deceleration factors (g's). For details, see Section 2.6.7.4.

The impact limiter load is considered to be uniformly applied over the end surface of the finite element model of the cask. The calculation of impact pressure loads is documented in Section 2.10.2.2.2. The following is a summary of the impact pressures applied to the exterior surface of the impacting end, for the different loading scenarios, with the corresponding design deceleration (g) values.

<u>LOADING CONDITION</u>	<u>IMPACT PRESSURE FOR 1g</u>	<u>DECELERATION (g)</u>
End impact with basket and fuel	42.35 psi	56.1
End impact with basket, no fuel	35.74 psi	49.4

For the end impact, with basket and fuel, a uniform pressure of 2376 psi ($[42.35 \text{ psi}][56.1 \text{ g}/1\text{g}]$) is applied on the exterior surface of the end of the finite element model of the cask.

This pressure value is calculated by dividing the total impact load ($[56.1 \text{ g}/1\text{g}][250,000 \text{ lb}] = 14.03 \times 10^6 \text{ lb}$) by the impact area ($p \times (43.35)^2 = 5903.8 \text{ in}^2$), which is the surface area of the end of the cask.

It should be noted that the design weight of the cask is 250,000 pounds, which includes the weight of the empty cask with impact limiters (194,000 lb), plus the weight of the cavity contents (56,000 lb) for the directly loaded fuel configuration. For those load conditions for which the cask contains no fuel, the basket (design weight = 17,000 lb) is still considered to be in the cask, resulting in a weight of 211,000 pounds for the empty cask with basket. The weights of the cavity contents for the Yankee-MPC canistered fuel and the Yankee-MPC canistered GTCC waste configurations are 55,590 pounds and 54,271 pounds, respectively.

5. Inertial body load - The inertial effects, which occur during the end impact, are represented by equivalent static forces, in accordance with D'Alembert's principle. Inertial body load includes the weight of the empty cask (194,000 lb) and the weight of the cavity contents (56,000 lb) for the directly loaded fuel configuration, which envelopes that of the Yankee-MPC canistered fuel or the Yankee-MPC canistered GTCC waste.

Inertia loads resulting from the weight of the empty cask are imposed by applying an appropriate deceleration factor to the cask mass. The applied decelerations are determined by considering the crush strength and the geometry of the impact limiters, as explained in Section 2.6.7.4.

The inertial load resulting from the 56,000-pound contents design weight is represented as an equivalent static pressure load uniformly applied on the interior surface of the impacting end of the cask. For the load case with no fuel in the cavity, the basket (design weight = 17,000 lb) is considered to be in the cask; the weight of the basket is represented in the ANSYS finite element model in the same manner as that of the contents.

The following is a summary of the inertial body load for a 1g deceleration and the design decelerations for the different loading scenarios. The calculations of content pressures is documented in Section 2.10.2.2.1.

<u>LOADING CONDITION</u>	<u>IMPACT PRESSURE DECELERATION</u>	
	<u>FOR 1g</u>	<u>(g)</u>
End impact with basket and fuel	14.14 psi	56.1
End impact with basket, no fuel	4.29 psi	49.4

In the ANSYS analyses, the inertial body loads are considered together with the impact loads. The results of the two simultaneous loadings are documented as "impact loads."

In all cases, the 30-foot end drop load condition for the canistered Yankee class fuel configuration is bounded by the analyses of the directly loaded fuel configuration. The primary basis for the validity of that statement is that the NAC-STC, with canistered Yankee class fuel, weighs essentially the same as the NAC-STC with directly loaded PWR fuel. Therefore, the crush deceleration from the cask impact limiters for the Yankee-MPC canistered configuration will be essentially equal to that for the NAC-STC directly loaded fuel configuration. The aluminum honeycomb cavity spacers' crush strength is less than that of the impact limiter redwood/balsa design so the spacers will crush first, providing initial deceleration prior to that produced by the impact limiters.

The primary stresses throughout the cask body are calculated for individual and combined loading conditions, for the directly loaded fuel configuration, which envelopes the Yankee-MPC canistered configuration. The individual primary loading conditions are: (1) internal pressure (including bolt preload); (2) top end impact (impact load only); and (3) bottom end impact (impact load only). The combined loading conditions for primary stress evaluations are the: (1) 30-foot top end impact with bolt preload and 50 psig internal pressure; (2) 30-foot top end impact with bolt preload and 12 psig internal pressure; (3) 30-foot top end impact (without contents) with bolt preload and 12 psig internal pressure; (4) 30-foot bottom end impact with bolt preload and 50 psig internal pressure; (5) 30-foot bottom end impact with bolt preload 12 psig internal pressure; and (6) 30-foot bottom end impact (without contents) with bolt preload and 12 psig internal pressure.

Because axisymmetry exists in the cask geometry and in the end-drop loading conditions, axisymmetric boundary conditions are represented in the formulation of the isoparametric elements. A longitudinal support is imposed on the corner node located in the non-impacting end of the cask, to prevent rigid body motion. When the cask system is in equilibrium (i.e., the inertial body loads match the impact loads exactly), then the reaction force at this support will be zero. An examination of the magnitude of the reaction forces provides a check of the validity of the finite element evaluation for the 30-foot end drop condition. The reaction at the longitudinal support is 2,582 pounds/radian for the 56.1g top end drop load condition. This means that the unbalanced force of the cask model system is only $(2582)(2\pi)/56.1 = 289$ pounds. Compared to

the cask design weight of 250,000 pounds, the unbalanced force is negligible, amounting to only 0.12 percent of the design weight of the cask.

The allowable stress limit criteria, for containment and noncontainment structures, are provided in Section 2.1.2. These criteria are used to determine the allowable stresses for each cask component, conservatively using the maximum operating temperature within a given component to determine the allowable stress throughout that component. Note that higher temperatures result in lower allowable stresses.

Stress results for the individual loading cases of internal pressure (including bolt preload) are documented in Tables 2.10.4-1 and 2.10.4-2. Stress results for the individual 30-foot top and bottom end drop impact loading cases are documented in Tables 2.10.4-13 and 2.10.4-14. These are nodal stress summaries obtained from the finite element analysis results. As described in Section 2.10.4, the nodal stresses are documented on the representative section cuts. Stress results for the combined loading conditions discussed above are documented in Tables 2.10.4-112 through 2.10.4-129. These tables document the primary, primary membrane (P_m), primary membrane plus primary bending ($P_m + P_b$), and critical P_m and $P_m + P_b$ stresses in accordance with the criteria presented in Regulatory Guide 7.6. As described in Sections 2.10.2.3 and 2.10.2.4, procedures have been implemented to document the nodal and sectional stresses as well as to determine the critical (maximum) stress summary for all cask components.

For the top end impact loading case, the maximum calculated membrane stress intensity is 12.6 ksi. The maximum calculated membrane plus bending stress intensity is 34.4 ksi. By comparison, for the combined loading case, including impact, bolt preload, and internal pressure; the maximum calculated primary membrane stress intensity is 16.4 ksi and the maximum calculated primary membrane plus primary bending stress intensity is 38.5 ksi. The maximum stress intensities due to impact alone are equal to 90 percent of the maximum primary stress intensities due to the combined loading. Therefore, it is concluded that the impact stresses are the governing factor for the 30-foot top end drop condition.

For the 30-foot top end drop scenario, ANSYS analyses were performed at the three different temperature conditions. The results from those three analyses show that the maximum $P_m + P_b$ stress intensities are 37.1 ksi, 38.5 ksi, and 36.2 ksi, as listed in respective Tables 2.10.4-116, 2.10.4-118 and 2.10.4-120.

These three stress results are essentially identical, with the difference between them being less than 6 percent. Since the allowable stress for a component is a function of the component temperature, with higher temperatures resulting in lower allowable stresses, the allowable stress will be lowest for temperature condition 1 because the highest component temperatures occur for condition 1. Therefore, it is concluded that the stress results from temperature condition 1 are the most critical for the end drop accident conditions. The allowable stresses for temperature condition 1 are conservatively used for all of the temperature condition analyses.

A similar set of ANSYS analyses was performed for the 30-foot bottom end drop case. The stress results follow the same pattern as the top end drop. The maximum $P_m + P_b$ stress intensities for the 30-foot bottom end drop are 22.7 ksi, 23.1 ksi, and 21.7 ksi, as listed in Tables 2.10.4-125, 2.10.4-127, and 2.10.4-129, respectively.

As shown in Tables 2.10.4-112 through 2.10.4-129, the margins of safety are positive for all of the end drop accident conditions. The most critically stressed component in the system is the inner lid, for the top end drop. The minimum margin of safety for the top end drop condition is found to be +0.8, as documented in Table 2.10.4-118. The minimum margin of safety for the bottom end drop condition is found to be +1.8, as documented in Table 2.10.4-127.

Satisfaction of the extreme total stress intensity range limit is demonstrated in Section 2.1.3.3. The documentation of the NAC-STC adequacy in satisfying the buckling criteria for the stresses of the end drop condition is presented in Section 2.10.5.

The NAC-STC maintains its containment capability and therefore satisfies the requirements of 10 CFR 71.73 for the hypothetical accident 30-foot end drop condition for the directly loaded fuel configuration, which envelopes the Yankee-MPC canistered fuel and Yankee-MPC canistered GTCC waste configurations for the 30-foot end drop conditions.

2.7.1.1.2 Thirty-Foot End Drop—CY-MPC Configuration

The NAC-STC loaded with the CY-MPC fuel basket is structurally evaluated for the hypothetical accident 30-foot end drop condition in accordance with the requirements of 10 CFR 71.73(c)(1). In this evaluation, the NAC-STC equipped with an impact limiter over each end and loaded with a CY-MPC canister, falls through a distance of 30 feet onto a flat, unyielding, surface.

The finite element analysis method is utilized to perform the end drop stress evaluations for the CY-MPC. With the exception of the loading, the CY-MPC model is the same as the model used to evaluate the Yankee-MPC. A description of the model is included in Section 2.10.2.1.1.

Boundary Conditions—CY-MPC Configuration End Drop Analysis

The maximum internal pressure for the CY-MPC system is 38.1 psig as shown in Section 3.4.4. Since the maximum internal pressure is less than the 50 psig design pressure used for the analyses presented in Sections 2.6 and 2.7, the analyses presented in Sections 2.6 and 2.7 bound the CY-MPC system.

Two cold environment cases are considered. The first case includes -40 °F ambient temperature, no solar insolation, maximum decay heat, and maximum internal pressure. Component temperatures for this case are less than the temperatures used for the NAC-STC analysis. Therefore, the Yankee-MPC analysis envelops the CY-MPC design. The second case, or minimum temperature condition, assumes -40°F ambient temperature, no solar insolation, no decay heat, and maximum internal pressure. An evaluation of the minimum temperature condition is not required since all component temperatures are at -40°F.

For the bottom and top end drops, a surface pressure load equivalent to the weight of the loaded canister and spacer (67,200 lb.) is applied to either the cask bottom or canister lid. The process for applying the pressure load is described in detail in Section 2.10.2.2.1. The pressure load is multiplied by an acceleration of 56.1g to account for the total impact load.

The allowable stress limit criteria, for containment and noncontainment structures, are provided in Section 2.1.2. These criteria are used to determine the allowable stresses for each cask component, conservatively using the maximum operating temperature within a given component to determine the allowable stress throughout that component. Note that higher temperatures result in lower allowable stresses.

Results—CY-MPC Configuration End Drop Analysis

Maximum stress intensities are obtained for the sections shown in Figure 2.7.1.1-1. The coordinate of each section is presented in Table 2.7.1.1-1. Tables 2.7.1.1-2 through 2.7.1.1-5 provide a stress summary at each of the sections listed in Table 2.7.1.1-1. As shown in Tables 2.7.1.1-2 through 2.7.1.1-5, the margins of safety are positive for all of the end drop accident conditions. The most critically stressed component in the system is the outer lid, for the top end

drop. The minimum margin of safety for the top end drop condition is found to be +1.2, as documented in Table 2.7.1.1-2. The minimum margin of safety for the bottom end drop condition is found to be +0.06 and occurs in the bottom plate, as documented in Table 2.7.1.1-5. These stresses occur at the center of the end plate and are artificially high due too the presence of a small hole modeled in the ends (ANSYS modeling technique).

The NAC-STC maintains its containment capability and therefore satisfies the requirements of 10 CFR 71.73 for the hypothetical accident 30-foot side drop condition for the CY-MPC fuel configuration, which envelopes the canistered fuel and canistered GTCC waste configurations for the 30-foot side drop conditions

Figure 2.7.1.1-1 Location of Sections for CY-MPC Configuration Stress Evaluation

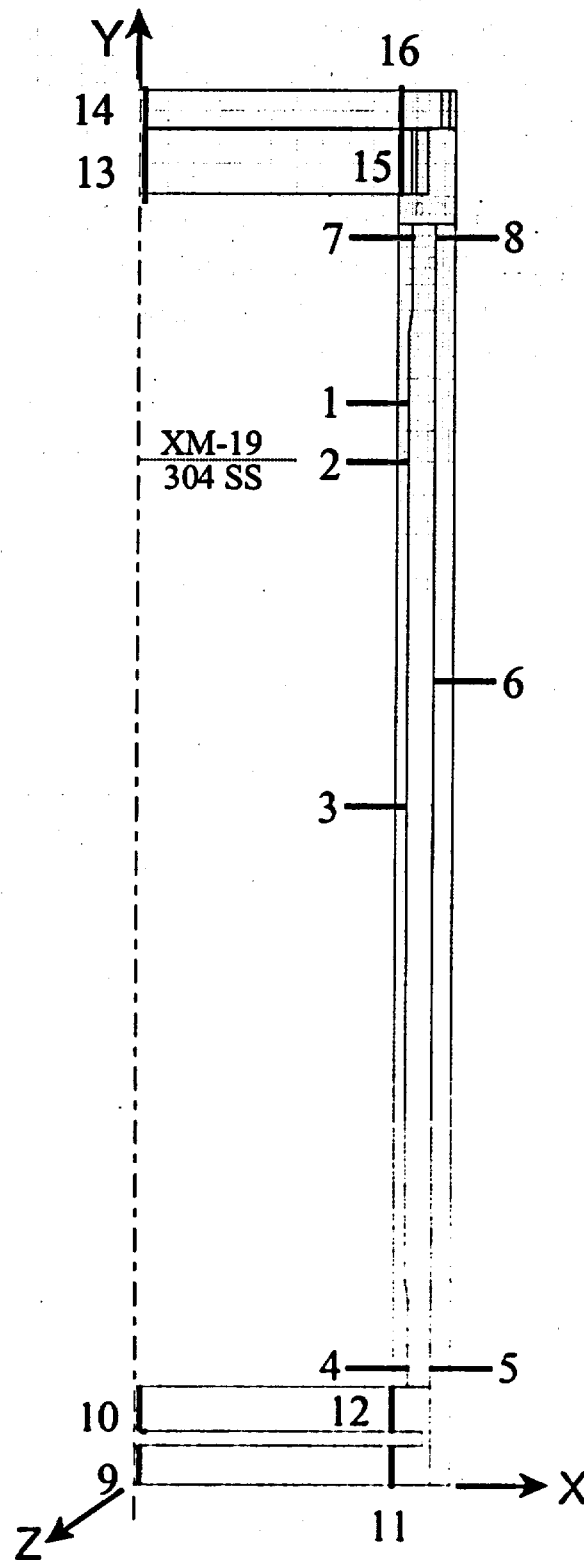


Table 2.7.1.1-1 NAC-STC Section Locations for CY-MPC Stress Evaluation (Maximums)

Section No.	Component Name and Material	Section Location (in.)							
		Inside Node	X	Y	Z	Outside Node	X	Y	Z
1	Transition Shell – XM-19	197	35.5	146.1	0.0	165	37	146.1	0.0
2*	Inner Shell – 304	196	35.5	142.0	0.0	164	37	142.0	0.0
3	Inner Shell – 304	189	35.5	94.2	0.0	157	37	94.2	0.0
4	Bottom Forging – 304	130	35.5	14.5	0.0	123	38	14.5	0.0
5	Outer Shell – 304	280	40.7	14.5	0.0	328	43	14.5	0.0
6	Outer Shell – 304	300	40.7	103.2	0.0	358	43	103.2	0.0
7	Top Forging – 304	271	35.5	173.2	0.0	265	37.5	173.2	0.0
8	Top Forging – 304	317	40.7	173.2	0.0	435	43.4	173.2	0.0
9	Bottom Plate – 304	1	0.5	0.0	0.0	6	0.5	5.45	0.0
10	Bottom Forging – 304	10	0.5	7.45	0.0	16	0.5	13.65	0.0
11	Bottom Plate – 304	22	35.5	0.0	0.0	32	35.5	5.45	0.0
12	Bottom Forging – 304	52	35.5	7.45	0.0	62	35.5	13.65	0.0
13	Inner Lid – 304	484	0.5	178.68	0.0	786	0.5	187.65	0.0
14	Outer Lid – 17-4	510	0.5	187.68	0.0	499	0.5	192.96	0.0
15	Inner Lid – 304	485	35.5	178.68	0.0	796	35.5	187.65	0.0
16	Outer Lid – 17-4	497	35.5	187.68	0.0	495	35.5	192.96	0.0

* This section is at the boundary of transition shell and inner shell.

Table 2.7.1.1-2 NAC-STC Critical P_m Stress Summary for CY-MPC; 30-ft Top End Drop

Section No.	P_m Stresses (ksi)						Stress Intensity Impact (ksi)	Stress Intensity Bolt Preload + Pressure** (ksi)	Stress Intensity Total (ksi)	Allowable Stress* (ksi)	Margin of Safety
	S_x	S_y	S_z	S_{xy}	S_{yz}	S_{xz}					
1	0.0	-4.4	0.0	0.0	0.0	0.0	4.4	1.9	6.3	65.2	9.3
2	0.0	-4.3	0.0	0.0	0.0	0.0	1.6	1.9	3.5	45.9	12.1
3	0.0	-3.5	0.0	0.0	0.0	0.0	3.5	1.9	5.4	45.9	7.5
4	-0.1	-1.5	0.5	-0.2	0.0	0.0	2.0	1.9	3.9	45.9	10.8
5	0.0	-0.6	0.4	0.0	0.0	0.0	1.1	1.9	3.0	45.9	14.3
6	0.0	-3.5	0.8	0.0	0.0	0.1	4.3	1.9	6.2	45.9	6.4
7	-0.5	-3.6	-0.5	0.1	0.0	-0.1	3.2	1.9	5.1	45.9	8.0
8	-0.3	-5.7	-0.1	-0.5	0.1	0.1	5.6	1.9	7.5	45.9	5.1
9	-0.1	-0.1	-1.1	0.0	0.0	-0.1	1.0	1.9	2.9	45.9	14.8
10	0.1	0.0	0.9	0.0	0.0	0.0	0.9	1.9	2.8	45.9	15.4
11	-0.5	0.0	-0.5	-0.2	0.0	0.0	0.6	1.9	2.5	45.9	17.4
12	0.4	-0.8	0.2	-0.3	0.0	0.0	1.3	1.9	3.2	45.9	13.3
13	-0.5	-6.9	-0.8	1.1	-0.1	0.0	6.8	1.9	8.7	45.9	4.3
14	-1.4	-20.4	-2.8	0.7	-0.1	-0.1	19.1	1.9	21.0	45.9	1.2
15	0.0	-2.9	-0.3	0.0	-0.3	0.0	3.0	1.9	4.9	45.9	8.4
16	-0.1	-3.9	0.0	-0.6	-0.3	0.0	4.1	1.9	6.0	45.9	6.7

* Allowable at 331°F (maximum temperature for inner shell) governed by 0.7Su.

** Based on internal pressure of 50 psi.

Table 2.7.1.1-3 NAC-STC Critical $P_m + P_b$ Stress Summary for CY-MPC; 30-ft Top End Drop

Section No.	P_m Stresses (ksi)						Stress Intensity Impact (ksi)	Stress Intensity Bolt Preload + Pressure** (ksi)	Stress Intensity Total (ksi)	Allowable Stress* (ksi)	Margin of Safety
	S_x	S_y	S_z	S_{xy}	S_{yz}	S_{xz}					
1	0.0	-4.6	0.0	0.0	0.0	0.0	4.6	1.9	6.5	93.2	13.3
2	0.0	-4.4	0.0	0.0	0.0	0.0	4.4	1.9	6.3	65.6	9.4
3	0.0	-3.5	0.0	0.0	0.0	0.0	1.2	1.9	3.1	65.6	20.2
4	0.0	-3.6	-0.1	-0.4	0.0	0.0	3.7	1.9	5.6	65.6	11.7
5	0.0	-2.1	0.0	-0.2	0.0	0.0	2.2	1.9	4.1	65.6	15.0
6	0.0	-3.5	0.8	0.0	0.0	0.1	4.4	1.9	6.3	65.6	9.4
7	-0.8	-6.1	-1.5	0.1	0.0	-0.2	5.3	1.9	7.2	65.6	8.1
8	0.1	-9.4	-1.0	-0.3	0.1	0.0	9.5	1.9	11.4	65.6	4.8
9	-0.9	-0.2	-5.6	0.0	0.0	-0.3	5.5	1.9	7.4	65.6	7.9
10	0.9	0.2	6.8	0.0	0.0	0.3	6.6	1.9	8.5	65.6	6.7
11	-1.8	0.0	-0.3	-0.2	0.0	0.1	1.8	1.9	3.7	65.6	16.7
12	2.4	0.3	0.5	-0.1	0.0	-0.1	2.1	1.9	4.0	65.6	15.4
13	7.9	-2.4	13.0	1.2	0.1	0.3	15.5	1.9	17.4	65.6	2.8
14	1.3	-18.4	2.6	1.1	0.7	0.1	21.1	1.9	23.0	65.6	1.9
15	-0.1	-2.9	2.0	0.6	-0.1	0.0	4.9	1.9	6.8	65.6	8.7
16	5.6	-3.6	4.5	0.0	-0.2	-0.4	9.4	1.9	11.3	65.6	4.8

* Allowable at 331°F (maximum temperature for inner shell) governed by 0.7Su.

** Based on internal pressure of 50 psi.

Table 2.7.1.1-4 NAC-STC Critical P_m Stress Summary for CY-MPC; 30-ft Bottom End Drop

Section No.	P_m Stresses (ksi)						Stress Intensity Impact (ksi)	Stress Intensity Bolt Preload + Pressure** (ksi)	Stress Intensity Total (ksi)	Allowable Stress* (ksi)	Margin of Safety
	S_x	S_y	S_z	S_{xy}	S_{yz}	S_{xz}					
1	0.0	-3.3	0.0	0.0	0.0	0.0	3.3	1.9	5.2	65.2	11.5
2	0.0	-3.4	0.0	0.0	0.0	0.0	3.4	1.9	5.3	45.9	7.7
3	0.0	-4.2	0.0	0.0	0.0	0.0	4.2	1.9	6.1	45.9	6.5
4	-0.6	-4.4	-1.1	-0.3	0.0	-0.1	3.8	1.9	5.7	45.9	7.1
5	0.0	-7.0	-0.8	0.8	0.0	0.0	7.2	1.9	9.1	45.9	4.0
6	0.0	-4.0	0.6	0.0	0.0	0.1	4.6	1.9	6.5	45.9	6.1
7	-0.1	-2.1	1.1	0.2	0.0	0.1	3.2	1.9	5.1	45.9	8.0
8	0.0	-1.6	1.1	-0.1	0.0	0.1	2.7	1.9	4.6	45.9	9.0
9	-0.8	-20.4	-5.9	-1.4	0.4	-0.3	19.9	1.9	21.8	45.9	1.1
10	0.2	-3.7	1.6	0.0	0.0	0.1	5.2	1.9	7.1	45.9	5.5
11	-0.8	-5.2	-1.1	-0.1	0.8	0.0	4.6	1.9	6.5	45.9	6.1
12	1.0	-2.0	1.1	0.2	0.0	0.0	3.1	1.9	5.0	45.9	8.2
13	-0.3	-0.7	-0.4	0.1	0.0	0.0	0.5	1.9	2.4	45.9	18.1
14	-0.3	-2.4	-0.5	0.1	0.0	0.0	2.1	1.9	4.0	45.9	10.5
15	-0.3	-0.8	-0.4	0.5	0.0	0.0	1.1	1.9	3.0	45.9	14.3
16	-0.1	-0.3	-0.1	0.1	0.0	0.0	0.3	1.9	2.2	45.9	19.9

* Allowable at 331°F (maximum temperature for inner shell) governed by 0.7Su.

** Based on internal pressure of 50 psi.

Table 2.7.1.1-5 NAC-STC Critical $P_m + P_b$ Stress Summary for CY-MPC; 30-ft Bottom End Drop

Section No.	P_m Stresses (ksi)						Stress Intensity Impact (ksi)	Stress Intensity Bolt Preload + Pressure** (ksi)	Stress Intensity Total (ksi)	Allowable Stress* (ksi)	Margin of Safety
	S_x	S_y	S_z	S_{xy}	S_{yz}	S_{xz}					
1	0.0	-3.5	-0.1	0.0	0.0	0.0	3.5	1.9	5.4	93.2	16.3
2	0.0	-3.5	0.0	0.0	0.0	0.0	3.5	1.9	5.4	65.6	11.1
3	0.0	-4.3	0.0	0.0	0.0	0.0	4.3	1.9	6.2	65.6	9.6
4	-1.1	-7.3	-2.2	-0.3	0.0	-0.3	6.3	1.9	8.2	65.6	7.0
5	0.2	-12.9	-2.3	0.3	0.0	-0.1	13.1	1.9	15.0	65.6	3.4
6	0.0	-4.0	0.6	0.0	0.0	0.1	4.6	1.9	6.5	65.6	9.1
7	0.0	-2.9	0.9	0.1	0.0	0.1	3.8	1.9	5.7	65.6	10.5
8	0.0	-3.6	0.6	0.3	0.0	0.1	4.2	1.9	6.1	65.6	10.8
9	-1.4	-60.7	-35.4	-3.2	1.0	-2.2	59.9	1.9	61.8	65.6	0.06
10	3.1	-0.6	23.0	0.0	0.0	1.1	23.6	1.9	25.5	65.6	1.6
11	4.1	-3.6	4.0	-0.8	0.6	-0.2	8.1	1.9	10.0	65.6	5.6
12	3.6	-1.7	2.5	0.5	0.1	-0.1	5.4	1.9	7.3	65.6	8.0
13	4.3	-1.2	6.7	0.2	0.1	0.1	7.9	1.9	9.8	65.6	5.7
14	2.4	-2.6	3.8	0.2	0.1	0.1	6.4	1.9	8.3	65.6	7.9
15	-0.6	-1.0	1.5	0.7	0.0	0.1	3.0	1.9	4.9	65.6	12.4
16	-0.1	-0.3	1.0	0.2	0.0	0.0	1.4	1.9	3.3	65.6	18.9

* Allowable at 331°F (maximum temperature for inner shell) governed by 0.7Su.

** Based on internal pressure of 50 psi.

THIS PAGE INTENTIONALLY LEFT BLANK

2.7.1.2 Thirty-Foot Side Drop

The NAC-STC is structurally evaluated for the hypothetical accident 30-foot side drop condition in accordance with the requirements of 10 CFR 71.73(c)(1). In this event the NAC-STC, equipped with an impact limiter over each end, falls through a distance of 30 feet onto a flat, unyielding, horizontal surface. The cask strikes the surface in a horizontal position; consequently, a side impact on the cask occurs. The types of loading involved in a side drop accident are closure lid bolt preload, internal pressure, thermal, impact load, and inertial body load. There are three credible side impact conditions to be considered, according to Regulatory Guide 7.8:

1. Side drop with 100°F ambient temperature, maximum decay heat load, and maximum solar insolation.
2. Side drop with -20°F ambient temperature, maximum decay heat load, and no solar insolation.
3. Side drop with -20°F ambient temperature, no decay heat load, and no solar insolation.

The finite element analysis method is utilized to perform the side drop stress evaluations for the NAC-STC. The side drop accident condition is analyzed using a three-dimensional structural model to accurately represent the non-axisymmetric loads involved in the side drop case. One-half of the cask is modeled as a three-dimensional structure with one plane of symmetry. The ANSYS STIF45 3-D solid element is the primary element type used in the model. In order to reduce the overall problem size, two three-dimensional models have been constructed for the directly loaded fuel configuration--the top fine mesh model and the bottom fine mesh model. A detailed description of the three-dimensional finite element models of the NAC-STC is presented in Section 2.10.2.1.2. The top model contains a fine mesh region at the upper half of the cask with a relatively coarse mesh at the bottom end; the bottom model contains a fine mesh region at the bottom end with relatively coarse mesh at the top end.

Both models are used in the side drop analyses to obtain the detailed stresses throughout the cask for the directly loaded fuel configuration. The stress results from the fine mesh portion of each model are then used to form the final stress summary. For the Yankee-MPC and CY-MPC canistered fuel configurations, the stress results are obtained from the single finite element model of that configuration.

2.7.1.2.1 Thirty-Foot Side Drop—NAC STC and Yankee-MPC Configurations

During a side impact event, the cask body experiences a lateral deceleration. Considering the cask as a free body, the impact limiters apply the load to the side of the cask (in the impact limiter contact area) to produce the deceleration. Since the deceleration represents an amplification factor for the inertial loading of the cask, the equivalent static method is adopted to do the impact evaluations. The analyses consider the behavior of the cask to be linearly elastic. Additionally, fabrication stresses are considered to be negligible (Section 2.6.11).

Five categories of load—closure lid bolt preload, internal pressure, thermal, impact, and body inertia—are considered on the cask:

1. Closure lid bolt preload - The required total bolt preload on the inner lid bolts is 42 (bolts) times 107,765 pounds/bolt or 4.51×10^6 pounds (Section 2.6.7.5.4.1). For the outer lid bolts, the total bolt preload is 36 (bolts) times 17,963 pounds/bolt or 6.44×10^5 pounds (Section 2.6.7.5.4.2). Bolt preload is applied to the model by imposing initial strains to the bolt shafts, as explained in Section 2.10.2.2.3.
2. Internal pressure - The cask internal pressure is temperature dependent and is evaluated in Section 3.4.4. Pressures of 50 psig and 12 psig are applied on the interior surfaces of the cask cavity for the hot ambient and cold ambient cases, respectively. These pressures envelope the calculated pressures for all cask configurations—directly loaded fuel (12 psig), Yankee-MPC canistered fuel (11.3 psig), and Yankee-MPC canistered GTCC waste (< 11.3 psig).
3. Thermal - The heat transfer analyses determine the cask temperature distributions for the following three combinations of ambient temperature, heat load, and solar insolation for directly loaded fuel:

Condition 1.	100°F ambient temperature, with maximum decay heat load, and maximum solar insolation.
Condition 2.	-20°F ambient temperature, with maximum decay heat load, and no solar insolation.

Condition 3. -20°F ambient temperature, with no decay heat load, and no solar insolation.

The cask temperatures calculated for each of the three thermal conditions discussed above are used in the ANSYS structural analyses to determine the values of the temperature-dependent material properties.

Additional heat transfer analyses were performed for the Yankee-MPC canistered fuel configuration as described in Section 2.6.7.2.

4. Impact loads - The impact loads are induced by the impact limiters acting on the cask during a side drop condition. The impact loads are determined from the energy absorbing characteristics of the impact limiters, as described in Section 2.6.7.4. The impact load is expressed in terms of the design cask weight (loaded or empty), multiplied by appropriate deceleration factors (g's). The 30-foot side drop evaluations conservatively consider a deceleration factor of 55g; the calculated deceleration value is 51.7g, as documented in Section 2.6.7.4, Table 2.6.7.4.1-3.

The impact limiter load is applied to the finite element model as a distributed pressure over the contact areas between the impact limiters and the cask. The contact area is defined based on the "crush" geometry of the impact limiter. The distribution of impact pressure is considered to be uniform in the longitudinal direction, and is considered to vary sinusoidally in the circumferential direction. A cosine-shaped pressure distribution is selected, which is peaked at the center, and spread over a 79.4-degree arc on either side of the centerline, around the circumference, as shown in Figure 2.10.2-32 of Section 2.10.2.2.1. The 79.4-degree arc is determined based on the impact limiter test results for a side drop crush geometry. The assumption of a "peaked" pressure distribution is a conservative, classical, stress analysis procedure. Since the center of gravity of the loaded cask is located within 1 inch of the cask middle plane, the impact load is considered to be evenly divided between the two limiters. The impact contact area for a side drop accident consists of the 12.0-inch overlapping region between the impact limiter and the cask, at each end of the cask.

The calculation to determine the pressure applied to the finite element model is documented in Section 2.10.2.2.2. The calculation is based on a 1g deceleration

condition. The following is a summary of the lateral impact pressures for the eight circumferential sectors:

ARC (deg)	LATERAL IMPACT PRESSURE FOR 1g	DECELERATION
	(psi)	(g)
0 - 8.3	163.22	55
8.3 - 17.0	158.67	55
17.0 - 26.2	149.06	55
26.2 - 35.8	133.98	55
35.8 - 45.9	113.17	55
45.9 - 56.5	86.69	55
56.5 - 67.7	54.99	55
67.7 - 79.4	18.96	55

The impact pressures used in the 30-foot side drop analyses are determined by multiplying the pressure values above by the deceleration factor (55g).

It should be noted that the design weight of the cask is 250,000 pounds, which includes the weight of the empty cask (194,000 lb), plus the weight of the cavity contents (56,000 lb), for the directly loaded fuel configuration, which envelopes the Yankee-MPC canistered fuel or Yankee-MPC GTCC waste configurations. For those load conditions in which the cask contains no fuel, the basket (design weight = 17,000 lb) is still considered to be in the cask, resulting in a weight of 211,000 pounds for the cask with basket.

5. Inertial body load - The inertial effects that occur during the impact are represented by equivalent static forces, in accordance with D'Alembert's principle. Inertial body load includes the weight of the empty cask (194,000 lb) and the weight of the cavity contents (56,000 lb) for the directly loaded fuel configuration, which envelopes that of the Yankee-MPC canistered fuel or the Yankee-MPC canistered GTCC waste.

Inertia loads resulting from the weight of the empty cask are imposed by applying an appropriate deceleration factor to the cask mass. The applied deceleration is 55g, and is applied as explained in the discussion of the impact loads.

The inertial load, resulting from the 56,000-pound contents weight, is represented as an equivalent static pressure applied on the interior surface of the cask for the directly loaded fuel configuration. Specifically, the equivalent static pressure is applied with a uniform distribution along the cavity length, and with a cosine-shaped distribution in the circumferential direction. The calculation of the contents pressure, as documented in Section 2.10.2.2.1, uses the identical method as that used in the determination of the impact pressures. In the case of no fuel in the cavity, the design weight of the basket (17,000 lb) is considered, and is represented in the same manner as that of the contents design weight. The following is a summary of the contents pressures for a 1g deceleration, for the eight circumferential sectors:

ARC (deg)	LATERAL CONTENTS PRESSURE FOR 1g	DECELERATION (g)
	(psi)	
0 - 8.3	6.51	55
8.3 - 17.0	6.33	55
17.0 - 26.2	5.95	55
26.2 - 35.8	5.34	55
35.8 - 45.9	4.51	55
45.9 - 56.5	3.46	55
56.5 - 67.7	2.19	55
67.7 - 79.4	0.76	55

Similarly, inertial load pressures are calculated for the Yankee-MPC canistered fuel configuration of the NAC-STC as described in Section 2.6.7.2.

The contents pressures considered in the 30-foot side drop analyses are determined by multiplying the pressure values above by the deceleration factor (55g).

In the ANSYS analyses, the inertial body loads are considered together with the impact loads. The results of the two simultaneous loadings are documented as "impact loads."

The stresses throughout the cask body are calculated for individual and combined loading conditions. The individual loading conditions are (1) internal pressure (including bolt preload); and (2) 30-foot side impact (impact load only). The combined loading condition is the 30-foot side impact with bolt preload and 50 psig internal pressure. This is the most critical combined loading condition for the 30-foot side drop, as will be shown in a discussion later in this report.

The finite element model has one plane of symmetry in the cask geometry and in the side drop loading conditions. Symmetric boundary conditions are applied to the cask finite element model by restraining the nodes on the symmetry plane to prevent translations in the direction normal to the symmetry plane. In addition, two nodes at the outer cask radius on the top and bottom ends of the cask, opposite the points of impact, are restrained laterally (in the drop direction) and the node at the top is restrained in the longitudinal direction to prevent rigid body motion. When the cask system is in equilibrium (i.e., the inertial body loads match the impact loads exactly), then the reaction forces at these supports will be zero. An examination of the magnitude of the reaction forces provides a check of the validity of the finite element evaluation for the 30-foot side drop condition. The sum of reactions in the cask lateral direction for the bottom model is 9,465 pounds, for the application of a 55g-load. This means that the unbalanced force of the cask model system is only $9465/55 = 172.1$ pounds. Compared to one-half of the design weight of the cask (125,000 lb), the unbalanced force is negligible, amounting to only 0.1 percent of the design weight of the cask. A similar check done for the top model indicates that the unbalanced force is 0.5 percent of the design weight, which is also negligible.

The allowable stress limit criteria, for containment and noncontainment structures, are provided in Section 2.1.2. These criteria are used to determine the allowable stresses for each cask component, conservatively using the maximum operating temperature within a given component to determine the allowable stress throughout that component. Note that higher component temperatures result in

lower allowable stresses. Table 2.10.2-5 documents the allowable stress values determined for each component, for temperature condition 1.

The stress results for the 30-foot side drop loading cases for the NAC-STC directly loaded fuel configuration are presented as described below.

Stress results for the individual internal pressure loading conditions are documented in Tables 2.10.4-1 and 2.10.4-2. Stress results for the individual 30-foot side impact loading condition are documented in Table 2.10.4-15. These are the nodal stress summaries obtained from the finite element analysis results. As described in Section 2.10.2.4.2, the nodal stresses are documented on the representative section cuts. Stress results for the combined loading condition are documented in Tables 2.10.4-130 through 2.10.4-140. These tables document--the primary stresses for the 0-degree circumferential location, the primary membrane (P_m) stresses for the 0-, 45.9-, 91.7-, and the 180-degree circumferential locations, the primary membrane plus primary bending ($P_m + P_b$) stresses for the 0-, 45.9-, 91.7-, and the 180-degree circumferential locations, and the critical P_m and critical $P_m + P_b$ stresses--in accordance with the criteria presented in Regulatory Guide 7.6. The stress results on the 0-, 45.9-, 91.7-, and the 180-degree circumferential locations document the stress variation in the circumferential direction. The circumferential locations are illustrated in Figure 2.10.2-8. As described in Sections 2.10.2.3 and 2.10.2.4, procedures have been implemented to document the nodal and sectional stresses as well as to determine the critical stress summary for all cask components.

Each of the stress summary tables for the directly loaded fuel configuration are prepared by considering the stress results of two analysis runs, the first using the top fine mesh model and the second using the bottom fine mesh model. The stress results from the fine mesh portion of each model are used to form the nodal and sectional stress summaries. For the critical stress summaries, stresses for the top forging, inner lid and outer lid are determined from the top fine mesh model results; stresses for the bottom plate and the bottom forging are calculated from the bottom fine mesh model results; stresses for the inner shell, the transition sections, and the outer shell are determined as the larger of the stress results from both models. In order to justify the use of stress results from both models for the side drop evaluation, comparisons are made on the combined loading (impact plus internal pressure)

stress results from the two models, at the middle section of the cask (Sections L and M in Figure 2.10.2-34, axial location of 96.15 inches from cask bottom). On the 0-degree, 45-degree, and 90-degree circumferential locations, the stress results from the two models show good agreement, with a difference of less than 10 percent. On the 180-degree circumferential location, where stresses are lower, the stress results from the two models are still reasonably comparable, with a difference of less than 15 percent. An additional check is performed for sections J and K (axial location of 54.90 inches), and sections N and O (axial location of 137.40 inches), which are about 40 inches away from the center of the cask (Figure 2.10.2-34). The stress results from the two models also show good agreement at these sections, with a difference of less than 10 percent for the 0-degree, 45.9-degree and 90-degree circumferential locations. Therefore, it is concluded that the combined stress results from the top fine mesh model and the bottom fine mesh model for the 30-foot side drop condition are valid and conservative.

There are three temperature conditions to be considered in the side drop evaluation. In order to determine the most critical temperature condition, two parametric studies are performed for the NAC-STC, using the three-dimensional bottom fine mesh model. The first parametric study compares the stress results for temperature condition 1 and temperature condition 2. The combined loading stress results show that the maximum stress intensities for conditions 1 and 2 are 34.1 ksi and 34.0 ksi, respectively. Since allowable stress is a function of temperature, higher component temperatures result in lower allowable stresses. The minimum margins of safety for conditions 1 and 2 are +0.87 and +0.93, respectively. It is, therefore, concluded that condition 1 is more critical than condition 2. The second parametric study compares the stress results between the analyses of conditions 1 and 3. The stress results indicate that the minimum margins of safety for temperature conditions 1 and 3 are +0.87 and +1.67, respectively. Therefore, condition 1 is more critical than condition 3. It is concluded, from the stress results of the parametric studies, that condition 1 is the most critical for the side drop accident condition. Therefore, only the stress results for temperature condition 1 for the 30-foot side drop are provided in the stress tables of this section.

It is worthwhile to mention that the most critical stress for the impact loading condition and that for the primary loading condition are essentially identical, with a maximum difference of 3 percent. Therefore it is concluded that the impact stresses are the governing factor, for the 30-foot side drop condition.

As shown in the critical P_m and $P_m + P_b$ stress summaries (Tables 2.10.4-133 and 2.10.4-134) for the directly loaded fuel configuration, the critical stresses for most of the cask components occur on the 0-degree circumferential location, which contains the line of impact. It is also observed that, for the cask inner shell, the maximum calculated stresses are located on the circumferential locations in the 56.5- to 67.7-degree region. This is because the maximum shearing stresses are located near the 56.5-degree circumferential location.

Similarly, the stress results for the Yankee-MPC canistered fuel configuration of the NAC-STC are presented in Tables 2.7.1.2-1 and 2.7.1.2-2. The section locations are defined in Figure 2.6.7.2-1. Only the inner and outer shells and their attachment regions to the top and bottom forgings are evaluated for the Yankee-MPC canistered fuel configuration because the Yankee-MPC canistered contents loading on the cask cavity does not significantly change the stresses in the end components of the cask from those stresses calculated for the directly loaded fuel configuration.

As shown in Tables 2.10.4-133 and 2.10.4-134, the margins of safety are positive for all of the 30-foot side drop accident conditions. The most critically stressed component in the system is the top forging. The minimum margin of safety for the side drop condition is found to be +0.4, as documented in Table 2.10.4-133 for the directly loaded fuel configuration. For the Yankee-MPC canistered fuel configuration, Tables 2.7.1.2-1 and 2.7.1.2-2 show that all margins of safety are positive with a minimum margin of safety, +0.2, located on the inner shell near the bottom.

Satisfaction of the extreme total stress intensity range limit is demonstrated in Section 2.1.3.3.

The documentation of the adequacy of the NAC-STC to satisfy the buckling criteria for the stresses of the side drop condition is presented in Section 2.10.5.

The NAC-STC maintains its containment capability and, therefore, satisfies the requirements of 10 CFR 71.73 for the 30-foot side drop hypothetical accident condition.

2.7.1.2.2 Thirty-Foot Side Drop—CY-MPC Configuration

The NAC-STC loaded with the CY-MPC canister is structurally evaluated for the hypothetical accident 30-foot side drop condition in accordance with the requirements of 10 CFR 71.73(c)(1). In this event the NAC-STC, equipped with an impact limiter over each end, falls through a distance of 30 feet onto a flat, unyielding, horizontal surface. The cask strikes the surface in a horizontal position; consequently, a side impact on the cask occurs. The types of loading involved in a side drop accident are closure lid bolt preload, internal pressure, thermal, impact load, and inertial body load. There are three credible side impact conditions to be considered, according to Regulatory Guide 7.8:

1. Side drop with 100°F ambient temperature, maximum decay heat load, and maximum solar insolation.
2. Side drop with -20°F ambient temperature, maximum decay heat load, and no solar insolation.
3. Side drop with -20°F ambient temperature, no decay heat load, and no solar insolation.

The finite element analysis method is utilized to perform the side drop stress evaluations for the CY-MPC. With the exception of the loading, the CY-MPC model is the same as the model used to evaluate the Yankee-MPC. A description of the model is included in Section 2.10.2.1.1.

Boundary Conditions—CY-MPC Configuration Side Drop Analysis

The maximum internal pressure for the CY-MPC system is 38.1 psig as shown in Section 3.4.4. Since the maximum internal pressure is less than the 50 psig design pressure used for the analyses presented in Sections 2.6 and 2.7, the analyses presented in Sections 2.6 and 2.7 bound the CY-MPC system.

Two cold environment cases are considered. The first case includes -40°F ambient temperature, no solar insolation, maximum decay heat, and maximum internal pressure. Component temperatures for this case are less than the temperatures used for the NAC-STC analysis. Therefore, the Yankee-MPC analysis envelops the CY-MPC design. The second case, or minimum temperature condition, assumes -40°F ambient temperature, no solar insolation, no

decay heat, and maximum internal pressure. An evaluation of the minimum temperature condition is not required since all component temperatures are at -40°F .

The inertial load, resulting from the 67,200-pound contents weight, is represented as an equivalent static pressure applied on the interior surface of the cask for the CY-MPC fuel configuration. Specifically, the equivalent static pressure is applied with a uniform distribution along the cavity length, and with a cosine-shaped distribution in the circumferential direction. Note that the weight of the canister lids is considered separately from the weight of the canister shell and fuel basket. This results in larger load in the region of the canister structural and shield lids. The contents pressures considered in the 30-foot side drop analyses are determined by multiplying the pressure values above by the deceleration factor (55g). In the ANSYS analyses, the inertial body loads are considered together with the impact loads. The results of the two simultaneous loadings are documented as "impact loads."

The stresses throughout the cask body are calculated for individual and combined loading conditions. The individual loading conditions are (1) internal pressure (including bolt preload); and (2) 30-foot side impact (impact load only). The combined loading condition is the 30-foot side impact with bolt preload and 50 psig internal pressure. The peak stress intensity from the internal pressure plus bolt preload is conservatively added to the sectional stresses from the cask body impact results.

The allowable stress limit criteria, for containment and noncontainment structures, are provided in Section 2.1.2. These criteria are used to determine the allowable stresses for each cask component, conservatively using the maximum operating temperature within a given component to determine the allowable stress throughout that component. Note that higher temperatures result in lower allowable stresses.

CY-MPC Configuration Side Drop Analysis Results

The stress results for the CY-MPC configuration of the NAC-STC are presented in Tables 2.7.1.2-4 and 2.7.1.2-5. The section locations are defined in Figure 2.7.1.2-1. The coordinates of each section is presented in Table 2.7.1.2-3. Only the inner and outer shells and their attachment regions to the top and bottom forgings are evaluated for the CY-MPC configuration because the canistered contents loading on the cask cavity does not significantly change the stresses in the end components of the cask from those stresses calculated for the directly loaded fuel configuration.

As shown in Tables 2.7.1.2-4 and 2.7.1.2-5, the margins of safety are positive for all of the 30-foot side drop accident conditions. The most critically stressed component in the system is the inner shell. The minimum margin of safety for the side drop condition is found to be +0.23 as documented in Table 2.7.1.2-5 for the CY-MPC configuration. Tables 2.7.1.2-4 and 2.7.1.2-5 show that all margins of safety are positive with a minimum margin of safety, +0.23, located on the inner shell near the bottom.

Satisfaction of the extreme total stress intensity range limit is demonstrated in Section 2.1.3.3.

The documentation of the adequacy of the NAC-STC loaded with a CY-MPC canister to satisfy the buckling criteria for the stresses of the side drop condition is presented in Section 2.10.5.

The CY-MPC canister maintains its containment capability and, therefore, satisfies the requirements of 10 CFR 71.73 for the 30-foot side drop hypothetical accident condition.

Figure 2.7.1.2-1 Location of Sections for NAC-STC Cask Body Stress Evaluation for CY-MPC

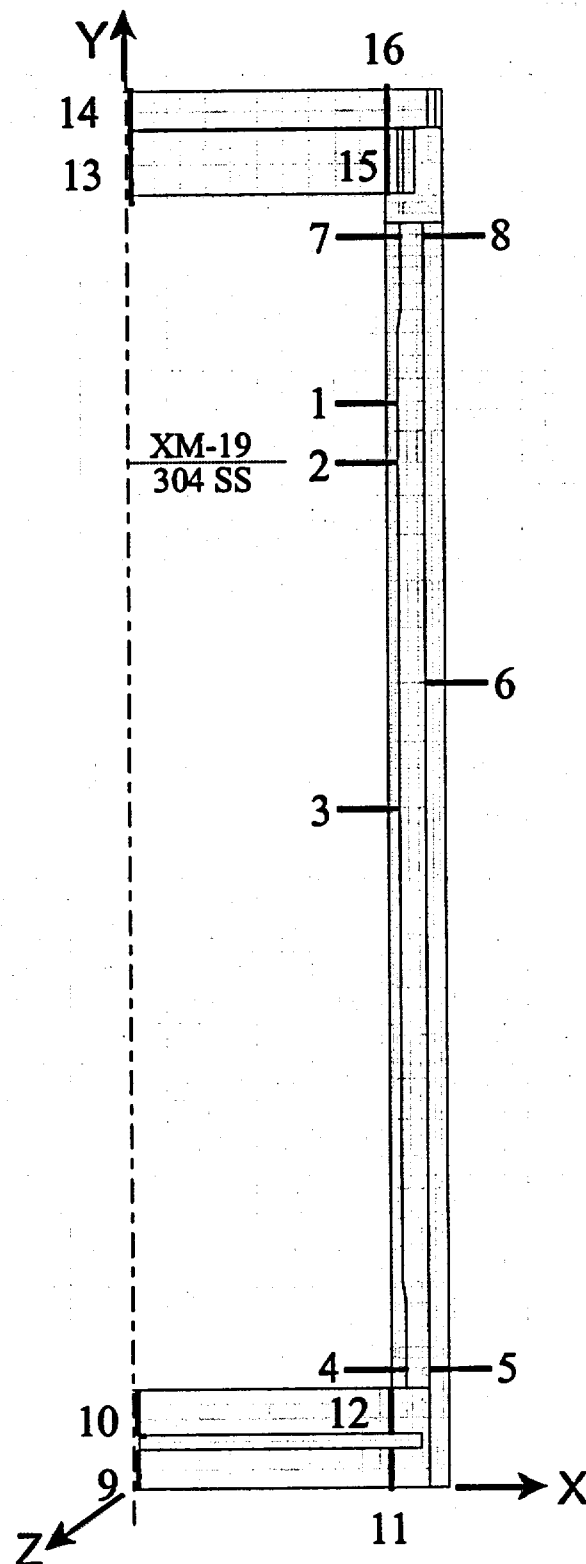


Table 2.7.1.2-1 Yankee-MPC Critical P_m Stress Summary; 30-ft Side Drop; Drop Orientation = 90°

Section No.	P_m Stresses (ksi)						Principal Stresses (ksi)			S.I.	S.I.** Bolt Preload	S.I.	Allowable Stress*	Margin of Safety
	S_x	S_y	S_z	S_{xy}	S_{yz}	S_{xz}	S1	S2	S3	Impact (ksi)	+ Pressure (ksi)	Total (ksi)	(ksi) $0.7S_u$	
1	-2.4	9.4	15.2	-0.2	-1.6	0.9	15.6	9.0	-2.4	18.1	1.9	20.0	65.7	2.3
2	-1.7	12.0	14.1	0.4	-1.3	0.7	14.7	11.5	-1.7	16.4	1.9	18.3	46.1	1.5
3	-1.1	20.9	6.5	0.0	0.1	0.4	20.9	6.5	-1.1	22.0	1.9	23.9	46.1	0.9
4	-0.4	-12.8	-16.2	3.2	0.9	-1.1	0.4	-13.1	-16.7	17.1	1.9	19.0	46.1	1.4
5	2.0	-2.3	-11.9	3.9	0.9	-0.9	4.3	-4.4	-12.1	16.5	1.9	18.4	46.1	1.5
6	-0.6	22.5	5.3	0.0	0.0	1.0	22.5	5.4	-0.8	23.3	1.9	25.2	46.1	0.8
7	0.0	-8.9	-10.4	-1.7	-0.7	-0.7	0.4	-8.8	-10.8	11.2	1.9	13.1	46.1	2.5
8	0.0	6.5	-3.6	-1.8	-0.7	-0.2	7.0	-0.4	-3.7	10.7	1.9	12.6	46.1	2.7

* Allowable at 311°F (maximum temperature for inner shell).

** Based on internal pressure of 50 psi.

Table 2.7.1.2-2 Yankee-MPC Critical $P_m + P_b$ Stress Summary; 30-ft Side Drop; Drop Orientation = 90°

Section No.	$P_m + P_b$ Stresses (ksi)						Principal Stresses (ksi)			S.I.	S.I. Bolt Preload	S.I.	Allowable Stress*	Margin of Safety
	S_x	S_y	S_z	S_{xy}	S_{yz}	S_{xz}	S1	S2	S3	Impact (ksi)	+ Pressure** (ksi)	Total (ksi)	(ksi) S_u	
1	-2.7	26.5	33.3	-0.2	-1.0	2.1	33.5	26.4	-2.8	36.3	1.9	38.2	94.0	1.5
2	-1.5	24.8	32.3	0.4	-0.8	2.0	32.5	24.8	-1.6	34.2	1.9	36.1	65.9	0.8
3	-1.0	29.8	29.1	0.0	0.0	1.9	29.8	29.2	-1.1	30.9	1.9	32.8	65.9	1.0
4	1.0	-51.8	-26.6	4.2	0.3	-1.8	1.4	-26.7	-52.1	53.5	1.9	55.4	65.9	0.2
5	3.0	-35.0	-20.3	1.1	0.3	-1.5	3.1	-20.4	-35.1	38.2	1.9	40.1	65.9	0.6
6	-0.5	34.1	34.6	0.0	0.1	2.8	34.8	34.1	-0.7	35.5	1.9	37.4	65.9	0.8
7	0.6	-21.6	-12.0	-2.4	0.0	-0.8	0.9	-12.0	-21.9	22.8	1.9	24.7	65.9	1.7
8	-1.2	17.7	-2.6	-2.4	-1.5	0.0	18.1	-1.5	-2.8	20.9	1.9	22.8	65.9	1.9

* Allowable at 311°F (maximum temperature for inner shell).

** Based on internal pressure of 50 psi.

Table 2.7.1.2-3 CY-MPC Configuration Section Locations for Stress Evaluation (Maximums)

Section No.	Component Name and Material	Section Location (in.)							
		Inside Node	X	Y	Z	Outside Node	X	Y	Z
1	Transition Shell – XM-19	197	35.5	146.1	0.0	165	37	146.1	0.0
2*	Inner Shell – 304	196	35.5	142.0	0.0	164	37	142.0	0.0
3	Inner Shell – 304	189	35.5	94.2	0.0	157	37	94.2	0.0
4	Bottom Forging – 304	130	35.5	14.5	0.0	123	38	14.5	0.0
5	Outer Shell – 304	280	40.7	14.5	0.0	328	43	14.5	0.0
6	Outer Shell – 304	300	40.7	103.2	0.0	358	43	103.2	0.0
7	Top Forging – 304	271	35.5	173.2	0.0	265	37.5	173.2	0.0
8	Top Forging – 304	317	40.7	173.2	0.0	435	43.4	173.2	0.0

* This section is at the boundary of transition shell and inner shell.

Table 2.7.1.2-4 CY-MPC Configuration Critical P_m Stress Summary; 30-ft Side Drop

Section No.	P _m Stresses (ksi)						Stress Intensity Impact (ksi)	Stress Intensity Bolt Preload + Pressure** (ksi)	Stress Intensity Total (ksi)	Allowable Stress* (ksi)	Margin of Safety
	S _x	S _y	S _z	S _{xy}	S _{yz}	S _{xz}					
1	-1.2	8.4	7.6	0.0	1.3	0.4	10.5	1.9	12.4	65.2	4.3
2	-1.0	10.6	6.7	-0.1	-1.2	0.2	12.0	1.9	13.9	45.9	2.3
3	-1.1	21.3	5.6	0.0	0.0	0.4	22.4	1.9	24.3	45.9	0.89
4	-0.3	-8.5	-14.7	4.1	1.0	-1.2	16.6	1.9	18.5	45.9	1.5
5	2.5	5.0	-11.3	4.4	0.5	-1.3	19.8	1.9	21.7	45.9	1.1
6	-0.6	24.1	5.2	0.0	0.0	0.9	24.9	1.9	26.8	45.9	0.71
7	-0.9	-10.7	-6.8	-3.6	-1.4	-0.5	12.6	1.9	14.5	45.9	2.2
8	-0.1	9.9	0.3	-1.8	-0.7	0.2	10.6	1.9	12.5	45.9	2.7

* Allowable at 331°F (maximum temperature for inner shell) governed by 0.7S_u.

** Based on internal pressure of 50 psi.

Table 2.7.1.2-5 CY-MPC Configuration Critical $P_m + P_b$ Stress Summary; 30-ft Side Drop

Section No.	P_m Stresses (ksi)						Stress Intensity Impact (ksi)	Stress Intensity Bolt Preload + Pressure** (ksi)	Stress Intensity Total (ksi)	Allowable Stress* (ksi)	Margin of Safety
	S_x	S_y	S_z	S_{xy}	S_{yz}	S_{xz}					
1	-1.0	13.7	21.1	0.0	-0.9	1.3	22.4	1.9	24.3	93.2	2.8
2	-0.8	15.7	21.2	-0.1	-0.8	1.2	22.2	1.9	24.1	65.6	1.7
3	-1.0	29.8	26.9	0.0	0.0	1.8	30.9	1.9	32.8	65.6	1.0
4	1.6	-48.8	-25.7	4.9	0.3	-2.1	51.5	1.9	53.4	65.6	0.23
5	1.8	36.7	-1.9	7.9	1.7	-0.8	40.9	1.9	42.8	65.6	0.53
6	-0.5	35.2	33.1	0.0	0.0	2.7	35.9	1.9	37.8	65.6	0.74
7	1.0	-22.9	-7.3	-4.8	-0.4	-0.7	25.8	1.9	27.7	65.6	1.4
8	-1.2	15.3	-0.9	-2.4	-2.0	0.2	17.5	1.9	19.4	65.6	2.4

* Allowable at 331°F (maximum temperature for inner shell) governed by 0.7Su.

** Based on internal pressure of 50 psi.

2.7.1.3 Thirty-Foot Corner Drop

The NAC-STC in the directly loaded fuel configuration is structurally evaluated for the hypothetical accident 30-foot corner drop condition in accordance with the requirements of 10 CFR 71.73(c)(1). In this event the NAC-STC, equipped with an impact limiter over each end, falls through a distance of 30 feet onto a flat, unyielding, horizontal surface. The cask strikes the surface on its top or bottom corner. The cask center of gravity is directly above the initial impact point for the corner drop condition. For the NAC-STC, an angle of 24 degrees from vertical is calculated for the corner drop orientation. The types of loading involved in a corner drop accident are closure lid bolt preload, internal pressure, thermal, impact load, and inertial body load. There are six credible corner impact conditions to be considered, according to Regulatory Guide 7.8.

1. Top corner drop with 100°F ambient temperature, maximum decay heat load, and maximum solar insolation.
2. Top corner drop with -20°F ambient temperature, maximum decay heat load, and no solar insolation.
3. Top corner drop with -20°F ambient temperature, no decay heat load, and no solar insolation.
4. Bottom corner drop with 100°F ambient temperature, maximum decay heat load, and maximum solar insolation.
5. Bottom corner drop with -20°F ambient temperature, maximum decay heat load, and no solar insolation.
6. Bottom corner drop with -20°F ambient temperature, no decay heat load, and no solar insolation.

The finite element analysis method is utilized to perform the corner drop stress evaluations for the NAC-STC. The corner drop accident conditions are analyzed using a three-dimensional structural model to accurately represent the non-axisymmetric loads involved in the corner drop case. One-half of the cask is modeled as a three-dimensional structure with one plane of

symmetry. The ANSYS STIF45 3-D solid element type is used in the model. Two finite element models are constructed; a top fine mesh model and a bottom fine mesh model. Each model is a complete representation of the cask, with a fine mesh region at the impacting end and with a relatively coarse mesh at the opposite end. The fine element mesh is modeled at the impacting end of the cask to provide detailed results in that region. The stresses predicted by the coarse element mesh at the non-impacting end of the model are not critical, so less detail is required. The detailed descriptions of the three-dimensional finite element models of the NAC-STC are described in Section 2.10.2.1.2.

Considering the cask as a free body, the impact limiter will apply the load to the cask impacting corner to produce the deceleration. Since the deceleration represents an amplification factor for the inertial loading of the cask, the equivalent static method is adopted to do the impact evaluations. The analyses consider the behavior of the cask to be linear elastic. Additionally, the fabrication stresses are considered to be negligible (Section 2.6.11).

Five categories of load—closure lid bolt preload, internal pressure, thermal, impact, and body inertia—are considered on the cask:

1. Closure lid bolt preload - The required total bolt preloads on the inner lid bolts and the outer lid bolts are 4.51×10^6 pounds and 6.02×10^5 pounds, respectively (Section 2.6.7.5). Bolt preload is applied to the model by imposing initial strains to the bolt shafts, as explained in Section 2.10.2.2.3. The bolts are modeled as beam (ANSYS STIF4) elements.
2. Internal pressure - The cask internal pressure is temperature dependent and is evaluated in Section 3.4.4. Pressures of 50 psig and 12 psig are applied on the interior surfaces of the cask cavity for the hot ambient and cold ambient cases, respectively. These pressures envelope the calculated pressures for all cask configurations—directly loaded fuel (12 psig), Yankee-MPC canistered fuel (11.3 psig), and Yankee-MPC canistered GTCC waste (< 11.3 psig).
3. Thermal - The heat transfer analyses performed in Sections 3.4.2 and 3.4.3 determine the cask temperature distributions for the following three combinations of ambient temperature, heat load, and solar insolation for directly loaded fuel:

Condition 1. 100°F ambient temperature, with maximum decay heat load, and maximum solar insolation.

Condition 2. -20°F ambient temperature, with maximum decay heat load, and no solar insolation.

Condition 3. -20°F ambient temperature, with no decay heat load, and no solar insolation.

The cask temperature distributions, calculated for each of the three thermal conditions, are used in the ANSYS structural analyses to determine the values of the temperature-dependent material properties such as modulus of elasticity, density, and Poisson's ratio. These temperatures are also used to evaluate the thermal stress effect on the cask.

4. Impact loads - The impact loads are produced by the impact limiter acting on the cask corner during a corner drop condition. The impact loads are determined from the energy absorbing characteristics of the impact limiters, as described in Section 2.6.7.4. The impact load is expressed in terms of the design cask weight (loaded or empty), multiplied by an appropriate deceleration factor (g's). The design deceleration factor of 55g is used for both top and bottom corner drops. This compares to the actual deceleration factors of 49.3g, and 43.6g, as documented in Section 2.6.7.4, Table 2.6.7.4.1-2.

The impact loads for the corner drop analyses have lateral and longitudinal components, which are calculated from the total impact loads. The lateral component is distributed as a pressure with a circumferential distribution (similar to the side drop pressure) over an arc of 0 to 79.4 degrees on each side of the impact centerline (Section 2.10.2.2.2). The longitudinal component has a uniform distribution on a sector of the impacting end of the cask, over the same arc of 0 to 79.4 degrees on each side of the impact centerline.

Section 2.10.2.2.2 documents the impact pressures for a cask design weight of 250,000 pounds and an impact limiter contact length of 24.0 inches (12.0 inches at each end). In the corner drop case the impact energy is absorbed by only one impact limiter and, hence, the corner drop lateral impact pressures are determined by multiplying the side drop impact limiter by 2 (to account for only half as much impact limiter area), and by multiplying by the sine of the drop angle. For example, the corner drop lateral impact

pressure, for the elements located between the 0- and 8.29-degree circumferential planes, is:

$$\begin{aligned}\text{Press}_1 &= (163.22)(2)(\sin 24^\circ) = 132.78 \text{ psi for 1g} \\ \text{Press}_{55} &= (132.78)(55\text{g}/1\text{g}) = 7303.0 \text{ psi for 55g}\end{aligned}$$

The following is a summary of the lateral impact pressures, for the elements at the various circumferential locations, for a 1g deceleration:

ARC (deg)	LATERAL IMPACT PRESSURE FOR 1g	DECELERATION
	(psi)	(g)
0 - 8.3	132.78	55
8.3 - 17.0	129.07	55
17.0 - 26.2	121.26	55
26.2 - 35.8	108.99	55
35.8 - 45.9	92.06	55
45.9 - 56.5	70.52	55
56.5 - 67.7	44.73	55
67.7 - 79.4	15.42	55

The longitudinal impact pressure is calculated as the cosine component of the total impact load, divided by the sector area within the 0- to 79.4-degree arc.

Therefore:

$$\begin{aligned}\text{Weight} &= 250,000 \text{ lb} \\ \text{Area} &= (79.4/180)(\pi)(43.35)^2 = 2604 \text{ in}^2 \\ \text{Press}_1 &= (250,000)(\cos 24^\circ)/2604 = 87.70 \text{ psi for 1g} \\ \text{Press}_{55} &= (87.70)(55\text{g}/1\text{g}) = 4824.0 \text{ psi for 55g}\end{aligned}$$

It should be noted that the design weight of the cask is 250,000 pounds, which includes the weight of the empty cask (194,000 lb) plus the weight of the cavity contents (56,000 lb).

5. Inertial body load - The inertial effects that occur during the impact are represented by equivalent static forces, in accordance with D'Alembert's principle. Inertial body load

includes the weight of the empty cask (194,000 lb) and the weight of the cavity contents (56,000 lb).

Inertia loads resulting from the weight of the empty cask are imposed by applying an appropriate deceleration factor to the cask mass. The lateral and longitudinal components of inertial loading are determined in the same manner as for the impact loading.

The inertial load resulting from the 56,000-pound contents weight is represented as an equivalent static pressure load with both lateral and longitudinal components applied on the interior surface of the cask. The lateral component is applied to the cask model with the same circumferential distribution as that for the side drop pressure (over an arc of 0 degrees to 79.4 degrees on each side of the impact centerline). The lateral component pressure is determined by ratioing the side drop contents pressure values (Section 2.10.2.2.1) by the deceleration factor and by the sine of the drop orientation angle. The longitudinal component has a uniform distribution over the cask cavity end. The longitudinal component pressure is calculated by ratioing the end drop contents pressure by the deceleration factor and by the cosine of the drop orientation angle. The total deceleration factor is constant at 55g for both the top and the bottom corner drops.

Section 2.10.2.2.1 contains the side drop contents pressures for a total contents weight of 56,000 pounds. The corner drop lateral contents pressure for the elements located between the 0- and 8.29-degree circumferential planes is therefore:

$$\begin{aligned}\text{Press}_1 &= (6.51)(\sin 24^\circ) &= 2.65 \text{ psi for } 1g \\ \text{Press}_{55} &= (2.65)(55g/1g) &= 146.0 \text{ psi for } 55g\end{aligned}$$

The following is a summary of the applied lateral contents pressures for the corner drop for the directly loaded fuel configuration, for the elements at the various circumferential locations, for a 1g deceleration.

ARC (deg)	LATERAL CONTENTS	
	PRESSURE FOR 1g (psi)	DECELERATION (g)
0 - 8.3	2.65	55
8.3 - 17.0	2.57	55
17.0 - 26.2	2.42	55
26.2 - 35.8	2.17	55
35.8 - 45.9	1.83	55
45.9 - 56.5	1.41	55
56.5 - 67.7	0.89	55
67.7 - 79.4	0.31	55

The longitudinal contents pressure is calculated from the longitudinal component of the total contents weight and the area over which it acts. Therefore:

$$\begin{aligned}
 \text{Weight} &= 56,000 \text{ lb} \\
 \text{Area} &= (p)(35.5)^2 = 3959 \text{ in}^2 \\
 \text{Press}_1 &= (56,000)(\cos 24^\circ)/3959 = 12.92 \text{ psi for 1g} \\
 \text{Press}_{55} &= (12.92)(55\text{g}/1\text{g}) = 711.0 \text{ psi for 55g}
 \end{aligned}$$

In the ANSYS analyses, the inertial body loads are considered together with the impact loads. The results of the two simultaneous loadings are documented as "impact loads".

The stresses throughout the cask body are calculated for individual and combined loading conditions. The individual loading conditions are: (1) internal pressure (including bolt preload); (2) 30-foot drop top corner impact (impact load only); and (3) 30-foot drop bottom corner impact (impact load only). The combined loading conditions are: (1) the 30-foot drop top corner impact with bolt preload and 50 psig internal pressure and (2) the 30-foot drop bottom corner impact with bolt preload and 50 psig internal pressure.

The model has one plane of symmetry in the cask geometry and in the corner drop loading conditions. Symmetric boundary conditions are applied to the cask finite element model by restraining the nodes on the symmetry plane to prevent translations in the direction normal to the

symmetry plane. In addition, two nodes at the outer cask radius on the top and bottom ends of the cask opposite the point of impact are restrained laterally; a longitudinal restraint is applied at one of the nodes opposite the end of impact, i.e., a bottom corner drop is axially restrained at the top node, and vice-versa. These lateral and axial restraints are only to prevent rigid body motion; there should be no significant reaction forces associated with these restraints. When the cask system is in equilibrium (i.e., the inertial body loads match the impact loads exactly), then the reaction forces at these supports will be zero. However, it is difficult to balance the impact limiter pressure resultant with the contents pressure and inertial body load resultant. An eccentricity between the two resultants induces a moment on the cask model. Therefore, non-zero reactions are found at the restraints. The reaction forces cause very high localized stresses (or stress singularities) in the model at the supports. These stresses are unrealistic and do not exist in the real cask. The stress singularity effect is minimized by distributing the reaction forces over the nodes in the top and bottom regions of the model. For the bottom corner drop, the reactions at the supports are 612 pounds laterally and zero longitudinally, for the application of a 55g deceleration. This means that the unbalanced force of the cask model system is only $612/55 = 11.1$ pounds. Compared to one-half of the design weight of the cask (125,000 lb), the unbalanced force is negligible, amounting to only 0.009 percent of the design weight of the cask. For the top corner drop, the reactions at the supports are 511 pounds laterally and zero longitudinally, for the application of a 55g deceleration. This means that the unbalanced force of the cask model system is only $511/55 = 9.3$ pounds. Compared to one-half of the design weight of the cask (125,000 lb), the unbalanced force is negligible, amounting to only 0.007 percent of the design weight of the cask.

The allowable stress limit criteria, for containment and non-containment structures, are provided in Section 2.1.2. These criteria are used to determine the allowable stresses for each cask component, conservatively using the maximum transport temperature within a given component to determine the allowable stress throughout that component. Note that higher component temperatures result in lower allowable stresses. Table 2.10.2-5 documents the allowable stress values determined for each component, for temperature condition 1.

Based on the discussion in Section 2.6.7.3, it is concluded that the 30-foot corner drop condition is enveloped by the 30-foot end and side drop analyses. Therefore, no additional analysis of the 30-foot corner drop condition is required for the Yankee-MPC or CY-MPC canistered fuel configurations of the NAC-STC. In all cases, the evaluations of the 30-foot corner drop load conditions for the Yankee-MPC and CY-MPC canistered configurations are bounded by the

30-foot corner drop analyses of the directly loaded fuel configurations. The primary basis for this conclusion is that the Yankee-MPC and CY-MPC canistered configurations weigh essentially the same as the directly loaded fuel configuration. Spacers in the cask cavity locate the package center of gravity for the Yankee-MPC and CY-MPC canistered fuel configurations at effectively the same location as that of the directly loaded fuel configuration.

Stress results for the individual loading cases of internal pressure (including bolt preload) are documented in Tables 2.10.4-1 and 2.10.4-2. Stress results for the individual 30-foot top and bottom corner drop impact loading cases are documented in Tables 2.10.4-16 and 2.10.4-17. These are the nodal stress summaries obtained from the finite element analysis results. As described in Section 2.10.2.4.2 and Section 2.10.4, the nodal stresses are documented on the representative section cuts. Primary stress results for the combined loading conditions discussed above are documented in Tables 2.10.4-141 and 2.10.4-152. All of the corner drop analyses are performed at temperature condition 1. The results from Sections 2.7.1.1 and 2.7.1.2 indicate that the stresses associated with temperature condition 1 yield the smallest margins of safety due to the effect of higher temperatures upon the allowable stresses.

These tables document the primary, primary membrane (P_m), primary membrane plus primary bending ($P_m + P_b$), and critical P_m and $P_m + P_b$ stresses in accordance with the criteria presented in Regulatory Guide 7.6. As described in Sections 2.10.2.3 and 2.10.2.4, procedures have been implemented to document the nodal and sectional stresses as well as to determine the critical stress summary for all cask components.

The P_m and the $P_m + P_b$ stresses documented in Tables 2.10.4-142 through 2.10.4-151 and 2.10.4-153 through 2.10.4-162 are stress results on the 0-, 45.9-, 91.7-, and the 180-degree circumferential locations. They indicate that the stress variations in the circumferential direction are similar between the top and the bottom corner drops. Furthermore, it is observed that the maximum calculated stresses are located on the circumferential locations in the 45.9- to 67.7-degree region. This is because the maximum shearing stresses are located near the 56.5-degree circumferential location. This shear stress, which is in the axial to circumferential location, is caused by the cantilever support from the impact limiter pressures and is compounded by the uneven distribution of the impact limiter pressure loading and the contents pressure loading.

The top corner drop cases result in higher maximum stress intensities than the bottom corner drop cases. For the individual impact loading cases, the maximum calculated membrane stress

intensity for the top corner drop is 33.7 ksi. The maximum calculated membrane plus bending stress intensity is 52.8 ksi. By comparison, for the combined loading case, including impact, bolt preload, and internal pressure, the maximum calculated P_m stress intensity is 33.4 ksi and the maximum calculated $P_m + P_b$ stress intensity is 51.8 ksi. The maximum stress intensity due to impact alone is 1.9 percent greater than the maximum stress intensities due to the combined loading. Therefore it is concluded that the impact case is the governing one for the 30-foot corner drop condition.

As shown in Tables 2.10.4-141 through 2.10.4-162, the margins of safety are positive for all of the corner drop accident conditions. The most critically stressed component is the inner lid for the top corner drop, and is the bottom forging for the bottom corner drop. The minimum margin of safety for the top corner drop condition is found to be +0.3, as documented in Table 2.10.4-145. The minimum margin of safety for the bottom corner drop condition is found to be +0.6, as documented in Table 2.10.4-156.

Satisfaction of the extreme total stress intensity range limit is demonstrated in Section 2.1.3.3.

The documentation of the adequacy of the NAC-STC to satisfy the buckling criteria for the stresses of the corner drop condition is presented in Section 2.10.5.

The NAC-STC maintains its containment capability and, therefore, satisfies the requirements of 10 CFR 71.73 for the 30-foot corner drop hypothetical accident condition.

2.7.1.4 Thirty-Foot Oblique Drop

The NAC-STC is structurally evaluated for the hypothetical accident 30-foot oblique drop condition in accordance with the requirements of 10 CFR 71.73. In this event the NAC-STC, equipped with an impact limiter over each end, falls through a distance of 30 feet onto a flat, unyielding, horizontal surface. The cask strikes the surface obliquely on its top or bottom corner. For the NAC-STC, orientation angles of 15 degrees and 75 degrees are evaluated for the oblique drops. These angles are determined to be the most critical oblique drop orientations, as demonstrated in the following discussion. This section presents the 30-foot oblique drop evaluation for the directly loaded fuel configuration and shows that for the NAC-STC Yankee-MPC and CY-MPC configurations, the side drop results bound the oblique drop results.

The types of loading involved in an oblique drop accident are closure lid bolt preload, internal pressure, thermal, impact load, and inertial body load. There are six credible oblique impact conditions to be considered, according to Regulatory Guide 7.8:

1. Top oblique drop with 100°F ambient temperature, maximum decay heat load, and maximum solar insolation.
2. Top oblique drop with -20°F ambient temperature, maximum decay heat load, and no solar insolation.
3. Top oblique drop with -20°F ambient temperature, no decay heat load, and no solar insolation.
4. Bottom oblique drop with 100°F ambient temperature, maximum decay heat load, and maximum solar insolation.
5. Bottom oblique drop with -20°F ambient temperature, maximum decay heat load, and no solar insolation.
6. Bottom oblique drop with -20°F ambient temperature, no decay heat load, and no solar insolation.

The finite element analysis method is utilized to perform the oblique drop stress evaluations for the NAC-STC. The oblique drop accident conditions are analyzed using a three-dimensional structural model to accurately represent the non-axisymmetric loads involved in the oblique drop case. One-half of the cask is modeled, as a three-dimensional structure with one plane of symmetry. The ANSYS STIF45 3-D solid element is the primary element type used in the model. Two finite element models are constructed--a top fine mesh model and a bottom fine mesh model. Each model is a complete representation of the cask with a fine mesh region at the impacting end and with a relatively coarse mesh at the opposite end. The fine element mesh density is modeled at the impacting end of the cask to provide detailed results in that region. The stresses predicted by the coarse element mesh, at the non-impacting end of the model, are not critical, so less detail is required. The detailed description of the three-dimensional finite element models of the NAC-STC are presented in Section 2.10.2.1.2.

During an impact event, the cask body will experience a deceleration in the oblique drop direction. Considering the cask as a free body, the impact limiter will apply the loads to the impacting corner to produce the deceleration. Since the deceleration represents an amplification factor for the inertial loading of the cask, the equivalent static method is adopted to do the impact evaluations. The analyses consider the behavior of the cask to be linear elastic. Additionally, the fabrication stresses are considered to be negligible (Section 2.6.11).

Five categories of load--closure lid bolt preload, internal pressure, thermal, impact, and body inertial--are considered on the cask:

1. Closure lid bolt preload - The required total bolt preloads on the inner lid bolts and the outer lid bolts are 4.51×10^6 pounds and 6.02×10^5 pounds, respectively. Bolt preload is applied to the model by imposing initial strains to the bolt shafts, as explained in Section 2.10.2.2.3. The bolts are modeled as beam (ANSYS STIF4) elements.
2. Internal pressure - The cask internal pressure is temperature dependent and is evaluated in Section 3.4.4. Pressures of 50 psig and 12 psig are applied on the interior surfaces of the cask cavity for the hot ambient and cold ambient cases, respectively. These pressures envelope the calculated pressures for all cask configurations--directly loaded fuel (12 psig), Yankee-MPC canistered fuel (11.3 psig), and Yankee-MPC canistered GTCC waste (< 11.3 psig).

3. Thermal - The heat transfer analyses performed in Sections 3.4.2 and 3.4.3 determine the cask temperature distributions for the following three combinations of ambient temperature, heat load, and solar insolation for directly loaded fuel:

Condition 1. 100°F ambient temperature, with maximum decay heat load, and maximum solar insolation.

Condition 2. -20°F ambient temperature, with maximum decay heat load, and no solar insolation.

Condition 3. -20°F ambient temperature, with no decay heat load, and no solar insolation.

The cask temperature distributions, calculated for each of the three thermal conditions, are used in the ANSYS structural analyses to determine the values of the temperature-dependent material properties.

4. Impact loads - The impact loads are produced by the impact limiter acting on the cask during an oblique drop condition. The impact loads are determined from the energy absorbing characteristics of the impact limiters, as described in Section 2.6.7.4. The impact load is expressed in terms of the design cask weight (loaded or empty), multiplied by an appropriate deceleration factor (g's).

The impact load is similar to that discussed in Section 2.7.1.3 and is applied to the cask model by the same method. The design deceleration factor of 55g is used for both the top and the bottom oblique drops. This compares to the actual deceleration factors of 51.6g, and 47.1g, respectively, for the 15-degree drop orientation, and to 28.7g, and 29.9g,

respectively, for the 75-degree drop orientation (Section 2.6.7.4). Section 2.10.2.2.2 documents the impact pressures for a cask design weight of 250,000 pounds and a total impact limiter length of 24.0 inches (12.0 inches at each end). In the oblique drop case the impact energy is absorbed by only one impact limiter, and hence the oblique drop lateral impact pressures are determined by multiplying the side drop impact pressures by 2 (to account for having only half as much impact limiter area), and by multiplying by the sine of the drop angle. For example, the oblique drop lateral impact pressure, for elements located between the 0-degree and the 8.29-degree circumferential planes is:

$$\text{Press}_1 = (163.22)(2)(\sin 15^\circ) = 84.49 \text{ psi for } 1g$$

$$\text{Press}_{55} = (84.49)(55g/1g) = 4647 \text{ psi for } 55g$$

The following are summaries of lateral impact pressures, for the elements on the various circumferential locations, for a 1g deceleration, at 15-degree and 75-degree drop orientation angles:

15-Degree Drop Orientation

ARC (deg)	LATERAL IMPACT PRESSURE FOR 1g	DECELERATION
	(psi)	(g)
0 - 8.3	84.49	55
8.3 - 17.0	82.13	55
17.0 - 26.2	77.16	55
26.2 - 35.8	69.35	55
35.8 - 45.9	58.58	55
56.9 - 56.5	44.87	55
56.5 - 67.7	28.47	55
67.7 - 79.4	9.81	55

75-Degree Drop Orientation

ARC (deg)	LATERAL IMPACT PRESSURE FOR 1g	DECELERATION
	(psi)	(g)
0 - 8.3	315.32	55
8.3 - 17.0	306.53	55
17.0 - 26.2	287.96	55
26.2 - 35.8	258.83	55
35.8 - 45.9	218.63	55
45.9 - 56.5	167.47	55
56.5 - 67.7	106.23	55
67.7 - 79.4	36.63	55

The longitudinal impact pressure is calculated as the longitudinal component of the total impact load, divided by the sector area within the 0- to 79.4-degree arc on each side of the impact centerline. Therefore, for the 15-degree drop orientation:

$$\begin{aligned}
 \text{Weight} &= 250,000 \text{ lb} \\
 \text{Area} &= (79.4/180)(\pi)(43.35)^2 = 2604 \text{ in}^2 \\
 \text{Press}_1 &= (250,000)(\cos 15^\circ)/2604 = 92.73 \text{ psi for 1g} \\
 \text{Press}_{55} &= (92.73)(55\text{g}/1\text{g}) = 5100 \text{ psi for 55g}
 \end{aligned}$$

The longitudinal impact pressure for the 75-degree drop orientation, calculated by the same method, is 24.85 psi for a 1g deceleration, and 1367 psi for a 55g deceleration.

It should be noted that the design weight of the cask is 250,000 pounds, which includes the weight of the empty cask (194,000 lb), plus the weight of the cavity contents (56,000 lb) for the directly loaded fuel configuration, which envelopes the Yankee-MPC canistered fuel or Yankee-MPC GTCC waste configurations.

5. Inertial body load - The inertial effects that occur during the impact are represented by equivalent static forces, in accordance with D'Alembert's principle. The inertial body load includes the weight of the empty cask (194,000 lb) and the weight of the cavity contents (56,000 lb). Inertia loads resulting from the weight of the empty cask are imposed by applying an appropriate deceleration factor to the cask mass. The lateral and longitudinal components of inertial loading are determined in the same manner as for the impacting loading.

The inertial load resulting from the 56,000-pound contents design weight is represented as an equivalent static pressure load with both lateral and longitudinal components applied on the interior surface of the cask for the directly loaded fuel configuration. The contents pressure loading is similar to that discussed in Section 2.10.2.2.1 and is applied to the cask model similarly to that in the side drop analyses. The lateral and longitudinal components of the contents pressure are determined in the same manner as for the corner drop analyses (Section 2.7.1.3). The total deceleration factor is constant at 55g for all of the top and bottom oblique drops.

Section 2.10.2.2.1 contains the side drop contents pressures for a total contents weight of 56,000 pounds. The oblique drop lateral contents pressure for elements located between the 0-degree and the 8.29-degree circumferential planes, for the 15-degree drop orientation, is therefore:

$$\begin{aligned}\text{Press}_1 &= (6.51)(\sin 15^\circ) &= 1.68 \text{ psi for } 1g \\ \text{Press}_{55} &= (1.68)(55g/1g) &= 92.4 \text{ psi for } 55g\end{aligned}$$

The following are summaries of the applied lateral contents pressures, for the elements at the various circumferential locations, for a 1g deceleration, at 15-degree and 75-degree drop orientation angles.

15-Degree Drop Orientation

LATERAL CONTENTS

ARC	PRESSURE FOR 1g	DECELERATION
<u>(deg)</u>	<u>(psi)</u>	<u>(g)</u>
0 - 8.3	1.68	55
8.3 - 17.0	1.64	55
17.0 - 26.2	1.54	55
26.2 - 35.8	1.38	55
35.8 - 45.9	1.17	55
56.9 - 56.5	0.90	55
56.5 - 67.7	0.57	55
67.7 - 79.4	0.20	55

75-Degree Drop Orientation

LATERAL CONTENTS

ARC	PRESSURE FOR 1g	DECELERATION
<u>(deg)</u>	<u>(psi)</u>	<u>(g)</u>
0 - 8.3	6.29	55
8.3 - 17.0	6.11	55
17.0 - 26.2	5.75	55
26.2 - 35.8	5.16	55
35.8 - 45.9	4.36	55
45.9 - 56.5	3.34	55
56.5 - 67.7	2.12	55
67.7 - 79.4	0.73	55

The longitudinal contents pressure is calculated as the longitudinal component of the total impact load, divided by the sector area within the 0- to 79.4-degree arc on each side of the impact centerline. Therefore, for the 15-degree drop orientation:

$$\begin{aligned}\text{Weight} &= 56,000 \text{ lb} \\ \text{Area} &= (p)(35.5)^2 = 3959 \text{ in}^2 \\ \text{Press}_1 &= (56,000)(\cos 15^\circ)/3959 = 13.66 \text{ psi for } 1g \\ \text{Press}_{55} &= (13.66)(55g/1g) = 751.3 \text{ psi for } 55g\end{aligned}$$

The longitudinal impact pressure for the 75-degree drop orientation, calculated by the same method, is 3.66 psi for 1g deceleration, and is 201.3 psi for 55g deceleration.

In the ANSYS analyses, the inertial body loads are considered together with the impact loads. The results of the two simultaneous loadings are documented as "impact loads."

The stresses throughout the cask body are calculated for individual and combined loading conditions. The individual loading conditions are: (1) the internal pressure (including bolt preload); (2) the 30-foot bottom 15-degree oblique drop impact (impact load only); (3) the 30-foot top 75-degree oblique drop impact (impact load only); and (4) the 30-foot bottom 75-degree oblique drop impact (impact load only). The combined loading conditions are: (1) the 30-foot bottom 15-degree orientation oblique impact with bolt preload and 50 psi internal pressure; (2) the 30-foot top 75-degree oblique drop impact with bolt preload and 50 psi internal pressure; and (3) the 30-foot bottom 75-degree oblique drop impact with bolt preload and 50 psi internal pressure.

The boundary conditions applied to the models are the same as those discussed in Section 2.7.1.3. The lateral and longitudinal restraints are only to prevent rigid body motion; there should be no significant reaction forces associated with these restraints. When the cask system is in equilibrium (i.e., the inertial body loads match the impact loads exactly), the reaction forces at these restraints will be zero. However, it is difficult to balance the impact limiter pressure resultant with the contents pressure and inertial body load resultant. An eccentricity between the two resultants induces a moment on the cask model. Therefore, non-zero reactions are found at the restraints. The reaction forces cause very high localized stresses (or stress singularities) in the model at the restraints. These stresses are unrealistic and do not exist in the real cask. The stress singularity effect is

minimized by distributing the reaction forces over the nodes in the top and bottom regions of the model. For the bottom 15-degree oblique drop, the reactions at the restraints are 136 pounds laterally and essentially zero longitudinally, for the application of a 55g deceleration factor. This means that the unbalanced force of the cask model system is only $136/55 = 2.5$ pounds. Compared to one-half of the cask design weight (125,000 lb), the unbalanced force is negligible, amounting to only 0.002 percent of the design weight of the cask. For the top 75-degree oblique drop, the reactions at the restraints are 2312 pounds laterally and essentially zero longitudinally, for the application of a 55g deceleration factor. This means that the unbalanced force of the cask model system is only $2312/55 = 42$ pounds. Compared to one-half of the cask design weight (125,000 lb), the unbalanced force is negligible, amounting to only 0.03 percent of the design weight of the cask. For the bottom 75-degree oblique drop, the reactions at the restraints are 2731 pounds laterally and essentially zero longitudinally, for the application of a 55 deceleration factor. This means that the unbalanced force of the cask model system is only $2731/55 = 50$ pounds. Compared to one-half of the cask design weight (125,000 lb), the unbalanced force is negligible, amounting to only 0.04 percent of the design weight of the cask.

The allowable stress limit criteria, for containment and noncontainment structures, are provided in Section 2.1.2. These criteria are used to determine the allowable stresses for each cask component, conservatively using the maximum transport temperature within a given component to determine the allowable stress throughout that component. Note that higher component temperatures results in lower allowable stresses. Table 2.10.2-5 documents the allowable stress values for each component for condition 1 temperatures.

Stress results for the directly loaded fuel configuration for the individual loading cases of internal pressure (including bolt preload) are documented in Tables 2.10.4-1 and 2.10.4-2. Stress results for the individual 30-foot top and bottom oblique drop impact loading cases are documented in Tables 2.10.4-18, 2.10.4-19, and 2.10.4-20. These are the nodal stress summaries obtained from the finite element analysis results. As described in Section 2.10.2.4.2 and Section 2.10.4, the nodal stresses are documented on the representative section cuts. Stress results for the combined loading conditions discussed above are documented in Tables 2.10.4-163 through 2.10.4-177. All the

oblique drop analyses are performed for temperature condition 1. The results from Sections 2.7.1.1 and 2.7.1.2 both indicate that the stresses associated with temperature condition 1 yield the smallest margins of safety as a result of the effect of higher temperatures upon the allowable stresses. These tables document the primary, primary membrane (P_m), primary membrane plus primary bending ($P_m + P_b$), and critical P_m and $P_m + P_b$ stresses in accordance with the criteria presented in Regulatory Guide 7.6. As described in Sections 2.10.2.3 and 2.10.2.4, procedures have been implemented to document the nodal and sectional stresses as well as to determine the critical stress summary for all cask components.

The critical oblique drop orientation is determined by the following considerations. First, the deceleration g-loads for different drop orientation angles between 0 and 90 degrees (in 15° increments) are determined by the computer program RBCUBED, as documented in Section 2.6.7.4. The g-load values are highest for the end drop ($f = 0^\circ$) and the side drop ($f = 90^\circ$) conditions and are lower for all of the angles in-between. From a plot of the g-load values versus drop orientation angle, it is expected that the most critical oblique drop angle will be adjacent to either the end drop or the side drop and, hence, the 15- and 75-degree oblique drop angles are chosen for further investigation. Also, SCANS (NUREG/CR-4554) analyses are performed for all oblique drop angles from 0 to 90 degrees, in 15-degree increments. A plot of the stress results from the SCANS analyses indicates that the 15-degree drop angle has the highest normal stress intensity, and that the 75-degree drop angle has the highest shear stress intensity; the stress results for the angles between 15 degrees and 75 degrees are all lower. Next, the stress results from the ANSYS analyses of the end, corner, and side drop conditions-- $f = 0$ degrees, 24 degrees, and 90 degrees, respectively--are reviewed. From the stress results documented in Sections 2.7.1.1, 2.7.1.2, and 2.7.1.3--and in Tables 2.10.4-112 through 2.10.4-162--it is observed that the maximum critical P_m and $P_m + P_b$ stresses are always higher for the corner ($f = 24^\circ$) and side ($f = 90^\circ$) drop conditions than for the end drop condition ($f = 0^\circ$). Thus, the results of the ANSYS analyses suggest that the 75-degree drop orientation will result in greater stresses than the 15-degree drop orientation.

Finally, ANSYS analyses are performed for both the 15-degree and 75-degree oblique drop conditions using the three-dimensional bottom fine mesh model. A comparison of the stress results indicates that the 75-degree oblique drop stress results are, in general, more critical than the 15-degree oblique drop stress results. In the few cases where the stresses on an individual cross-section are higher for the 15-degree drop than for the 75-degree drop, the difference between the stress results is negligible. Therefore it is concluded that the 75-degree drop orientation is more critical than the 15-degree drop orientation. For this reason, only the 75-degree drop analysis is performed for the top oblique drop condition. Thus, the determination that the 75-degree orientation is the most critical oblique drop orientation is based upon: (1) the observation that the impact g-loads are highest for drop orientations near 0 degrees and 90 degrees; (2) SCANS analyses for all angles from 0 degrees to 90 degrees, in 15-degree increments, indicate that the 15-degree drop orientation has the highest normal stress intensity and that the 75-degree drop orientation has the highest shear stress intensity; (3) the stress results for the 24-degree and the 90-degree drop orientations are higher than those for the 0-degree drop orientation; and (4) the direct comparison of stress results, between the 15-degree and the 75-degree drop orientations, using the three-dimensional bottom fine mesh model. Based on these observations, the stress results from the oblique drop orientations other than 75 degrees will be lower and, therefore, are not considered further.

The 75-degree top oblique drop case results in higher maximum stress intensities than the other oblique drop cases. For the individual impact loading cases, the maximum calculated membrane stress intensity for the 75-degree top oblique drop is 34.8 ksi. The maximum calculated membrane plus bending stress intensity is 44.6 ksi. By comparison, for the combined loading case, the maximum calculated P_m stress intensity is 34.8 ksi and the maximum calculated $P_m + P_b$ stress intensity is 44.5 ksi. Therefore, it is concluded that the impact case is the governing one for the 30-foot oblique drop condition.

As shown in Tables 2.10.4-166 through 2.10.4-177, the margins of safety are positive for all of the oblique drop accident conditions for the directly loaded fuel configuration. The most critically stressed component in the system, for the top 75-degree oblique drop, is the top forging. The minimum margin of safety for the top oblique drop condition is +0.4, as documented in Table 2.10.4-171. For the bottom oblique drop, the most critically stressed component in the system is the bottom forging. The minimum margin of safety for the bottom oblique drop condition is +0.6, as documented in Table 2.10.4-167.

As described in this section, the directly loaded fuel configuration of the NAC-STC was analyzed for the 30-foot oblique drop conditions and the 75-degree (from vertical) cask drop orientation was determined to be the critical oblique drop orientation. The maximum component stresses are summarized as follows:

<u>Stress Type</u>	30' Side Drop Condition 1		30' Bottom 75° Drop Condition 1		30' Top 75° Drop Condition 1	
	<u>Section ID</u>	<u>S.I.</u>	<u>Section ID</u>	<u>S.I.</u>	<u>Section ID</u>	<u>S.I.</u>
P_m	401 - 1 (Table 2.10.4-133)	36.0	12880-12877 (Table 2.10.4-166)	4.0	403-3 (Table 2.10.4-171)	34.8
$P_m + P_b$	403 - 3 (Table 2.10.4-134)	49.4	880-877 (Table 2.10.4-167)	5.1	404-4 (Table 2.10.4-172)	44.5

The maximum primary membrane and primary membrane plus bending stresses occur in component 6 (Figure 2.10.2-33) for the 30-foot side, 30-foot bottom 75-degree, and 30-foot top 75-degree drop conditions. These results show that the 30-foot side drop condition envelopes the most critical 30-foot oblique drop conditions (75-degree top and bottom) for the directly loaded fuel configuration of the NAC-STC. Based on the demonstration of the structural adequacy of the NAC-STC in the Yankee-MPC and CY-MPC configurations presented in Sections 2.7.1.1 and 2.7.1.2, and the fact that the same cask body used in the Yankee-MPC and CY-MPC configurations is analyzed and approved for the transport of directly loaded fuel, it is concluded that the 30-foot oblique drop condition is enveloped by the 30-foot side drop analysis and no further evaluation of the Yankee-MPC and CY-MPC canistered configurations of the NAC-STC for the 30-foot oblique drop condition is required.

Satisfaction of the extreme total stress intensity range limit is demonstrated in Section 2.1.3.3.

The documentation of the adequacy of the NAC-STC to satisfy the buckling criteria for the stresses of the oblique drop condition is presented in Section 2.10.5.

The NAC-STC maintains its containment capability and, therefore, satisfies the requirements of 10 CFR 71.73 for the 30-foot oblique drop hypothetical accident condition.

2.7.1.5 Lead Slump Resulting From a Cask Drop Accident

Following a drop accident, there may be a reduction in the shielding capability of the NAC-STC as a result of lead slump. Some of the fuel also may rupture. The analysis for this accident assumes that all of the fuel rods are ruptured. The three drop accidents evaluated are the bottom end drop, the side drop and the bottom corner drop. The effect of the lead slump that could result from the bottom end drop or the side drop is calculated in this section. The dose rate that could occur as a result of the corner drop is bounded by that for the bottom end drop accident.

Since the previous sections demonstrated that the Yankee-MPC and CY-MPC canistered fuel design is bounded by the NAC-STC directly loaded fuel design, the lead slump results presented herein for the directly loaded fuel design also bound the Yankee-MPC and CY-MPC canistered fuel design. Additionally, the heat load of the fuel transported in the Yankee-MPC and CY-MPC canistered fuel design is less than the 26 kW heat load considered for this evaluation.

The maximum lead slump occurs during the 30-foot bottom end drop accident. The worst case is to assume that the radial gap that exists as a result of the lead contraction following lead pour is completely filled by slumping lead leaving a voided region at the top of the lead annulus adjacent to the upper end-fitting. Prior to lead pour, the inner and outer shells of the cask are heated to approximately the temperature of the molten lead to minimize thermal stress effects. During cooldown, the contraction of the lead shell is significantly greater than that of the stainless steel inner and outer shells due to the difference in material coefficients of thermal expansion; the lead pour continues to fill the contraction gap as the lead solidifies at 620°F. As the stainless steel and lead shells cool down from 620°F to 70°F, a gap is formed. For the cold accident transport conditions (26-kilowatt heat load and -20°F ambient temperature), the shells heat up to an average temperature of 245°F with the gap partially closing. This condition represents the maximum source of radiation combined with its associated maximum contraction gap.

The hypothesized lead slump calculated for the 30-foot end drop accident is 1.73 inches. This calculated worst case value of 1.73 inches is conservative when considering details of the temperature dependent interaction of the lead gamma shield and both inner and outer steel shells. Differential axial growth between the lead and the steel will reduce and potentially eliminate the radial gap at both ends of the annulus. In addition to this effective increase in lead volume, the slumping action resulting from the 30-foot hypothetical end drop, defined by the detailed finite element analysis presented in Section 2.10.9, shows that the friction forces resulting from

differential thermal expansion and lead material properties mitigates the slumping of the lead. Therefore, the dose rate calculation based on the 1.73 inches of lead slump is conservative. Calculations were performed with the three-dimensional Monte Carlo shielding code MORSE (West). The height of the lead at the top of the lead annulus was reduced by 1.73 inches (Figure 5.3-6). The calculated dose rate at 1 meter from the cask surface is 192.55 mrem/hour with the highest contribution, 173.15 mrem/hour, from the end-fitting gamma. The second highest contribution, 8.62, is from the plenum spring gamma (see Table 5.1-6).

Thus, the hypothetical accident dose rate limits of 10 CFR 71.51 are satisfied. The results of this analysis are presented in Table 5.1-6.

For a 30-foot side drop accident, the lead may tend to slump into the lower portion of the annulus between the inner and outer shells; thus, a reduction in the thickness of lead shielding may occur on the upper side of the cask.

An evaluation of the lead slump for the side drop accident indicates that the nominal lead thickness of 3.20 inches (at the transition regions near the top and bottom end of the inner shell) may be reduced by a maximum of 0.88 inch. This calculated worst case value of 0.88 inches is conservative for the same reasons presented above for the end drop condition. The loss of a 0.88-inch thickness of lead will result in an increase in the primary gamma surface dose rate, which is calculated below:

$$\frac{D_{\text{accident}}}{D_{\text{normal}}} = (2)^{0.88/0.4} = 4.59$$

The surface dose rate along the lead annulus is highest during normal transport conditions at the fuel midplane. The primary gamma contribution at 1 meter from the cask surface at the fuel midplane would increase by a factor of 4.59 based on a half value layer for lead of 0.4 inch. There is no change in the neutron, secondary gamma and stainless steel gamma dose rate contributions as a result of this accident because they are not significantly affected by a change in lead thickness. The change to the fuel midplane dose rate contribution from the end-fittings is not considered because of their distance from the location of interest. Based on the values found in Table 5.1-9, the total dose rate 1 meter from the cask surface at the fuel midplane under these conditions would be:

$$\begin{aligned} D_{\text{total}} &= (13.53)(4.59) + (3.28)(4.59) + 1.49 \\ &= 62.1 \text{ (fuel gamma)} + 15.06 \text{ (grid spacer gamma)} + 1.49 \\ &\quad \text{(neutron)} \\ &= 78.65 \text{ mrem/hour} \end{aligned}$$

Thus, the dose rate limits of 10 CFR 71.51 are satisfied. The results of this analysis are presented in Table 5.1-6. The analysis shows that the loss of lead shielding resulting from a lead slump accident will not result in a substantial loss in shielding effectiveness and that the dose rates from this accident are small when compared to the allowable dose rates for a hypothetical accident.

THIS PAGE INTENTIONALLY LEFT BLANK

2.7.1.6 Closure Analysis - Hypothetical Accident Conditions

Section 2.6.7.5 provides a general description of the analysis approaches employed to demonstrate the structural integrity of the NAC-STC closure assembly for both normal conditions of transport and hypothetical accident conditions. The materials of construction and the geometry of the components of the closure assembly are also identified in Sections 2.6.7.5 and 2.6.7.5.1.

As discussed in Section 2.6.7.5.2, the analysis of the NAC-STC closure assembly must demonstrate that the inner and outer lids and bolts satisfy two criteria: (1) calculated maximum stresses must be less than the allowable stress limit (material yield strength is conservatively selected); and (2) lid deformation and/or rotation at the o-ring locations must be less than the elastic rebound of the o-rings.

Finite element evaluation of the closure is performed using the ANSYS computer program and a two-dimensional axisymmetric model. Three 10 CFR 71 hypothetical accident condition loadings are conservatively considered: (1) impact limiter crush pressure on the outer lid; (2) pin puncture on the outer lid; and (3) impact of the cavity contents on the inner lid. The inner and outer lids and bolts are evaluated at a temperature of 200°F.

2.7.1.6.1 Finite Element Model

2.7.1.6.1.1 Description

The components of the NAC-STC closure assembly that are considered in the finite element model include the outer lid, the inner lid and NS-4-FR neutron shielding material, the stainless steel coverplate, and the inner and outer lid bolts.

The finite element model of the NAC-STC closure is constructed utilizing the ANSYS PREP7 routine. Because both the geometric configuration and the loading conditions on the closure are axisymmetric, a two-dimensional axisymmetric model is adequate. The finite element model is shown in Figures 2.7.1.6-1 through 2.7.1.6-3. The model utilizes ANSYS STIF42 elements for the lids and STIF1 elements for the bolts. In addition, the interface between the outer lid, the inner lid, and the top forging is represented by two-dimensional interface (gap) elements (STIF12) with the coefficient of friction set to zero.

The gap elements represent two surfaces that may maintain or break physical contact, and may slide relative to each other. Note that the gap element is only capable of supporting compression in the direction normal to the surfaces and friction in the tangential directions. The gap elements transmit compressive loadings, if the surfaces are in contact, but permit no tensile load. This means that the gap elements allow the interface surfaces of the lids to separate from each other, and move relative to each other with no friction.

A large gap element stiffness is specified to maintain the boundary between the interfacing surfaces for compressive loadings.

The NS-4-FR neutron shielding material is considered to be bonded to the steel; which means that common nodes were used to connect two adjacent materials. Its compression modulus of elasticity, 0.56×10^6 psi, is two percent of the modulus of elasticity for steel and too low to have any significant effect on the flexural properties of the inner lid.

The inner and outer lid bolts are modeled as spar elements. The inner lid bolt is connected to the countersink in the lid and to the cask body at the bolt centerline. The outer lid bolt is connected to the countersink in the lid and to the top forging at the bolt centerline. The cross-sectional properties of the bolts are input to ANSYS on a "per radian" basis. The bolt preloads are applied to the finite element model as initial strains on the beam elements.

The material properties of the closure components are presented in Section 2.3.

2.7.1.6.2 Loading Conditions

The NAC-STC closure is analyzed for structural adequacy under hypothetical accident conditions in accordance with 10 CFR 71.73. The three critical accidents considered in the analyses are the 30-foot top end drop and the 30-foot top corner drop in accordance with 10 CFR 71.73(c)(1), and the pin puncture in accordance with 10 CFR 71.73(c)(2).

2.7.1.6.2.1 Loading Condition 1: 30-Foot Top End Drop

During a 30-foot top end drop, the cask (with its attached transport impact limiters) falls through a distance of 30 feet onto a flat, unyielding, horizontal surface. The cask strikes the surface in a vertical position and, consequently, a flat end impact on the top impact limiter occurs. The

compression of the impact limiter energy-absorbing material produces compressive bearing pressure on the top surface of the outer lid.

The nominal dynamic crush strength of the energy absorbing material (redwood) in the end region of the NAC-STC transport impact limiter is 1260 psi. A fabrication tolerance of ± 10 percent on the crush strength of the impact limiter material may produce a maximum crush strength equal to 1390 psi. This 1390 psi maximum crush strength occurs as a uniformly distributed, normal bearing pressure load on the top surface of the outer lid. This analysis conservatively uses a bearing pressure of 2376 psi, equivalent to a 56.1g top end impact.

In addition, during the accident, the empty fuel basket and fuel/basket spacer, which are assumed to be in the cask cavity are restrained/decelerated by the inner lid, producing a bearing pressure on the bottom surface of the inner lid. The mass of the basket and spacer, subjected to a 56.1g design deceleration, produces a uniformly distributed bearing pressure of 800 psi on the inside surface of the inner lid. The internal pressure of the cask is about 47 psi, making the total pressure on the inside surface of the inner lid 847 psi. The finite element model with boundary conditions is shown in Figure 2.7.1.6-1.

The 30-foot top end drop for the NAC-STC directly loaded fuel configuration bounds the Yankee-MPC canistered fuel configuration, since the Yankee-MPC canistered contents weight is equal to or less than that of the directly loaded fuel configuration under all scenarios. Additionally, for the Yankee-MPC canistered fuel configuration, the aluminum honeycomb spacers provide additional fuel basket deceleration at impact, further reducing the impact on the cask ends.

2.7.1.6.2.2 Loading Condition 2: Pin Puncture

The NAC-STC outer lid is analyzed for structural adequacy in accordance with the requirements of 10 CFR 71.73(c)(2) for puncture under hypothetical accident conditions. The cask is assumed to be inverted, with the lid downward, when dropped from a height of 1 meter (40 in) onto a 15-centimeter (6-in) diameter, mild steel bar oriented vertically on an unyielding surface.

During the impact, the puncture pin is considered to apply a pressure of 47,000 psi (assumed dynamic flow stress of mild steel) in the inward normal direction on the outer lid over a 6-inch

diameter region at the centerline of the exterior surface. The presence of the top impact limiter is conservatively ignored.

The force exerted by the pin on the cask is:

$$F = (p)(3)^2(47,000)$$

$$= 1.329 \times 10^6 \text{ lb}$$

The deceleration of the cask is:

$$a = \frac{F}{W}g$$

$$= 5.3g$$

where

$$W = 250,000 \text{ lb}$$

Since the weight (250,000 lb) for the directly loaded fuel configuration envelopes that of the Yankee-MPC canistered fuel configuration of the NAC-STC, the existing pin puncture analysis bounds the Yankee-MPC canistered fuel configuration.

The uniformly distributed internal pressure exerted by the spacer, the fuel assemblies and the basket on the inner lid is:

$$p = \frac{(56,350)(5.3)}{\frac{\pi}{4}(71)^2}$$

$$= 75.7 \text{ psi}$$

The finite element model with boundary conditions is shown in Figure 2.7.1.6-2.

2.7.1.6.2.3 Loading Condition 3: 30-Foot Top Corner Drop

During a 30-foot top corner drop, the cask (with its attached transport impact limiters) falls through a distance of 30 feet onto a flat, unyielding horizontal surface. As the corner of the impact limiter contacts the flat, unyielding surface, the cask body impacts on the inside diameter of the impact limiter and the cask cavity contents (spacer, basket and fuel assemblies) impact on the inside surface of the inner lid. The design deceleration of 55g (actual impact load = 44.2g, Table 2.6.7.4.1-2) acting on the cavity contents produces a pressure on the inner surface of the inner lid of:

$$p = \frac{56,350 \times 55}{(\pi)(35.50)^2}$$
$$= 785 \text{ psi}$$

Adding the contents pressure to the design internal pressure of 45 psig brings the total pressure on the inner lid to 830 psi. The bearing pressure of the impact limiter on the external surface of the outer lid and the outer lid are conservatively neglected. 847 psi internal pressure, representing 56.1g is conservatively applied to the inner lid. The finite element model with boundary conditions is shown in Figure 2.7.1.6-3.

The 30-foot top corner drop for the directly loaded fuel configuration bounds the Yankee-MPC canistered fuel design, as the total contents weight is equal to, or less than, that of the directly loaded fuel configuration under all accident scenarios. Additionally, the Yankee-MPC canistered fuel configuration includes aluminum honeycomb spacers in the cask cavity that provide additional fuel basket deceleration at impact.

2.7.1.6.3 Analysis Results

Based on the discussion presented for the Yankee-MPC canistered fuel configuration in Section 2.7.1.6.2, the results presented in this subsection for the NAC-STC directly loaded fuel configuration bound the Yankee-MPC canistered fuel configuration.

Table 2.7.1.6-1 provides a summary of the resulting stresses and deformations for the inner and outer lids as determined by the ANSYS finite element analyses for the three loading conditions

defined in Section 2.7.1.6.2. Both the stress and the deformation/rotation limit criteria are satisfied for the inner and the outer lids.

The maximum calculated stress in the outer lid is 52,042 psi, which results in a minimum margin of safety of +0.87 when evaluated with respect to material yield strength for load condition 2, pin puncture on the outer lid. Note that this evaluation is very conservative and that when the outer lid stress results are compared to non-containment structural criteria for the maximum primary membrane stress of 24 ksi with allowable of $0.7S_u$ and the maximum primary membrane plus bending stress of 52 ksi with allowable of S_u , the respective margins of safety are 2.94 and 1.59. The maximum out-of-plane rotational movement of the outer lid is 0.001 inch for load condition 1, impact limiter crush pressure on the outer lid. This elastic deformation is less than the elastic rebound of the Type 321 stainless steel o-ring material (0.005 inches); therefore, the seal is maintained.

The maximum calculated von Mises stress in the inner lid is 22,284 psi, which results in a minimum margin of safety of +0.12 when evaluated with respect to the material yield strength for load condition 1, neglecting impact limiter crush pressure on the outer lid. Note that this evaluation is very conservative and that when the inner lid stress results are compared to containment structural criteria for the maximum primary membrane stress of 2 ksi with allowable $2.4 S_m$ and the maximum primary membrane plus bending stress of 18 ksi with allowable of S_u , the respective margins of safety are +24.0 and +2.66. The maximum out-of-plane rotational movement of the inner lid is 0.0053 inch for load condition 3, impact of the cavity contents on the inner lid. This rotational movement of 0.0053 inches is calculated for a loading condition that is 27 percent larger than the conservatively postulated loading from the corner drop configuration. The corner drop loading configuration has conservatively ignored the outer lid stiffening effects on the top forging and the impact limiter loading on the top forging. Adjusting this displacement for the ratio of load, 44.2/56.1, Section 2.7.1.6.2.3, the displacement of the inner lid at the sealing surface becomes 0.0042 inches which is less than the elastic rebound of the metallic o-ring (0.005 inches). The analyses of the inner and outer lid bolts are presented in Section 2.7.1.6.4.

2.7.1.6.4 Lid Bolt Analysis

The NAC-STC inner and outer lid bolts are preloaded at installation to ensure that the sealing function of the o-rings located in the inner and the outer lids is maintained. The lid bolts are

installed with a torque that is calculated to produce a total tensile load that is not less than the total load on the lid; that is, the sum of: (1) internal pressure force on the lid; (2) o-ring compression forces; (3) inertial weight of the lid (calculated weight multiplied by the impact load factor); and (4) inertial weight of any other components that can contact the lid calculated weight multiplied by the impact load factor). Since the total bolt preload exceeds the total load on the lid, there is no movement of the lid relative to its mating component and the status of the seal at the o-ring(s) is maintained.

Inner and outer lid bolt evaluations are prepared for a complete range of impact orientations, from an end impact at 0 degrees to a flat side impact at 90 degrees, in 5-degree increments. Loads are derived from the hypothetical accident impact accelerations summarized in Table 2.6.7.4.1-3. Where necessary, impact accelerations have been interpolated at 5-degree increments from those values given in Table 2.6.7.4.1-2.

The bounding load condition for the NAC-STC inner lid bolt evaluation is the combined weight of the loaded Yankee-MPC canister, canister spacers, and inner lid multiplied by the acceleration factors applicable to the redwood impact limiter as summarized in Tables 2.6.7.4.1-1 through 2.6.7.4.1-3. Although the loaded CY-MPC canister configuration is heavier, the lower acceleration factor developed by the balsa impact limiters (Tables 2.6.7.4.2-1 and 2.6.7.4.2-2) results in a lower impact load on the inner lid bolts. Using the values from the tables, the Yankee-MPC end drop impact load is $(66,690 \times 56.1g =) 3.74 \times 10^6$ lbs. The corresponding CY-MPC impact load is $(77,885 \times 42.4 =) 3.30 \times 10^6$ lbs.

Hypothetical accident condition results are summarized in Tables 2.7.1.6-2 and 2.7.1.6-3 corresponding to a "hot" initial condition and a "cold" initial condition, respectively, for the inner lid bolts. The details of this analytic evaluation are described and example calculations are performed in Section 2.10.8 for hypothetical accident conditions. Similarly, Tables 2.7.1.6-4 and 2.7.1.6-5 summarize the analysis results corresponding to a "hot" condition and a "cold" condition, respectively, for the outer lid bolts. The "hot" condition bolt temperature is taken as 200°F, as summarized in Table 3.4.5. The "cold" condition bolt temperature is assumed to be -20°F, per regulatory requirements. Physical properties for the SB-637, Grade N07718 nickel alloy and the SA-564, H1150, 17-4PH stainless steel bolt materials are conservatively taken at 270°F for both the "hot" and "cold" condition. As defined within Table 2.1.2-1, the allowable bolt stresses are taken as the material yield strength, S_y , yielding allowable direct tension stresses of 141.7 ksi for the inner lid bolts; and 94.2 ksi for the outer lid bolts. Based on these thorough

evaluations, the inner lid bolts and the outer lid bolts incur maximum stress intensities that result in positive margins of safety as shown:

$$\text{For inner lid bolts: } M.S. = (141,700/92,870) - 1 = +0.53$$

$$\text{For outer lid bolts: } M.S. = (94,200/72,305) - 1 = +0.30$$

The bolt engagements may be evaluated by calculating shear stresses within the SA-336, Type 304 end forging and inner lid forging materials. At 270°F, the allowable shear stress is $0.42S_u$, or 26.4 ksi, according to Table 2.1.2-1. The maximum bolt tension loads in the inner and outer lid bolts are 138,541 pounds and 39,672 pounds (Section 2.6.7.5.4), respectively. The shear area per inch of engagement for 1 1/2 - 8UN internal threads is 3.792 square inches (Section 2.6.7.5.4). The total thread engagement length is 2.39 inches for the inner lid bolts.

The shear stress and the margin of safety for the inner lid bolts are:

$$\begin{aligned} S_s &= P/A = 138,541/(3.792)(2.39) \\ &= 15,287 \text{ psi} \end{aligned}$$

$$M.S. = (26,400/15,287) - 1 = +0.72$$

For the outer lid bolts, the shear area per inch of engagement for 1-8 UNC internal threads is 2.325 square inches (Section 2.6.7.5.4). The total thread engagement length is 2.0 inches. The shear stress and the margin of safety for the outer lid bolts are:

$$\begin{aligned} S_s &= P/A = 39,672/(2.325)(2.0) \\ &= 8,532 \text{ psi} \end{aligned}$$

$$M.S. = (26,400/8,532) - 1 = + 12.09$$

2.7.1.6.5 Conclusions

Using consistently conservative assumptions, the NAC-STC closure assembly is shown to satisfy the performance and structural integrity requirements of CFR 71.73(c)(1) for hypothetical accident conditions.

The inner and outer lid bolts are analyzed for the thermal (fire) accident condition in Section 2.7.3.4.

Figure 2.7.1.6-1 Finite Element Model - Lid Assembly (Loading Condition 1 - 56.1g Top Impact)

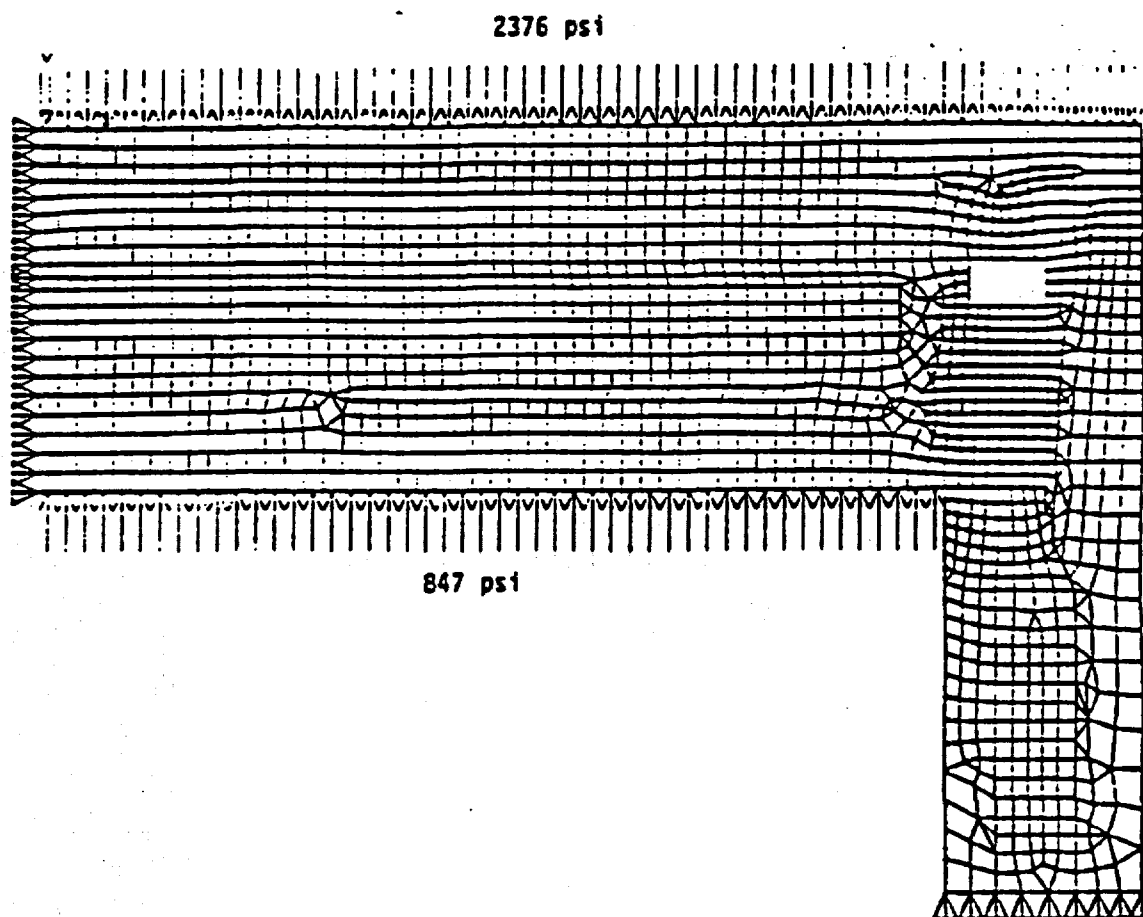


Figure 2.7.1.6-2 Finite Element Model - Lid Assembly (Loading Condition 2 - Pin Puncture)

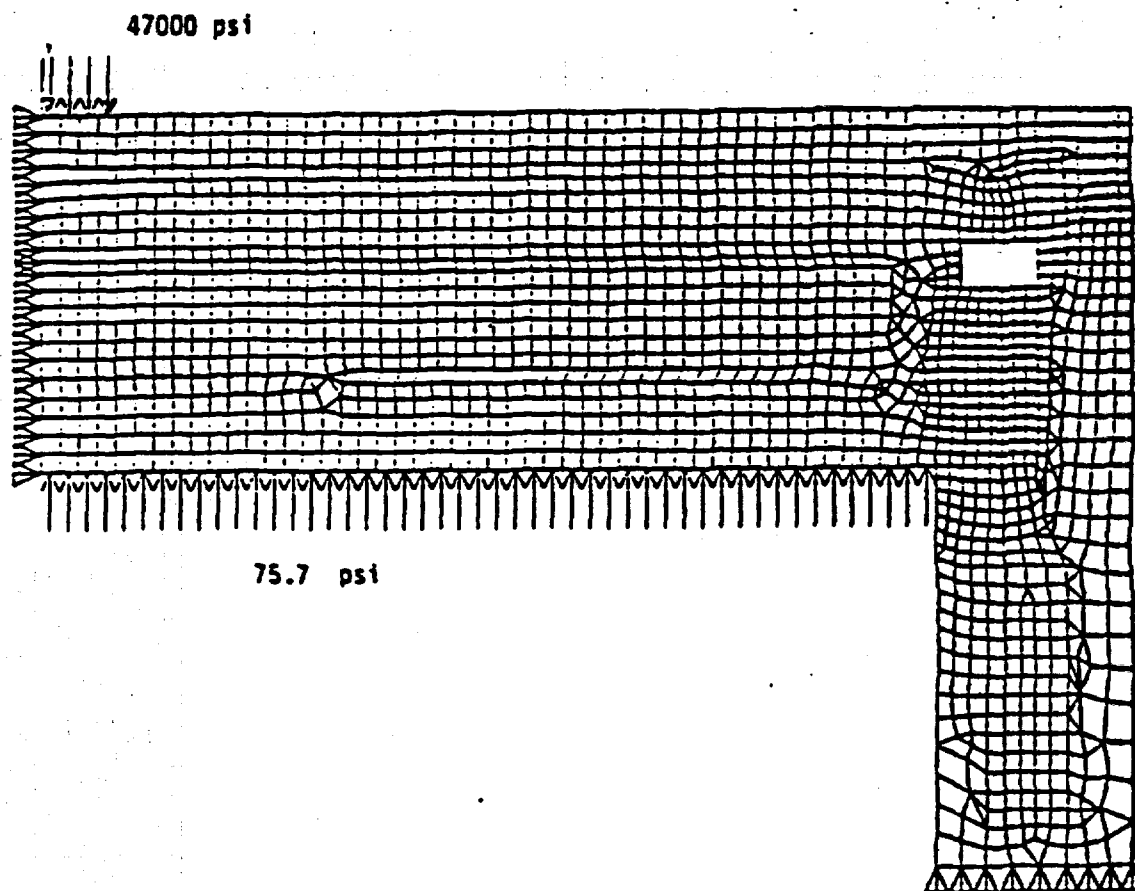


Figure 2.7.1.6-3 Finite Element Model - Lid Assembly (Loading Condition 3 - 56.1g Top Impact of Cavity Contents Plus Internal Pressure)

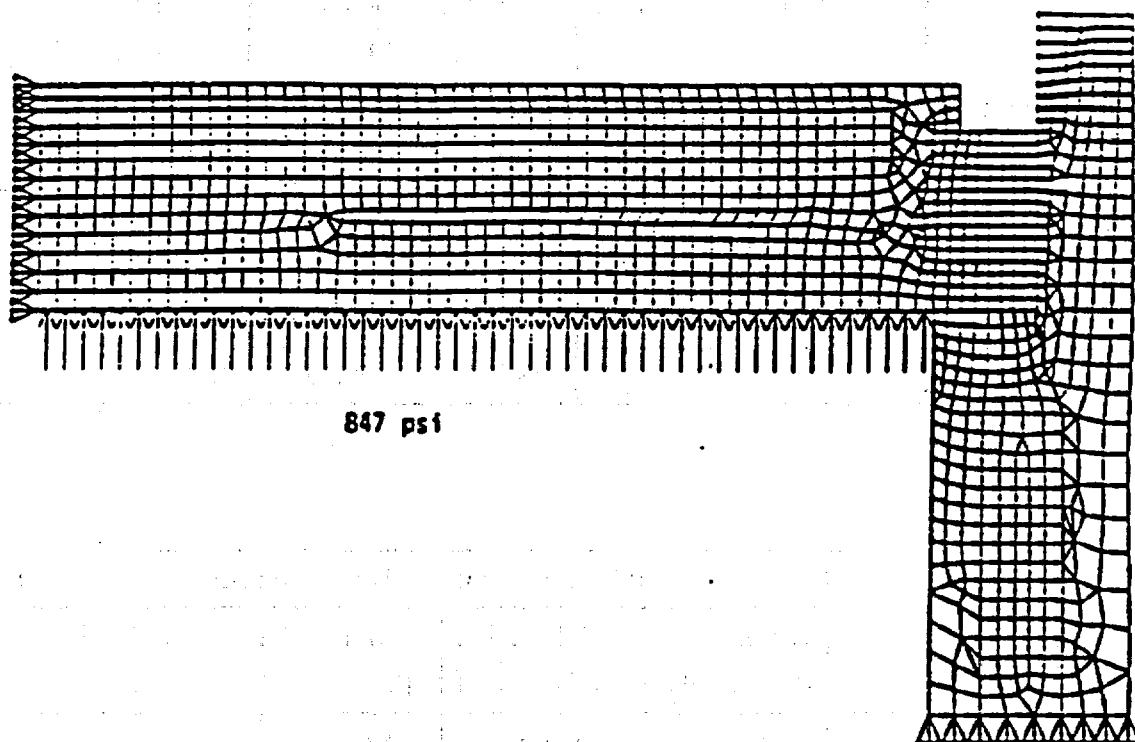


Table 2.7.1.6-1 Stress Summary - Accident Analyses of the NAC-STC Inner and Outer Lids

Load Condition	Maximum Von Mises Stress					
	Outer Lid ($S_y = 97.1 \text{ ksi @ } 200^\circ\text{F}$)		Inner Lid ($S_y = 25.0 \text{ ksi @ } 200^\circ\text{F}$)		Displacement at O-ring Location (inches)	
	Stress (psi)	Margin of Safety	Stress (psi)	Margin of Safety	Inner Lid	Outer Lid
1	19,647	+4.94	22,284	+0.12	0.003	0.001
2	52,042	+0.87	20,312	+0.23	0.0016 2	0.00016
3	-	-	22,080	+0.13	0.0053	

Load Condition	Maximum Primary Membrane Stress			
	Outer Lid 17-4 PH St. Stl. ($0.7S_u = 94.5 \text{ ksi @ } 200^\circ\text{F}$)		Inner Lid Type 304 St. Stl. ($2.4S_m = 48.0 \text{ ksi @ } 200^\circ\text{F}$)	
	Stress (psi)	Margin of Safety	Stress (psi)	Margin of Safety
1	1,530	+Large	882	+Large
2	24,000	+2.94	2,000	+Large
3	-	-	147	+Large

Table 2.7.1.6-1 Stress Summary - Accident Analyses of the NAC-STC Inner and Outer Lids (Continued)

Load Condition	Maximum Primary Membrane Plus Primary Bending Stress			
	Outer Lid 17-4 PH St. Stl. ($S_u = 135$ ksi @ 200°F)		Inner Lid Type 304 St. Stl. ($S_u = 66.2$ ksi @ 200°F)	
	Stress (psi)	Margin of Safety	Stress (psi)	Margin of Safety
1	19,647	+5.87	18,088	+2.66
2	52,042	+1.59	12,000	+4.52
3	-	-	16,029	+5.13

Table 2.7.1.6-2 NAC-STC "Hot" Inner Lid Bolt Analysis (Hypothetical Accident Condition)

Nominal Bolt Diameter (in):	1.5	Longitudinal Weight (lb):	66,690
Number of Bolts:	42	Lateral Weight (lb):	10,690
Service Stress, S_y (psi):	141,700		
Bolt Expansion (in/in):	7.30E-06 at a 270°F		
Bolt Modulus of Elasticity (ksi):	27,950 Service Temp.		
Lid Expansion (in/in):	8.94E-06	CALCULATED LOADS & STIFFNESS	
Lid Modulus of Elasticity (ksi):	27,180	Bolt Thermal Load (lb):	13,703
Bolt Stress Area (in ²):	1.492	Bolt Preload (lb):	115,066
		Bolt Static Load (lb):	9,036
Maximum Pressure (psig):	45.3	Bolt Stiffness (lb/in):	4.57E+06
Seal Diameter (in):	73.247	Lid Stiffness (lb/in):	5.40E+07
Preload Torque (ft/lb):	2740 at room temperature		
Nominal Room Temp. °F:	70		
Bolt Circle Diameter (in):	75.31		
Lid Diameter (in):	79.00		

Angle wrt. Vert. (deg)	Impact Accel. ¹ (g)	LOAD (lbs)				STRESS (psi)					Margin of Safety
		Impact		Bolt Tension		Direct Tension	Shear	Principal		Stress Intens.	
		Tension	Shear	Applied	Net			S2	S1		
0 End	56.1	98115	0	98115	136425	91437	0	0	91437	91437	0.55
5 (+)	54.7	116201	1213	116201	138541	92856	813	-7	92863	92870	0.53
10 (+)	53.3	111933	2356	111933	138208	92633	1579	-27	92659	92686	0.53
15 (+)	51.9	106903	3419	106903	137815	92369	2292	-57	92426	92483	0.53
20 (+)	50.4	100994	4387	100994	137354	92060	2941	-94	92154	92248	0.54
24 Corner	49.3	96041	5104	96041	136968	91801	3421	-127	91929	92056	0.54
30 (+)	49.5	91414	6299	91414	136607	91560	4222	-194	91754	91948	0.54
35 (+)	49.6	86641	7241	86641	136234	91310	4853	-257	91567	91824	0.54
40 (+)	49.8	81351	8148	81351	135822	91033	5461	-326	91360	91686	0.55
45 (+)	49.9	75243	8981	75243	135345	90714	6019	-398	91111	91509	0.55
50 (+)	50.1	68673	9768	68673	134832	90370	6547	-472	90842	91314	0.55
55 (+)	50.2	61401	10466	61401	134265	89990	7015	-544	90533	91077	0.56
60 (+)	50.4	53738	11109	53738	133667	89589	7446	-615	90204	90818	0.56
65 (+)	50.5	45511	11649	45511	133025	89159	7808	-679	89837	90516	0.57
70 (+)	50.7	36978	12126	36978	132359	88713	8127	-738	89451	90190	0.57
75 (+)	50.8	28037	12489	28037	131662	88245	8371	-787	89032	89819	0.58
80 (+)	51.0	18885	12784	18885	130948	87766	8568	-829	88595	89424	0.58
85 (+)	51.1	9497	12957	9497	130215	87276	8684	-856	88131	88987	0.59
90 Side	51.3	0	13057	0	129474	86779	8751	-874	87653	88526	0.60

1 See Section 2.6.7.4 for impact acceleration details.

Table 2.7.1.6-3 NAC-STC "Cold" Inner Lid Bolt Analysis (Hypothetical Accident Condition)

Nominal Bolt Diameter (in):	1.5	Longitudinal Weight (lb):	66,690
Number of Bolts:	42	Lateral Weight (lb):	10,690
Service Stress, S_y (psi):	141,700		
Bolt Expansion (in/in):	7.30E-06 at a 270°F		
Bolt Modulus of Elasticity (ksi):	27,950 Service Temp.		
Lid Expansion (in/in):	8.94E-06		
Lid Modulus of Elasticity (ksi):	27,180		
Bolt Stress Area (in ²):	1.492		
		CALCULATED LOADS & STIFFNESS	
Maximum Pressure (psig):	45.3	Bolt Thermal Load (lb):	0
Seal Diameter (in):	73.247	Bolt Preload (lb):	115,066
Preload Torque (ft/lb):	2740 at room temperature	Bolt Static Load (lb):	9,036
Nominal Room Temp. °F:	70	Bolt Stiffness (lb/in):	4.57E+06
Bolt Circle Diameter (in):	75.31	Lid Stiffness (lb/in):	5.40E+07
Lid Diameter (in):	79.00		

Angle wrt. Vert. (deg)	Impact Accel. ¹ (g)	LOAD (lbs)				STRESS (psi)					Margin of Safety
		Impact		Bolt Tension		Direct Tension	Shear	Principal		Stress Intens.	
		Tension	Shear	Applied	Net			S2	S1		
0 End	40.6	73503	0	73503	120801	80966	0	0	80966	80966	0.75
5 (+)	41.3	87735	916	87735	122617	82183	614	-5	82187	82182	0.72
10 (+)	42.0	88202	1856	88202	122653	82207	1244	-19	82226	82245	0.72
15 (+)	42.7	87953	2813	87953	122634	82194	1885	-43	82237	82281	0.72
20 (+)	43.4	86967	3778	86967	122557	82143	2532	-78	82221	82299	0.72
24 Corner	44.0	85716	4555	85716	122459	82077	3053	-113	82191	82304	0.72
30 (+)	44.7	82550	5689	82550	122212	81912	3813	-177	82089	82266	0.72
35 (+)	45.3	79130	6613	79130	121945	81733	4433	-240	81972	82212	0.72
40 (+)	45.9	74980	7509	74980	121621	81516	5033	-310	81825	82135	0.73
45 (+)	46.5	70116	8369	70116	121242	81261	5609	-385	81647	82032	0.73
50 (+)	47.0	64423	9164	64423	120798	80964	6142	-463	81427	81890	0.73
55 (+)	47.6	58221	9924	58221	120314	80639	6652	-545	81184	81729	0.73
60 (+)	48.2	51392	10624	51392	119781	80282	7121	-627	80909	81536	0.74
65 (+)	48.8	43979	11257	43979	119203	79894	7545	-706	80601	81307	0.74
70 (+)	49.4	36029	11815	36029	118582	79479	7919	-781	80260	81041	0.75
75 (+)	50.0	27596	12293	27596	117924	79038	8239	-850	79887	80737	0.76
80 (+)	50.5	18700	12658	18700	117230	78572	8484	-906	79478	80384	0.76
85 (+)	51.1	9497	12957	9497	116512	78091	8684	-954	79045	79999	0.77
90 Side	51.7	0	13159	0	115771	77595	8820	-990	78584	79574	0.78

1 See Section 2.6.7.4 for impact acceleration details.

Table 2.7.1.6-4 NAC-STC "Hot" Outer Lid Bolt Analysis (Hypothetical Accident Condition)

Nominal Bolt Diameter (in):	1	Longitudinal Weight (lb):	18,985
Number of Bolts:	38	Lateral Weight (lb):	8,120
Service Stress, S_y (psi):	94,200		
Bolt Expansion (in/in):	5.90E-06 at a 270°F		
Bolt Modulus of Elasticity (ksi):	27,300 Service Temp.		
Lid Expansion (in/in):	5.90E-06	CALCULATED LOADS & STIFFNESS	
Lid Modulus of Elasticity (ksi):	27,300	Bolt Thermal Load (lb):	0
Bolt Stress Area (in ²):	0.606	Bolt Preload (lb):	38,810
		Bolt Static Load (lb):	4,000
Maximum Pressure (psig):	7.35	Bolt Stiffness (lb/in):	5.49E+08
Seal Diameter (in):	81.81	Lid Stiffness (lb/in):	6.83E+07
Preload Torque (ft/lb):	600		
Nominal Room Temp. °F:	70		
Bolt Circle Diameter (in):	83.7		
Lid Diameter (in):	86.7		

Angle wrt. Vert. (deg)	Impact Accel. ¹ (g)	LOAD (lbs)				STRESS (psi)					Margin of Safety
		Impact		Bolt Tension		Direct Tension	Shear	Principal		Stress Intens.	
		Tension	Shear	Applied	Net			S2	S1		
0 End	56.1	30468	0	30468	39077	64483	0	0	64483	64483	0.46
5 (+)	54.7	34483	1075	34483	39672	65465	1774	-48	65513	65561	0.44
10 (+)	53.3	33198	2088	33198	39577	65309	3445	-181	65490	65672	0.43
15 (+)	51.9	31706	3030	31706	39466	65126	5000	-382	65508	65889	0.43
20 (+)	50.4	29953	3888	29953	39336	64911	6416	-628	65539	66167	0.42
24 Corner	49.3	28484	4523	28484	39227	64730	7483	-849	65580	66429	0.42
30 (+)	49.5	27112	5583	27112	39125	64562	9212	-1289	65851	67139	0.40
35 (+)	49.6	25696	6417	25696	39019	64388	10589	-1697	66085	67782	0.39
40 (+)	49.8	24127	7220	24127	38903	64196	11915	-2140	66336	68476	0.38
45 (+)	49.9	22316	7959	22316	38768	63973	13133	-2591	66564	69155	0.36
50 (+)	50.1	20367	8657	20367	38623	63734	14285	-3055	66789	69844	0.35
55 (+)	50.2	18211	9275	18211	38462	63469	15306	-3498	66967	70465	0.34
60 (+)	50.4	15938	9845	15938	38293	63190	16246	-3932	67122	71054	0.33
65 (+)	50.5	13498	10323	13498	38112	62891	17035	-4318	67208	71526	0.32
70 (+)	50.7	10967	10748	10967	37923	62580	17733	-4875	67255	71931	0.31
75 (+)	50.8	8315	11068	8315	37726	62254	18264	-4962	67217	72179	0.31
80 (+)	51.0	5601	11329	5601	37524	61921	18694	-5206	67127	72333	0.30
85 (+)	51.1	2817	11482	2817	37317	61579	18947	-5363	66942	72305	0.30
90 Side	51.3	0	11571	0	37107	61233	19094	-5466	66699	72165	0.31

1 See Section 2.6.7.4 for impact acceleration details.

Table 2.7.1.6-5 NAC-STC "Cold" Outer Lid Bolt Analysis (Hypothetical Accident Condition)

Nominal Bolt Diameter (in):	1	Longitudinal Weight (lb):	16,985
Number of Bolts:	36	Lateral Weight (lb):	8,120
Service Stress, S_y (psi):	84,200		
Bolt Expansion (in/in):	5.90E-06 at a 270°F		
Bolt Modulus of Elasticity (ksi):	27,300 Service Temp.		
Lid Expansion (in/in):	5.90E-06		
Lid Modulus of Elasticity (ksi):	27,300		
Bolt Stress Area (in ²):	0.606		
		CALCULATED LOADS & STIFFNESS	
Maximum Pressure (psig):	7.35	Bolt Thermal Load (lb):	0
Seal Diameter (in):	81.81	Bolt Preload (lb):	36,810
Preload Torque (ft/lb):	600	Bolt Static Load (lb):	4,000
Nominal Room Temp. °F:	70	Bolt Stiffness (lb/in):	5.49E+06
Bolt Circle Diameter (in):	83.7	Lid Stiffness (lb/in):	6.83E+07
Lid Diameter (in):	86.7		

Angle wrt. Vert. (deg)	Impact Accel. ¹ (g)	LOAD (lbs)				STRESS (psi)					Margin of Safety
		Impact		Bolt Tension		Direct Tension	Shear	Principal		Stress Intens.	
		Tension	Shear	Applied	Net			S2	S1		
0 End	40.6	23155	0	23155	38533	63585	0	0	63585	63585	0.48
5 (+)	41.3	26021	812	26021	39043	64428	1340	-28	64456	64484	0.46
10 (+)	42.0	26159	1645	26159	39054	64445	2715	-114	64559	64673	0.46
15 (+)	42.7	26085	2493	26085	39048	64436	4113	-262	64697	64959	0.45
20 (+)	43.4	25793	3348	25793	39026	64400	5525	-471	64871	65341	0.44
24 Corner	44.0	25422	4037	25422	38999	64354	6661	-682	65037	65719	0.43
30 (+)	44.7	24483	5041	24483	38929	64239	8319	-1060	65299	66359	0.42
35 (+)	45.3	23469	5861	23469	38854	64115	9671	-1427	65542	66969	0.41
40 (+)	45.9	22238	6655	22238	38762	63964	10981	-1833	65796	67629	0.39
45 (+)	46.5	20795	7416	20795	38655	63786	12238	-2267	66054	68321	0.38
50 (+)	47.0	19107	8121	19107	38529	63579	13401	-2709	66288	68997	0.37
55 (+)	47.6	17267	8795	17267	38392	63353	14513	-3166	66520	69686	0.35
60 (+)	48.2	15242	9415	15242	38241	63105	15537	-3618	66722	70340	0.34
65 (+)	48.8	13044	9976	13044	38078	62835	16462	-4052	66886	70938	0.33
70 (+)	49.4	10686	10470	10686	37902	62545	17278	-4456	67001	71456	0.32
75 (+)	50.0	8185	10893	8185	37716	62238	17976	-4819	67057	71876	0.31
80 (+)	50.5	5546	11218	5546	37520	61914	18511	-5112	67026	72139	0.31
85 (+)	51.1	2817	11482	2817	37317	61579	18947	-5363	66942	72305	0.30
90 Side	51.7	0	11661	0	37107	61233	19243	-5545	66778	72323	0.30

1 See Section 2.6.7.4 for impact acceleration details.

THIS PAGE INTENTIONALLY LEFT BLANK

2.7.2 Puncture

The puncture accident outlined in 10 CFR 71 Subpart F requires that the NAC-STC suffer no loss of containment as a result of a 40-inch free fall onto an upright 6-inch diameter mild steel bar (puncture pin), which is supported on an unyielding surface. The impact orientation of the cask is required to be such that maximum damage is inflicted upon the cask.

The maximum cask damage will result from direct impacts of the puncture pin on the following locations: (1) cask side - midpoint, (2) center of the cask lid, (3) center of the cask bottom, and (4) cask port covers. Since an impact at any other location is less severe, the NAC-STC is analyzed for the puncture accident at these four locations.

The canistered Yankee class fuel configuration of the NAC-STC has essentially the same weight and center of gravity location as does the directly loaded fuel configuration. Therefore, the puncture evaluations for the directly loaded fuel configuration are not affected by consideration of canistered fuel or GTCC waste in the cavity of the NAC-STC.

The first of the two main parts of the report is a description of the current state of the world. This part is divided into two sections: a description of the current state of the world and a description of the current state of the world.

The second of the two main parts of the report is a description of the future state of the world. This part is divided into two sections: a description of the future state of the world and a description of the future state of the world.

The third of the two main parts of the report is a description of the current state of the world. This part is divided into two sections: a description of the current state of the world and a description of the current state of the world.

THIS PAGE INTENTIONALLY LEFT BLANK

2.7.2.1 Puncture - Cask Side Midpoint

2.7.2.1.1 Discussion

The NAC-STC is analyzed for structural adequacy in accordance with the requirements of 10 CFR 71 for puncture (hypothetical accident condition). The cask is assumed to be in a horizontal position and dropped through a distance of 40 inches onto a 6-inch diameter, mild steel bar oriented vertically on an unyielding surface. The NAC-STC is analyzed for a cask weight of 250,000 lbs to bound the directly loaded and Yankee-MPC configurations, and for a weight of 260,000 lbs to bound the CY-MPC configuration. The static structural evaluation of the cask is performed by classical analysis and the use of relations derived from destructive testing.

2.7.2.1.2 Analysis Description

Figure 2.7.2.1-1 illustrates the local cask midpoint section that is evaluated for this analysis. It is composed of the initial 2.65-inch design thickness, Type 304 stainless steel outer shell, a 3.70-inch thick chemical lead middle shell, and a 1.50-inch thick, Type 304 stainless steel inner shell.

During impact, the puncture pin is considered to apply a force, based on its assumed 47,000 psi dynamic flow stress, of 1.329×10^6 pounds ($47,000 \times \pi \times 6^2/4$) to the cask outer shell midpoint in the inward normal direction. The neutron shield is conservatively not considered.

2.7.2.1.3 Detailed Analysis

For an impact occurring on the cask side, the required local cask outer shell thickness (t_r) for puncture integrity is calculated according to the Nelms equation (Shappert) as:

$$t_r = \left[\frac{W}{S_u} \right]^{0.71} = 2.58 \text{ in}$$

where

$$\begin{aligned} W &= \text{cask design weight} = 250,000 \text{ lb} \\ S_u &= \text{cask outer shell ultimate tensile strength at } 292^\circ\text{F} \\ &= 66,400 \text{ psi} \end{aligned}$$

for the CY-MPC configuration

$$t_r = \left[\frac{W}{S_u} \right]^{0.71} = 2.64 \text{ in}$$

where

$$\begin{aligned} W &= \text{cask design weight} = 260,000 \text{ lb} \\ S_u &= \text{cask outer shell ultimate tensile strength at } 294^\circ\text{F} \\ &= 66,400 \text{ psi} \end{aligned}$$

From the free body diagram in the sketch that follows, it can be determined that:

$$\text{Deceleration} = \frac{\text{Applied Load}}{\text{Cask Design Weight}} = \frac{1.329 \times 10^6}{250,000} = 5.32 \text{ g}$$

letting $W_B = W_L$ (Redwood Impact Limiters)

$$\begin{aligned} W_B &= (\text{weight of bottom assembly and limiter}) \times 5.32 \text{ g} \\ &= (20,990 + 8865)(5.32) \\ &= 158,829 \text{ lb} \end{aligned}$$

$$\begin{aligned} W_L &= (\text{weight of cask lids and upper limiter}) \times 5.32 \text{ g} \\ &= 158,829 \text{ lb} \end{aligned}$$

P = distributed linear load (lb/in)

$$= \frac{(250,000)(5.32) - (2)(158,829)}{192.96}$$

$$= 5,246 \text{ lb/in}$$

Then the maximum moment and shear are:

$$M_{\max} = 96.48 W_L + 0.50 P (96.48)^2 = 3.97 \times 10^7 \text{ in-lb}$$

$$V_{\max} = (1.329 \times 10^6)(0.50) = 6.645 \times 10^5 \text{ lb}$$

For the CY-MPC:

$$\text{Deceleration} = \frac{\text{Applied Load}}{\text{Cask Design Weight}} = \frac{1.329 \times 10^6}{260,000} = 5.11 \text{ g}$$

letting $W_B = W_L$ (Balsa Impact Limiters)

$$\begin{aligned} W_B &= (\text{weight of bottom assembly and limiter}) \times 5.11 \text{ g} \\ &= (20,990 + 6000)(5.11) \\ &= 137,920 \text{ lb} \end{aligned}$$

$$\begin{aligned} W_L &= (\text{weight of cask lids and upper limiter}) \times 5.11 \text{ g} \\ &= 137,920 \text{ lb} \end{aligned}$$

P = distributed linear load (lb/in)

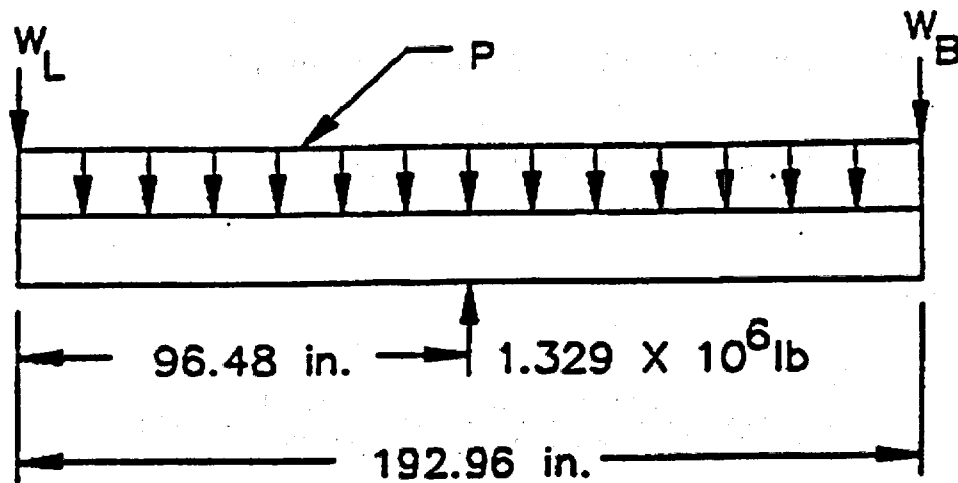
$$= \frac{(260,000)(5.11) - (2)(137,920)}{192.96}$$

$$= 5456 \text{ lb/in}$$

Then the maximum moment and shear are:

$$M_{\max} = 96.48 W_L + 0.50 P (96.48)^2 = 3.87 \times 10^7 \text{ in-lb}$$

$$V_{\max} = (1.329 \times 10^6)(0.50) = 6.645 \times 10^5 \text{ lb}$$



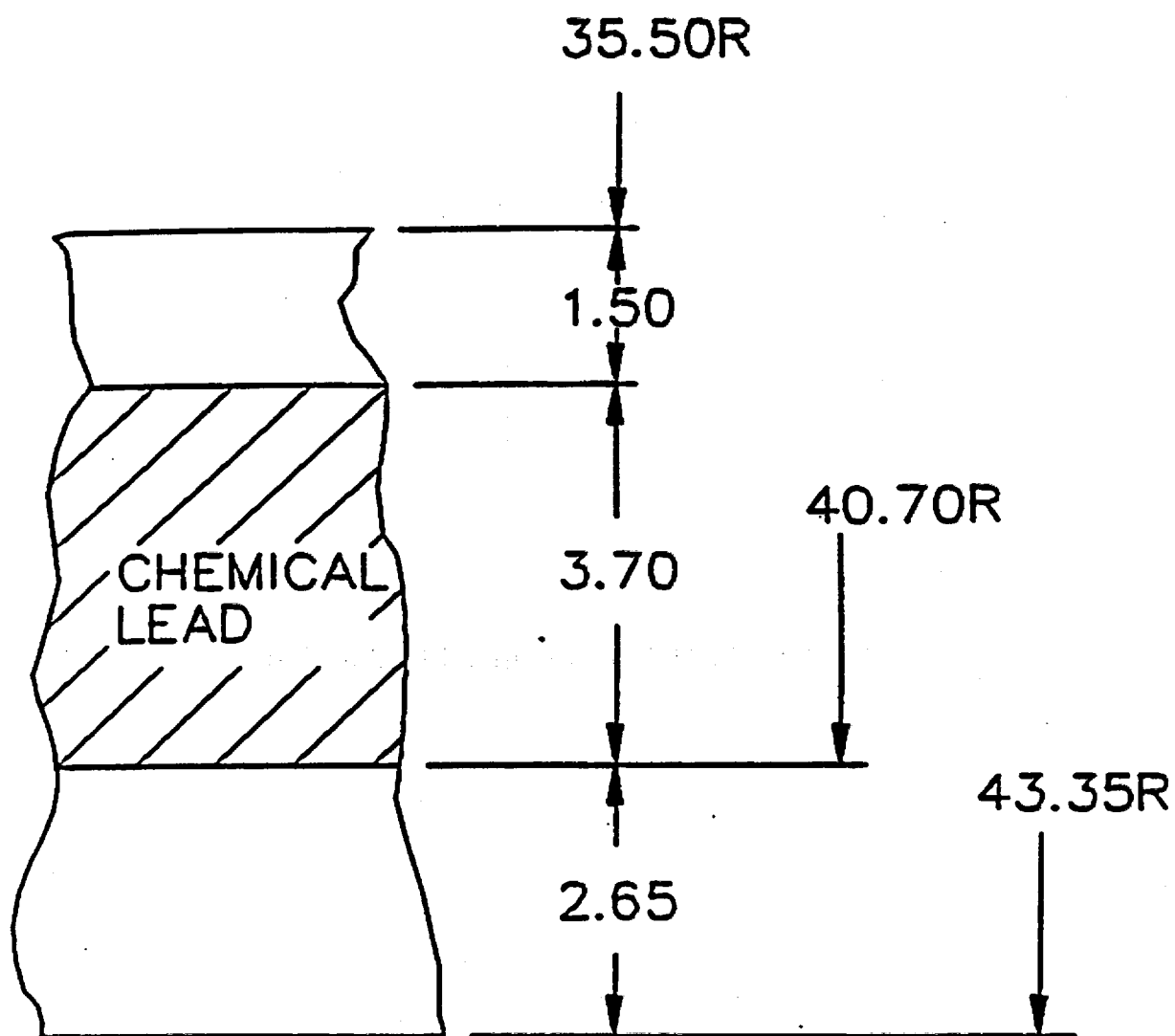
Cask Side Midpoint Puncture - Free Body Diagram

Since this loading is bounded by the 30-foot side drop loading (i.e., a cask deceleration force of $1.375 \times 10^7 \text{ lb}$, which produces $M_{\max} = 3.32 \times 10^8 \text{ in-lb}$ and $V_{\max} = 6.875 \times 10^6 \text{ lb}$), the overall cask stresses are bounded by the 30-foot side drop, disregarding the local stresses in the area of the puncture pin. Since the outer shell thickness is 2.65 inches, Nelms Equation, the margin of safety, based on thickness, is +0.03 for NAC-STC and +0.004 for CY-MPC.

2.7.2.1.4 Conclusion

For the pin puncture event at the cask midpoint, local deformation may occur in the region of the impact; however, the cask is demonstrated to have sufficient thickness to resist puncture. Therefore, the NAC-STC satisfies the requirements of 10 CFR 71 for consideration of puncture at the midpoint.

Figure 2.7.2.1-1 NAC-STC Midpoint Section



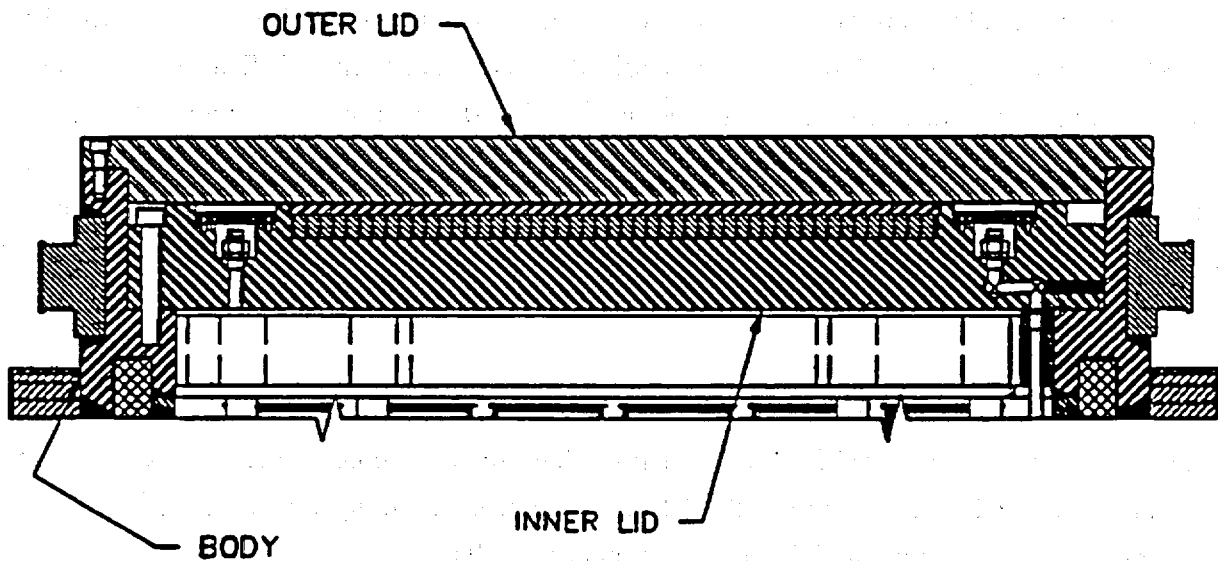
THIS PAGE INTENTIONALLY LEFT BLANK

2.7.2.2 Puncture - Center of Outer Lid

Discussion

The NAC-STC closure lids are analyzed for structural adequacy in accordance with the requirements of 10 CFR 71 for puncture (hypothetical accident condition). The cask is assumed to be inverted, with the lids downward, when dropped through a distance of 40 inches onto a 6-inch diameter, mild steel bar oriented vertically on an unyielding surface. The structural evaluation of the cask lid is performed by finite element analysis and the use of relations derived from destructive testing.

The main closure of the NAC-STC consists of an assembly of a bolted inner lid and a bolted outer lid. The Type 304 stainless steel inner lid is bolted to the top forging by forty-two 1 1/2 - 8 UN bolts fabricated from SB-637, Grade N07718 nickel alloy steel bolting material and is sealed by a metallic o-ring. The 17-4 PH stainless steel outer lid is bolted to the top forging by thirty-six 1-8 UNC bolts fabricated from 17-4 PH stainless steel and is sealed to the top forging by a metallic o-ring.



Assembly for NAC-STC Body and Lids

Lid Geometry

The main body of the inner lid is 9.0 inches thick and 79.0 inches in diameter. A 3.0-inch thick, 4.03-inch wide integral outer rim on the top of the inner lid encloses a 2.0-inch thick layer of NS-4-FR neutron shielding material and a 1.0-inch thick, Type 304 stainless steel coverplate.

The outer lid is a plate consisting of a 5.25-inch thick central main body having a 79.08-inch diameter and a 2.50-inch thick integral outer flange having an outside diameter of 86.70 inches. There is a 0.06-inch gap between the inner lid and the outer lid.

2.7.2.2.1 NAC-STC and Yankee-MPC Configuration Outer Lid Puncture Evaluation

Lid Analysis Considerations

The lid analysis must demonstrate that the lids and bolts satisfy two criteria: (1) calculated maximum stresses must be less than the allowable stress limit; the material yield strength is conservatively selected; and (2) lid deformation and/or rotation at the o-ring locations must be less than the elastic rebound of the o-rings.

Finite element evaluations of the combination of the inner and outer lids are performed using ANSYS computer program and a two-dimensional axisymmetric model. During the impact, the puncture pin is considered to apply a pressure of 47,000 psi (assumed dynamic flow stress of mild steel) on the cask lid at the centerline of the exterior surface in the inward normal direction. This is the critical load location on the outer lid because the maximum bending stress and edge rotation occur in the lid. The presence of an impact limiter is conservatively ignored. The lids and bolts are evaluated at a temperature of 200°F.

Finite Element Model Description

The components of the NAC-STC lid assembly that are considered in the finite element model include the outer lid, the inner lid, the NS-4-FR neutron shielding material, the stainless steel coverplate, the top forging, and the inner and outer lid bolts.

The finite element model of the NAC-STC lids is constructed utilizing the ANSYS PREP7 routine. Because both the geometric configuration and loading conditions on the lids are axisymmetric, a two-dimensional axisymmetric model is adequate to represent the lids. The finite element model is shown in Figure 2.7.2.2-1. The model contains ANSYS STIF42 elements for the lids and STIF3 elements for the bolts. In addition, the interfaces between the outer lid, the

inner lid, and the top forging are represented by two-dimensional interface (gap) elements (STIF12) with the coefficient of friction set to zero.

The gap elements represent two surfaces that may maintain, or break, physical contact and may slide relative to each other. Note that the gap element is only capable of supporting compression in the direction normal to the surfaces and friction in the tangential directions. Depending on whether or not there is contact between the two surfaces, the gap elements transmit compressive loadings, but permit no tensile load. This means that the gap elements allow the lid surfaces to separate relative to each other. With the coefficient of friction set to zero, no friction force is developed.

A large gap element stiffness is specified to maintain the boundary between the interfacing surfaces for compressive loadings.

The NS-4-FR neutron shielding material is considered to be bonded to the steel. With respect to a finite element model analysis "bonded" means the use of common nodes to connect two adjacent materials. Its modulus of elasticity, 0.56×10^6 psi, is two percent of the modulus of elasticity for steel and too low to have any significant effect on the flexural properties of the inner lid.

The lid bolts are modeled as spar elements. The outer lid bolt is connected to the countersink in the lid and to the cask body at the bolt centerline. The cross-sectional properties of the bolts are input on a "per radian" basis. The bolt preloads are applied to the finite element model as initial strains on the beam elements.

The material properties of the lids and bolts are from Section 2.3.

Loading Condition

The NAC-STC outer lid is analyzed for structural adequacy in accordance with the requirement of 10 CFR 71, puncture (hypothetical accident condition). During the impact, the puncture pin is considered to apply a pressure of 47,000 psi (assumed dynamic flow stress of mild steel) in the inward normal direction on the outer lid over a 6-inch diameter region at the centerline of the exterior surface. The presence of the top impact limiter is conservatively ignored.

The force exerted by the pin on the cask is:

$$F = (\pi)(3)^2(47,000)$$

$$= 1.329 \times 10^6 \text{ lb}$$

The deceleration of the cask is:

$$\begin{aligned} a &= \frac{F}{W} g \\ &= 5.3 \text{ g} \end{aligned}$$

where W is equal to 250,000 lb

The uniformly distributed internal pressure exerted by the spacer, basket, and fuel on the inner lid is:

$$\begin{aligned} p &= \frac{(56,350)(5.3)}{(\pi/4)(71)^2} \\ &= 75.7 \text{ psi} \end{aligned}$$

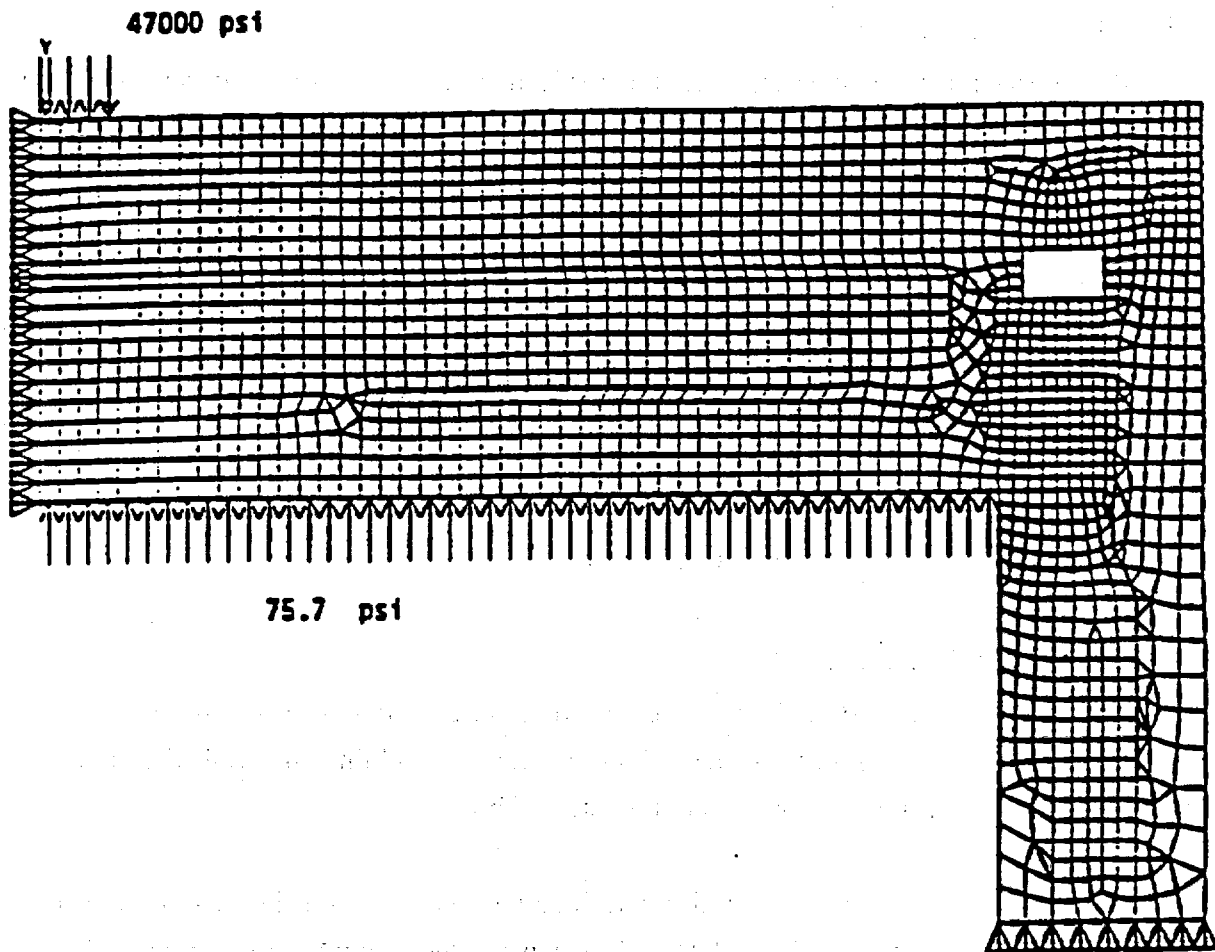
Analysis Results

The ANSYS finite element analysis of the NAC-STC closure lids for the pin puncture loading produced the results as summarized in this section.

The maximum primary membrane plus bending calculated stress in the outer lid is 52,000 psi. The ultimate strength of the 17-4 PH stainless steel is 135 ksi at 200°F, providing a margin of safety of +1.59. The maximum gap at the location of the outer o-ring on the outer lid as a result of the out-of-plane rotation of the outer lid is 0.00016 inch. This elastic, short-duration deformation is less than the elastic rebound of the metallic o-ring material (0.005 inches); therefore, the seal is maintained.

The maximum primary membrane plus bending calculated stress in the inner lid is 12,000 psi. The ultimate strength of the Type 304 stainless steel is 66.2 ksi at 200°F, providing a margin of safety of +4.52. The maximum gap at the location of the o-rings on the inner lid as a result of the out-of-plane rotation of the edge of the inner lid is 0.00162 inch. This short duration, elastic deformation is less than the elastic rebound of the metallic o-ring material (0.005 inch). The positive margins of safety on the stresses and the small displacements of the lids at the o-ring locations satisfy both stress and displacement/ rotation limit criteria for the lids. Therefore, the NAC-STC satisfies the requirements of 10 CFR 71 for consideration of puncture at the cask closure lids.

Figure 2.7.2.2-1 Finite Element Model - Lid Assembly - Yankee-MPC Pin Puncture



2.7.2.2.2 CY-MPC Configuration Outer Lid Puncture Evaluation

Lid Analysis Considerations

The lid analysis must demonstrate that the lids and bolts satisfy two criteria: (1) calculated maximum stresses must be less than the allowable stress limit; and (2) lid deformation and/or rotation at the o-ring locations must be less than the elastic rebound of the o-rings.

Finite element evaluations of the combination of the inner and outer lids are performed using ANSYS computer program and a two-dimensional axisymmetric model. During the impact, the puncture pin is considered to apply a pressure of 47,000 psi (assumed dynamic flow stress of mild steel) on the cask lid at the centerline of the exterior surface in the inward normal direction. This is the critical load location on the outer lid because the maximum bending stress and edge rotation occur in the lid. The presence of an impact limiter is conservatively ignored. The lids and bolts are evaluated at a temperature of 250°F.

Finite Element Model Description

The components of the NAC-STC lid assembly that are considered in the finite element model include the outer lid, the inner lid, the NS-4-FR neutron shielding material, the stainless steel coverplate, the top forging, and the inner and outer lid bolts.

Because both the geometric configuration and loading conditions on the lids are axisymmetric, the finite element model of the NAC-STC lids is constructed as a two-dimensional axisymmetric model. The finite element model is shown in Figure 2.7.2.2-2. The model contains ANSYS PLANE42 elements for the lids and cask and BEAM3 elements for the bolts. In addition, the interfaces between the outer lid, the inner lid, and the top forging are represented by two-dimensional interface (gap) elements (CONTAC52) with the coefficient of friction set to zero.

The gap elements represent two surfaces that may maintain, or break, physical contact and may slide relative to each other. Note that the gap element is only capable of supporting compression in the direction normal to the surfaces. Depending on whether or not there is contact between the two surfaces, the gap elements transmit compressive loads, but permit no tensile load. A gap element stiffness of 10E9 in-lbs and 1E8 in-lbs is specified for the inner bolt region and outer bolt region, respectively. For the gaps located at the bolting surfaces, the initial gap is specified to be zero. Gap elements are specifically located at the o-ring locations for evaluation of the final

gap. For other surfaces, the initial gap is defined by the initial relative location of the nodes connected, a gap stiffness of 1E6 in-lbs is used.

The NS-4-FR neutron shielding material is considered to be bonded to the steel. With respect to a finite element model analysis "bonded" means the use of common nodes to connect two adjacent materials. Its modulus of elasticity, 0.56×10^6 psi, is two percent of the modulus of elasticity for steel and too low to have any significant effect on the flexural properties of the inner lid.

The lid bolts are modeled as beam elements. The outer lid bolt is connected to the countersink in the lid and to the cask body at the bolt centerline. The bolt preloads are applied to the finite element model as initial strains on the beam elements.

The material properties of the lids and bolts are from Section 2.3.

Loading Condition

The NAC-STC outer lid is analyzed for structural adequacy in accordance with the requirement of 10 CFR 71, puncture (hypothetical accident condition). During the impact, the puncture pin is considered to apply a pressure of 47,000 psi (assumed dynamic flow stress of mild steel) in the inward normal direction on the outer lid over a 6-inch diameter region at the centerline of the exterior surface. The presence of the top impact limiter is conservatively ignored.

The force exerted by the pin on the cask is:

$$F = (\pi)(3)^2(47,000)$$

$$= 1.329 \times 10^6 \text{ lb}$$

The deceleration of the cask is:

$$a = \frac{F}{W} \times g = 5.11 \text{ g (5.3g conservatively used)}$$

where W is equal to 260,000 lbs

The uniformly distributed internal pressure exerted by the spacer, basket, and fuel on the inner lid is:

$$p = \frac{(68,000)(5.3)}{(\pi/4)(71)^2} = 91.0 \text{ psi}$$

Analysis Results

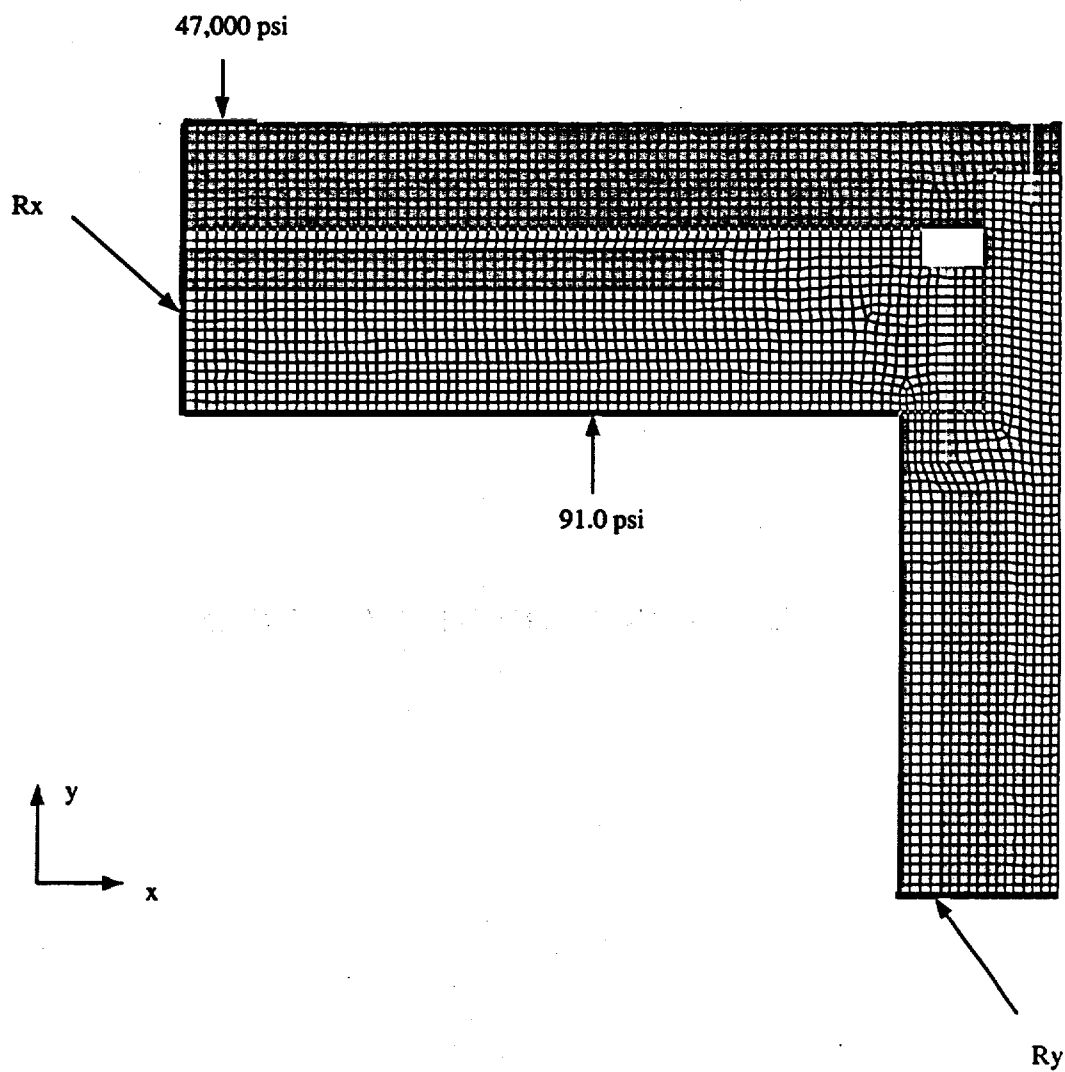
The ANSYS finite element analysis of the NAC-STC closure lids for the pin puncture loading produced the results as summarized in this section.

The maximum primary membrane plus bending calculated stress in the outer lid is 81,300 psi. The ultimate strength of the 17-4 PH stainless steel is 135 ksi at 250°F, providing a margin of safety of +0.66. The maximum gap at the location of the outer o-ring on the outer lid as a result of the out-of-plane rotation of the outer lid is 0.004 inch. This elastic, short-duration deformation is less than the elastic rebound of the metallic o-ring material (0.005 inches); therefore, the seal is maintained.

The maximum primary membrane plus bending calculated stress in the inner lid is 23,300 psi. The ultimate strength of the Type 304 stainless steel is 63.8 ksi at 250°F, providing a margin of safety of +1.73. The maximum gap at the location of the o-rings on the inner lid as a result of the out-of-plane rotation of the edge of the inner lid is 0.00001 inch. This short duration, elastic deformation is less than the elastic rebound of the metallic o-ring material (0.005 inch).

The positive margins of safety on the stresses and the small displacements of the lids at the o-ring locations satisfy both stress and displacement/ rotation limit criteria for the lids. Therefore, the NAC-STC satisfies the requirements of 10 CFR 71 for consideration of puncture at the cask closure lids.

Figure 2.7.2.2-2 Lid Assembly Finite Element Model—CY-MPC Pin Puncture



THIS PAGE INTENTIONALLY LEFT BLANK

2.7.2.3 Puncture - Center of Cask Bottom

2.7.2.3.1 Discussion

The NAC-STC bottom is analyzed for structural adequacy in accordance with the requirements of 10 CFR 71 for puncture (hypothetical accident condition). The cask is assumed to be vertical and upright when dropped through a distance of 40 inches onto a 6-inch diameter, mild steel bar oriented vertically on an unyielding surface. The NAC-STC is analyzed for a cask weight of 250,000 lb. and 260,000 lb. to bound the current STC design and the CY-MPC configuration. The structural evaluation of the cask bottom is performed by classical elastic analysis and the use of relations derived from destructive testing.

2.7.2.3.2 Analysis Description

The cask bottom geometry shown in Figure 2.7.2.3-1 depicts a 5.45-inch thick outer plate and a 6.20-inch thick inner plate enclosing a 2.0-inch thick layer of NS-4-FR neutron shield material. The plates are made from Type 304 stainless steel. The layer of neutron shield material has a 78.88-inch diameter. The temperature-dependent material properties in Section 2.3 are used in this analysis.

During the impact, the puncture pin is considered to apply a pressure of 47,000 psi (assumed dynamic flow stress of mild steel) on the cask bottom exterior surface in the inward normal direction. The presence of an impact limiter is conservatively ignored.

Vertical and rotational restraints are provided at the 78.88-inch diameter for the composite section by the outer ring of stainless steel, which has an outside diameter of 86.70 inches.

2.7.2.3.3 Detailed Analysis

For the loading and displacement boundary conditions described, the bending behavior of the bottom plates can be assessed by applying formulas from Case 7, (Roark, 4th. ed., page 218) for a fixed edge circular plate, with a concentric uniform load (q) over a circular area of radius (r).

Because of the relatively high stiffness of the NS-4-FR material in compression, any normal displacement of the outer plate due to an inward load on its exterior face will cause a corresponding displacement in the inner plate, as shown in the following analysis.

The bearing stresses in the NS-4-FR material caused by the pin load of 47,000 psi, assuming a 45-degree distribution of pressure through the outer plate to the NS-4-FR, is:

$$\begin{aligned} p &= [(3.0)^2 / (8.45)^2] (47,000) \\ &= 5924 \text{ psi} \end{aligned}$$

This is less than the 8,780 psi yield compressive strength of the NS-4-FR material. The compression deformation of the 2-inch thick NS-4-FR is:

$$\begin{aligned} e &= p(2)/E \\ &= 0.02 \text{ in} \end{aligned}$$

where $E = 561,000$ psi, the compression modulus of the NS-4-FR.

Conservatively consider that the pin load on the exterior face of the outer plate is equally shared by the outer and inner plates. Then, the effective load on the outer plate is $47,000/2$, or 23,500 psi.

The maximum stress at the center of the outer plate is given by:

$$\begin{aligned} S_r = S_t &= \frac{3 q \gamma^2}{2 m t^2} \left[(m + 1) \ln \left(\frac{a}{\gamma} \right) + (m + 1) \left(\frac{\gamma^2}{4 a^2} \right) \right] \\ &= 35,103 \text{ psi} \end{aligned}$$

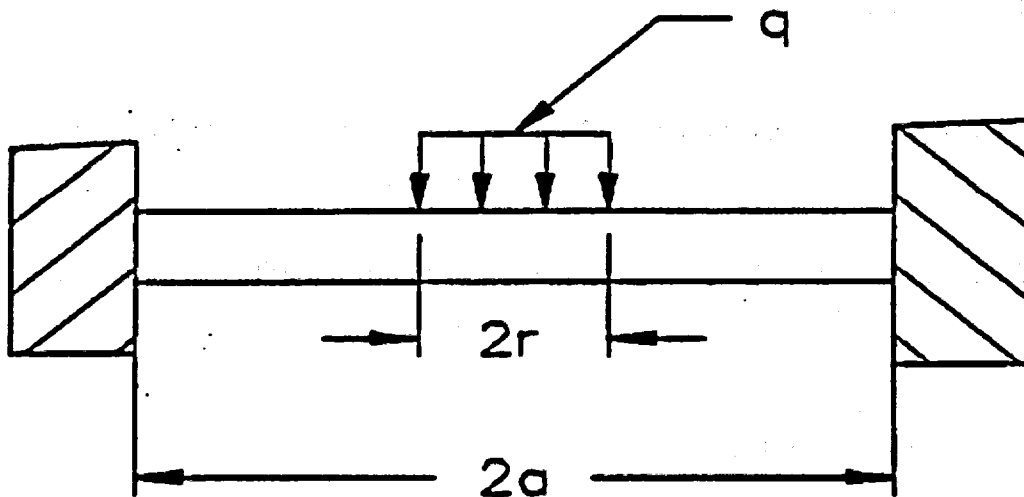
where:

$$\begin{aligned} q &= 23,500 \text{ psi} \\ \gamma &= 3 \text{ in} \\ \nu &= 0.275 \\ m &= 1/\nu = 3.636 \\ t &= 5.45 \text{ in} \\ a &= 39.44 \text{ in} \end{aligned}$$

The punching shear stress around the periphery of the pin is:

$$S_s = \frac{qY}{2t}$$

$$= 6468 \text{ psi}$$



Bottom Plate Loading Diagram

Since the maximum temperature of the cask bottom is less than 420°F for the 100°F ambient temperature hot case, the minimum ultimate strength (S_u) and design stress intensity (S_m) are 64,200 and 18,460 psi, respectively. For accident conditions, the section stress intensity resulting from $P_m + P_b$ stresses must not exceed 64,200 psi (lesser value of $3.6 S_m$ or S_u); the section stress intensity resulting from P_m stress must not exceed 44,900 psi (lesser value of $2.4 S_m$ or $0.7 S_u$). Averaging the radial bending stress and the tangential bending stresses at the center of the outer plate, the cross section primary bending stresses are:

$$S_t = S_r = \frac{S_r}{2} = 17,552 \text{ psi}$$

Conservatively, combining the bending stresses and the shear stress, the maximum stress is:

$$S_{\text{max}} = \left[\frac{(S_r' + S_t')^2}{2} + S_s^2 \right]^{0.5} = 25,651 \text{ psi}$$

Then the maximum stress intensity and margin of safety associated with $P_m + P_b$ stresses are:

$$S.I. = 2S_{\text{max}} = 51,302 \text{ psi}$$

$$M.S. = \frac{S_u}{S.I.} - 1 = +0.25$$

Clearly, the addition of S_s and S_t for the P_m stress intensity is less critical than the above stress combination.

The required local bottom plate thickness (t_r) for puncture integrity is calculated according to Shappert as:

$$t_r = \left[\frac{W}{S_u} \right]^{0.71} = 2.60 \text{ in}$$

where:

W = cask design weight = 250,000 lb

S_u = 65,200 psi (bottom plate ultimate tensile strength at 350°F)

$$M.S. = \frac{5.45}{2.60} - 1 = +1.10$$

For the CY-MPC configuration:

$$t_r = \left[\frac{W}{S_u} \right]^{0.71} = 2.67 \text{ in}$$

where:

W = cask design weight = 260,000 lb

$$S_u = 65,200 \text{ psi (bottom plate ultimate tensile strength at 350°F)}$$

$$MS = \frac{5.45}{2.67} - 1 = +1.04$$

The puncture pin load applied to the cask is:

$$\begin{aligned} F_{pp} &= \pi r^2 S_{DFS} \\ &= 1.329 \times 10^6 \text{ lb} \end{aligned}$$

where:

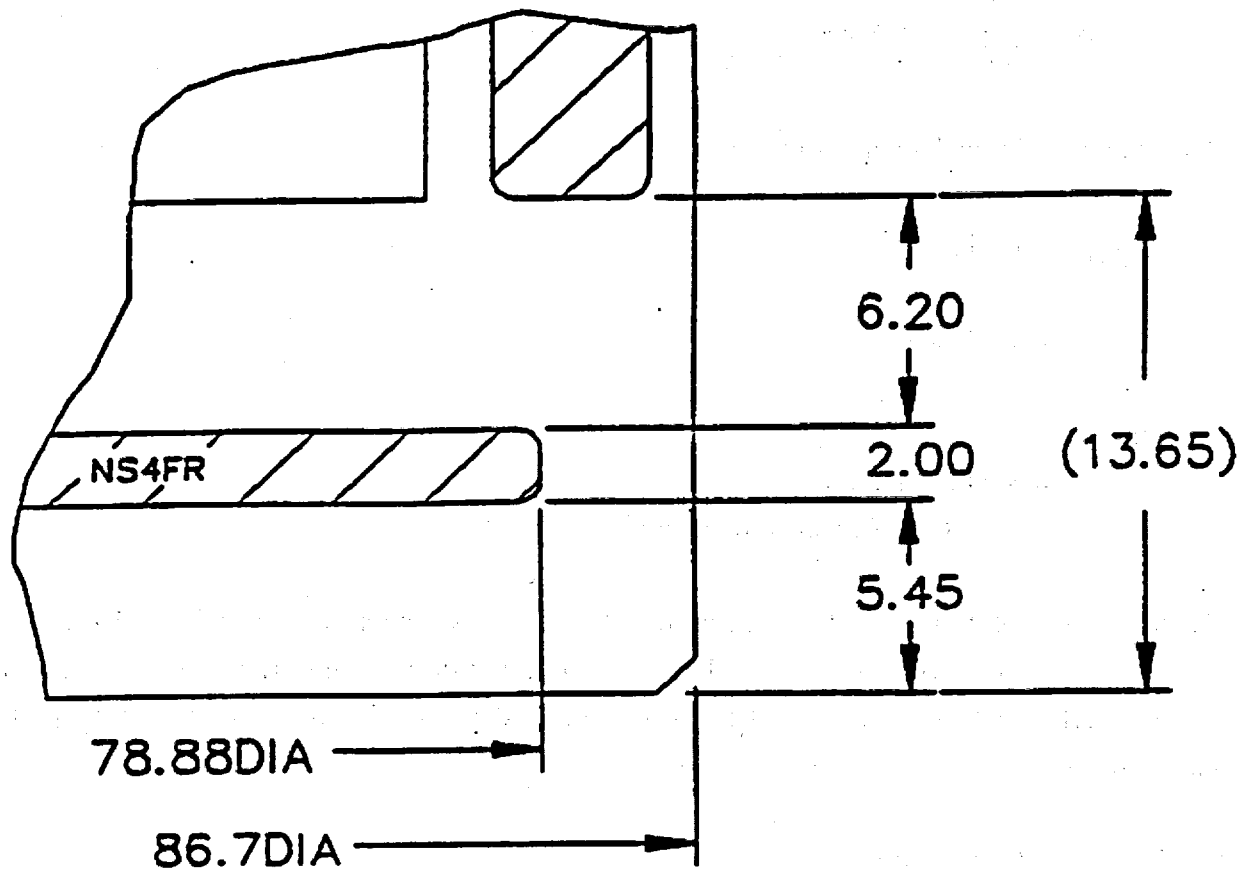
$$\begin{aligned} r &= 3.0 \text{ in (pin radius)} \\ S_{DFS} &= 47,000 \text{ psi (assumed dynamic flow stress)} \end{aligned}$$

Then, for static equilibrium, the cask deceleration force is a maximum of 1.329×10^6 pounds. Since this loading is bounded by the 30-foot bottom end drop loading (i.e., a cask deceleration force of 1.12×10^7 lb), the cask stresses are bounded by the 30-foot bottom end drop stress calculations.

2.7.2.3.4 Conclusion

For a pin puncture impact on the cask bottom, local deformation may occur in the region of the impact. However, using a conservative loading, it is determined that (1) the minimum margin of safety is +0.25, (2) the bottom plate puncture resistance exceeds puncture requirements, and (3) overall cask stresses are enveloped by the 30-foot bottom end drop analysis. Therefore, the NAC-STC satisfies the requirements of 10 CFR 71 for consideration of puncture on the cask bottom.

Figure 2.7.2.3-1 NAC-STC Bottom Design Configuration



2.7.2.4 Puncture - Port Cover

The port cover of the NAC-STC is analyzed for structural adequacy in accordance with the requirements of 10 CFR 71 for puncture (hypothetical accident condition). The cask is assumed to be in a horizontal position and dropped through a distance of 40 inches onto a 6-inch diameter, mild steel bar oriented vertically on an unyielding surface. The structural evaluation of the port cover is performed by classical elastic analysis methods.

2.7.2.4.1 Analysis Description

The port cover geometry shown in Figure 2.7.2.4-1 is typical for the two port cover locations in the top forging of the cask. Each cover centerline is located 16.4 inches axially below the top of the outer lid. In this region, the cask body is a Type 304 stainless steel ring in excess of 7 inches thick. The port cover material is SA-705, Type 630, precipitation-hardened stainless steel. The vent and drain ports are located in the inner lid where they are protected by the outer lid during normal operation. Therefore, they are not subject to pin puncture loading. The temperature-dependent material properties presented in Section 2.3 are used in this analysis.

During the impact, the puncture pin is considered to apply a pressure of 47,000 psi (assumed dynamic flow stress of mild steel) on the port cover and the surrounding exterior surface of the cask in the inward normal direction.

The port cover rotation at its mating surface with the cask body is restrained by the bolted flange configuration of the cover. The port cover is also restrained from rotation in its flange region due to the puncture pin pressure acting on its exterior surface.

2.7.2.4.2 Detailed Analysis

2.7.2.4.2.1 Local Impact Region - Port Cover

For the loading and displacement boundary conditions described, the bending behavior of the port cover is assessed by applying formulas from Case 6 (Roark, 4th ed., page 217) for a uniformly loaded circular plate with fixed edges. The maximum radial stresses and the inward deflection of the port cover are, respectively:

$$S_r = \frac{3qa^2}{4t^2} = 74,569 \text{ psi}$$

$$y = \frac{3qa^4(1-\nu^2)}{16Et^3} = 0.0013 \text{ in}$$

where:

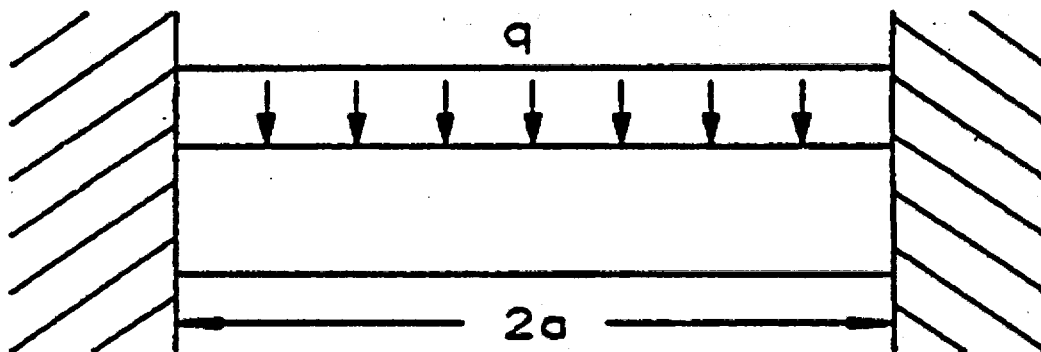
$$q = 47,000 \text{ psi}$$

$$a = 1.469 \text{ in}$$

$$t = 1.01 \text{ in}$$

$$E = 27.6 \times 10^6 \text{ psi (at } 200^\circ\text{F)}$$

$$\nu = \text{Poisson's ratio} = 0.287$$



Port Cover Plate Loading Diagram

Since the maximum port cover temperature is less than 300°F for the 100°F ambient temperature hot case (Section 3.4.2), the yield strength of the port cover (conservatively based on 300°F) is 93,000 psi. Therefore, the minimum margin of safety is +0.25. Since the clearance between the port cover and the valve exceeds 0.0013 inch, the port cover does not contact the valve during impact.

2.7.2.4.2.2 Local Impact Region - Upper Ring

Locally, the potential puncture pin force due to its dynamic flow stress is:

$$F_{pp} = (3)^2 \pi (47,000) = 1.329 \times 10^6 \text{ lb}$$

This force, acting on the 7.85-inch thick stainless steel cask body, produces a maximum shear stress:

$$S_s = F_{pp} / [6\pi(7.85)] = 8,982 \text{ psi}$$

As a result of the port cover being recessed 0.06 inches below the cask exterior surface, bearing impact is limited to the annular ring surrounding the port cover (i.e., from 4.53-inch to 6.00-inch diameter), the bearing stress on the cask is:

$$S_{br} = F_{pp} / 0.25 \pi [(6.00)^2 - (4.53)^2] = 109,317 \text{ psi}$$

If deformation of the cask and/or pin permits the pin to impact the top of the port cover, the bearing area increases to:

$$\begin{aligned} A_b &= 0.25\pi [(6.00)^2 - (4.53)^2 + (4.50)^2 - (2.875)^2] - 0.75\pi (.45)^2 \\ &= 21.09 \text{ in}^2 \end{aligned}$$

Then, the bearing stress on the cask and on the port cover is:

$$S_{br} = \frac{F_{pp}}{A_b} = 63,016 \text{ psi}$$

The allowable dynamic yield bearing stress of Type 304 stainless steel is 65,130 psi; i.e., $1.67 \times 39,000$ psi dynamic yield strength (MIL-HDBK-5A). The allowable dynamic ultimate bearing stress of Type 304 stainless steel is 132,000 psi; i.e., $2.0 \times 66,000$ psi ultimate tensile strength (MIL-HDBK-5A). Thus, the minimum yield margin of safety is +0.03 and the ultimate margin of safety is +1.09 for the bearing stress state at the cask and port cover mating surface.

For the port cover material, the yield strength is 93,000 psi (Section 2.7.2.4.2.1). The bearing stress of 63,016 psi results in a yield margin of safety of +0.48.

2.7.2.4.2.3 Cask Body Stresses

The NAC-STC is analyzed for structural adequacy during a puncture pin impact on a port cover. The cask is assumed to be in a horizontal position and dropped through a distance of 40 inches, impacting the pin on a port cover, which is located near the upper end of the cask. The static structural evaluation of the cask is performed by classical elastic analysis methods.

During an impact, the puncture pin is considered to apply a total force of 1.329×10^6 pounds (Figure 2.7.2.4-2) to the cask at the port cover in the inward normal direction assuming a pin dynamic flow stress of 47,000 psi. Vertical restraint is provided by the bottom impact limiter and the puncture pin located 16.4 inches from the top of the outer lid.

For the loading and displacement boundary conditions described, the free body diagram (Figure 2.7.2.4-2) is evaluated. For static equilibrium, the cask deceleration force (F_g) and reaction (R_r) are determined by solving the following simultaneous equations:

$$1.329 \times 10^6 - F_g + R_r = 0$$

$$F_g (85.80) - 176.62 R_r = 0$$

then

$$F_g = 2.585 \times 10^6 \text{ lb}$$

$$R_r = 1.256 \times 10^6 \text{ lb}$$

Since this loading is bounded by the 30-foot side drop loading (a cask deceleration force of 1.35×10^7 lb; Section 2.7.1.2), the cask stresses for the puncture pin impact are bounded by the 30-foot side drop accident.

2.7.2.4.3 Conclusion

For the pin puncture event, local deformation may occur in the region of impact. However, it is demonstrated by use of conservative loading that: (1) the minimum margin of safety is +0.03 for local stresses; (2) the port cover seals are maintained; and (3) cask bending stresses are enveloped by the 30-foot side drop analysis. Therefore, the NAC-STC satisfies the requirements of 10 CFR 71 for puncture of the cask at the port cover.

Figure 2.7.2.4-1 Port Cover Geometry

**FIGURE WITHHELD AS SENSITIVE
UNCLASSIFIED INFORMATION**

Figure 2.7.2.4-2 Puncture of Cask at Port Cover Location (Free body Diagram)

**FIGURE WITHHELD AS SENSITIVE
UNCLASSIFIED INFORMATION**

THIS PAGE INTENTIONALLY LEFT BLANK

2.7.2.5 Puncture Accident - Shielding Consequences

In order to comply with 10 CFR 71, calculations were performed for the hypothetical accidents described in Section 2.7. In this case, a puncture occurs, which causes a localized reduction in the cask shielding. The resulting dose rates are bounded by the loss of neutron shield accident dose rates, which do not exceed the limits of 10 CFR 71.51. Details of the shielding analysis are presented in Section 5.4.

THIS PAGE INTENTIONALLY LEFT BLANK

2.7.2.6 Puncture - Conclusion

The analyses of Section 2.7.2 demonstrate the structural and shielding adequacy of the NAC-STC for a puncture pin impact on the (1) cask side midpoint, (2) center of cask closure, (3) center of cask bottom, and (4) cask port cover. Therefore, the NAC-STC satisfies the structural and the shielding requirements of 10 CFR 71 for the puncture event.

THIS PAGE INTENTIONALLY LEFT BLANK

2.7.3 Thermal

2.7.3.1 Discussion

For the hypothetical fire accident condition, the NAC-STC cask body performs its protection and containment functions identically for both the directly loaded fuel and the canistered fuel or GTCC waste configurations. However, for the fire accident event the canistered configuration components have the advantage of not heating up as rapidly as the fuel and basket in the directly loaded fuel configuration, due to the presence of the canister shell and the gaps, each side of the shell in the heat flow path of the canistered configuration. During the cooldown period following the actual fire, the reverse situation exists so that the canistered configuration contents and basket do not cool down as rapidly as the fuel and basket do in the directly loaded fuel configuration.

The temperature and pressure evaluations of the directly loaded fuel and the canistered fuel configurations of the NAC-STC are presented in Sections 3.5.1, 3.5.3 and 3.5.4.

The NAC-STC is analyzed for structural adequacy in accordance with the requirements of 10 CFR 71.73(c)(3), Thermal, hypothetical accident conditions. The cask is assumed to be subjected to a fire, which produces a surrounding environment of 1475°F for a period of 30 minutes. The thermal evaluation of the hypothetical fire transient is presented Section 3.5. The structural evaluation of the NAC-STC for the Thermal (fire) accident is performed in this section.

THIS PAGE INTENTIONALLY LEFT BLANK

2.7.3.2 Pressure Stress Evaluation

The maximum Thermal (fire) accident condition temperatures, which are calculated in Section 3.5, are summarized in Table 3.5-1 for the various cask components. From Section 3.5.4, the maximum internal cask cavity pressure resulting from the fire transient is 65.5 psig, 42.5 psig and 56 psig for the directly loaded fuel, the Yankee-MPC canistered fuel configuration, and the CY-MPC canistered fuel configuration, respectively. These pressures are based on the assumption that the canister containment fails during the fire transient. The NAC-STC is conservatively evaluated for an internal pressure of 125 psig to protect against an unanticipated pressure buildup. The canister is evaluated for an internal pressure of 50 psig.

Stresses for lid bolt preload plus an internal pressure of 50 psig are calculated at 11 locations on the containment vessel in Section 2.6.1 (Table 2.10.4-1). Table 2.7.3.2-1 presents a tabulation of the principal stresses, the stress intensity, the allowable stress intensity, and the margin of safety at each of those locations for an internal pressure of 125 psig for the directly loaded fuel configuration of the NAC-STC; the tabulated stresses are conservatively calculated by ratioing: $S_{125} = (S_{50})(125/50)$. The allowable stress intensities are based on Table 2.1.1-1 for containment structures for hypothetical accident conditions. Tables 2.7.3.2-2 and 2.7.3.2-3 present a tabulation of the principal stresses, stress intensities, allowable stress intensities and margins of safety at 11 locations in the canister (see Figure 2.6.13.3-1). The stresses are calculated by ratioing: $S_{50} = (S_{20})(50/20)$ from Tables 2.6.13.4-1 and 2.6.13.4-2. The allowable stresses are based on Table 2.1.1-1 for Type 304L stainless steel.

The maximum deflection of the inner lid resulting from the 125 psig pressure is 0.0135 inch. Therefore, there is no loading in the outer lid bolts resulting from a 125 psig internal pressure because of a 0.06 inch gap between the outer and the inner lids.

The stress in the inner lid bolts resulting from a 125 psig internal pressure is:

$$\begin{aligned} S_{BI} &= (\pi/4)(72.331)^2(125)/(42)(1.492) \\ &= 8,197 \text{ psi} \end{aligned}$$

The accident condition allowable stress for the inner lid bolts at 400°F is 138,600 psi (S_y), so the margin of safety for the inner lid bolts is:

$$M.S. = (109,600/8197) - 1 = +Large$$

Therefore, the NAC-STC satisfies the accident condition stress intensity limits for the maximum internal cavity pressure that occurs during the Thermal (fire) accident for both the directly loaded fuel configuration and the canistered fuel configuration.

Table 2.7.3.2-1 Cask Internal Pressure Stress Summary - Thermal Accident (125 psig)

Section	Node	Principal Stresses (ksi)				Allowable	Margin
		S1	S2	S3	S.I (ksi)	S.I. ¹ (ksi)	of Safety
A5	5	1.50	1.50	0.00	1.50	48.0	+Large
C1	251	3.00	1.50	0.75	2.25	48.0	+Large
F1	251	3.00	1.50	0.75	2.25	69.6	+Large
H4	584	2.50	1.75	0.00	2.50	69.6	+Large
J1	971	2.75	1.00	-0.25	3.00	48.0	+Large
L1	1601	2.75	1.00	-0.25	3.00	48.0	+Large
N1	2216	2.75	1.00	-0.25	3.00	48.0	+Large
P4	2549	2.50	1.50	0.00	2.50	69.6	+Large
R4	2774	1.75	0.50	-2.75	4.50	69.6	+Large
V7	3617	1.00	-0.50	-3.50	4.50	94.5	+Large
X7	2807	0.75	0.75	0.00	0.75	94.5	+Large

¹ Conservatively assume primary membrane stress intensity.

Table 2.7.3.2-2 Canister Pressure Stress Summary - Thermal Accident (50 psig)
(Primary Membrane Stress)

Section	S1	Principal Stresses		S.I. (ksi)	Allowable S.I. (ksi)	Margin of Safety
		(ksi) S2	S3			
1	13.332	4.032	-3.355	16.69	35.5	1.12
2	7.210	-4.170	-5.785	13.0	35.5	1.73
3	2.782	1.375	-.005	2.79	35.5	11.7
4	1.151	.962	.317	0.83	35.5	41.7
5	.820	.682	-1.102	1.92	35.5	17.5
6	.302	-.214	-.948	1.25	35.5	27.4
7	1.070	.364	-.317	1.39	35.5	24.5
8	1.071	.343	-.194	1.26	35.5	27.2
9	3.470	1.693	-1.817	5.29	35.5	5.71
10	0.39	-.065	-.074	0.11	42.0	321.7
11	.182	.182	.001	0.18	35.5	196.2

Table 2.7.3.2-3 Canister Pressure Stress Summary - Thermal Accident (50 psig)
(Primary Membrane Stress + Bending Stress)

Section	S1	Principal Stresses (ksi) S2	S3	S.I. (ksi)	Allowable S.I. (ksi)	Margin of Safety
1	3.18	0.35	-18.61	21.8	53.3	1.44
2	3.80	-15.79	-39.95	43.8	53.3	0.21
3	2.81	1.38	-0.017	2.83	53.3	17.8
4	0.95	0.78	-0.032	0.98	53.3	53.4
5	5.17	2.15	-0.65	5.82	53.3	8.15
6	-0.58	-3.08	-2.50	2.50	53.3	20.3
7	3.87	1.63	-0.135	4.01	53.3	12.3
8	0.61	-0.26	-1.49	2.10	53.3	24.4
9	42.42	41.35	2.36	40.06	53.3	+0.33
10	-0.12	-2.98	-3.01	2.89	63.0	17.4
11	0.33	0.33	0.01	0.32	53.3	Large

THIS PAGE INTENTIONALLY LEFT BLANK

2.7.3.3 Thermal Stress Evaluation

Differential thermal expansion stresses and through-thickness thermal gradient stresses are induced in the NAC-STC as a result of the Thermal (fire) accident event. All of these thermal stresses are classified as secondary, displacement-limited stresses according to the "ASME Boiler and Pressure Vessel Code." Limits on secondary stresses do not apply for accident conditions (Table 2.1.2-1); the secondary stresses, in themselves, do not compromise the integrity of the cask. To satisfy the requirement regarding the extreme total stress intensity range that is specified in Paragraph C.7 of Regulatory Guide 7.6 (as discussed in Section 2.1.3.3), a finite element analysis is performed to determine the maximum stresses associated with the Thermal (fire) accident transient event.

The thermal analysis of the NAC-STC for the Thermal (fire) accident is presented in Section 3.5. The thermal analysis is performed using the ANSYS finite element computer code. Based on the evaluations performed in Sections 2.6.7.4.7 and 2.10.6, the impact limiters remain attached in position on the NAC-STC throughout the sequence of hypothetical accidents defined in 10 CFR 71.73. Therefore, the impact limiters are included in the finite element thermal analysis model.

The ANSYS finite element computer program is used to calculate the thermal stresses in the NAC-STC for the Thermal (fire) accident. The analysis uses the two-dimensional, axisymmetric finite element model that is described in detail in Section 2.10.2.1.1. The finite element model is constructed of two-dimensional, isoparametric solid elements with two-dimensional beam elements representing the lid bolts and two-dimensional gap elements simulating the interfaces between the lids and the body and between the shielding materials and the body. The model described in Section 2.10.2.1.1 is modified to allow the beam elements representing the bolt head to be coupled in the vertical direction to the solid elements representing the lids.

Time history results of the Thermal (fire) hypothetical accident transient analysis show that maximum gradients occur at 30 minutes into the event (when impinging flame terminates). Accordingly, temperatures at the 30-minute time step are taken

from the appropriate ANSYS file generated by the thermal analysis in Section 3.5 and are linearly interpolated for the proper nodal locations of the structural analysis finite element model. A uniform temperature of 70°F is input as the initial stress free condition of the structural finite element model. Temperature dependent material properties are input in tabular form to allow ANSYS to use the correct properties for each nodal temperature. The temperature dependent material properties are obtained from the "ASME Boiler and Pressure Vessel Code, Section III, Division 1": "Appendix I" for temperatures less than or equal to 800°F. For temperatures over 800°F material properties are obtained from "ASME Boiler and Pressure Vessel Code, Section III, Division 1, Subsection NH" and Section II, Part D, Subpart 2." For material properties not explicitly covered by the code, extrapolated values are used.

The maximum primary plus secondary nodal stress components and principal stresses, calculated by ANSYS in the NAC-STC containment vessel for the directly loaded fuel configuration for the 30-minute time step of the Thermal (fire) Accident, are summarized in Table 2.10.4-178. The detailed results of the ANSYS stress calculations for the NAC-STC during the Thermal (fire) Accident are contained in Tables 2.10.4-178 through 2.10.4-180. Based on the temperature comparison that is discussed in Section 3.5.3 for the canistered fuel configuration and the temperatures tabulated in Table 2.7.3.2-1, the components within the canister (support disk and aluminum heat transfer disk) have higher temperatures than the directly loaded fuel basket, but the cask components (containment boundary) have lower temperatures. Therefore, the thermal evaluation of the canistered fuel configuration of the NAC-STC cask is bounded by that of the directly loaded fuel configuration.

To conservatively evaluate the stress state in the NAC-STC as specified in Paragraph C.7 of Regulatory Guide 7.6, the maximum primary plus secondary (P+Q) stress intensity in the NAC-STC containment vessel for the Thermal Accident will be used (92.2 ksi at Location R on the containment vessel). It is demonstrated in other sections of this Safety Analysis Report that the maximum combined primary membrane plus primary bending stress intensities for all of the other normal conditions of transport and hypothetical accident conditions satisfy Regulatory Guide 7.6, i.e. they are less than $1.0 S_u$. It is, therefore, conservative to assume that the maximum allowable value for the primary stresses, $1.0 S_u$, actually develops within the NAC-STC containment vessel.

The maximum S_u value for the NAC-STC containment vessel material at Location R is 100.0 ksi (Type XM-19 stainless steel). Adding this maximum S_u value to the maximum P+Q stress

intensity calculated for the Thermal Accident at Location R, the total primary plus secondary stress intensity is $92.2 + 100.0 = 192.2$ ksi. The maximum possible stress intensity range is twice this value, or $(2)(192.2) = 384.4$ ksi. The appropriate alternating stress is one-half of this value, or $S_{alt} = (0.5)(384.4) = 192.2$ ksi. To account for the temperature effects, the variation in modulus of elasticity of the material is factored into the calculation as follows:

$$\begin{aligned} S_{alt}(850^{\circ}\text{F}) &= (E_{70}/E_{850})(S_{alt}) \\ &= [28.3 \times 10^6 / 23.8 \times 10^6](192.2) \\ &= 228.5 \text{ ksi} \end{aligned}$$

At 850°F , "ASME Boiler and Pressure Vessel Code, Section III, Division 1, Subsection NH" limits the strain range of Type 316 stainless steel to 0.04080 inch/inch, and the strain range of Type 304 stainless steel to 0.04825 inch/inch. This analysis conservatively applies a strain range limit of 0.0303 inch/inch. For the modulus of elasticity at 850°F of 23,800 ksi, the S_{alt} at 10 cycles is $(0.0303)(23,800 \text{ ksi})$ or 721.1 ksi.

$$\text{M.S.} = (721.1/228.5) - 1 = +2.15$$

Considering the conservative assumptions that were used in the preceding evaluation, i.e. (1) use of the allowable primary stress rather than the actual value; (2) assuming fully reversing primary and secondary stress states to determine stress intensity ranges; and (3) assuming that the worst case primary stresses occur simultaneously with the worst case fire transient stresses, it is apparent that the actual margin of safety is significantly larger than +2.15. Thus, the requirements of Paragraph C.7 of Regulatory Guide 7.6 are satisfied.

THIS PAGE INTENTIONALLY LEFT BLANK

2.7.3.4 Bolts - Closure Lids (Thermal Accident)

During the thermal (fire) hypothetical accident, the NAC-STC inner lid bolts and outer lid bolts are calculated to experience a maximum average temperature of 335°F. This ANSYS analysis of the closure lids and bolts was performed using an average temperature of 310°F. The effect on the stress results due to the temperature difference of 25°F (335-310) is insignificant since the increase of the coefficient of thermal expansion (thermal stress) for the bolt material is less than 0.5%.

The maximum thermal gradients occur at the end of the fire (30 minutes), which produces the largest differential thermal growth between the inner and outer lids of the cask body. Using the results of the ANSYS analysis at the end of the fire (30 minutes), the maximum membrane and bending stresses for the lid bolts, including the combined effects of the 125 psig internal pressure, o-ring compression forces, bolt preload, and thermal accident conditions, are determined as shown in Figure 2.7.3.4-1 to be:

<u>Bolt Location</u>	<u>Maximum Membrane + Bending (ksi)</u>
Inner Lid Bolts:	90.5 + 6.3 = 96.8
Outer Lid Bolts:	82.3 + 1.6 = 83.9

Based on the yield stress at 335°F, the margins of safety are:

Inner Lid bolts (SB-637 Grade N07718)

$$\text{M.S.} = \frac{139.9}{96.8} - 1 = +0.45$$

Outer Lid bolts (17-4PH Stainless Steel)

$$\text{M.S.} = \frac{918}{83.9} - 1 = +0.09$$

Figure 2.7.3.4-1 Bolt Stress - Thermal (Fire) Accident

```

POST1 -INP=
PSBI

PRINT ELEMENT STRESS ITEMS PER ELEMENT
***** POST1 ELEMENT STRESS LISTING *****
LOAD STEP 1 ITERATION= 50 SECTION= 1
TIME= 0. LOAD CASE= 1

ELEM SDI SBI SBJ
2536 13362. 6331.6 -0.36972E-10
2540 15093. -1606.6 -0.16853E-10
2843 0. -0.27634E-10 3928.8
2844 -0.10730E-09 6089.6 0.29950E-10
2845 82316. -1606.6 -1606.6
2846 0.12982E-09 0.20382E-11 12067.
2847 -0.19442E-09 11432. 0.64312E-10
2848 90483. 6331.6 6331.6

MINIMUMS
ELEMENT 2847 2840 2843
VALUE -0.19442E-09 -1606.6 -1606.6

MAXIMUMS
ELEMENT 2848 2847 2846
VALUE 90483. 11432. 12067.
POST1 -INP=
PRINT NODE LISTING
***** POST1 NODE LISTING *****

NODE X Y Z THX THY THXZ
3057 35.206 187.40 0. 0.000 0.000 0.000
3058 35.206 188.40 0. 0.000 0.000 0.000
7024 37.655 176.90 0. 0.000 0.000 0.000
7064 37.655 179.40 0. 0.000 0.000 0.000
9000 33.705 192.78 0. 0.000 0.000 0.000
9001 35.206 192.78 0. 0.000 0.000 0.000
9002 36.455 192.78 0. 0.000 0.000 0.000
9003 36.833 185.40 0. 0.000 0.000 0.000
9004 37.655 185.40 0. 0.000 0.000 0.000
9005 38.608 185.40 0. 0.000 0.000 0.000
POST1 -INP=
5

PRINT ELEMENT LISTING
***** POST1 ELEMENT LISTING *****
ELEM TYPE STIF MAT ESTS NODES
2536 3 3 13 0 7064 7024
2540 3 3 12 0 3058 3057
2843 3 3 12 0 9000 9001
2844 3 3 12 0 9001 9002
2845 3 3 12 0 9001 3058
2846 3 3 12 0 9003 9004
2847 3 3 12 0 9006 9005
2848 3 3 12 0 9006 7064
POST1 -INP=

POST DATA FILE= 12
LOAD STEP= 1
ITERATION= 50
CURRENT INPUT FILE= 05
GEOMETRY STORED FOR 3059 NODES 2842 ELEMENTS
***** STRESS DEFINITIONS *****
LABEL STIF ITEM

```

OUTER LID BOLT
INNER LID BOLT

2.7.3.5 Performance Summary - Thermal Accident

The NAC-STC satisfies all licensing and performance criteria for the Thermal (fire) accident; thus, containment of the cask contents is ensured.

THIS PAGE INTENTIONALLY LEFT BLANK

2.7.3.6 Conclusion

The NAC-STC cask shells, lids, and lid bolts are demonstrated to be structurally adequate against loss of containment. Therefore, the NAC-STC cask satisfies 10 CFR 71 structural requirements for the fire accident scenario.

95, 100, 105

100, 105

THIS PAGE INTENTIONALLY LEFT BLANK

2.7.4 Crush

In accordance with 10 CFR 71.73(c)(2) and IAEA Safety Series No. 6, paragraph 627(c), this test is not applicable to the NAC-STC because the mass of the cask and contents is greater than 500 kilograms (1100 lb) and the cask and contents have an overall density greater than 1000 kilograms/cubic meter (62.4 lbs/ft³).

10/10/2004 10:10:10 AM

10/10/2004 10:10:10 AM

THIS PAGE INTENTIONALLY LEFT BLANK

2.7.5 Immersion - Fissile Material

According to the requirements of 10 CFR 71.73(c)(5), a package containing fissile material, where water inleakage has not been assumed for criticality analysis, must be subjected to water pressure equivalent to immersion under a head of water of at least 0.9 meters (3 feet) for a period of 8 hours. This immersion is the fifth test in the Hypothetical Accident sequence of tests for the package. Paragraph No. 633 of IAEA Safety Series No. 6 specifies the same requirements for the international shipment of radioactive materials. A head of water of 0.9 meters (3 feet) is equivalent to an external pressure of $(3)(0.433) = 1.3$ psig.

The analyses presented in Sections 2.7 through 2.7.3 document that the NAC-STC maintains containment of the package contents for the sequence of Hypothetical Accident tests - free drop, puncture, and fire - that precede the immersion test. The outer lid is shown to be structurally adequate for a maximum external dynamic crush pressure of the top impact limiter of 2376 psi (Section 2.7.1.6). For the 2.65-inch thick outer shell with a mean radius of 42.03 inches, an external pressure of 1.3 psig produces a negligible compressive hoop stress. According to the manufacturer's specifications, the metallic o-rings used in the NAC-STC are adequate for pressures in excess of 5000 psi. Therefore, the NAC-STC satisfies the immersion requirement of 10 CFR 71.73(c)(5) for a package containing fissile material.

The criticality analyses of both the directly loaded fuel configuration and the canistered fuel configuration do assume water inleakage, so containment of the package contents is an additional safety consideration.

THIS PAGE INTENTIONALLY LEFT BLANK

2.7.6 Immersion - All Packages

According to the requirements of 10 CFR 71.73(c)(6), a package must be subjected to water pressure equivalent to immersion under a head of water of at least 15 meters (50 ft) for a period of 8 hours. Paragraph 630 of IAEA Safety Series No. 6 requires that a package be immersed under a head of water of at least 200 meters (656 ft) for a period of not less than 1 hour. A head of water of 200 meters (656 ft) is equivalent to an external pressure of $(656)(0.433) = 284$ psig. Also, 10 CFR 71.61 requires that a package's undamaged containment system be able to withstand an external water pressure of 290 psi for a period of not less than one hour without collapse, buckling or inleakage of water.

The outer lid is shown to be structurally adequate for a maximum external dynamic crush pressure of the top impact limiter of 2376 psi (Section 2.7.1.6). For the 2.65-inch thick outer shell with a mean radius of 42.03 inches, an external pressure of 290 psig produces a compressive hoop stress of -4599 psi, which is much less than the material yield strength. According to the manufacturer's specifications, the metallic o-rings used in the NAC-STC are adequate for pressures in excess of 5000 psi.

Therefore, the NAC-STC satisfies all of the immersion requirements for a package that is used for the international shipment of radioactive materials.

THIS PAGE INTENTIONALLY LEFT BLANK

2.7.7 Damage Summary

The analysis results reported in Sections 2.7.1 through 2.7.6 are summarized in Tables 2.7.7-1 through 2.7.7-3.

These results indicate that the damage incurred by the NAC-STC during the hypothetical accident is minimal and does not diminish the cask's ability to maintain the containment boundary. A 30-foot drop or a 40-inch pin puncture accident may damage the neutron shield and result in a reduction in the cask's neutron shielding ability. However, the gamma shielding remains intact to provide sufficient shielding to satisfy the accident shielding criteria. (Section 2.7.1.5 discusses the shielding consequences of the drop accidents).

Also, in a 30-foot hypothetical drop accident, the impact limiters may crush to a maximum depth of 31.6 inches, and the lead may slump to a maximum of 1.73 inches. These potential consequences have no adverse structural effects.

Based on the analyses of Sections 2.7 through 2.7.6, the NAC-STC fulfills the structural and shielding requirements of 10 CFR 71 for all of the hypothetical accident conditions.

Table 2.7.7-1 Summary of Maximum Calculated Stresses - 30-Foot Free Drop

30-Foot Drop	Conditions [*]					Maximum Calculated Stress		Allowable Stress	Margin Of
	1	2	3	4	5	Type	Value (ksi)	(ksi)	Safety
Containment ^{**}	✓	✓	✓	✓	✓	P_m	16.4	48.0	+1.9
(on end)	✓	✓	✓	✓	✓	$P_m + P_b$	38.5	69.8	+0.8
Noncontainment ^{***}	✓	✓	✓	✓	✓	P_m	12.5	44.9	+2.6
(on end)	✓	✓	✓	✓	✓	$P_m + P_b$	23.1	64.2	+1.8
Containment ^{**}	✓	✓	✓	✓	✓	P_m	36.0	49.3	+0.4
(on side)	✓	✓	✓	✓	✓	$P_m + P_b$	49.4	70.9	+0.4
	✓	✓	✓	✓	✓		55.4	65.9	+0.2 ^{****}
Noncontainment ^{***}	✓	✓	✓	✓	✓	P_m	24.8	44.9	+0.8
(on side)	✓	✓	✓	✓	✓	$P_m + P_b$	34.1	64.2	+0.9
	✓	✓	✓	✓	✓		37.4	65.9	+0.8 ^{****}
Containment ^{**}	✓	✓	✓	✓	✓	P_m	34.8	49.3	+0.4
(oblique)	✓	✓	✓	✓	✓	$P_m + P_b$	51.8	69.8	+0.3
Noncontainment ^{***}	✓	✓	✓	✓	✓	P_m	24.1	44.9	+0.9
(oblique)	✓	✓	✓	✓	✓	$P_m + P_b$	40.3	64.2	+0.6

Conditions are:

1. Ambient Temperature (100°F)
2. Insolance (-20°F)
3. Decay Heat
4. Internal Pressure
5. Weight of Contents

^{**} The containment structure includes the inner lid, top forging, inner shell, and bottom inner forging.

^{***} The noncontainment structure includes the outer lid, the outer shell, the bottom outer forging, and the bottom plate.

^{****} These stresses correspond to the canistered fuel configuration.

Table 2.7.7-2 Summary of Maximum Calculated Stresses - Puncture

40 Inch Drop	Conditions [*]					Maximum Calculated Stress		Allowable Stress		Margin Of
	1	2	3	4	5	Type	Value (ksi)	Type	Value (ksi)	Safety
Containment ^{**}										
(inner lid)	✓	✓	✓	✓	✓	$P_a + P_b$	12.0	1.0 S_u	66.2	+4.52
Noncontainment ^{***}										
(on mid-length)	✓	✓	✓		✓	-	-	-		+0.03 ^{****}
Noncontainment ^{***}										
(on bottom center)	✓	✓	✓			$P_a + P_b$	51.3	1.0 S_u	64.2	+0.25
(outer lid center)	✓	✓	✓	✓	✓	$P_a + P_b$	52.0	1.0 S_u	135.0	+1.59

^{*} Conditions

1. Ambient Temperature (100°F)
2. Insulance (-20°F)
3. Decay Heat
4. Internal Pressure
5. Weight of Contents

^{**} The containment structure includes the inner lid, top forging, inner shell, and bottom inner forging.

^{***} The noncontainment structure includes the outer lid, the outer shell, the bottom outer forging and the bottom plate.

^{****} Result obtained from the displacement criteria, not from the stress criteria.

Table 2.7.7-3 Summary of Maximum Calculated Stresses - Thermal (Fire) Accident

40 Inch Drop	Conditions*					Maximum Calculated Stress		Allowable Stress		Margin Of Safety
	1	2	3	4	5	Type	Value (ksi)	Type	Value (ksi)	
Containment**										
(top forging)			✓	✓	✓	$P_m + P_b + Q$	228.5	S_{sk}	721.1	+2.15
Noncontainment***										
(outer shell)			✓	✓	✓	$P_m + P_b + Q$	216.2	S_{sk}	721.1	+2.33
Inner Lid Bolts			✓	✓	✓	$P_m + Q$	96.8	S_y	140.9	+0.45
Outer Lid Bolts			✓	✓	✓	$P_m + Q$	83.9	S_y	93.0	+0.11

* Conditions

1. Ambient Temperature (100°F)
2. Insolation (-20°F)
3. Decay Heat
4. Internal Pressure
5. Weight of Contents

** The containment structure includes the inner lid, top forging, inner shell, and bottom inner forging.

*** The noncontainment structure includes the outer lid, the outer shell, the bottom outer forging and the bottom plate.

2.7.8 Directly Loaded Fuel Basket Analysis - Accident Conditions

The hypothetical accident condition analyses of the directly loaded fuel basket are presented in this section. The accident condition analyses of the canistered fuel basket and GTCC waste basket are presented in Sections 2.7.9 and 2.7.10, respectively.

The directly loaded fuel basket for the NAC-STC is designed to contain 26 PWR fuel assemblies, each of which produces a 0.85-kilowatt heat load. The basket structure has a right circular cylinder configuration and consists of 26 square fuel tubes supported by 31 circular support disks, a circular top and bottom plate, which are retained by six threaded rods with spacer nuts. The structural design of the NAC-STC 26 PWR fuel assembly basket is illustrated in Figure 2.7.8-1.

Each fuel tube has an 8.78-inch square inside dimension, a 0.142-inch thick wall, and can hold one intact PWR fuel assembly. The fuel assemblies together with the tubes are laterally supported in square holes in the stainless steel support disks. Each circular support disk is 0.5 inches thick, 70.86 inches in diameter, and has 26 holes that are each 9.234 inches square. There are two different web widths in the support disks. One web width is 1.47 inches between the holes, and the other web width is 3.27 inches between the holes. The top and bottom plates are both 1.0 inch thick and have the same diameter as the support disks. The disks are spaced and retained at 4.87-inch center-to-center intervals by threaded rods and spacer nuts at six locations near the periphery of each disk to form an integral basket assembly. The fuel basket contains the fuel and is enclosed by the inner shell of the cask.

The material of the support disks is 17-4 PH stainless steel. The top plate and the bottom plate are fabricated from Type 304 stainless steel. The 26 square fuel tubes are made from Type 304 stainless steel encasing BORAL. The threaded rods and spacer nuts are fabricated from 17-4 PH stainless steel. The fuel tubes are not structural components; and are not considered in the basket evaluation. The primary function of the threaded rods and spacer nuts is to locate and structurally assemble the circular support disks, heat transfer disks, and the top and bottom plates to form an integral assembly. The threaded rods and spacer nuts carry the inertial weight of the support disks heat transfer disks, endplate and their own inertial weight for a 30-foot end drop accident loading condition. The end drop loading condition of the threaded rods and spacer nuts represents classical closed form analysis and they are evaluated independent of the finite element

basket model. The support disks structural evaluation is performed using a finite element model of a single disk. Figure 2.7.8-2 shows a support disk cross-sectional configuration.

The directly loaded fuel basket is evaluated for the normal conditions of transport loads in Section 2.6.12 and is evaluated for the hypothetical accident loads in this section. Both stress analyses and buckling evaluations are performed and documented in the subsequent sections. In addition to structural analysis of the basket components qualified to ASME Code, Section III, Division 1, Subsection NG, "Core Support Structures," an evaluation of the stainless steel/BORAL composite fuel tube has been performed for a postulated impact load.

Figure 2.7.8-1 NAC-STC Directly Loaded 26 PWR Fuel Assembly Basket

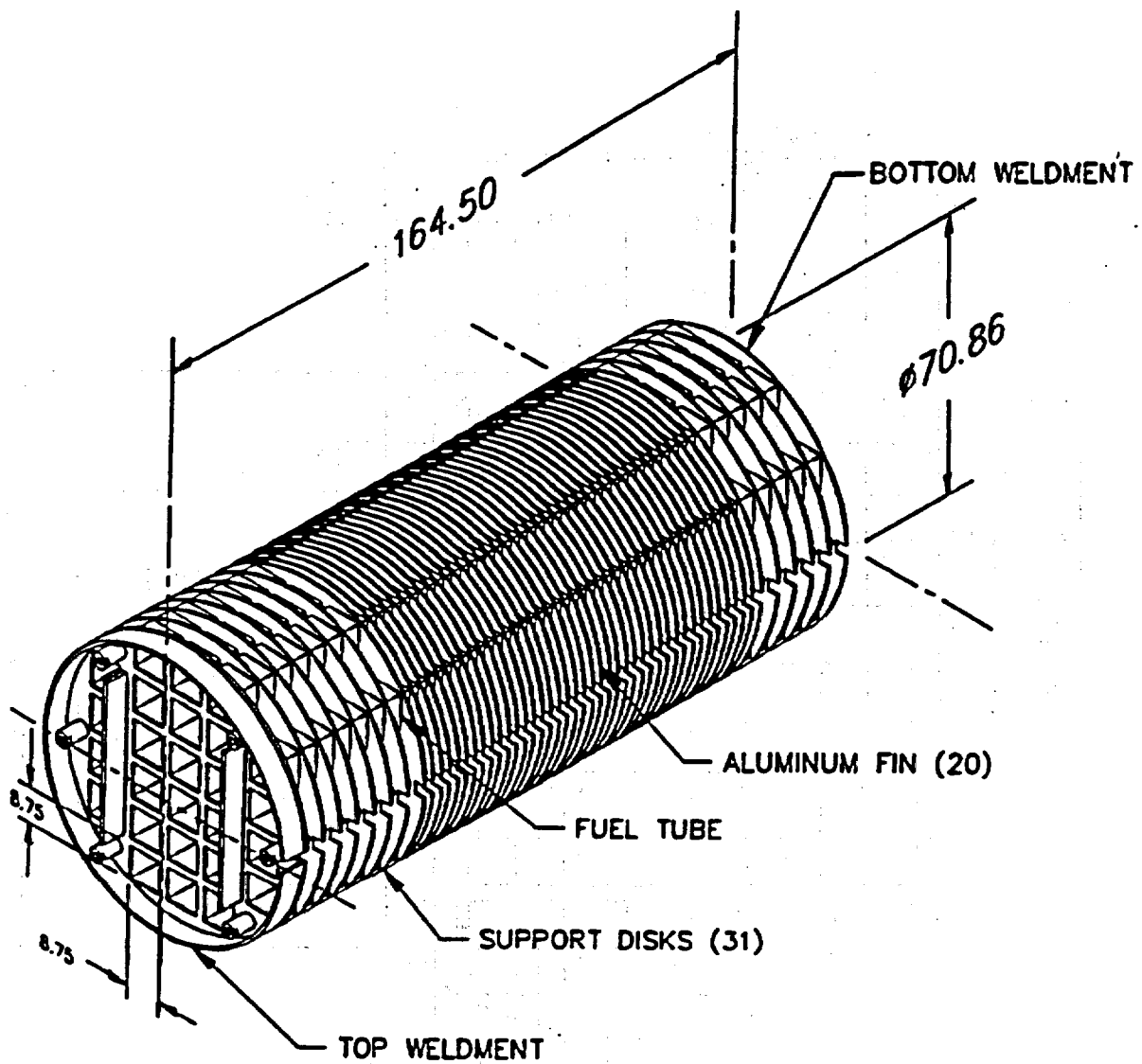


Figure 2.7.8-2 Support Disk Cross-Sectional Configuration for Directly Loaded Fuel
Configuration

**FIGURE WITHHELD AS SENSITIVE
UNCLASSIFIED INFORMATION**

2.7.8.1 Stress Evaluation of Support Disk - Directly Loaded Fuel Configuration

To determine the structural adequacy of the support disks in the 26 PWR fuel assembly basket, the drop accident impact load is evaluated for all cask orientations. The drop accident impact load is analyzed for a 30-foot side drop and a 30-foot end drop and conservatively combined using the square root sum of the squares of the resultant maximum nodal stress intensity values to assure all included orientations are enveloped. A quasi-static impact load equal to the weight of the fuel and tubes multiplied by a 55 g amplification factor is applied to the support disk structure to simulate the side drop accident condition. However, since the support disk does not carry load from the fuel assemblies in the vertical direction, analysis of the 30-foot end drop is limited to consideration of the 56.1 g out-of-plane inertial load from the mass of a single support disk. The 55 g and 56.1 g amplification factors are design values which envelope the calculated deceleration values in Section 2.6.7.4 for a 30-foot drop accident condition. For the side drop condition, the fuel assembly loads are transmitted in direct compression through the tube wall to the web structure of each support disk. These loads are transmitted to the inner shell of the cask by the 31 support disks, the top plate and the bottom plate.

The weights of the PWR fuel assemblies and the basket structure (the support disks and fuel tubes) are applied as a 55 g impact load to simulate a side drop accident scenario for the basket assembly. The value of 55 g for the impact loading is the NAC-STC design deceleration force for a 30-foot side drop accident condition. The support disk configuration (Figure 2.7.8-2) is analyzed for nine drop orientations: 0, 15, 30, 37, 45, 60, 64, 75, and 90 degrees, to bound the possible maximum stress cases. The drop orientations are identified in Figure 2.7.8.1-1. As shown in Figure 2.7.8.1-1 drop orientation, 37 degrees and 64 degrees respectively put each of the support disk ligaments in direct impact.

A finite element analysis is performed, utilizing the ANSYS computer code, to calculate the stresses in a support disk. In accordance with ASME Code, Section III, Subsection NG criteria, the maximum primary stress intensity calculated in the support disk is compared to the allowable stress limit, $0.7S_u$, where S_u is conservatively defined for this analysis evaluation as the material ultimate strength

at a maximum temperature of 600°F. The maximum temperature in the basket support disk is 498°F (Table 3.4-1). Analyses are conservatively performed by calculating the total primary stress intensity at a node point for combined membrane and bending and then employing the 0.7 S_u allowable at 600°F. This enveloping method is conservative since further stress classification dictates that the membrane stress, P_m and the primary membrane plus primary bending stress, $P_m + P_b$ is lower than the total calculated maximum stress intensity, SI , at a node point. The margin of safety is conservatively obtained by evaluating the allowable for the smaller primary membrane stress, 0.7 S_u relative to the total combined primary membrane plus bending stress intensity at a single node. According to the ASME Code, Section III, Division 1, Subsection NG, the allowable for membrane plus bending stress ($P_m + P_b$) is S_u . Using this conservative enveloping methodology to evaluate the fuel basket structural integrity results in large margins of safety. These results document that the fuel basket does not yield under any imposed design load.

2.7.8.1.1 Finite Element Model Description

Two types of finite element analyses were performed for the NAC-STC 26 PWR basket support disk evaluations for hypothetical accident conditions: one for the 30-foot side drop impact condition; and a second for the evaluation of the 30-foot end drop impact condition.

The temperature distribution on the support disk is determined in a separate thermal analysis which uses a three-dimensional finite element model representing one-quarter of the cask. The thermal analysis model is documented in detail in Section 3.4.

The finite element model for the 30-foot side drop impact analysis has the same mesh arrangement and element types as that of the finite element model used for the 1-foot side drop analysis shown in Figure 2.6.12.2-2. The stiffness of the gap elements is 1.0E+6 pounds/inch, as discussed in Section 2.6.12.2.

The finite element model for the 30-foot end drop impact analysis has the same mesh arrangement and element type as that of the finite element model used for

the 1-foot end drop analyses shown in Figure 2.6.12.2-1. The end drop inertial loading is applied in the cask longitudinal direction (lateral to the plane of the support disks). The support disks are separated by spacer nuts on threaded rods at six locations near the periphery of the disks. Displacement restraints are applied at the nodes on the support disk model where the six threaded rods are located.

2.7.8.1.2 Impact Loading Conditions

The lateral impact load applied on the support disk for a side drop accident, includes the inertial weights of the fuel assemblies, the stainless steel tubes, one aluminum heat transfer disk, and the support disk itself. The loads are amplified to account for the side drop impact, a 55 g load factor is used to amplify the weight of the basket components. The load corresponding to the support disk weight is included as the inertial loading resulting from a 55 g acceleration for both the 30-foot side drop and the 30-foot end drop accident conditions.

Each fuel assembly is conservatively assumed to weigh 1525 pounds and is 159.20 inches long. The stainless steel fuel tube has an 8.78-inch square inside dimension and a 9.064-inch square outside dimension. The load at each support disk hole is calculated in Section 2.7.8.1.3.1.

The amplified load from the fuel and the fuel tubes is uniformly applied in the plane of the support disk at the bottom of each hole for the 0-degree and the 90-degree drop orientations. For the other side drop orientations, the load is distributed along the two lower sides of each hole. The mass of the aluminum heat transfer fin is lumped equally at each of the threaded rod locations.

2.7.8.1.2.1 Side Drop Analysis Results

Finite element stress analyses are performed for the 55 g side impact load cases for nine different impact orientations--0, 15, 30, 37, 45, 60, 64, 75, and 90 degrees, as shown in Figure 2.7.8.1-1. The stress evaluations are performed in accordance with the ASME Code, Section III, Division 1, Subsection NG.

The locations of the 20 highest nodal SI stresses in the support disk for each of the nine side impact orientations evaluated are shown in Figures 2.7.8.1-2 through 2.7.8.1-10. Tables 2.7.8.1-1 through 2.7.8.1-9, respectively, provide tabulations of the nodal SI stresses at the 20 locations of maximum stress in the support disk for each of the nine side impact orientations. The tables also show the margin of safety for each analysis location for the 55 g side impact load condition. Table 2.7.8.1-10 presents a summary of the maximum stress locations and margins of safety for the 55 g side impact analysis for the nine impact orientations.

The conservative stress limit chosen for this evaluation of the support disk is $0.7 S_u$. The material ultimate strength value is taken at the enveloping temperature of 600°F. Then the allowable stress intensity becomes $(0.7)(126.7) = 88.7$ ksi.

The total impact loading applied to the finite element model of the support disk is verified in Section 2.7.8.1.3.3 by comparing the reaction forces calculated by ANSYS to those calculated by classical methods. The analysis in Section 2.7.8.1.3.4 evaluates the effect of the stress concentration at the threaded rod holes in the support disk. The minimum margin of safety calculated for the maximum nodal SI stress with a stress concentration factor of 3.0 applied at the threaded rod hole location in the support disk is +3.9, using the stresses resulting from the 55-g side impact load case.

The minimum calculated margin of safety in the support disk of the NAC-STC 26 PWR basket is +0.8 for the 30-degree drop orientation at node number 565 (Figure 2.7.8.1-4) for the 55 g side impact load condition. In addition to the ASME Code, Subsection NG criteria adopted as the design code for the fuel basket, it is noted that the yield strength of 17-4 PH stainless steel at the bounding temperature of 500°F (Table 3.4-1) is 87.0 ksi and, therefore, for the highest impact stress of 50.6 ksi, the basket will not yield. Therefore, the support disks in the NAC-STC 26 PWR fuel basket are structurally adequate for a 55 g side impact load condition.

2.7.8.1.2.2 End Drop Analysis Results

The support disks of the NAC-STC fuel basket are spaced by threaded rods and spacer nuts positioned at six locations near the periphery of each disk. An ANSYS structural analysis is performed to evaluate the effect of a 30-foot end drop impact (out-of-plane loading) on the support disks in the NAC-STC with the cask in the vertical position. The ANSYS eight-node brick element (STIF45) is used in the model as shown in Figure 2.7.8.1-11. The end drop impact loading is applied in the cask longitudinal direction (perpendicular to the plane of the support disk). A load factor of 56.1 g is applied to the mass of the support disk. The value of 56.1 g is the maximum deceleration of the NAC-STC for a 30-foot end drop impact (Table 2.6.7.4-2). Displacement restraints are applied in the ANSYS model at the nodes where the six threaded rods with spacer nuts are located.

Table 2.7.8.1-11 presents a summary of the 20 highest nodal stress intensity results in the support disk for the 30 foot end drop load. Figure 2.7.8.1-12 presents the location of these 20 nodes. The minimum margin of safety is +1.6 for the maximum stress of 36.2 ksi, when evaluated with respect to the conservative NG criteria of $0.7 S_u$, where S_u is defined at the node temperature for steady state design basis heat load.

As stated in Section 2.7.8.1, the maximum nodal stress intensity for the side drop, 50.6 ksi at 30 degrees, is combined with the maximum nodal stress intensity for the end drop (36.2 ksi) using the square root sum of the squares assuring a conservative envelope of the stress in the basket support disk under any drop orientation. Using this methodology, the conservative envelope of stress intensity is 62.2 ksi, which is less than the allowable of $0.7 S_u$ and the material yield strength. Yield strength of 17-4 PH stainless steel at the basket bounding temperature of 500°F (Table 3.4-1) is 87.0 ksi. Therefore, under end drop accident conditions, the fuel basket support disks do not yield and demonstrate significant margin of safety.

2.7.8.1.2.3 Support Disk Web Stresses for a 30-Foot Side Drop Condition

The support disk is analyzed for nine drop orientations in Section 2.7.8.1.2.1. The 20 maximum stress intensities for each drop orientation are listed in Tables 2.7.8.1-1 through 2.7.8.1-9. In this section, a supplementary detailed stress evaluation of the support disk webs is presented for the same drop orientations summarized in Section 2.7.8.1.2.1.

The locations of the nodal stresses in the support disk webs for each of the nine 1-foot side impact orientations evaluated are shown in Figure 2.7.8.1-13. Tables 2.7.8.1-12 through 2.7.8.1-20 provide tabulations of the nodal stress intensities at the defined node locations on the web for each of the nine impact orientations. The tables also show the margin of safety for each analysis location for the 55 g side impact load condition. The minimum margin of safety for this summarized node stress intensity relative to $0.7 S_u$ at 600°F for the support disk web of the NAC-STC PWR basket for a 30-foot side drop is +2.8 for the 90-degree drop orientation. This margin of safety is greater than the evaluation of maximum stress in the support disk presented in Section 2.7.8.1.2.1 and continues to demonstrate the significant structural integrity of the NAC-STC fuel basket.

2.7.8.1.2.4 Support Disk Shear Stresses for a 30-Foot Side Drop and a 30-Foot End Drop Condition

The maximum stress intensity for the 30-foot side drop is reported in Table 2.7.8.1-3 as 50.58 ksi, (30° drop orientation). Similarly, the maximum stress intensity for the 30-foot end drop is also reported in Table 2.7.8.1-11 as 36.20 ksi. Therefore, the maximum enveloping shear stress anywhere in the basket support disk is $50.58/2 = 25.29$ ksi.

According to the ASME Code, Section III, Division 1, Subsection NG, "Core Support Structures," the allowable hypothetical accident loading shear stress is $0.42 S_u$. The ultimate stress S_u for 17-4 PH at the bounding operating temperature of 600°F is 126.7 ksi.

Minimum margin of safety for shear is

$$\begin{aligned} \text{M.S.} &= \frac{(2)(0.42S_u)}{SI} - 1 \\ &= \frac{(2)(0.42)(126.7)}{50.58} - 1 = \underline{+1.1} \end{aligned}$$

Therefore, the structural adequacy of the NAC-STC fuel basket support disk design for the normal conditions of transport 30-foot side drop and 30-foot end drop is demonstrated.

2.7.8.1.3 Supplemental Data - Support Disk Analysis

2.7.8.1.3.1 Calculation of Pressure Loadings

Purpose: Determination of the impact pressure loadings on the 26 PWR fuel assembly basket for the side drop condition in the ANSYS analysis.

Solution: I = Length of fuel = 159.20 in
W = Weight of one fuel assembly = 1525 lb
W/L = Unit weight = 1525/159.20 = 9.579 lb/in

The weight (W_c) of the tube per linear inch is:

$$\begin{aligned} W_{\text{tube}} &= 141 \text{ lb} \\ L_{\text{tube}} &= 154.7 \text{ in} \\ W_c &= \frac{141}{154.7} \\ &= 0.911 \text{ lb/in} \end{aligned}$$

"Fuel assembly plus tube" weight per linear inch is:

$$9.579 + 0.911 = 10.490 \text{ lb/in}$$

Distributing the combined weight as a pressure load considering a 4.88-inch spacing between two adjacent support disks and a 55-g load factor:

$$P = \frac{(10.490)(4.88)(55)}{(9.234)(0.5)} = 609.8 \text{ psi}$$

For the 0-degree drop use:

$$P_x = 609.8 \text{ psi}$$

For a 90-degree drop use:

$$P_y = 609.8 \text{ psi}$$

For a q-degree drop use:

$$P_x = (609.8)(\cos q)$$

$$P_y = (609.8)(\sin q)$$

2.7.8.1.3.2 Calculation of Lump Masses of the Aluminum Heat Transfer Disk and the Six Threaded Rods and Spacers

The masses of the aluminum heat transfer disk and the six threaded rods and spacer nuts are lumped into the finite element model at the threaded rod locations on the support disk for both the 18.1 g and 55 g side drop analyses. The lump masses applied to the model through ANSYS pointwise generalized mass element (STIF21) is 0.0613 pounds mass.

2.7.8.1.3.3 Verification of Impact Load Applied on the ANSYS Model

The total impact pressure applied on the model is verified by comparing the reaction forces from the ANSYS results versus the hand-calculated method. The 90-degree side drop evaluation is used as an example.

From the ANSYS result, the total reaction force per disk is: $F_y = 94,520 \text{ lb}$

Therefore, total weight = $94,520/55 = 1718.55 \text{ lb}$.

This load is verified by the classical-calculation method as described below:

Weight of each support disk = 245.19 lb

Weight of aluminum heat transfer disk
and six threaded rods per support disk = 142.074 lb

Weight of 26 "fuel assemblies plus tubes" = $(26)(4.88)(10.49)$
= $1330.97 \text{ lb/support disk}$

Total weight = $245.19 + 1330.97 + 142.074 = 1718.234 \text{ lb}$

Total load = 1718.234 lb

The difference between the classical-calculation total load (1718 lb) and the ANSYS total load of 1718.6 pounds is negligible (0.034%).

2.7.8.1.3.4 Evaluation of Stress Concentration at the Threaded Rod Hole Areas in the Support Disks

There are six holes near the periphery of each support disk for the installation of the threaded rods and spacer nuts. The stress concentration effect at these areas is evaluated.

From the ANSYS stress results for the 55-g side impact load condition, the nodal stresses (SI) at the threaded rod hole areas for different loading conditions are listed below.

Nodal SI Stresses (psi)
(55-g Side Impact)

Node ¹ Temp	65	374	732	1041	1708	2375
0.7S _u ²	376	405	376	405	405	405
Orientation	92.58	91.88	92.58	91.88	91.88	91.88
0	6.3	3.2	1.4	1.3	3.2	1.3
15	5.9	3.9	1.3	1.7	3.8	1.2
30	5.4	3.8	1.3	2.1	4.3	1.4
37	5.1	3.7	1.3	2.4	4.6	1.7
45	4.6	3.6	1.3	2.6	5.0	2.0
60	3.5	3.0	1.2	2.8	5.6	2.5
64	3.2	2.7	1.2	2.8	5.7	2.6
75	2.2	1.7	1.2	2.5	6.1	2.5
90	1.2	1.4	1.2	1.4	4.7	4.7
Max SI	6.3	3.9	1.4	2.8	6.1	4.7
MS ³	2.7	4.9	15.5	7.2	2.8	3.9

¹ Node numbers in the finite element model at the threaded rod hole location.

² S_u is the ultimate strength of 17-4 PH stainless steel.

³ Margin of Safety, MS is calculated with respect to 1/3 of the allowable strength to account for stress concentration factor around the holes.

Considering a stress concentration factor of 4.0, the minimum margin of safety for the threaded rod hole areas is +2.7, and occurs at the threaded rod located on node 65 for the 0-degree side drop orientation.

Figure 2.7.8.1-1 Support Disk Drop Orientations

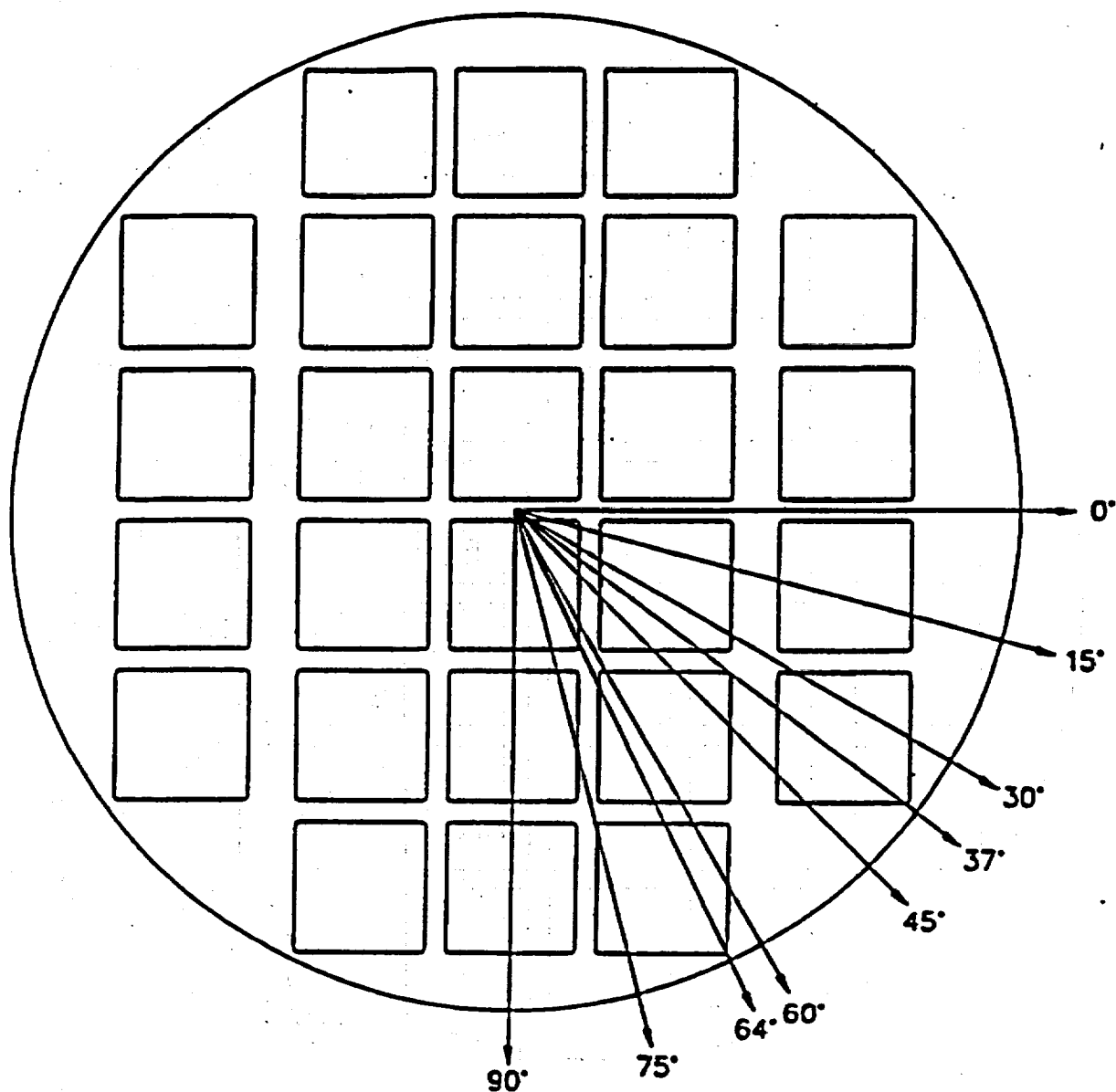


Figure 2.7.8.1-2 Locations of 20 Maximum Nodal SI Stresses - 55-g Side Drop Impact (0° Drop Orientation)

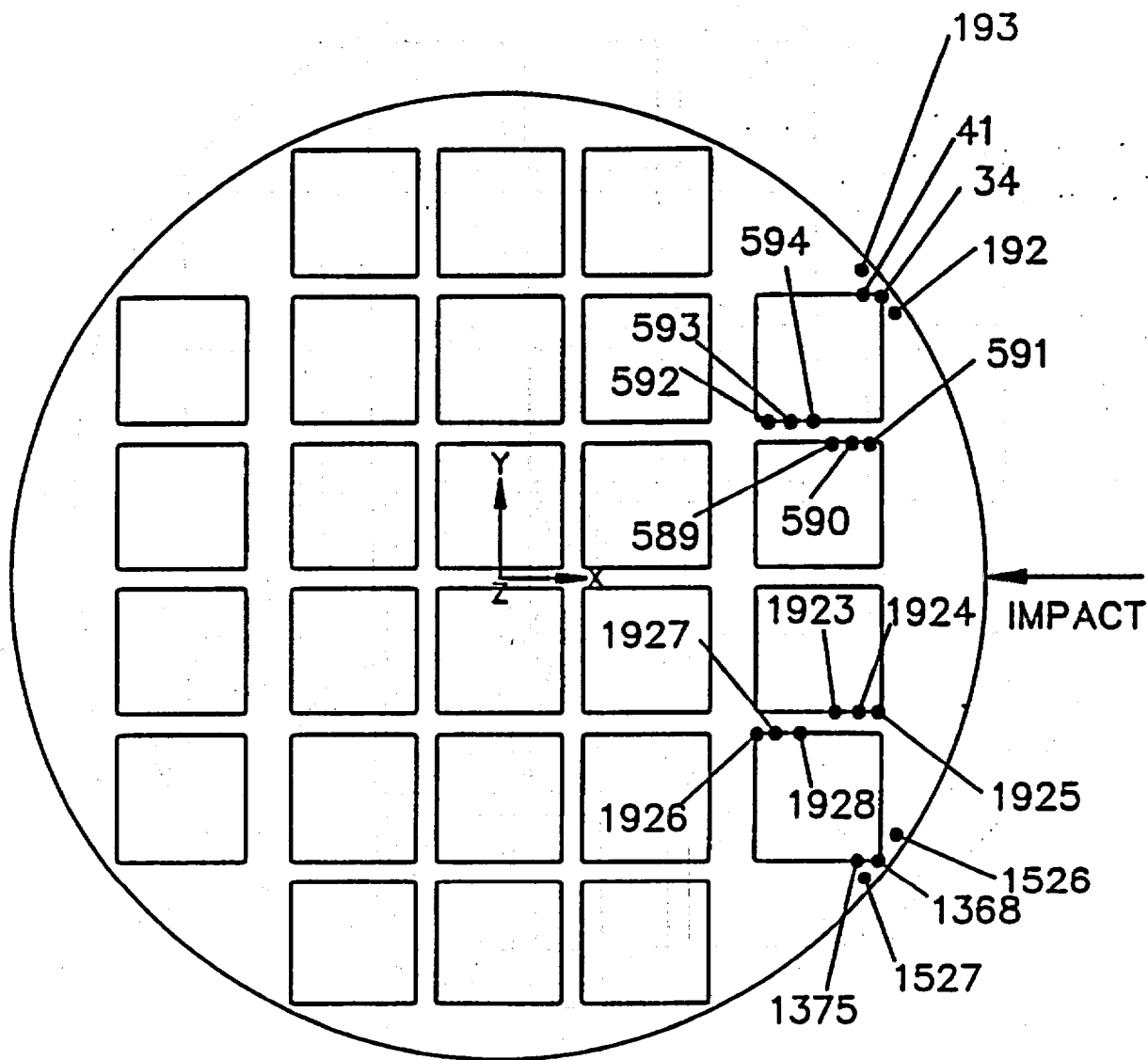


Figure 2.7.8.1-3 Locations of 20 Maximum Nodal SI Stresses - 55-g Side Drop Impact (15° Drop Orientation)

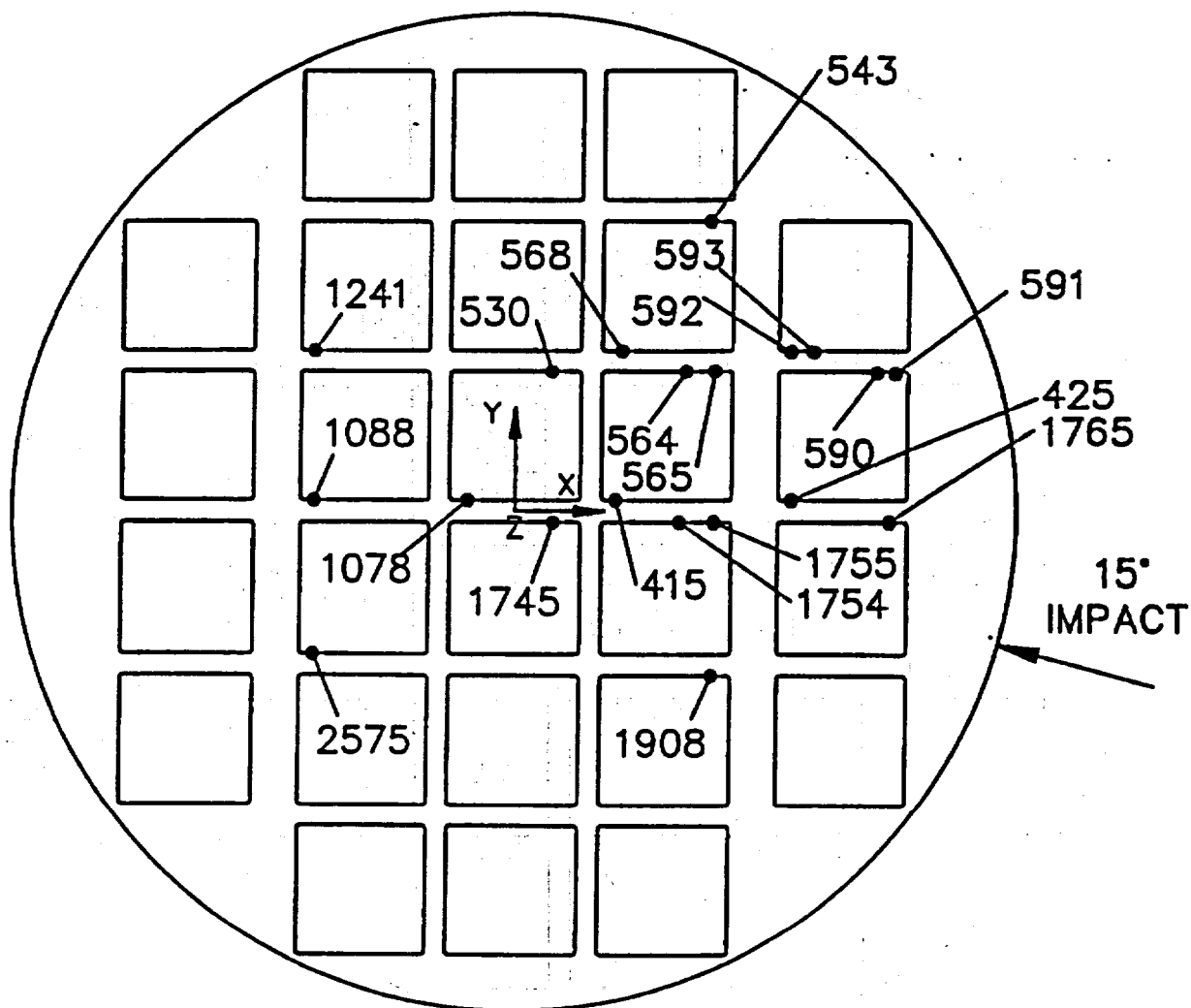


Figure 2.7.8.1-4 Locations of 20 Maximum Nodal SI Stresses - 55-g Side Drop Impact (30° Drop Orientation)

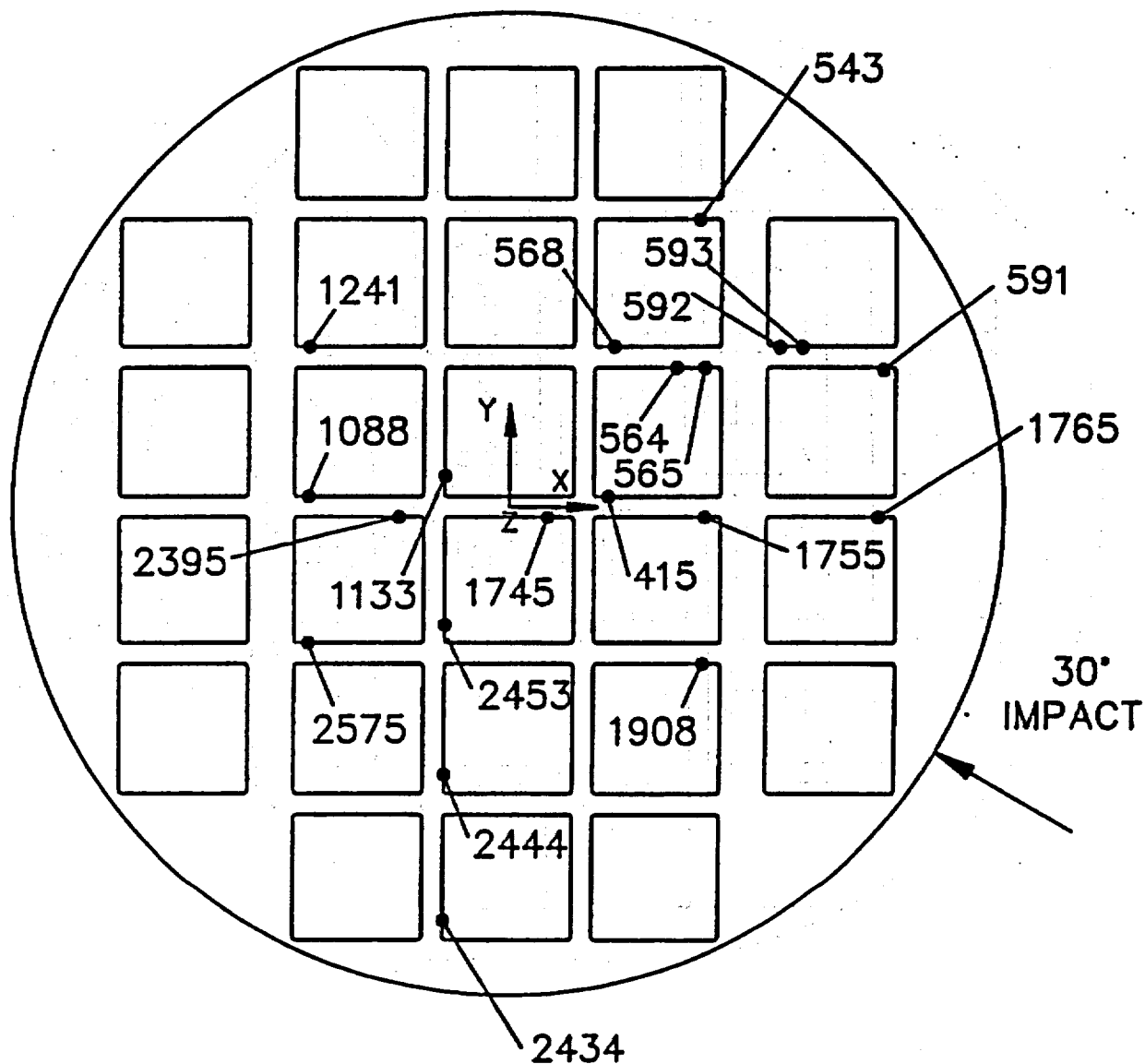


Figure 2.7.8.1-5 Locations of 20 Maximum Nodal SI Stresses - 55-g Side Drop Impact (37° Drop Orientation)

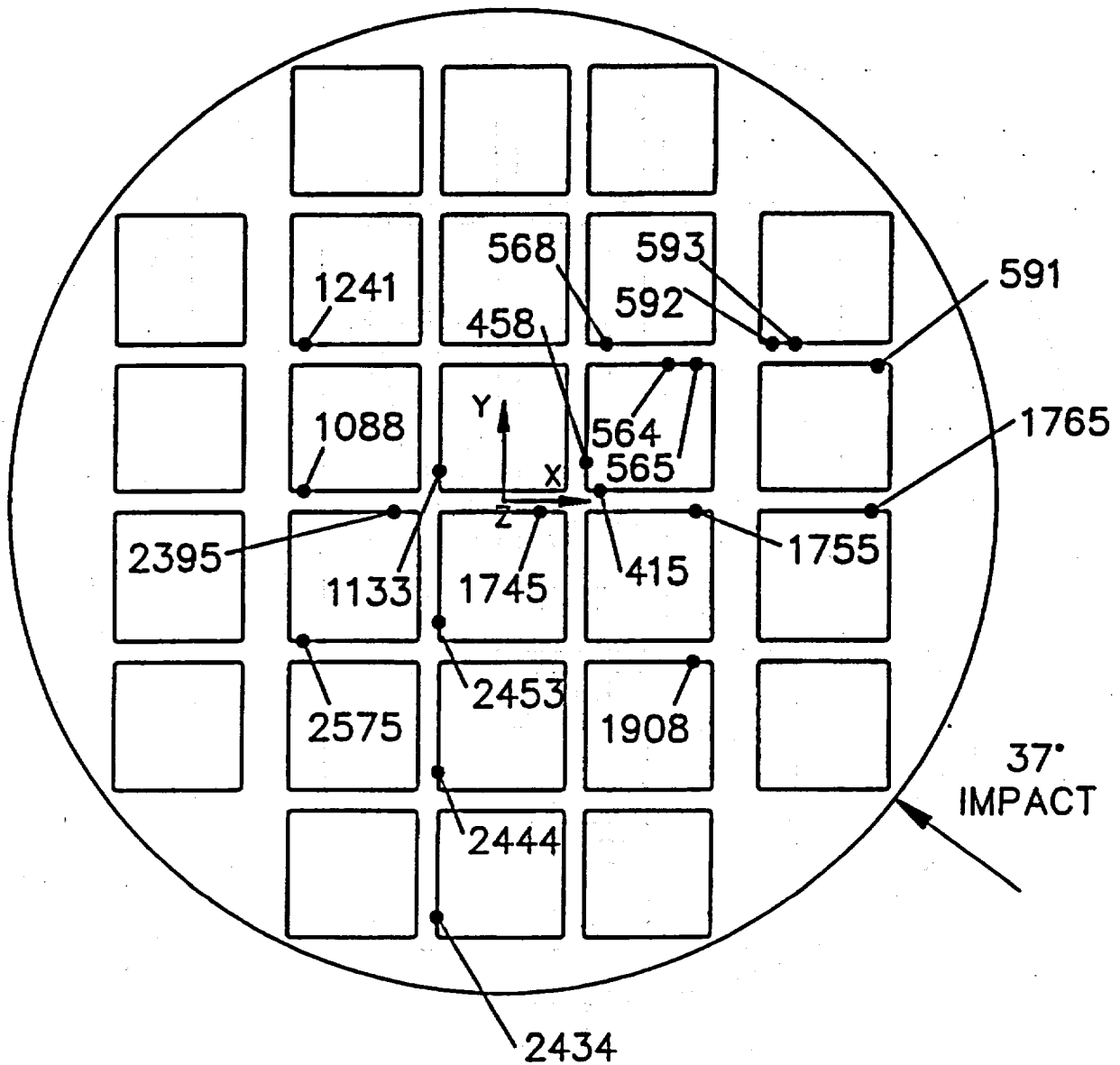


Figure 2.7.8.1-6 Locations of 20 Maximum Nodal SI Stresses - 55-g Side Drop Impact (45° Drop Orientation)

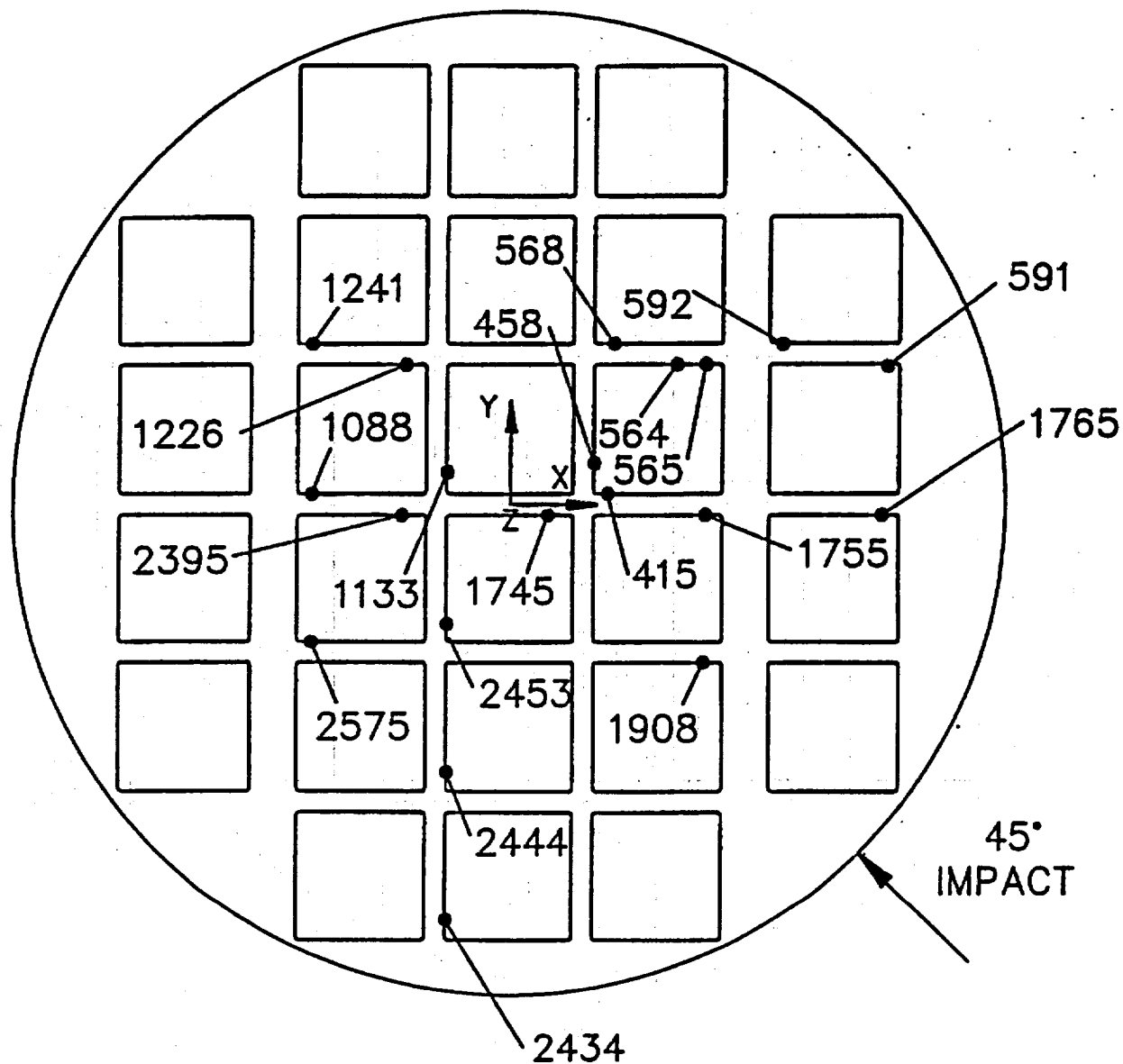


Figure 2.7.8.1-7 Locations of 20 Maximum Nodal Stresses - 55-g Side Drop Impact (60° Drop Orientation)

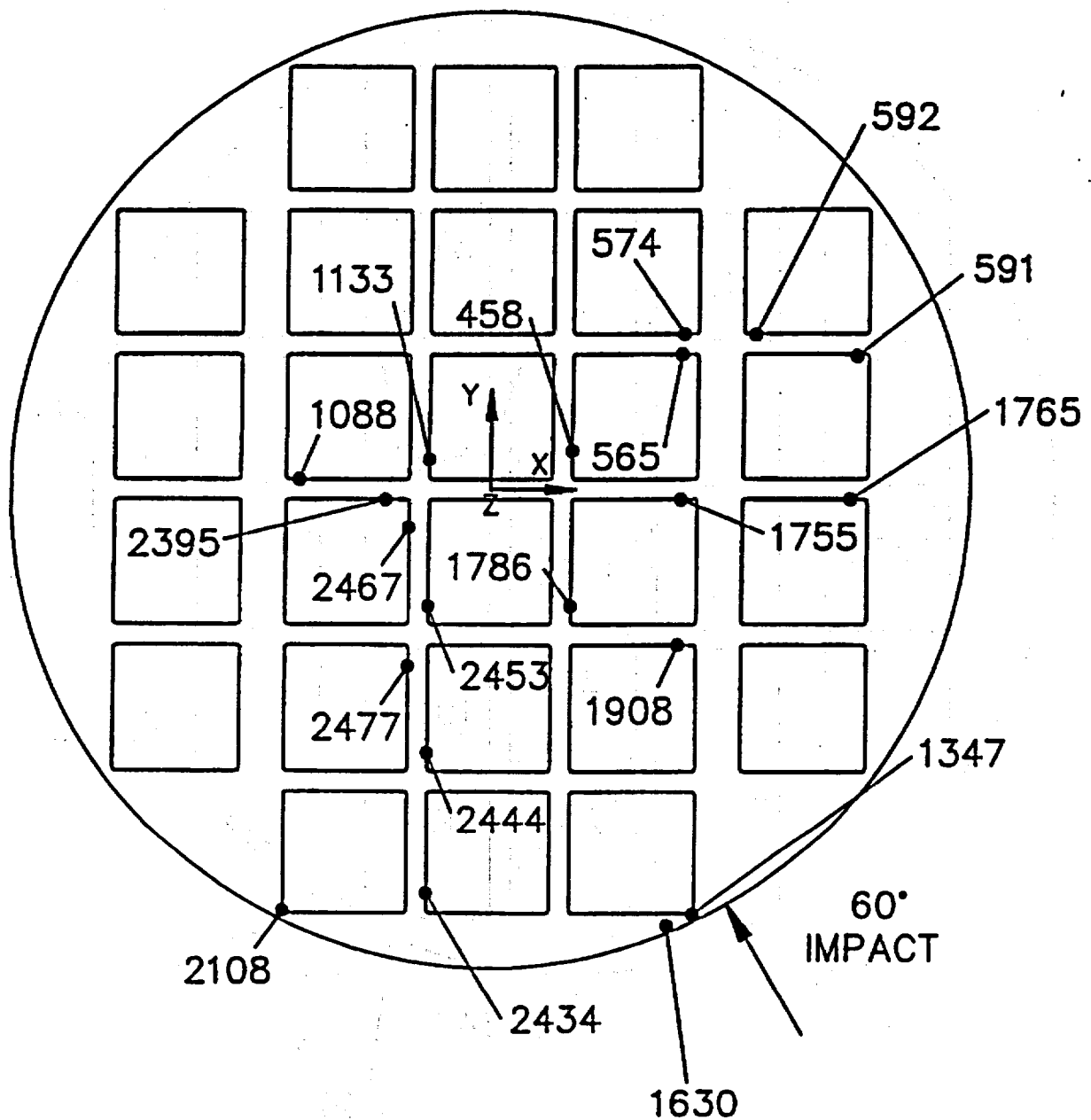


Figure 2.7.8.1-8 Locations of 20 Maximum Nodal SI Stresses - 55-g Side Drop Impact (64° Drop Orientation)

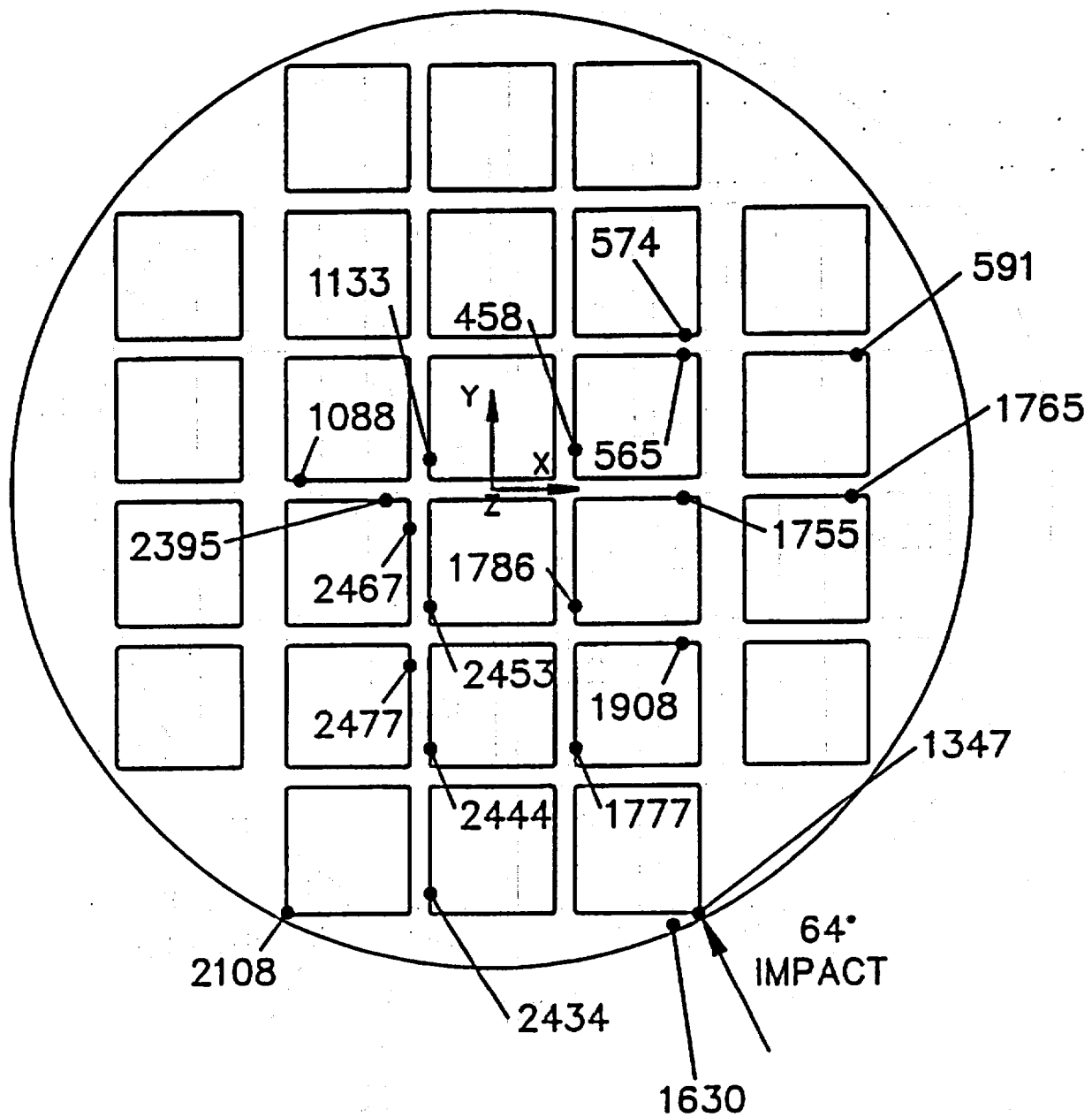


Figure 2.7.8.1-9 Locations of 20 Maximum Nodal SI Stresses - 55-g Side Drop Impact (75° Drop Orientation)

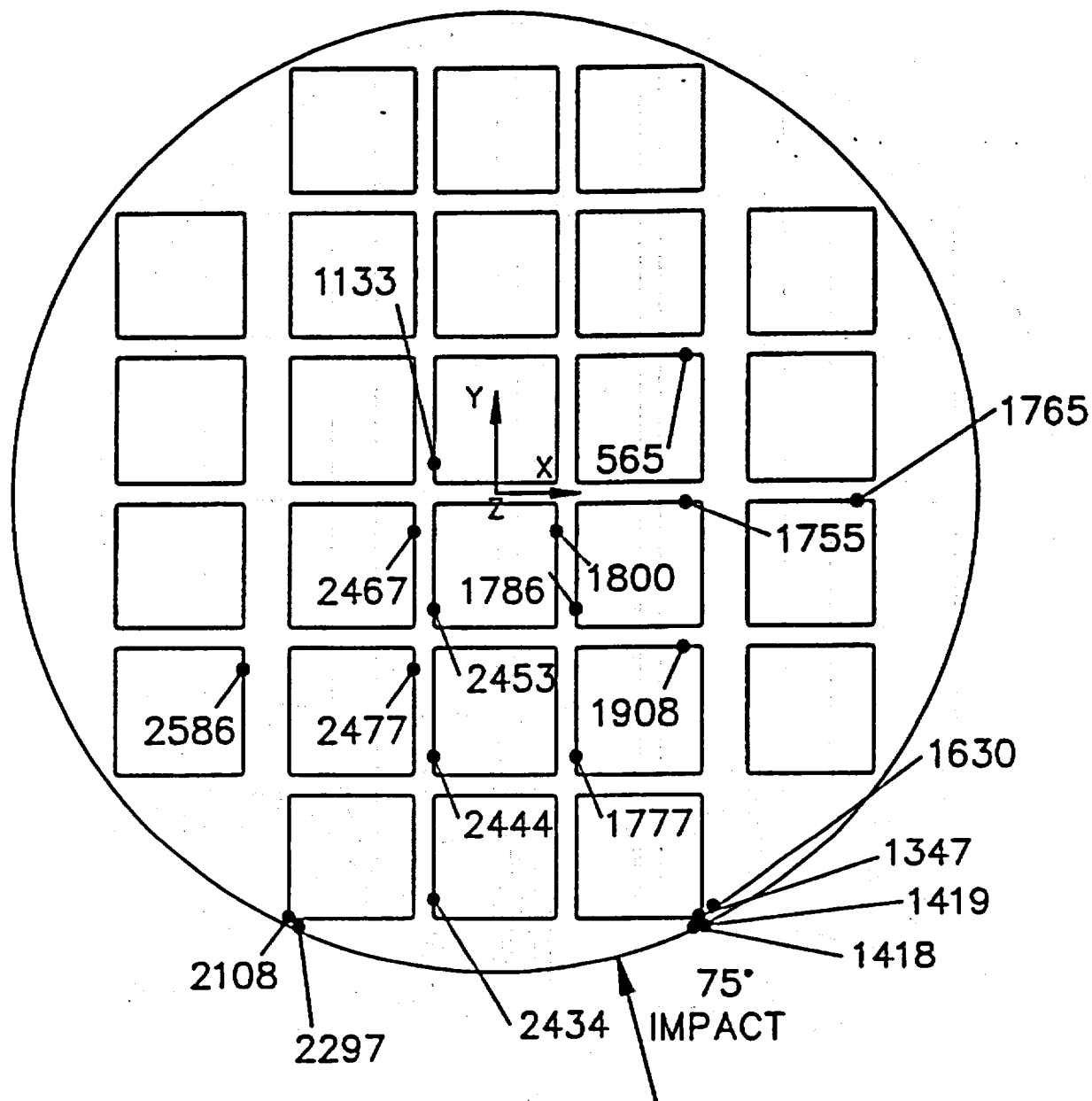


Figure 2.7.8.1-10 Locations of 20 Maximum Nodal SI Stresses - 55-g Side Drop Impact (90° Drop Orientation)

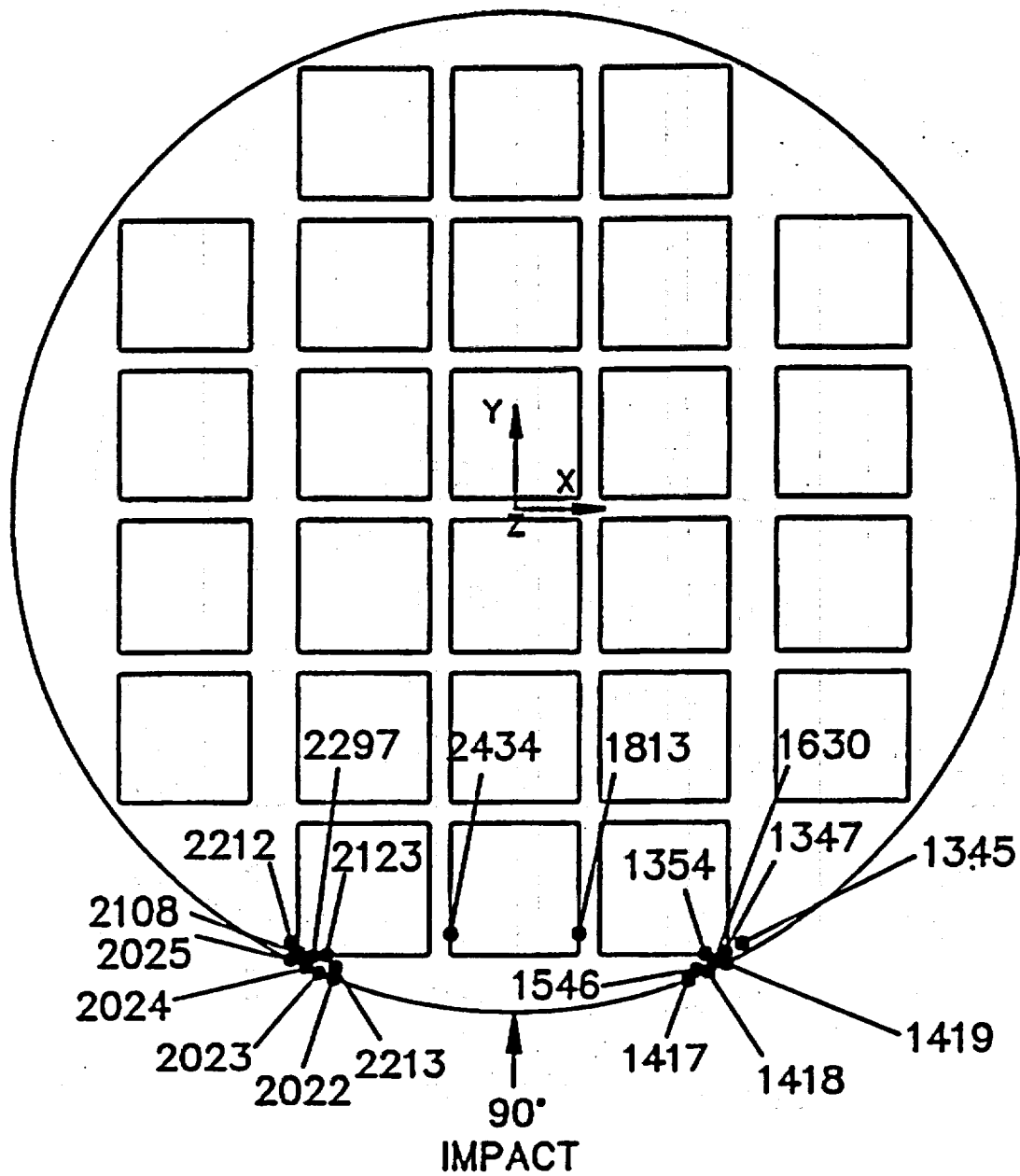


Figure 2.7.8.1-11 Finite Element Model for the Basket Support Disk End Drop

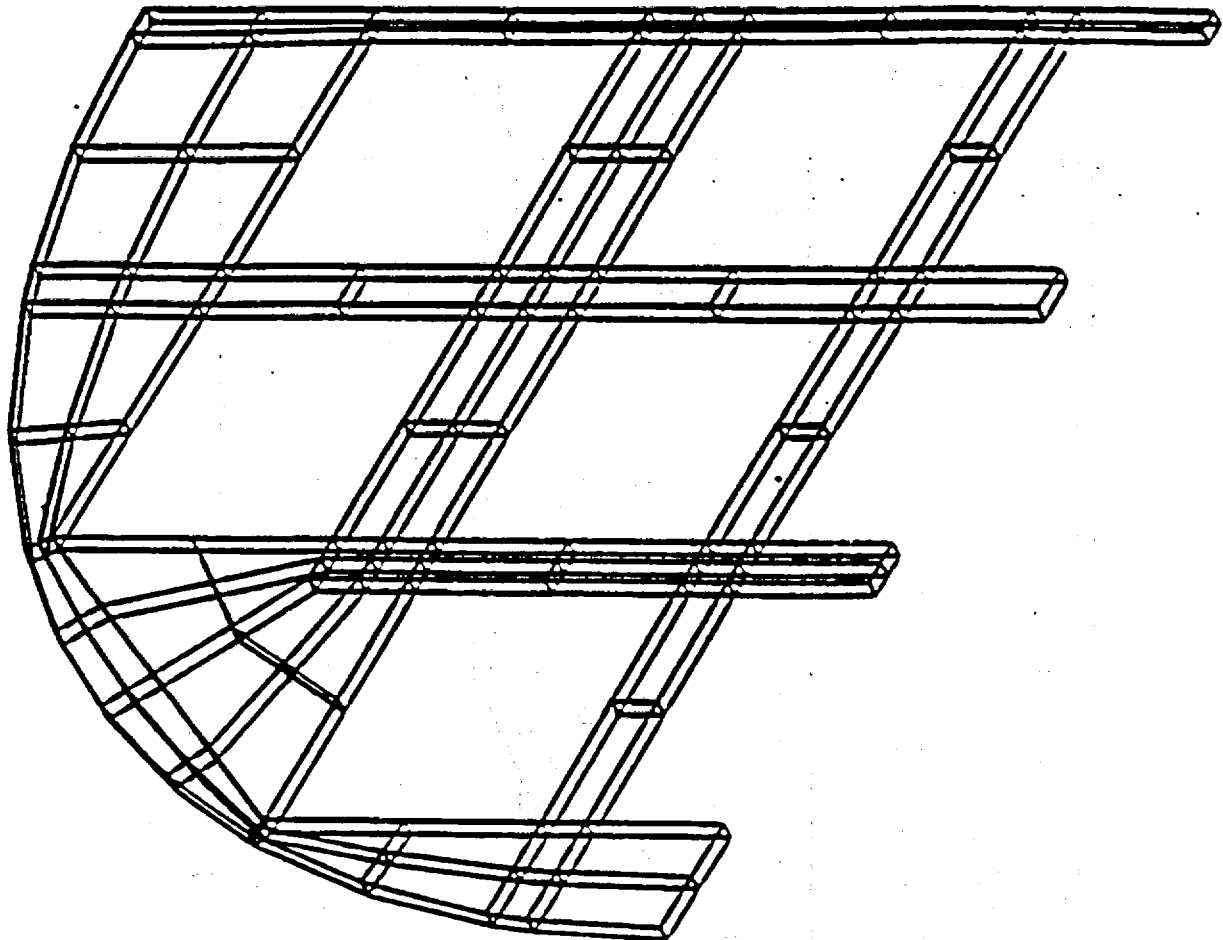


Figure 2.7.8.1-12. Locations of the 20 Maximum Nodal SI Stresses - 56.1-g End Drop

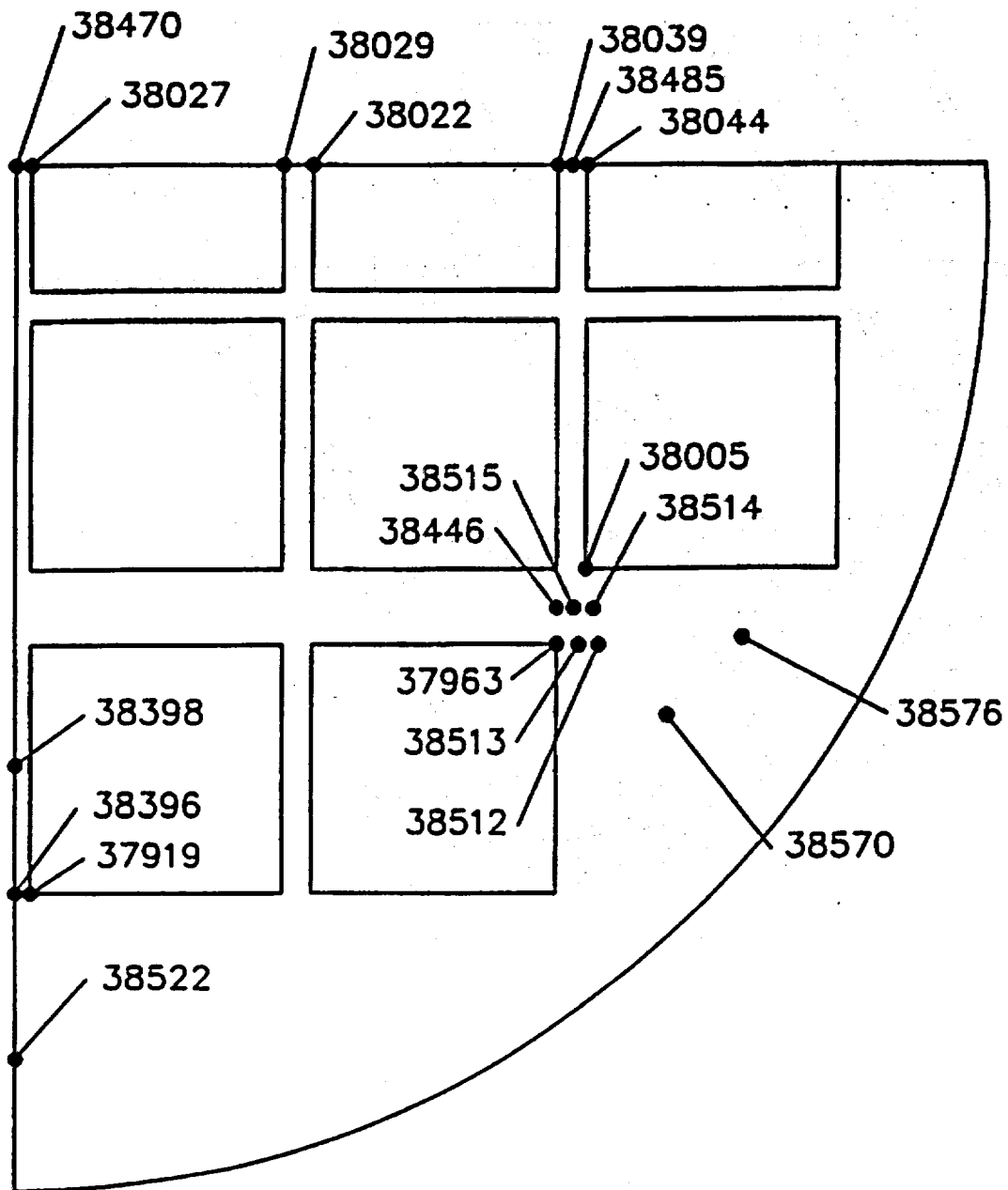


Figure 2.7.8.1-13 Node Point Locations for Basket Web Stress Summaries

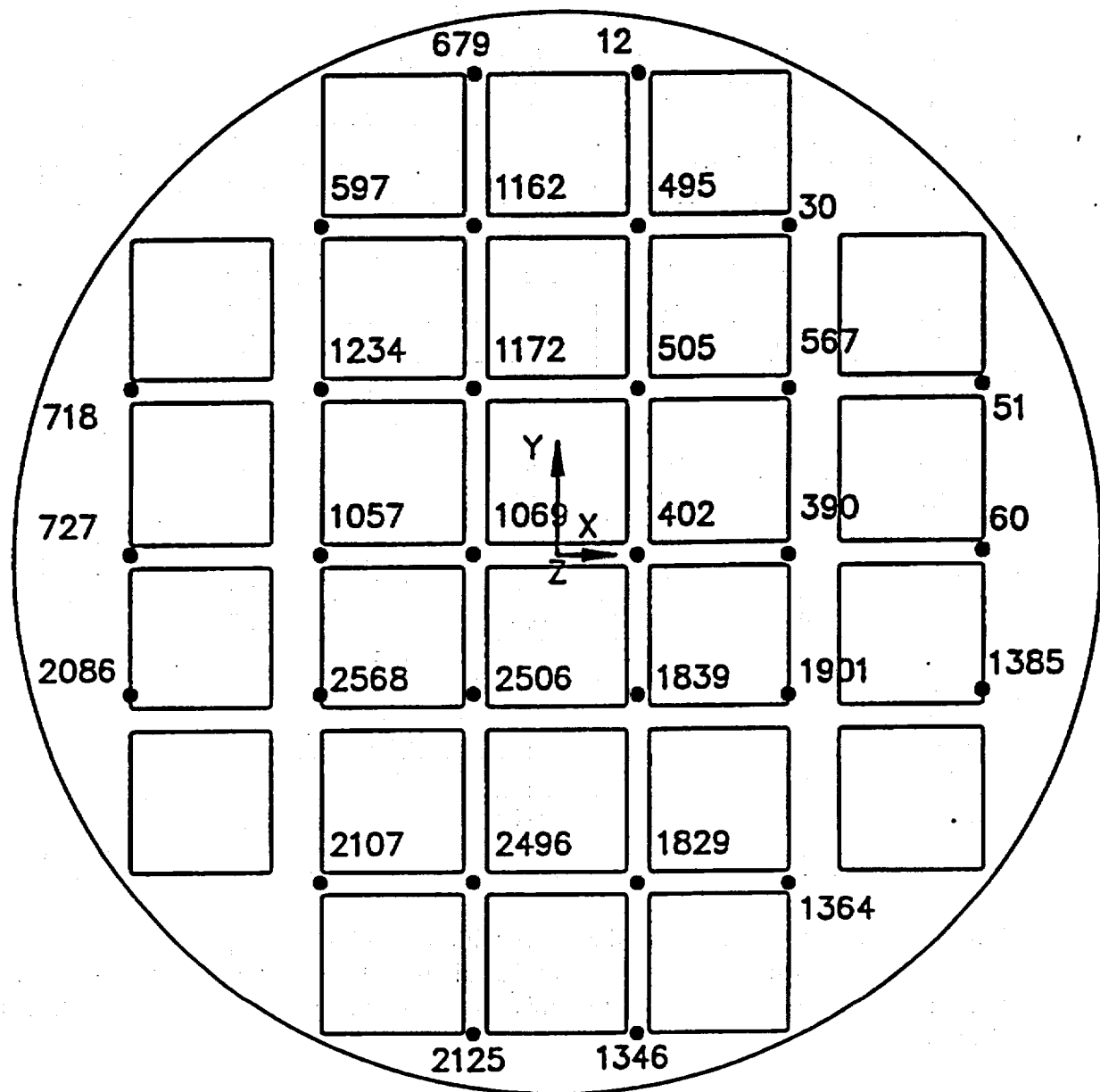


Table 2.7.8.1-1 Basket 55-g Side Impact Stresses for 0-Degree Drop Orientation

Node No. ¹	S _x (ksi)	S _y (ksi)	S _z (ksi)	S _{xy} (ksi)	SI (ksi)	MS ²
1368	-18.9	-18.2	0.0	-11.2	31.7	1.8
34	-18.9	-18.2	0.0	11.2	31.7	1.8
591	-29.2	0.9	0.0	1.1	30.3	1.9
1925	-29.2	0.9	0.0	-1.1	30.2	1.9
592	-29.5	0.5	0.0	1.1	30.2	1.9
1926	-29.5	0.5	0.0	-1.1	30.2	1.9
593	-25.4	0.2	0.0	0.2	25.6	2.5
1927	-25.4	0.2	0.0	-0.2	25.6	2.5
590	-25.3	0.2	0.0	0.2	25.5	2.5
1924	-25.3	0.2	0.0	-0.2	25.5	2.5
1527	-18.3	-12.9	0.0	-7.4	25.2	2.5
193	-18.3	-12.9	0.0	7.4	25.2	2.5
594	-24.2	-0.1	0.0	0.5	24.2	2.7
1928	-24.2	-0.1	0.0	-0.5	24.2	2.7
589	-24.1	-0.1	0.0	0.5	24.2	2.7
1923	-24.1	-0.1	0.0	-0.5	24.2	2.7
1526	-9.7	-16.0	0.0	-9.2	24.1	2.7
192	-9.7	-16.0	0.0	9.2	24.1	2.7
1375	-21.0	-5.0	-0.0	-6.9	23.9	2.7
41	-21.0	-5.0	0.0	6.9	23.9	2.7

- ¹ Stress components are listed for the nodes with the 20 highest impact nodal point stress intensity values (see Figure 2.7.8.1-2 for locations of these nodes). Note that S_x is the stress in the radial direction, S_y is the stress in the circumferential direction and S_{xy} is the shearing stress.
- ² The allowable stress is 0.7 S_u. S_u is the ultimate strength of 17-4 PH stainless steel at a bounding 600°F. S_u = 126.7 ksi.

Table 2.7.8.1-2 Basket 55-g Side Impact Stresses for 15-Degree Drop Orientation

Node No. ¹	S _x (ksi)	S _y (ksi)	S _z (ksi)	S _{xy} (ksi)	SI (ksi)	MS ²
565	-48.4	0.8	0.0	2.6	49.5	0.8
1755	-44.0	0.6	0.0	2.3	44.9	1.0
591	-42.6	1.4	0.0	2.3	44.3	1.0
592	-40.1	1.1	0.0	1.6	41.4	1.1
568	-36.2	2.4	0.0	2.0	38.9	1.3
1908	-37.8	0.6	0.0	2.0	38.6	1.3
1088	-36.1	1.5	0.0	1.7	37.7	1.3
415	-35.0	2.3	0.0	1.8	37.5	1.4
1241	-35.7	1.6	0.0	1.7	37.5	1.4
564	-36.8	-0.3	0.0	2.2	37.2	1.4
1765	-35.0	1.1	0.0	1.7	36.3	1.4
2575	-32.6	1.6	0.0	1.5	34.3	1.6
1754	-33.8	-0.1	0.0	1.7	34.1	1.6
543	-31.6	1.9	0.0	2.2	33.8	1.6
593	-33.5	0.0	0.0	0.8	33.7	1.6
1745	-32.5	0.9	0.0	1.8	33.6	1.6
590	-33.1	0.0	0.0	1.3	33.4	1.6
425	-32.2	0.7	0.0	1.1	33.1	1.7
1078	-29.9	2.5	0.0	1.4	32.6	1.7
530	-31.1	1.1	0.0	1.9	32.4	1.7

- ¹ Stress components are listed for the nodes with the 20 highest impact nodal point stress intensity values (see Figure 2.7.8.1-3 for locations of these nodes). Note that S_x is the stress in the radial direction, S_y is the stress in the circumferential direction and S_{xy} is the shearing stress.
- ² The allowable stress is 0.7 S_u. S_u is the ultimate strength of 17-4 PH stainless steel at a bounding 600°F, S_u = 126.7 ksi.

Table 2.7.8.1-3 Basket 55-g Side Impact Stresses for 30-Degree Drop Orientation

Node No. ¹	S _x (ksi)	S _y (ksi)	S _z (ksi)	S _{xy} (ksi)	SI (ksi)	MS ²
565	-49.1	1.2	0.0	3.0	50.6	0.8
1755	-44.7	1.0	0.0	2.8	46.0	0.9
591	-44.0	1.5	0.0	2.8	45.9	0.9
592	-39.4	1.0	0.0	1.3	40.6	1.2
1908	-37.9	1.0	0.0	2.4	39.1	1.3
1765	-36.0	1.2	0.0	2.2	37.5	1.4
568	-34.7	2.3	0.0	1.7	37.2	1.4
1088	-35.6	1.5	0.0	1.4	37.2	1.4
1241	-34.8	1.4	0.0	1.4	36.4	1.4
564	-35.8	-0.5	0.0	2.5	36.3	1.4
415	-33.5	2.4	0.0	1.5	36.1	1.5
1745	-32.5	1.5	0.0	2.2	34.2	1.6
2395	-31.7	2.1	0.0	2.6	34.2	1.6
1133	2.6	-30.9	0.0	2.8	34.0	1.6
2575	-32.1	1.7	0.0	1.2	33.9	1.6
593	-33.7	-0.2	0.0	0.8	33.8	1.6
2453	1.2	-32.1	0.0	2.7	33.7	1.6
2444	0.7	-32.5	0.0	2.6	33.5	1.6
2434	1.5	-31.6	0.0	2.5	33.5	1.6
543	-30.8	2.1	0.0	2.5	33.3	1.7

¹ Stress components are listed for the nodes with the 20 highest impact nodal point stress intensity values (see Figure 2.7.8.1-4 for locations of these nodes). Note that S_x is the stress in the radial direction, S_y is the stress in the circumferential direction and S_{xy} is the shearing stress.

² The allowable stress is 0.7 S_u. S_u is the ultimate strength of 17-4 PH stainless steel at a bounding 600°F, S_u = 126.7 ksi.

Table 2.7.8.1-4 Basket 55-g Side Impact Stresses for 37-Degree Drop Orientation

Node No. ¹	S _x (ksi)	S _y (ksi)	S _z (ksi)	S _{xy} (ksi)	SI (ksi)	MS ²
565	-48.7	1.3	0.0	3.2	50.5	0.8
592	-44.2	1.5	0.0	3.0	46.1	0.9
1755	-44.5	1.2	0.0	2.9	46.0	0.9
592	-38.7	1.0	0.0	1.2	39.9	1.2
1908	-37.5	1.2	0.0	2.6	39.0	1.3
1765	-36.1	1.2	0.0	2.4	37.7	1.4
1088	-35.2	1.5	0.0	1.2	36.8	1.4
568	-33.6	2.3	0.0	1.6	36.0	1.5
1241	-34.2	1.4	0.0	1.3	35.7	1.5
2444	0.5	-34.6	0.0	2.5	35.5	1.5
564	-34.9	-0.5	0.0	2.6	33.4	1.5
2453	1.0	-33.7	0.0	2.6	35.2	1.5
415	-32.5	2.5	0.0	1.3	35.1	1.5
2395	-32.0	2.3	0.0	2.8	34.8	1.5
1133	2.5	-31.9	0.0	2.7	34.8	1.6
2434	1.6	-32.4	0.0	2.4	34.4	1.6
1745	-32.2	1.7	0.0	2.3	34.2	1.6
2575	-31.8	1.7	0.0	1.1	33.6	1.6
458	3.1	-29.9	0.0	3.0	33.6	1.6
593	-33.3	-0.2	0.0	0.8	33.4	1.7

¹ Stress components are listed for the nodes with the 20 highest impact nodal point stress intensity values (see Figure 2.7.8.1-5 for locations of these nodes). Note that S_x is the stress in the radial direction, S_y is the stress in the circumferential direction and S_{xy} is the shearing stress.

² The allowable stress is 0.7 S_u. S_u is the ultimate strength of 17-4 PH stainless steel at a bounding 600°F, S_u = 126.7 ksi.

Table 2.7.8.1-5 Basket 55-g Side Impact Stresses for 45-Degree Drop Orientation

Node No. ¹	S _x (ksi)	S _y (ksi)	S _z (ksi)	S _{xy} (ksi)	SI (ksi)	MS ²
565	-47.7	1.5	0.0	3.3	49.6	0.8
591	-43.9	1.5	0.0	3.2	45.9	0.9
1755	-43.9	1.3	0.0	3.1	45.6	0.9
1908	-36.7	1.4	0.0	2.7	38.5	1.3
592	-37.4	1.0	0.0	1.1	38.5	1.3
1765	-36.0	1.3	0.0	2.6	37.6	1.4
2444	0.3	-36.5	0.0	2.5	37.2	1.4
2453	0.8	-35.2	0.0	2.6	36.4	1.4
1088	-34.4	1.5	0.0	1.1	36.0	1.5
1133	2.3	-32.6	0.0	2.6	35.3	1.5
2395	-32.1	2.6	0.0	3.0	35.2	1.5
2434	1.7	-33.1	0.0	2.3	35.1	1.5
1241	-33.1	1.3	0.0	1.1	34.5	1.6
458	2.9	-30.8	0.0	2.9	34.2	1.6
568	-31.8	2.2	0.0	1.4	34.2	1.6
564	-33.3	-0.6	0.0	2.8	33.8	1.6
1745	-31.4	2.0	0.0	2.5	33.4	1.6
415	-30.9	2.5	0.0	1.1	33.5	1.6
1226	-30.2	2.3	0.0	3.0	33.0	1.6
2575	-31.2	1.7	0.0	0.9	33.0	1.7

- ¹ Stress components are listed for the nodes with the 20 highest impact nodal point stress intensity values (see Figure 2.7.8.1-6 for locations of these nodes). Note that S_x is the stress in the radial direction, S_y is the stress in the circumferential direction and S_{xy} is the shearing stress.
- ² The allowable stress is 0.7 S_u. S_u is the ultimate strength of 17-4 PH stainless steel at a bounding 600°F, S_u = 126.7 ksi.

Table 2.7.8.1-6 Basket 55g Side Impact Stresses for 60-Degree Drop Orientation

Node No. ¹	S _x (ksi)	S _y (ksi)	S _z (ksi)	S _{xy} (ksi)	SI (ksi)	MS ²
565	-42.7	2.0	0.0	3.4	45.2	1.0
1755	-41.1	1.7	0.0	3.3	43.3	1.0
591	-40.5	1.5	0.0	3.3	42.6	1.1
2444	0.0	-38.5	0.0	2.2	38.8	1.3
2453	0.5	-36.6	0.0	2.3	37.4	1.4
2108	-21.6	-20.1	0.0	12.0	36.9	1.4
1908	-34.4	1.7	0.0	2.9	36.6	1.4
1765	-34.9	1.3	0.0	2.3	36.6	1.4
2434	1.8	-33.4	0.0	1.9	35.5	1.5
1133	1.8	-32.7	0.0	2.3	34.8	1.6
1347	-27.1	-11.1	0.0	-12.0	34.7	1.6
2395	-30.8	3.0	0.0	3.3	34.4	1.6
458	2.4	-31.3	0.0	2.5	34.1	1.6
2467	2.7	-31.2	0.0	1.3	34.0	1.6
1630	-28.2	-7.7	0.0	-10.5	33.5	1.6
2477	1.7	-31.8	0.0	0.9	33.5	1.6
1088	-31.8	1.4	0.0	0.8	33.2	1.7
1786	0.9	-31.9	0.0	2.2	33.1	1.7
574	29.4	-2.7	0.0	3.2	32.7	1.7
592	-31.9	0.7	0.0	0.8	32.7	1.7

¹ Stress components are listed for the nodes with the 20 highest impact nodal point stress intensity values (see Figure 2.7.8.1-7 for locations of these nodes). Note that S_x is the stress in the radial direction, S_y is the stress in the circumferential direction and S_{xy} is the shearing stress.

² The allowable stress is 0.7 S_u. S_u is the ultimate strength of 17-4 PH stainless steel at a bounding 600°F, S_u = 126.7 ksi.

Table 2.7.8.1-7 Basket 55-g Side Impact Stresses for 64-Degree Drop Orientation

Node No. ¹	S _x (ksi)	S _y (ksi)	S _z (ksi)	S _{xy} (ksi)	SI (ksi)	MS ²
565	-40.4	2.1	0.0	3.3	43.0	1.1
1755	-39.9	1.8	0.0	3.3	42.1	1.1
591	-38.1	1.6	0.0	3.3	40.2	1.2
2444	-0.5	-38.7	0.0	2.1	38.9	1.3
2108	-22.6	-20.4	0.0	12.4	37.9	1.3
2453	0.4	-36.7	0.0	2.2	37.3	1.4
1765	-34.2	1.3	0.0	2.9	36.0	1.5
1908	-33.5	1.8	0.0	3.0	35.8	1.5
1347	-27.8	-11.6	0.0	-12.2	35.6	1.5
2434	1.8	-33.2	0.0	1.8	35.3	1.5
2467	2.6	-31.7	0.0	1.4	34.5	1.6
1630	-28.9	-7.9	0.0	-10.8	34.4	1.6
1133	1.6	-32.2	0.0	2.1	34.2	1.6
2477	1.7	-32.4	0.0	1.0	34.2	1.6
2395	-30.0	3.1	0.0	3.3	33.8	1.6
458	2.2	-31.1	0.0	2.4	33.7	1.6
1786	0.8	-32.1	0.0	2.2	33.2	1.7
574	29.6	-2.5	0.0	3.2	32.8	1.7
1777	0.2	-31.6	0.0	1.9	32.1	1.8
1088	-30.6	1.4	0.0	0.7	32.0	1.8

- ¹ Stress components are listed for the nodes with the 20 highest impact nodal point stress intensity values (see Figure 2.7.8.1-8 for locations of these nodes). Note that S_x is the stress in the radial direction, S_y is the stress in the circumferential direction and S_{xy} is the shearing stress.
- ² The allowable stress is 0.7 S_u. S_u is the ultimate strength of 17-4 PH stainless steel at a bounding 600°F, S_u = 126.7 ksi.

Table 2.7.8.1-8 Basket 55-g Side Impact Stresses for 75-Degree Drop Orientation

Node No. ¹	S _x (ksi)	S _y (ksi)	S _z (ksi)	S _{xy} (ksi)	SI (ksi)	MS ²
2108	-25.4	-20.9	0.0	13.4	40.5	1.2
2444	-0.2	-38.5	0.0	1.9	38.6	1.3
1347	-29.1	-12.9	0.0	-13.0	37.8	1.3
1755	-33.7	2.1	0.0	3.2	36.4	1.4
1630	-30.3	-8.6	0.0	-11.5	36.3	1.4
2453	0.7	-35.8	0.0	2.0	36.1	1.5
2477	1.6	-33.7	0.0	1.2	35.4	1.5
2467	2.4	-32.6	0.0	1.6	35.2	1.5
565	-31.7	2.3	0.0	3.1	34.5	1.6
2434	1.8	-32.3	0.0	1.5	34.4	1.6
2297	-25.2	-10.9	0.0	12.2	34.0	1.6
1908	-30.2	2.1	0.0	3.0	32.8	1.7
1786	0.5	-32.0	0.0	1.9	32.6	1.7
1777	-0.3	-32.0	0.0	1.6	32.2	1.8
1800	2.1	-29.4	0.0	1.3	31.7	1.8
1419	-25.3	-11.4	0.0	-10.7	31.4	1.8
2586	-28.5	2.3	0.0	3.2	31.4	1.8
1765	-29.0	1.5	0.0	2.9	31.1	1.9
1418	-25.9	-8.1	0.0	-10.8	31.0	1.9
1133	1.1	-29.6	0.0	1.7	30.9	1.9

¹ Stress components are listed for the nodes with the 20 highest impact nodal point stress intensity values (see Figure 2.7.8-9 for locations of these nodes). Note that S_x is the stress in the radial direction, S_y is the stress in the circumferential direction and S_{xy} is the shearing stress.

² The allowable stress is 0.7S_u. S_u is the ultimate strength of 17-4 PH stainless steel at a bounding 600°F, S_u = 126.7 ksi.

Table 2.7.8.1-9 Basket 55-g Side Impact Stresses for 90-Degree Drop Orientation

Node No. ¹	S _x (ksi)	S _y (ksi)	S _z (ksi)	S _{xy} (ksi)	SI (ksi)	MS ²
2108	-32.6	-17.9	0.0	15.2	44.6	1.0
1347	-32.6	-17.9	0.0	-15.2	44.6	1.0
2297	-33.7	-10.8	0.0	13.6	41.5	1.1
1630	-33.7	-10.8	0.0	-13.6	41.5	1.1
2024	-29.5	-10.1	0.0	12.7	35.9	1.5
1418	-29.5	-10.1	0.0	-12.7	35.9	1.5
2025	-27.8	-14.9	0.0	11.9	35.4	1.5
1419	-27.8	-14.9	0.0	-11.9	35.4	1.5
2123	-30.9	-3.5	0.0	7.8	33.9	1.6
1354	-30.9	-3.5	0.0	-7.7	33.9	1.6
2023	-28.3	-5.6	0.0	9.8	32.0	1.8
1417	-28.3	-5.6	0.0	-9.8	32.0	1.8
2212	-21.0	-17.2	0.0	10.2	31.4	1.8
1545	-21.0	-17.2	0.0	-10.2	31.4	1.8
2213	-25.9	-5.2	0.0	8.1	29.4	2.0
1546	-25.9	-5.2	0.0	-8.1	29.4	2.0
2022	-25.0	-3.7	0.0	7.1	27.3	2.2
1416	-25.0	-3.7	0.0	-7.1	27.3	2.2
1813	1.6	-25.1	0.0	-0.8	27.0	2.3
2434	1.6	-25.1	0.0	0.8	27.0	2.3

- ¹ Stress components are listed for the nodes with the 20 highest impact nodal point stress intensity values (see Figure 2.7.8.1-10 for locations of these nodes). Note that S_x is the stress in the radial direction, S_y is the stress in the circumferential direction and S_{xy} is the shearing stress.
- ² The allowable stress is 0.7S_u. S_u is the ultimate strength of 17-4 PH stainless steel at a bounding 600°F, S_u = 126.7 ksi.

Table 2.7.8.1-10 Summary of Basket 55-g Side Impact Analysis Results

Drop Orientation (deg)	Maximum Nodal SI Stress ¹ (ksi)	Temperature ² (°F)	Allow Stress ³ (ksi)	Margin of Safety
0	31.74	600	88.69	1.8
15	49.52	600	88.69	0.79
30	50.58	600	88.69	0.75
37	50.46	600	88.69	0.76
45	49.63	600	88.69	0.79
60	45.15	600	88.69	0.96
64	42.97	600	88.69	1.06
75	40.50	600	88.69	1.19
90	44.57	600	88.69	0.99

¹ The maximum stress documented is the stress intensity.

² Conservative envelope temperature of the support disk.

³ The allowable stress is $0.7S_u$. S_u is the ultimate strength of 17-4 PH steel alloy $S_u = 126.7$ ksi at 600°F.

Table 2.7.8.1-11 End Drop Impact (56.1 g) Basket Stresses

Node No. ¹	S _x (ksi)	S _y (ksi)	S _z (ksi)	S _{xy} (ksi)	S _{yz} (ksi)	S _{zx} (ksi)	SI (ksi)	MS ²
38512	-21.9	-23.7	5.2	1.9	4.8	-0.1	36.2	1.6
38522	-9.2	-7.0	-1.2	-7.0	-13.2	-2.0	32.6	1.9
38513	-11.3	-14.7	3.6	4.0	-2.4	-2.1	31.2	2.0
38570	-10.4	-11.0	-1.5	1.3	-8.7	3.3	29.8	2.2
38396	-9.4	-23.4	-0.7	5.5	6.8	-0.5	28.9	2.3
38514	-17.3	-15.8	1.4	1.6	2.7	2.5	28.7	2.3
37963	-8.1	-12.9	1.5	8.0	2.3	-2.9	27.7	2.4
37919	-7.6	-16.9	0.1	4.3	-4.4	-0.6	26.0	2.6
38515	-22.6	-20.0	-2.7	1.1	-2.3	4.1	24.9	2.9
38027	-2.0	18.7	-1.8	-0.5	-0.4	2.1	22.7	3.2
38576	-10.8	-16.3	-2.6	2.9	3.2	-1.4	22.6	3.2
38470	-2.3	18.0	-2.1	0.0	0.3	-2.3	22.5	3.2
38005	-14.4	-13.1	-0.1	4.2	2.0	-1.7	22.4	3.2
38029	0.4	20.3	-0.6	0.2	-0.2	-1.4	21.9	3.3
38032	0.3	20.1	-0.7	-0.1	0.1	1.4	21.7	3.3
38039	0.1	21.6	0.2	0.2	-0.2	0.1	21.7	3.4
38044	-0.1	21.2	0.0	0.2	0.1	-0.1	21.3	3.4
38485	-0.2	20.9	0.0	0.2	0.0	0.0	21.2	3.5
38446	-18.6	-14.5	-1.8	4.0	0.2	-0.5	21.2	3.5
38398	2.2	-12.7	1.9	-1.7	-3.1	2.1	20.3	3.6

¹ Stress components are listed for the nodes with the 20 highest impact nodal point stress intensity values (see Figure 2.7.8.1-12 for locations of these nodes). Note that S_x is the stress in the radial direction, S_y is the stress in the circumferential direction and S_z is the stress in the longitudinal direction.

² The allowable stress is 0.7S_u at the node temperature for the steady state design basis heat load heat transfer analysis.

Table 2.7.8.1-12 Basket Web Stress 55-g Side Impact for 0-Degree Orientation

Node No. ¹	S _x (ksi)	S _y (ksi)	S _z (ksi)	S _{xy} (ksi)	SI (ksi)	MS ²
402	-14.3	3.9	0.0	0.0	18.2	3.9
390	-14.4	2.4	0.0	0.0	16.9	4.2
1901	-13.7	3.1	0.0	0.0	16.9	4.3
567	-13.7	3.1	0.0	0.0	16.9	4.3
60	-16.0	-4.6	0.0	0.0	16.5	4.4
1839	-12.5	3.6	0.0	1.2	16.4	4.4
505	-12.5	3.6	0.0	-1.2	16.4	4.4
51	-14.9	-5.7	0.0	-0.1	15.6	4.7
1385	-14.9	-5.7	0.0	0.1	15.6	4.7
1829	-8.2	2.8	0.0	1.4	11.3	6.8
495	-8.2	2.8	0.0	-1.4	11.3	6.8
1069	-9.9	1.2	0.0	0.0	11.2	6.9
2506	-8.2	0.7	0.0	0.9	9.2	8.7
1172	-8.2	0.7	0.0	-0.9	9.2	8.7
1364	-7.2	-0.4	0.0	1.0	8.4	9.6
30	-7.2	-0.4	0.0	-1.0	8.4	9.6
1057	-6.1	-3.6	0.0	-0.1	6.3	13.0
2568	-4.8	-3.6	0.0	0.2	5.3	15.8
1234	-4.8	-3.6	0.0	-0.2	5.3	15.8
2496	-4.1	0.1	0.0	0.9	4.7	18.0
1162	-4.1	0.1	0.0	-0.9	4.7	18.0
727	-2.8	-1.7	0.0	0.0	3.0	28.8
697	-1.7	0.5	0.0	-0.2	2.3	36.9
2107	-1.7	0.5	0.0	0.2	2.3	37.0
1346	0.0	1.0	0.0	0.5	2.1	40.4
12	0.0	1.0	0.0	-0.5	2.1	40.4
2125	-0.3	-0.3	0.0	0.4	2.0	43.2
679	-0.3	-0.3	0.0	-0.4	2.0	43.2
718	-0.8	-1.2	0.0	-0.1	1.4	61.4
2086	-0.8	-1.2	0.0	0.1	1.4	61.4

¹ Stress components are listed for the nodes with the 20 highest impact nodal point stress intensity values (see Figure 2.7.8.1-13 for locations of these nodes). Note that S_x is the stress in the radial direction, S_y is the stress in the circumferential direction and S_{xy} is the shearing stress.

² The allowable stress is 0.7S_u. S_u is the ultimate strength of 17-4 PH stainless steel at a bounding 600°F, S_u = 126.7 ksi.

Table 2.7.8.1-13 Basket Web Stress 55-g Side Impact for 15-Degree Orientation

Node No. ¹	S _x (ksi)	S _y (ksi)	S _z (ksi)	S _{xy} (ksi)	SI (ksi)	MS ²
402	-13.0	0.5	0.0	-7.2	19.8	3.5
505	-10.8	0.9	0.0	-7.9	19.8	3.5
567	-12.8	2.5	0.0	-0.8	17.4	4.1
1069	-8.8	-1.7	0.0	-7.7	16.8	4.3
390	-13.5	1.2	0.0	-0.8	16.8	4.3
1172	-6.9	-0.8	0.0	-7.8	16.8	4.3
1839	-11.5	-0.3	0.0	-5.7	16.1	4.5
60	-15.3	-4.1	0.0	-0.3	16.0	4.5
51	-14.8	-4.9	0.0	-0.7	15.9	4.6
1901	-12.5	0.3	0.0	-0.7	14.9	5.0
495	-5.3	0.6	0.0	-6.6	14.5	5.1
2506	-7.3	-3.6	0.0	-6.5	13.8	5.4
1385	-12.9	-4.9	0.0	-0.4	13.6	5.5
1162	-2.0	-0.2	0.0	-6.5	13.1	5.8
1364	-8.8	2.3	0.0	-0.4	11.8	6.5
2496	-4.7	-5.5	0.0	-5.5	11.5	6.6
1829	-9.0	-1.6	0.0	-4.1	11.6	6.6
30	-4.8	-5.1	0.0	-2.2	9.8	8.0
2125	-0.3	-5.1	0.0	-0.8	8.9	8.9
1057	-5.6	-3.2	0.0	-1.2	8.2	9.8
1234	-3.8	-2.6	0.0	-1.3	7.8	10.4
2568	-5.0	-3.6	0.0	-1.1	7.4	10.9
697	-0.4	3.7	0.0	-1.7	6.9	11.9
2107	-2.6	-2.9	0.0	-1.6	6.3	13.0
1346	-1.0	-2.9	0.0	-0.4	5.8	14.2
12	-0.9	0.2	0.0	-1.4	3.3	25.5
727	-2.5	-1.4	0.0	-0.5	3.2	26.3
679	-0.1	0.1	0.0	-1.3	3.1	27.4
718	-0.1	0.1	0.0	-0.7	2.4	35.6
2086	-1.3	-1.9	0.0	-0.4	2.4	36.1

¹ Stress components are listed for the nodes with the 20 highest impact nodal point stress intensity values (see Figure 2.7.8.1-13 for locations of these nodes). Note that S_x is the stress in the radial direction, S_y is the stress in the circumferential direction and S_{xy} is the shearing stress.

² The allowable stress is 0.7S_u. S_u is the ultimate strength of 17-4 PH stainless steel at a bounding 600°F, S_u = 126.7 ksi.

Table 2.7.8.1-14 Basket Web Stress 55-g Side Impact for 30-Degree Orientation

Node No. ¹	S _x (ksi)	S _y (ksi)	S _z (ksi)	S _{xy} (ksi)	SI (ksi)	MS ²
505	-9.4	-0.8	0.0	-8.1	18.5	3.8
402	-11.3	-2.0	0.0	-7.5	17.7	4.0
1172	-5.9	-2.4	0.0	-7.9	16.3	4.5
1069	-7.4	-4.3	0.0	-7.9	16.2	4.5
567	-11.5	1.8	0.0	-0.7	16.2	4.5
390	-12.2	0.4	0.0	-0.7	15.4	4.8
51	-13.6	-4.1	0.0	-0.7	15.2	4.8
60	-13.9	-3.4	0.0	-0.3	14.8	5.0
2506	-5.5	-7.2	0.0	-6.8	14.4	5.1
1839	-9.5	-3.8	0.0	-5.9	14.1	5.3
495	-4.1	-0.2	0.0	-6.5	13.6	5.5
2496	-2.7	-10.1	0.0	-5.2	13.6	5.5
1901	-10.8	-0.6	0.0	-0.6	13.4	5.6
1162	-1.2	-0.8	0.0	-6.2	12.5	6.1
1385	-11.3	-4.2	0.0	-0.4	12.1	6.4
2125	-4.6	-8.5	0.0	-0.4	10.4	7.5
1829	-7.0	-5.9	0.0	-3.8	10.3	7.6
30	-3.6	-6.2	0.0	-2.2	10.2	7.7
1364	-7.7	1.0	0.0	-0.4	9.9	7.9
2107	-1.3	-6.9	0.0	-1.6	8.5	9.4
1057	-5.0	-4.0	0.0	-1.5	8.0	10.2
1346	-3.9	-6.2	0.0	-0.3	7.7	10.6
1234	-3.3	-2.8	0.0	-1.5	7.5	10.9
2568	-4.1	-4.7	0.0	-1.3	7.2	11.2
697	-0.3	4.2	0.0	-1.8	6.9	11.9
727	-2.2	-1.3	0.0	-0.8	3.6	23.3
12	-0.6	0.1	0.0	-1.3	3.1	27.9
2086	-1.3	-2.0	0.0	-0.8	3.0	28.4
718	0.1	0.2	0.0	-0.9	2.9	29.4
679	0.2	0.1	0.0	-1.2	2.9	30.0

¹ Stress components are listed for the nodes with the 20 highest impact nodal point stress intensity values (see Figure 2.7.8.1-13 for locations of these nodes). Note that S_x is the stress in the radial direction, S_y is the stress in the circumferential direction and S_{xy} is the shearing stress.

² The allowable stress is 0.7S_u. S_u is the ultimate strength of 17-4 PH stainless steel at a bounding 600°F, S_u = 126.7 ksi.

Table 2.7.8.1-15 Basket Web Stress 55-g Side Impact for 37-Degree Orientation

Node No. ¹	S _x (ksi)	S _y (ksi)	S _z (ksi)	S _{xy} (ksi)	SI (ksi)	MS ²
505	-8.5	-1.6	0.0	-8.2	17.8	4.0
402	-10.3	-3.2	0.0	-7.7	16.9	4.3
1069	-6.7	-5.5	0.0	-8.0	16.1	4.5
1172	-5.3	-3.1	0.0	-8.0	16.1	4.5
567	-10.6	1.4	0.0	-0.7	15.4	4.8
2506	-4.6	-8.8	0.0	-6.9	15.2	4.8
2496	-1.9	-12.1	0.0	-5.1	15.1	4.9
390	-11.3	0.0	0.0	-0.6	14.6	5.1
51	-12.7	-3.5	0.0	-0.7	14.6	5.1
60	-12.9	-2.9	0.0	-0.3	14.2	5.3
1839	-8.4	-5.3	0.0	-6.0	13.7	5.5
495	-3.3	-0.6	0.0	-6.4	13.1	5.8
1901	-9.9	-1.0	0.0	-0.5	12.6	6.1
1162	-0.8	-1.1	0.0	-6.1	12.2	6.3
2125	-5.9	-10.0	0.0	-0.4	11.5	6.7
1385	-10.3	-3.7	0.0	-0.4	11.3	6.9
1829	-6.1	-7.7	0.0	-3.7	10.7	7.3
30	-2.9	-6.7	0.0	-2.1	10.5	7.5
2107	-0.9	-8.6	0.0	-1.6	9.9	7.9
1364	-7.1	0.5	0.0	-0.4	9.0	8.9
1346	-5.0	-7.5	0.0	-0.3	8.8	9.1
1057	-4.6	-4.3	0.0	-1.6	7.9	10.2
1234	-3.0	-2.9	0.0	-1.6	7.3	11.2
2568	-3.7	-5.1	0.0	-1.4	7.3	11.2
697	-0.2	4.4	0.0	-1.8	6.9	11.8
727	-2.1	-1.2	0.0	-0.9	3.9	21.8
2086	-1.2	-2.1	0.0	-0.9	3.3	26.0
718	0.2	0.4	0.0	-1.0	3.1	27.2
12	-0.5	0.0	0.0	-1.2	2.9	29.1
679	0.2	-0.1	0.0	-1.2	2.7	31.3

¹ Stress components are listed for the nodes with the 20 highest impact nodal point stress intensity values (see Figure 2.7.8.1-13 for locations of these nodes). Note that S_x is the stress in the radial direction, S_y is the stress in the circumferential direction and S_{xy} is the shearing stress.

² The allowable stress is 0.7S_u. S_u is the ultimate strength of 17-4 PH stainless steel at a bounding 600°F, S_u = 126.7 ksi.

Table 2.7.8.1-16 Basket Web Stress 55-g Side Impact for 45-Degree Orientation

Node No. ¹	S _x (ksi)	S _y (ksi)	S _z (ksi)	S _{xy} (ksi)	SI (ksi)	MS ²
505	-7.2	-2.5	0.0	-8.2	17.1	4.2
2496	-1.0	-14.1	0.0	-4.9	16.8	4.3
1069	-5.7	-6.7	0.0	-8.1	16.3	4.5
402	-8.9	-4.5	0.0	-7.7	16.2	4.5
2506	-3.6	-10.4	0.0	-7.0	16.6	4.5
1172	-4.5	-3.9	0.0	-7.9	15.9	4.6
567	-9.4	0.8	0.0	-0.6	14.2	5.3
51	-11.4	-2.7	0.0	-0.8	13.8	5.4
390	-10.1	-0.4	0.0	-0.6	13.7	5.5
1839	-7.0	-7.0	0.0	-6.1	13.5	5.6
60	11.7	2.2	0.0	-0.3	13.5	5.6
2125	-7.2	-11.5	0.0	-0.3	12.9	5.9
495	-2.4	-1.1	0.0	-6.2	12.5	6.1
1162	-0.3	-1.5	0.0	-5.9	11.8	6.5
1829	-4.9	-9.7	0.0	-3.5	11.6	6.6
1901	-8.6	-1.4	0.0	-0.4	11.6	6.7
2107	-0.4	-10.3	0.0	-1.6	11.6	6.7
30	-2.1	-7.2	0.0	-2.0	10.7	7.3
1385	-9.1	-3.0	0.0	-0.4	10.3	7.6
1346	-6.2	-9.0	0.0	-0.3	10.1	7.8
1364	-6.3	-0.2	0.0	-0.5	8.1	10.0
1057	-4.1	-4.5	0.0	-1.7	7.8	10.4
2568	-3.1	-5.5	0.0	-1.6	7.3	11.1
1234	-2.6	-2.8	0.0	-1.7	7.1	11.5
697	-0.1	4.7	0.0	-1.8	6.9	11.9
727	-1.9	-1.2	0.0	-1.1	4.2	20.4
2086	-1.2	-2.2	0.0	-1.1	3.6	23.8
718	0.2	0.6	0.0	-1.1	3.4	25.3
12	-0.4	-0.1	0.0	-1.1	2.8	30.8
679	0.3	-0.1	0.0	-1.1	2.6	33.0

¹ Stress components are listed for the nodes with the 20 highest impact nodal point stress intensity values (see Figure 2.7.8.1-13 for locations of these nodes). Note that S_x is the stress in the radial direction, S_y is the stress in the circumferential direction and S_{xy} is the shearing stress.

² The allowable stress is 0.7S_u. S_u is the ultimate strength of 17-4 PH stainless steel at a bounding 600°F, S_u = 126.7 ksi.

Table 2.7.8.1-17 Basket Web Stress 55-g Side Impact for 60-Degree Orientation

Node No. ¹	S _x (ksi)	S _y (ksi)	S _z (ksi)	S _{xy} (ksi)	SI (ksi)	MS ²
2496	0.4	-17.1	0.0	-4.5	19.9	3.5
2506	-1.6	-12.8	0.0	-6.9	18.0	3.9
1069	-3.5	-8.6	0.0	-8.0	16.8	4.3
505	-4.2	-4.1	0.0	-7.8	15.6	4.7
402	-5.6	-6.7	0.0	-7.7	15.5	4.7
1172	-2.3	-5.1	0.0	-7.5	15.3	4.8
2125	-9.0	-13.7	0.0	-0.2	15.0	4.9
1839	-4.2	-9.7	0.0	-6.0	14.3	5.2
2107	0.3	-12.9	0.0	-1.5	14.2	5.2
1829	-2.8	-12.9	0.0	-3.2	13.9	5.4
1346	-8.0	-11.3	0.0	-0.3	12.4	6.2
60	-8.7	-0.7	0.0	-0.3	11.9	6.4
390	-7.2	-1.1	0.0	-0.5	11.5	6.7
51	-7.7	-1.6	0.0	-0.7	11.3	6.9
567	-6.1	-0.9	0.0	-0.5	11.2	6.9
495	-0.7	-1.9	0.0	-5.6	11.2	6.9
1162	0.5	-1.9	0.0	-5.2	10.8	7.3
30	-0.7	-7.2	0.0	-1.8	10.6	7.4
1901	-6.0	-2.2	0.0	-0.3	9.7	8.1
1385	-6.3	-1.4	0.0	-0.4	8.4	9.6
2568	-2.0	-6.1	0.0	-1.7	7.4	11.0
1057	-2.9	-4.6	0.0	-1.9	7.3	11.2
1364	-4.8	-1.3	0.0	-0.6	6.8	12.1
697	0.0	4.7	0.0	-1.7	6.5	12.7
1234	-1.5	-2.3	0.0	-1.9	6.4	13.0
727	-1.4	-0.9	0.0	-1.3	4.5	18.8
2086	-1.1	-2.3	0.0	-1.3	4.0	21.1
718	0.5	1.1	0.0	-1.3	3.7	23.2
12	-0.2	-0.3	0.0	-0.9	2.5	34.0
679	0.5	-0.1	0.0	-0.9	2.4	36.6

¹ Stress components are listed for the nodes with the 20 highest impact nodal point stress intensity values (see Figure 2.7.8.1-13 for locations of these nodes). Note that S_x is the stress in the radial direction, S_y is the stress in the circumferential direction and S_{xy} is the shearing stress.

² The allowable stress is 0.7S_u. S_u is the ultimate strength of 17-4 PH stainless steel at a bounding 600°F, S_u = 126.7 ksi.

Table 2.7.8.1-18 Basket Web Stress 55-g Side Impact for 64-Degree Orientation

Node No. ¹	S _x (ksi)	S _y (ksi)	S _z (ksi)	S _{xy} (ksi)	SI (ksi)	MS ²
2496	0.7	-17.6	0.0	-4.4	20.5	3.3
2506	-1.0	-13.3	0.0	-6.9	18.5	3.8
1069	-2.8	-9.0	0.0	-7.9	17.0	4.2
2125	-9.4	-14.1	0.0	-0.2	15.5	4.7
402	-4.9	-7.3	0.0	-7.6	15.4	4.7
505	-3.2	-4.6	0.0	-7.5	15.1	4.9
1172	-1.6	-5.3	0.0	-7.3	15.1	4.9
2107	0.5	-13.5	0.0	-1.5	14.8	5.0
1839	-3.4	-10.3	0.0	-6.0	14.7	5.0
1829	-2.3	-13.6	0.0	-3.1	14.5	5.1
1346	-8.4	-11.8	0.0	-0.3	12.9	5.9
60	-7.7	-0.3	0.0	-0.3	11.3	6.8
390	-6.3	-1.3	0.0	-0.5	10.8	7.2
495	-0.4	-2.1	0.0	-5.3	10.7	7.3
1162	0.6	-2.0	0.0	-5.0	10.3	7.6
567	-5.0	-1.6	0.0	-0.5	10.3	7.6
30	-0.4	-6.9	0.0	-1.6	10.3	7.6
51	-6.3	-2.1	0.0	-0.7	10.1	7.8
1901	-5.2	-2.4	0.0	-0.3	9.3	8.6
1385	-5.5	-0.9	0.0	-0.4	7.9	10.2
2568	-1.7	-6.1	0.0	-1.7	7.5	10.8
1057	-2.4	-4.5	0.0	-1.9	7.1	11.5
1364	-4.3	-1.6	0.0	-0.6	6.5	12.6
697	-0.1	4.6	0.0	-1.7	6.2	13.3
1234	-1.1	-2.0	0.0	-1.9	6.1	13.7
727	-1.1	-0.8	0.0	-1.3	4.5	18.8
2086	-1.1	-2.3	0.0	-1.3	4.1	20.6
718	0.6	1.3	0.0	-1.3	3.7	23.1
12	-0.1	-0.3	0.0	-0.9	2.5	34.9
679	0.5	-0.2	0.0	-0.8	2.3	37.8

¹ Stress components are listed for the nodes with the 20 highest impact nodal point stress intensity values (see Figure 2.7.8.1-13 for locations of these nodes). Note that S_x is the stress in the radial direction, S_y is the stress in the circumferential direction and S_{xy} is the shearing stress.

² The allowable stress is 0.7S_u. S_u is the ultimate strength of 17-4 PH stainless steel at a bounding 600°F, S_u = 126.7 ksi.

Table 2.7.8.1-19 Basket Web Stress 55-g Side Impact for 75-Degree Orientation

Node No. ¹	S _x (ksi)	S _y (ksi)	S _z (ksi)	S _{xy} (ksi)	SI (ksi)	MS ²
2496	1.5	-18.8	0.0	-4.0	22.0	3.0
2506	0.7	-14.4	0.0	-6.5	20.1	3.4
1069	-0.2	-10.0	0.0	-7.3	17.6	4.1
2125	-10.2	-15.0	0.0	-0.2	16.3	4.4
1829	-0.7	-15.3	0.0	-2.9	16.3	4.4
1839	-0.9	-12.0	0.0	-5.8	16.2	4.5
2107	0.9	-14.7	0.0	-1.5	16.1	4.5
402	-1.4	-8.8	0.0	-7.0	15.8	4.6
1346	-9.3	-12.9	0.0	-0.3	14.1	5.3
1172	0.2	-5.9	0.0	-6.3	14.0	5.3
505	-0.5	-5.7	0.0	-6.4	13.7	5.5
495	0.0	-2.5	0.0	-4.3	9.1	8.8
390	-2.9	-2.7	0.0	-0.4	8.7	9.2
1162	0.5	-2.1	0.0	-4.1	8.6	9.3
30	-0.1	-5.3	0.0	-1.2	8.6	9.3
567	-1.9	-3.3	0.0	-0.2	8.4	9.6
60	-3.9	-1.0	0.0	-0.1	8.2	9.8
1901	-2.7	-3.1	0.0	-0.2	8.1	9.9
2568	-0.7	-5.8	0.0	-1.7	7.4	11.0
51	-2.5	-3.2	0.0	-0.5	7.3	11.2
1385	-3.1	0.2	0.0	-0.4	6.6	12.4
1057	-0.8	-3.8	0.0	-1.9	6.2	13.3
1364	-3.1	-2.4	0.0	-0.6	6.0	13.7
697	-0.2	3.8	0.0	-1.4	5.1	16.2
1234	-0.1	-1.2	0.0	-1.8	5.0	16.9
2086	-0.9	-1.9	0.0	-1.4	4.2	20.0
727	-0.2	-0.1	0.0	-1.3	4.2	20.1
718	0.7	1.8	0.0	-1.2	3.5	24.4
12	-0.1	-0.5	0.0	-0.7	2.3	37.0
679	0.6	-0.2	0.0	-0.7	2.1	41.4

¹ Stress components are listed for the nodes with the 20 highest impact nodal point stress intensity values (see Figure 2.7.8.1-13 for locations of these nodes). Note that S_x is the stress in the radial direction, S_y is the stress in the circumferential direction and S_{xy} is the shearing stress.

² The allowable stress is 0.7S_u. S_u is the ultimate strength of 17-4 PH stainless steel at a bounding 600°F, S_u = 126.7 ksi.

Table 2.7.8.1-20 Basket Web Stress 55-g Side Impact for 90-Degree Orientation

Node No. ¹	S _x (ksi)	S _y (ksi)	S _z (ksi)	S _{xy} (ksi)	SI (ksi)	MS ²
1829	4.1	-18.8	0.0	0.5	23.1	2.8
2496	4.1	-18.8	0.0	-0.5	23.1	2.8
1839	4.8	-15.0	0.0	0.5	19.8	3.5
2506	4.8	-15.0	0.0	-0.5	19.8	3.5
1346	-11.1	-14.9	0.0	-0.1	16.2	4.5
2125	-11.1	-14.9	0.0	0.1	16.2	4.5
402	2.2	-10.8	0.0	0.4	13.0	5.8
1069	2.2	-10.8	0.0	-0.4	13.0	5.8
1364	1.8	-10.9	0.0	0.3	12.9	5.9
2107	1.8	-10.9	0.0	-0.3	12.9	5.9
2568	2.5	-4.9	0.0	-0.9	7.7	10.6
1901	2.5	-4.9	0.0	0.9	7.7	10.6
1172	-0.5	-6.5	0.0	-0.2	6.7	12.3
505	-0.5	-6.5	0.0	0.2	6.7	12.3
1057	0.6	-3.8	0.0	-0.9	4.9	17.0
390	0.6	-3.8	0.0	0.9	4.9	17.0
1234	-0.9	-2.8	0.0	-1.0	3.4	25.3
567	-0.9	-2.8	0.0	1.0	3.4	25.3
697	-1.2	-0.3	0.0	-0.2	2.8	31.0
30	-1.2	-0.3	0.0	0.2	2.8	31.1
1162	-0.8	-2.6	0.0	0.3	2.7	32.4
495	-0.8	-2.6	0.0	-0.3	2.7	32.4
2086	1.3	-0.3	0.0	-0.8	2.5	35.0
1385	1.3	-0.3	0.0	0.8	2.5	35.0
727	0.3	-0.1	0.0	-0.8	1.7	50.0
60	0.3	-0.1	0.0	0.8	1.7	50.0
51	-0.8	-0.5	0.0	0.7	1.7	50.4
718	-0.8	-0.6	0.0	-0.7	1.7	50.4
679	0.3	-0.6	0.0	0.2	0.9	96.5
12	0.3	-0.6	0.0	-0.2	0.9	96.5

¹ Stress components are listed for the nodes with the 20 highest impact nodal point stress intensity values (see Figure 2.7.8.1-13 for locations of these nodes). Note that S_x is the stress in the radial direction, S_y is the stress in the circumferential direction and S_{xy} is the shearing stress.

² The allowable stress is 0.7S_u. S_u is the ultimate strength of 17-4 PH stainless steel at a bounding 600°F, S_u = 126.7 ksi.

THIS PAGE INTENTIONALLY LEFT BLANK

2.7.8.2 Stress Evaluation of the Directly Loaded Fuel Basket Threaded Rods and Spacer Nuts - Accident Condition

In accordance with 10 CFR 71.73(c)(1), a spent-fuel shipping cask is subject to a free drop from a height of 30 feet onto a flat, unyielding surface. The design deceleration for the NAC-STC for the hypothetical accident 30-foot end drop is 56.1g (Table 2.6.7.4.1-2).

For a bottom end drop, the threaded rods and spacer nuts are loaded with the weight of the 31 support disks, the top plate, the 20 aluminum heat transfer disks, and the weights of the threaded rods and spacer nuts. These loads are calculated as follows:

Total weight of basket	=	16,350 lb
Less weight of bottom plate	=	-645 lb
Less weight of fuel tubes	=	<u>-3,666 lb</u>
1g load on the tie rods and spacer nuts	=	12,039 lb
Accident load on tie rods and spacer nuts	=	(12,039)(56.1)
	=	675,388 lb

The effective area of one threaded rod and spacer nut at each of the six locations supporting the weight of the support disks is equivalent to the gross area of the square spacer nut and is calculated as:

$$A = (2.5)(2.5)$$
$$= 6.25 \text{ in}^2$$

The average compressive stress in the threaded rods and spacer nuts is:

$$S_c = \frac{675,388}{(6)(6.25)}$$
$$= 18,010 \text{ psi}$$

Then, the margin of safety is:

$$\text{M.S.} = \frac{0.7S_u}{S_c} - 1 = \underline{+4.11}$$

where

$$S_u = 131.43 \text{ ksi}$$

(17-4 PH stainless steel at 405°F)

Therefore, the threaded rods and spacer nuts are structurally adequate for a 56.1 g end impact.

2.7.8.3 Assessment of Buckling – Directly Loaded Fuel Basket

During the impact of the NAC-STC cask onto an unyielding surface, the basket will be subjected to compressive loading in the plane of the support disks. Depending on the orientation of the basket, loads acting perpendicular to the plane of the support disk (out of plane) will also be applied. These compressive loadings in conjunction with out of plane bending require that buckling of the basket be a design consideration.

To ensure the stability of the basket, the design of the NAC-STC fuel basket is evaluated using Subsection NF of the ASME Boiler and Pressure Vessel Code, Section III, Division 1. The stability of the basket is maintained by 31 17-4 PH steel support disks and six 17-4 PH threaded tie rods. These two components are evaluated separately.

2.7.8.3.1 Assessment of Buckling of the 17-4 PH Stainless Steel Support Disks

The loads of interest are those generated during a lateral impact of any arbitrary angle (other than an end drop). During the lateral impact, the weight of the fuel assembly is transferred to the support disks. The webs of the support disks furthest away from the plane of impact will experience the least loading while the webs nearest the plane of impact which are transferring the weight of the fuel assemblies will be subjected to maximum compression. Loads in the webs of the fuel basket disk transferring the impact forces can be represented as a direct stress (i.e., uniaxial stress). This characterization categorizes the web as a linear support (Section NF-3300).

Within the design rules for linear supports, two levels of loadings are required to be addressed; Service Level A and B loadings, which corresponds to normal transport, and Service Level D loadings, which is associated with the 30 foot (9 meter) drop.

The forces acting on the basket are derived from the deceleration of the basket. The decelerations corresponding to the 30 foot (9 meter) drop are at least 2.8 times larger than the decelerations corresponding to the 1 foot drop. In comparing the allowables for the Service Level D loads to

loads to the allowables for the Service Level A and B Loads, the maximum increase of allowables is 1.7 (NF-3341.1). The Service Level D loading is the limiting condition.

To address the accident condition, Section NF-3340 can be applied which uses limit analyses to establish allowable loads acting on the support disks. Since out of plane loading is present, the governing conditions are detailed in equations (6), (7) and (8) of Section NF-3342.2.

Equation (6) of NF-3342.2 (b)(3) is specified as

$$\frac{P}{P_{cr}} + \frac{C_m M}{[1 - (P/P_{cr})] M_m} \leq 1.0$$

where:

P = the load acting in the plane of the web

The maximum compressive load is experienced by the web when the cask is subjected to a side impact. The web with the maximum load is the web nearest the plane of impact. The maximum number accumulation of fuel assembly weights is five. Other basket orientations yield a lower accumulation of weights.

The weight of the fuel assemblies and fuel tubes have a weight per unit length of 10.579 lb/in. Since the centerline to centerline distance of the disks is 4.87 inches, the maximum compressive load due to ten fuel assemblies is (5)(10.579)(4.87) or 257.6 pounds.

Additionally, the weights of the webs are also accumulative. This is conservatively considered in this calculation as the addition of eleven webs or 23.07 lbs.

The total amplified load (55g) is (55)(257.6 + 23.07) or 15.44 kips.

P = 15.44 kips

$$P_{cr} = 1.7 A F_a$$

where:

$$\begin{aligned} A &= \text{cross sectional area of the web} = (1.5)(.5) \\ A &= .75 \text{ in}^2 \end{aligned}$$

$$F_a = \text{as defined by equation (4) in NF-3322.1(c)(1) for non-austenitic stainless steels}$$

$$F_a = \frac{[1 - (Kl/r)^2 / 2C_c^2] S_y}{5/3 + [3(Kl/r) / 8C_c] - [(Kl/r)^3 / 8C_c^3]}$$

where:

$$Kl/r = \text{slenderness ratio.}$$

For the weak axis of bending, the radius of gyration is 0.1443 for the 1.5 inch wide and 0.5 inch thick web.

The length (l) of the unbraced span is 9.2 inches, which is the length of the slot containing the fuel assembly.

The factor K is taken to be 0.7 (AISC Steel Construction Manual, 8th edition), which corresponds to the condition of the bottom web. For this particular web, one end is connected to the edge of the basket and the other end is considered to be pinned.

$$l/r = 63.78$$

$$Kl/r = 44.6$$

$$\begin{aligned} S_y &= \text{yield strength at temperature (400 °F)} \\ S_y &= 89.8 \text{ ksi} \end{aligned}$$

$$C_c = \sqrt{2\pi^2 E / S_y}$$

At 400° for 17-4 PH (SA 693, Type 630), $E = 26,500$ ksi, $S_y = 89.8$ ksi

$$C_c = 76.32 \text{ (Note that } l/r < C_c \text{ for NF-3342.2 (b)(1))}$$

substituting into the expression for F_a ,

$$F_a = 40.02 \text{ ksi}$$

$$P_{cr} = 51.02 \text{ kips}$$

$$C_m = \text{interaction coefficient} = 1.0 \text{ (conservatively)}$$

$$M = \text{maximum bending moment due to the out of plane bending}$$

The moment (M) acting out of plane is due to the axial component of the deceleration. The maximum deceleration for any side or oblique drop, other than the end drop, is 55g. The maximum moment is computed by considering the web with the maximum compression as a simple span beam. Using a length of 9.204 inches, and 0.283 lb/in^3 as the density for steel, the maximum moment acting on the web is:

$$M = 123.5 \text{ lb-in}$$

$$P_e = 1.92 A F_e'$$

where F_e' is defined by equation NF-3322.1 (e)

$$F_e' = \frac{12\pi^2 E}{23 K l / r}$$

$$F_e' = 68.60$$

$$P_e = 1.92 (1.5 \times 5)(68.6)$$

$$P_e = 98.78$$

$$M_p = S_y Z$$

where:

$$Z = \text{plastic section modulus for the weak axis bending (1.5 inch width, .5 inch thickness), from Roark for a rectangular cross section}$$

$$Z = 0.25 (1.5) (0.5^2) = 0.09375 \text{ inch}^3$$

$$M_p = 8.4188 \text{ kip-in}$$

The maximum critical moment that can be resisted by a plastically designed member in the absence of axial load, M_m

$$M_m = M_p \left(1.07 - \frac{(1/r \sqrt{S_y})}{3160} \right)$$

$$M_m = 0.8787 M_p$$

$$M_m = 7.398 \text{ in-kip}$$

By substituting the computed quantities into equation (6) of NF-3342.2 (b)(3),

$$\frac{15.44}{51.02} + \frac{(1)(0.1235)}{(1 - 15.44/98.78)7.398} \leq 1.0$$

$$0.283 \leq 1.0$$

The margin of safety is:

$$M.S. = \frac{1.0}{0.283} - 1 = \underline{+2.53}$$

The first term in the above equation is also equation (5) of NF-3342.2 (b)(2) and the corresponding margin of safety is $51.02/15.44 - 1$, or +2.30.

Equation (7) of NF-3342.2 (b)(3) is specified as:

$$\frac{P}{P_y} + \frac{M}{1.18 M_p} \leq 1.0$$

where:

P_y = the axial plastic load = yield strength times cross sectional area

P_y = 67.35 kips

substituting

$$\frac{15.44}{67.35} + \frac{0.1235}{1.18(8.4188)} \leq 1.0$$

$$0.242 \leq 1.0$$

The margin of safety is:

$$\text{M.S.} = 1.0/0.242 - 1 = \underline{+3.13}$$

Also note for this equation, that for $M = 0.1235$ kip-in and $M_p = 8.4188$ kip-in, $M < M_p$ for which the margin of safety is:

$$\text{M.S.} = 8.4188/0.1235 - 1 = \underline{+67.1}$$

2.7.8.3.2 Assessment of Buckling of the 17-4 PH Threaded Rods

2.7.8.3.2.1 Maximum Compressive Load

The maximum compressive load applied to the threaded rods are during the 30 foot (9 meter) end drop, which corresponds to a maximum deceleration of 56.1 g's.

During the end impact, the weight of the support disks, aluminum heat transfer disks, are transferred to the threaded rods. The forces due to the weight of the fuel assemblies is transmitted directly to the end plate of the cask cavity.

The threaded rods transferring the load can be represented as a direct stress (i.e., uniaxial stress). This characterization categorizes the rod as a linear support (Section NF-3300).

To address the accident condition, Section NF-3340 can be applied which uses limit analyses to establish allowable loads acting on the support disks. Since out of plane loading is not present, the governing conditions are detailed in equation (5) of Section NF-3342.2, which specifies the allowable compressive force (P_{cr}).

$$P_{cr} = 1.7 A F_a$$

The maximum force ($P_{max} \leq P_{cr}$) transmitted to a threaded rod is based on the weight of the basket less the weight of the fuel tubes and the bottom weldment (The bottom weldment weighs 660 pounds while the top weldment weighs 974 pounds). The total weight transmitted by the six rods is 12,024 pounds.

The design of the basket is not sufficiently symmetrical to distribute the loading to the threaded rods in an equal fashion. To determine the distribution of the loads to the threaded rods in an end drop orientation, a finite element model of a single support disk was generated. The model of the entire disk shown in Figure 2.7.8.3-1 uses the ANSYS plate element (STIF63). The material properties for 17-4 PH employed in the model corresponds to the maximum basket temperature at 500°F. While the temperature does vary throughout the basket, the effect on the variation

of the modulus of elasticity and the corresponding effect on the load distribution to the rods is considered to be insignificant.

The support of the threaded rod is simulated by restraining the out of plane degree of freedom at the centerline of the location of the threaded rod connection with the support disk. A 1g load was applied to the elements comprising the support disk. The nodal reactions were used to determine the load distribution to the threaded rods. The four threaded rods at location A in Figure 2.7.8.3-1 have the same reaction value and carry 74.5% of the weight of the support disk, 18.6% per rod. The remaining two threaded rods, which are also of equal value carry 25.5% of the weight of the disk, 12.8% per rod. The limiting load for the threaded rod is 18.6% of the weight of the support disk.

The maximum load to be considered for the threaded rod is 12,024 pounds amplified by 56.1 g and factored by 0.186, or $P_{\max} = 125.63$ kips.

The axial compressive stress permitted in the threaded rod, F_a , is computed in the same manner as in Section 2.7.8.3.1. In the section of the threaded rod experiencing the maximum compressive load, the span is considered as a simple span configuration and the length corresponds to the centerline to centerline distance between the support disks. The simple span condition requires the effective length factor, K , to equal 1.0 (AISC Steel Construction Code, Eight Edition). Using the minor diameter to compute the radius of gyration, $Kl/r = 13.279 < C_c$. Using $C_c = 76.32$, F_a is determined to be 51.08 ksi and P_{cr} is 154.58 kips.

The margin of safety for equation (5) of NF-3342.2 is:

$$M.S. = 154.58/125.63 - 1 = \underline{+0.23}$$

2.7.8.3.2.2 Maximum Combined Axial and Bending Loads

In drop orientations other than the end drop, the aluminum heat transfer disks, which are supported by the threaded rods, will exert a lateral component on the threaded rods. This will induce bending moment into the threaded rod. It is assumed that the entire weight of one aluminum heat transfer disk will be carried by a single threaded rod carrying the maximum compressive load. This is conservative since the location of the closest aluminum fin to the

bottom of the cask will only experience the weight of 20 support disks instead of 31 disks as in this calculation.

The combined loading is governed by equations NF-3342.2 (6) and (7).

For equation NF-3342.2 (6),

$$\frac{P}{P_{cr}} + \frac{C_m M}{[1 - (P/P_{cr})] M_m} \leq 1.0$$

Assuming that the mass of the heat transfer disk acts as a point load at the mid span, the maximum moment for a simple span beam is:

$$M = F l / 4$$

where:

$$F = \text{weight of the heat transfer disk times the lateral deceleration}$$

As the cask assumes other angles, the maximum deceleration varies. Since the maximum decelerations decrease from 56.1 g's at 0° (end drop) to 33.8 g's at 60°, it is conservative to assume the maximum deceleration is 56.1 g's. The lateral deceleration is $56.1 \sin q$, where q is the angle measured from the vertical to the centerline of the cask body. The weight of the aluminum heat transfer disk is 105 pounds.

$$F = 56.1 (.105) \sin q \text{ (kips)}$$

$$l = 4.88 \text{ inches}$$

$$M = 7.186 \sin q \text{ (kip-in)}$$

The axial load on the rod at some angle of notation, q , is determined by $125.63 \cos q$ kips, then P in the above equation is $125.63 \cos q$.

$$P_e = 1.92 A F_e'$$

where F_{e-} is defined by equation NF-3322.1 (e)

$$F_{e-} = \frac{12\pi^2 E}{23(Kl/r)^2}$$

$$F_{e-} = 773.87$$

$$P_e = 1.92 A F_e'$$

$$P_e = 2644.78$$

$$M_p = S_y Z$$

where

$$Z = \text{plastic modulus for the weak axis M bending} \\ 1.333 R^3$$

$$Z = 1.333 (.735)^3 \text{ inch}^3$$

$$M_p = 47.53 \text{ kip-in}$$

The maximum critical moment that can be resisted by a plastically designed member in the absence of axial load, $M_m = M_p$

$$M_m = 47.53 \text{ kip-in}$$

By substituting the computed quantities into equation (6) of NF-3342.2,

$$\frac{125.63 \cos 0}{154.54} + \frac{(1)(7.186 \sin 0)}{(1 - 125.63 \cos 0 / 2644.78) 47.53} \leq 1.0$$

or

$$0.81272 \cos \theta + \frac{0.1512 \sin \theta}{1 - .0475 \cos \theta} \leq 1.0$$

It is necessary to determine the angle θ which maximizes the left side of the inequality. The maximum ratio of 0.828 occurs at $\theta = 11.0^\circ$.

The margin of safety for equation NF-3342.2 (6) is:

$$\text{M.S.} = 1.0/0.828 - 1 = \underline{+0.21}$$

Equation (7) of NF-3342.2 is specified as:

$$\frac{P}{P_y} + \frac{M}{1.18 M_p} \leq 1.0$$

where:

P_y = the axial plastic load = yield strength times cross sectional area

$$P_y = (1.78)(89.8) \text{ kips}$$

$$P_y = 159.84 \text{ kips}$$

substituting

$$\frac{125.63 \cos \theta}{159.84} + \frac{(1)(7.186 \sin \theta)}{1.18(47.53)} \leq 1.0$$

or

$$0.7856 \cos \theta + 0.1281 \sin \theta \leq 1.0$$

By taking the derivative and setting it to zero the maximum angle is determined to be $\theta = 9.26^\circ$.

Substituting for $\theta = 9.26$, Equation (7) of NF-3342.2 becomes:

$$0.796 \leq 1.0$$

The margin of safety for equation NF-3342.2 (7) is:

$$\text{M.S.} = 1.0/0.796 - 1 = \underline{+0.26}$$

Also note that for $M = 1.156$ kip-in and $M_p = 47.53$ kip-in, $M < M_p$ for which the margin of safety is:

$$\text{M.S.} = 47.53/1.156 - 1 = \underline{+40.12}$$

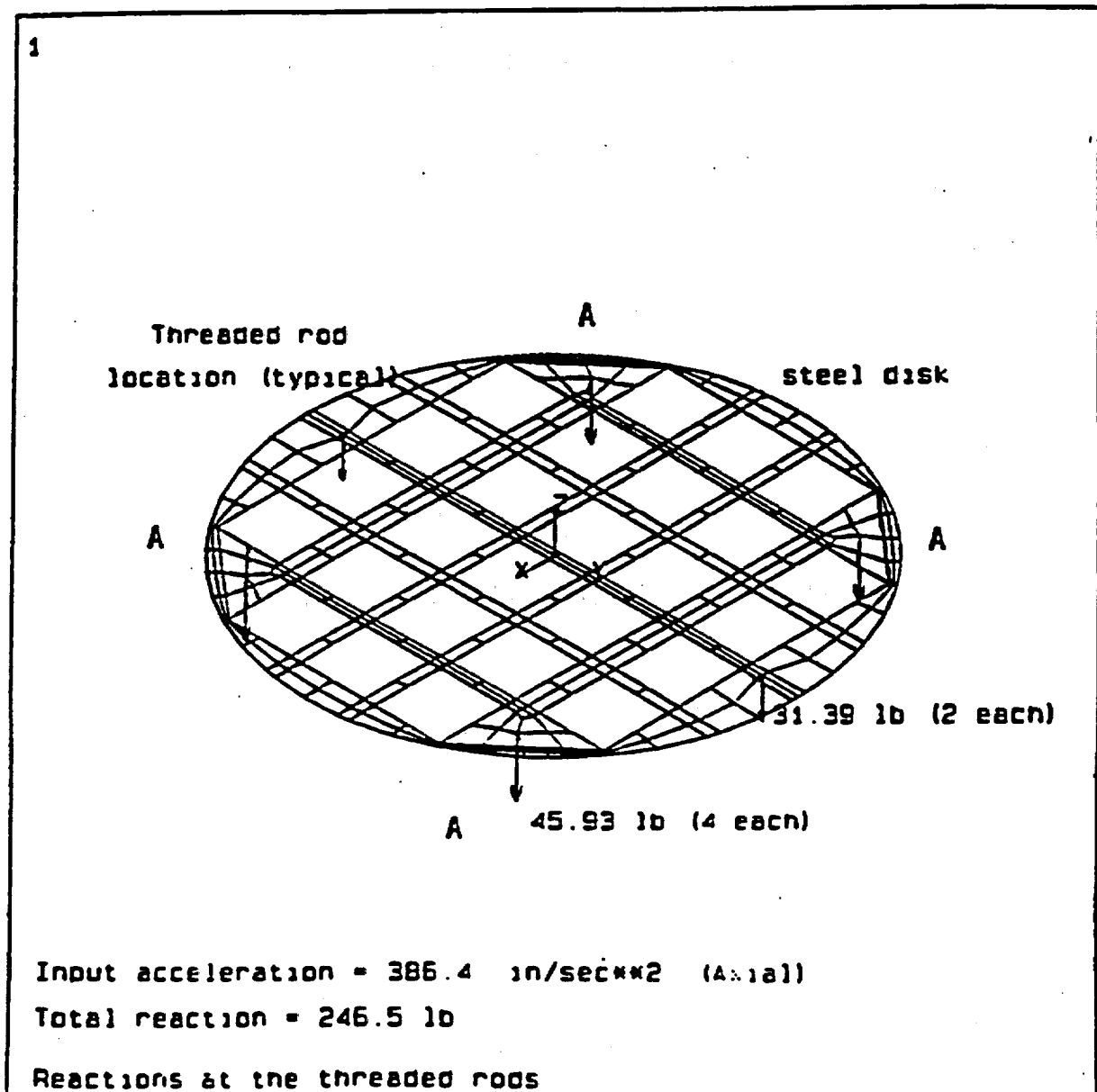
2.7.8.3.3 Summaries of Margins for NF-3400 Evaluation of Buckling

For the 17-4 PH stainless steel support disk and threaded rod, the margins of safety are summarized below:

<u>Equation</u>	<u>Support Disk</u>	<u>Threaded Rod</u>
NF-3342.2 (5)	+2.30	+0.23
NF-3342.2 (6)	+2.11	+0.21
NF-3342.2 (7)	+3.13	+0.26

Based on Subsection NF-3340 of the ASME Boiler and Pressure Vessel Code, Section III, the NAC 17-4 PH stainless steel basket design will maintain stability against buckling for the hypothetical 30 foot (9 meter) drop onto an unyielding surface.

Figure 2.7.8.3-1 Finite Element Model of a Support Disk



THIS PAGE INTENTIONALLY LEFT BLANK

2.7.8.4 Directly Loaded Fuel Basket Fuel Tube Analysis

The fuel tube provides a foundation and sealed cavity to mount BORAL poison plates within the fuel basket structure and does not provide a structural function relative to the support of the fuel assembly. The fuel tube design is presented in Figure 2.7.8.4-1. To ensure that the fuel tube remains functional when the cask is subjected to design load conditions, a structural evaluation of the tube has been performed for both the end and side impact load conditions.

2.7.8.4.1 Fuel Tube End Impact Analysis

During the postulated cask end impact, fuel assemblies are supported by the cask bottom plate for the bottom end drop and the inner lid for the top end drop. Fuel assembly load is not carried by the fuel tubes. Therefore, evaluation of the fuel tube for the end impact load is performed considering the weight of the fuel tube subjected to the cask deceleration carried by the minimum tube cross section. The tube minimum cross section is located at the contact point of the tube with the bottom weldment. From the dimensions of the tube shown in Figure 2.7.8.4-1 the minimum cross section area is:

$$\begin{aligned}\text{Area} &= (\text{Thickness})(\text{Mean Perimeter}) \\ &= [0.048][(4)(8.876 - 0.048) - 1] \\ &= 1.647 \text{ in}^2\end{aligned}$$

The total bearing load on the tube during the cask bottom end impact is 7910 pounds, (56.1 g x 141 lb). The maximum compressive and bearing stress in the fuel tube is 4800 psi, (7910/1.647). Limiting the compressive stress level in the tube to the material yield strength ensures the tube remains in position when the cask is subjected to the postulated end drop. Type 304 stainless steel yield strength is 19,400 psi at a conservatively high temperature of 500°F for the axial location on the fuel tube, which has the minimum cross section area. Using this criteria to evaluate the tube for the end drop load, a positive margin of safety of +3.04 is achieved.

2.7.8.4.2 Fuel Tube Side Impact Analysis

During the cask side impact load configuration the fuel tube is supported by the fuel basket 31 stainless steel support disks. The fuel basket support disks are spaced at 4.37 inches, which is less than one half of the fuel tube width of 8.88 inches, and provide support for the full length of the fuel tube. Considering the fuel tube subjected to the 55 g side impact deceleration and the 31 support locations provided by the basket support disks, the fuel tube shear stress is:

$$\text{Impact Shear Load} = (55)(141)/31 = 250 \text{ lb}$$

$$\text{Shear Area of Tube} = (0.048)(8.88)(2) = 1.17 \text{ in}^2$$

$$\text{Shear Stress of Tube} = 250/1.17 = 213 \text{ psi}$$

The ultimate strength (S_u) of Type 304 stainless steel at 500°F is 63,500 psi. The allowable shear stress of the tube wall material is $0.42S_u = 26.7$ ksi which results in a large positive margin of safety. It is evident from the conservative evaluation of the tube loading resulting from its own mass during the side impact configuration that the tube structure will maintain position and function.

In addition to the above evaluation, the load transfer of a fuel assembly to the fuel basket support disk when the cask is subjected to a side impact will be through direct bearing and compression of the distributed load of the fuel assembly through the fuel tube to the support disk web. For purposes of the tube evaluation, two load conditions and tube wall thicknesses are evaluated. One analysis postulates that the fuel assembly grid is located at the center of the span between the support disks and produces a localized distributed load over the effective area of the grid. The second analysis considers the fuel assembly load as a distributed pressure on the inside tube surface. The fuel tube structural performance is nonlinear when subjected to either of the postulated impact loadings and is not adequately evaluated using classical methods. Therefore, a finite element model of the tube is developed representing three support disk tube span lengths and analyzed for the imposed loading of the fuel assembly grid at mid-span of the modeled central span

to evaluate maximum accumulated plastic strain. The finite element model was then modified to consider the main tube wall thickness of 0.048 inches as the only material subjected to a distributed pressure load representative of the fuel assembly deceleration of 55g. Figure 2.7.8.4-2 presents the half symmetry fuel tube finite element model for the maximum plastic strain fuel tube grid loading evaluation. Figure 2.7.8.4-3 presents the half symmetry fuel tube finite element model used for the maximum plastic stress fuel assembly distributed loading evaluation. Fuel assembly stiffness is not considered in the development of the imposed load to the fuel tube for either of the two analyses.

The tube is modeled with the ANSYS plastic, quadrilateral shell element (STIF43) with large deflection capability. All energy is absorbed into tube strain by conservatively fixing the displacement of the tube at support disk spacing perpendicular to the direction of load. Material properties reported in NUREG/CR-0481, SAND 77-1872, "An Assessment of Stress-Strain Data Suitable for Finite-Element Elastic-Plastic Analysis of Shipping Containers," are used in these analyses.

Results from the maximum plastic strain evaluation, which loaded the grid surface area and absorbed all energy into the tube wall produced a strain level of 0.036 inch/inch as summarized in Table 2.7.8.4-1. Type 304 stainless steel is a material with high ductility and capacity to absorb significant strain without failure. ASME material specification requirements dictate 40 percent minimum elongation for the defined tube structural material. The maximum strain level of 0.036 inch/inch, or 3.6 percent demonstrates that the fuel tube maintains functional capacity when considering assembly deceleration at the localized fuel assembly grid locations.

Results from the 55g fuel assembly distributed load on the main tube wall, 0.048 inch thick, verifies that the maximum plastic stress in the tube is less than 31 ksi. This maximum plastic stress is local to the sections of the tube resting on the steel support disks. Over 72 percent of the tube does not exceed the material yield strength. Figure 2.7.8.4-4 depicts the elastic-plastic stress distribution over the fuel tube subjected to the side drop distributed pressure load. The maximum plastic stress is more than a factor of two less than the tube wall material minimum ultimate strength of 63.5 ksi.

Defining acceptable elastic-plastic response at one half the material performance permits margins of safety to be evaluated with significant margin beyond the chosen limits relative to actual material failure. Using this methodology to evaluate total cumulative strain shows a margin of safety of:

$$\text{M.S.} = \frac{40/2}{4} - 1 = 4.0$$

Similarly, the margin of safety for elastic-plastic stress becomes:

$$\text{M.S.} = \frac{(63.5 - 19.4)}{(31 - 19.4)} - 1 = 0.9$$

More than 72 percent of the tube wall is below the material yield strength. Both evaluations of maximum cumulative plastic strain and maximum elastic-plastic stress result in significant margin when evaluated with respect to an allowable chosen to be 50 percent of the material allowable plastic response.

It is evident from both the maximum cumulative strain, and the elastic-plastic stress analyses that the tube position within the support basket is maintained.

Assurance that the BORAL poison remains within the sealed casing has been evaluated considering loads produced by the BORAL and skin mass decelerated by 55g's being maintained by the seal weld. Total load and resultant stress is calculated as follows:

$$F = \text{Volume} \times \text{Density} \times 55$$

$$\begin{aligned} F_{\text{BORAL}} &= (8.18 \times 0.075 \times 4.37) \times 0.10 \times 55 \\ &= 14.7 \text{ pounds} \end{aligned}$$

$$\begin{aligned} F_{\text{Skin}} &= ([9.064 - 2(0.019 + 0.075 + 0.13)] \times 0.019 \times 4.37) \times 0.288 \times 55 \\ &= 11.3 \text{ pounds} \end{aligned}$$

Total load per inch of seal weld becomes:

$$\begin{aligned} F_{\text{Weld}} &= (F_{\text{BORAL}} + F_{\text{Skin}}) / \text{weld length} \\ &= (14.7 + 11.3) / (2 \times 4.37) \\ &= 2.97 \text{ pounds / inch} \end{aligned}$$

The fuel tube skin seal weld provides more material thickness than the skin material thickness. Material stress is calculated based on the thickness of the stainless steel skin. Using the load per unit length acting at the weld area, calculated above, the stress produced in the skin along the seal weld in the stainless steel skin is:

$$S_{\text{Seal}} = 2.97 / 1 \times 0.019 = 156 \text{ psi}$$

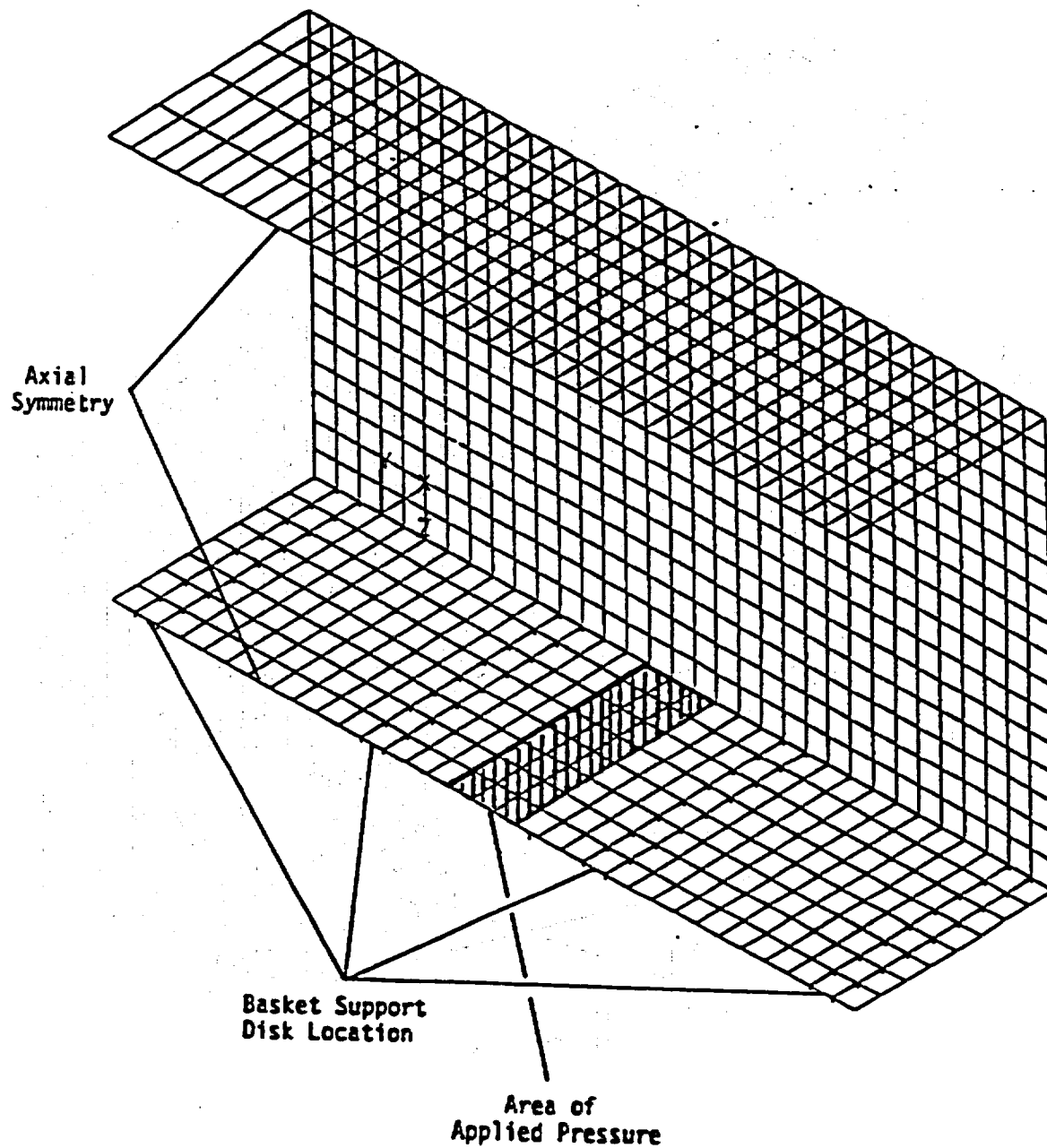
This additional load and material stress, 156 psi, transferred into the main tube wall analyzed for cumulative plastic strain and maximum elastic-plastic stress with a maximum stress intensification factor of 4 remains insignificant relative to the margins of 4.0 and 0.9 respectively. Therefore, it is evident that the fuel tube will remain in position within the fuel basket assembly and that the sealed BORAL remains within the sealed cavity on each outer surface of the tube wall.

This evaluation shows that the impact stress in the seal weld would be less than 200 psi. Therefore the seal weld and outer skin will maintain confinement of the BORAL material.

Figure 2.7.8.4-1 Fuel Tube Configuration

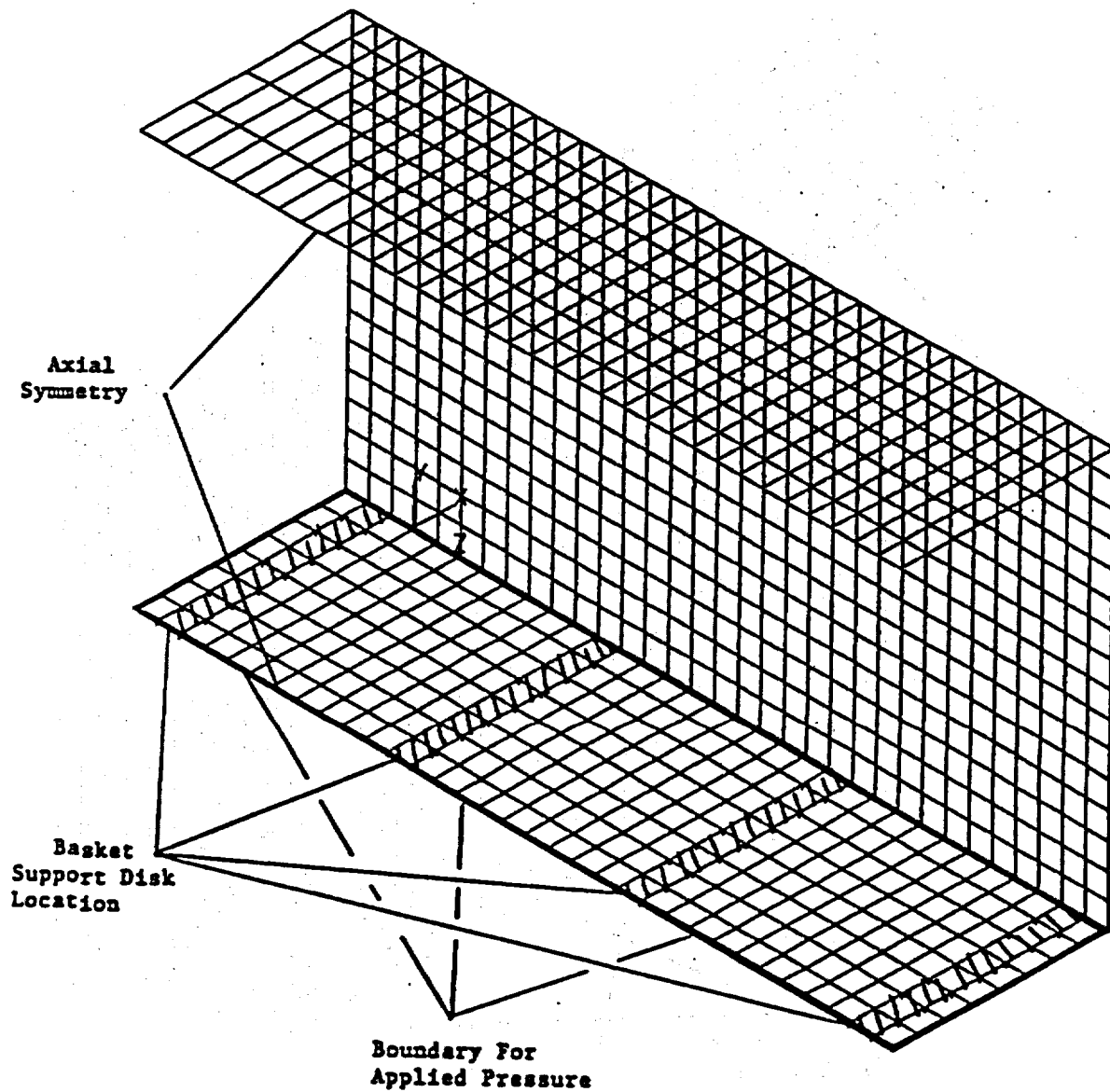
**FIGURE WITHHELD AS SENSITIVE
UNCLASSIFIED INFORMATION**

Figure 2.7.8.4-2 Fuel Tube Finite Element Model Grid Loading



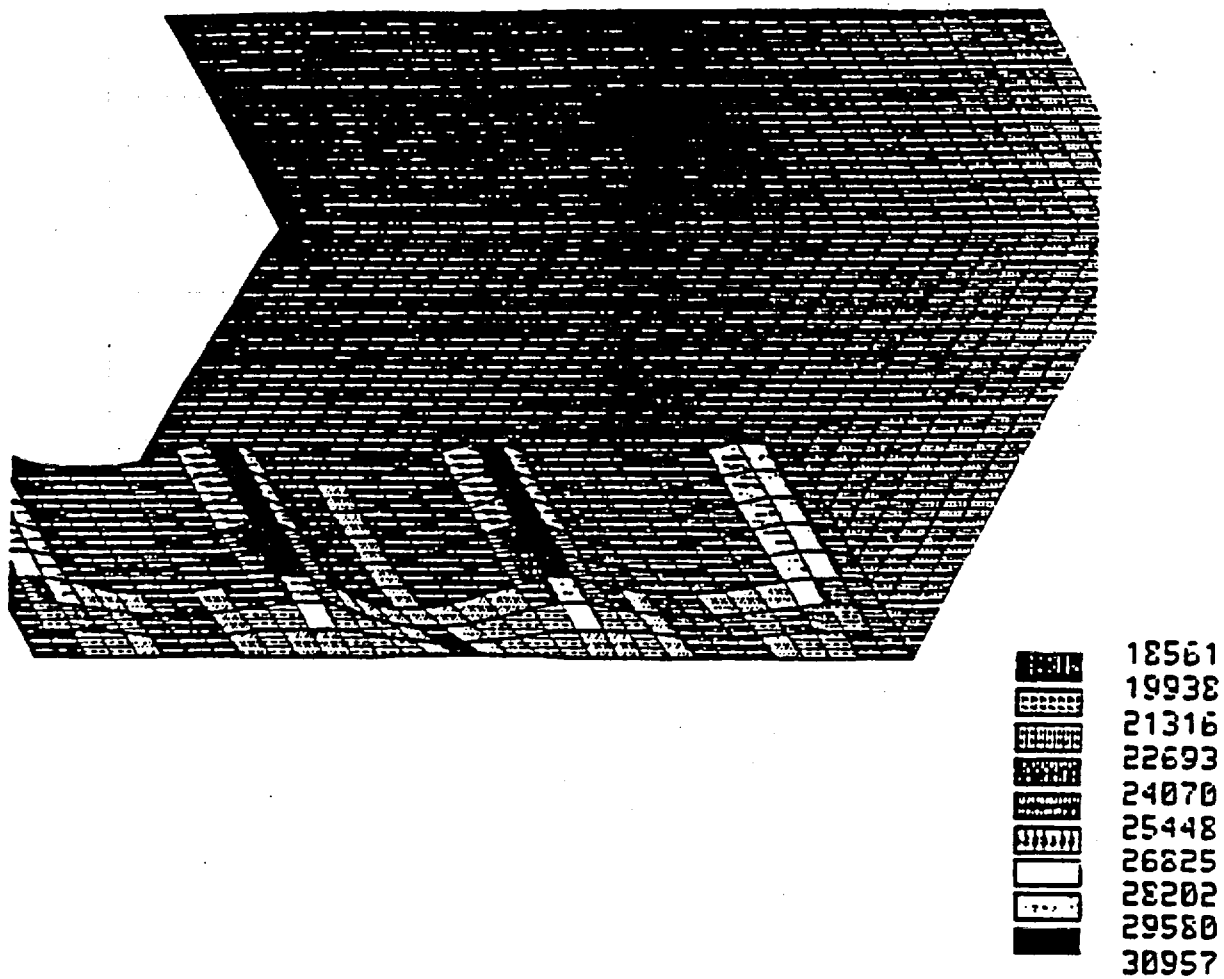
Note: Tube Wall Cumulative Strain Evaluation Considers the Main Tube Wall and Skin Encasement, $t = 0.048 + 0.019 = 0.067$ inches

Figure 2.7.8.4-3 Fuel Tube Finite Model Distributed Pressure Loading



Note: Tube Wall Stress Evaluation Considers the Main Tube Wall Only, $t = 0.048$ inches

Figure 2.7.8.4-4 Elastic-Plastic Stress Distribution



Note: 55g Fuel Assembly Distributed Load

Table 2.7.8.4-1 Ten Highest Strain Points for Total Energy Analysis

ELEMENT	STRAIN IN/IN
51	0.0356
1	0.0356
54	0.0354
4	0.0354
57	0.0354
7	0.0354
60	0.0350
10	0.0350
63	0.0348
13	0.0348

2.7.8.5 Directly Loaded Fuel Basket Weldment Analysis for 30-Foot End Drop

The response of the top and the bottom weldment plates of the fuel basket assembly to a 56.1g accident condition deceleration load are examined. The top and bottom weldment plates are both 1-inch thick and fabricated from SA 240, Type 304 stainless steel. The top weldment supports its own weight as well as the weight of the 26 fuel tubes (without the fuel assemblies) during a 30-foot top end drop. Similarly the bottom weldment supports its own weight and also the weight of the 26 fuel tubes (without the fuel assemblies) during a 30-foot bottom end drop. The responses of the end plates to the 30-foot end drop are analyzed using ANSYS STIF63 three-dimensional, six degrees of freedom, elastic quadrilateral shell elements. The finite element model for both weldment plates and the corresponding boundary condition of each weldment plate are shown in Section 2.6.12.13, Figure 2.6.12.13-1 through Figure 2.6.12.13-3. The evaluation is based on material properties of SA 240, Type 304 at a conservative temperature of 500°F. The hottest steel support disk during normal transport conditions is 498°F, see Table 3.4-1.

The primary membrane plus primary bending stress in the top weldment plate for the 30-foot top end drop is 61.9 ksi. The primary membrane plus primary bending stress in the bottom weldment plate for the 30-foot bottom end drop is 51.3 ksi. At 500°F, the accident condition stress allowable, S_u is 63.5 ksi. The minimum margin of safety for the top weldment plate and the bottom weldment plate are +0.03 and +0.24 respectively. Therefore, the structural adequacy of the NAC-STC fuel basket weldment end plates for the accident condition of transport is demonstrated.

2.7.9 Yankee-MPC Fuel Basket Analysis - Accident Conditions

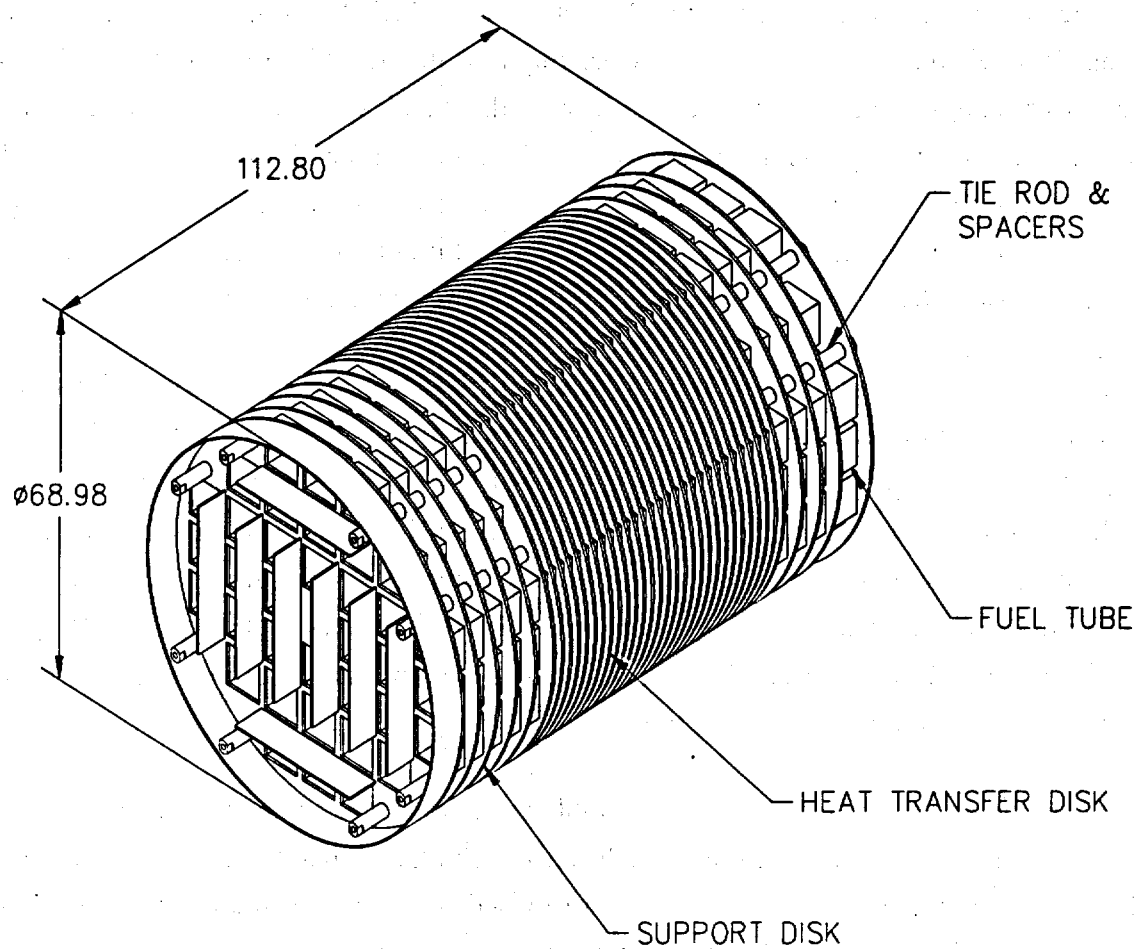
The Yankee-MPC fuel basket is designed to accommodate up to 36 fuel assemblies. The basket is a right cylinder structure and is fabricated with the following components: 36 square fuel tubes, 22 circular support disks, 14 heat transfer disks, 8 tie rods with split spacers, and two end weldment plates. The basket components and their geometry are illustrated in Figure 2.7.9-1 and Figure 2.6.14-2. Each fuel tube has a 7.80-inch square inside dimension, 0.141-inch thick composite wall, and holds the design basis Yankee Class fuel assembly. Figure 2.6.14-3 shows the details of the stainless steel tube with the encased BORAL. The fuel tubes are open at each end; therefore, longitudinal fuel assembly loads are imparted to the cask body and not the fuel basket structure. The fuel assemblies, together with the tubes are laterally supported in the holes in the stainless steel support disks. Each support disk is 0.5 inches thick, 69.15 inches in diameter and has 37 holes that are each 8.254 inches square. There are three web thicknesses in the support disks; 0.875 inch, 0.810 inch, and 0.75 inch. The widest web is nearest the center of the basket, the web decreases in width towards the outer radius of the basket. The support disks are equally spaced at 4.41 inches except for the disk nearest the bottom weldment, which is spaced 6.50 inches from the bottom weldment plate. The weldments are geometrically similar to the support disks and are 1 inch thick and 68.98 inches in diameter. The tie rod has 3.0 inches of 1 1/8-8 UN-2B threads at the upper end of the rod, which corresponds to the top of the basket. Fourteen (14) aluminum heat transfer disks are located at the mid-section of the cavity to fully optimize the passive heat rejection from the package. Each heat transfer disk is 0.50 inch thick, 68.87 inches in diameter, and has 37 holes that are 8.224 inches square. There are three different web widths, 0.905 inches, 0.84 inches and 0.78 inches. The widest aluminum web is nearest the center of the basket to optimize the passive heat rejection. The dimensional differences between the heat transfer disk and the support disk accommodates the different rate of thermal growth between aluminum and stainless steel preventing interference between the tube, the support disk, and heat transfer disks. The heat transfer disks, which serve no structural function, are supported by the eight tie rods with split spacers. The center hole of the support and heat transfer disks is not accessible as the center hole position is blocked by the top end weldment plate, which has only 36 fuel tube positions.

The fuel basket contains the fuel and is laterally supported by the canister shell. The 22 support disks and two (2) end plates are fabricated from Type 17-4 PH and Type 304 stainless steels, respectively. The 14 heat transfer disks are fabricated from Type 6061-T651 aluminum alloy. The 36 fuel tubes are fabricated from Type 304 stainless steel. The tie rods and spacers are

fabricated from Type 304 stainless steel. The stainless steel tubes are not considered to be a structural component with respect to the disks and are not included in the basket or weldment analyses. The primary function of the split spacers and the threaded top nut is to locate and structurally assemble the support disks, heat transfer disks and the top and bottom weldment plates into an integral assembly. The spacers carry the inertial weight of the support disks, heat transfer disks, one end plate, and their own inertial weight for a hypothetical accident condition, 30-foot end drop. The end drop loading of the split spacers and tie rods represent a classical closed form structural analysis. Therefore the only component that requires a detailed finite element analysis is the support disk.

The fuel basket is evaluated for the hypothetical accident condition loads in this section and is evaluated for the normal transport loads in Section 2.6.14.

Figure 2.7.9-1 Yankee-MPC Fuel Basket Assembly



2.7.9.1 Detailed Analysis – Yankee-MPC Fuel Basket

Based on criticality control requirements, the Yankee-MPC basket design criteria requires the maintenance of fuel support and control of spacing of the fuel assemblies for all load conditions. The structural design criteria for the fuel basket is the ASME Boiler and Pressure Vessel Code, Section III, Division 1, Subsection NG, "Core Support Structures." Consistent with this criteria, the main structural component in the fuel basket, the stainless steel support disk, is shown to have a maximum primary membrane stress intensity less than the allowable stress limit, defined as $0.7 S_u$, for the accident condition. Likewise the primary membrane plus bending stress intensity is shown to be less than the allowable stress limit, defined as $1.0 S_u$. The value of S_u is defined at conservatively high temperatures for the component being analyzed.

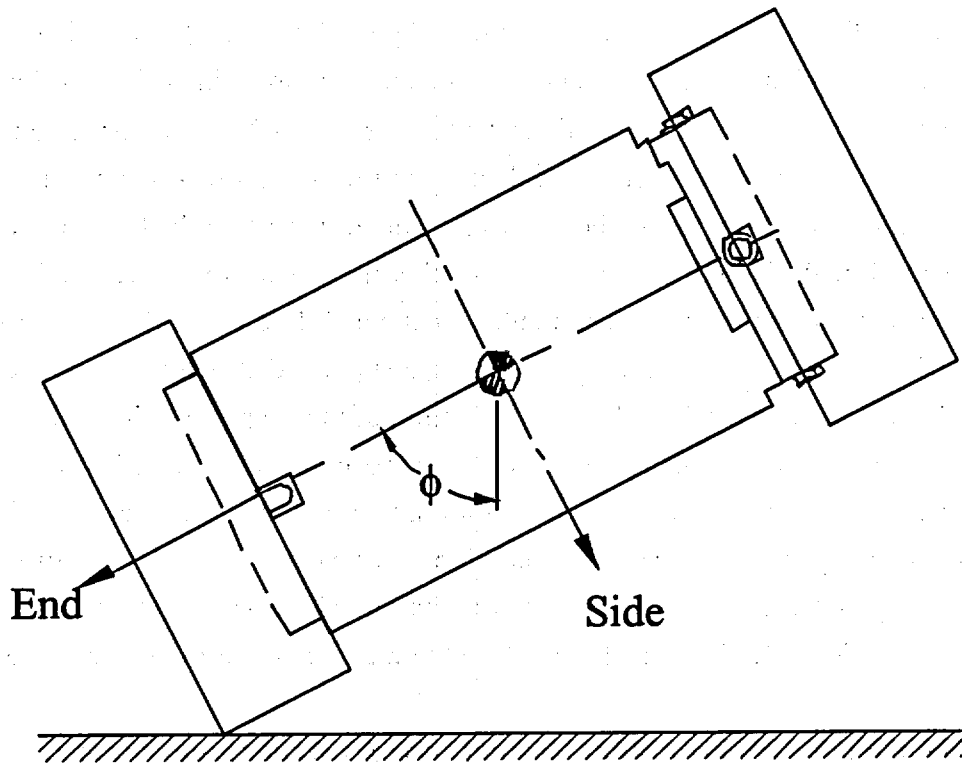
The structural evaluation for the support disks considers various cask drop orientations as well as various basket drop orientations. The cask drop orientation is defined in Figure 2.7.9.1-1; end drop ($\phi=0^\circ$), side drop ($\phi=90^\circ$) and off-angle drops ($0^\circ < \phi < 90^\circ$). For the side drop conditions, three basket drop orientations (0° , 22.9° , and 45°) are considered, as shown in Figure 2.6.14.1-1. Angles of 22.9° and 45° were selected because minimum web thickness occurs at those orientations. A parametric study in Section 2.10.11.1 indicates that the 22.9° drop case is bounded by the 45° drop case. Therefore, detailed analysis is performed for the 0° and 45° basket orientations for side drop conditions.

In the side drop, the loads of the fuel assemblies are transferred into the plane of the support disks, from which they are transmitted to the canister shell, and then to the cask body (cask inner shell). In the end drop, the support disks are loaded by their own inertial weight and do not experience load from the guided, but free standing fuel assemblies.

Finite element models are used to perform analyses for end drop and side drop conditions using the ANSYS program. Off-angle drops are evaluated by combining the results from the analyses for the end and side drop conditions (Section 2.7.9.1.4). Note that the methodology used for the off-angle drop evaluation is very conservative given the g loads decrease significantly for off-angle drop orientations (see Table 2.6.7.4.1-3).

In addition to the load from inertial weight, the analyses also consider the stresses due to differential thermal expansion for the buckling evaluation.

Figure 2.7.9.1-1 Cask Orientation



2.7.9.1.1 Finite Element Model Description – Yankee-MPC Fuel Basket

Three finite element models were generated to analyze the canistered Yankee class fuel basket for accident conditions; one for the end drop (Figure 2.6.14.2-1), in which the loads are perpendicular to the plane of the disk and two for the side drop, in which the loads act in the plane of the disk, for two basket orientations, 0° (Figure 2.6.14.2-2) and 45° (Figure 2.6.14.2-3). These are the same models used for the evaluation of the support disk for normal conditions of transport. All models accommodate thermal expansion effects using the temperature distribution from the thermal analysis and the coefficient of thermal expansion. See Section 2.6.14.2 for detailed description of the models. The model for the end drop conditions is constructed using ANSYS SHELL63 elements. It consists of a single support disk with a thickness of 0.5 inch. The finite element models for the side drop evaluation of the support disks are three dimensional models and include the lower section of the canister and cask as well as 14 of the support disks. Similar to the consideration of the normal condition, two bounding thermal conditions (2 and 3) are used in the analysis of the accident condition. See Section 2.6.14.3 for discussion of the thermal considerations. Allowable stresses are determined based on conservative temperatures of 539° F (see Section 2.6.14.3) for Thermal Condition 2 and -40° F for Thermal Condition 3.

To determine the most critical regions, a series of cross sections are considered. The section locations are identified in Figures 2.6.14.2-9 and 2.6.14.2-10 for the 0° and 45° basket drop cases, respectively. Tables 2.6.14.2-1 and 2.6.14.2-2 list the coordinate location of the cross section end points.

2.7.9.1.2 Stress Evaluation of the Yankee-MPC Support Disk for a 30-Foot End Drop Condition

The support disks of the Yankee-MPC fuel basket are located by 8 tie rods with spacers. A structural analysis is performed using ANSYS to evaluate the effect of a 30-foot end drop impact, which corresponds to the most severe out-of-plane loading. The model described in Section 2.7.9.1.1 is used in conjunction with a 56.1g deceleration. Linearized stresses at the cross sections identified in Figure 2.6.14.2-9 are compared to stress allowables per ASME Code, Section III, Subsection NG.

The stress evaluation results for the 30-foot end drop condition are:

Thermal Condition	P_m		P_m+P_b	
	Stress Intensity (ksi)	M.S.	Stress Intensity (ksi)	M.S.
2	0	N/A	52.9	1.42
3	0	N/A	53.9	1.51

The margin of safety (M.S.) is:

$$M.S. = (\text{Allowable Stress}/\text{Stress Intensity}) - 1,$$

where the allowable stress is $1.0 S_u$ for 17-4PH Type 630 stainless steel.

The minimum margin of safety is +1.42. The P_m stresses in the support disk for end drop conditions are essentially zero because there is no in-plane loading. Tables 2.7.9.1.2-1 and 2.7.9.1.2-2 list the 40 highest P_m+P_b stress intensities for thermal conditions 2 and 3, respectively.

Table 2.7.9.1.2-1 $P_m + P_b$ Stresses for the Yankee-MPC Support Disk—30-Foot End Drop
Thermal Condition 2

Section	Sx (ksi)	Sy (ksi)	Sxy (ksi)	Stress Intensity (ksi)	Allowable Stress (ksi)	Margin of Safety
50	-52.7	-5.6	-3.3	52.9	127.8	1.42
46	-52.6	-17.9	1.3	52.6	127.8	1.43
19	-18.3	-52.5	-0.3	52.5	127.8	1.44
5	-52.4	-27.8	0.1	52.4	127.8	1.44
30	-6.1	-51.5	2.9	51.7	127.8	1.47
56	-18.3	-51.6	0.5	51.6	127.8	1.48
9	-51.3	-19.0	-0.1	51.3	127.8	1.49
7	-51.2	-18.8	-0.6	51.3	127.8	1.49
4	-27.4	-51.2	-0.2	51.2	127.8	1.49
42	-50.8	-27.6	1.0	50.9	127.8	1.51
11	-50.6	-5.9	2.7	50.8	127.8	1.52
3	-50.3	-27.8	-0.2	50.3	127.8	1.54
67	-6.4	-46.7	-1.8	46.8	127.8	1.73
79	-0.1	-46.5	0.3	46.5	127.8	1.75
103	-46.4	0.0	0.3	46.4	127.8	1.75
13	-45.7	-6.6	1.3	45.8	127.8	1.79
94	-45.6	-0.1	-0.1	45.6	127.8	1.80
80	-0.1	-45.5	-0.2	45.5	127.8	1.81
104	-45.5	-0.1	-0.2	45.5	127.8	1.81
95	-44.5	-0.1	-0.2	44.5	127.8	1.87
78	-0.1	-44.0	0.3	44.0	127.8	1.90
102	-44.0	-0.1	0.3	44.0	127.8	1.90
93	-43.8	-0.1	0.1	43.8	127.8	1.92
77	-6.3	-35.1	-10.2	38.3	127.8	2.34
66	-35.1	-6.3	-10.2	38.3	127.8	2.34
89	-0.6	-37.7	-3.3	38.0	127.8	2.36
88	-0.5	-37.5	1.4	37.5	127.8	2.41
20	-37.2	-28.2	0.0	37.2	127.8	2.43
45	-28.1	-36.9	1.0	37.0	127.8	2.46
87	-0.3	-36.0	0.8	36.0	127.8	2.55
82	0.3	-35.7	-0.5	36.0	127.8	2.55
37	8.8	-25.9	3.9	35.5	127.8	2.60
81	0.2	-35.2	-0.3	35.4	127.8	2.61
53	-26.3	8.1	-4.3	35.4	127.8	2.61
106	-34.8	0.4	1.4	35.3	127.8	2.62
107	-34.0	0.5	-3.3	35.1	127.8	2.64
83	0.5	-33.9	2.9	34.9	127.8	2.66
97	-34.4	0.3	-0.7	34.7	127.8	2.68
105	-34.4	0.2	0.8	34.6	127.8	2.69
96	-34.4	0.2	-0.2	34.6	127.8	2.69

Note: See Figure 2.6.14.2-9 for section locations and definition of coordinate system.

Table 2.7.9.1.2-2 $P_m + P_b$ Stresses for the Yankee-MPC Support Disk—30-Foot End Drop Thermal Condition 3

Section	Sx (ksi)	Sy (ksi)	Sxy (ksi)	Stress Intensity (ksi)	Allowable Stress (ksi)	Margin of Safety
5	-53.9	-28.5	0.0	53.9	135.0	1.51
46	-53.1	-18.3	1.6	53.1	135.0	1.54
19	-18.8	-52.9	-0.6	52.9	135.0	1.55
50	-52.6	-5.8	-3.1	52.8	135.0	1.56
4	-28.1	-52.4	-0.4	52.4	135.0	1.58
42	-52.0	-28.3	1.2	52.1	135.0	1.59
56	-18.7	-52.0	0.6	52.0	135.0	1.60
9	-51.7	-19.5	-0.2	51.7	135.0	1.61
7	-51.7	-19.2	-0.9	51.7	135.0	1.61
30	-6.3	-51.4	2.7	51.6	135.0	1.62
3	-51.5	-28.5	-0.3	51.5	135.0	1.62
11	-50.5	-6.1	2.5	50.7	135.0	1.66
79	-0.1	-46.7	0.3	46.7	135.0	1.89
103	-46.7	0.0	0.3	46.7	135.0	1.89
67	-6.6	-46.5	-1.7	46.6	135.0	1.90
94	-45.8	-0.1	-0.1	45.8	135.0	1.95
13	-45.6	-6.8	1.2	45.6	135.0	1.96
80	-0.1	-45.3	-0.2	45.3	135.0	1.98
78	-0.1	-45.3	0.3	45.3	135.0	1.98
104	-45.3	-0.1	-0.2	45.3	135.0	1.98
102	-45.3	-0.1	0.3	45.3	135.0	1.98
93	-45.0	-0.1	0.1	45.0	135.0	2.00
95	-44.3	-0.1	-0.2	44.3	135.0	2.05
20	-38.2	-28.4	-0.2	38.2	135.0	2.53
45	-28.3	-37.9	1.2	38.0	135.0	2.55
88	-0.5	-37.7	1.7	37.8	135.0	2.57
89	-0.6	-37.5	-3.1	37.8	135.0	2.57
77	-6.1	-34.3	-9.9	37.4	135.0	2.61
66	-34.3	-6.1	-9.9	37.4	135.0	2.61
87	-0.3	-36.9	1.0	36.9	135.0	2.66
81	0.2	-36.1	-0.5	36.3	135.0	2.72
82	0.3	-36.0	-0.7	36.3	135.0	2.72
106	-35.1	0.3	1.7	35.6	135.0	2.79
105	-35.3	0.2	1.0	35.5	135.0	2.80
96	-35.3	0.2	-0.3	35.5	135.0	2.80
37	8.7	-25.6	3.8	35.1	135.0	2.85
8	-27.5	-35.0	-0.4	35.0	135.0	2.85
97	-34.7	0.3	-0.9	35.0	135.0	2.86
53	-26.0	7.9	-4.2	35.0	135.0	2.86
107	-33.8	0.5	-3.1	34.9	135.0	2.87

Note: See Figure 2.6.14.2-9 for section locations and definition of coordinate system.

2.7.9.1.3 Stress Evaluation of the Yankee-MPC Support Disk for a 30-Foot Side Drop Load Condition

To determine the structural adequacy of the Yankee-MPC support disk in the canistered Yankee class fuel basket for the 30-foot side drop impact load condition, a quasi-static impact load equal to the weight of the fuel and tubes multiplied by a 55g amplification factor is applied to the support disk structure. The inertial loading of the support disk is also included via the density input for the 17-4 PH stainless steel. The fuel assembly load is transmitted in direct compression through the tube wall to the web structure of the support disk. A finite element analysis is performed using the three dimensional support disk side model described in Section 2.7.9.1.1. As discussed in Section 2.7.9.1, two bounding cases of basket orientation (0° and 45°) are considered in the analysis. The material properties are evaluated at two thermal conditions: Thermal Condition 2, the cold condition (-40°F with 12.5 kW heat load) which has the largest change in temperature from the center of the basket to the outer edge and Thermal Condition 3, extreme cold (-40°F ambient with no heat load). Linearized stresses of the cross-sections (Figures 2.6.14.2-9 and 2.6.14.2-10) at the five critical disks (Section 2.6.14.2 and Figure 2.6.14.2-8) are compared to the stress allowable per the ASME Code, Section III, Subsection NG. The allowable stress is $0.7S_u$ for P_m , and $1.0 S_u$ for $P_m + P_b$ stresses, respectively.

The stress evaluation results for the 30-foot side drop condition are summarized in Table 2.7.9.1.3-1. The minimum margin of safety is +0.19, which occurs in disk No. 2 for the 45° basket drop orientation (Thermal Condition 2). For the 0° basket drop orientation, the highest P_m stress intensities occur in Disk No. 1 and the highest $P_m + P_b$ stress intensities occur in Disk No. 5 (Thermal Condition 2). Tables 2.7.9.1.3-2 through 2.7.9.1.3-5 list the 40 highest P_m stress intensities for Disk No. 1 (Thermal Conditions 2 and 3) and $P_m + P_b$ stress intensities for Disk No. 5 (Thermal Conditions 2 and 3). For the 45° basket drop orientation, the highest P_m stress intensities occur in Disk No. 3 and the highest $P_m + P_b$ stress intensities occur in Disk No. 2 (Thermal Condition 2). Tables 2.7.9.1.3-6 through 2.7.9.1.3-9 list the 40 highest P_m stress intensities for Disk No. 3 and the 40 highest $P_m + P_b$ stress intensities for Disk No. 2 (Thermal Conditions 2 and 3).

Table 2.7.9.1.3-1 Summary of Maximum Yankee-MPC Support Disk Stresses for 30-Foot Side Drop

Thermal Condition	Disk Number	P _m		P _m +P _b	
		S.I. (ksi)	M.S.	S.I. (ksi)	M.S.
0° BASKET DROP ORIENTATION					
2	1	47.7	0.87	62.6	1.04
	2	44.7	1.00	61.4	1.08
	3	40.7	1.20	67.5	0.89
	4	38.2	1.34	73.1	0.75
	5	39.1	1.29	73.3	0.74
3	1	48.2	0.96	63.2	1.14
	2	45.1	1.10	61.4	1.20
	3	40.9	1.31	67.1	1.01
	4	38.1	1.48	72.7	0.86
	5	39.0	1.42	72.9	0.85
45° BASKET DROP ORIENTATION					
2	1	41.9	1.13	106.0	0.21
	2	42.4	1.11	107.0	0.19
	3	45.5	0.97	105.7	0.21
	4	45.1	0.98	106.2	0.20
	5	45.1	0.98	106.2	0.20
3	1	42.1	1.24	108.0	0.25
	2	42.5	1.22	109.3	0.24
	3	45.4	1.08	107.7	0.25
	4	44.8	1.11	108.2	0.25
	5	44.9	1.10	108.3	0.25

Table 2.7.9.1.3-2 P_m Stresses for the Yankee-MPC Support Disk—30-Foot Side Drop, 0° Basket Orientation, Thermal Condition 2, Disk Number 1

Section	Sx (ksi)	Sy (ksi)	Sxy (ksi)	Stress Intensity (ksi)	Allowable Stress (ksi)	Margin of Safety
49	20.1	-27.6	0.1	47.7	89.4	0.87
60	24.6	-22.3	-0.1	46.9	89.4	0.91
45	25.1	-21.6	-0.4	46.7	89.4	0.91
64	13.7	-28.7	0.1	42.4	89.4	1.11
71	21.9	-17.7	0.0	39.6	89.4	1.26
56	20.9	-15.7	-0.1	36.7	89.4	1.44
53	-22.9	-33.5	-0.2	33.5	89.4	1.67
92	0.0	-33.5	-0.2	33.5	89.4	1.67
51	-28.2	-33.4	-0.2	33.4	89.4	1.68
67	21.5	-10.8	-0.1	32.3	89.4	1.77
4	18.5	-12.7	0.0	31.2	89.4	1.87
66	-24.2	-15.7	-10.1	30.9	89.4	1.90
72	8.6	-19.5	3.0	28.7	89.4	2.11
91	0.0	-28.6	0.1	28.6	89.4	2.13
62	-17.9	-28.6	0.1	28.6	89.4	2.13
41	9.2	-18.7	-0.4	27.9	89.4	2.20
8	21.0	-6.7	0.0	27.8	89.4	2.22
65	-2.6	-27.1	3.2	27.5	89.4	2.25
90	0.0	-27.5	0.1	27.5	89.4	2.25
47	-18.6	-27.4	0.1	27.4	89.4	2.26
63	8.3	-18.1	3.0	27.1	89.4	2.30
19	17.4	-9.6	-0.1	27.0	89.4	2.31
48	7.9	-18.3	3.1	26.9	89.4	2.33
10	-24.5	-6.6	0.0	24.5	89.4	2.65
23	21.1	-3.3	0.0	24.4	89.4	2.67
61	8.6	-14.8	-3.2	24.3	89.4	2.69
12	23.3	-0.8	0.0	24.1	89.4	2.71
30	19.6	-4.0	0.1	23.6	89.4	2.79
50	-2.6	-22.7	-3.5	23.3	89.4	2.85
46	8.3	-13.7	-3.2	22.9	89.4	2.90
88	0.0	-22.3	-0.1	22.3	89.4	3.02
58	-20.8	-22.2	-0.1	22.2	89.4	3.02
6	-22.1	-12.5	0.0	22.1	89.4	3.05
21	-21.7	-9.4	-0.1	21.7	89.4	3.12
28	-21.7	-10.7	-0.1	21.7	89.4	3.12
2	-21.6	-18.6	-0.4	21.6	89.4	3.14
87	0.0	-21.5	-0.4	21.5	89.4	3.15
43	-8.9	-21.5	-0.4	21.5	89.4	3.16
52	-2.3	-20.1	3.3	20.7	89.4	3.32
69	-20.6	-17.6	0.0	20.6	89.4	3.35

Note: See Figure 2.6.14.2-9 for section locations and definition of coordinate system.

Table 2.7.9.1.3-3 $P_m + P_b$ Stresses for the Yankee-MPC Support Disk—30-Foot Side Drop, 0° Basket Orientation, Thermal Condition 2, Disk Number 5

Section	Sx (ksi)	Sy (ksi)	Sxy (ksi)	Stress Intensity (ksi)	Allowable Stress (ksi)	Margin of Safety
65	-69.4	-37.7	11.7	73.3	127.8	0.74
52	-66.5	-29.0	8.6	68.3	127.8	0.87
50	-64.3	-31.8	-9.5	66.9	127.8	0.91
26	53.7	20.3	6.1	54.7	127.8	1.33
72	44.1	-7.6	-3.4	52.1	127.8	1.45
13	51.5	9.5	3.4	51.8	127.8	1.47
63	45.7	-5.9	-0.9	51.6	127.8	1.47
104	-49.4	-2.4	3.3	49.6	127.8	1.57
107	-49.0	-2.3	3.4	49.2	127.8	1.60
24	48.4	7.8	2.9	48.6	127.8	1.63
11	48.1	8.1	-3.2	48.3	127.8	1.64
48	39.3	-8.5	-1.0	47.8	127.8	1.67
33	47.3	3.1	3.5	47.5	127.8	1.69
51	-36.5	-32.3	-12.5	47.1	127.8	1.71
70	41.5	-4.9	-0.1	46.4	127.8	1.75
59	43.9	-1.6	0.7	45.5	127.8	1.81
61	36.7	-8.5	0.3	45.2	127.8	1.83
71	18.6	-26.2	-2.4	45.0	127.8	1.84
68	41.5	-2.9	-0.6	44.4	127.8	1.88
9	44.0	3.9	2.1	44.1	127.8	1.90
46	38.4	-4.7	-0.2	43.1	127.8	1.96
22	42.4	4.6	-2.5	42.6	127.8	2.00
57	37.7	-4.7	-0.3	42.4	127.8	2.02
60	20.4	-18.9	4.6	40.4	127.8	2.16
7	40.2	3.2	-2.2	40.3	127.8	2.17
62	-26.6	-33.7	9.2	40.0	127.8	2.19
53	-23.9	-34.3	-9.5	39.9	127.8	2.20
67	21.5	-16.9	5.0	39.7	127.8	2.22
45	16.9	-21.9	4.3	39.7	127.8	2.22
31	38.9	1.4	1.5	38.9	127.8	2.28
29	38.0	-0.6	-0.9	38.7	127.8	2.30
20	38.6	1.5	1.3	38.7	127.8	2.30
3	35.3	-3.2	-0.2	38.5	127.8	2.32
56	19.6	-17.4	-5.1	38.4	127.8	2.33
64	0.7	-37.5	1.1	38.2	127.8	2.34
95	34.3	-2.1	3.2	37.1	127.8	2.45
98	34.1	-2.3	3.3	36.9	127.8	2.46
49	7.3	-28.6	-2.2	36.2	127.8	2.53
47	-23.9	-29.4	8.8	35.8	127.8	2.57
37	34.9	10.8	4.0	35.6	127.8	2.59

Note: See Figure 2.6.14.2-9 for section locations and definition of coordinate system.

Table 2.7.9.1.3-4 P_m Stresses for the Yankee-MPC Support Disk—30-Foot Side Drop, 0° Basket Orientation, Thermal Condition 3, Disk Number 1

Section	Sx (ksi)	Sy (ksi)	Sxy (ksi)	Stress Intensity (ksi)	Allowable Stress (ksi)	Margin of Safety
49	20.4	-27.8	0.1	48.2	94.5	0.96
45	25.3	-21.8	-0.4	47.1	94.5	1.01
60	24.6	-22.4	-0.2	47.0	94.5	1.01
64	13.8	-28.7	0.1	42.6	94.5	1.22
71	21.8	-17.5	0.0	39.3	94.5	1.40
56	20.8	-15.8	-0.1	36.6	94.5	1.58
53	-23.0	-33.8	-0.2	33.8	94.5	1.80
92	0.0	-33.7	-0.2	33.7	94.5	1.80
51	-28.1	-33.7	-0.2	33.7	94.5	1.81
67	21.4	-10.6	-0.1	32.0	94.5	1.95
4	18.7	-12.8	0.0	31.5	94.5	2.00
66	-24.1	-15.7	-10.1	30.9	94.5	2.06
91	0.0	-28.7	0.1	28.7	94.5	2.29
62	-17.9	-28.6	0.1	28.6	94.5	2.30
72	8.7	-19.3	2.9	28.6	94.5	2.31
41	9.4	-18.9	-0.4	28.3	94.5	2.34
8	21.1	-6.9	-0.1	28.0	94.5	2.37
90	0.0	-27.7	0.1	27.7	94.5	2.41
47	-18.7	-27.7	0.1	27.7	94.5	2.41
65	-2.3	-27.2	3.2	27.6	94.5	2.43
63	8.4	-18.2	3.0	27.3	94.5	2.47
48	7.9	-18.4	3.1	27.1	94.5	2.49
19	17.3	-9.7	-0.1	26.9	94.5	2.51
10	-24.8	-6.8	-0.1	24.8	94.5	2.81
61	8.7	-14.8	-3.2	24.3	94.5	2.88
23	20.9	-3.4	0.0	24.3	94.5	2.88
12	23.3	-0.9	-0.1	24.2	94.5	2.90
50	-2.3	-22.8	-3.5	23.3	94.5	3.05
30	19.5	-3.8	0.1	23.3	94.5	3.05
46	8.4	-13.8	-3.2	23.1	94.5	3.08
88	0.0	-22.3	-0.2	22.3	94.5	3.23
6	-22.3	-12.7	0.0	22.3	94.5	3.23
58	-20.7	-22.3	-0.2	22.3	94.5	3.24
2	-21.9	-18.8	-0.4	21.9	94.5	3.32
87	0.0	-21.8	-0.4	21.8	94.5	3.34
43	-9.1	-21.7	-0.4	21.7	94.5	3.35
21	-21.7	-9.5	-0.1	21.7	94.5	3.36
28	-21.7	-10.5	-0.1	21.7	94.5	3.36
52	-2.0	-20.3	3.3	20.9	94.5	3.53
69	-20.4	-17.4	0.0	20.4	94.5	3.62

Note: See Figure 2.6.14.2-9 for section locations and definition of coordinate system.

Table 2.7.9.1.3-5 $P_m + P_b$ Stresses for the Yankee-MPC Support Disk—30-Foot Side Drop, 0° Basket Orientation, Thermal Condition 3, Disk Number 5

Section	Sx (ksi)	Sy (ksi)	Sxy (ksi)	Stress Intensity (ksi)	Allowable Stress (ksi)	Margin of Safety
65	-68.9	-37.8	11.7	72.9	135.0	0.85
52	-66.2	-29.1	8.6	68.1	135.0	0.98
50	-64.1	-31.9	-9.5	66.7	135.0	1.02
26	53.0	20.1	6.0	54.1	135.0	1.50
63	45.8	-6.1	-0.9	52.0	135.0	1.60
72	44.0	-7.5	-3.3	52.0	135.0	1.60
13	51.3	9.3	3.4	51.6	135.0	1.62
104	-49.1	-2.4	3.3	49.3	135.0	1.74
107	-48.7	-2.3	3.4	49.0	135.0	1.76
11	48.4	8.1	-3.2	48.6	135.0	1.78
48	39.6	-8.6	-1.0	48.2	135.0	1.80
24	47.9	7.6	2.9	48.1	135.0	1.81
33	46.9	3.1	3.5	47.2	135.0	1.86
51	-36.4	-32.5	-12.5	47.1	135.0	1.87
70	41.3	-4.9	0.0	46.2	135.0	1.92
61	37.2	-8.4	0.2	45.6	135.0	1.96
59	43.6	-1.8	0.7	45.4	135.0	1.98
71	18.7	-25.9	-2.4	44.8	135.0	2.01
68	41.6	-2.7	-0.7	44.4	135.0	2.04
9	43.9	3.7	2.1	44.0	135.0	2.07
46	38.8	-4.8	-0.2	43.5	135.0	2.10
57	37.9	-4.7	-0.3	42.6	135.0	2.17
22	42.4	4.5	-2.5	42.6	135.0	2.17
60	20.5	-19.3	4.6	40.9	135.0	2.30
7	40.4	3.2	-2.1	40.5	135.0	2.33
53	-24.0	-34.5	-9.5	40.1	135.0	2.36
45	17.0	-22.1	4.3	40.1	135.0	2.37
62	-26.4	-33.7	9.2	40.0	135.0	2.38
67	21.4	-16.9	5.0	39.6	135.0	2.41
3	35.6	-3.2	-0.2	38.8	135.0	2.48
31	38.6	1.4	1.5	38.7	135.0	2.49
64	1.0	-37.5	1.1	38.5	135.0	2.50
29	38.0	-0.5	-1.0	38.5	135.0	2.50
56	19.6	-17.3	-5.1	38.3	135.0	2.52
20	38.2	1.2	1.3	38.3	135.0	2.53
98	34.0	-2.2	3.3	36.9	135.0	2.66
95	34.1	-2.1	3.2	36.8	135.0	2.66
49	7.6	-28.7	-2.3	36.6	135.0	2.69
47	-23.8	-29.5	8.8	35.8	135.0	2.77
37	34.7	10.8	4.0	35.4	135.0	2.81

Note: See Figure 2.6.14.2-9 for section locations and definition of coordinate system.

Table 2.7.9.1.3-6 P_m Stresses for the Yankee-MPC Support Disk—30-Foot Side Drop, 45° Basket Orientation, Thermal Condition 2, Disk Number 3

Section	Sx (ksi)	Sy (ksi)	Sxy (ksi)	Stress Intensity (ksi)	Allowable Stress (ksi)	Margin of Safety
52	23.7	-21.2	3.5	45.5	89.4	0.97
25	-25.8	15.9	-1.0	41.7	89.4	1.14
21	-28.9	10.5	0.0	39.4	89.4	1.27
39	-19.9	-38.6	-0.8	38.7	89.4	1.31
50	-33.0	-21.1	-1.2	33.1	89.4	1.70
28	-32.9	-15.3	-1.1	33.0	89.4	1.71
58	-3.9	-27.1	-11.7	33.0	89.4	1.71
32	-32.5	-9.7	-0.8	32.6	89.4	1.75
48	16.1	-15.4	3.6	32.3	89.4	1.77
59	-20.8	5.7	-8.5	31.4	89.4	1.84
17	-25.5	5.1	0.0	30.6	89.4	1.92
49	-11.2	-30.3	-1.4	30.4	89.4	1.95
46	-19.7	5.6	-8.1	30.1	89.4	1.97
29	-14.7	-27.5	-1.1	27.6	89.4	2.24
20	-6.3	19.7	4.5	27.5	89.4	2.25
27	-15.3	-1.8	11.6	26.8	89.4	2.33
45	-1.6	23.6	4.3	26.6	89.4	2.37
40	-15.7	4.8	-7.5	25.4	89.4	2.52
24	-9.0	14.2	4.3	24.7	89.4	2.62
30	12.6	-9.8	3.9	23.7	89.4	2.77
44	-22.2	-0.2	-1.4	22.3	89.4	3.01
54	0.2	-7.7	-10.3	22.1	89.4	3.04
92	-1.6	-21.2	-1.1	21.2	89.4	3.21
43	-7.0	-21.1	-0.5	21.1	89.4	3.23
26	-4.6	15.1	3.5	20.9	89.4	3.28
31	-10.4	9.0	3.7	20.7	89.4	3.32
10	-13.0	7.5	-1.1	20.7	89.4	3.33
23	17.1	15.8	3.3	19.8	89.4	3.51
42	16.9	5.0	4.4	18.3	89.4	3.88
19	15.8	10.4	4.4	18.3	89.4	3.89
5	-3.3	12.2	4.6	18.0	89.4	3.98
6	-13.6	4.1	0.3	17.8	89.4	4.04
85	-1.6	15.9	-1.0	17.6	89.4	4.08
13	-0.1	16.2	3.0	17.3	89.4	4.16
57	-5.7	-16.4	-1.4	16.6	89.4	4.39
37	-14.8	-10.9	3.0	16.4	89.4	4.46
76	-14.1	-1.9	-4.9	15.9	89.4	4.64
80	-1.6	-15.3	-1.1	15.4	89.4	4.81
61	-15.1	-0.5	-0.9	15.1	89.4	4.91
55	-0.9	-14.8	-2.2	15.1	89.4	4.92

- Note:
1. See Figure 2.6.14.2-10 for section locations.
 2. Stress components are based on the coordinate system shown in Figure 2.6.14.2-10, rotated 45°.

Table 2.7.9.1.3-7 P_m+P_b Stresses for the Yankee-MPC Support Disk—30-Foot Side Drop, 45° Basket Orientation, Thermal Condition 2, Disk Number 2

Section	Sx (ksi)	Sy (ksi)	Sxy (ksi)	Stress Intensity (ksi)	Allowable Stress (ksi)	Margin of Safety
19	45.1	105.6	10.0	107.2	127.8	0.19
42	43.8	100.8	9.7	102.4	127.8	0.25
24	-97.8	-14.5	1.5	97.8	127.8	0.31
20	-96.7	-11.8	-1.4	96.8	127.8	0.32
30	-11.7	-95.5	0.9	95.5	127.8	0.34
53	-94.4	-24.0	6.7	95.0	127.8	0.34
4	40.9	91.2	7.7	92.3	127.8	0.38
52	-0.5	-90.2	0.4	90.2	127.8	0.42
5	-89.4	-18.3	0.7	89.4	127.8	0.43
48	-3.7	-87.1	-0.2	87.1	127.8	0.47
31	-82.4	-13.6	-0.1	82.4	127.8	0.55
37	-79.7	-22.6	7.7	80.7	127.8	0.58
45	74.5	51.2	11.6	79.3	127.8	0.61
26	-72.1	5.9	-2.1	78.1	127.8	0.64
33	-76.6	-16.0	3.2	76.8	127.8	0.66
51	-75.0	-15.1	0.7	75.0	127.8	0.70
54	-10.4	-46.3	-31.3	72.2	127.8	0.77
23	38.3	69.4	9.8	72.2	127.8	0.77
9	-71.5	-17.2	2.6	71.6	127.8	0.78
21	-11.4	47.5	-7.2	60.6	127.8	1.11
60	-54.7	-39.5	10.2	59.8	127.8	1.14
56	-58.0	-19.3	7.9	59.6	127.8	1.15
62	-58.2	-10.8	1.6	58.2	127.8	1.20
13	-51.2	3.2	-1.4	54.5	127.8	1.35
59	-52.5	-26.3	4.4	53.2	127.8	1.40
47	-48.1	-33.1	8.2	51.8	127.8	1.47
8	25.6	50.2	5.2	51.2	127.8	1.49
12	25.6	48.5	7.1	50.5	127.8	1.53
3	-48.3	-33.8	4.5	49.6	127.8	1.58
85	-0.3	48.1	-1.1	48.5	127.8	1.64
32	-44.7	-28.0	8.1	48.0	127.8	1.66
75	47.2	5.4	-2.4	47.3	127.8	1.70
92	-2.9	-46.7	-1.3	46.7	127.8	1.73
82	1.0	46.2	0.2	46.2	127.8	1.77
46	-45.3	-21.8	3.4	45.8	127.8	1.79
39	-21.4	-42.3	-8.9	45.6	127.8	1.80
25	-34.2	10.2	4.8	45.4	127.8	1.81
106	-45.4	-4.3	0.1	45.4	127.8	1.81
17	-8.5	34.1	-6.7	44.7	127.8	1.86
80	-3.1	-44.6	-1.1	44.6	127.8	1.86

Note: 1. See Figure 2.6.14.2-10 for section locations.
2. Stress components are based on the coordinate system shown in Figure 2.6.14.2-10, rotated 45°.

Table 2.7.9.1.3-8 P_m Stresses for the Yankee-MPC Support Disk—30-Foot Side Drop, 45° Basket Orientation, Thermal Condition 3, Disk Number 3

Section	Sx (ksi)	Sy (ksi)	Sxy (ksi)	Stress Intensity (ksi)	Allowable Stress (ksi)	Margin of Safety
52	23.8	-21.0	3.5	45.4	94.5	1.08
25	-25.6	16.0	-1.0	41.6	94.5	1.27
21	-28.8	10.6	0.1	39.4	94.5	1.40
39	-20.1	-38.9	-1.0	39.0	94.5	1.42
50	-33.2	-20.9	-1.2	33.3	94.5	1.84
28	-33.1	-15.1	-1.1	33.2	94.5	1.85
59	-21.9	6.0	-9.0	33.1	94.5	1.85
58	-4.1	-27.1	-11.7	32.8	94.5	1.88
32	-32.4	-9.4	-0.8	32.5	94.5	1.91
48	16.1	-15.2	3.6	32.1	94.5	1.94
17	-25.8	5.1	0.1	30.9	94.5	2.06
49	-11.3	-30.3	-1.4	30.4	94.5	2.11
46	-19.8	5.7	-8.2	30.3	94.5	2.12
20	-6.4	19.8	4.6	27.8	94.5	2.41
29	-14.8	-27.5	-1.0	27.6	94.5	2.43
45	-1.7	23.9	4.3	27.0	94.5	2.50
40	-16.6	5.0	-8.0	26.9	94.5	2.52
27	-15.3	-1.8	11.5	26.6	94.5	2.55
24	-8.8	13.9	4.3	24.3	94.5	2.89
30	12.7	-9.5	3.9	23.6	94.5	3.01
44	-22.4	-0.2	-1.3	22.5	94.5	3.19
43	-7.1	-21.4	-0.5	21.4	94.5	3.41
54	0.4	-7.7	-9.8	21.3	94.5	3.44
31	-10.5	9.2	3.7	21.0	94.5	3.49
92	-1.6	-21.0	-1.1	21.0	94.5	3.49
26	-4.6	15.1	3.5	20.8	94.5	3.54
10	-13.1	7.5	-1.1	20.6	94.5	3.58
23	17.3	15.9	3.3	20.0	94.5	3.72
19	16.0	10.5	4.5	18.5	94.5	4.12
42	16.9	5.0	4.5	18.4	94.5	4.12
5	-3.3	12.2	4.7	18.2	94.5	4.19
85	-1.6	16.0	-1.0	17.7	94.5	4.35
6	-13.6	4.1	0.4	17.7	94.5	4.35
13	-0.1	16.0	3.0	17.2	94.5	4.51
57	-5.8	-16.4	-1.4	16.6	94.5	4.70
37	-14.9	-10.6	3.0	16.4	94.5	4.75
76	-14.1	-1.9	-4.8	15.8	94.5	4.99
80	-1.6	-15.1	-1.0	15.2	94.5	5.22
55	-1.0	-14.7	-2.2	15.1	94.5	5.26
60	-3.3	-15.0	0.7	15.1	94.5	5.28

Note: 1. See Figure 2.6.14.2-10 for section locations.
2. Stress components are based on the coordinate system shown in Figure 2.6.14.2-10, rotated 45°.

Table 2.7.9.1.3-9 $P_m + P_b$ Stresses for the Yankee-MPC Support Disk—30-Foot Side Drop, 45° Basket Orientation, Thermal Condition 3, Disk Number 2

Section	Sx (ksi)	Sy (ksi)	Sxy (ksi)	Stress Intensity (ksi)	Allowable Stress (ksi)	Margin of Safety
19	46.0	107.7	10.1	109.3	135.0	0.24
42	44.5	102.9	9.8	104.5	135.0	0.29
20	-98.9	-12.6	-1.3	98.9	135.0	0.37
24	-98.5	-15.3	1.6	98.6	135.0	0.37
30	-12.1	-96.6	0.9	96.6	135.0	0.40
4	42.0	94.2	7.7	95.3	135.0	0.42
53	-94.5	-23.8	6.6	95.1	135.0	0.42
5	-92.2	-19.4	0.8	92.2	135.0	0.46
52	-0.5	-90.3	0.4	90.3	135.0	0.50
48	-4.0	-88.0	-0.2	88.0	135.0	0.53
31	-83.5	-13.9	-0.1	83.5	135.0	0.62
37	-80.8	-22.6	7.7	81.8	135.0	0.65
45	75.8	52.2	11.8	80.7	135.0	0.67
26	-71.5	5.9	-2.1	77.5	135.0	0.74
33	-76.9	-16.5	3.3	77.0	135.0	0.75
51	-75.8	-15.1	0.7	75.8	135.0	0.78
9	-72.9	-18.5	2.9	73.0	135.0	0.85
23	38.8	69.5	9.8	72.4	135.0	0.86
54	-10.2	-44.7	-29.8	68.9	135.0	0.96
60	-57.5	-41.9	10.9	63.0	135.0	1.14
21	-10.8	49.3	-7.1	61.7	135.0	1.19
56	-58.7	-19.1	7.9	60.2	135.0	1.24
62	-59.3	-12.0	1.8	59.4	135.0	1.27
59	-55.3	-27.9	4.7	56.1	135.0	1.41
13	-51.0	3.1	-1.4	54.2	135.0	1.49
3	-51.2	-35.1	4.7	52.5	135.0	1.57
47	-48.5	-33.3	8.3	52.1	135.0	1.59
8	26.0	50.0	5.3	51.1	135.0	1.64
12	25.5	48.0	7.1	50.1	135.0	1.70
85	-0.3	48.3	-1.1	48.7	135.0	1.77
32	-44.8	-29.1	8.0	48.2	135.0	1.80
75	47.2	5.4	-2.5	47.4	135.0	1.85
6	6.3	46.6	-3.2	46.8	135.0	1.88
92	-2.9	-46.6	-1.3	46.6	135.0	1.90
82	1.1	46.6	0.2	46.6	135.0	1.90
17	-8.1	36.0	-6.7	46.1	135.0	1.93
46	-45.6	-21.9	3.4	46.1	135.0	1.93
39	-21.6	-42.6	-9.3	46.1	135.0	1.93
2	-38.5	-41.2	5.8	45.9	135.0	1.94
106	-45.6	-4.3	0.2	45.6	135.0	1.96

Note: 1. See Figure 2.6.14.2-10 for section locations.
2. Stress components are based on the coordinate system shown in Figure 2.6.14.2-10, rotated 45°.

2.7.9.1.4 Stress Evaluation of the Yankee-MPC Support Disk for 30-Foot Off-Angle Drop Load Condition

This section documents the methodology used to calculate the stresses associated with off-angle impacts of the transport cask (Figure 2.7.9.1-1). The results show that the stress criteria is met for all off-angle conditions. Note that the methodology used for the off-angle drop evaluation is very conservative since the g loads decrease significantly for off-angle drop orientations (Table 2.6.7.4.1-3).

To evaluate off-angle impacts, the stress components (i.e., S_x , S_y , S_{xy}) are combined from the side drop and end drop cases for both the 0° basket drop orientation and the 45° basket drop orientation (Figure 2.6.14.1-1). The stresses are combined according to the various cask drop angles ($\phi = 0^\circ, 24^\circ, 30^\circ, 45^\circ, 60^\circ, 73^\circ, 75^\circ, 77^\circ, 80^\circ, 83^\circ, 85^\circ, 88^\circ$ and 90°) for all five critical support disks (Figure 2.6.14.2-8). The normal stresses (S_x and S_y) and the shear stress (S_{xy}) for a drop with an angle of ϕ (Figure 2.7.9.1-1) are calculated by the following equations:

$$S_{x(\phi)} = S_{x(\text{end})}\cos\phi + S_{x(\text{side})}\sin\phi,$$

$$S_{y(\phi)} = S_{y(\text{end})}\cos\phi + S_{y(\text{side})}\sin\phi,$$

$$S_{xy(\phi)} = S_{xy(\text{end})}\cos\phi + S_{xy(\text{side})}\sin\phi,$$

where:

$S_{x(\text{end})}$, $S_{y(\text{end})}$, and $S_{xy(\text{end})}$ are the sectional stresses resulting from the Support Disk End Drop Model, and $S_{x(\text{side})}$, $S_{y(\text{side})}$, and $S_{xy(\text{side})}$ are the section stresses resulting from the Support Disk Side Drop Model.

Off-angle principle stresses (i.e., S_1 , S_2) are calculated by using the following equation:

$$S_1, S_2 = \frac{S_{x(\phi)} + S_{y(\phi)}}{2} \pm \sqrt{\left(\frac{S_{x(\phi)} - S_{y(\phi)}}{2}\right)^2 + S_{xy(\phi)}^2}$$

Once the off-angle principle stresses are calculated, new stress intensities (SI) can be calculated. Summaries of the maximum support disk stress intensities in the 30-foot off-angle drop conditions are given in Table 2.7.9.1.4-1.

Table 2.7.9.1.4-1 Yankee-MPC Support Disk Stress Summary for the 30-Foot Off-Angle Drop

Stress State	Thermal Condition	Section	Cask Drop Angle (°)	Disk Number	S _x (ksi)	S _y (ksi)	S _{xy} (ksi)	Stress Intensity (ksi)	Allowable Stress ⁴ (ksi)	Margin of Safety
0° BASKET DROP ORIENTATION										
P _m	2	49	90	1	20.1	-27.6	0.1	47.7	89.4	0.87
P _m +P _b	2	50	45	4	-82.7	-26.3	-9.0	84.1	127.8	0.52
P _m	3	49	90	1	20.4	-27.8	0.1	48.2	94.5	0.96
P _m +P _b	3	50	45	4	-82.6	-26.5	-8.9	84.0	135.0	0.60
45° BASKET DROP ORIENTATION										
P _m	2	52	90	3	23.7	-21.2	3.5	45.5	89.4	0.97
P _m +P _b	2	19	60	2	48.3	117.7	8.8	118.8	127.8	0.08
P _m	3	52	90	3	-23.8	-21.0	3.5	45.3	94.5	1.08
P _m +P _b	3	19	60	2	49.2	119.7	9.0	120.9	135.0	0.12

Notes:

1. P = Primary Stress, P_m + P_b = Primary Membrane + Bending Stress.
2. See Figures 2.6.14.2-9 and 2.6.14.2-10 for section location.
3. See Figure 2.7.9.1-1 for definition of cask drop angle.
4. See Figure 2.6.14.2-8 for disk number.
5. Allowable Stress for 17-4PH, Type 630 stainless steel:

For P_m, S_{allow} = 0.7 S_u = 89.4 ksi at 539°F
= 94.5 ksi at -40°F

For P_m + P_b, S_{allow} = S_u = 127.8 ksi at 539°F
= 135.0 ksi at -40°F

2.7.9.2 Stress Evaluation of the Yankee-MPC Tie Rods and Spacers for a 30-Foot End Drop Load Condition

In accordance with 10 CFR 71.73(c)(1), a spent-fuel shipping cask is subject to a free drop from a height of 30 feet onto a flat, unyielding surface. The design deceleration for the NAC-STC for the hypothetical accident 30-foot end drop is 56.1 g (Table 2.6.7.4.1-2).

The structural capacity of the spacers supporting the basket is evaluated by hand calculations using classical analysis. Accident loading due to the 30-foot drop of the fuel basket is compared to the stress limit of $0.7 S_u$ in accordance with Article NF 1440 of the ASME Code, assuming membrane stresses.

No detailed evaluation of the tie rods is required. The tie rods serve basket assembly purposes and are not part of the load path for the condition evaluated. The tie rods are loaded during fabrication by a 190 ft-lbs preload. Under drop conditions, the preload will be reduced. The tie rod design is, therefore, acceptable by inspection.

During the end drop, the spacers are loaded with the weight of 22 support disks, the aluminum heat transfer disks, one end plate, and the weight of the spacers. The load is resisted by the effective area of 8 spacers. The compressive stresses are calculated on the effective area of the spacer.

The material allowable stress was conservatively selected at a temperature of 500°F. The temperature near the outer edge of the support disks (at the tie rods) is 387.9°F.

2.7.9.2.1 Design Criteria

Stress limits = $0.7 S_u$ (accident condition)
(more limiting than $2.4 S_m$)
Loading criteria (g) = 56.1g (accident condition)
Evaluation temperature = 500°F

Canister Basket Parameters

Fuel basket weight = 9,530 lbs
Bottom weldment weight = 438 lbs
Fuel tube weight (36 tubes) = 2,164 lbs
Rod diameter = 1.13 in
Spacer outer diameter = 2.50 in

Materials

Tie rod = SA 479 Type 304 Stainless Steel

Spacer = A511 Type 304 Stainless Steel

Material Allowable

Type 304 SS = $S_m = 17,500$ psi (500°F)

= $S_u = 63,500$ psi (500°F)

2.7.9.2.2 30-Foot End Drop Condition - Results

The deceleration assumed for the canister basket in the 30-foot end drop is 56.1g. The spacers are loaded with the weight of the 22 support disks, the aluminum heat transfer disks, one end plate and the weight of the spacers. These loads are calculated as:

Total weight of basket = 9,530 lbs

Less weight of bottom weldment = -438 lbs

Less weight of fuel tubes = -2,164 lbs

Therefore,

1-g load on spacers = 6,928 lbs

Applied g level = 56.1g

Therefore,

Accident condition load on spacers = $6,928 \times 56.1$

= 388,661 lbs

The effective area of one spacer at each of eight locations supporting the weight of the support disks is equal to the net area of the spacer and is calculated as:

$$A = \frac{3.14 \times (2.5^2 - 1.25^2)}{4}$$
$$= 3.68 \text{ in}^2$$

The average compressive stress, S_c , in the spacer is:

$$S_c = \frac{388,661}{8 \times 3.68}$$

= 13,202 psi.

The allowable stress for Type 304 SS under accident conditions of transport is $0.7 S_u$.

$$\begin{aligned} S_u &= 63,500 \text{ psi} \\ 0.7 S_u &= 0.7 \times 63,500 \\ &= 44,450 \text{ psi} \end{aligned}$$

The margin of safety (MS), which is defined as $\frac{0.7S_u}{S_c} - 1$, is calculated as:

$$\frac{44,450}{13,202} - 1 = 2.37$$

Therefore, the spacers are structurally adequate for a 56.1g end impact under accident conditions.

2.7.9.3 Yankee-MPC Basket Support Disk - Buckling Evaluation (Accident Conditions)

The Yankee-MPC support disk is subjected to compressive and/or inertia loads during a 30-foot drop of the NAC-STC cask onto an unyielding surface. Depending on the cask orientation for the 30-foot drop impact, the support disk may have both in-plane and out-of-plane loads applied to it. The in-plane loads (basket side impact component) apply compressive forces and in-plane (strong axis) bending moments on the support disk and the out-of-plane inertial loads (basket end-impact component) produce out-of-plane (weak axis) bending moments on the support disk. Buckling of the support disk is evaluated in accordance with the methods and acceptance criteria of NUREG/CR-6322.

The margin of safety is calculated based on the Interaction Equations 31 and 32 in NUREG/CR-6322. These two equations adopt the "Limit Analysis Design" approach for structural members subjected to stresses beyond the yield limit of the material, i.e., for members deformed elastically as a result of axial load or bending moment. Other equations applicable to the calculations are listed later in this section.

The maximum forces and moments are determined from the finite element analysis stress results for the Support Disk End-Drop Model as well as the Support Disk Side Drop Model (two different basket orientations, 0° and 45°). The buckling evaluations account for both in-plane

(about the strong axis of the web) and out-of-plane (about the weak axis of the web) buckling modes. Evaluation of strong axis buckling is performed only for the side drop condition since it is the governing case (side drop always produces maximum compressive force and strong axis bending moment). Evaluation for weak axis buckling is performed for several cask drop angles (Figure 2.7.9.1-1).

Methodology and equations for the buckling evaluation are summarized as follows.

Symbols and Units

- P = applied axial compressive loads, kips
- M = applied bending moment, kips-inch
- P_a = allowable axial compressive load, kips
- P_{cr} = critical axial compression load, kips
- P_e = Euler buckling loads, kips
- P_y = average yield load, equal to profile area times specified minimum yield stress, kips
- C_c = column slenderness ratio separating elastic and inelastic buckling
- C_m = coefficient applied to bending term in interaction equation
- M_m = critical moment that can be resisted by a plastically designed member in the absence of axial load, kip-in.
- M_p = plastic moment, kip-in.
- F_a = axial compressive stress permitted in the absence of bending moment, ksi
- F_e = Euler stress for a prismatic member divided by factor of safety, ksi
- k = ratio of effective column length to actual unsupported length
- l = unsupported length of member, in.
- r = radius of gyration, in.
- S_y = yield strength, ksi
- A = cross sectional area of member, in²
- Z_x = plastic section modulus, in³
- λ = allowable reduction factor, dimensionless.

From NUREG/CR-6322, the following equations are used to evaluate the support disk for accident condition of transport:

$$\frac{P}{P_{cr}} + \frac{C_m M}{M_m \left[1 - \frac{P}{P_e} \right]} \leq 1.0$$

$$\frac{P}{P_y} + \frac{M}{1.18 M_p} \leq 1.0$$

where: $P_{cr} = 1.7 \times A \times F_a$

$$F_a = \frac{P_a}{A} \quad \text{for} \quad P_a = P_y \left[\frac{1 - \frac{\lambda^2}{4}}{1.11 + 0.5\lambda + 0.17\lambda^2 - 0.28\lambda^3} \right]$$

$$\text{and} \quad \lambda = \frac{1}{\pi} \left(\frac{kl}{r} \right) \sqrt{\frac{S_y}{E}}$$

$$F_e = \frac{\pi^2 \cdot E}{130 \cdot \left(\frac{k \cdot l}{r} \right)^2}$$

$$P_e = 1.92 \times A \times F_e$$

$$P_y = S_y \times A$$

$$C_m = 0.85 \text{ for members with joint translation (sideways).}$$

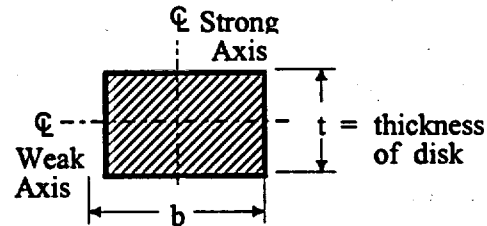
$$M_p = S_y \times Z_x$$

$$M_m = M_p \cdot \left(1.07 - \frac{\left(\frac{1}{r} \right) \cdot \sqrt{S_y}}{3160} \right) \leq M_p$$

Buckling evaluation is performed for all sections of disk ligaments (Figures 2.6.14.2-9 and 2.6.14.2-10). Using the cross-sectional stresses calculated at each of the sections for each loading condition, the maximum corresponding compressive forces (P) and bending moment (M) are determined as follows:

$$P = \sigma_m A,$$

$$M = \sigma_b S,$$



where, σ_m is the membrane stress, σ_b is the strong axis bending stress or weak axis bending stress, A is the area ($b \times t$), and S is the section modulus ($tb^2/6$ for strong axis bending and $bt^2/6$ for weak axis bending).

To determine the margin of safety:

$$P_1 = P/P_{cr} \quad M_1 = \frac{C_m M}{(1 - P/P_{cr}) M_m} \quad (P_1 + M_1 \leq 1) \quad (\text{Eq. 31, NUREG/CR-6322})$$

$$\text{and} \quad P_2 = P/P_y \quad M_2 = \frac{M}{1.18 M_p} \quad (P_1 + M_1 \leq 1) \quad (\text{Eq. 32, NUREG/CR-6322})$$

The margins of safety are calculated as:

$$MS1 = \frac{1}{P_1 + M_1} - 1$$

$$MS2 = \frac{1}{P_2 + M_2} - 1$$

The side drop conditions (cask drop angle $\phi=90^\circ$) are the governing conditions for strong axis buckling evaluation since the axial compression for (P) and the strong axis bending moment (M) decrease with the drop angle. Weak axis buckling evaluation is performed for several drop angles ($\phi=0^\circ, 24^\circ, 30^\circ, 45^\circ, 60^\circ, 73^\circ, 75^\circ, 77^\circ, 80^\circ, 83^\circ, 85^\circ, 88^\circ$ and 90°). For the evaluation of

off-angle drop cases, the forces (P) and bending moments (M) used for the buckling evaluation (weak axis only) are determined as follows:

$$P = P_{\text{side}} \sin \phi$$

$$M = M_{\text{end}} \cos \phi$$

where:

P_{side} is the compression force from the Side Drop cases

M_{end} is the weak axis bending moment from the End Drop cases

ϕ is the cask drop angle (Figure 2.7.9.1-1)

The results of buckling evaluations for the support disks for the 30-foot drop condition are summarized below. The minimum margin of safety is +0.15 for the strong axis buckling evaluation and +0.78 for weak axis buckling evaluation. As the tables demonstrate, the support disks meet the requirements of NUREG/CR-6322.

Stress State	Thermal Condition	Section Number	Drop Angle	Disk Number	P (kip)	P_{cr} (kip)	M (in-kip)	M_p (in-kip)	M_m (in-kip)	MS1	MS2
Strong Axis, 30-Foot Drop, 0° Basket Drop Orientation											
P	2	65	90	4	6.78	36.23	2.40	6.06	5.80	0.80	0.83
P+Q	2	65	90	4	6.37	36.23	2.54	6.06	5.80	0.77	0.81
P	3	65	90	4	6.69	43.52	2.39	7.38	6.99	1.19	1.25
P+Q	3	65	90	5	7.92	43.52	2.47	7.38	6.99	1.01	1.06
Strong Axis, 30-Foot Drop, 45° Basket Drop Orientation											
P	2	52	90	4	7.84	36.24	3.56	6.06	5.80	0.30	0.35
P+Q	2	52	90	3	9.43	36.24	3.89	6.06	5.80	0.15	0.20
P	3	52	90	4	7.73	43.54	3.56	7.39	6.99	0.58	0.65
P+Q	3	52	90	4	7.60	43.54	3.41	7.39	6.99	0.64	0.71
Weak Axis, 30-Foot Drop, 0° Basket Drop Orientation											
P	2	50	30	4	3.40	30.40	1.40	4.00	3.60	1.16	1.47
P+Q	2	56	30	1	4.90	32.80	1.80	4.40	3.90	0.78	1.06
P	3	50	30	4	3.30	36.20	1.40	4.90	4.40	1.61	2.03
P+Q	3	50	30	5	4.00	36.20	1.40	4.90	4.40	1.48	1.89
Weak Axis, 30-Foot Drop, 45° Basket Drop Orientation											
P	2	19	24	1	1.70	32.80	1.60	4.40	3.90	1.43	1.74
P+Q	2	19	24	1	1.70	32.80	1.90	4.40	3.90	1.16	1.44
P	3	19	24	1	1.80	39.10	1.60	5.30	4.70	1.89	2.32
P+Q	3	19	24	1	1.80	39.10	1.60	5.30	4.70	1.89	2.32

Notes:

1. P = Primary Stress, P+Q = Primary + Secondary Stresses.
2. See Figures 2.6.14.2-9 and 2.6.14.2-10 for section location.
3. See Figure 2.7.9.1-1 for definition of cask drop angle.
4. See Figure 2.6.14.2-8 for disk number.

2.7.9.4 : Yankee-MPC Fuel Tube Analysis

The fuel tube provides a foundation and sealed cavity to mount BORAL neutron poison plates within the fuel basket structure. It does not provide a structural function relative to the support of the fuel assembly. The fuel tube configuration is shown in Figure 2.7.9.4-1. To ensure that the fuel tube remains functional when the cask is subjected to design load conditions, a structural evaluation of the tube has been performed for both the end and side impact load conditions.

2.7.9.4.1 Fuel Tube Side Impact Analysis

Detailed finite element analysis and classical hand calculations were performed for the fuel tubes for the directly loaded NAC-STC system as documented in Section 2.7.8.4. By comparing the design parameters (dimensions, weight, etc.) of the fuel tube for the canistered fuel to those of fuel tubes for the NAC-STC system, it is concluded that the analyses for the directly loaded uncanistered NAC-STC envelope the design conditions for the fuel tube of the canistered fuel system.

A comparison of the design parameters for the fuel tube of the canistered Yankee class system and the fuel tube of the directly loaded NAC-STC system is shown below:

	<u>Canistered</u>	<u>Directly Loaded</u>
Fuel Tube Material (Stainless steel)	Type 304	Type 304
Fuel Tube Thickness (inch)	0.048	0.048
Fuel Tube Inside Dimension (inch)	7.80	8.78
Fuel Tube Weight (lb)	59.	141.
Fuel Assembly Weight (lb)	900.	1,525
No. of Support Disks	22	31
Fuel Weight Supported by one Disk (lb)	41 (900/22)	49 (1,525/31)
Spacing Between Support Disk (inch)	3.91	4.37

2.7.9.4.2 End Impact Evaluation

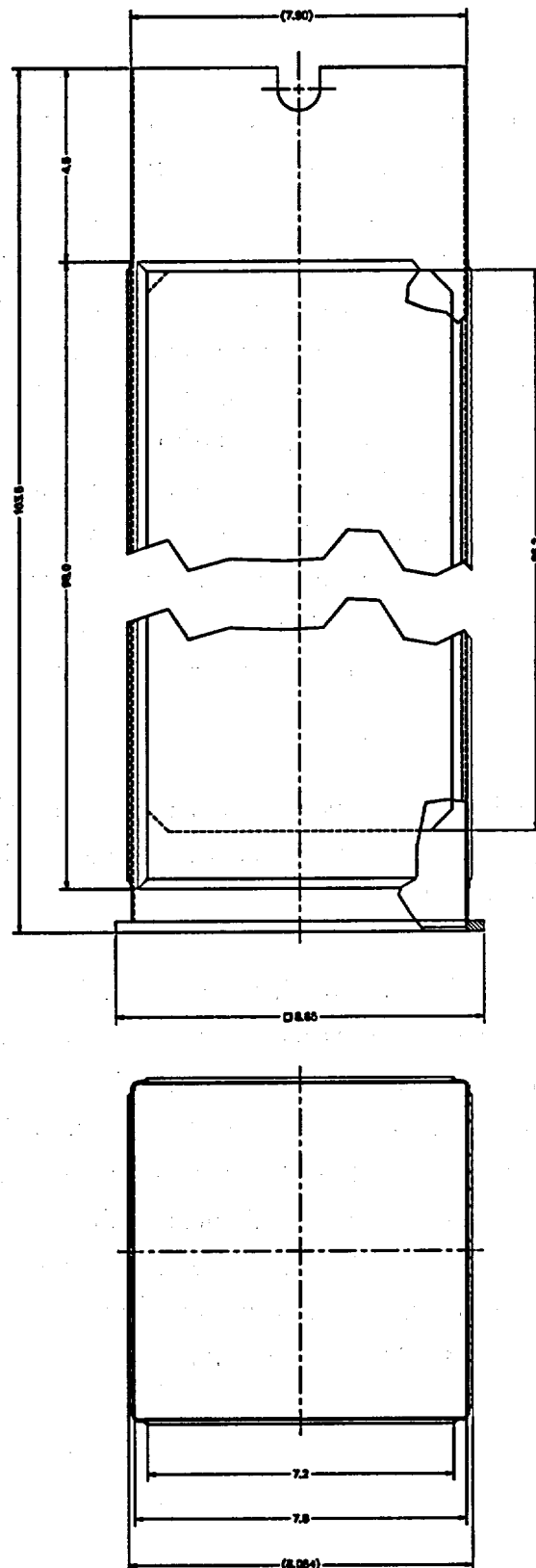
The fuel tube end impact analysis for the directly loaded fuel basket configuration of the NAC-STC is documented in Section 2.7.8.4.1. The bearing stress during an end impact condition are proportional to the tube weight, tube cross-sectional area and the design g-load. Since the weight and center of gravity location of the canistered fuel configuration is essentially the same as that of the directly loaded fuel configuration, the same design g-loads (56.1g for end drop and 55g for side drop) are applicable to the canistered basket/tubes. Based on the fuel tube dimensions and loading data presented above, the bearing stress for an end impact condition for the canistered fuel tube is:

$$(S_{br})_{\text{directly loaded}} (59/141) (8.78/7.8) = 0.47 (S_{br})_{\text{directly loaded}}$$

From Section 2.7.8.4.1, the calculated $(S_{br})_{\text{directly loaded}} = 4.8$ ksi, while the allowable stress (material yield strength) is 19.4 ksi.

Therefore, the canistered fuel tube stress is well below its allowable stress limit during an end impact accident condition.

Figure 2.7.9.4-1 Yankee-MPC Fuel Tube Configuration



2.7.9.5 Yankee-MPC Basket Weldment Analysis for 30-Foot End Drop

The response of the top and the bottom weldment plates of the Yankee-MPC fuel basket assembly to a 56.1g accident condition deceleration load is examined. Two finite element models representing the PWR basket top and bottom weldments were constructed for structural evaluation. The structural evaluations were performed at normal condition temperatures; therefore, prior to the structural evaluation portion of the analyses, the steady-state temperature distribution in the top and bottom weldment models was determined by applying fixed temperatures to the outer circular edge and a volumetric heat generation rate to all of the elements, then solving for the intermediate temperatures. The fixed temperature of the outer edge of the top and bottom weldments was assumed to be equal to the maximum temperature of the canister lid/bottom plate. During the temperature solution portion of the analyses, the finite element models were constructed using ANSYS three-dimensional thermal shell elements (SHELL57). During the structural evaluation portion of the analyses, the finite element models were constructed using ANSYS three-dimensional, six-degrees-of-freedom, elastic shell elements (SHELL63). The finite element models represent one-quarter sections of the weldments.

The responses of the top and bottom weldments to a hypothetical accident 30-foot end drop were investigated using these two finite element models. For the 30-foot end drop evaluation, a deceleration load of 56.1g was used.

Both the top and bottom weldments are 0.5-inch thick and fabricated from SA240, Type 304 stainless steel. The top weldment supports its own weight and 36 fuel tubes (without the fuel assemblies) during a top end drop. Eight structural ribs, eight tie-rod ends, and a circumferential ring support the top weldment and its loads during a top end drop. These structural components are modeled as zero-translation restraints in the direction of the end drop. The finite element models of the top weldment and bottom weldment with the applied structural boundary conditions are presented in Figures 2.7.9.5-1 and 2.7.9.5-3, respectively. The finite element models of the top weldment and the bottom weldment with the applied structural forces is presented in Figures 2.7.9.5-2 and 2.7.9.5-4, respectively.

Figure 2.7.9.5-1 Yankee-MPC Top Weldment Finite Element Model with Structural Boundary Conditions

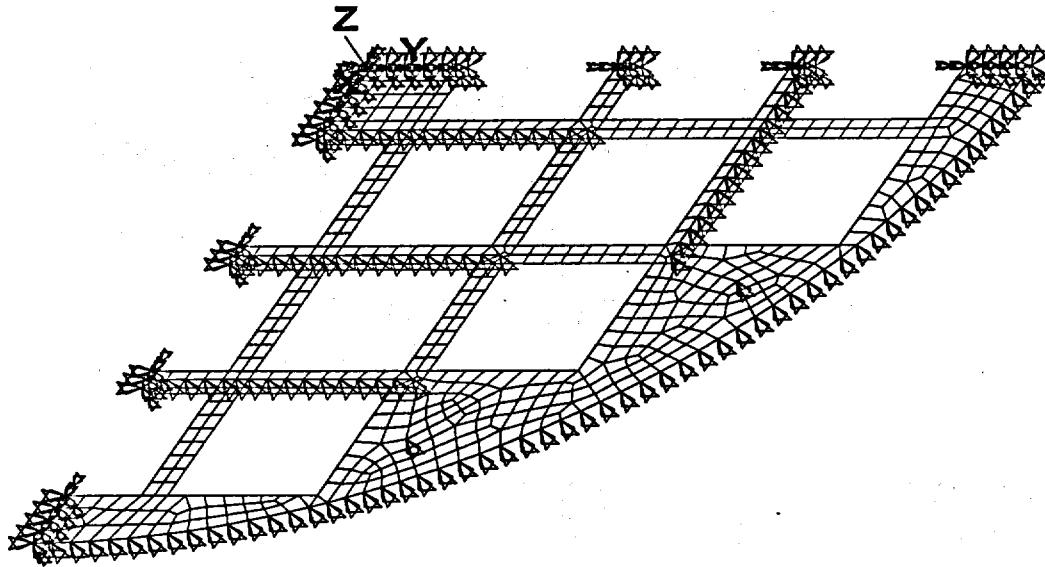


Figure 2.7.9.5-2 Yankee-MPC Top Weldment Finite Element Model with Structural Applied Loads

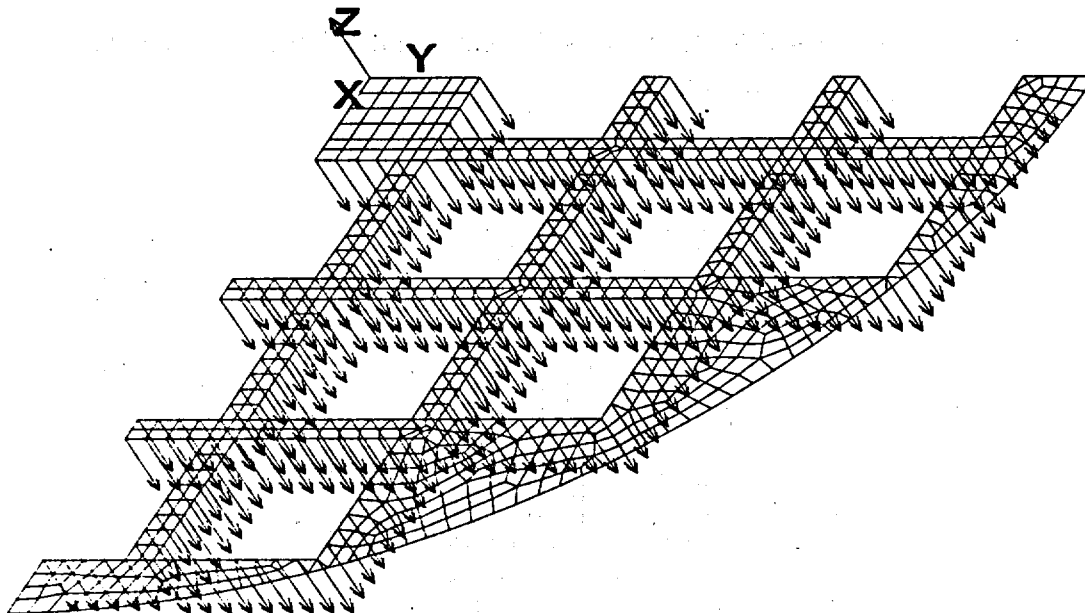


Figure 2.7.9.5-3 Yankee-MPC Bottom Weldment Finite Element Model with Structural Boundary Conditions

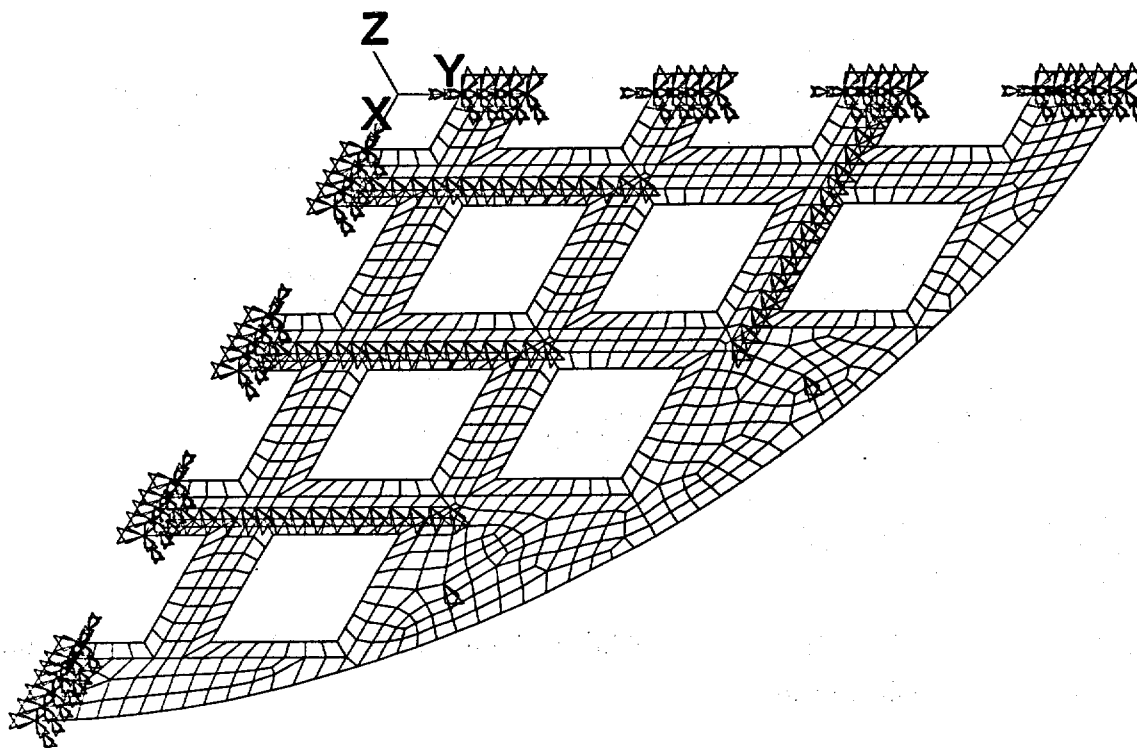
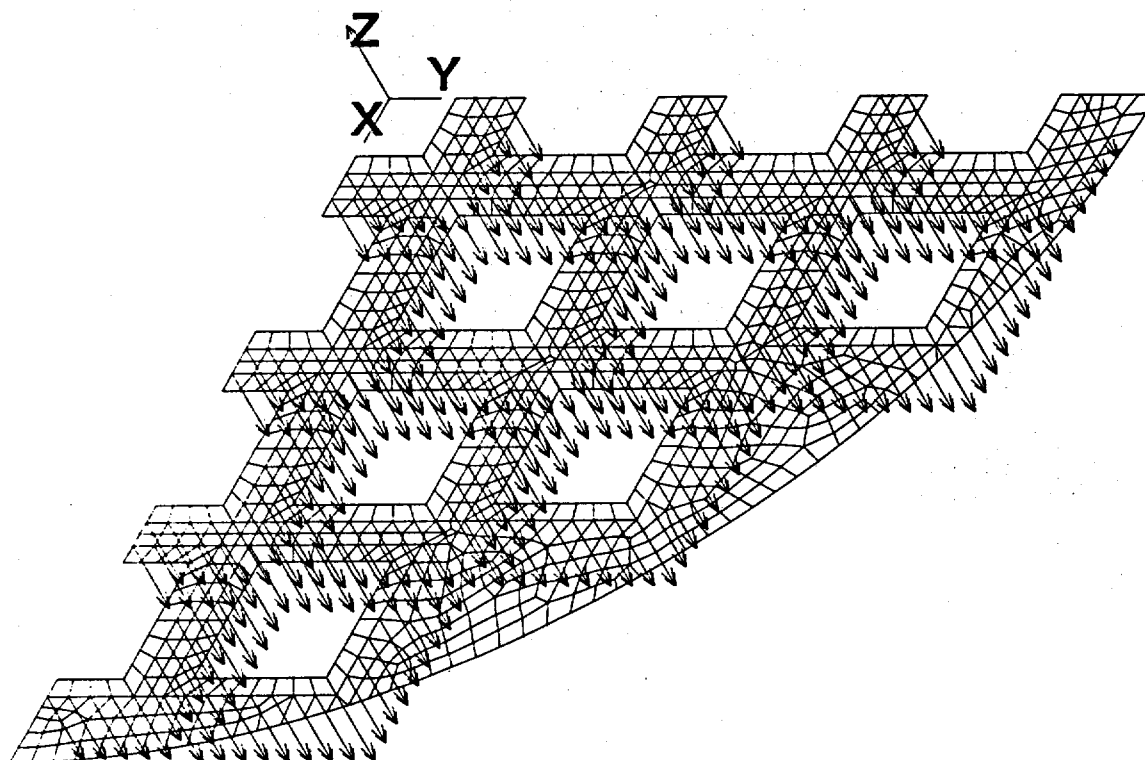


Figure 2.7.9.5-4 Yankee-MPC Bottom Weldment Finite Element Model with Structural Applied Conditions



2.7.9.5.1 Results of Yankee-MPC Fuel Basket Weldment Analyses (30-Foot End Drop)

The maximum stress intensity (SI), for primary membrane plus primary bending ($P_m + P_b$), for the 30-foot end drop analysis is 58.0 ksi for the top weldment and 48.1 ksi for the bottom weldment as shown in the table below.

Because there is a large radial temperature gradient through the weldments, the maximum stress intensities do not occur at the maximum temperature of the models, and it is overly conservative to compare these stress intensities to stress allowables based upon the maximum temperature. Therefore, the stress evaluation was performed on a nodal basis. That is, using ANSYS, the maximum stress at each node in each model was compared to the maximum allowable stress at the temperature of the node being evaluated.

For hypothetical accident conditions, the following criteria was used in evaluating the top and bottom weldments nodal stress intensities:

$$P_m + P_b < 3.6S_m \text{ or } S_u, \text{ whichever is less.}$$

(Note: For Type 304 stainless steel in these temperature ranges, S_u is smaller than $3.6S_m$.)

The margin of safety (MS) is calculated as:

$$\text{M.S.} = (\text{Allowable Stress} / \text{Nodal Stress Intensity}) - 1$$

The minimum margins of safety for each weldment for the end drop condition are:

Component/Condition	$P_m + P_b$ (ksi)	Nodal Temp. (°F)	S_u (ksi)	M.S.
Top Weldment/30-ft. Drop	58.0	223	69.9	+0.20
Bottom Weldment/30-ft. Drop	48.1	257	68.1	+0.42

2.7.9.5.2 Yankee-MPC Top Weldment Structural Rib Buckling Evaluation

The structural ribs on the top weldment are subjected to axial loads during a top end drop. End constraints on the ribs during a top end drop consist of: fixed at the end welded to the top weldment, and free at the other end. Because there are no closed solutions readily available for

evaluating a plate for buckling loads with end constraints matching those of the top weldment ribs, a closed-form solution for the buckling of a column was used to analyze a 1-inch section of one of the ribs.

For a column under axial loading with one end fixed and the other end free, the critical load (P_{cr}) is determined by:

$$P_{cr} = \frac{\pi^2 EI}{(KL)^2}$$

where:

I = moment of inertia,

E = modulus of elasticity,

L = length of the column, and

K = effective length factor ($K = 2$ for a column with one end fixed and the other free).

Evaluating a 1-inch section of one of the ribs at the maximum weldment temperature of 540°F yields:

$$P_{cr} = \frac{\pi^2 (25.6 \times 10^6 \text{ lb/in}^2) \frac{1}{12} (1.0 \text{ in}) (0.38 \text{ in})^3}{(2 \times 6.80 \text{ in})^2} = 6,241 \text{ lb}$$

For the 30-foot top end drop, the sum of the forces on the nodes representing the ribs is a maximum of 3,681 lbs. Thus, the maximum load (P) on a 1-inch section of one of the structural ribs is:

$$P = \frac{3,681}{27.5/2} (1) = 268 \text{ lb}$$

Thus, the margin of safety (MS) for buckling of one of the structural ribs of the top weldment during a 30-foot top end drop is:

$$\text{M.S.} = \frac{6,241}{268} - 1 = 22.3$$

2.7.9.5.3 Conclusions

As shown in this section, both the top and bottom weldments maintain positive margins of safety when subjected to the 30-foot end drop conditions. As shown in the top weldment structural rib buckling calculation, the actual maximum load (P) on one of the structural ribs of the top weldment during a 30-foot drop is much less than the predicted buckling load (P_{cr}). Therefore, the top and bottom weldments are structurally adequate.

THIS PAGE INTENTIONALLY LEFT BLANK

2.7.10 Greater Than Class C (GTCC) Basket Analysis - Accident Conditions

The Greater Than Class C (GTCC) basket is evaluated against the requirements of the ASME Code, Section III, Subsection NF (component supports), to ensure that the basket components are structurally adequate for loads imposed during normal conditions of transport in Section 2.6.16 and during hypothetical accident conditions in this section. The evaluation of the GTCC waste basket support disks and the support wall for the 30-ft end drop and side drop accident conditions are presented in this section. As discussed in Section 2.6.16.1, an evaluation of the tubes is not required for accident conditions. Load amplification factors of 55 g and 56.1 g are used for side drop and end drop conditions respectively. Accident condition allowable stresses are based on the normal condition of transport (Level A) in NF-3322 with a factor of 1.7 (NF-3341.1).

The evaluation of the Yankee-MPC and CY-MPC GTCC baskets is provided in Sections 2.7.10.1 and 2.7.10.2, respectively.

2.7.10.1 Yankee-MPC GTCC Basket Evaluation

Support Disk

In the side drop condition, the total basket and contents weight is shared by the eight (8) stainless steel disks. Due to the rigidity of the 2.5-inch thick support wall, the bending and shear stresses over the cross sections of the GTCC basket are not a concern. The in-plane compressive stress on the disk is the limiting factor and is evaluated to demonstrate structural integrity. Loads contributed to the in-plane stress are from the weights of one section (15.60 inches) of the 24 waste containers (baffles), 24 tubes, the wall and one disk. The weights are summarized as:

weight of one disk	= 3,373/8	= 422 pounds
weight of tube contributing to the disk load	= 5,935/7	= 848 pounds
weight of wall contributing to the disk load	= (5,478+8,116+3,507)/7	= 2443 pounds
weight of waste contributing to the disk load	= 12,341/7	= 1763 pounds
TOTAL		= 5476 pounds

The load, P , resulting from the 55 g deceleration experienced during the side drop is:

$$P = (55)(5,476) = 301,180 \text{ lbs.}$$

The lower portion of the disk (26.4-in. wide, 1-in. thick, and 6.5-in. high) is considered to be a column subjected to the axial force, P . The width of 26.4-in. is determined by considering a contact angle of 45° (between disk and canister shell during drop conditions). The cross-section area, A , considered for the load is:

$$A = (1.0)(26.4) = 26.4 \text{ in}^2$$

The normal conditions allowable stress, F_a , for an axially loaded compression member is given by NF-3322.1(c)(2).

$$F_a = S_y \left(0.47 - \frac{Kl/r}{444} \right) = 8,331 \text{ psi,}$$

where,

$$K = 0.8 \text{ for the end conditions,}$$

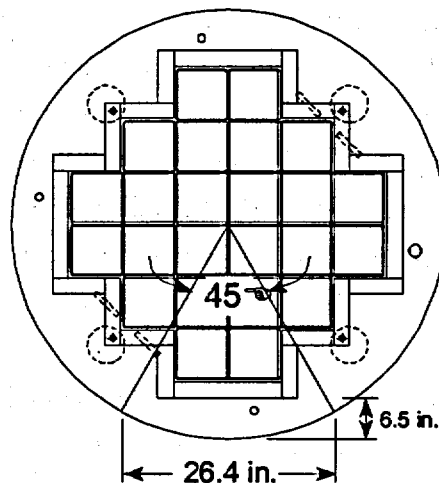
$$l = 6.5, \text{ length of disk to shell,}$$

$$r = \frac{d}{\sqrt{12}} = 0.29.$$

$$\text{Therefore, } Kl/r = 18 < 120.$$

The allowable load across the section is calculated to be

$$P_y = 1.7 A F_a = (1.7)(26.4)(8331) = 373,895 \text{ lb.}$$



The margin of safety is:

$$M.S. = \left(\frac{P_Y}{P} \right) - 1 = \left(\frac{373,895}{301,180} \right) - 1 = +0.24.$$

Side Drop Bearing Stress

In the side drop condition, the weight of the GTCC contents and eight (8) 1-inch thick support disks and the 2.5-inch thick plates that comprise the basket walls transmit the load to the canister shell through the 1-inch thick support disks. As computed in Section 2.7.10.1, the total impact load experienced by a single support disk, when factored by 55 g, is 301,180 pounds. This is conservative because according to NF-3223.1, the bearing load evaluation is not required for service level D accident conditions. The bearing stress evaluation is the load divided by the area of contact between the 1-inch support disks and the canister shell. A 45 degree total angular contact is assumed for which the corresponding area of contact is:

$$A_c = \pi D t \theta = 27.08 \text{ in}^2.$$

where,

$$D = \text{support disk diameter} = 68.98 \text{ in.},$$

$$t = \text{support disk thickness} = 1.0 \text{ in.},$$

$$\theta = \text{ratio for contact angle} = 45/360 = 0.125.$$

This corresponds to a bearing stress (S_{br}) of

$$S_{br} = \frac{301,180}{27.08} = 11,121 \text{ psi.}$$

The allowable for the bearing stress for a normal condition of transport loading condition is $S_y = 19,400$ psi. Based on the conservative accident condition loading of 55 g, the margin of safety is computed as

$$M.S. = \left(\frac{19,400}{11,121} \right) - 1 = +0.74.$$

Support Wall - Side Drop Evaluation

In the side drop orientation, the load of the GTCC waste and tubes is transferred into the 2.5-inch thick support walls. This develops a bending stress in the support wall. The deceleration of the contents and basket is 55 g. Considering the load of waste baffle and tubes to be transmitted uniformly to the support walls, the maximum moment in the wall is

$$M_{\max} = \frac{55(w)(L)^2}{8} = 531,878 \text{ in-lb.}$$

where,

$$w = (5,935 + 5,478 + 8,116 + 3,507 + 12,341)/111.3 = 317.9 \text{ pounds/inch, which is the weight of the baffle, tubes and support wall per unit length and,}$$

$$L = 15.60, \text{ distance between the support disks.}$$

The calculation of the sectional modulus ($S = 970 \text{ in}^3$) of the support wall conservatively considers the lower portion of the 2.5-inch thick wall only. The bending stress is

$$f_b = \frac{531,799}{970} = 548 \text{ psi.}$$

The allowable is

$$1.7 \times 0.6 S_y = (1.7)(0.6)(19,400) = 19,788 \text{ psi.}$$

The margin of safety is:

$$M.S. = \left(\frac{19,788}{548} \right) - 1 = +35.1$$

The maximum shear stress is considered to be the load transferred to a single disk divided by the cross sectional area (A_s) of the lower section of 2.5-inch thick wall.

$$A_s = 22.09(2.5) = 55.225 \text{ in}^2$$

Using the distributed weight of 317.9 pounds/inch

$$f_v = \frac{0.5(55)(317.9)(15.6)}{55.225} = 2,470 \text{ psi.}$$

The allowable shear is $F_v = 1.7 \times 0.4S_y = (1.7)(0.4)(19400) = 13,192 \text{ psi}$, and the margin of safety is

$$\text{M.S.} = \left(\frac{13,192}{2,470} \right) - 1 = +4.3.$$

Support Wall - End Drop Evaluation

In the end drop orientation, the weight of eight 1-inch thick support disks and the 2.5-inch thick plates that comprise the basket walls transmit the load to the canister end through the 2.5-inch thick plates. This represents a total weight of 20,474 pounds ($5,478 + 8,116 + 3,507 + 3,373$). The GTCC waste and tubes are free standing and will be supported by the canister ends directly.

The axial compressive stress evaluation is the total load times the deceleration (56.1g) divided by the area of contact between the 2.5-inch thick plates and the canister end. The cross sectional area of the wall is computed as the perimeter of the 2.5-inch plates,

$$A = (16)(2.5)(8.44) + (4)(2.5)(22.09) = 558.5 \text{ in}^2.$$

The applied force, P , resulting from the 56.1 g deceleration experienced during the end drop is:

$$P = (56.1)(20,474) = 1,148,591 \text{ lbs.}$$

The allowable stress, F_a , for an axially loaded compression member is given by NF-3322.1(c)(2).

$$F_a = S_y \left(0.47 - \frac{Kl/r}{444} \right) = 8,542 \text{ psi,}$$

where,

$K = 0.65$ for the end conditions,

$l = 14.6$, distance between disks,

$$r = \frac{d}{\sqrt{12}} = 0.72.$$

$d = 1.0$, thickness of support disk

Therefore, $Kl/r = 13.18 < 120$.

The allowable load across the section is calculated to be

$$P_y = 1.7 A F_a = 1.7(558.5)(8,542) = 8,110,202 \text{ lb}$$

and the associated margin of safety is

$$M.S. = \left(\frac{8,110,202}{1,148,591} \right) - 1 = +6.1.$$

The Yankee-MPC GTCC basket support wall is adequate based on the above calculation.

Basket Support Disk - End Drop Evaluation

In the end drop orientation, the weight of a 1-inch thick support disk will produce a bending moment and shear force in the 3/8 inch weld at the support disk/wall interface. To simplify the evaluation, a 1-inch by 1-inch section is considered. The axial force, F_y , on the weld is

$$F_y = \frac{Wg}{L} = \left(\frac{(422)(56.1)}{235.6} \right) = 100.5 \text{ lb,}$$

where,

$$W = 422 \text{ lb, the weight of one disk,}$$

$$L = 4(25.15) + 16(8.44), \text{ the perimeter of the weld,}$$

$$g = 56.1 \text{ g.}$$

The bending moment, M , at the weld is

$$M = F_y \left(\frac{d}{2} \right) = 602.8 \text{ inch - pounds,}$$

where,

$$d = \frac{68.96}{2} - \sqrt{\left(\frac{39.03}{2} \right)^2 + \left(\frac{22.15}{2} \right)^2} = 12 \text{ inch, the greatest radial distance to the outer edge of the disk.}$$

$$A_w = 2(1) = 2 \text{ in.}$$

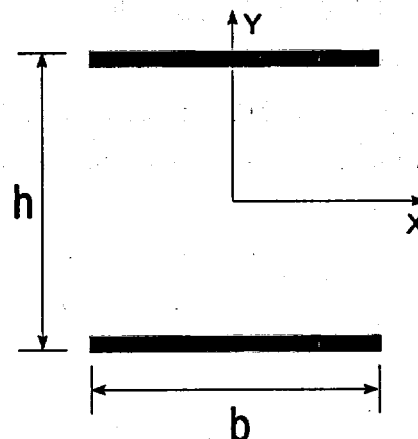
The section modulus, S_w , for the weld cross-section is

$$S_w = bh = 1 \text{ in.}^2,$$

where,

$$b = 1 \text{ in.},$$

$$h = 1 \text{ in.}$$



Therefore, the resulting bending force is calculated to be

$$F_b = \frac{M}{S_w} = 602.8 \frac{\text{lb}}{\text{in}}$$

and the shear force is

$$F_v = \frac{F_y}{A_w} = 50.3 \frac{\text{lb}}{\text{in.}}$$

Therefore, the resulting shear force applied to the weld is

$$F_r = \sqrt{F_b^2 + F_v^2} = 604.9 \frac{\text{lb}}{\text{in.}}$$

The allowable shear stress in the base metal at the weld junction is

$$F_a = (1.7)(0.4)F_y = (1.7)(0.4)(19,400) = 13,192 \text{ lb/in}^2.$$

The required weld size is calculated as follows:

$$\frac{F_r}{F_a} = \frac{604.9}{13,192} = 0.05 \text{ in.} < \frac{3}{8} \text{ in.}$$

The required weld is less than the actual 3/8-inch weld. The support disk has larger cross-sectional area and moment of inertia than the weld and therefore is qualified by comparison to the weld. No further evaluation is required.

2.7.10.2 CY-MPC GTCC Basket Analysis – Accident Conditions

The CY-MPC GTCC basket is evaluated against the requirements of the ASME Code, Section III, Subsection NF (component supports), to ensure that the basket components are structurally adequate for loads imposed during normal conditions of transport (presented in Section 2.6.18) and hypothetical accident conditions (presented in this Section).

The CY-MPC GTCC basket is designed to transport up to 24 containers of GTCC waste. The basket (shield shell weldment) is constructed with 2.25-inch thick SA240 Type 304 stainless steel plates that form walls in an octagon configuration. A total of 9 circular disks, also of Type 304 stainless steel material with 69.15-inch diameter and 1-inch thickness provide support to the basket wall structure. The disks are spaced 17.0 inches center-to-center and are welded to the wall structure with circumferential fillet welds. The GTCC waste containers (tube array weldment) are positioned and supported using 24 stainless steel tubes that are located within the welded wall structure.

Each stainless steel tube has an 8.72-inch square inside dimension, a 0.25-inch thick wall, and can hold one waste container. The tubes inside the basket are stacked together with a maximum of 6 tubes in a row and are welded together around the perimeter at 12 locations. The basket wall and circular disks support the tubes when in a horizontal orientation. The ends of the basket are enclosed by the canister, which provides end support to tubes in non-horizontal orientations.

Tube Array Weldment

The tube array weldment is not required to maintain structural integrity during accident conditions of transport. Therefore, no analysis of the Tube Array Weldment is presented in this section.

Shield Shell Weldment Evaluation

The shield shell weldment is required to maintain structural integrity during accident conditions of transport.

End Drop Analysis

During an end drop the entire weight of the shield shell weldment applies a compressive load at the base of the shell weldment. The shield shell weldment consists of the octagon shell and the nine support disks. The weight of the assembly is, conservatively:

$$W = 19,500 + 9 \times 250 = 21,750 \text{ lbs}$$

where

19,500 lb. = weight of octagon shell (19,047 lb. actual)

250 lb. = weight of support disk (222 lb. actual)

The cross sectional area of the shell weldment at the base is:

$$A = 2.25 \times [4 \times (18.28 + 22.66 - 8)] = 296 \text{ in}^2$$

The stress at the base of the assembly is:

$$S_s = \frac{60 \times 21,750}{296} = 4,408 \text{ psi}$$

For a bounding temperature of 400°F where $S_m = 18,700$ psi, the margin of safety is:

$$MS = \frac{2.4 \times 18,700}{4,408} - 1 = +\text{large}$$

Side Drop Analysis

For a side-drop scenario, a three-dimensional periodic finite element model of the shell assembly is used, Figure 2.7.10.2-1. The model represents an 8.50-inch segment of the assembly. The model is constructed of SOLID45 elements. CONTAC52 elements are used at the periphery of the support disk to represent a gap between the basket and canister and the gap between the

canister shell and the transport cask inner liner. Note that the interface with the canister is conservatively not modeled.

Boundary conditions for the finite element model are shown in Figure 2.7.10.2-2. Pressure loads are applied as shown in Figure 2.7.10.2-2 to represent the weight of the loaded tube weldment (The tube array weldment weight is 11,353 lbs and the weight of the waste is 20,230 lbs.). The pressure load is applied as a triangular distribution for a 45° basket orientation. This angle is used to maximize the bending in the shell. The triangular load distribution is used to represent the loading of the tube array.

Using a temperature distribution obtained from the CY-MPC GTCC thermal analysis, the shell assembly model is analyzed for two thermal conditions using ambient temperatures of 100°F and - 40°F. The finite element model considers the 45° basket orientation with a 55g acceleration.

The maximum primary membrane sectional stress in the shell assembly is 35.1 ksi. The allowable stress is 45.9 ksi (0.7Su). This results in a margin of safety of +0.31. The maximum primary membrane plus bending sectional stress in the shell assembly is 57.2 ksi, with an allowable stress of 65.6 ksi (Su). The resulting margin of safety is +0.14. A temperature of 325°F is used to establish the allowable stress, which is conservative, compared to the calculated temperature of 318°F. The maximum stress occurs in the shell support disk.

Figure 2.7.10.2-1 CY-MPC GTCC Basket Shield Shell Assembly Finite Element Model

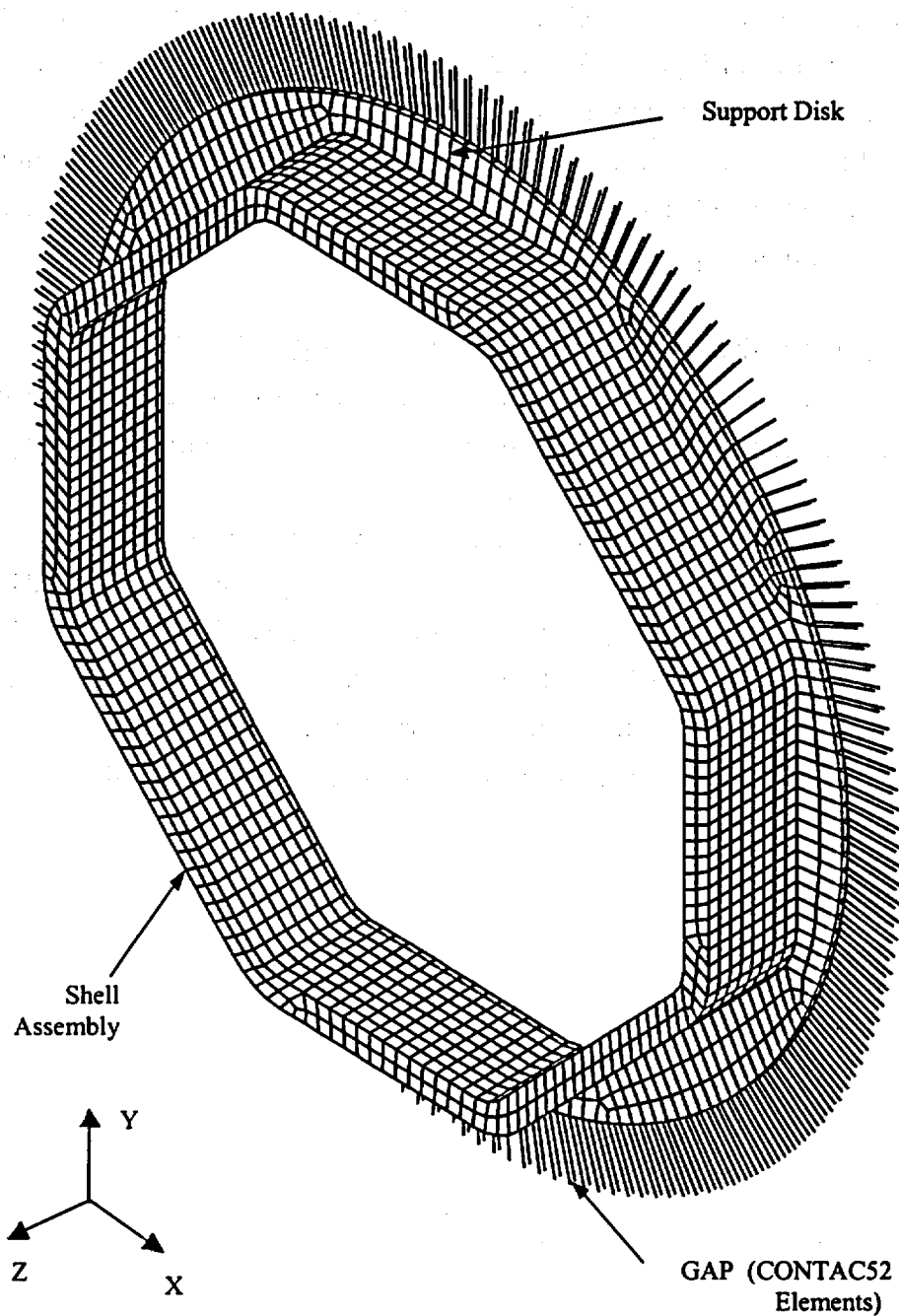
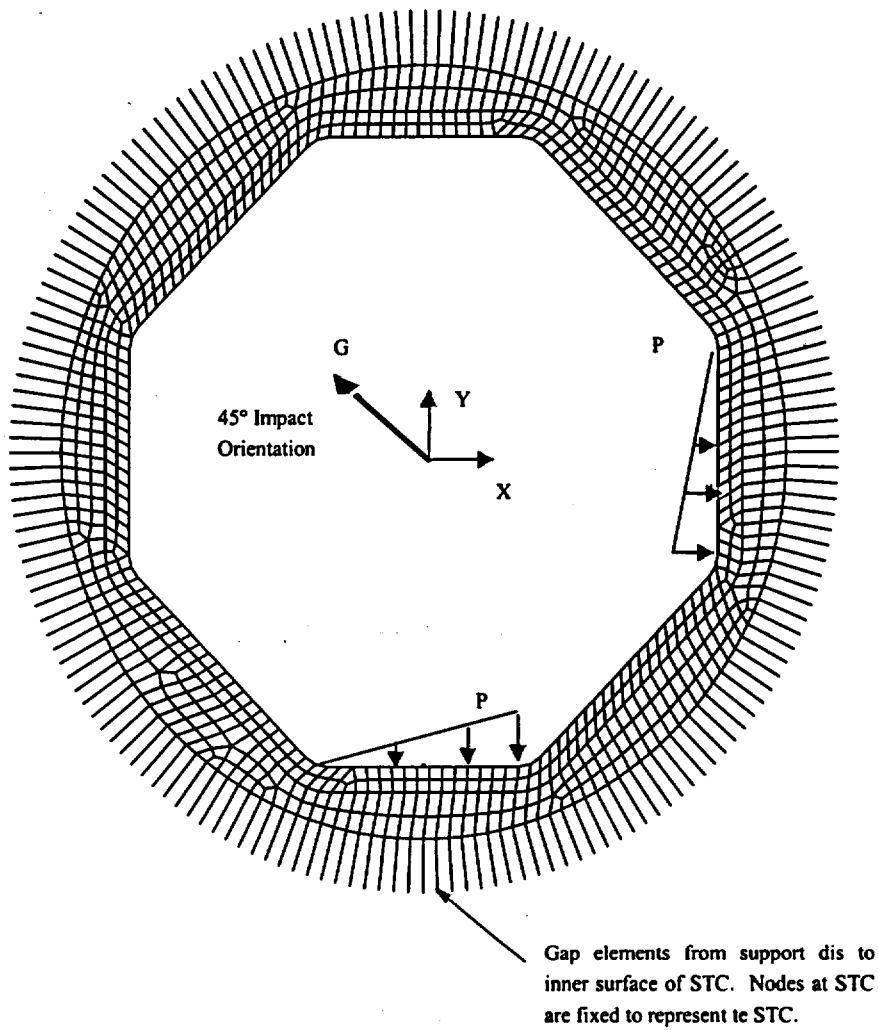


Figure 2.7.10.2-2 CY-MPC GTCC Basket Shell Assembly Loading and Boundary Conditions



THIS PAGE INTENTIONALLY LEFT BLANK

2.7.11 Yankee-MPC Transportable Storage Canister Analysis – Accident Conditions

This section presents the evaluation of the transportable storage canister for the hypothetical accident conditions. The evaluation for normal conditions of transport is presented in Section 2.6.13.

The canistered fuel, or the canistered GTCC waste, configuration consists of the canister together with the top and bottom transport spacers. The spacers position the canister in the NAC-STC cavity to ensure that the center of gravity of the NAC-STC in the canistered configuration is the same as that for the directly loaded fuel configuration.

The principal components of the canister are the canister shell, including the bottom plate, the fuel basket or GTCC waste basket, the shield lid, and the structural lid. A description of the geometry and materials of construction of the canister, baskets, and spacers are provided in Section 1.2.1.2.8.

The general arrangement of the canister, depicted with the fuel basket, is shown in Figure 2.6.13-1. The individual components of the canister are depicted in Figure 2.6.13-2.

A drop accident stress evaluation is performed for the 30-foot side drop condition, and for the 30-foot top and bottom end drop conditions. The stress intensities resulting from these two evaluations bound those that result from the 30-foot corner and oblique drop conditions. This conclusion is based on the analysis results for the directly loaded fuel configurations described in Sections 2.6.12, 2.7.1.3, 2.7.1.4, and 2.7.8.

The transport spacers may crush under the corner, oblique and end drop conditions. In crushing, they reduce the total g load on the fuel or GTCC waste canister that would occur in the hypothetical accident conditions. However, no credit is taken for the presence of the aluminum honeycomb spacers. All of the impact g load - 55 g for the side drop, and 56.1 g for the end drops - is assumed to be applied to the canister. Consequently, the end drop analyses are conservative.

2.7.11.1 Canister - Accident Analysis Description

The canister is a right-circular shell fabricated from rolled 5/8-inch thick, Type 304L stainless steel plate. It is closed on its bottom end with a Type 304L stainless steel circular plate that is 1-inch thick. The canister is closed at the top end by a 5-inch thick, Type 304 stainless steel shield lid, which is seal welded to the canister shell. The shield lid is covered by a 3-inch thick, Type 304L, stainless steel structural lid welded to the canister shell at its top inside edge. The loaded canister is lifted using 6 hoist rings threaded into the top of the structural lid. The canister is the defined confinement boundary for spent fuel or GTCC waste contents during long-term storage, and it is the defined containment boundary for Reconfigured Fuel Assemblies during transport, satisfying the requirements of 10 CFR 71.63(b) for a separate inner container. No credit is taken for containment by the canister for the transport of intact fuel assemblies or GTCC waste. Containment of these contents for transport is provided by the NAC-STC, using the same containment boundary defined for the directly loaded fuel configuration.

The structural design criteria for the canister is the ASME Code Section III, Subsection NB, "Class 1 Components." Consistent with this criteria, the structural components of the canister (shell, bottom plate, and structural lid) are shown to satisfy the allowable stress intensity limits presented in Table 2.1.2-1.

The canister is evaluated using the ANSYS finite element program for the 30-foot drop conditions in the end and side impact orientations. The ANSYS finite element model is the same as that used for the evaluation of the 1-foot drop impacts evaluated for normal conditions of transport. The model is described in Section 2.6.13.2. As described in Section 2.6.13.2, the COMBIN40 elements used between the structural and shield lids and for the backing ring are assigned a gap sizes of 1E-8 inches. The maximum gap size is 0.08 inches. However, use of the smaller gap size results in the highest stresses at critical sections, resulting in the lowest margin of safety. All gap-spring elements are assigned a stiffness of 1E8 lb/in.

2.7.11.2 Analysis Results

The detailed results of the analysis for the 30-foot side, and top and bottom end drops are presented in Tables 2.7.11-1 through 2.7.11-6. The force summation for the side drop analyses indicated that the weight of the canister and contents was 4.86% less than actual (i.e., the

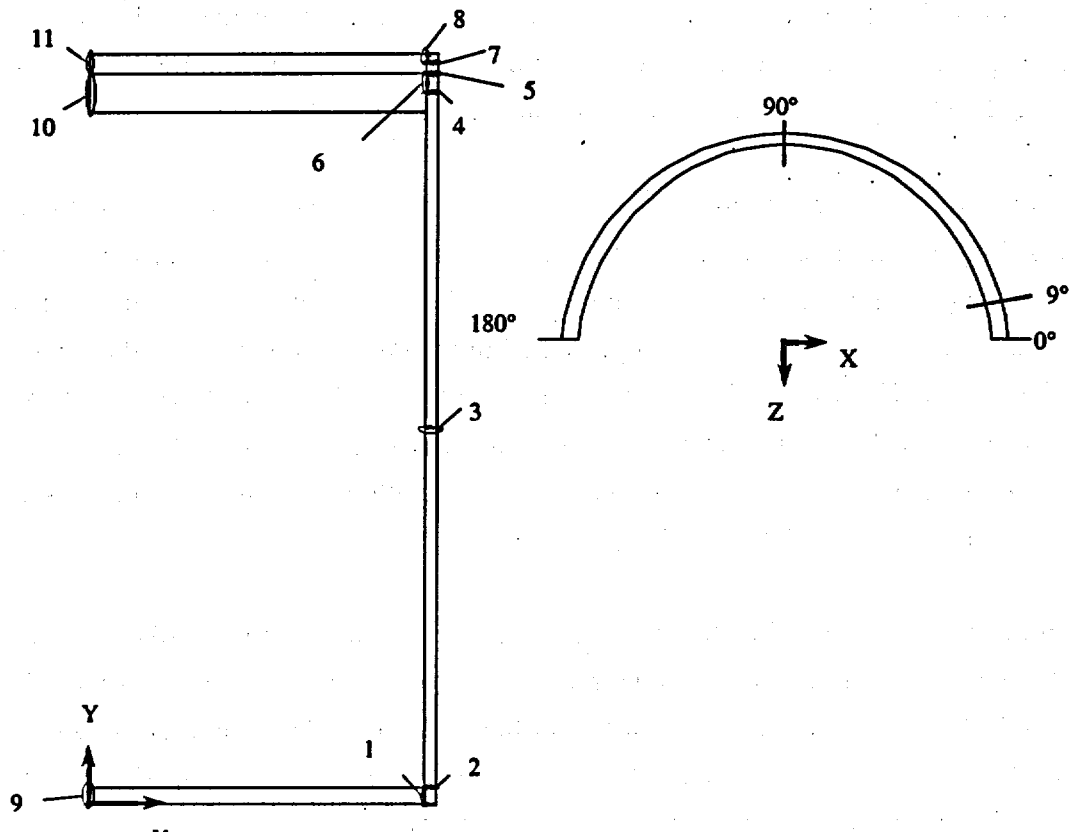
modeled weight (26,098 pounds) was less than the calculated weight (27,365 pounds) by 4.86%). Consequently, the stresses presented in the tables for the side drop, are scaled up 4.86% from those same stresses calculated by the finite element model. The section stresses presented in the tables are identified by a section number. A cross-section of the canister showing the section numbers is presented in Figure 2.7.11-1. A summary of the canister minimum Margins of Safety for the evaluated drop conditions is shown in Table 2.7.11-7.

For the top and bottom end drops, the stresses are essentially uniform around the circumference. For the side drop, the stresses vary around the circumference. Therefore, the circumferential angle at which the maximum stress occurs is noted in the table, (in parentheses) beside the section number. The allowable stresses presented in the tables are for Type 304L stainless steel, except for section 10, which is for Type 304 stainless steel. These allowables are evaluated at 350°F (maximum calculated temperature in the canister is 338°F). The allowable stress for P_m stresses is defined as the lesser of $2.4 S_m$ or $0.7 S_u$. The allowable stress for the $P_m + P_b$ stresses is defined as the lesser of $3.6 S_m$ or $1.0 S_u$.

The minimum margin of safety for the evaluated side and end drops is +0.69 for the primary membrane stress (P_m) in the 30-foot side impact, using the minimum gap size of 1×10^{-8} inches at Section 8. The minimum margin of safety for the evaluated side and end drops is +0.83 for the primary membrane stress at the same section, assuming the maximum gap size of 0.08 inches. Consequently, use of the minimum gap size is conservative.

The canister structural lid closure weld is specifically evaluated for the hypothetical accident conditions. The lid weld is identified as Section 8 in Figure 2.7.11-1. The structural lid weld has a root and final weld surface Liquid Penetrant examination performed in accordance with ASME, Section V, Article 6. Upon completion, the weld is ultrasonically examined in accordance with ASME Section V, Article 5, or multi-pass liquid penetrant examined in accordance with ASME Section V, Article 6. In accordance with NRC guidance, if a multi-pass liquid penetrant examination is performed on the structural lid closure weld, two separate weld stress reduction factors are applied to the structural lid canister shell weld – a 0.8 factor to conservatively consider the weld configuration and a 0.8 factor per NRC ISG-4, Item 5. Thus, a total weld stress reduction factor of 0.64 (0.8×0.8) is applied to the stress allowable for the structural lid weld. The canister closure weld evaluation for accident conditions is presented in Section 2.7.11.4. The evaluation, which is based on the finite element analysis stress result as shown in Section 2.7.11.2, shows a minimum margin of safety of +0.69 for the weld.

Figure 2.7.11-1 Identification of the Sections for Evaluating the Linearized Stresses in the Canister



Section	Node 1		Node 2	
	X	Y	X	Y
1	34.695	0.000	34.695	1.000
2	34.695	1.000	35.320	1.000
3	34.695	57.269	35.320	57.269
4	34.695	118.000	35.320	118.000
5	34.695	119.000	35.320	119.000
6	34.695	118.000	34.695	119.000
7	34.695	121.120	35.320	121.120
8	34.695	121.120	34.695	122.000
9	0.000	0.000	0.000	1.000
10	0.000	114.000	0.000	119.000
11	0.000	119.000	0.000	122.000

Table 2.7.11-1 Canister, 30-Foot Side Drop (Primary Membrane Stress) (psi)

Section No.	Component Stresses						Principal Stresses			S.I.	Allow. Stress	Margin of Safety
	SX	SY	SZ	SXY	SYZ	SXZ	S1	S2	S3			
1(0°)	-14680.4	1080.1	-9311.6	-235.5	-21.1	-904.6	1083.2	-9163.7	-14827.2	15917.7	39000	1.45
2(0°)	-3395.4	62.4	-7415.7	-314.3	-438.9	-478.6	111.6	-3358.7	-7501.7	7612.8	39000	4.12
3(180°)	-4.6	-1213.2	586.7	0.1	-4.0	-45.8	590.3	-8.1	-1213.2	1802.5	39000	20.64
4(9°)	-16945.4	3043.0	-4750.2	-336.0	2851.1	2020.7	3978.4	-5329.0	-17301.9	21276.1	39000	0.83
5(0°)	-10863.5	1232.1	-7804.7	-1756.4	1333.8	92.4	1662.0	-7961.0	-11146.6	12803.4	39000	2.05
6(0°)	-23467.7	-3813.8	-11125.6	-2768.3	1168.1	38.0	-3262.2	-11293.4	-23855.7	20594.5	39000	0.89
7(9)	-11503.1	654.7	-4158.7	-31.6	1865.5	961.7	1299.2	-4673.6	-11639.5	12939.7	39000	2.01
8(0°)	-19367.6	-4979.8	-8614.2	-982.6	865.8	-756.5	-4697.7	-8785.2	-19472.5	14774.8	24960*	0.69
9	-2146.5	-15.3	1105.2	-2.9	-14.7	-78.0	1107.3	-15.5	-2148.6	3255.9	39000	10.98
10	-1032.3	-8.4	331.8	-59.4	-2.9	-27.1	332.3	-4.9	-1036.3	1368.4	45640	32.35
11	-1131.4	-1.3	373.3	-25.5	-5.1	-32.8	374.1	-0.7	-1132.5	1506.8	39000	24.88

* Includes two stress reduction factors for weld: $0.8 \times 0.8 = 0.64$ (See Section 2.7.11.4).

Table 2.7.11-2 Canister, 30-Foot Side Drop (Primary Membrane Plus Primary Bending Stress) (psi)

Section No.	Component Stresses						Principal Stresses			S.I.	Allow. Stress	Margin of Safety
	SX	SY	SZ	SXY	SYZ	SXZ	S1	S2	S3			
1(0°)	-24841.3	457.1	-12761.5	-195.8	106.1	-824.5	459.5	-12709.0	-24904.3	25365.6	58500	1.31
2(0°)	-2630.9	-1326.5	-8993.8	-290.8	-641.0	-126.3	-1218.5	-2682.3	-9050.5	7832.0	58500	6.47
3(0°)	89.9	2039.5	3198.2	2.7	38.7	156.9	3207.7	2038.5	81.9	3125.9	58500	17.71
4(9°)	-13894.0	9446.8	-2019.6	93.3	2241.9	2829.1	9886.2	-1813.0	-14533.6	24421.9	58500	1.40
5(0°)	-14261.0	2077.3	-6923.9	-2052.1	1046.5	-15.1	2446.4	-7037.2	-14512.6	16966.3	58500	2.45
6(0°)	-32968.0	-7832.0	-15215.2	-4140.9	1477.5	185.3	-6920.8	-15456.4	-33639.1	26718.3	58500	1.19
7(9°)	-9079.8	4969.3	-1993.4	53.6	1402.0	1674.6	5250.3	-1894.8	-9460.5	14711.9	58500	2.98
8(0°)	-28144.4	-7245.8	-12646.1	-2107.7	1351.6	-307.9	-6716.3	-12971.2	-28354.1	21643.1	37440*	0.73
9	-2172.7	-33.2	1088.4	-2.9	-14.9	-75.6	1089.5	-33.5	-2174.8	3264.3	58500	16.92
10	-1360.0	-10.9	297.9	-63.0	-2.9	-40.8	299.0	-8.0	-1364.2	1663.1	65200	38.20
11	-1344.3	-1.2	354.1	-25.6	-5.0	-39.5	355.1	-0.7	-1346.4	1700.8	58500	33.40

* Includes two stress reduction factors for weld: $0.8 \times 0.8 = 0.64$ (See Section 2.7.11.4).

Table 2.7.11-3 Canister, 30-Foot Bottom End Drop (Primary Membrane Stress) (psi)

Section No.	Component Stresses						Principal Stresses			S.I.	Allow. Stress	Margin of Safety
	SX	SY	SZ	SXY	SYZ	SXZ	S1	S2	S3			
1	-70.7	-1971.0	-361.1	176.2	70.3	22.4	-51.8	-360.9	-1990.0	1938.0	39000.0	19.12
2	289.7	-5185.0	-1182.0	91.4	54.3	94.4	297.4	-1187.0	-5187.0	5485.0	39000.0	6.11
3	2.1	-4867.0	0.9	0.0	0.2	0.0	2.1	0.9	-4867.0	4869.0	39000.0	7.01
4	-2131.0	-2251.0	-1084.0	0.0	734.3	0.0	-729.3	-2131.0	-2605.0	1876.0	39000.0	19.79
5	2510.0	-2096.0	-1535.0	-310.9	-0.9	278.1	2549.0	-1553.0	-2117.0	4667.0	39000.0	7.36
6	551.9	1897.0	-676.0	15.4	84.7	-106.6	1900.0	561.0	-688.0	2588.0	39000.0	14.07
7	-3028.0	979.9	-1533.0	-368.1	39.6	55.9	1014.0	-1531.0	-3063.0	4077.0	39000.0	8.57
8	588.3	-3496.0	-2019.0	466.6	119.6	210.4	659.5	-2031.0	-3554.0	4214.0	24960.0*	4.92
9	82.5	-682.0	94.2	6.5	58.3	-0.5	98.5	82.5	-686.4	785.0	39000.0	48.68
10	183.8	-98.9	168.1	43.7	-77.1	5.7	195.2	183.5	-125.7	320.9	45640.0	141.22
11	-469.6	-9.4	-467.5	48.0	-75.2	-1.2	7.4	-470.1	-483.8	491.2	39000.0	78.40

* Includes two stress reduction factors for weld: $0.8 \times 0.8 = 0.64$ (See Section 2.7.11.4).

Table 2.7.11-4 Canister, 30-Foot Bottom End Drop (Primary Membrane Plus Primary Bending Stress) (psi)

Section No.	Component Stresses						Principal Stresses			S.I.	Allow. Stress	Margin of Safety
	SX	SY	SZ	SXY	SYZ	SXZ	S1	S2	S3			
1	398.0	-2678.0	-380.7	125.9	67.7	37.0	405.2	-380.8	-2685.0	3090.0	58500.0	17.93
2	-1988.0	-7553.0	85.1	0.0	-32.4	0.0	85.2	-1988.0	-7553.0	7638.0	58500.0	6.66
3	2.1	-4867.0	2.9	1.1	0.4	-0.1	3.0	2.1	-4867.0	4870.0	58500.0	11.01
4	-2259.0	-3096.0	-704.5	0.0	805.1	0.0	-458.8	-2259.0	-3342.0	2883.0	58500.0	19.29
5	1450.0	-10380.0	-4379.0	304.5	3.7	410.7	1486.0	-4407.0	-10390.0	11880.0	58500.0	3.92
6	3324.0	5269.0	932.2	817.6	53.3	-170.6	5567.0	3041.0	917.1	4650.0	58500.0	11.58
7	-2361.0	8380.0	938.8	-472.4	41.6	196.1	8401.0	950.4	-2393.0	10790.0	58500.0	4.42
8	4403.0	-1585.0	-491.6	605.7	160.4	345.7	4490.0	-503.9	-1659.0	6149.0	37440.0*	5.09
9	105.1	-686.4	100.3	8.1	60.4	-1.7	106.1	104.0	-691.1	797.2	58500.0	72.38
10	6941.0	230.8	6895.0	28.2	-72.6	35.9	6960.0	6876.0	229.9	6730.0	65200.0	8.69
11	-4093.0	-195.3	-4098.0	47.4	-79.5	-18.6	-193.1	-4079.0	-4115.0	3922.0	58500.0	13.92

* Includes two stress reduction factors for weld: $0.8 \times 0.8 = 0.64$ (See Section 2.7.11.4).

Table 2.7.11-5 Canister, 30-Foot Top End Drop (Primary Membrane Stress) (psi)

Section No.	Component Stresses						Principal Stresses			S.I.	Allow. Stress	Margin of Safety
	SX	SY	SZ	SXY	SYZ	SXZ	S1	S2	S3			
1	68.2	-371.6	-91.0	-74.7	-19.4	7.7	81.2	-90.6	-385.0	466.2	39000.0	82.66
2	-130.9	110.4	271.9	-75.3	-8.3	-28.6	273.9	131.9	-154.5	428.5	39000.0	90.02
3	-2.9	-975.6	1104.0	0.0	-0.1	-87.6	1110.0	-9.8	-975.6	2086.0	39000.0	17.70
4	185.3	-1596.0	-207.6	-108.1	-29.1	23.1	193.4	-208.6	-1603.0	1796.0	39000.0	20.71
5	-244.0	-1458.0	-78.9	0.0	-55.0	0.0	-76.7	-244.0	-1460.0	1384.0	39000.0	27.18
6	-84.0	-969.1	-40.4	0.0	-65.6	0.0	-35.8	-84.0	-973.7	937.9	39000.0	40.58
7	-18.5	-1372.0	-204.8	2.2	-21.7	-3.1	-18.5	-204.5	-1372.0	1354.0	39000.0	27.80
8	-9.6	-1177.0	-128.4	-6.9	-12.4	-1.4	-9.5	-128.3	-1178.0	1168.0	24960.0*	20.37
9	-3.5	-11.4	-3.7	-25.0	73.7	0.0	70.4	-3.5	-85.5	155.8	39000.0	249.32
10	2.6	-619.2	9.4	-2.6	5.6	-0.6	9.5	2.5	-619.3	628.8	45640.0	71.58
11	-22.9	-703.7	5.2	-2.3	-5.5	-1.9	5.4	-23.0	-703.8	709.1	39000.0	54.00

* Includes two stress reduction factors for weld: $0.8 \times 0.8 = 0.64$ (See Section 2.7.11.4).

Table 2.7.11-6 Canister, 30-Foot Top End Drop (Primary Membrane Plus Primary Bending Stress) (psi)

Section No.	Component Stresses						Principal Stresses			S.I.	Allow. Stress	Margin of Safety
	SX	SY	SZ	SXY	SYZ	SXZ	S1	S2	S3			
1	-217.7	-703.2	-2.5	-49.8	-15.1	-8.6	-1.9	-212.9	-708.6	706.7	58500.0	81.78
2	-84.3	1053.0	572.2	-92.6	-3.7	-51.7	1061.0	576.2	-95.8	1156.0	58500.0	49.61
3	-7.8	-973.9	1117.0	0.3	-0.2	-89.1	1124.0	-14.8	-973.9	2098.0	58500.0	26.88
4	-502.0	-2503.0	98.7	0.0	-82.4	0.0	101.3	-502.0	-2505.0	2607.0	58500.0	21.44
5	-29.7	-1643.0	-310.5	-74.7	-31.4	25.3	-23.8	-312.3	-1647.0	1623.0	58500.0	35.04
6	-227.9	-1240.0	-231.6	0.0	-33.7	0.0	-227.9	-230.4	-1241.0	1013.0	58500.0	56.75
7	-17.4	-1481.0	-246.9	-20.4	-23.0	-10.0	-16.7	-246.9	-1482.0	1465.0	58500.0	38.93
8	27.1	-1150.0	-107.9	5.8	-7.2	4.9	27.3	-108.0	-1150.0	1177.0	37440.0*	30.81
9	1221.0	66.5	1214.0	-25.0	73.7	12.9	1232.0	1209.0	61.3	1171.0	58500.0	48.96
10	95.9	-619.9	105.1	-0.8	11.4	0.5	105.3	95.9	-620.1	725.4	65200.0	88.88
11	-8.2	-704.4	12.6	3.5	9.8	0.0	12.8	-8.2	-704.6	717.3	58500.0	80.56

* Includes two stress reduction factors for weld: $0.8 \times 0.8 = 0.64$ (See Section 2.7.11.4).

Table 2.7.11-7 Summary of Minimum Margin of Safety for Canister 30-Foot Drops

Drop Orientation	Loading Condition	Stress Evaluated	Minimum Margin of Safety	Section No.*
Bottom end	30-ft. impact + pressure (0 psi)	P_m	4.92	8
Bottom end	30-ft. impact + pressure (0 psi)	$P_m + P_b$	3.92	5
Side	30-ft. impact + pressure (20 psi)	P_m	0.69	8
Side	30-ft. impact + pressure (20 psi)	$P_m + P_b$	0.73	8
Top end	30-ft. impact + pressure (20 psi)	P_m	17.70	3
Top end	30-ft. impact + pressure (20 psi)	$P_m + P_b$	21.44	4

* See Figure 2.7.11-1 for section locations.

2.7.11.3 Canister Buckling Evaluation for the 30-Foot End Drop

The canister shell is axially loaded by the weights of the structural lid, the shield lid, and the inertial weight of the shell during a 30-foot end drop impact. The impact load amplification factor is 56.1g's. The shell is evaluated as an unsupported, right circular cylinder using a critical buckling load per Blake, 2nd Edition, "Practical Stress Analysis in Engineering Design."

$$S_{cr} = \frac{E(0.605 - 10^{-7} M^2)}{M(1 + 0.004\phi)}$$
$$= 40.3 \text{ ksi}$$

The canister material is Type 304L stainless steel. Conservatively assume the material temperature to be at 400°F for the accident condition.

$$E = 26.5E+03 \text{ ksi} \quad R = (69.39 + 0.625)/2$$
$$= 35.01 \text{ inches (mid-radius of the canister shell)}$$
$$S_y = 17.5 \text{ ksi} \quad t = 0.625 \text{ inches. (thickness of the canister)}$$
$$\phi = E/S_y \quad \text{and} \quad M = R/t$$
$$= 1514.3 \quad = 56.0$$

The axial compression load in the canister shell is:

$$P_a = [(\pi/4) (69.03^2) (8)(0.291) + (\pi/4) (70.64^2 - 69.39^2) (121.5)(0.291)] (56.1)$$
$$P_a = 761,457 \text{ pounds}$$

and the axial compression stress is:

$$S_a = \frac{P_a}{(\pi/4)(70.64^2 - 69.39^2)}$$
$$S_a = 5.540 \text{ psi}$$

The margin of safety is:

$$(S_{cr}/S_a) - 1 = + 6.3$$

2.7.11.4 Canister Closure Weld Evaluation – Accident Conditions

2.7.11.4.1 Stress Evaluation for the Canister Closure Weld

The closure weld for the canister is a partial penetration weld with a thickness of 0.9 inches. The evaluation of this weld, in accordance with NRC guidance, is to incorporate two separate weld stress reduction factors: a 0.8 factor based on weld type and a second 0.8 factor based on NRC ISG-4, Item 5. These two weld stress reduction factors are incorporated by applying a factor of 0.64 (0.8×0.8) to the stress allowable for this weld.

The stresses for the canister are evaluated using sectional stresses as permitted by Subsection NB. The canister stress results from Section 2.7.11.2 are used for evaluation. The location of the section for the canister weld evaluation is shown in Figure 2.7.11-1 and corresponds to Section 8. The P_m and $P_m + P_b$ stress intensity for Section 8 and the associated allowables are listed below. The factored allowables, incorporating a 0.64 stress reduction factor, and the resulting margin of safety are:

STRESS TYPE	Analysis Stress Intensity (ksi)	0.64 x Allowable Stress (ksi)	Margin of Safety
P_m	14.77	24.96	0.69
$P_m + P_b$	21.64	37.44	0.73

This confirms that the canister closure weld is acceptable for the accident conditions.

2.7.11.4.1 Critical Flaw Size for the Canister Closure Weld

The closure weld for the canister is comprised of multiple weld beads using a compatible weld material for Type 304L stainless steel. An allowable (critical) flaw evaluation has been performed to determine the critical flaw size in the weld region. The result of the flaw evaluation is used to define the minimum flaw size, which must be identifiable in the nondestructive examination of the weld. Due to the inherent toughness associated with Type 304L stainless steel, a limit load analysis is used in conjunction with a J-integral/tearing modulus approach.

The safety margins used in this evaluation correspond to the stress limits contained in Section XI of the ASME Code.

The stress component used in the evaluation for the critical flaw size is the radial stress component in the weld region of the structural lid. For an accident (Level D) event, in accordance with ASME Code Section XI, a safety factor of $\sqrt{2}$ is required. For the purpose of identifying the stress for the flaw evaluation, the weld region corresponding to Section 8 in Figure 2.7.11-1 is considered. From additional post processing of the tipover analysis, the maximum tensile radial stress is 4.4 ksi. To perform the flaw evaluation, a 10 ksi stress is conservatively used, resulting in a significantly larger safety factor than the required safety factor of $\sqrt{2}$. Using 10 ksi as the basis for the evaluation, the minimum detectable flaw size is 0.52 inch for a flaw that extends 360 degrees around the circumference of the canister. Stress components for the circumferential and axial directions are also determined, which would be associated with flaws oriented in the radial or horizontal directions, respectively. The maximum stress for these components is 0.6 ksi, which is enveloped by the stress value of ksi used for the critical flaw evaluation for radial directions. The 360-degree flaw employed for the circumferential direction is considered to be bounding with respect to any partial flaw in the weld, which could occur in the radial and horizontal directions. Therefore, using a minimum detectable flaw size of 3/8 inch is acceptable, since it is less than the very conservatively determined 0.52-inch critical flaw size.

2.7.11.5 Dynamic Loading Effect - Structural Lid Weld

In a top end impact accident of the NAC-STC, the fuel assemblies and the basket in the canister bear against the canister shield lid. That load is transmitted to the shield lid weld, to the canister shell, and to the canister structural lid. The impact load occurs for a duration of approximately 100 milliseconds and, depending on the stiffness of the load path, dynamic amplification may occur. Two types of analyses are performed to evaluate the dynamic effect on the stresses at the canister/structural lid weld: 1) a static analysis using an axial acceleration of 45g; and 2) a transient analysis in which the loading is the time varying acceleration (45g maximum) associated with the compression of the top impact limiter. Note that 45g is selected as being equivalent to the axial component of the acceleration for the 30-foot top corner drop based on the impact limiter analysis (see Table 2.6.7.4.1-3).

2.7.11.5.1 Model Description

The analyses for this evaluation use a two-dimensional model of the upper portion of the canister, which includes the shield lid and the structural lid, as well as the upper 33 inches of the canister shell. ANSYS axisymmetric PLANE42 elements are used in the model. This model is shown in Figure 2.7.11.5-1 and was extracted from the three-dimensional model described in Section 2.6.13.2 for the canister. Instead of using the three-dimensional SOLID45 elements, only one-half of the cross-section of the model in the X-Y plane is required to form the two-dimensional axisymmetric model. The same configuration and stiffness of gap elements between the structural lid and the cask body, between the structural lid and the shield lid, and between the lids and the canister shell, as described in Section 2.6.13.2, are used in this two-dimensional evaluation.

This evaluation addresses an axial load component only. In reviewing the development of the axial load by the fuel, the fuel mass remains constant, and its load on the inner surface of the shield lid is based on the acceleration at each time step. For this reason, the fuel assemblies are represented as a uniform pressure on the inner surface of the shield lid for the static analysis. Also included in the uniform pressure applied to the inner surface of the shield lid is the weight of the basket. For the transient dynamic analysis, the pressure is allowed to vary as the acceleration time history (ATH), which is obtained from the impact limiter analysis for the 30-foot top corner drop. The ATH for this evaluation is shown in Figure 2.7.11.5-2. To restrain the model in the vertical direction, the free end of the gap elements attached to the outer surface of the structural lid are restrained.

To examine the sensitivity of the stiffness for the gap elements between the structural lid and the cask body, two additional values of gap stiffness are considered: a value of 50% of the nominal value and a value of 200% of the nominal value. For each additional case, both the static and the dynamic solutions are recalculated.

To compare the loads transmitted through the structural lid weld, the stress intensities in the weld are calculated for the individual cases. To evaluate the dynamic effect, the ratio of the calculated dynamic stress to the calculated static stress (SDLF) is computed for each time step.

2.7.11.5.2 Analysis Results

Since the transient dynamic analysis is initiated as a stress-free condition, the SDLF starts with a zero value. As the impact event proceeds, the SDLF increases to its maximum value and then returns to zero a value at the end of the event. The maximum values are presented below for the three gap-stiffness cases.

Results of the Evaluation of the Dynamic Loading of the Canister Structural Lid Weld

Case-Gap Stiffness	Maximum SDLF
Nominal stiffness value	1.006
200% of the nominal value	1.007
50% of the nominal value	1.005

The time history of the SDLF, which corresponds to the analysis using the nominal gap stiffness, is shown in Figure 2.7.11.5-3. The results indicate that the effect of dynamic loading is minimal, which is due to the large stiffness associated with the shield lid and the structural lid.

Figure 2.7.11.5-1 Two-Dimensional Axisymmetric Model of the Upper Section of the Yankee-MPC Canister

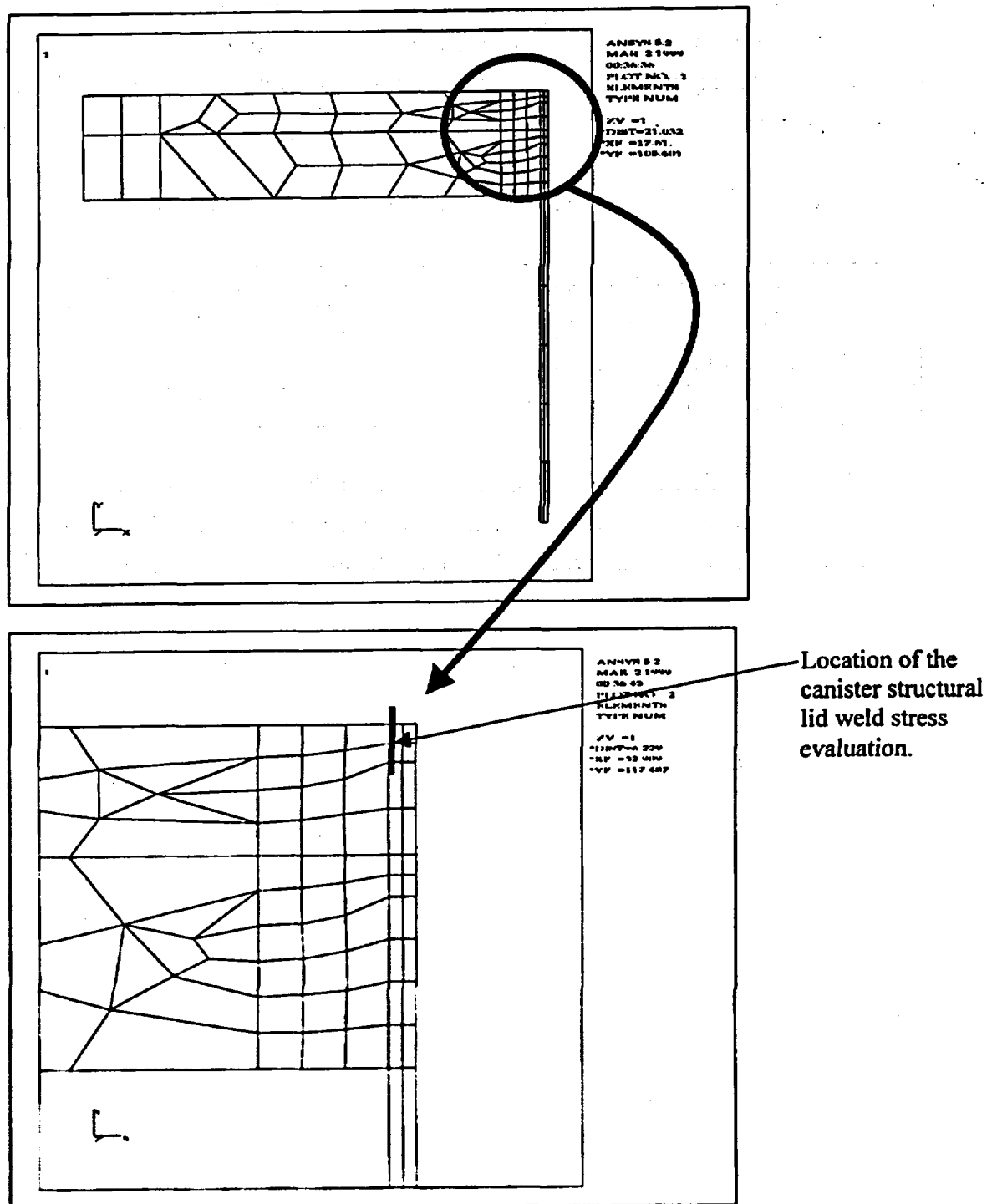


Figure 2.7.11.5-2 Axial Acceleration (g) Time History for a Top End Impact, Yankee-MPC Canister

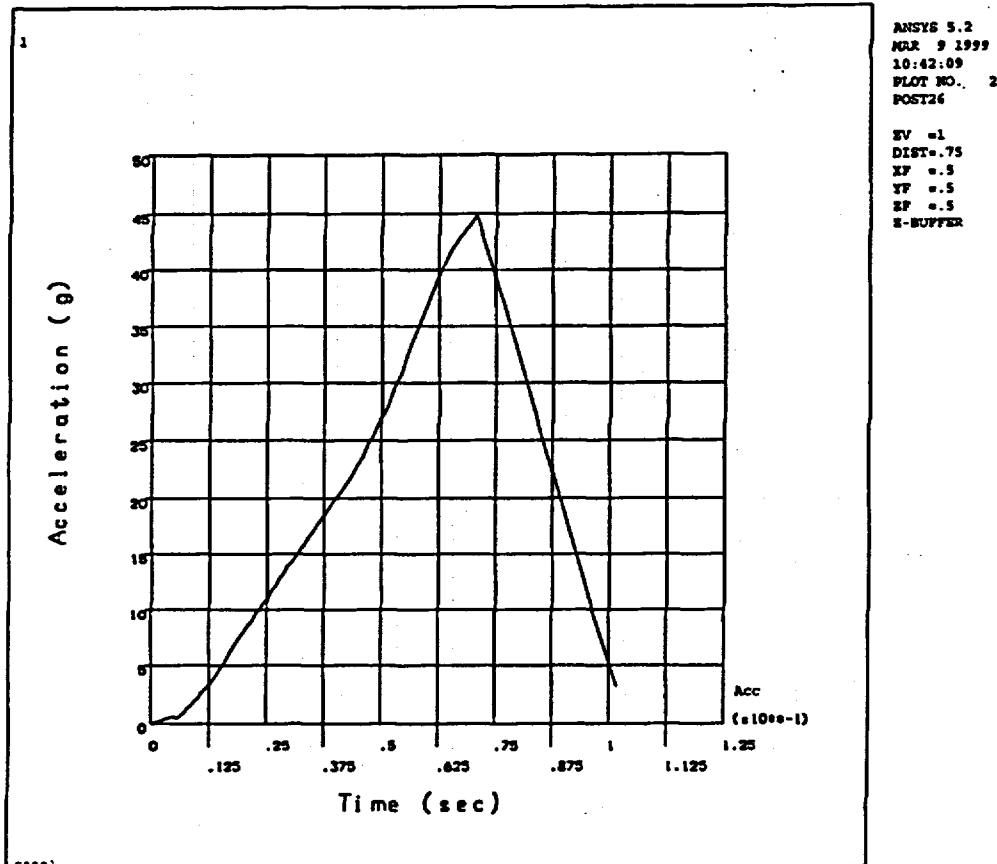
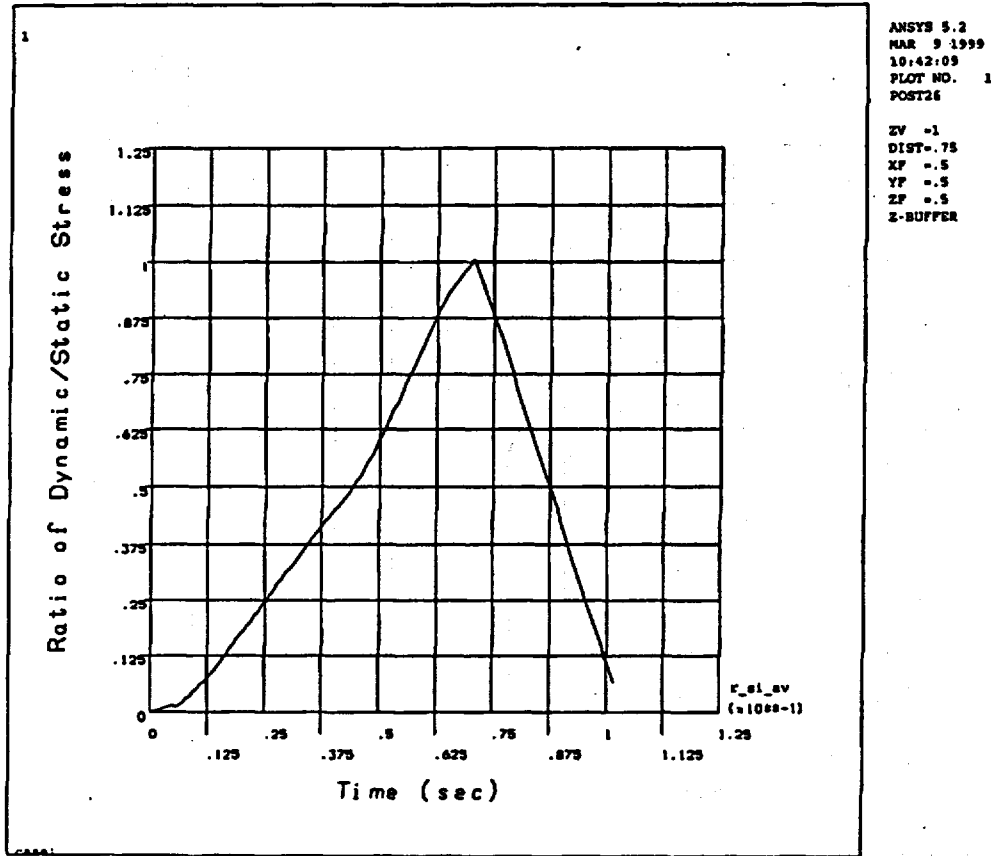


Figure 2.7.11.5-3 Time History for the Ratio of the Dynamic Stress to the Static Stress (SDLF) for the Yankee-MPC Canister Structural Lid Weld (Nominal Gap Stiffness Value)



2.7.12 CY-MPC Transportable Storage Canister Analysis – Accident Conditions

This section presents the evaluation of the CY-MPC transportable storage canister for the hypothetical accident conditions. The evaluation for normal conditions of transport is presented in Section 2.6.15.

The principal components of the canister are the canister shell, including the bottom plate, the fuel basket, the shield lid, and the structural lid. A description of the geometry and materials of construction of the canister, baskets, and spacer are provided in Section 1.2.1.2.8.

The general arrangement of the canister, depicted with the fuel basket, is shown in Figure 2.7.13-1.

A drop accident stress evaluation is performed for the 30-foot side drop condition, and for the 30-foot top and bottom end drop conditions. The stress intensities resulting from these two evaluations bound those that result from the 30-foot corner and oblique drop conditions. This conclusion is based on the analysis results for the directly loaded fuel configurations described in Sections 2.6.12, 2.7.1.3, 2.7.1.4, and 2.7.8.

The canister spacer in the cask cavity may crush during the corner, oblique and end drop loading conditions. In crushing, it will reduce the total g load on the fuel and canister that would occur in the hypothetical accident conditions. However, no credit is taken for the presence of the canister spacer. All of the impact g load - 55 g for the side drop, and 56.1 g for the end drops - is assumed to be applied to the canister.

2.7.12.1 Canister - Accident Analysis Description

The canister is a right-circular shell fabricated from rolled 5/8-inch thick, Type 304L stainless steel plate. It is closed on its bottom end with a Type 304L stainless steel circular plate that is 1.75-inches thick. The canister is closed at the top end by a 5-inch thick, Type 304 stainless steel shield lid, which is seal welded to the canister shell. The shield lid is covered by a 3-inch thick, Type 304L, stainless steel structural lid welded to the canister shell at its top inside edge. The canister is the defined confinement boundary for spent fuel or GTCC waste contents during long-term storage, and it is the defined containment boundary for intact fuel and Reconfigured Fuel Assemblies during transport, satisfying the requirements of 10 CFR 71.63(b) for a separate

inner container. The NAC-STC cask, using the same containment boundary defined for the directly loaded fuel configuration, provides the primary containment boundary in transport.

The structural design criteria for the canister is the ASME Code Section III, Subsection NB, "Class 1 Components." Consistent with this criteria, the structural components of the canister (shell, bottom plate, and structural lid) are shown to satisfy the allowable stress intensity limits presented in Table 2.1.2-1.

The canister is evaluated using the ANSYS finite element program for the 30-foot drop conditions in the end and side impact orientations. The ANSYS finite element model is the same as that used for the evaluation of the 1-foot drop impacts evaluated for normal conditions of transport. The model is described in Section 2.6.15.2. As described in Section 2.6.15.2, the COMBIN40 elements used between the structural and shield lids and for the backing ring are assigned a gap sizes of 1E-8 inches. The maximum gap size is 0.08 inches. However, use of the smaller gap size results in the highest stresses at critical sections, resulting in the lowest margin of safety. All gap-spring elements are assigned a stiffness of 1E8 lb/in.

2.7.12.2 Analysis Results

The detailed results of the analysis for the 30-foot side, and top and bottom end drops are presented in Tables 2.7.12-1 through 2.7.12-6. The section stresses presented in the tables are identified by a section number. A cross-section of the canister showing the section numbers is presented in Figure 2.7.12-1. A summary of the canister minimum Margins of Safety for the evaluated drop conditions is shown in Table 2.7.12-7.

For the top and bottom end drops, the stresses are essentially uniform around the circumference. For the side drop, the stresses vary around the circumference. Therefore, the circumferential angle at which the maximum stress occurs is noted in the table, (in parentheses) beside the section number. The allowable stresses presented in the tables are for Type 304L stainless steel, except for section 10, which is for Type 304 stainless steel. These allowables are evaluated at 350°F (maximum calculated temperature in the canister is 349°F). The allowable stress for P_m stresses is defined as the lesser of $2.4 S_m$ or $0.7 S_u$. The allowable stress for the $P_m + P_b$ stresses is defined as the lesser of $3.6 S_m$ or $1.0 S_u$.

The canister structural lid closure weld is specifically evaluated for the hypothetical accident conditions. The lid weld is identified as Section 8 in Figure 2.7.12-1. The structural lid weld has a root and final weld surface Liquid Penetrant examination performed in accordance with ASME Code, Section V, Article 6. The weld is ultrasonically examined in accordance with ASME Code Section V, Article 5, or multi-pass liquid penetrant examined in accordance with ASME Code Section V, Article 6. In accordance with NRC guidance, if a multi-pass liquid penetrant examination is performed on the structural lid closure weld, a weld stress reduction factor is applied to the structural lid canister shell weld – a 0.8 factor to conservatively consider the weld configuration, in accordance with NRC ISG-4, Item 5. Thus, a weld stress reduction factor of 0.8 is applied to the stress allowable for the structural lid weld. The canister closure weld evaluation for accident conditions is presented in Section 2.7.12.4. The evaluation, which is based on the finite element analysis stress result as shown in Section 2.7.12.2, shows a minimum margin of safety of +0.65 for the weld.

2.7.12.3 Canister Buckling Evaluation for the 30-Foot End Drop

The canister shell is axially loaded by the weights of the structural lid, the shield lid, and the inertial weight of the shell during a 30-foot end drop impact. The impact load amplification factor is 56.1g's. The shell is evaluated as an unsupported, right circular cylinder using a critical buckling load per Blake, 2nd Edition, "Practical Stress Analysis in Engineering Design."

$$S_{cr} = \frac{E(0.605 - 10^{-7} M^2)}{M(1 + 0.004\phi)}$$
$$= 40.3 \text{ ksi}$$

The canister material is Type 304L stainless steel. Conservatively assume the material temperature to be at 400°F for the accident condition.

$$E = 26.5E+03 \text{ ksi} \quad R = (69.39 + 0.625)/2$$
$$= 35.01 \text{ inches (mid-radius of the canister shell)}$$
$$S_y = 17.5 \text{ ksi} \quad t = 0.625 \text{ inches (thickness of the canister)}$$
$$\phi = E/S_y \quad \text{and} \quad M = R/t$$
$$= 1514.3 \quad = 56.0$$

The axial compression load in the canister shell is:

$$P_a = [(\pi/4) (69.03^2) (8)(0.291) + (\pi/4)(70.64^2 - 69.39^2)(151.75)(0.291)] (56.1)$$

$$P_a = 829,350 \text{ pounds}$$

and the axial compression stress is:

$$S_a = \frac{P_a}{(\pi/4)(70.64^2 - 69.39^2)}$$

$$S_a = 6,033 \text{ psi}$$

The margin of safety is:

$$(S_{cr}/S_a) - 1 = + 5.7$$

2.7.12.4 CY-MPC Canister Closure Weld Evaluation – Accident Conditions

2.7.12.4.1 Stress Evaluation for the CY-MPC Canister Closure Weld

The closure weld for the canister is a partial penetration grooveweld. The evaluation of this weld, in accordance with NRC guidance, incorporates a weld stress reduction factor of 0.8 based on NRC ISG-4, Item 5. The weld stress reduction factor is incorporated by applying a factor of 0.8 to the stress allowable for this weld.

The stresses for the canister are evaluated using sectional stresses as permitted by Subsection NB. The canister stress results from Section 2.7.12.2 are used for evaluation. The location of the section for the canister weld evaluation is shown in Figure 2.7.12-1 and corresponds to Section 8. The P_m and $P_m + P_h$ stress intensity for Section 8 and the associated allowables are listed below. The factored allowables, incorporating a 0.8 stress reduction factor, and the resulting margin of safety are:

Stress Type	Analysis Stress Intensity (ksi)	0.8 x Allowable Stress (ksi)	Margin of Safety
P_m	15.14	31.2	1.06
$P_m + P_b$	20.89	46.8	1.24

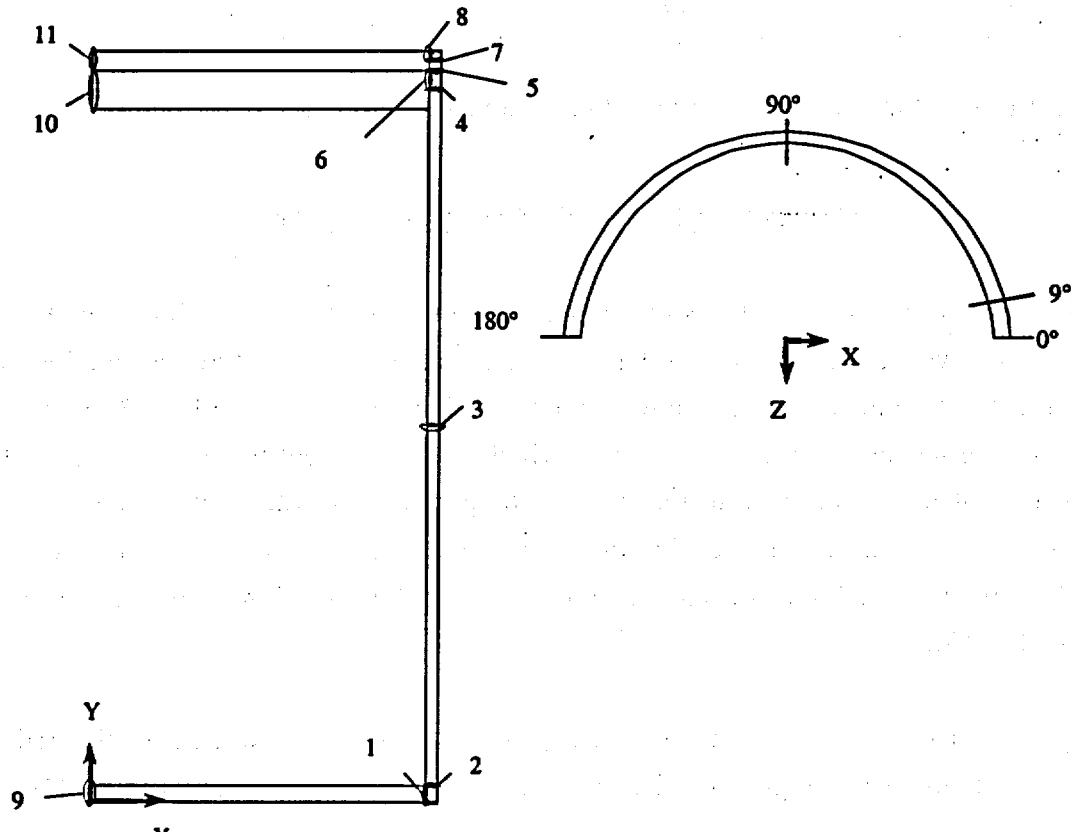
This confirms that the canister closure weld is acceptable for the accident conditions.

2.7.12.4.2 Critical Flaw Size for the Canister Closure Weld

The closure weld for the canister is comprised of multiple weld beads using a compatible weld material for Type 304L stainless steel. An allowable (critical) flaw evaluation has been performed to determine the critical flaw size in the weld region. The result of the flaw evaluation is used to define the minimum flaw size, which must be identifiable in the nondestructive examination of the weld. Due to the inherent toughness associated with Type 304L stainless steel, a limit load analysis is used in conjunction with a J-integral/tearing modulus approach. The safety margins used in this evaluation correspond to the stress limits contained in Section XI of the ASME Code.

The stress component used in the evaluation for the critical flaw size is the radial stress component in the weld region of the structural lid. For an accident (Level D) event, in accordance with ASME Code Section XI, a safety factor of $\sqrt{2}$ is required. For the purpose of identifying the stress for the flaw evaluation, the weld region corresponding to Section 8 in Figure 2.7.12-1 is considered. From additional post processing of the tipover analysis, the maximum tensile radial stress is 2.6 ksi. To perform the flaw evaluation, a 10 ksi stress is conservatively used, resulting in a significantly larger safety factor than the required safety factor of $\sqrt{2}$. Using 10 ksi as the basis for the evaluation, the minimum detectable flaw size is 0.52 inch for a flaw that extends 360 degrees around the circumference of the canister. Stress components for the circumferential and axial directions are also determined, which would be associated with flaws oriented in the radial or horizontal directions, respectively. The maximum stress for these components is 0.7 ksi, which is enveloped by the stress value used for the critical flaw evaluation for the radial direction. The 360-degree flaw employed for the circumferential direction is considered to be bounding with respect to any partial flaw in the weld, which could occur in the radial and horizontal directions. Therefore, using a minimum detectable flaw size of 3/8 inch is acceptable, since it is less than the very conservatively determined 0.52-inch critical flaw size.

Figure 2.7.12-1 Identification of the Sections for Evaluating the Linearized Stresses in the CY-MPC Canister



Section	Node 1		Node 2	
	X	Y	X	Y
1	34.695	0.00	34.695	1.75
2	34.695	1.75	35.32	1.75
3	34.695	72.75	35.32	75.75
4	34.695	148.25	35.320	148.25
5	34.695	148.75	35.320	148.75
6	34.695	148.25	34.695	148.75
7	34.695	150.87	35.320	150.87
8	34.695	150.87	34.695	151.75
9	0.10	0.00	0.10	1.75
10	0.10	143.75	0.10	148.73
11	0.10	148.77	0.10	151.75

Table 2.7.12-1 CY-MPC Canister, 30-Foot Side Drop (Primary Membrane Stress) (ksi)

Section No.	Component Stresses						S.I.	Allow. Stress	Margin of Safety
	SX	SY	SZ	SXY	SYZ	SXZ			
1(0°)	-14.2	0.9	-9.5	0.1	-0.2	-0.8	15.19	39	1.57
2(9°)	3	1.4	-4.3	-0.2	-1.3	-1.7	8.38	39	3.65
3(18°)	-0.9	2.4	1.1	0	0.1	0.7	3.54	39	10.03
4(9°)	-21.9	4.1	-8.3	-1.7	2.5	1.3	26.8	39	0.46
5(0°)	-18.2	2.6	-10	-4.8	1.4	1	23.19	39	0.68
6(0°)	-28.9	-6.9	-13.3	-6	1.2	0.8	25.25	39	0.54
7(9°)	-16.0	1.0	-7.7	0.3	1.7	0.5	17.3	39	1.25
8(0°)	-20.4	-5.7	-9.5	-1.2	0.8	-0.5	15.14	31.2*	1.06
9	-2	0.1	0.9	0.1	0	0	2.85	39	12.67
10	-1	0	0.3	-0.1	0	0	1.29	39	29.26
11	-1.2	0	0.4	0	0	0	1.64	39	22.85

* Includes a stress reduction factor for the weld of 0.8 (See Section 2.7.12.4).

Table 2.7.12-2 CY-MPC Canister, 30-Foot Side Drop (Primary Membrane Plus Primary Bending Stress) (ksi)

Section No.	Component Stresses						S.I.	Allow. Stress	Margin of Safety
	SX	SY	SZ	SXY	SYZ	SXZ			
1(0°)	-24.9	0.2	-13	0.8	0	-0.5	25.16	58.5	1.33
2(36°)	-1.9	-16.9	-4.6	-0.3	1.1	-4.2	18.14	58.5	2.22
3(0°)	-1.1	2.8	2.8	0	0	0.5	4.02	58.5	13.54
4(9°)	-20.0	11.7	-6.7	-0.6	2.8	2.4	32.6	58.5	0.79
5(0°)	-16.5	6.6	-10.3	-3.1	1.9	1.2	24.38	58.5	1.4
6(0°)	-35.6	-9.2	-15.8	-6	1.5	0.8	29.16	58.5	1.01
7(9°)	-14.0	6.1	-6.4	0.9	1.5	1.4	20.6	58.5	1.84
8(0°)	-30	-10.1	-13.7	-2.5	1.4	0	20.89	46.8*	1.24
9	-2.2	0.1	0.9	0.1	0	0	3.08	58.5	17.98
10	-1.2	0	0.4	-0.1	0	0	1.6	58.5	35.63
11	-1.4	0	0.4	0	0	0	1.82	58.5	31.09

* Includes a stress reduction factor for the welds of 0.8 (See Section 2.7.12.4).

Table 2.7.12-3 CY-MPC Canister, 30-Foot Bottom End Drop Without Internal Pressure
(Primary Membrane Stress) (ksi)

Section No.	Component Stresses						S.I.	Allow. Stress	Margin of Safety
	SX	SY	SZ	SXY	SYZ	SXZ			
1	0	-2	-0.3	-0.1	0	0	2.04	39	18.2
2	0.4	-5.1	-1	-0.2	0	-0.1	5.54	39	6.0
3	0	-4.8	0	0	0	0	4.83	39	7.1
4	-1.2	-3.2	-2.8	-0.9	0.1	-0.1	2.64	39	13.8
5	3.1	-2.3	-1.5	0.5	0	-0.3	5.48	39	6.1
6	1.4	3.1	-0.5	0.4	0.1	-0.2	3.67	39	9.6
7	-3.4	1.2	-1.5	-0.3	0	0.1	4.59	39	7.5
8	0.3	-3.3	-2	-0.5	0.1	-0.2	3.78	31.2*	7.3
9	0.1	-0.8	0.1	0	0	0	0.83	39	45.7
10	0.3	-0.1	0.3	0	0	0	0.35	39	109.6
11	-0.4	-0.1	-0.4	0	0	0	0.31	39	125.5

* Includes a stress reduction factor for the weld of 0.8 (See Section 2.7.12.4).

Table 2.7.12-4 CY-MPC Canister, 30-Foot Bottom End Drop (Primary Membrane Plus Primary Bending Stress) (ksi)

Section No.	Component Stresses						S.I.	Allow. Stress	Margin of Safety
	SX	SY	SZ	SXY	SYZ	SXZ			
1	0.1	-2.7	-0.4	-0.3	0	0	2.81	58.5	19.8
2	0.2	-7.1	-1.5	-0.1	0	-0.1	7.28	58.5	7.0
3	0	-4.8	0	0	0	0	4.83	58.5	11.1
4	-0.8	-6.6	-3.6	-1.2	0.1	-0.2	6.29	58.5	8.3
5	1.1	-11.6	-4.6	-0.4	0	-0.4	12.77	58.5	3.6
6	4.9	6.2	1.2	1.3	0.1	-0.3	5.84	58.5	9.0
7	-2	9.8	1.2	-0.5	0	0.2	11.77	58.5	4.0
8	4.3	-0.4	-0.4	-0.6	0.1	-0.3	4.95	46.8*	8.5
9	0.1	-0.8	0.1	0	0	0	0.93	58.5	61.7
10	5.8	-0.1	5.8	0	0	0	5.85	58.5	9.0
11	-3.9	0	-3.9	0	0	0	3.89	58.5	14.0

* Includes a stress reduction factor for the weld of 0.8 (See Section 2.7.12.4).

Table 2.7.12-5 CY-MPC Canister, 30-Foot Top End Drop (Primary Membrane Stress) (ksi)

Section No.	Component Stresses						S.I.	Allow. Stress	Margin of Safety
	SX	SY	SZ	SXY	SYZ	SXZ			
1	0	-0.8	-0.3	-0.1	0	0	0.8	39	47.6
2	-0.4	0.5	1	-0.1	0	-0.1	1.46	39	25.8
3	0	-1.4	1.1	0	0	-0.1	2.51	39	14.5
4	0.3	-2.4	-0.3	-0.2	0	0	2.68	39	13.6
5	-0.2	-2.2	-0.4	-0.1	0	0	1.94	39	19.1
6	-0.1	-1.1	-0.1	-0.2	0	0	1.11	39	34.0
7	0	-2	-0.3	0	0	0	1.94	39	19.1
8	0	-1.5	-0.2	0	0	0	1.47	31.2*	20.2
9	-0.1	0	-0.1	0	0	0	0.1	39	391
10	0	-0.8	0	0	0	0	0.78	39	48.7
11	0	-0.8	0	0	0	0	0.76	39	50.2

* Includes a stress reduction factor for the weld of 0.8 (See Section 2.7.12.4).

Table 2.7.12-6 CY-MPC Canister, 30-Foot Top End Drop (Primary Membrane Plus Primary Bending Stress) (ksi)

Section No.	Component Stresses						S.I.	Allow. Stress	Margin of Safety
	SX	SY	SZ	SXY	SYZ	SXZ			
1	-0.5	-1.9	0.3	0	0	0	2.27	58.5	24.8
2	-0.2	3.6	1.9	-0.3	0	-0.2	3.94	58.5	13.9
3	0	-1.4	1.1	0	0	-0.1	2.52	58.5	22.2
4	0.1	-3.6	-0.7	-0.1	0	0.1	3.69	58.5	14.9
5	-0.1	-3	-0.6	-0.2	0	0	2.95	58.5	18.9
6	0.4	-1	0.1	-0.2	0	0	1.44	58.5	39.7
7	0	-2.3	-0.4	0	0	0	2.22	58.5	25.4
8	0.1	-1.4	-0.1	0	0	0	1.5	46.8*	30.2
9	-3	0	-3	0	0	0	3.04	58.5	18.2
10	0.2	-0.8	0.2	0	0	0	0.96	58.5	60.0
11	0.1	-0.7	0	0	0	0	0.8	58.5	71.9

* Includes a stress reduction factor for the weld of 0.8 (See Section 2.7.12.4).

Table 2.7.12-7 Summary of Minimum Margin of Safety for CY-MPC Canister 30-Foot Drops

Drop Orientation	Loading Condition	Stress Evaluated	Minimum Margin of Safety	Section No.*
Bottom end	30-ft. impact + pressure (0 psi)	P_m	6.0	2
Bottom end	30-ft. impact + pressure (0 psi)	$P_m + P_b$	3.6	5
Side	30-ft. impact + pressure (20 psi)	P_m	0.46	4
Side	30-ft. impact + pressure (20 psi)	$P_m + P_b$	0.79	4
Top end	30-ft. impact + pressure (20 psi)	P_m	13.6	4
Top end	30-ft. impact + pressure (20 psi)	$P_m + P_b$	13.9	2

* See Figure 2.7.12-1 for section locations.

2.7.13 CY-MPC Fuel Basket Analysis - Accident Conditions

There are two different NAC-STC canistered fuel basket assemblies for Connecticut Yankee class fuel. The first fuel basket is designed to accommodate up to 24 fuel assemblies. The second fuel basket is designed to accommodate up to 26 fuel assemblies. The 26-fuel assembly basket supports the maximum load with the minimum structure. Therefore, only the 26-fuel assembly basket is considered in this analysis.

The fuel basket assembly analyzed herein is a right cylinder structure and is fabricated with the following components: 26 square fuel tubes, 28 circular support disks, 27 heat transfer disks, 6 tie rods with split spacers, and two end weldment plates.

The basket components and their geometry are illustrated in Figure 2.7.13-1 and Figure 2.7.13-2. The basket contains two sizes of fuel tubes. There are 22 standard and 4 oversized fuel tubes. The standard fuel tube has an 8.72-inch square inside dimension, 0.141-inch thick composite wall. The oversized fuel tube has a 9.12-inch square inside dimension, a 0.141-inch thick composite wall. Both fuel tubes hold the design basis Connecticut Yankee Class fuel assembly. The fuel tubes are open at each end. Therefore, longitudinal fuel assembly loads are imparted to the cask body and not the fuel basket structure.

The fuel assemblies, together with the tubes are laterally supported in the holes in the stainless steel support disks. Each support disk is 0.5 inches thick, 69.15 inches in diameter and has 26 holes. There are 22 holes that are each 9.17 inches square and 4 holes that are 9.57 inches square. There are four web thicknesses in the support disks; 1.50 inch, 1.25 inch, 1.10 inch, and 1.00 inch. The widest web is nearest the center of the basket, the web decreases in width towards the outer radius of the basket. The support disks are equally spaced at 4.09 inches.

The weldments are geometrically similar to the support disks and are 68.98 inches in diameter and .50 in thick. The top weldment includes support ribs and an outer ring. The bottom weldment includes support ribs and tie rod support bosses. The total heights of the top and bottom weldments are 6.8 and 2.0 inches, respectively.

Twenty-seven (27) aluminum heat transfer disks are interleaved with the support disks to fully optimize the passive heat rejection from the package. Each heat transfer disk is 0.50-inch thick, 68.9 inches in diameter, and has 26 holes for the fuel tubes. There are 22 standard holes that are 9.14 inches square and 4 oversized holes that are 9.54 inches square. There are five different web widths,

1.56 inches, 1.46 inches, 1.26 inches, 1.16 inches, and 1.06 inches. The widest aluminum web is nearest the center of the basket to optimize passive heat rejection. The dimensional differences between the heat transfer disk and the support disk accommodates the different rate of thermal growth between aluminum and stainless steel preventing interference between the tube, the support disk, and heat transfer disks. The heat transfer disks, which serve no structural function, are supported by the six (6) tie rods with split spacers. Each tie rod has 3.0 inches of 1 5/8-8 UN-2A threads at the upper end of the rod, which thread into the top nuts that clamp against the top weldment. The fuel basket contains the fuel and is laterally supported by the canister shell.

The 28 support disks and 2 end weldments are fabricated from 17-4 PH and Type 304 stainless steels, respectively. The 27 heat transfer disks are fabricated from Type 6061-T651 aluminum alloy. The 26 fuel tubes are fabricated from Type 304 stainless steel. The tie rods and spacers are fabricated from Type 304 stainless steel. The stainless steel tubes are not considered to be a structural component with respect to the disks and are not included in the basket or weldment analyses. The primary function of the split spacers and the threaded top nut is to locate and structurally assemble the support disks, heat transfer disks and the top and bottom weldment plates into an integral assembly. The spacers carry the inertial weight of the support disks, heat transfer disks, one end plate, and their own inertial weight for a normal transport condition 1-foot end drop. The end drop loading of the split spacers and tie rods represent a classical closed form structural analysis. Therefore the only component that requires a detailed finite element analysis is the support disk.

The fuel basket is evaluated for the hypothetical accident loads in this section and is evaluated for the normal transport condition in Section 2.6.16.

Figure 2.7.13-1 CY-MPC Canistered Fuel Basket

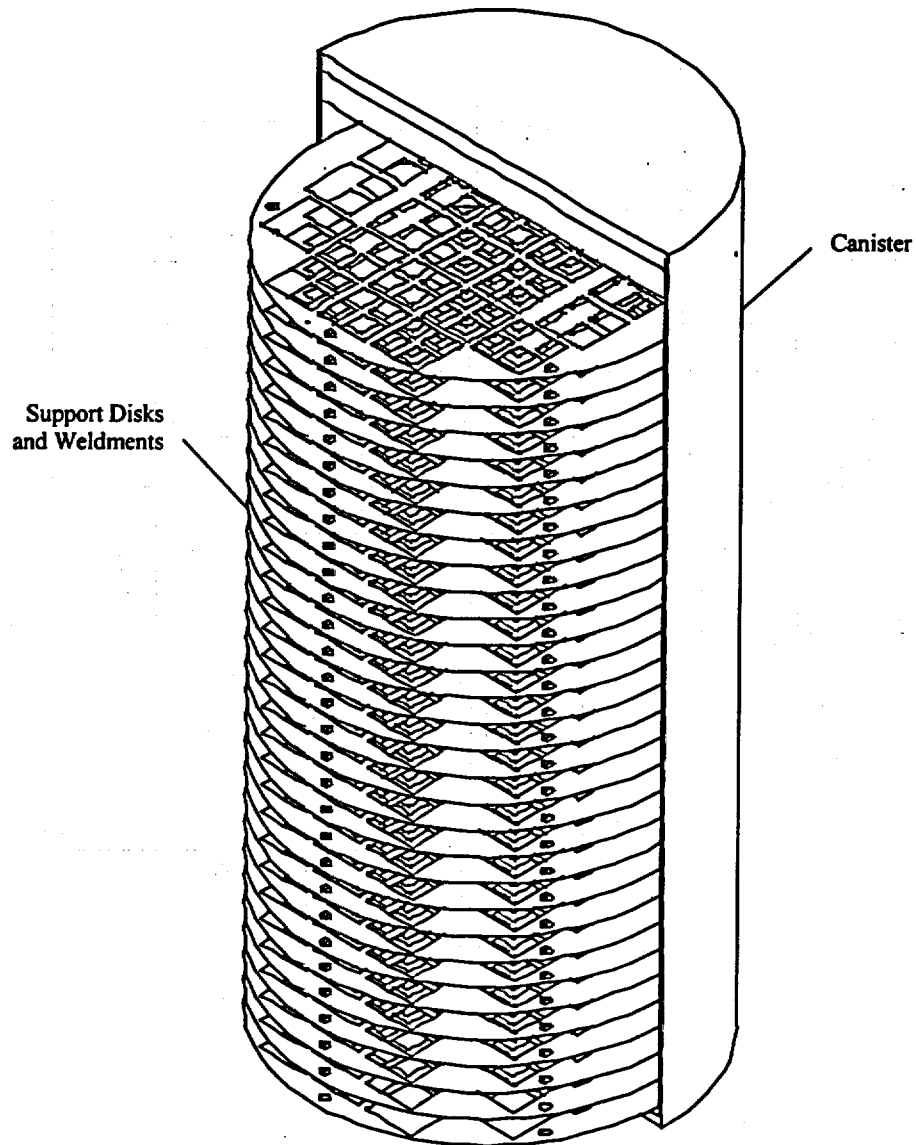
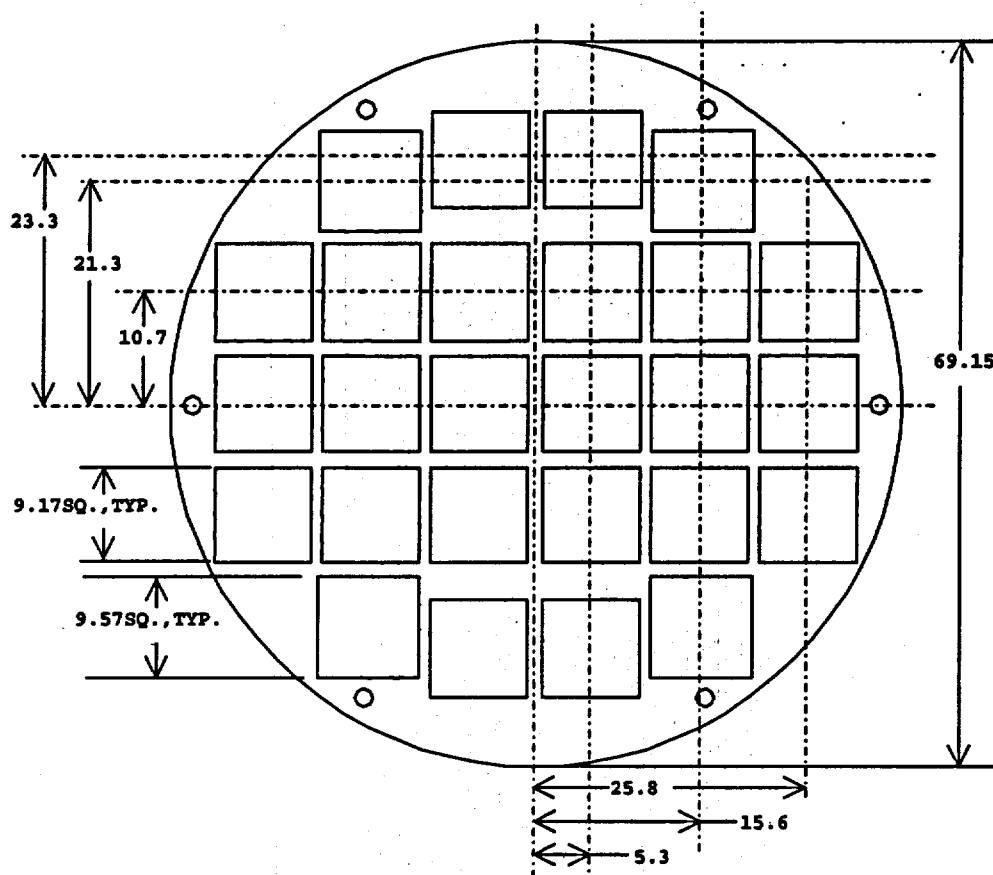


Figure 2.7.13-2 CY-MPC Basket Support Disk Configuration



2.7.13.1 Stress Evaluation of CY-MPC Support Disk

Based on criticality control requirements, the canistered fuel basket design criteria requires the maintenance of fuel support and control of spacing of the fuel assemblies for all load conditions. The structural design criteria for the fuel basket is the ASME Boiler and Pressure Vessel Code, Section III, Division 1, Subsection NG, "Core Support Structures." Consistent with this criteria, the main structural component in the fuel basket, the stainless steel support disk, is shown to have a maximum primary membrane stress intensity less than the allowable stress limit, defined as $0.7 S_u$, for the accident condition. Likewise the primary membrane plus bending stress intensity is shown to be less than the allowable stress limit, defined as $1.0 S_u$. The value of S_u is defined at conservatively high temperatures for the component being analyzed.

For the side drop conditions, four basket drop orientations (0° , 38° , 63° , and 90°) are considered, as shown in Figure 2.7.13.1-1. Angles of 38° and 63° were selected because minimal web thickness occurs at these orientations.

In the side drop, the loads of the fuel assemblies are transferred into the plane of the support disks, from which they are transmitted to the canister shell, and then to the cask body (cask inner shell). In the end drop, the support disks are loaded only by their own inertial mass and do not experience load from the guided, but free standing fuel assemblies.

Finite element models are used to perform analyses for end drop and side-drop conditions using the ANSYS program. In addition to the load from inertial weight, the analyses also consider the stresses due to differential thermal expansion.

Analyses for combined, or oblique angle drops are also performed. The stresses due to the side and end drop load conditions are combined according to the cask angle, as shown in Figure 2.7.13.1-2.

Figure 2.7.13.1-1 Basket Drop Orientations

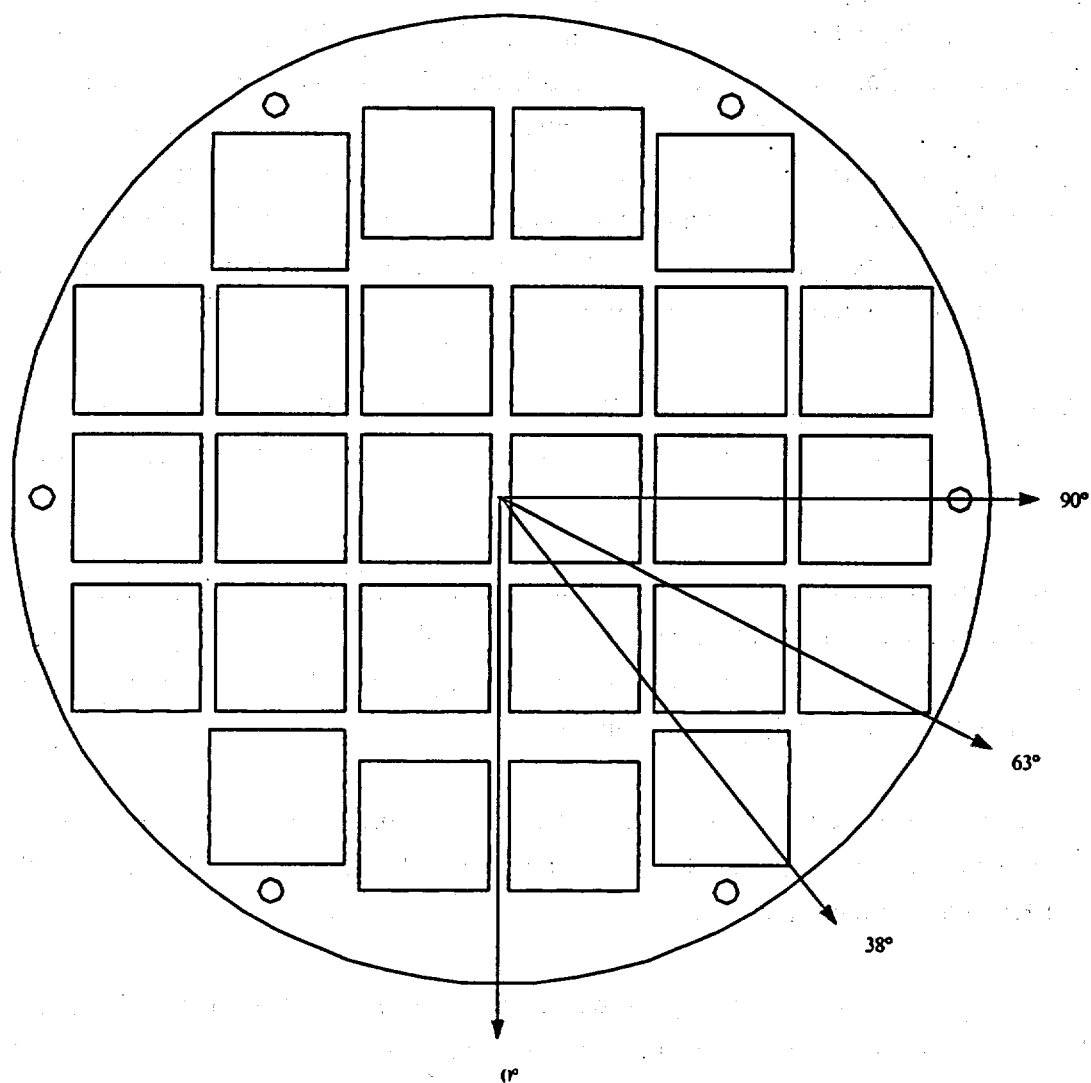
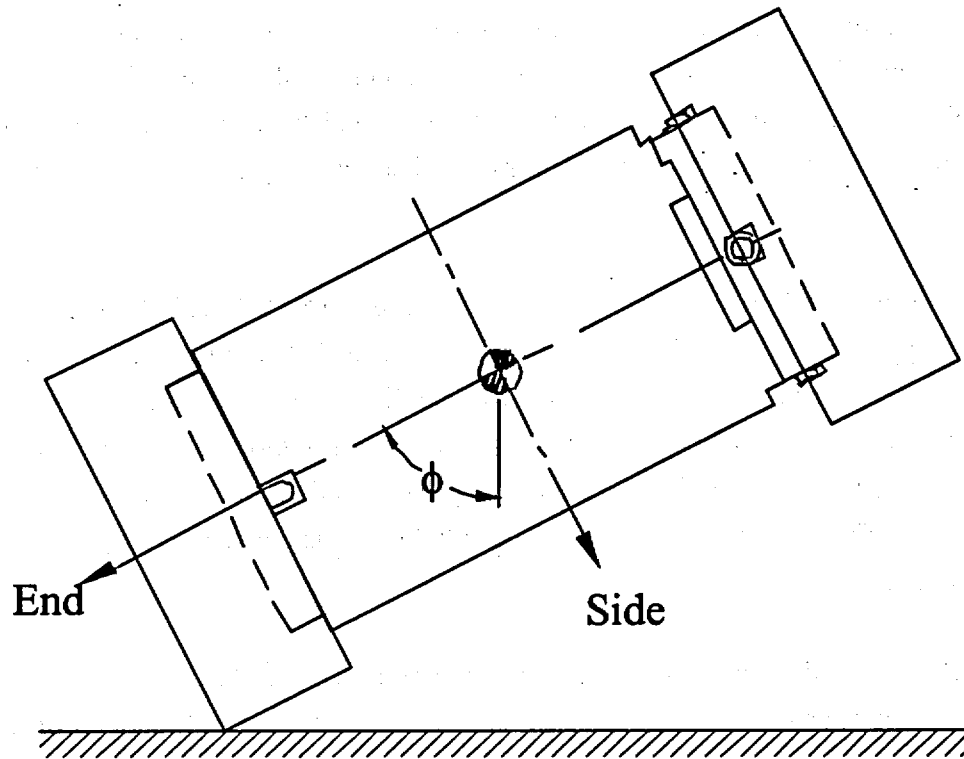


Figure 2.7.13.1-2 Cask Orientation



2.7.13.1.1 Finite Element Model Description - CY MPC Fuel Basket

Two finite element models were generated to analyze the CY-MPC fuel basket for the normal operating conditions. The first model simulates the side drop (Figure 2.6.16.2-1) at the basket orientations shown in Figure 2.7.13.1-1. The second model simulates the end drop. These results are then combined to simulate various oblique drops. All calculations accommodate thermal expansion effects using the temperature distribution from the thermal analysis and the coefficient of thermal expansion.

The model for the end drop simulation is constructed using ANSYS SHELL63 elements. It consists of a single support disk with a thickness of 0.5 inch. The shell elements accommodate the out-of-plane bending, which is present in the end-drop condition. The support disk is restrained in the direction of the drop by the split spacers on the six tie rods. Therefore, the nodes corresponding to the location of the tie rods are restrained in the out of plane direction (the cask axial direction) as well as all 5 remaining DOF to stabilize the model. The only loading is the inertial weight of the support disk in the out-of-plane direction.

The finite element model for the side-drop evaluation of the support disk is a three-dimensional model and includes a slice, or section of the canister and cask as well as a single support disk. The canister and the cask body are included in the model to more accurately simulate the boundary conditions for the support disk. The top and bottom portions of the canister and transport cask are not considered in this analysis. Neglecting these end effects is conservative because it allows slightly more deformation of the canister shell and the support disks. In the support disk side drop models, the canister shell and the cask body are modeled with SOLID45 elements. To increase the accuracy of the analysis, the element size is reduced towards the intersections of the ligaments.

While the cask, canister and support disk are modeled explicitly, the impact limiters are represented by CONTAC52 elements. Cask and impact limiter modeling reflect the same approach as described in Section 2.6.7.4. The load from each fuel assembly is modeled as a line-pressure on the inner surfaces of each support disk opening.

To determine the most critical regions, a series of 131 cross sections are considered. To aid in the identification of these sections, Figure 2.6.16.2-5 shows the section locations on a support disk for all of the side drop cases. Table 2.6.16.2-1 lists the geometric locations of the end points for each cross section.

2.7.13.1.2 Stress Evaluation of CY-MPC Support Disk for a 30-Ft End Drop Condition

Six (6) tie rods locate the support disks of the CY-MPC fuel basket with spacers. A structural analysis is performed using ANSYS to evaluate the effect of a 30-foot end drop impact, which corresponds to the most severe out-of-plane loading under hypothetical accident conditions. The model described in Section 2.7.13.1.1 is used with a 56.1g deceleration. Linearized stresses at the cross sections identified in Figure 2.6.16.2-5 are compared to stress allowables in accordance with the ASME Code, Section III, Subsection NG. Tables 2.7.13.1.2-1 and 2.7.13.1.2-2 list the 10 highest P_m and $P_m + P_b$ stress intensities, respectively.

The worst case results for the 30-foot end drop condition are summarized as:

P_m		$P_m + P_b$	
Stress Intensity (ksi)	M.S.	Stress Intensity (ksi)	M.S.
72.4	.23	103.2	.24

The margin of safety (M.S.) is calculated as: $M.S. = (\text{Stress Allowable}/\text{Stress Intensity}) - 1$.

Table 2.7.13.1.2-1 P_m Stresses for CY-MPC Support Disk – 30 Foot End Drop

Section*	Sx (ksi)	Sy (ksi)	Sxy (ksi)	Stress Intensity (ksi)	Allowable Stress (ksi)	Margin of Safety
61	66.6	-5.3	19.4	72.4	89.3	0.23
63	67.1	-5.3	-18.3	72.1	89.3	0.24
1	67.2	-4.8	-18.7	72.7	91.7	0.26
3	66.7	-5.2	19.3	72.6	91.7	0.26
131	17.7	20.6	-16.3	50.3	91.1	0.81
111	2.5	-44.0	3.0	44.2	89.3	1.02
129	-39.5	6.0	-13.3	44.2	89.3	1.02
125	-39.5	6.2	-13.4	44.2	90.2	1.04
62	28.1	13.9	-0.2	42.0	89.3	1.13
93	1.0	-41.3	-3.4	41.6	89.5	1.15

* See Figure 2.6.16.2-5 for section locations and definition of coordinate system.

Table 2.7.13.1.2-2 P_m+P_b Stresses for CY-MPC Support Disk—30-Foot End Drop

Section*	Sx (ksi)	Sy (ksi)	Sxy (ksi)	Stress Intensity (ksi)	Allowable Stress (ksi)	Margin of Safety
61	89.0	-18.7	34.6	103.2	127.6	0.24
63	89.0	-19.0	-31.9	101.4	127.6	0.26
3	88.7	-18.4	34.0	102.5	131.1	0.28
1	89.2	-17.9	-32.1	101.5	131.1	0.29
76	6.5	-52.6	17.1	65.3	127.8	0.96
93	4.8	-53.0	-16.7	65.0	127.8	0.97
94	6.4	-52.5	-16.7	64.6	127.6	0.98
111	4.9	-55.9	15.3	63.6	127.6	1.01
131	21.1	25.2	-17.5	52.8	130.2	1.47
129	-44.9	10.0	-14.0	49.9	127.6	1.56

* See Figure 2.6.16.2-5 for section locations and definition of coordinate system.

2.7.13.1.3 Stress Evaluation of CY MPC Support Disk for a 30-Ft Side Drop Condition

The structural adequacy of the support disk in the CY-MPC fuel basket for the 30-foot side-drop impact load condition was determined. A quasi-static impact load equal to the weight of the fuel and tubes multiplied by a 55g-amplification factor is applied to the support disk structure. The inertial loading of the support disk is also included via the density input for the 17-4 PH stainless steel. The fuel assembly load is transmitted in direct compression through the tube wall to the web structure of the support disk. A finite element analysis is performed using the three-dimensional support disk side model described in Section 2.7.13.1.1. As discussed in Section 2.7.13.1, four bounding cases of basket orientation (0° , 38° , 63° , and 90°) are considered in the analysis. The material properties are evaluated at a combined worst case thermal condition. This condition is based on the maximum support disk temperature from Thermal Condition 1 and the maximum temperature gradient across the disk from Thermal Condition 2. Linearized stresses at 131 cross-sections (see Figure 2.6.16.2-5) are compared to the stress allowable per the ASME Code, Section III, Subsection NG. The allowable stress is $0.7S_u$ for P_m , and $1.0 S_u$ for $P_m + P_b$ stresses, respectively.

The stress evaluation results for the 30-foot side-drop condition are summarized in Table 2.7.13.1.3-1. The minimum margin of safety is +0.26, which occurs for the 38° basket drop orientation. Tables 2.7.13.1.3-2 through 2.7.13.1.3-9 list the 30 highest P_m and $P_m + P_b$ stress intensities for each basket orientation considered.

Table 2.7.13.1.3-1 Summary of CY-MPC Support Disk Stresses for 30-Foot Side Drop

P_m		P_m+P_b	
Section	Margin of Safety	Section	Margin of Safety
0° Basket Orientation			
11	1.14	1	1.48
13	1.16	3	1.50
1	1.49	11	1.64
3	1.50	9	1.65
9	1.59	13	1.67
38° Basket Orientation			
73	0.80	1	0.26
1	1.43	2	0.58
6	1.74	13	0.61
7	1.92	26	0.62
13	2.08	11	0.63
63° Basket Orientation			
73	1.06	43	0.62
24	1.61	106	0.72
39	1.62	13	0.72
108	1.77	3	0.72
66	2.02	28	0.73
90° Basket Orientation			
108	0.87	129	1.18
90	0.88	108	1.49
105	1.55	90	1.52
87	1.56	44	1.66
110	1.95	24	1.69

Note: See Figure 2.6.16.2-5 for section locations and definition of coordinate system.

Table 2.7.13.1.3-2 P_m Stresses for CY-MPC Support Disk 30-Foot Side Drop,
0° Basket Orientation

Section	Sx (ksi)	Sy (ksi)	Sxy (ksi)	Stress	Allowable	Margin of Safety
				Intensity (ksi)	Stress (ksi)	
11	-21.2	-21.0	2.0	42.3	90.6	1.14
13	-21.1	-20.7	-1.9	41.9	90.6	1.16
1	-31.5	-5.4	0.7	36.9	91.7	1.49
3	-31.4	-5.3	-0.7	36.7	91.7	1.50
9	-31.2	-3.8	-0.4	35.1	90.9	1.59
7	-31.1	-2.9	0.0	34.0	90.9	1.67
5	-33.3	0.1	0.0	33.3	91.6	1.75
12	-21.3	-9.6	0.0	30.9	90.7	1.93
27	-18.4	-12.0	0.0	30.3	89.6	1.96
4	-30.4	0.0	-1.1	30.5	91.3	1.99
6	-30.3	0.0	1.1	30.4	91.3	2.00
131	-27.2	11.2	7.6	30.3	91.1	2.01
26	-15.3	-12.8	1.1	28.2	89.6	2.18
28	-15.3	-12.7	-1.1	28.0	89.6	2.20
8	-26.1	14.7	0.0	26.1	90.9	2.49
73	-17.5	-8.3	1.1	25.9	90.6	2.50
66	-17.4	-8.3	-1.1	25.8	90.6	2.51
2	-25.4	-0.9	0.0	26.3	92.4	2.51
17	-25.4	0.0	0.0	25.4	90.1	2.55
16	-24.2	0.0	-0.9	24.2	90.1	2.72
18	-24.1	0.0	0.9	24.2	90.1	2.73
69	-19.4	-3.8	-1.2	23.4	90.7	2.88
70	-19.3	-3.9	1.2	23.3	90.7	2.89
42	-13.7	-8.8	0.0	22.6	89.3	2.96
22	-21.6	11.2	0.0	21.6	89.7	3.15
32	-20.1	0.0	0.0	20.1	89.3	3.45
21	-20.0	13.1	1.0	20.1	89.7	3.46
85	-16.7	-3.2	1.4	20.1	89.6	3.46
84	-16.7	-3.2	-1.4	20.1	89.6	3.46
23	-19.9	13.0	-1.0	20.1	89.7	3.47

Note: See Figure 2.6.16.2-5 for section locations and definition of coordinate system.

Table 2.7.13.1.3-3 P_m Stresses for CY-MPC Support Disk 30-Foot Side Drop,
38° Basket Orientation

Section	Sx (ksi)	Sy (ksi)	Sxy (ksi)	Stress	Allowable	Margin of Safety
				Intensity (ksi)	Stress (ksi)	
73	-50.1	2.7	3.8	50.4	90.6	0.80
1	-19.0	-18.8	-0.5	37.8	91.7	1.43
6	-32.8	0.4	-3.9	33.4	91.3	1.74
7	-17.7	-13.3	1.3	31.1	90.9	1.92
13	-23.5	-5.9	1.1	29.4	90.6	2.08
24	-12.7	28.0	3.8	28.9	89.6	2.10
39	-7.0	27.1	4.4	28.0	89.3	2.19
114	-25.6	-1.6	1.2	27.3	89.3	2.27
121	22.7	3.4	3.9	27.2	89.3	2.28
5	-25.7	0.3	-4.9	27.2	91.6	2.36
38	-13.2	23.3	6.5	26.5	89.3	2.37
23	-19.3	21.5	5.9	26.3	89.7	2.40
88	-23.8	9.2	6.5	26.2	89.6	2.42
103	-20.3	8.8	9.4	25.6	89.3	2.48
66	24.8	-2.7	1.7	25.0	90.6	2.63
14	-13.1	-11.5	1.6	24.8	90.4	2.65
64	-14.7	-9.1	3.4	24.7	90.4	2.66
18	-23.6	0.3	-3.2	24.2	90.1	2.73
106	-18.7	12.5	7.1	23.4	89.3	2.82
91	-20.4	12.2	5.7	23.4	89.6	2.83
3	-23.3	11.9	-1.3	23.4	91.7	2.91
70	-20.2	0.3	5.0	22.2	90.7	3.08
109	-14.9	15.5	6.6	21.8	89.3	3.09
9	-21.8	9.5	2.2	22.2	90.9	3.09
108	4.7	13.7	4.3	20.4	89.3	3.37
55	7.1	13.2	0.9	20.3	89.3	3.40
2	-19.3	-1.5	-1.4	21.0	92.4	3.40
17	-18.0	0.3	-5.0	20.4	90.1	3.41
12	-15.2	-5.3	0.4	20.5	90.7	3.42
8	-20.0	13.9	1.6	20.4	90.9	3.46

Note: See Figure 2.6.16.2-5 for section locations and definition of coordinate system.

Table 2.7.13.1.3-4 P_m Stresses for CY-MPC Support Disk 30-Foot Side Drop,
63° Basket Orientation

Section	Sx (ksi)	Sy (ksi)	Sxy (ksi)	Stress	Allowable	Margin of Safety
				Intensity (ksi)	Stress (ksi)	
73	-43.7	10.0	3.4	44.0	90.6	1.06
24	-7.6	33.7	4.1	34.3	89.6	1.61
39	-3.2	33.3	4.8	34.0	89.3	1.62
108	11.4	19.7	4.4	32.2	89.3	1.77
66	28.7	1.0	1.8	30.0	90.6	2.02
121	20.6	7.9	3.0	29.1	89.3	2.06
54	1.5	25.9	3.2	28.1	89.3	2.18
90	8.9	17.0	2.9	26.6	89.6	2.37
109	-16.5	22.1	6.1	26.1	89.3	2.43
110	-0.3	25.4	-1.7	25.6	89.3	2.49
106	-19.4	18.0	6.4	25.1	89.3	2.56
91	-20.7	19.5	5.0	25.1	89.6	2.56
38	-7.9	22.1	6.9	24.9	89.3	2.58
88	-21.5	15.4	5.6	24.8	89.6	2.61
75	7.6	17.3	0.4	24.9	90.4	2.63
103	-17.7	13.0	8.4	24.0	89.3	2.71
102	10.1	9.2	7.1	24.0	89.3	2.72
23	-11.7	20.8	6.1	23.8	89.7	2.76
105	6.5	15.2	4.3	23.3	89.3	2.84
1	-8.2	-15.2	-1.1	23.5	91.7	2.90
92	-0.3	22.7	-0.9	22.7	89.5	2.94
111	-9.4	22.3	-0.4	22.3	89.3	3.00
6	-21.3	0.5	-4.1	22.4	91.3	3.07
114	-20.2	-1.1	1.6	21.5	89.3	3.15
107	-0.2	20.8	-2.6	21.2	89.3	3.21
55	7.8	12.8	0.5	20.5	89.3	3.35
129	-8.3	18.6	-3.9	19.9	89.3	3.48
130	-15.4	7.0	7.6	19.9	90.1	3.53
99	11.8	5.2	5.0	19.7	89.3	3.53
64	-15.0	-3.9	3.0	19.8	90.4	3.57

Note: See Figure 2.6.16.2-5 for section locations and definition of coordinate system.

Table 2.7.13.1.3-5 P_m Stresses for CY-MPC Support Disk 30-Foot Side Drop,
90° Basket Orientation

Section	Sx (ksi)	Sy (ksi)	Sxy (ksi)	Stress	Allowable	Margin of Safety
				Intensity (ksi)	Stress (ksi)	
108	23.9	23.8	0.9	47.8	89.3	0.87
90	23.7	23.8	-0.9	47.6	89.6	0.88
105	16.4	18.6	0.6	35.0	89.3	1.55
87	16.4	18.6	-0.6	35.1	89.6	1.56
110	-0.1	30.3	-0.3	30.3	89.3	1.95
92	-0.1	30.3	0.3	30.3	89.5	1.96
39	9.2	20.5	2.6	30.1	89.3	1.96
29	9.2	20.5	-2.5	30.2	89.6	1.97
44	9.2	19.4	-1.6	28.8	89.3	2.10
14	9.7	19.1	-1.5	29.0	90.4	2.12
24	9.2	19.3	1.6	28.7	89.6	2.12
129	-19.9	20.2	-8.5	28.6	89.3	2.13
54	8.2	19.8	1.1	28.0	89.3	2.18
109	-10.7	26.7	0.9	26.7	89.3	2.34
102	13.8	12.8	0.9	26.7	89.3	2.35
91	-10.5	26.7	-0.9	26.7	89.6	2.35
84	13.8	12.8	-0.8	26.6	89.6	2.36
107	0.0	24.9	-0.3	24.9	89.3	2.59
89	0.0	24.9	0.3	24.9	89.6	2.60
130	-16.0	20.6	5.8	24.5	90.1	2.68
111	-13.0	23.6	-0.5	23.6	89.3	2.78
93	-12.4	23.6	0.6	23.7	89.5	2.78
75	4.9	17.8	0.9	22.8	90.4	2.97
99	13.8	8.2	0.6	22.1	89.3	3.04
81	13.8	8.3	-0.5	22.1	89.6	3.05
123	4.0	17.8	-0.3	21.9	89.3	3.08
106	-14.7	21.7	0.6	21.8	89.3	3.10
88	-14.8	21.7	-0.6	21.8	89.6	3.11
104	0.0	19.5	-0.4	19.5	89.3	3.58
86	0.0	19.5	0.4	19.5	89.7	3.60

Note: See Figure 2.6.16.2-5 for section locations and definition of coordinate system.

Table 2.7.13.1.3-6 $P_m + P_b$ Stresses for CY-MPC Support Disk 30-Foot Side Drop,
0° Basket Orientation

Section	Sx (ksi)	Sy (ksi)	Sxy (ksi)	Stress Intensity (ksi)	Allowable Stress (ksi)	Margin of Safety
1	-52.8	1.6	-0.2	52.8	131.1	1.48
3	-52.5	1.4	0.2	52.5	131.1	1.50
11	-34.9	-13.7	3.1	49.0	129.4	1.64
9	-49.0	0.0	-0.2	49.0	129.8	1.65
13	-34.6	-13.5	-3.0	48.5	129.4	1.67
7	-48.4	2.2	0.0	48.4	129.8	1.68
66	-37.5	15.4	-5.3	38.7	129.4	2.34
131	-34.4	14.6	10.2	38.8	130.2	2.36
73	-37.3	14.9	5.1	38.4	129.4	2.37
81	-33.6	18.9	-3.8	34.6	128.0	2.70
21	-32.9	21.8	-4.6	34.6	128.1	2.71
23	-32.6	21.5	4.6	34.3	128.1	2.74
88	-33.3	18.6	3.8	34.2	128.0	2.74
67	-24.3	-9.7	1.1	34.1	129.5	2.80
72	-24.1	-9.9	-1.1	34.0	129.5	2.81
5	-33.4	0.1	0.0	33.4	130.9	2.92
124	-22.1	15.2	-13.7	32.9	130.3	2.97
70	-14.8	-16.5	-3.8	32.2	129.6	3.02
69	-14.6	-16.6	3.8	32.1	129.6	3.03
4	-32.0	0.0	-1.1	32.1	130.4	3.06
6	-31.9	0.0	1.1	32.0	130.4	3.08
12	-21.4	-9.6	-2.2	31.3	129.6	3.14
27	-18.4	-11.9	0.1	30.3	128.1	3.22
82	-18.2	-12.0	0.3	30.2	128.0	3.24
26	-24.6	-5.4	1.6	30.1	128.0	3.25
28	-24.3	-5.5	-1.6	29.9	128.0	3.28
87	-17.9	-12.0	-0.3	29.9	128.0	3.28
8	-26.2	14.8	-6.6	29.2	129.9	3.44
85	-11.1	-16.0	-1.2	27.2	128.1	3.70
84	-11.0	-16.1	1.3	27.2	128.1	3.71

Note: See Figure 2.6.16.2-5 for section locations and definition of coordinate system.

Table 2.7.13.1.3-7 $P_m + P_b$ Stresses for CY-MPC Support Disk 30-Foot Side Drop,
38° Basket Orientation

Section	Sx (ksi)	Sy (ksi)	Sxy (ksi)	Stress	Allowable	Margin of Safety
				Intensity (ksi)	Stress (ksi)	
1	-103.2	4.3	6.9	103.7	131.1	0.26
2	-83.5	14.5	-2.8	83.6	132.1	0.58
13	-80.3	20.4	1.5	80.4	129.4	0.61
26	-78.0	49.7	5.1	78.8	128.0	0.62
11	-79.2	24.2	3.4	79.5	129.4	0.63
41	-77.1	51.7	5.5	78.2	127.6	0.63
3	-78.5	25.3	-9.6	80.2	131.1	0.63
7	-78.5	6.2	7.0	79.2	129.8	0.64
28	-77.8	38.3	3.0	78.0	128.0	0.64
43	-77.1	44.5	4.1	77.6	127.6	0.64
12	-78.0	19.7	-1.1	78.0	129.6	0.66
100	-76.2	38.1	4.2	76.6	127.6	0.66
82	-76.3	36.1	3.8	76.7	128.0	0.67
99	75.8	-38.1	4.1	76.2	127.6	0.67
42	-73.2	58.8	1.9	73.4	127.6	0.74
106	-71.6	30.2	1.8	71.7	127.6	0.78
81	70.9	-38.4	4.9	71.6	128.0	0.79
52	-70.5	30.5	-1.1	70.6	127.6	0.81
88	-70.4	23.2	0.4	70.4	128.0	0.82
103	-67.9	47.2	4.4	68.8	127.6	0.85
70	-67.9	3.3	0.1	67.9	129.6	0.91
105	-65.9	57.5	2.8	66.8	127.6	0.91
66	67.5	-35.6	-1.3	67.5	129.4	0.92
73	-66.7	5.6	-6.7	67.4	129.4	0.92
67	-67.3	13.7	2.5	67.5	129.5	0.92
102	-54.0	61.9	7.3	66.3	127.6	0.92
84	-62.8	58.9	4.5	65.8	128.1	0.95
51	-63.7	36.5	4.5	64.5	127.6	0.98
69	-64.9	22.2	-0.3	64.9	129.6	1.00
87	-64.0	50.7	1.5	64.1	128.0	1.00

Note: See Figure 2.6.16.2-5 for section locations and definition of coordinate system.

Table 2.7.13.1.3-8 $P_m + P_b$ Stresses for CY-MPC Support Disk 30-Foot Side Drop, 63° Basket Orientation

Section	Sx (ksi)	Sy (ksi)	Sxy (ksi)	Stress	Allowable	Margin of Safety
				Intensity (ksi)	Stress (ksi)	
43	-78.5	54.5	2.6	78.8	127.6	0.62
106	-74.1	40.7	0.4	74.1	127.6	0.72
13	-75.1	31.1	0.6	75.1	129.4	0.72
3	-74.0	30.4	-9.7	76.0	131.1	0.72
28	-74.0	47.1	1.7	74.1	128.0	0.73
41	73.1	-41.4	4.4	73.7	127.6	0.73
1	-74.3	3.3	5.6	74.7	131.1	0.75
99	71.1	-25.7	2.6	71.3	127.6	0.79
129	-40.3	47.7	-26.5	70.8	127.6	0.80
100	-70.2	41.4	2.2	70.4	127.6	0.81
105	68.8	-26.0	4.0	69.2	127.6	0.84
2	-71.4	18.8	-2.6	71.5	132.1	0.85
88	-68.6	33.7	-0.6	68.6	128.0	0.87
42	-67.1	63.3	0.8	67.2	127.6	0.90
26	-66.7	50.0	3.0	67.2	128.0	0.91
82	-65.7	38.6	1.8	65.8	128.0	0.95
73	-65.2	18.7	-6.6	66.1	129.4	0.96
81	65.1	-23.6	2.7	65.2	128.0	0.96
11	65.4	-33.4	3.6	65.8	129.4	0.97
103	-63.7	52.7	3.3	64.6	127.6	0.97
44	-62.7	33.7	1.2	62.7	127.6	1.03
12	-63.2	24.0	-0.8	63.2	129.6	1.05
102	60.3	-39.0	5.7	61.8	127.6	1.06
52	-60.5	23.9	0.8	60.5	127.6	1.11
66	60.8	-20.8	-2.4	60.9	129.4	1.13
108	58.2	-15.6	3.6	58.5	127.6	1.18
40	58.1	-17.2	1.4	58.1	127.6	1.20
87	57.4	-24.3	3.9	57.8	128.0	1.21
25	57.7	-13.6	1.4	57.7	128.0	1.22
37	-33.2	56.7	3.4	57.2	127.6	1.23

Note: See Figure 2.6.16.2-5 for section locations and definition of coordinate system.

Table 2.7.13.1.3-9 $P_m + P_b$ Stresses for CY-MPC Support Disk 30-Foot Side Drop,
90° Basket Orientation

Section	Sx (ksi)	Sy (ksi)	Sxy (ksi)	Stress	Allowable	Margin of Safety
				Intensity (ksi)	Stress (ksi)	
129	-35.3	38.5	-21.7	58.6	127.6	1.18
108	31.2	19.9	-1.9	51.3	127.6	1.49
90	30.6	20.1	1.9	50.8	128.0	1.52
44	41.2	6.8	-0.9	48.0	127.6	1.66
24	40.5	7.1	0.9	47.6	128.0	1.69
39	26.9	16.1	1.8	43.2	127.6	1.95
29	27.1	16.0	-1.8	43.2	128.0	1.96
105	23.3	14.8	-1.5	38.2	127.6	2.34
130	-25.7	27.7	11.8	38.5	128.8	2.34
87	23.0	15.0	1.5	38.1	128.0	2.36
14	10.4	22.9	-3.3	34.0	129.2	2.80
43	30.6	2.4	0.9	33.0	127.6	2.86
23	30.4	2.6	-0.9	33.0	128.1	2.88
54	8.6	22.8	3.6	32.3	127.6	2.95
110	-0.1	31.7	-0.4	31.7	127.6	3.02
111	-15.6	27.6	-8.1	31.7	127.6	3.03
92	-0.1	31.6	0.3	31.6	127.9	3.04
93	-14.6	27.4	8.4	31.6	127.8	3.05
109	-17.9	29.3	-2.8	29.9	127.6	3.26
91	-17.2	29.0	2.8	29.6	128.0	3.32
38	17.7	11.9	0.2	29.5	127.6	3.32
28	18.0	11.7	-0.2	29.6	128.0	3.32
40	-28.3	14.5	-2.4	28.7	127.6	3.44
106	-21.5	25.3	-4.7	28.4	127.6	3.49
20	-28.1	14.4	2.4	28.5	128.0	3.49
88	-21.2	25.1	4.7	28.3	128.0	3.52
102	8.3	18.1	2.5	26.9	127.6	3.74
84	8.5	17.9	-2.4	26.9	128.1	3.76
41	-25.5	21.2	-2.6	26.7	127.6	3.78
42	-19.8	24.9	-3.1	26.4	127.6	3.83

Note: See Figure 2.6.16.2-5 for section locations and definition of coordinate system.

2.7.13.1.4 Stress Evaluation of CY-MPC Support Disk for 30-Ft Oblique Drop

This section documents the methodology used to calculate the stresses associated with oblique impacts of the transport cask (Figure 2.7.13.1-2). The results show that the stress criteria are met for all oblique conditions. Note that the methodology used for the off-angle drop evaluation is very conservative since the g loads decrease significantly for oblique drops (Section 2.6.7.4).

To evaluate oblique impacts, the stress components (i.e., S_x , S_y , S_{xy}) are combined from the side drop and end drop cases for both the 0° the 38° basket drop orientations (Figure 2.7.13.1-1). The stresses are combined according to the following cask drop angles: $\phi = 0^\circ, 24^\circ, 30^\circ, 45^\circ, 60^\circ, 73^\circ, 75^\circ, 77^\circ, 80^\circ, 83^\circ, 85^\circ, 88^\circ$ and 90° . Note that the 0° and 90° cask drop angles are equivalent to the end- and side- drop cases, respectively. The normal stresses (S_x and S_y) and the shear stress (S_{xy}) for a drop with an angle of ϕ (Figure 2.7.13.1-2) are calculated using the following equations:

$$S_{x(\phi)} = S_{x(\text{end})} \cos \phi + S_{x(\text{side})} \sin \phi,$$

$$S_{y(\phi)} = S_{y(\text{end})} \cos \phi + S_{y(\text{side})} \sin \phi,$$

$$S_{xy(\phi)} = S_{xy(\text{end})} \cos \phi + S_{xy(\text{side})} \sin \phi,$$

where:

$S_{x(\text{end})}$, $S_{y(\text{end})}$, and $S_{xy(\text{end})}$ are the sectional stresses resulting from the Support Disk End Drop Model, and $S_{x(\text{side})}$, $S_{y(\text{side})}$, and $S_{xy(\text{side})}$ are the section stresses resulting from the Support Disk Side Drop Model.

Off-angle principle stresses (i.e., S_1 , S_2) are calculated by using the following equation:

$$S_1, S_2 = \frac{S_{x(\phi)} + S_{y(\phi)}}{2} \pm \sqrt{\left(\frac{S_{x(\phi)} - S_{y(\phi)}}{2}\right)^2 + S_{xy(\phi)}^2}$$

Once the principle stresses are calculated, new stress intensities (SI) can be calculated. Summaries of the maximum support-disk stress-intensities in the 30-foot oblique drop conditions are given in Table 2.7.13.1.4-1.

Table 2.7.13.1.4-1 CY-MPC Support Disk Stress Summary for the 30-Foot Oblique Drop

Stress State	Section	Cask Drop Angle (°)	S _x (ksi)	S _y (ksi)	S _{xy} (ksi)	Stress Intensity (ksi)	Allowable Stress (ksi)	Margin of Safety
0° BASKET DROP ORIENTATION								
P _m	61	0	66.6	-5.3	19.4	83.5	89.3	0.07
P _m +P _b	61	0	89.0	-18.7	34.6	116.5	127.6	0.09
38° BASKET DROP ORIENTATION								
P _m	61	0	66.6	-5.3	19.4	83.5	89.3	0.07
P _m +P _b	61	30	109.9	-36.4	-31.7	128.7	131.1	0.02

Notes:

1. P_m = Primary Membrane Stress, P_m + P_b = Primary Membrane + Bending Stress.
2. See Figure 2.6.16.2-5 for section locations.
3. See Figure Figure 2.7.13.1-2 for definition of cask drop angle.
4. Allowable Stress for 17-4PH, Type 630 stainless steel:

For P_m, S_{allow} = 0.7 S_u = 89.4 ksi at 539°F
= 94.5 ksi at -40°F

For P_m + P_b, S_{allow} = S_u = 127.8 ksi at 539°F
= 135.0 ksi at -40°F

2.7.13.2 Stress Evaluation of Tie Rods and Spacers for 30-Foot End Drop Load Condition for the CY-MPC

Tie Rod Evaluation

The tie rods serve basket assembly purposes and are not loaded during drop conditions; therefore, no further analysis is required.

Spacer Evaluation

Six tie rods and cylindrical spacers, to maintain disk spacing, connect the basket support disks and heat transfer disks. In a side drop, the load path is through the support disks into the canister wall. In an end drop, the load path is through the spacers to either the canister lid or bottom depending on the drop orientation. The load comprises the weight of the top or bottom weldment (depending on the drop orientation), the weight of the support and heat transfer disks, and the weight of the spacers and washers. The weight of the fuel assemblies is transmitted directly into the canister lid or bottom because the fuel tubes in the basket are open at both ends. In drop orientations between a side drop and an end drop, only a portion of the load acts along the tie rod axis. Thus, the end drop is the critical loading condition for the spacers. The bottom-end drop is the governing case because the top weldment is heavier than the bottom weldment.

During an end drop, the 6 split spacers at the bottom of the heat transfer disk array are loaded by the top weldment, the 27 heat transfer disks, the spacers and washers above, and the 27 support disks above the lowest split spacer at the bottom of the heat transfer disk array. The total weight on the split spacers is 8,225 lbs.

The initial tie rod pre-load tension will be diminished by the compressive effect of the end drop. However, for conservatism, the total compression (2,011 lbs.) induced by the 50 ± 10 ft-lb bolt torque will be included in the load on the split spacers.

The maximum total load (P_{ssp}) on the split spacer is, for accident conditions:

$$P_{ssp} = 2,011 + (8,225) \times 60/6 = 84,261 \text{ lb, use } 100,000 \text{ lb}$$

Note: 60g conservatively used to bound 56g-end drop load

The stress (σ_{ssp}) is determined by applying the total load to the cross-sectional area (A_{ssp}) of the split spacer. A_{ssp} is conservatively taken as the area of the decreased diameter section.

$$\sigma_{ssp} = \frac{P_{ssp}}{A_{ssp}} = \frac{100,000 \text{ lb}}{2.45 \text{ in.}^2} = 40,816 \text{ psi}$$

Where

$$A_{ssp} = \frac{\pi}{4} (2.50^2 - 1.77^2) = 2.45 \text{ in.}^2$$

The margin of safety (MS) is:

$$MS = \frac{0.7S_u}{\sigma_{ssp}} - 1 = \frac{0.7(64,400)}{40,816} - 1 = +0.10 \text{ (Accident condition, } 400^\circ\text{F)}$$

The load on the bottom spacers comprises the weight of the top weldment, the weight of the support and heat transfer disks, and the weight of the spacers and washers.

During a bottom end drop, the 6 bottom spacers are loaded by the top weldment, the 27 heat transfer disks, the spacers and washers above, and the 28 support disks. The total weight on the spacers is 9,874 lbs.

The initial tie rod pre-load, tension, will be diminished by the compressive effect of the end drop. However, for conservatism, the total compression (2,011 lbs.) induced by the 50±10 ft-lb bolt torque will be included in the load on the bottom spacers.

The maximum total load (P_{bsp}) on the bottom spacer is:

$$P_{bsp} = 2,011 + (9,874) \times 60/6 = 100,751 \text{ lbs., use } 101,000 \text{ lbs.}$$

Note: 60g conservatively used to bound 56g-end drop load

The stress on the bottom spacer is:

$$\sigma_{ssp} = \frac{P_{bsp}}{A_{bsp}} = \frac{101,000 \text{ lbs}}{4.03 \text{ in.}^2} = 25,062 \text{ psi}$$

Where

$$A_{bsp} = \frac{\pi}{4} (2.875^2 - 1.77^2) = 4.03 \text{ in.}^2$$

The margin of safety (MS) is:

$$MS = \frac{0.7S_u}{\sigma_{bsp}} - 1 = \frac{0.7(64,400)}{25,062} - 1 = +0.80 \text{ (Accident condition, 400°F)}$$

THIS PAGE INTENTIONALLY LEFT BLANK

2.7.13.3 CY-MPC Fuel Basket Support Disk – Buckling Evaluation (Accident Condition)

The buckling evaluation of the support disk web is based on the Interaction Equations 31 and 32 in NUREG/CR-6322. These two equations adopt the "Limit Analysis Design" approach for structural members subjected to stresses beyond the yield limit of the material, i.e., for members deformed elastically as a result of axial load or bending moment. Other equations applicable to the calculations are listed later in this section.

The maximum forces and moments are determined from the finite element analysis stress results for the Support Disk End-Drop Model as well as the Support Disk Side Drop Models (four different basket orientations, 0°, 38°, 63°, and 90°). The buckling evaluations account for both in-plane (about the strong axis of the web) and out-of-plane (about the weak axis of the web) buckling modes. The methodology and equations used for the buckling evaluation are summarized as follows:

Symbols and Units

- P = applied axial compressive loads, kips
- M = applied bending moment, kips-inch
- P_a = allowable axial compressive load, kips
- P_{cr} = critical axial compression load, kips
- P_e = Euler buckling loads, kips
- P_y = average yield load, equal to profile area times specified minimum yield stress, kips
- C_c = column slenderness ratio separating elastic and inelastic buckling
- C_m = coefficient applied to bending term in interaction equation
- M_m = critical moment that can be resisted by a plastically designed member in the absence of axial load, kip-in.
- M_p = plastic moment, kip-in.
- F_a = axial compressive stress permitted in the absence of bending moment, ksi
- F_e = Euler stress for a prismatic member divided by factor of safety, ksi
- k = ratio of effective column length to actual unsupported length
- l = unsupported length of member, in.
- r = radius of gyration, in.
- S_y = yield strength, ksi
- A = cross sectional area of member, in²
- Z_x = plastic section modulus, in³
- λ = allowable reduction factor, dimensionless.

From NUREG/CR-6322, the following equations are used to evaluate the support disk for normal condition of transport:

$$\frac{P}{P_{cr}} + \frac{C_m M}{\left[1 - \frac{P}{P_e}\right] M_m} \leq 1.0 \quad (\text{Eq. 31, NUREG/CR-6322})$$

$$\frac{P}{P_y} + \frac{M}{118 M_p} \leq 1.0 \quad (\text{Eq. 32, NUREG/CR-6322})$$

where: $P_{cr} = 1.7 \times A \times F_a$

$$F_a = \frac{\left[1 - \frac{1}{2} \left(\frac{k \cdot \ell}{r \cdot C_c}\right)^2\right] \cdot S_y}{\frac{5}{3} + \frac{3}{8} \left(\frac{k \cdot \ell}{r \cdot C_c}\right) - \frac{1}{8} \left(\frac{k \cdot \ell}{r \cdot C_c}\right)^3} \quad \text{for } \frac{k \cdot \ell}{r} < C_c = \sqrt{2 \cdot \pi^2 \frac{E}{S_y}}$$

$$P_e = 1.92 \times A \times F_e$$

$$F_e = \frac{\pi^2 \cdot E}{1.92 \left(\frac{k \cdot \ell}{r}\right)^2} \quad (\text{non-austenitic})$$

$$P_y = S_y \times A$$

$C_m = 0.85$ for members with joint translation (sideways).

$$M_p = S_y \times Z_x$$

$$M_m = M_p \cdot \left(1.07 - \frac{\left(\frac{1}{r}\right) \cdot \sqrt{S_y}}{3160}\right) \leq M_p$$

Buckling evaluations are performed on all sections in the disk ligaments defined in Figure 2.6.16.2-5. Using the cross-sectional stresses calculated at each of the sections for each loading condition the maximum corresponding compressive forces (P) and bending moment are determined as follows,

$$P = \sigma_m A,$$

$$M = \sigma_b A,$$

where, σ_m is the membrane stress, σ_b is the strong axis bending stress or weak axis bending stress, A is the area ($b \times t$), and S is the section modulus ($tb^2/6$ for strong axis bending and $bt^2/6$ for weak axis bending).

To determine the margin of safety:

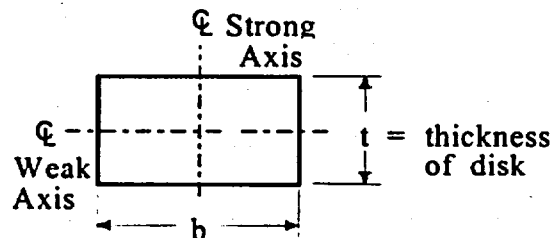
$$P_1 = P/P_{cr} \quad M_1 = \frac{C_m M}{(1 - P/P_{cr})M_m} \quad (P_1 + M_1 \leq 1) \quad (\text{Eq. 31, NUREG/CR-6322})$$

$$\text{and} \quad P_2 = P/P_y \quad M_2 = \frac{M}{1.18 M_p} \quad (P_1 + M_1 \leq 1) \quad (\text{Eq. 32, NUREG/CR-6322})$$

The margins of safety are:

$$MS1 = \frac{1}{P_1 + M_1} - 1$$

$$MS2 = \frac{1}{P_2 + M_2} - 1$$



The side drop conditions are the governing conditions for strong axis buckling evaluation since the axial compressive force (P) and the strong axis bending moment (M) decrease with the drop angle. Therefore, evaluation of strong axis buckling is performed for side-drop conditions only.

Buckling analysis was completed only for the 38° basket orientation because this is the worst case angle (See Section 2.7.13.1). The minimum margin of safety is +0.34, which occurs at section number 1. The results for the 20 worst-case sections are summarized in Table 2.7.13.3-1.

Table 2.7.13.3-1 NUREG/CR 6322 Buckling Analysis for CY-MPC Support Disk 30-Foot Side Drop, 38° Basket Orientation

Sect.	P (kip)	Pcr (kip)	Py (kip)	M (in-kip)	Mp (in-kip)	Mm (in-kip)	MS1	MS2
1	10.44	59.07	49.07	8.49	13.49	13.22	0.35	0.34
13	12.90	58.15	48.30	5.74	13.28	13.02	0.64	0.58
2	14.51	87.24	67.61	12.04	25.36	25.36	0.74	0.62
3	12.81	59.07	49.07	5.57	13.49	13.22	0.70	0.64
7	9.71	58.35	48.47	6.13	13.33	13.07	0.73	0.69
28	8.25	57.25	47.54	6.33	13.07	12.83	0.74	0.71
12	11.43	85.12	65.94	11.76	24.73	24.73	0.84	0.73
43	4.85	56.89	47.23	6.89	12.99	12.75	0.82	0.81
11	2.94	58.14	48.29	7.45	13.28	13.02	0.85	0.86
26	2.88	57.25	47.54	7.33	13.07	12.83	0.85	0.87
42	6.73	83.16	64.40	12.04	24.15	24.15	0.97	0.90
41	0.97	56.89	47.23	7.60	12.99	12.75	0.90	0.94
52	5.52	83.16	64.40	11.85	24.15	24.15	1.06	0.99
8	14.98	85.35	66.13	8.01	24.80	24.80	1.20	1.00
9	12.00	58.35	48.47	3.85	13.33	13.07	1.15	1.03
27	9.43	83.72	64.85	9.24	24.32	24.32	1.28	1.14
111	12.98	83.16	64.40	7.55	24.15	24.15	1.35	1.14
23	10.59	57.31	47.59	3.76	13.09	12.84	1.27	1.15
22	11.39	83.83	64.93	8.32	24.35	24.35	1.32	1.15
21	4.41	57.31	47.59	5.46	13.09	12.84	1.26	1.24

Note: See Figure 2.6.16.2-5 for section locations and definition of coordinate system.

2.7.13.4 Fuel Tube Analysis—CY-MPC

The fuel tube provides a foundation and sealed cavity to mount BORAL poison plates within the fuel basket structure. The fuel tube does not serve a structural function relative to the support of the fuel assembly. To ensure that the fuel tube remains functional when the cask is subjected to design load conditions, a structural evaluation of the tube is performed for both end and side-impact load conditions.

Fuel Tube End-Impact Analysis

During the postulated cask end impact, the cask bottom for the bottom-end drop, and the lid for the top-end drop support the CY fuel assemblies. The fuel tubes do not carry fuel assembly load. Therefore, evaluation of the fuel tube for the end-impact load is performed by considering the weight of the fuel tube subjected to the cask deceleration carried by the minimum tube cross-sectional area. The minimum cross-sectional area is located at the contact point of the tube with the bottom weldment. The minimum cross-sectional area is

$$MS = \frac{8,650}{3,565.3} - 1 = 1.43$$

The total bearing load on the tube during the cask bottom-end impact is 6,820 psi, (55g x 124 lbs). The maximum compressive and bearing stress is $(6,820 / 1.76) = 3,875$ psi. Limiting the compressive stress level to the material yield strength ensures that the tube remains in position when the cask is subjected to the postulated end-drop. Type 304 stainless steel yield strength is 17,300 psi at a conservatively high temperature of 750°F for the axial location on the fuel tube that has the minimum cross-sectional area. The margin of safety is

$$MS = \frac{17,300}{3,875} - 1 = +3.46$$

Fuel Tube Side-Impact Analysis

During the cask side-impact load configuration, the fuel tube is supported by the fuel basket's support disks. The support disks support the full length of the fuel tube, and are spaced at 4.59 inches (center-to-center) which is about one-half of the fuel tube width. Considering the fuel tube is subjected to a 60g side-impact deceleration and the 28 support locations provided by the basket support disk, the fuel tube shear stress is

$$\begin{aligned}\text{Impact Shear Load} &= 55 \times 1590 / 28 = 3,123.2 \text{ lbs} \\ \text{Shear Load} &= 3123.2 \text{ lbs} \\ \text{Area} &= 0.048 \times 9.12 \times 2 = 0.876 \text{ in}^2 \\ \text{Shear Stress} &= 3123.2 / 0.876 = 3,565.3 \text{ psi}\end{aligned}$$

Using an allowable shear stress equivalent to half the yield strength of the tube, 8650 psi (17,300 / 2), the margin of safety is

$$MS = \frac{8,650}{3,565.3} - 1 = 1.43 @ 750^\circ\text{F}$$

The conservative evaluation of the tube loading resulting from its own mass during a side-impact configuration indicates that the tube structure will maintain position and will function.

For transport and storage, the bounding load is the 30-foot side drop condition for transport (55g). ANSYS Finite Element program was used to perform the elastic-plastic analysis on the fuel tubes. ANSYS plastic quadrilateral (SHELL43) shell elements were used to model the fuel tube walls of thickness 0.048 inches. The CY basket's fuel tube is 131.95 inch long and supported by 0.5 inch thick support disks at a 4.59 inch pitch. The BORAL plate (0.075 inch) and stainless steel cover plate (0.018 inch) are conservatively not included in the model. The multi-linear kinematic hardening (kinh) option is used for the non-linear material properties. The stress-strain curve for Type 304 SS is used (R1).

Two loading cases were analyzed: pressure loading and grid loading. Note that only a quarter-symmetry periodic section of the fuel tube was modeled for both the cases (Figure 2.7.13.4-1).

For the pressure loading case, surface pressures were applied to the inside bottom surface of the fuel tubes. The distributed load of the fuel assembly on the fuel tube wall was modeled as a surface pressure loading, determined as follows:

$$\text{Impact Pressure} = \frac{gW_f}{w_f L_f} = 72.67 \text{ psi}$$

where:

$$\begin{aligned}g &= \text{acceleration load} = 55 \text{ g} \\ W_f &= \text{weight of fuel assembly} = 1590 \text{ lbs} \\ L_f &= \text{length of fuel tube} = 131.95 \text{ in} \\ w_f &= \text{width of fuel tube} = 9.12 \text{ in}\end{aligned}$$

For the grid loading case, a bounding load condition for the grid loading case model is simulated by applying a constant displacement of 0.08 inch in the negative Y direction to the nodes corresponding to the grid location in the model. It is assumed that the fuel assembly grid spacer is rigid and therefore a constant displacement is conservatively applied.

From the elastic-plastic analyses of the CY-MPC fuel tube, the maximum equivalent plastic stress is 24,060 psi for the uniform loading case and 30,970 psi for the grid loading case.

Conservatively, comparing the plastic stress of the CY-MPC to the allowable stress of 63,100 psi at 750°F for Type 304 SS, provides margins of safety of:

$$\text{Pressure Loading: } MS = \frac{63,100}{24,060} - 1 = 1.62$$

$$\text{Grid Loading: } MS = \frac{63,100}{30,970} - 1 = 1.04$$

The maximum total strain is 0.019 for CY-MPC fuel tube for the uniform loading case and 0.047 for the grid loading case, as shown in Figures 2.7.13.4-2 and 2.7.13.4-3.

Defining the acceptable elastic-plastic response of the stainless steel as one-half the material failure strain of 0.4 in/in at 750°F (R2). Using this methodology to evaluate total cumulative strain shows margins of safety of:

$$\text{Pressure Loading: } MS = \frac{0.4/2}{0.019} - 1 = 9.53 \text{ at } 750^\circ\text{F}$$

$$\text{Grid Loading: } MS = \frac{0.4/2}{0.047} - 1 = 3.26 \text{ at } 750^\circ\text{F}$$

Similarly, the margin of safety for elastic-plastic stress becomes:

$$\text{Pressure Loading: } MS = \frac{63,100 - 17,300}{24,060 - 17,300} - 1 = 5.78 \text{ at } 750^\circ\text{F}$$

$$\text{Grid Loading: } MS = \frac{63,100 - 17,300}{30,970 - 17,300} - 1 = 2.35 \text{ at } 750^\circ\text{F}$$

Where the yield strength of Type 304 SS at 750°F is 17,300 psi.

The total displacements of the fuel tube are 0.17 inch for the pressure loading case and 0.08 inch for the grid loading case.

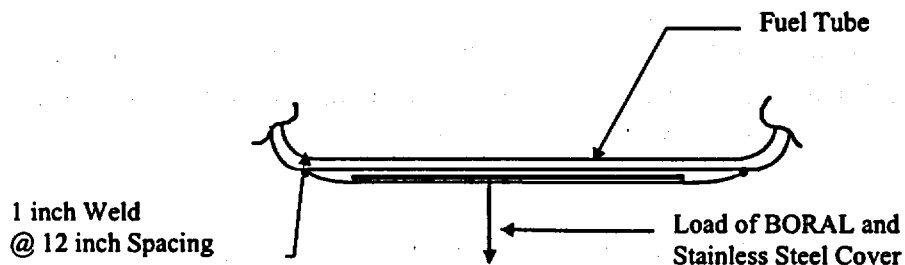
Both the maximum total equivalent strain and the elastic-plastic stress analyses indicate that the tube position within the support basket is maintained.

Maximum displacement in the fuel tube was averaged to determine the average displacement. The averaging technique was based on the parabolic shape of the displaced fuel tube bottom wall. The maximum displacement (D) is as follows:

Pressure Loading: $D = (2/3)(\text{max displacement}) = (2/3)(0.17) = 0.113 \text{ inch}$

Grid Loading: $D = (2/3)(\text{max displacement}) = (2/3)(0.08) = 0.053 \text{ inch}$

Assurance that the BORAL poison remains within the sealed casing is evaluated by considering that loads produced by the BORAL and skin mass decelerated by 55g are maintained by the seal weld.



Load exerted by BORAL/Stainless Steel skin is given as follows:

$$F_{b/ss} = g\rho t w l$$

where:

- g = acceleration due to gravity = 55 g
- ρ = density of material
 - = 0.098 lb/in³ (BORAL, aluminum density is conservatively used)
 - = 0.291 lb/in³ (stainless steel)

t = thickness of material
= 0.075 in (BORAL)
= 0.018 (stainless steel)
w = width of material
= 8.54 in (BORAL) (9.22-0.34x2)
= 9.05 in (stainless steel) (9.22-0.18x2+0.075x2)
l = length of material section = 12.0 in

Loads on a 1-inch weld for a 12-inch section:

$$F_b = 55 \times 0.098 \times 0.075 \times 8.54 \times 12.0 = 41.43 \text{ lbs}$$
$$F_{ss} = 55 \times 0.291 \times 0.018 \times 9.05 \times 12.0 = 31.29 \text{ lbs}$$

Total load (F_t) on a 1-inch section of fuel tube seal weld:

$$P = 41.43 + 31.29 = 72.72 \text{ lbs}$$

$$\text{Weld stress, } \sigma = \frac{P}{A} = \frac{72.72/2}{1 \times 0.018} = 2,020 \text{ psi}$$

Based on the weld material being Type 304 SS the margin of safety is:

$$\sigma_{\text{yield}} = 17,300 \text{ psi @ } 750^\circ\text{F}$$
$$MS = \frac{17,300}{2,020} - 1 = +7.56$$

Figure 2.7.13.4-1 CY-MPC Fuel Tube Finite Element Model

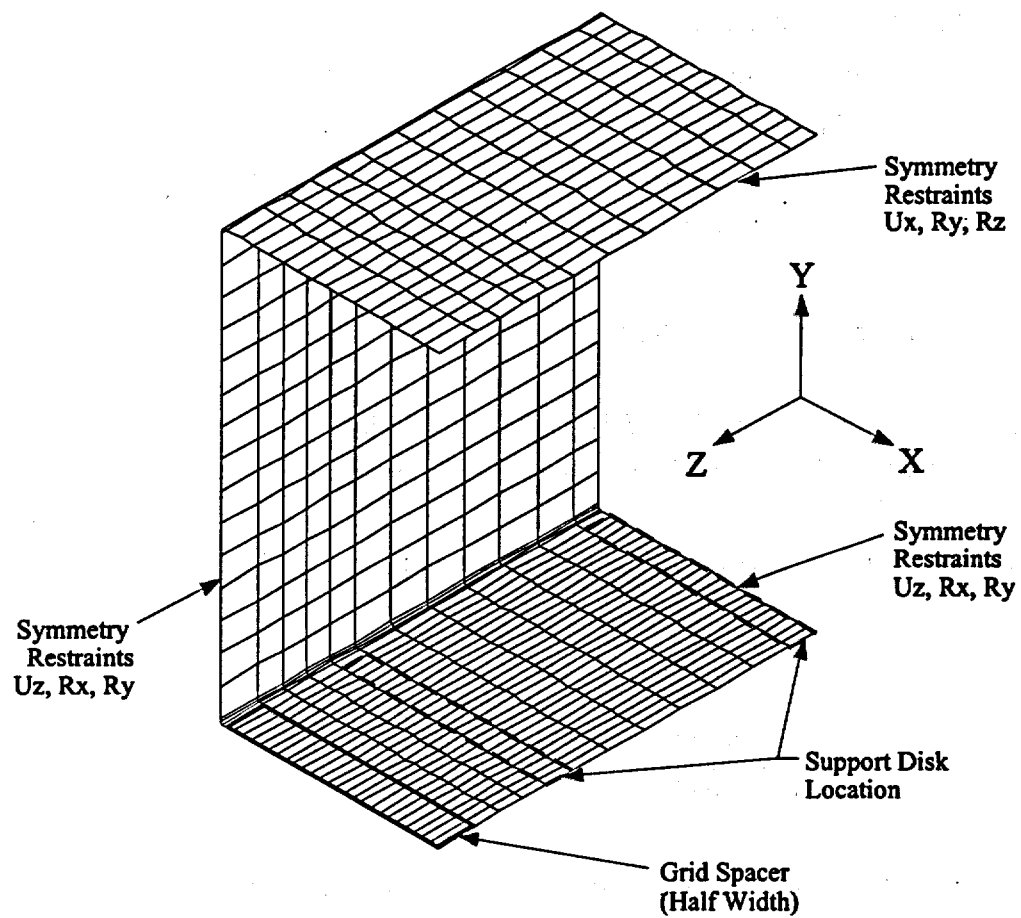


Figure 2.7.13.4-2 CY-MPC Fuel Tube Analysis Results – Total Equivalent Strain (Uniform Loading)

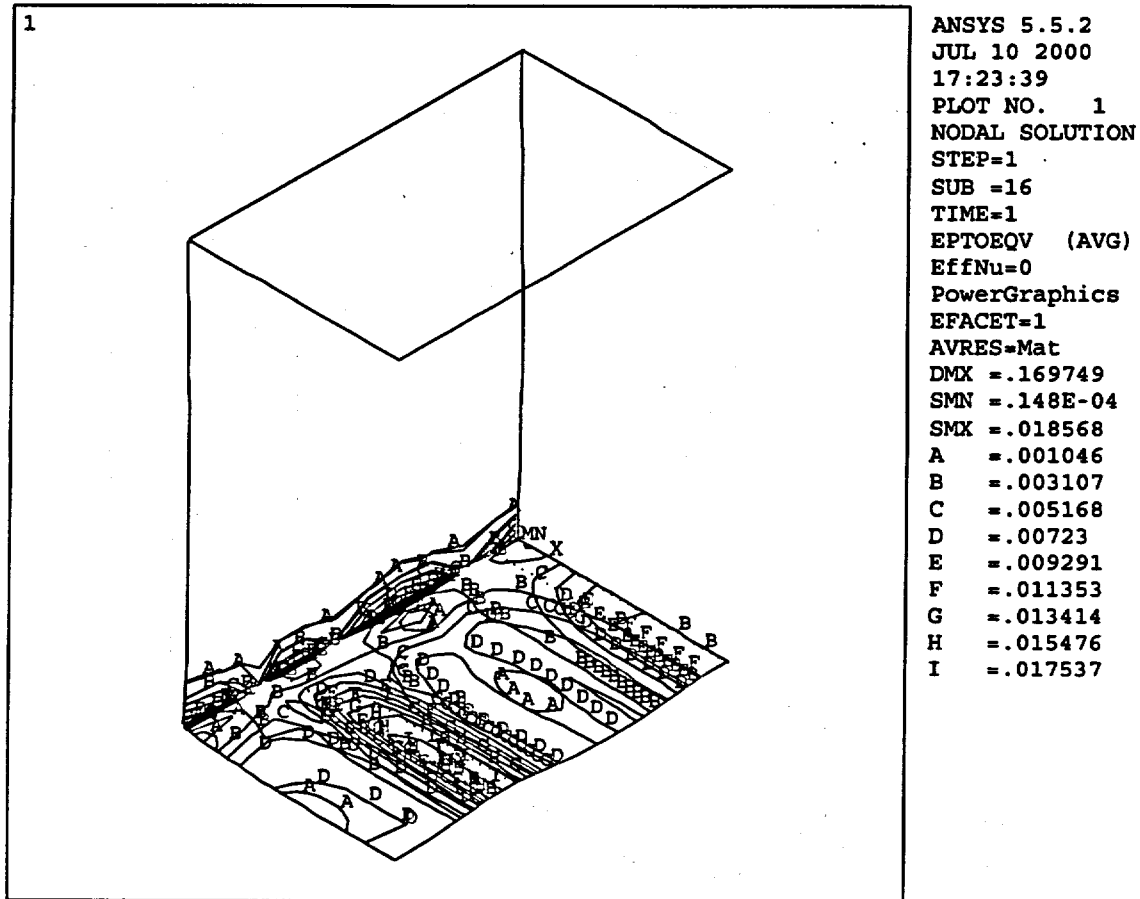
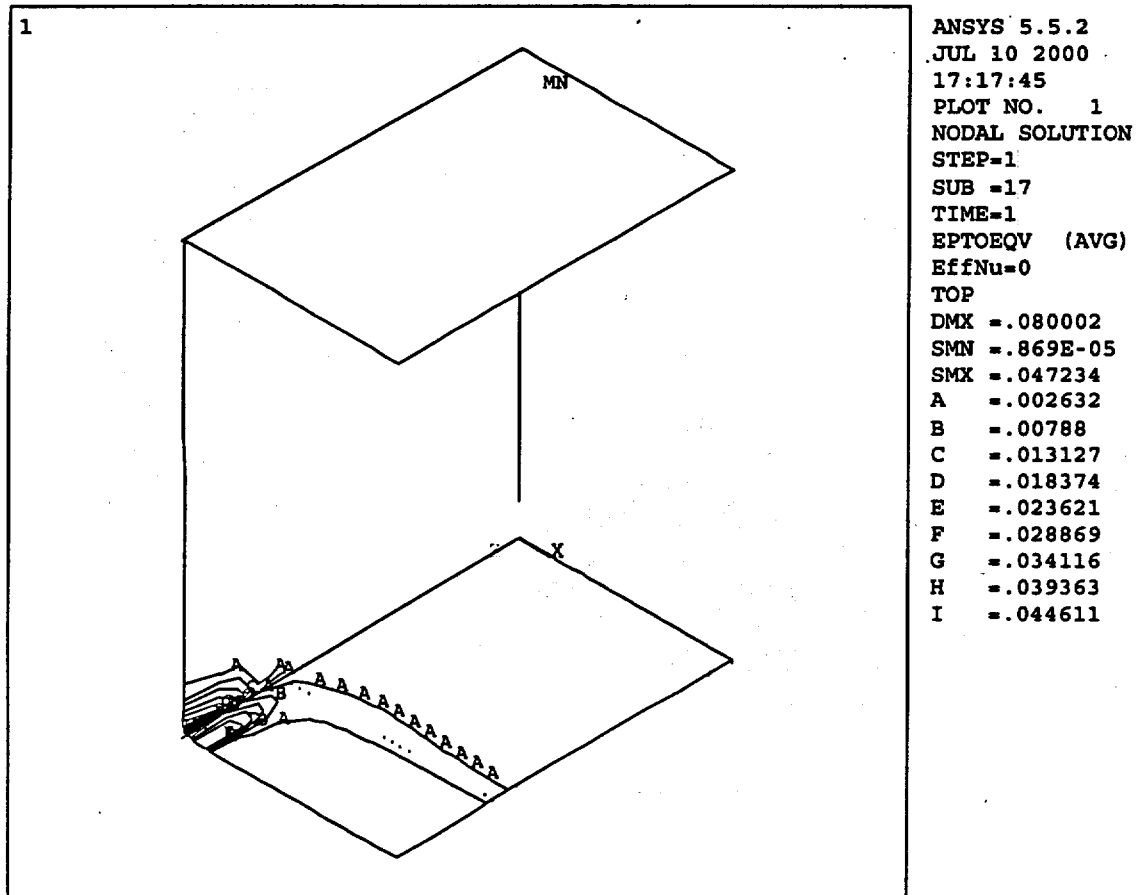


Figure 2.7.13.4-3 CY-MPC Fuel Tube Analysis Results – Total Equivalent Strain (Grid Loading)



2.7.13.5 CY-MPC Fuel Basket Weldment Analysis for 30-Foot End Drop

Two ANSYS finite element models (one for each weldment) are constructed for structural evaluation of the CY-MPC top and bottom weldments when subjected to 1-foot (presented in Section 2.6.16) and 30-foot drop (presented in this Section) conditions. Because of symmetry of the geometry of the weldments and the symmetry of the loading during end-drop conditions, the FE models represent quarter and half sections of the bottom and top weldments, respectively.

The top and bottom weldments are 0.5-inch thick plates of Type 304 stainless steel. The weldments support their own weight plus the weight of 26 fuel assembly tubes. A finite element analysis is performed for both weldments, since the support for each weldment is different due to the location of the support ribs for each. Both models use the SHELL63 element, which permits out of plane loading. Figures 2.7.13.5-1 and 2.7.13.5-2 show the finite element models for the weldments. The ribs supporting the weldment plates were also represented by SHELL63. The top weldment is constrained in the axial direction at the tie rod locations. The bottom weldment is constrained in the axial direction at the support ribs. Evenly distributed nodal forces around the periphery of the fuel assembly slot represent the force on the weldment from each fuel tube. The application of the nodal loads at the slot periphery is accurate since the tube weight is transmitted to the edge of the slot, which provides support to the fuel tubes in the end drop condition. An acceleration of 60g is applied to bound both the transport and storage end-drop conditions.

This analysis demonstrates that the weldment design satisfies the primary membrane (P_m) and the primary membrane plus bending ($P_m + P_b$) stress criteria.

The weldments are shown to satisfy the stress criteria in ASME Code, Section III Division I, Subsection NG. The margins of safety are conservatively evaluated at the maximum temperature of 500°F. The calculated temperatures and margins of safety are:

Component	Stress (ksi) $P_m + P_b$	Stress Allowable (ksi)	M.S.
Top Weldment	57.62	63.0	+0.09
Bottom Weldment	47.19	63.0	+0.34

Figure 2.7.13.5-1 Finite Element Model of the CY-MPC Top Weldment

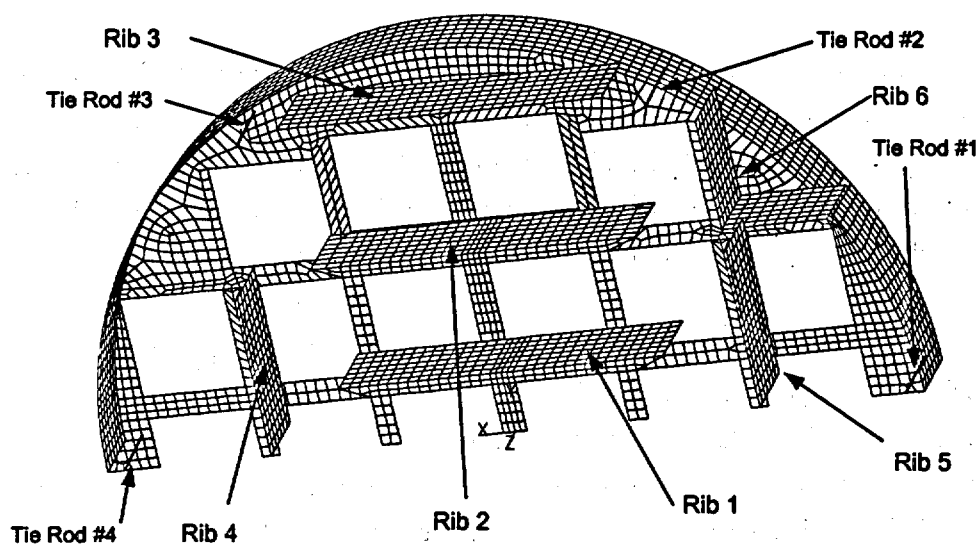
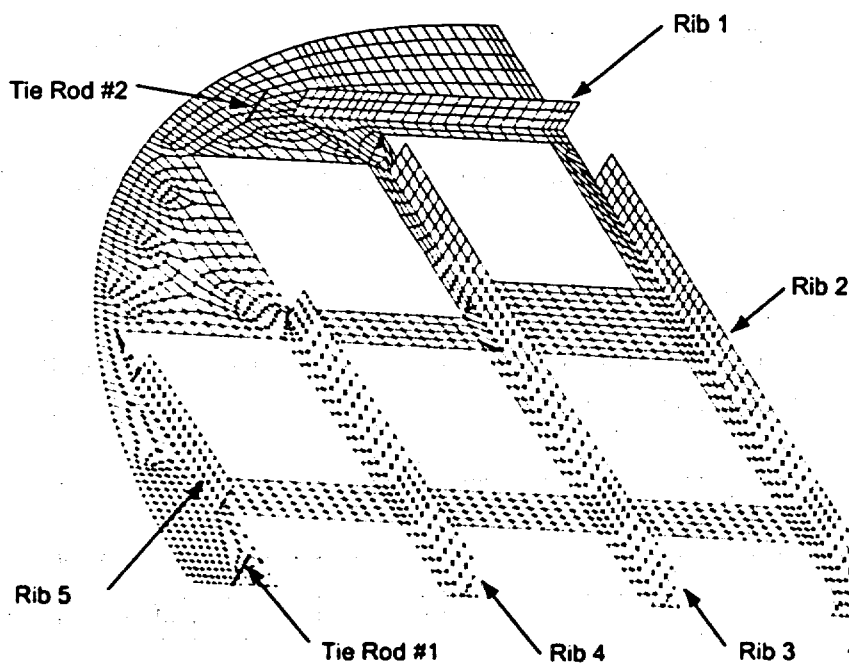


Figure 2.7.13.5-2 Finite Element Model of the CY-MPC Bottom Weldment



2.7.14 CY-MPC Reconfigured Fuel Assembly and Damaged Fuel Can Evaluation – Accident Conditions

The CY-MPC reconfigured fuel assembly and damaged fuel can are evaluated for the hypothetical accident conditions using 60g impact accelerations for the end-drop and side-drop impacts. Material properties for the reconfigured fuel assembly are taken at 750°F. Material properties for the damaged fuel can are taken at 600°F. These temperatures envelope all operating condition temperatures.

2.7.14.1 CY-MPC Reconfigured Fuel Assembly Weldment Evaluation

End Impact

For the end impact, the corner angles are evaluated to the criteria specified in NUREG/CR-6322, "Buckling Analysis of Spent Fuel Basket." Length (L) for both corner angles and tubes is conservatively taken as the length of the tube divided into five equal spans by the tube support grids, $L=135.09/5 = 27.02$ inches.

Corner Angle

For Service Level D, the corner angles are evaluated for axial compression in accordance with NUREG/CR-6322 and ASME Code Section III, Appendix F-1334.3.

Because Subsection F-1334.3 specifies no criteria for austenitic stainless steel, the following method from NUREG/CR-6322 is used to determine the criteria for the hypothetical accident condition.

The austenitic stainless steel criteria for the hypothetical accident condition can be expressed as:

$$SS_{\text{Level D}} = \left(\frac{SS}{CS} \right)_{\text{Level A}} \times CS_{\text{Level D}} \quad (\text{NUREG/CR-6322 Equation 39})$$

where SS and CS stand for stainless steel and carbon steel, respectively.

The maximum allowable stress for stainless steel ($F_a = 6,424.4 \text{ lb/in}^2$) for Level A (normal) conditions was determined previously. The allowable axial load ($P_{\text{SS-normal}}$) can be determined using the relation:

$$P_{\text{SS-normal}} = F_a \times A = 6,424.4 \text{ lb/in}^2 \times 0.715 \text{ in}^2 = 4,593.4 \text{ lb}$$

The maximum allowable axial load ($P_{CS-normal}$) for carbon steel ($S_y = 25.8$ ksi) can be determined using NUREG/CR-6322 Equation 22 as:

$$F_a = \frac{\left[1 - \frac{1}{2} \left(\frac{Kl}{rC_c} \right)^2\right] S_y}{\frac{5}{3} + \frac{3}{8} \frac{Kl}{rC_c} - \frac{1}{8} \left(\frac{Kl}{rC_c} \right)^3} = \frac{0.9498(25,800)}{1.667 + 0.1188 - .0039} = 13,752.1 \text{ psi}$$

where,

$$\frac{Kl}{r} = 43.8 < C_c = \sqrt{2\pi^2 \frac{E}{S_y}} = 138.85.$$

$$E = 25.2E3 \text{ ksi}$$

$$P_{CS-normal} = F_a A = 13,752.1 \text{ lb/in.}^2 (0.715 \text{ in.}^2) = 9,832.8 \text{ lb}$$

The maximum allowable axial compressive load ($P_{CS-accident}$) for carbon steel accident conditions using NUREG/CR-6322 Equation 33 is:

$$P_{CS-accident} = \frac{\left(1 - \frac{\lambda^2}{4}\right) P_y}{1.11 + 0.50\lambda + 0.17\lambda^2 - 0.28\lambda^3} = \frac{0.9502(18,447.0)}{1.11 + 0.223 + 0.0338 - 0.0249} = 13,399.8 \text{ lb}$$

where,

$$P_y = \text{the average yield load } (S_y \times A = 25,800 \text{ ksi} \times 0.715 \text{ in.}^2 = 18,447.0 \text{ lb})$$

$$\lambda = \frac{1}{\pi} \left(\frac{Kl}{r} \right) \sqrt{\frac{S_y}{E}} = \frac{1}{\pi} (43.8) \sqrt{\frac{25.8}{25.2e3}} = 0.4461 \quad 0 \leq 0.4461 \leq 1$$

Using NUREG/CR-6322 Equation 39 to determine the allowable load for stainless steel Level D (accident) conditions:

$$SS_{Level D} = \left(\frac{SS}{CS} \right)_{Level A} \times CS_{Level D} \quad (\text{NUREG/CR-6322 Equation 39})$$

and

$$P_{SS-Level D} = \frac{P_{SS-Level A}}{P_{CS-Level A}} \times P_{CS-Level D} = \frac{4,593.4}{9,832.8} \times 13,399.8 = 6,259.7 \text{ lb}$$

The load (P_{60g}) on each corner angle for the hypothetical accident condition is:

$$P_{60g} = \frac{225 \text{ lb}(60g)}{4} = 3,375 \text{ lb}$$

The margin of safety (MS) for the hypothetical accident condition is:

$$MS = \frac{P}{P_{60g}} - 1 = \frac{6,259.7}{3,375} - 1 = +0.85$$

2.7.14.1.1 CY-MPC Reconfigured Fuel Assembly Tube Evaluation

For Service Level D, accident conditions, the tubes are evaluated for axial compression in accordance with NUREG/CR-6322 and ASME Code Section III, Appendix F-1334.3.

Because Subsection F-1334.3 specifies no criteria for austenitic stainless steel, the following method from NUREG/CR-6322 is used to determine the criteria for the hypothetical accident condition (Service Level D).

The austenitic stainless steel criteria for the hypothetical accident condition can be expressed as:

$$SS_{Level D} = \left(\frac{SS}{CS} \right)_{Level A} \times CS_{Level D} \quad (\text{NUREG/CR-6322 Equation 39})$$

where SS and CS stand for stainless steel and carbon steel, respectively.

The maximum allowable Service Level A (normal conditions) stress for stainless steel ($F_a = 2,750 \text{ lb/in.}^2$) was determined previously. The allowable axial load ($P_{SS-Level A}$) can be determined using the relation:

$$P_{SS-normal} = F_a \times A = 2,750 \text{ lb/in.}^2 \times 0.0580 \text{ in.}^2 = 159.5 \text{ lb}$$

The maximum allowable Service Level A axial load ($P_{CS-Level A}$) for carbon steel can be determined as:

$$F_a = \frac{12}{23} \frac{\pi^2 E}{\left(\frac{KL}{r}\right)^2} = \frac{12}{23} \frac{\pi^2 (25.2E6)}{(144.57^2)} = 6,208.7 \text{ psi} \quad (\text{NUREG/CR-6322 Equation 23})$$

where,

$$\frac{KL}{r} = 144.57 > C_c = \sqrt{2\pi^2 \frac{E}{S_y}} = 138.85$$

$$S_y = 25.8 \text{ ksi}$$

$$E = 25.2E3 \text{ ksi}$$

$$P_{CS-normal} = F_a A = 6,208.7 \text{ lb/in.}^2 (0.0580 \text{ in.}^2) = 360.1 \text{ lb}$$

The maximum allowable axial compressive load ($P_{CS-Level D}$) for carbon steel Level D conditions is:

$$P_{CS-accident} = \frac{2P_y}{3\lambda^2} = \frac{2(1496.4)}{3(1.472^2)} = 460.4 \text{ lb} \quad (\text{NUREG/CR-6322 Equation 35})$$

where,

$$P_y = \text{the average yield load } (S_y \times A = 25,800 \text{ ksi} \times 0.0580 \text{ in.}^2 = 1,496.4 \text{ lb})$$

$$\lambda = \frac{1}{\pi} \left(\frac{KL}{r} \right) \sqrt{\frac{S_y}{E}} = \frac{1}{\pi} (144.57) \sqrt{\frac{25.8}{25.2E3}} = 1.472 > \sqrt{2}$$

Using NUREG/CR-6322 Equation 39 to determine the allowable load for stainless steel Service Level D conditions:

$$SS_{Level D} = \left(\frac{SS}{CS} \right)_{Level A} \times CS_{Level D} \quad (\text{NUREG/CR-6322 Equation 39})$$

$$P_{SS-Level D} = \frac{P_{SS-Level A}}{P_{CS-Level A}} \times P_{CS-Level D} = \frac{159.5}{360.1} \times 460.4 = 203.9 \text{ lb}$$

The load (P_{60g}) on each tube for the hypothetical accident condition is:

$$P_{60g} = 2.27 \text{ lb}(60g) = 136.2 \text{ lb}$$

The margin of safety (MS) for the hypothetical accident condition is:

$$MS = \frac{P}{P_{60g}} - 1 = \frac{203.9}{136.2} - 1 = +0.50$$

Side Impact

The reconfigured fuel assembly corner angles and tubes are each evaluated as a continuous beam supported at 6 places-the top and bottom housings and 4 intermediate tube support grids. The beam model for the corner angle is analyzed with a uniformly distributed load that is the self-weight of the angle multiplied by the acceleration factor (60g). The beam model for the tube is analyzed with a uniformly distributed load comprising the weight of the fuel rods and the self weight of the tube multiplied by an acceleration factor (60g).

Corner Angle

The corner angle length between the top and bottom housing is approximately 135.09 inches. The four intermediate tube support grids divide the corner angle into five equal spans approximately 27.02 inches long.

The maximum moment (M_{max}) in the corner angle is:

$$M_{max} = 0.0779wl^2 = 0.0779(0.2033)(27.02^2)(60g) = 694 \text{ lb-in.}$$

The maximum shear force (V) in the corner angle is:

$$V = \frac{23}{38}(wl) = \frac{23}{38}(0.2033)(27.02)(60g) = 200 \text{ lb}$$

The maximum bending stress (σ_b) is:

$$\sigma_b = \frac{M_{max} \times c}{I} = \frac{694(1.431)}{0.272} = 3,652 \text{ psi}$$

The maximum shear stress (τ) is:

$$\tau = \frac{V}{A} = \frac{200}{0.715} = 280 \text{ psi}$$

The combined stress is:

$$\sigma_{1,2} = \frac{\sigma_b}{2} \pm \sqrt{\left(\frac{\sigma_b}{2}\right)^2 + \tau^2} = \frac{3,652}{2} \pm \sqrt{\left(\frac{3,652}{2}\right)^2 + (280)^2} = 1,826 \pm 1,847 \text{ psi}$$

$$\sigma_1 = 3,673 \text{ psi}$$

$$\sigma_2 = -21 \text{ psi}$$

The maximum combined stress is:

$$\sigma_{\max} = |\sigma_1 - \sigma_2| = 3,694 \text{ psi}$$

The margin of safety MS is:

$$MS = \frac{3.6S_m}{\sigma_{\max}} - 1 = \frac{3.6(15,600)}{3,694} - 1 = +14.2$$

2.7.14.1.2 CY-MPC Reconfigured Fuel Assembly Tube Evaluation – Corner Angle

The tube length between the top and bottom housing is approximately 135.09 inches. The four intermediate tube support grids divide the tube into five equal spans approximately 27.02 inches long.

The maximum moment (M_{\max}) in the tube is:

$$M_{\max} = 0.0779wl^2 = 0.0779(0.076)(27.02^2)(60g) = 260 \text{ lb-in.}$$

The maximum shear force (V) in the tube is:

$$V = \frac{23}{38}(wl) = \frac{23}{38}(0.076)(27.02)(60g) = 75 \text{ lb}$$

The maximum bending stress (σ_b) is:

$$\sigma_b = \frac{M_{\max} \times c}{I} = \frac{260(0.28125)}{.002026} = 35,498 \text{ psi}$$

The maximum shear stress (τ) is:

$$\tau = \frac{V}{A} = \frac{75}{0.0580} = 1,293 \text{ psi}$$

The combined stress is:

$$\sigma_{1,2} = \frac{\sigma_b}{2} \pm \sqrt{\left(\frac{\sigma_b}{2}\right)^2 + \tau^2} = \frac{35,498}{2} \pm \sqrt{\left(\frac{35,498}{2}\right)^2 + (1,293)^2} = 17,749 \pm 17,796 \text{ psi}$$

$$\sigma_1 = 35,545 \text{ psi}$$

$$\sigma_2 = -47 \text{ psi}$$

The maximum combined stress is:

$$\sigma_{\max} = |\sigma_1 - \sigma_2| = 35,592 \text{ psi}$$

The margin of safety MS is:

$$MS = \frac{3.6S_m}{\sigma_{\max}} - 1 = \frac{3.6(15,600)}{35,592} - 1 = +0.58$$

2.7.14.1.3 CY-MPC Reconfigured Fuel Assembly Tube Support Grid Evaluation

Analysis of the reconfigured fuel assembly support grid uses an ANSYS finite element model to evaluate the stresses during impact conditions. The model consists of 1/2 of the support grid and is used to evaluate both side and end impacts. The support grid plate is 0.5 inches thick and constructed of 304 stainless steel. Figure 2.7.14-1 shows a plot of the finite element model. The regions where the support grid is welded to the corner angles are shown on the figure as heavy lines. These weld regions are fixed in the appropriate directions to represent the fixity of the angles. A plane of symmetry also exists and is appropriately constrained.

End Drop

During the end drop, the model is loaded using a static gravity load of 60g in the vertical direction (z). For accident conditions the addition of thermal stresses to the primary stresses is not required.

The peak nodal stress calculated for the 60g loading is 5,482 psi. The Service level D (accident) allowable stress at 750°F is $3.6 \times 15,600 = 56,160$ psi and the resulting margin of safety is +9.2.

Side Drop

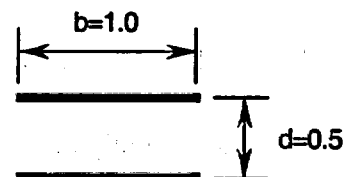
During the side-drop, the model (same as used in end-drop) is loaded using a static gravity load of 60g.

The peak nodal stress calculated for the 60g side loading is 43,812 psi. The Service level D allowable stress at 750°F is $3.6 \times 15,600 = 56,160$ psi and the resulting margin of safety is +0.28.

2.7.14.1.4 CY-MPC Reconfigured Fuel Assembly Weld Analysis

Maximum forces and moments for analysis of the welds joining the tube support grids to the corner angles are taken from the finite element analysis output. Each support grid is welded to the four corner angles with 1/8-in. fillet welds one inch in length both top and bottom. Using Blodgett's (R1) method of considering the weld as a line, the bending force (F_b) on the weld per inch of length is determined as follows:

$$F_b = \frac{M}{S_w} = \frac{46.0 \text{ lb} \cdot \text{in.}}{0.5 \text{ in.}^2} = 92.0 \text{ lb/in.}$$



The shear force (F_v) is:

$$F_v = \frac{V}{A_w} = \frac{51.2 \text{ lb}}{2.0 \text{ in.}} = 25.6 \text{ lb/in.}$$

where

$$S_w = b \times d$$

$$A_w = 2 \times b$$

The resultant force (F) on the weld is:

$$F = \sqrt{F_b^2 + F_v^2} = 95.5 \text{ lb}$$

The effective throat thickness of the 1/8-in. fillet weld is $0.707(0.125 \text{ in.}) = 0.088 \text{ in.}$, the effective throat area is $0.088 \text{ in.}^2/\text{in.}$, and the stress (f) in the weld is:

$$f = \frac{F}{nA} = \frac{95.5 \text{ lb/in.}}{0.4(0.088 \text{ in.}^2/\text{in.})} = 2,713.1 \text{ psi}$$

where

$n = 0.4$ is the minimum quality factor for a Category E Type V weld per ASME Code Section III-NG.

The margin of safety (MS) is determined on the basis of the parent metal yield strength:

$$MS = \frac{3S_m}{f} - 1 = \frac{3.6(15,600) \text{ psi}}{(2,713.1)} - 1 = +\text{large}$$

2.7.14.2 CY-MPC Damaged Fuel Can – Accident Conditions

The CY-MPC damaged fuel can is evaluated for hypothetical accident conditions of concrete cask 6-inch drop and the tip-over event. The concrete cask 30-foot drop is evaluated considering a 60g end-impact and a 60g side-impact.

A bounding temperature of 600°F is used for accident conditions. Material properties for ASME SA240/SA479 Type 304 Stainless Steel, ASME Code Section III, Subsection NG, are:

S_u	63.3 ksi
S_y	18.6 ksi
S_m	16.7 ksi
E	25.2×10^3 ksi

The weight of the damaged fuel can top assembly (lid) is 19.46 lbs, and the weight of the can weldment is 91.6 pounds. Twenty-five lbs and 95 lbs are used in the analysis for the top assembly and can weldment, respectively.

2.7.14.2.1 CY-MPC Damaged Fuel Can Tube Body Evaluation – Side Impact

The majority of the tube body is contained within the fuel tube in the basket assembly. Because both the tube body and the fuel tube have square cross sections, they will be in full contact (for 131.95 in. longitudinally) during the side impact and no significant bending stress will be introduced into the tube body. The last 4.55 in. of the body tube and the 5.0-in. length of the side plates will be unsupported past the fuel tube flange in the side impact configuration.

The tube body will be evaluated as a cantilevered beam with the combined weight (P) of the overhanging tube body, side plates and lid assembly multiplied by a deceleration factor of 60g. The 60g deceleration conservatively bounds the maximum deceleration of 55g for the cask side drop accident (Section 2.6.7.4).

The maximum bending stress (f_b) is determined as follows:

$$f_b = \frac{M_{\max} c}{I} = \frac{20,055(4.44)}{22.95} \cong 3,880 \text{ psi}$$

where:

$$M_{\max} = Pg \times L = 35(60)(9.55) = 20,055 \text{ lb}\cdot\text{in.}$$

$$g = 60$$

The shear stress (τ) is:

$$\tau = \frac{Pg}{A} = \frac{35(60)}{1.766} \cong 1,189 \text{ psi}$$

$$\sigma_1, \sigma_2 = \frac{1}{2} \left(f_b \pm \sqrt{f_b^2 + 4\tau^2} \right) = \frac{1}{2} \left(3,880 \pm \sqrt{3,880^2 + 4(1,189)^2} \right) \cong 4,215 \text{ psi and } -335 \text{ psi}$$

The stress intensity (σ_{\max}) = $|\sigma_1 - \sigma_2| = 4,550 \text{ psi}$

The Margin of Safety (MS) is:

$$MS = \frac{1.0 S_u}{\sigma_{max}} - 1 = \frac{1.0(63,300)}{4,550} - 1 = +12.9$$

2.7.14.2.2 CY-MPC Damaged Fuel Can Weld Evaluation

The welds joining the tube body to the side plates are full penetration welds (Type III, ASME Code Section III, Subsection NG paragraph NG-3352.3). Per Table NG-3352-1 (ASME Code Section III, Subsection NG), the weld quality factor (n) for a Type III weld with visual surface inspection is 0.5.

The margin of safety (MS) for the weld is:

$$MS = \frac{(1.0)n \cdot S_u}{\sigma_{max}} - 1 = \frac{(1.0)(0.5)(63,300 \text{ psi})}{4,550} - 1 = +5.9$$

2.7.14.2.3 CY-MPC Damaged Fuel Can Tube Body Evaluation – End Impact

For the bottom end impact, the tube body is subjected to the weight of the top assembly (lid), the side plates, and its self-weight. Because the top assembly is heavier, the bottom end drop is the governing case for tube body compression. The can contents bear against the bottom assembly through which the loads are transferred to the canister bottom plate.

The compressive load (P) on the tube body is:

$$P = 5,982.6 \text{ lb; use } 7,500 \text{ lb for evaluation}$$

The compressive stress (S_c) in the tube body is:

$$S_c = \frac{P}{A} = \frac{7,500 \text{ lb}}{1.766 \text{ in.}^2} \cong 4,247 \text{ psi}$$

The margin of safety (MS) is:

$$MS = \frac{0.7 S_u}{S_c} - 1 = \frac{0.7(63,300) \text{ psi}}{4,247 \text{ psi}} - 1 = +9.4$$

2.7.14.2.4 Tube Body Buckling Evaluation

The tube is evaluated, using the Euler formula, to determine the critical buckling load (P_{cr}):

$$P_{cr} = \frac{\pi^2 EI}{L_e^2} = \frac{\pi^2 (25.2 \times 10^6) (22.95)}{2(136.5)^2} = 76,587 \text{ lb}$$

where:

$$E = 25.2 \times 10^6 \text{ psi}$$

$$I = \frac{8.88^4 - 8.78^4}{12} = 22.95 \text{ in}^4$$

$$L_e = 2L \text{ (worst case condition)}$$

$$L = \text{unsupported tube body length (136.5 in.)}$$

Because the maximum compressive load (7,500 lb under the accident condition) is much less than the critical buckling load (76,587 lb) the tube has adequate resistance to buckling.

2.7.14.2.5 CY-MPC Damaged Fuel Can Lid Evaluation—End Impact

During a bottom end impact, the top lid will be subjected to bending stresses caused by the weight of the top lid. The top lid assembly conservatively weighs 25 lbs. Under a 60g load, the load on the plate is 1,500 lbs or $(1,500/8.77^2) \approx 20$ psi. The maximum stress for the lid is calculated by conservatively assuming a unit width simply supported beam 8.77-inches long with a thickness of 0.75-inches.

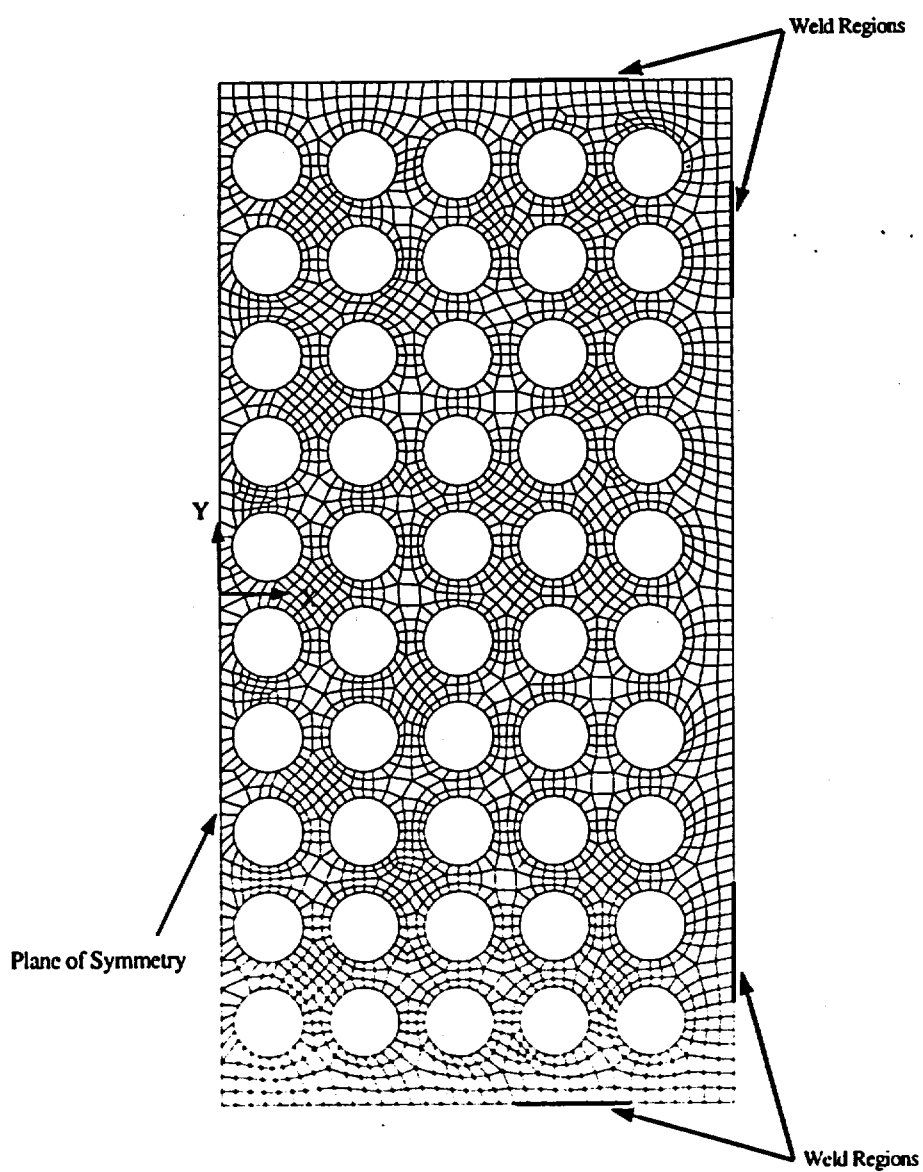
$$M = \frac{20(8.77^2)}{8} = 192.3 \text{ in} \cdot \text{lbs}$$

$$S_b = \frac{6(192.3)}{1.0(0.75^3)} = 2,051 \text{ psi}$$

The Margin of Safety is:

$$MS = \frac{2.4(16,700)}{2,051} - 1 = + \text{Large}$$

Figure 2.7.14-1 CY-MPC Reconfigured Fuel Assembly Tube Support Grid Finite Element Model



THIS PAGE INTENTIONALLY LEFT BLANK

2.8 Special Form

This section is not applicable to the NAC-STC because the fuel to be transported in the cask fails to satisfy the definition in 10 CFR 71.4 for special form radioactive material.

THIS PAGE INTENTIONALLY LEFT BLANK